

AD-A274 464



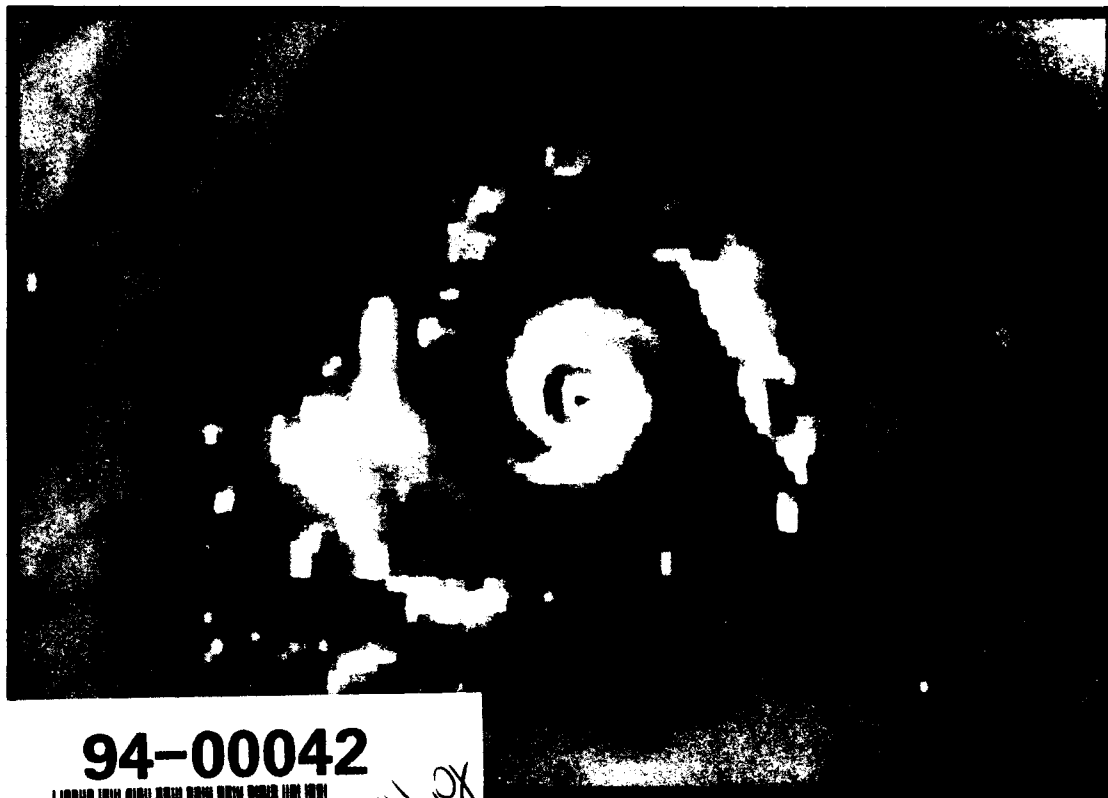
3

DTIC

JAN 04 1994

1992

ANNUAL TROPICAL CYCLONE REPORT



94-00042



2/1/98

JOINT TYPHOON WARNING CENTER
GUAM, MARIANA ISLANDS

DISTRIBUTION STATEMENT A

Approved for public release

Distribution Statement A

94 1 03 050

**Best
Available
Copy**

FRONT COVER CAPTION: An unusual picture of the concentric eye walls of Super Typhoon Gay (31W) as viewed by the passive microwave imager aboard the Defense Meteorological Satellite Program (DMSP) spacecraft on 191826Z November. The dense cirrus overcast that masks the outer concentric eye wall is transparent in the microwave spectrum, but would be opaque in the visual and infrared. The Meteorological Imagery, Data Display, and Analysis System (MIDDAS) combined the data from three channels (85 GHz horizontally polarized, 85 GHz vertically polarized, and 37 GHz vertically polarized) to make this multispectral image.

DTIC QUALITY INSPECTED 8

Accession For	
NTIS GRA&I	<input checked="" type="checkbox"/>
DTIC TAB	<input type="checkbox"/>
Unannounced	<input type="checkbox"/>
Justification	
By _____	
Distribution/	
Availability Codes	
Dist	Avail and/or Special
A-1	

**U. S. NAVAL OCEANOGRAPHY COMMAND CENTER
JOINT TYPHOON WARNING CENTER
COMNAVMARIANAS
PSC 489, BOX 12
FPO AP 96536-0051**

DONALD A. MAUTNER

**CAPTAIN, UNITED STATES NAVY
COMMANDING OFFICER**

CHARLES P. GUARD

**LIEUTENANT COLONEL, UNITED STATES AIR FORCE
DIRECTOR, JOINT TYPHOON WARNING CENTER
COMMANDER, DETACHMENT 1, 633d OPERATIONS SUPPORT SQUADRON**



STAFF

JOINT TYPHOON WARNING CENTER

LCDR	ANTHONY A. MARTINEZ	USN	TDO, DEPUTY DIRECTOR
*LCDR	ROBERT L. BEARD	USN	TDO, DEPUTY DIRECTOR
CAPT	STEPHEN C. HALLIN	USAF	TDO, TECHNIQUE DEVELOPMENT
CAPT	JOHN S. SHATTUCK	USAF	TDO
LT	THOMAS H. CECERE	USN	TDO
LT	GREGORY SALVATO	USN	TDO
**LT	STACY R. STEWART	USNR	TDO
*LT	DAVID J. STREMLER	USN	TDO
AG2	RONALD H. BRYAN	USN	TDA, LPO
AG3	BONNIE J. CAMPBELL	USN	TDA, STATISTICS
*AG3	HOLLY L. HOULIHAN	USN	TDA, STATISTICS
AG3	MARK A. WIREMAN	USN	TDA
*SRA	JANET E. KEMBLE	USAF	TDA
*AGAN	PHARAOH J. BELL	USN	TDA
*A1C	TIMOTHY J. GALLAGHER	USAF	TDA, STATISTICS
A1C	SEAN R. VOLOM	USAF	TDA
A1C	STACY L. SIMON	USAF	TDA

DET 1, 633 OSS

*CAPT	DANIEL N. SHOEMAKER	USAF	TDO, TECHNIQUE DEVELOPMENT
*CAPT	ROBERT G. HUDSON	USAF	OIC, USPACOM SAT NETWORK
CAPT	CHRISTOPHER K. BROOKS	USAF	OIC, USPACOM SAT NETWORK
1LT	SCOTT C. JACOBS	USAF	DATA DEVELOPMENT
MSGT	JOY L. HARDING	USAF	SAT FORECASTER; NCOIC
TSGT	PHILLIP A. ROSEBERRY	USAF	SAT FORECASTER
TSGT	TERESA A. deBOER	USAF	SAT FORECASTER
TSGT	WILLIAM GATES, JR.	USAF	SAT FORECASTER
TSGT	JEFFREY E. OAKES	USAF	SAT FORECASTER
TSGT	THEODORE V. MUSTAIKES, JR.	USAF	SAT FORECASTER
TSGT	JAMES G. BROCK	USAF	SAT FORECASTER
*TSGT	DANILO O. MONTILLANO	USAF	CHIEF INFORMATION MANAGEMENT
SSGT	VINCENT T. AGUON	USAF	CHIEF INFORMATION MANAGEMENT
*SSGT	RAYMOND L. SOUZA, JR.	USAF	SAT FORECASTER
*SSGT	DANIEL T. EBBERT	USAF	SAT FORECASTER

ATCR STAFF

CAPT	ELIZABETH B. BORELLI	USAF	TDO, BEST TRACK OFFICER, EDITOR
CAPT	DAN B. MUNDELL	USAF	TDO, STATISTICS OFFICER
MR	FRANK H. WELLS	USN	TECHNICAL EDITOR
*SGT	BRIAN L. McDONALD	USAF	SENIOR TDA, GRAPHICS
*SGT	CARLOS A. DELANUEZ	USAF	TDA, GRAPHICS
*SRA	CORNELIUS MASSEY	USAF	TDA, GRAPHICS
AG3	DAVID L. HAZEL	USN	TDA, GRAPHICS, STATISTICS

ONR POST - DOCTORATE FELLOW

DR	MARK A. LANDER	UNIVERSITY OF GUAM
----	----------------	--------------------

* TRANSFERRED DURING 1992

** ACTIVE DUTY TRAINING

FOREWARD

The Annual Tropical Cyclone Report is prepared by the staff of the Joint Typhoon Warning Center (JTWC), a combined Air Force/Navy organization operating under the command of the Commanding Officer, U.S. Naval Oceanography Command Center/Joint Typhoon Warning Center, Guam. The JTWC was founded 1 May 1959 when the Commander-in-Chief Pacific (USCINCPAC) forces directed that a single tropical cyclone warning center be established for the western North Pacific region. The operations of JTWC are guided by CINCPAC Instruction (CINCPACINST) 3140.1V.

The mission of JTWC is multifaceted and includes:

1. Continuous monitoring of all tropical weather activity in the Northern and Southern Hemispheres, from 180° east longitude westward to the east coast of Africa, and the prompt issuance of appropriate advisories and alerts when tropical cyclone development is anticipated.

2. Issuance of warnings on all significant tropical cyclones in the above area of responsibility.

3. Determination of requirements for tropical cyclone reconnaissance and assignment of appropriate priorities.

4. Post-storm analysis of significant tropical cyclones occurring within the western North Pacific and North Indian Oceans, which includes an in-depth analysis of tropical cyclones of note and all typhoons.

5. Cooperation with the Naval Research Laboratory, Monterey, California on operational evaluation of tropical cyclone models and forecast aids, and the development of new techniques to support operational forecast scenarios.

Changes this year include: 1) wind area radius threshold of 30kt on warnings increased to 35kt ; and, 2) 36-hour forecasts added to

western North Pacific and North Indian Ocean tropical cyclone warnings.

Special thanks to: the men and women of the Alternate Joint Typhoon Warning Center for standing in for JTWC which was incapacitated for 11 days after Typhoon Omar's passage; Fleet Numerical Oceanography Center for their unfaltering operational and software support; the Naval Research Laboratory for their dedicated research and forecast improvement initiatives; the Air Force Global Weather Central for continued satellite support and microwave development efforts; the 633d Communications Squadron, Operating Location Charlie and the Operations and Equipment Support departments of the Naval Oceanography Command Center, Guam for their high quality support; all the men and women of the ships and facilities ashore throughout the JTWC AOR, and especially on Guam, who took the observations and communicated them with pride that became the basis for our analyses, forecasts and post analyses; the staff at National Oceanic and Atmospheric Administration (NOAA) National Environmental Satellite, Data, and Information Service (NESDIS) for their tropical cyclone position and intensity support; the personnel of Tropical Cyclone Motion-1992 (TCM-92) for sharing their data and understanding of tropical cyclones; the personnel of the Pacific Fleet Audio-Visual Center, Guam for their assistance in the reproduction of satellite imagery for this report; the Navy Publications and Printing Service Branch Office, Guam; Dr. Bob Abbey and the Office of Naval Research for their support to the University of Guam for the Post-Doctorate Fellow at JTWC; Dr. Mark Lander for his training efforts, suggestions and valuable insights; and AG3 Dave Hazel for his excellent support with the desktop publishing system and graphics.

EXECUTIVE SUMMARY

The Joint Typhoon Warning Center, Guam (JTWC) experienced the busiest year in its 33-year history during 1992, eclipsing the record-setting 1991 year by 250 warnings. In addition to the massive warning workload, the Center also supported several contingencies and scientific field experiments, and endured the assault of five typhoons in less than a 3-month period that included Typhoon Omar which blasted Guam with 105-kt sustained winds and caused \$457 million in damages to the island. JTWC warnings were crucial to the safe deployment of ships, aircraft and personnel involved with Operations RESTORE HOPE, FULL ACCOUNTING, and PROVIDE COMFORT. JTWC's participation in such experiments as the TCM-92 (a Naval Postgraduate School/ONR-sponsored mini-field experiment), GTE/PEM-West (a NASA atmospheric chemistry field expedition), and TOGA COARE (an international air-sea interaction field experiment) greatly contributed to the success of each.

In 1992, JTWC issued 1405 warnings, significantly surpassing the 1990 and 1991 records of 1139 and 1155 warnings, respectively. Of the 159 days of the year JTWC was in warning status, 75 of those days had at least two storms, 27 days at least three storms at the same time, and 3 days had four storms occurring simultaneously. JTWC's track forecast performance in 1992 for the western North Pacific was the third best in Center's history, despite the workload. When compared to the climatology-persistence model, CLIPER,

JTWC forecasts were 24 percent better across the board, indicating that JTWC forecasts were very good despite a relatively difficult forecast year. In the Southern Hemisphere, forecast errors for the second straight year were below normal, and in the North Indian Ocean the forecast errors were smaller than the long term average for 24 hours, although for 48 and 72 hours they were slightly larger. Intensity forecast errors for western North Pacific tropical cyclones were smaller than average at 24 hours and 48 hours, but showed no improvement over the long term mean at 72 hours.

JTWC and its Air Force satellite reconnaissance component, Det 1, 633d Operations Support Squadron, continued to improve capabilities through the acquisition and exploitation of new technology. The Meteorological Imagery, Data Display, and Analysis System (MIDDAS) gained the capability to process and display all polar orbiting satellite data in addition to geostationary data. The Mission Sensor Tactical Imaging Computer (MISTIC) gained the capability to co-register microwave imager data with conventional infrared data. JTWC was also able to routinely obtain worldwide microwave imager data from FNOC and manipulate it on the MISTIC. And the Naval Research Lab began work on the SPAWRSYSCOM-funded follow-on system to the current Automated Tropical Cyclone Forecast System (ATCF).

TABLE OF CONTENTS

	Page
FOREWORD	iii
EXECUTIVE SUMMARY	iv
1. OPERATIONAL PROCEDURES	1
1.1 General	1
1.2 Data Sources	1
1.3 Communications	2
1.4 Data Displays	5
1.5 Analyses	5
1.6 Forecast Procedures	5
1.7 Warnings	8
1.8 Prognostic Reasoning Messages	9
1.9 Tropical Cyclone Formation Alerts	9
1.10 Significant Tropical Weather Advisories	9
2. RECONNAISSANCE AND FIXES	11
2.1 General	11
2.2 Reconnaissance Availability	11
2.3 Satellite Reconnaissance Summary	11
2.4 Radar Reconnaissance Summary	15
2.5 Tropical Cyclone Fix Data	15
3. SUMMARY OF NORTHWEST PACIFIC AND NORTH INDIAN OCEAN TROPICAL CYCLONES	19
3.1 General	19
3.2 Western North Pacific Tropical Cyclones	24

INDIVIDUAL TROPICAL CYCLONES

<u>Tropical Cyclone</u>	<u>Author</u>	<u>Page</u>	<u>Tropical Cyclone</u>	<u>Author</u>	<u>Page</u>
(01W) TY Axel	Stremmer.....	36	(17W) TY Ryan	Mundell.....	92
(01C) TS Ekeka	Mundell.....	42	(18W) TY Sibyl	Borelli.....	96
(02W) TY Bobbie	Borelli.....	44	(19W) TY Ted	Cecere.....	100
(03W) TY Chuck	Borelli.....	48	(20W) TS Val	Salvato.....	105
(04W) TS Deanna	Borelli.....	51	(21W) TS Ward	Mundell.....	107
(05W) TY Eli	Martinez.....	53	(22W) TS Zack	Borelli.....	110
(06W) TS Faye	Cecere.....	56	(23W) STY Yvette	Cecere.....	112
(07W) TY Gary	Mundell.....	58	(24W) TY Angela	Salvato.....	116
(08W) TS Helen	Salvato.....	61	(25W) TY Brian	Mundell.....	120
(09W) TS Irving	Cecere.....	63	(26W) TY Colleen	Borelli.....	126
(10W) TY Janis	Martinez.....	67	(27W) TS Dan	Mundell.....	130
(11W) TY Kent	Salvato.....	70	(28W) STY Elsie	Cecere.....	136
(12W) TY Lois	Mundell.....	73	(29W) TD 29W	Borelli.....	139
(13W) TS Mark	Borelli.....	75	(30W) TY Forrest	Salvato.....	141
(14W) TS Nina	Cecere.....	77	(31W) STY Gay	Shattuck.....	145
(15W) TY Omar	Martinez.....	79	(32W) TY Hunt	Borelli.....	152
(16W) TS Polly	Salvato.....	88			

3.3 North Indian Ocean Tropical Cyclones	<u>Page</u> 155
INDIVIDUAL TROPICAL CYCLONES	
<u>Name</u>	<u>Page</u>
TC 01B.....	158
TC 02A	160
TC 03B.....	162
TC 04B.....	164
TC 05B.....	166
TC 06A	168
TC 07B.....	170
TC 08B.....	172
TC 09B.....	174
TC 10B.....	176
TC 11A	178
TC 12A	180
Forrest (30W).....	141
4. SUMMARY OF SOUTH PACIFIC AND SOUTH INDIAN OCEAN TROPICAL CYCLONES	183
4.1 General.....	183
4.2 South Pacific and South Indian Ocean Tropical Cyclones	183
5. SUMMARY OF FORECAST VERIFICATION	191
5.1 Annual Forecast Verification	169
5.2 Comparison of Objective Techniques	205
5.3 Testing and Results	208
6. TROPICAL CYCLONE WARNING VERIFICATION STATISTICS	213
6.1 General	213
6.2 Warning Verification Statistics.....	213
7. TROPICAL CYCLONE SUPPORT SUMMARY	249
BIBLIOGRAPHY	257
APPENDIX A - Definitions.....	259
APPENDIX B - Names for Tropical Cyclones.....	262
APPENDIX C - Contractions	263
APPENDIX D - Past Annual Tropical Cyclone Reports	266
APPENDIX E - Distribution List	267

1. OPERATIONAL PROCEDURES

1.1 GENERAL

The Joint Typhoon Warning Center (JTWC) provides a variety of routine products and services to the organizations within its area of responsibility (AOR), including:

1.1.1 SIGNIFICANT TROPICAL WEATHER ADVISORY — Issued daily or more frequently as needed, to describe all tropical disturbances and their potential for further development during the advisory period. A separate bulletin is issued for the western Pacific and the Indian Ocean.

1.1.2 TROPICAL CYCLONE FORMATION ALERT — Issued when synoptic or satellite data indicate that the development of a significant tropical cyclone is likely within 12 to 24 hours in a specified area.

1.1.3 TROPICAL CYCLONE/ TROPICAL DEPRESSION WARNING — Issued periodically throughout each day to provide forecasts of position, intensity, and wind distribution for tropical cyclones in JTWC's AOR.

1.1.4 PROGNOSTIC REASONING MESSAGES — Issued with warnings for tropical depressions, tropical storms, typhoons and super typhoons in the western North Pacific to discuss the rationale for the content of JTWC's warnings.

1.1.5 PRODUCT CHANGES — The contents and availability of the above JTWC products are set forth in USCINCPACINST 3140.1V. Changes to USCINCPACINST 3140.1V, and JTWC products and services are proposed and discussed at the Annual Tropical Cyclone Conference.

1.2 DATA SOURCES

1.2.1 COMPUTER PRODUCTS — Numerical and statistical guidance are available from the USN Fleet Numerical Oceanography Center (FNOC) at Monterey, California. These products along with selected ones from the National Meteorological Center (NMC) are received through the Naval Environmental Data Network (NEDN), the Naval Environmental Satellite Network (NESN), and by microcomputer dial-up connections using military and commercial telephone lines. Numerical guidance is also received from international sources as well.

1.2.2 CONVENTIONAL DATA — These data sets are comprised of land and shipboard surface observations, and enroute meteorological observations from commercial and military aircraft (AIREPS) recorded within six hours of synoptic times, and cloud-motion winds derived from satellite data. The conventional data is hand- and computer-plotted, and hand-analyzed in the tropics for the surface/gradient and 200-mb levels. These analyses are prepared twice daily from 0000Z and 1200Z synoptic data. Also, FNOC supplies JTWC with computer generated analyses and prognoses, from 0000Z and 1200Z synoptic data, at the surface, 850-mb, 700-mb, 500-mb, 400-mb, and 200-mb levels, deep-layer-mean winds, wind shear, and geopotential height change charts.

1.2.3 SATELLITE RECONNAISSANCE — Meteorological satellite imagery recorded at USAF/USN ground sites and USN ships supply day and night coverage in JTWC's AOR. Interpretation of these satellite data provides tropical cyclone positions and estimates of current and forecast intensities. The USAF tactical satellite sites and Air Force Global Weather Central currently receive and analyze special

sensor microwave/imager (SSM/I) data to provide locations of tropical cyclones of which the center is obscured by cirrus clouds and estimates of 35-kt (18 m/sec) wind radii near tropical cyclones. Use of satellite reconnaissance is discussed further in section 2.3, Satellite Reconnaissance Summary.

1.2.4 RADAR RECONNAISSANCE — Land-based radar observations are used to position tropical cyclones. Once a well-defined tropical cyclone moves within the range of land-based radar sites, radar reports are invaluable for determination of position and movement. JTWC's use of radar reports during 1992 is discussed in section 2.4, Radar Reconnaissance Summary.

1.2.5 AIRCRAFT RECONNAISSANCE — Until the summer of 1987, dedicated aircraft reconnaissance was used routinely to locate and determine the wind structure of tropical cyclones. Now aircraft fixes are only available via radar reports from transiting jet aircraft or from weather reconnaissance aircraft involved in dedicated research. Four fixes were received from the WC-130 supporting the Tropical Cyclone Motion-1992 (TCM-92) experiment.

1.2.6 DRIFTING METEOROLOGICAL BUOYS — In 1989, the Commander, Naval Oceanography Command put the NAVOCEANCOM Integrated Drifting Buoy Plan (1989-1994) into action to meet USCINPACFLT requirements that included tropical cyclone warning support. In 1992, 19 drifting buoys, which included 16 mini-meteorological (MINI-MET) and three larger TOGA buoys, were deployed during the WESTPAC tropical cyclone season by a Naval Oceanographic Office-contracted C-130 aircraft.

These buoys transmit data to NOAA's TIROS-N polar orbiting satellites, which in turn both store and immediately retransmit the data. If the satellite retransmission can be received by

Guam, JTWC acquires the drifting buoy data directly via a Local User's Terminal (LUT). Additionally, the data stored aboard the satellites are recovered via Service ARGOS, processed, and then distributed to operational centers worldwide over the Global Telecommunications System (GTS), and Automated Weather Network (AWN) via the NWS Telecommunications Gateway in Silver Springs, Maryland.

1.2.7 AUTOMATED METEOROLOGICAL OBSERVING STATIONS (AMOS) — Through a cooperative effort between the Naval Oceanography Command, the Department of the Interior, and NOAA (NWS) to increase data available for tropical analysis and forecasting, a network of 20 AMOS stations is being installed in the Micronesian islands. (Previous to this effort, two sites were installed in the Northern Mariana Islands at Saipan and Rota through a joint venture between the Navy and NOAA (NWS).) JTWC receives data from all AMOS sites via the AWN under the KWBC bulletin headers SMPW01, SIPW01 and SNPW01 (SXYM10 for Tinian and Rota). Since September of 1991, the capability to transmit data via System ARGOS and NOAA polar orbiting satellites has been available as a backup to regular data transmission to GOES West and more recently, for sites to the west of Guam, to Japanese GMS. ARGOS upgrades to existing sites are also being accomplished as the opportunity arises. An AMOS summary appears in Table 1-1.

1.3 COMMUNICATIONS

Primary communications support is provided by the Naval Telecommunications Center (NTCC), Nimitz Hill, a component of the Naval Computers and Telecommunications Area Master Station, Western Pacific (NCTAMS WESTPAC). In addition, JTWC uses several other communications systems.

1.3.1 AUTOMATED DIGITAL NETWORK (AUTODIN) — AUTODIN is used for dissemination of warnings, alerts and other related bulletins to Department of Defense (DOD) and other U.S. Government installations. These messages are relayed for further transmission over Navy Fleet Broadcasts, and Coast Guard continuous wave Morse code and voice broadcasts. AUTODIN messages can be relayed to commercial telecommunications for delivery to non-DOD users. Inbound message traffic for JTWC is received via AUTODIN addressed to NAVOCEANCOMCEN GU//JTWC// or DET 1 633 OSS NIMITZ HILL GU//CC//.

1.3.2 AUTOMATED WEATHER NETWORK (AWN) — The AWN provides weather data over the Pacific Meteorological Data System (PACMEDS). The PACMEDS, operational at

JTWC since April 1988, allows Pacific-Theater agencies to receive weather information at a 1200 baud rate. JTWC uses a software package called AWNCOM/WINDS on a microcomputer to send and receive data via the PACMEDS. Through recent hardware and software upgrades, this system provides effective storage and manipulation of the large volume of meteorological reports available from throughout JTWC's vast AOR. Through the AWN, JTWC has access to data available on the Global Telecommunications System (GTS). JTWC's AWN station identifier is PGTW.

1.3.3 DEFENSE SWITCHED NETWORK (DSN) — DSN, formerly AUTOVON, is a worldwide, general purpose, switched telecommunications network for the DOD. The network provides a rapid and vital voice link for

Table 1-1 AUTOMATED METEOROLOGICAL OBSERVING STATIONS SUMMARY

<u>Site</u>	<u>Location</u>	<u>Callsign</u>	<u>ID#</u>	<u>Report</u>	<u>Installed</u>
Saipan*	15.2°N, 145.7°E	15D151D2	----	ARC	1986
Rota	14.2°N, 145.2°E	15D16448	91221	ARC	1987
Faraulep**	8.1°N, 144.6°E	FARP2	52005	C-MAN/ARGOS	1988
Enewetak	11.4°N, 162.3°E	ENIP2	91251	C-MAN/ARGOS	1989
Ujae***	8.9°N, 165.8°E	UJAP2	91365	C-MAN	1989
Pagan	18.1°N, 145.8°E	PAGP2	91222	C-MAN/ARGOS	1990
Kosrae	5.3°N, 163.0°E	KOSP2	91355	C-MAN/ARGOS	1990
Mili	6.1°N, 171.8°E	MILP2	91377	C-MAN	1990
Oroluk	7.6°N, 155.1°E	ORKP2	91343	C-MAN	1991
Pingelap	6.3°N, 160.7°E	PIGP2	91352	C-MAN/ARGOS	1991
Ulul	8.7°N, 149.7°E	----	91328	C-MAN/ARGOS	1992
Tinian*	15.0°N, 145.6°E	15D151D2	91231	ARC	1992

* Saipan site relocated to Tinian and commissioned on 1 June 1992.

** The prototype site on Faraulep was destroyed on 28 November 1991 by Super Typhoon Owen.

*** Ujae site was destroyed on 18 November 1992 by Super Typhoon Gay.

ARC = Automated Remote Collection system (via GOES West)

C-MAN = Coastal-Marine Automated Network (via GOES West or GMS)

ARGOS = System ARGOS data collection (via NOAA's TIROS-N)

JTWC to communicate tropical cyclone information to DOD installations. The DSN telephone numbers for JTWC are 344-4224 or 344-5240.

1.3.4 NAVAL ENVIRONMENTAL DATA NETWORK (NEDN) — The NEDN is the primary link to FNOC to obtain computer-generated analyses and prognoses. It is also a backup communications line for requesting and receiving the objective tropical cyclone forecast aids from FNOC's mainframe computers. The NEDN allows JTWC to communicate directly to the other Naval Oceanography Command Centers around the world.

1.3.5 PUBLIC DATA NETWORK (PDN) — A commercial packet switching network that provides low-speed interactive transmission to users of FNOC products. The PDN is now the primary method for JTWC to request and receive FNOC-produced objective tropical cyclone forecast aids. The PDN allows direct access of FNOC products via the Automated Tropical Cyclone Forecast (ATCF) system. The PDN also serves as an alternate method of obtaining FNOC analyses and forecast fields. TYMNET is the contractor providing PDN services between FNOC and JTWC.

1.3.6 DEFENSE DATA NETWORK (DDN) — The DDN is a DOD computer communications network utilized to exchange data files. Because the DDN has links, or gateways, to non-military information networks, it is frequently used to exchange data with the research community. JTWC's internet address is 26.19.0.250 and its E-Mail account is jtops@nocc.navy.mil. The Det 1, 633d OSS address is admin@nocc.navy.mil.

1.3.7 TELEPHONE FACSIMILE — TELEFAX provides the capability to rapidly scan and transmit, or receive, documents over commercial telephone lines or DSN. TELEFAX is used

to disseminate tropical cyclone advisories and warnings to key agencies on Guam and, in special situations, to DOD, other U.S. Government agencies, and the other Micronesian Islands. Inbound documents for JTWC are received at (671) 344-4032 or (671) 344-6143.

1.3.8 NAVAL ENVIRONMENTAL SATELLITE NETWORK (NESN) — The NESN's primary function is to pass satellite data from the satellite global data base at FNOC to regional centers. Similarly, it can pass satellite data from NOCC/JTWC to FNOC or other regional centers. The NESN's carrier circuit serves as a backup to the NEDN.

1.3.9 AIRFIELD FIXED TELECOMMUNICATIONS NETWORK (AFTN) — AFTN was installed at JTWC in January 1990. Though it is primarily for the exchange of aviation information, weather information and warnings are also distributed via this network. It also provides point-to-point communication with other warning agencies not connected to the AWN or GTS. JTWC's AFTN identifier is PGUMYMYT.

1.3.10 LOCAL USER TERMINAL (LUT) — JTWC uses a LUT, provided by the Naval Oceanographic Office, as the primary means of receiving real-time data from drifting meteorological buoys and ARGOS-equipped AMOS via the polar orbiting NOAA TIROS-N satellites.

1.3.11 COMPUTER FACSIMILE — The NOCC/JTWC Rapid Response Team (RRT) uses a microcomputer to automatically transmit facsimile messages to agencies on Guam and the Northern Marianas when a typhoon threatens the Mariana Islands. The RRT can be reached at (671) 344-7116 or (671) 344-7119.

1.3.12 TELEX — NOCC/JTWC's address for inbound TELEX messages is 197873NOCC GU.

1.4 DATA DISPLAYS

1.4.1 NAVAL ENVIRONMENTAL DISPLAY STATION (NEDS) — The NEDS receives, processes, stores, displays and prints copies of FNOC environmental products. It drives the fleet facsimile broadcast and can also be used to generate the requests for objective tropical cyclone forecast techniques.

1.4.2 AUTOMATED TROPICAL CYCLONE FORECAST SYSTEM (ATCF) — The ATCF is a software program that assists the Typhoon Duty Officer (TDO) in the preparation, formatting, and dissemination of tropical cyclone alerts and warnings. It cuts message preparation time and reduces the number of corrections to JTWC's alerts and warnings. The ATCF automatically displays: the working and objective best tracks, forecasts of track, intensity, and wind distribution; information from computer generated forecast aids and products from other agencies; and computes the myriad statistics calculated by JTWC. Links have been established through a Local Area Network (LAN) to the NOCC Operations watch team to facilitate the generation of tropical cyclone warning graphics for the fleet facsimile broadcasts, for NOCC's local metwatch program and warning products for Micronesia. A module permits satellite reconnaissance fixes to be input from Det 1, 633d OSS into the LAN. Several other modules are still under development including: direct links to NTCC, the LUT, and AWNCOM/WINDS.

1.4.3 NAVAL SATELLITE DISPLAY SYSTEM (NSDS) — The NSDS functions as a display of FNOC-stored Defense Meteorological Satellite Program (DMSP) imagery and low resolution geostationary imagery. It is the primary means for JTWC to directly observe areas of cloudiness in the western Indian Ocean.

1.4.4 NAVAL SATELLITE DISPLAY SYSTEM-GEOSTATIONARY (NSDS-G) — The NSDS-G is NOCC's primary geostationary imagery processing and display system. It can be used to process high resolution geostationary imagery for tropical cyclone positions and intensity estimates for the western Pacific Ocean should the Meteorological Imagery, Data Display, and Analysis System (MIDDAS) fail.

1.5 ANALYSES

The JTWC Typhoon Duty Officer (TDO) routinely performs manual streamline analyses of composite surface/gradient-level (3000 ft (914 m)) and upper-tropospheric (centered on the 200-mb level) data for 0000Z and 1200Z each day. Manual sea-level pressure analyses concentrating on the mid-latitudes are available from the NOCC Operations watch team. Computer analyses of the surface, 925-, 850-, 700-, 500-, 400-, and 200-mb levels, deep-layer-mean winds, frontal boundaries depiction, 1000-200 mb/400-200 mb/and 700-400 mb wind shear, 500 mb and 700 mb 24-hour height change, and a variety of other meteorological displays are available from the 0000Z and 1200Z FNOC data bases. Additional sectional charts at intermediate synoptic times and auxiliary charts, such as station-time plot diagrams, time-height cross section charts and pressure-change charts, are analyzed during periods of significant tropical cyclone activity.

1.6 FORECAST PROCEDURES

1.6.1 INITIAL POSITIONING — The warning position is the best estimate of the center of the surface circulation at synoptic time. It is estimated from an analysis of all fix information received from one hour before to one and one-half hours after that synoptic time. The analysis is aided by a computer-generated objective best track scheme that weights fix information based on its statistical accuracy. The TDO includes

synoptic observations and other information to adjust the position, testing consistency with the past direction, speed of movement and the influence of the different scales of motions. If the fix data are not available due to reconnaissance platform malfunction or communication problems, or are considered unrepresentative, synoptic data and/or extrapolation from previous fixes are used.

1.6.2 TRACK FORECASTING — In preparing the JTWC official forecast, the TDO evaluates a wide variety of information, and employs a number of objective and subjective techniques. Because tropical cyclone track forecasting has and continues to require a significant amount of subjective input from the TDO, detailed aspects of the forecast-development process will vary somewhat from TDO to TDO, particularly with respect to the weight given to any of the available guidance. JTWC uses a standardized, three-phase tropical cyclone motion forecasting process to improve not only track forecast accuracy, but also intensity forecast accuracy and forecast-to-forecast consistency.

1.6.2.1 Field Analysis Phase — Navy Operational Global Atmospheric Prediction System (NOGAPS) analyses and prognoses at various levels are evaluated for position, development, and movement of not only the tropical cyclone, but also relevant synoptic features such as: 1) subtropical ridge circulations, 2) mid-latitude short/long-wave troughs and associated weaknesses in the subtropical ridge, 3) monsoon surges, 4) influences of cyclonic cells in the Tropical Upper Tropospheric Trough (TUTT), 5) other tropical cyclones, and 6) the distribution of sea surface temperature. This process permits the TDO to develop an initial impression of the environmental steering influences to which the tropical cyclone is and will be subjected to as depicted by NOGAPS. The NOGAPS analyses are then compared to the

hand-plotted and analyzed charts prepared by the TDO and to the latest satellite imagery in order to determine how well the NOGAPS initialization process has conformed to the available synoptic data, and how well the resultant analysis fields agree with the synoptic situation inferred from the imagery. Finally, the TDO compares both the computer and hand-analyzed charts to monthly climatology in order to make a preliminary determination as to what degree the tropical cyclone is and will continue to be (according to NOGAPS) subjected to a climatological or nonclimatological synoptic environment. Noting latitudinal and longitudinal displacements of subtropical ridge and long-wave mid-latitude features is of particular importance, and will partially determine the relative weights given to climatologically- or dynamically-based objective forecast guidance.

1.6.2.2 Objective Techniques Analysis Phase — After displaying the latest set of forecasts given by JTWC's suite of objective techniques, the TDO then evaluates the pattern produced by the set of forecasts according to the following principles. First, the degree to which the current situation is considered to be and will continue to be climatological is further refined by comparing the forecasts of the climatology-based objective techniques, dynamically-based techniques, and past motion of the present storm. This assessment partially determines the relative weighting given the different classes of objective techniques. Second, the spread of the pattern determined by the set of objective forecasts is used to provide a measure of the predictability of subsequent motion, and the advisability of including a low or moderate probability alternate forecast scenario in the prognostic reasoning message or warning (outside the western North Pacific). The spread of the objective techniques pattern is typically small well-before or well-after recurvature (providing high forecast confidence) and large near the decision-point of recurvature or non-recurvature, or dur-

ing a quasi-stationary or erratic movement phase (increasing the likelihood of alternate scenarios).

1.6.2.3 Construct Forecast Phase — The TDO then constructs the JTWC official forecast giving due consideration to the: 1) extent to which the synoptic situation is, and is expected to remain, climatological, 2) past statistical performance of the various objective techniques on the current storm, and 3) known properties of individual objective techniques given the present synoptic situation or geographic location. The following guidance for weighting the objective techniques is applied:

a) Weight persistence strongly in the first 12 to 24 hours of the forecast period.

b) Give significant weight to the last JTWC forecast at all forecast times, unless there is significant evidence to warrant a departure. (Also consider the latest forecasts from regional warning centers, if applicable.)

c) Give more weight to the techniques that have been performing well on the current tropical cyclone and/or are expected to perform well in the current and expected synoptic situation.

d) Stay within the "envelope" determined by the spread of objective techniques forecasts unless there is a specific reason for not doing so (e.g., all objective forecasts start out at a significant angle relative to past motion of the current tropical cyclone).

1.6.3 INTENSITY FORECASTING — The empirically derived Dvorak (1984) technique is used as a first guess for the intensity forecast. The TDO then adjusts the forecast after evaluating climatology and the synoptic situation. An interactive conditional climatology scheme allows the TDO to define a situation similar to the system being forecast in terms of location, time of year, current intensity, and intensity trend. Synoptic influences such as the location of major troughs and ridges, and the position and intensity of the TUTT all play a large part

in intensifying or weakening a tropical cyclone. JTWC incorporates a checklist into the intensity forecast procedure. Such criteria as upper-level outflow patterns, neutral points, sea-surface temperatures, enhanced monsoonal or cross-equatorial flow, and vertical wind shear are evaluated for their tendency to enhance or inhibit normal development, and are incorporated into the intensity forecast process through locally developed thumb rules. In addition to climatology and synoptic influences, the first guess is modified for interactions with land, with other tropical cyclones, and with extratropical features. Climatological and statistical methods are also used to assess the potential for rapid intensification (Mundell, 1990).

1.6.4 WIND-RADII FORECASTING — Since the loss of dedicated aircraft reconnaissance in 1987, JTWC has turned to other data sources for determining the radii of winds around tropical cyclones. The determination of wind radii forecasts is a three-step process:

(a) First, low-level satellite drift winds, microwave imager 35 kt wind speed analysis (See Chapter 2), and synoptic data are used to derive the current wind distribution.

(b) Next the first guess of the radii is determined from statistically-derived empirical wind radii models. JTWC currently uses three models: the Tsui model, the Huntley model, and the Martin-Holland model. The latter model uses satellite-derived parameters to determine the size and shape of the wind profile associated with a particular tropical cyclone. The Martin-Holland model also incorporates latitude and speed of motion to produce an asymmetrical wind distribution. These models provide wind distribution analyses and forecasts that are primarily influenced by the intensity forecasts. The analyses are then adjusted based on the actual analysis from step (a), and the forecasts are adjusted appropriately.

(c) Finally, synoptic considerations, such as the interaction of the cyclone with mid-latitude

pressure cells, are used to fine-tune the forecast wind radii.

1.6.5 EXTRATROPICAL TRANSITION —

When a tropical cyclone moves into the mid-latitudes, it often enters an environment that is detrimental to the maintenance of the tropical cyclone's structure and energy-producing mechanisms. The effects of cooler sea surface temperatures, cooler and dryer environmental air, and strong vertical wind shear all act to convert the tropical cyclone into an extratropical cyclone. JTWC indicates that this conversion process is occurring by stating that the tropical cyclone is "becoming extratropical." JTWC will indicate that the conversion is expected to be complete by stating that the system has "become extratropical." When a tropical cyclone is forecast to become extratropical, JTWC coordinates the transfer of responsibility with the appropriate regional Naval Oceanography Command Center, which assumes warning responsibilities for the extratropical system.

1.6.6 TRANSFER OF WARNING RESPONSIBILITIES — JTWC coordinates the transfer of warning responsibility for tropical cyclones entering or exiting its AOR. For tropical cyclones crossing 180° east longitude in the North Pacific Ocean, JTWC coordinates with the Central Pacific Hurricane Center (CPHC), Honolulu via the Naval Western Oceanography Center (NWOC), Pearl Harbor, Hawaii. For tropical cyclones crossing 180° east longitude in the South Pacific Ocean, JTWC coordinates with the NWOC, which has responsibility for the Southeastern Pacific.

Whenever a tropical cyclone threatens Guam, files are electronically transferred from JTWC to the Alternate Joint Typhoon Warning Center (AJTWC) collocated with NWOC. In the event that JTWC should become incapacitated, the AJTWC assumes JTWC's functions. Assistance in determining satellite reconnais-

sance requirements, and in obtaining the resultant data, is provided by the weather unit supporting the 15th Air Base Wing, Hickam AFB, Hawaii.

1.7 WARNINGS

JTWC issues two types of warnings: Tropical Cyclone Warnings and Tropical Depression Warnings.

1.7.1 TROPICAL CYCLONE WARNINGS -

These are issued when a closed circulation is evident and maximum sustained winds are forecast to reach 34 kt (18 m/sec) within 48 hours, or when the tropical cyclone is in such a position that life or property may be endangered within 72 hours.

Each Tropical Cyclone Warning is numbered sequentially and includes the following information: the current position of the surface center; an estimate of the position accuracy and the supporting reconnaissance (fix) platform(s); the direction and speed of movement during the past six hours (past 12 hours in the Southern Hemisphere); and the intensity and radial extent of over 35-, 50-, and 100-kt (18-, 26-, and 51 m/sec) surface winds, when applicable. At forecast intervals of 12, 24, 36, 48, and 72 hours (12, 24, and 48 hours in the Southern Hemisphere), information on the tropical cyclone's anticipated position, intensity and wind radii is provided. Vectors indicating the mean direction and mean speed between forecast positions are included in all warnings. In addition, a 3-hour extrapolated position is provided in the remarks section.

Warnings in the western North Pacific and North Indian Oceans are issued every six hours (unless an amendment is required) valid at standard synoptic times: 0000Z, 0600Z, 1200Z and 1800Z (every 12 hours: 0000Z, 1200Z or 0600Z, 1800Z in the Southern Hemisphere). All warnings are released to the communications network no earlier than synoptic time and

no later than synoptic time plus two and one-half hours, so that recipients are assured of having all warnings in hand by synoptic time plus three hours (0300Z, 0900Z, 1500Z and 2100Z). By area, the warning bulletin headers are: WTIO31-35 PGTW for northern latitudes from 35° to 100° east longitude, WTPN31-36 PGTW for northern latitudes from 100° to 180° east longitude, WTXS31-36 PGTW for southern latitudes from 35° to 135° east longitude, and WTPS31-35 PGTW for southern latitudes from 135° to 180° east longitude.

1.7.2 TROPICAL DEPRESSION WARNINGS

— These are issued only for western North Pacific tropical depressions that are not expected to reach the criteria for Tropical Cyclone Warnings, as mentioned above. The depression warning contains the same information as a Tropical Cyclone Warning except that the Tropical Depression Warning is issued every 12 hours (unless an amendment is required) at standard synoptic times and extends in 12-hour increments only through 36 hours.

Both Tropical Cyclone and Tropical Depression Warning forecast positions are later verified against the corresponding best track positions (obtained during detailed post-storm analyses) to determine the most probable path and intensity of the cyclone. A summary of the verification results for 1992 is presented in Chapter 5, Summary of Forecast Verification.

1.8 PROGNOSTIC REASONING MESSAGES

These plain language messages provide meteorologists with the rationale for the JTWC forecasts for tropical cyclones in the western North Pacific Ocean. They also discuss alternate forecast scenarios, if changing conditions indicate such potential. Prognostic reasoning messages (WDPN31-36 PGTW) are prepared to complement tropical cyclone (but not tropical depression) warnings. In addition to these mes-

sages, prognostic reasoning information is provided in the remarks section of all types of warnings when significant forecast changes are made or when deemed appropriate by the TDO.

1.9 TROPICAL CYCLONE FORMATION ALERTS

Tropical Cyclone Formation Alerts are issued whenever interpretation of satellite imagery and other meteorological data indicates that the formation of a significant tropical cyclone is likely. These alerts will specify a valid period, usually not exceeding 24 hours, and must either be canceled, reissued, or superseded by a warning prior to expiration. By area, the Alert bulletin headers are: WTIO21-25 PGTW for northern latitudes from 35° to 100° east longitude, WTPN21-26 PGTW for northern latitudes from 100° to 180° east longitude, WTXS21-26 PGTW for southern latitudes from 35° to 135° east longitude, and WTPS21-25 PGTW for southern latitudes from 135° to 180° east longitude.

1.10 SIGNIFICANT TROPICAL WEATHER ADVISORIES

This product contains a description of all tropical disturbances in JTWC's AOR and their potential for further (tropical cyclone) development. In addition, all tropical cyclones in warning status are briefly discussed and referenced.

Two separate messages are issued daily, and each is valid for a 24-hour period. The Significant Tropical Weather Advisory for the Western Pacific Ocean is issued by 0600Z. The Significant Tropical Weather Advisory for the Indian Ocean is issued by 1800Z. These are reissued whenever the situation warrants. For each suspect area, the words "poor", "fair", or "good" are used to describe the potential for development. "Poor" will be used to describe a tropical disturbance in which the meteorological conditions are currently unfavorable for

development. "Fair" will be used to describe a tropical disturbance in which the meteorological conditions are favorable for development, but significant development has not commenced or is not expected to occur in the next 24 hours. "Good" will be used to describe the potential for development of a disturbance covered by an Alert. By area, the advisory bulletin headers are: ABPW10 PGTW for northern latitudes from 100° to 180° east longitude and southern latitudes from 135° to 180° east longitude and ABIO10 PGTW for northern latitudes from 35° to 100° east longitude and southern latitudes from 35° to 135° east longitude.

2. RECONNAISSANCE AND FIXES

2.1 GENERAL

JTWC depends primarily on two reconnaissance platforms, satellite and radar, to provide necessary, accurate, and timely meteorological information in support of advisories, alerts and warnings. In data-rich areas, synoptic data are also used to supplement the above. As in past years, the optimal use of all available reconnaissance resources to support JTWC's products remains a primary concern. Weighing the specific capabilities and limitations of each reconnaissance platform, and the tropical cyclone's threat to life and property both afloat and ashore, continue to be important factors in careful product preparation.

2.2 RECONNAISSANCE AVAILABILITY

2.2.1 SATELLITE — Fixes from Air Force/Navy ground sites and Navy ships supply day and night coverage in JTWC's AOR. Interpretation of this satellite imagery yields tropical cyclone positions, and estimates of current and forecast intensities using the Dvorak technique. The Special Sensor Microwave/Imager (SSM/I) data are used to determine the extent of the 35-kt (18-m/sec) winds near the tropical cyclone and to aid in tropical cyclone positioning, especially when the center is obscured by clouds.

2.2.2 RADAR — Interpretation of land-based radar, which remotely senses and maps precipitation within tropical cyclones, provides positions in the proximity (usually within 175 nm (325 km) of radar sites in the Philippine Islands, Taiwan, Hong Kong, China, Japan, South Korea, Kwajalein, Guam, Thailand, Australia, and India.

2.2.3 AIRCRAFT - Four tropical cyclone fixes

were received from the weather reconnaissance aircraft associated with the TCM-92 mini-field experiment conducted at JTWC from 21 July to 20 August 1992.

2.2.4 SYNOPTIC — JTWC also determines tropical cyclone positions based on the analysis of surface/gradient-level synoptic data. These positions are an important supplement to fixes provided by remote sensing platforms, and become invaluable in situations where neither satellite nor radar fixes are available or representative.

2.3 SATELLITE RECONNAISSANCE SUMMARY

The Air Force provides satellite reconnaissance support to JTWC through the DMSP Tropical Cyclone Reporting Network (DMSP Network), which consists of tactical sites and a centralized facility. The personnel of Det 1, 633 OSS (hereafter referred to as Det 1), collocated with JTWC at Nimitz Hill, Guam, coordinate required tropical cyclone reconnaissance support with the following units:

15 ABW/WE, Hickam AFB, Hawaii
18 OSS/WE, Kadena AB, Japan
603 ACCS/WE, Osan AB, Republic of Korea
Air Force Global Weather Central,
Offutt AFB, Nebraska

The tactical sites provide a combined coverage from polar orbiting satellites that includes most of the western North Pacific, from near the international date line westward to Southeast Asia. The Naval Oceanography Command Detachment, Diego Garcia, furnishes interpretation of low resolution NOAA polar orbiting satellite coverage in the central Indian Ocean, and Navy ships equipped for direct satellite readout contribute supplementary support.

Also, civilian contractors with the U.S. Army at Kwajalein Atoll provide satellite fixes on tropical cyclones in the Marshall Islands that supplement Det 1's satellite coverage.

Additionally, DMSP low resolution satellite mosaics are available from the FNOC via the NEDN and NESN lines. These mosaics are used to metwatch the areas not included in the area covered by the DMSP tactical sites. They provide JTWC forecasters with the capability to "see" what AFGWC's satellite image analysts have been fixing, after the fact.

In addition to polar orbiter imagery, Det 1 uses high resolution geostationary imagery to support the reconnaissance mission. Animation of these geostationary images is invaluable for determining the location of cloud system centers and their motion, particularly in the formative stages. Animation is also valuable in assessing environmental, or ambient, changes affecting tropical cyclone behavior. Det 1 is able to receive and process high resolution digital geostationary data through its Meteorological Imagery, Data Display and Analysis System (MIDDAS), and through the Navy's Geostationary Satellite Receiving System (GSRS). Det 1 can process imagery on a daily basis from at least four polar orbiting and one geostationary spacecraft.

AFGWC is the centralized member of the DMSP network. In support of JTWC, AFGWC processes stored imagery from DMSP and NOAA spacecraft. Imagery is recorded by the various spacecraft as they orbit the earth, and is later relayed to AFGWC by a network of communication satellites and command readout sites. This enables AFGWC to obtain the recorded coverage necessary to fix all tropical cyclones within JTWC's AOR.

The hub of the DMSP network is Det 1. Based on available satellite coverage, Det 1 is responsible for coordinating satellite reconnaissance requirements with JTWC and tasking the individual network sites for the necessary tropical cyclone fixes, current intensity estimates,

and SSM/I surface wind information. When a particular satellite pass is selected to support the development of JTWC's next tropical cyclone warning, two sites are tasked to fix the tropical cyclone from the same pass. This "dual-site" concept provides the necessary redundancy that virtually guarantees JTWC a satellite fix to support each warning. It also supplies independent assessments of the same data to provide JTWC forecasters a measure of confidence in the location and intensity information.

The network provides JTWC with several products and services. The main service is to monitor the AOR for indications of tropical cyclone development. If development is suspected, JTWC is notified. Once JTWC issues either a Tropical Cyclone Formation Alert or a warning, the network provides tropical cyclone positions and current intensity estimates, with a forecast intensity estimate implied in the intensity estimation code. Each satellite-derived tropical cyclone position is assigned a Position Code Number (PCN), which is a measure of positioning confidence. The PCN is determined by a combination of (1) the availability of visible landmarks in the image that can be used as references for precise gridding and (2) the degree of organization of the tropical cyclone's cloud system (Table 2-1). Once the tropical cyclone's intensity is assessed as having reached 50 knots (26 m/sec), information of the distribution of 35-kt (18-m/sec) winds is provided using SSM/I data. Through the technique development efforts at AFGWC, a PCN has been developed to indicate the confidence in microwave imagery-derived position reports.

TABLE 2-1 POSITION CODE NUMBERS (PCN)

PCN	METHOD FOR CENTER DETERMINATION/GRIDDING
1	EYE/GEOGRAPHY
2	EYE/EPHEMERIS
3	WELL DEFINED CIRCULATION CENTER/GEOGRAPHY
4	WELL DEFINED CIRCULATION CENTER/EPHEMERIS
5	POORLY DEFINED CIRCULATION CENTER/GEOGRAPHY
6	POORLY DEFINED CIRCULATION CENTER/EPHEMERIS

Det 1 provides at least one estimate of the tropical cyclone's current intensity every 6 hours once JTWC is in alert or warning status. Current intensity estimates are made using the Dvorak (1975, 1984) technique for both visible and enhanced infrared imagery (Figure 2-1). On mature tropical cyclones, the enhanced infrared technique is preferred due to its objectivity; however, the visible technique is used to supplement this information during the daylight hours, primarily as a measure of consistency. The standard relationship between tropical cyclone "T-number", maximum sustained surface wind speed, and minimum sea-level pressure (Atkinson and Holliday, 1977) for the Pacific is shown in Table 2-2. For subtropical cyclones, intensity estimates are made using the Hebert and Poteat (1975) technique.

2.3.1 SATELLITE PLATFORM SUMMARY

Figure 2-2 shows the status of operational polar orbiting spacecraft. Of the four NOAA spacecraft in orbit, NOAA 10, 11, and 12 provided imagery throughout 1992, while NOAA 9 remained in a standby mode.

Of the four DMSP spacecraft: F8 provided only horizontally polarized 85 GHz channel

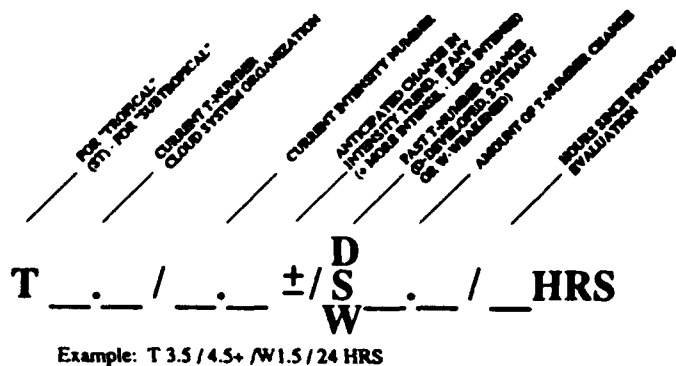


Figure 2-1. Dvorak code for communicating estimates of current and forecast intensity derived from satellite data. In the example, the current "T-number" is 3.5, but the current intensity is 4.5. The cloud system has weakened by 1.5 "T-numbers" since the previous evaluation conducted 24-hours earlier. The plus (+) symbol indicates an expected reversal of the weakening trend or very little further weakening of the tropical cyclone during the next 24-hour period.

from its SSM/I sensor; F9 failed on 21 February 1992; F10 supplied imagery, but continued to present satellite analysts with gridding problems due to the eccentricity of its orbit; and, F11 performed well all year.

2.3.2 STATISTICAL SUMMARY

During 1992, information from the DMSP network was the primary input to JTWC's warnings. Virtually all warnings were based on satellite reconnaissance data. JTWC received a total of 5557 satellite fixes during 1992: of these, 3663 were for the western North Pacific, 438 for the North Indian Ocean, and 1456 for the Southern Hemisphere. Of all the fixes, 37 percent were from polar orbiters and 63 percent were from the geostationary platform. Once again, there was an increase in the total number of fixes over the previous year. This is attributable to an increased use of the MIDDAS, which was tasked heavily for hourly positions when tropical cyclones approached major DOD facilities or heavily populated areas.

No DMSP network site experienced significant outages in 1992, compared to the 51 percent down-time reported for 1991. At Nimitz Hill, during periods when the site temporarily could only receive data, but not produce a film copy, the MIDDAS ingested the data and provided the needed images, preventing impacts experienced in the pre-MIDDAS period. A

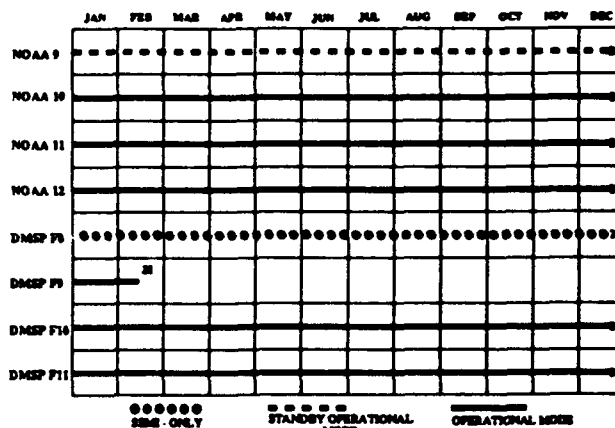


Figure 2-2. Polar orbiting spacecraft status for 1992.

comparison of satellite fixes from all data sources with their corresponding best track positions is shown in Table 2-3.

2.3.3 APPLICATION OF NEW TECHNOLOGY

By early 1992, all tactical sites in the DMSP network had received the Mission Sensor Tactical Imaging Computer (MISTIC) for processing the SSM/I, however, the AFGWC Tropical Section continued to provide the majority of the SSM/I support to JTWC. High resolution, 256 gray shade, SSM/I data became available at AFGWC for interpretation via AFGWC's Satellite Data Handling System on 1 March 1992. AFGWC, Det 1, and 18 OSS/WE (Kadena AB) provided bulletins to JTWC describing the distribution of 35-kt (18-m/sec) winds near tropical cyclones. The MISTIC II, which is an expanded and upgraded version of the MISTIC system, was to be installed at the tactical network sites in early 1993. MISTIC II is designed to supply co-registered OLS and full resolution, 256 gray shade, SSM/I data.

2.3.4 FUTURE OF SATELLITE RECONNAISSANCE

The MIDDAS, which was formally accepted for operational use by Det 1 on 1 April 1992, has proven invaluable for providing JTWC with tailored satellite support. Work on the development and application of more user-friendly, interactive software designed for the MIDDAS continues. The Det 1 goal is to establish a fully integrated satellite system with interfaces to the Automated Weather Distribution System (AWDS), NEXRAD, MIDDAS, MISTIC II, TESS 3, and the MARK IVB.

Plans and work have progressed on installation of the MARK IVB at DMSP network sites. Projected completion dates for the Nimitz Hill, Hickam AFB, and Kadena AB sites will be in 1994. Until the projected October 1993 installation of AWDS, conventional weather data will continue to come through the Automated Weather Network (AWN).

TABLE 2-2 MAXIMUM SUSTAINED WIND SPEED (KT) AS A FUNCTION OF DVORAK CURRENT AND FORECAST INTENSITY NUMBER AND MINIMUM SEA-LEVEL PRESSURE (MSLP)

TROPICAL CYCLONE INTENSITY NUMBER	WIND SPEED	MSLP (MB) (NW PACIFIC)
0.0	25	- - - -
0.5	25	- - - -
1.0	25	- - - -
1.5	25	- - - -
2.0	30	1000
2.5	35	997
3.0	45	991
3.5	55	984
4.0	65	976
4.5	77	966
5.0	90	954
5.5	102	941
6.0	115	927
6.5	127	914
7.0	140	898
7.5	155	879
8.0	170	858

2.4 RADAR RECONNAISSANCE SUMMARY

Fourteen of the 33 significant tropical cyclones in the western North Pacific during 1992 passed within range of land-based radar with sufficient precipitation and organization to be fixed. A total of 364 land-based radar fixes were logged at JTWC, and one airborne radar fix was provided by a TCM-92 WC-130 aircraft.

The WMO radar code defines three categories of accuracy: good [within 10 km (5 nm)], fair [within 10 - 30 km (5 - 16 nm)], and poor [within 30 - 50 km (16 - 27 nm)]. Of the 363 radar fixes encoded in this manner, 132 were good, 102 were fair, and 129 were poor. Excellent support for the radar network through timely and accurate radar fix positioning

allowed JTWC to track and forecast tropical cyclone movement during even the most erratic track changes. Ten radar reports were logged for tropical cyclones in the North Indian Ocean, and none were logged for tropical cyclones in the Southern Hemisphere.

Due to the loss of radar at Andersen AFB, Guam during Typhoon Omar, the NEXRAD installation was accelerated to occur in February 1993. During the period without weather radar coverage on Guam, supplemental data was provided from the Federal Aviation Administration's Center-Radar Approach Control located on Andersen AFB.

2.5 TROPICAL CYCLONE FIX DATA

Table 2-4A delineates the number of fixes per platform for each individual tropical cyclone for the western North Pacific. Totals and percentages are also indicated. Similar information is provided for the North Indian Ocean in Table 2-4B, and for the South Pacific and South Indian Oceans in Table 2-4C.

TABLE 2-3 MEAN DEVIATION (NM) OF ALL SATELLITE DERIVED TROPICAL CYCLONE POSITIONS FROM JTWC BEST TRACK POSITIONS (NUMBER OF CASES IN PARENTHESES)

NORTHWEST PACIFIC OCEAN				
PCN	1982-1991 AVERAGE		1992 AVERAGE	
1&2	13.5	(5136)	15.5	(972)
3&4	20.9	(5456)	27.4	(942)
5&6	36.2	(11919)	43.3	(1749)
Totals:	27.13	(22511)	31.8	(3663)
NORTH INDIAN OCEAN				
PCN	1982-1991 AVERAGE		1992 AVERAGE	
1&2	13.5	(134)	12.6	(33)
3&4	29.4	(89)	35.8	(28)
5&6	39.6	(978)	34.2	(377)
Totals:	36.0	(1201)	32.6	(438)
WESTERN SOUTH PACIFIC AND SOUTH INDIAN OCEAN				
PCN	1982-1991 AVERAGE		1992 AVERAGE	
1&2	16.3	(1556)	14.3	(415)
3&4	26.9	(1299)	27.0	(369)
5&6	35.9	(7275)	38.2	(672)
Totals:	31.7	(10130)	28.6	(1456)

TABLE 2-4A

1992 NORTHWEST PACIFIC OCEAN FIX PLATFORM SUMMARY

NORTHWEST PACIFIC		SATELLITE	RADAR	SYNOPTIC	AIRCRAFT	TOTAL
TS Ekeka	(01C)	88	0	0	0	88
TY Axel	(01W)	123	0	0	0	123
TY Bobbie	(02W)	120	43	2	0	165
TY Chuck	(03W)	90	0	0	0	90
TS Deanna	(04W)	101	0	0	0	101
TY Eli	(05W)	88	0	2	0	90
TS Faye	(06W)	56	0	0	0	56
TY Gary	(07W)	88	12	4	0	104
TS Helen	(08W)	37	0	0	0	37
TY Irving	(09W)	61	31	3	0	95
TY Janis	(10W)	119	71	7	1	198
STY Kent	(11W)	217	37*	0	1	255
TS Lois	(12W)	114	0	0	1	115
TS Mark	(13W)	81	4	20	0	105
TS Nina	(14W)	45	0	0	0	45
STY Omar	(15W)	249	20	0	0	269
TS Polly	(16W)	104	4	4	0	112
TY Ryan	(17W)	196	11	0	0	207
TY Sibyl	(18W)	120	0	0	0	120
TY Ted	(19W)	109	0	5	0	114
TS Val	(20W)	67	0	1	0	68
TY Ward	(21W)	113	0	0	0	113
TS Zack	(22W)**	77	0	0	0	77
STY Yvette	(23W)	178	0	0	0	178
TY Angela	(24W)**	122	0	5	0	127
TY Brian	(25W)	147	13	0	0	160
TY Colleen	(26W)	160	0	0	0	160
TY Dan	(27W)	123	0	0	0	123
STY Elsie	(28W)	154	26	0	0	180
TD 29W	(29W)	14	0	0	0	14
TY Forrest	(30W)	133	14	0	0	147
STY Gay	(31W)	282	56	1	0	339
TY Hunt	(32W)	99	21	0	0	120
Totals:		3875	363	54	3	4295
Percentage of Total:		90%	8%	1%	0%	100%

* One Airborne radar fix included

** Regenerated

TABLE 2-4B

1992 NORTH INDIAN OCEAN FIX PLATFORM SUMMARY

<u>NORTH INDIAN OCEAN</u>	<u>SATELLITE</u>	<u>RADAR</u>	<u>SYNOPTIC</u>	<u>TOTAL</u>
TC 01B (01B)	52	0	0	52
TC 02A (02A)	32	10	0	42
TC 03B (03B)	28	0	1	29
TC 04B (04B)	28	0	0	28
TC 05B (05B)	17	0	0	17
TC 06A (06A)	14	0	1	15
TC 07B (07B)	24	0	0	24
TC 08B (08B)	16	0	0	16
TC 09B (09B)	63	0	0	63
TC 10B (10B)	41	0	2	43
TC 11A (11A)	20	0	0	20
TC 12A (12A)	25	0	0	25
Forrest (30W)	<u>79</u>	<u>0</u>	<u>0</u>	<u>79</u>
Totals:	439	10	4	453
Percentage of Total:	97%	2%	1%	100%

TABLE 2-4C 1992 SOUTH PACIFIC AND SOUTH INDIAN OCEANS FIX PLATFORM SUMMARY

<u>TROPICAL CYCLONES</u>	<u>SATELLITE</u>	<u>SYNOPTIC</u>	<u>RADAR</u>	<u>TOTAL</u>
TC 01S - - - -	17	0	0	17
TC 02S - - - -	32	0	0	32
TC 03P Tia	95	0	0	95
TC 04S - - - -	25	0	0	25
TC 05S Graham	110	0	0	110
TC 06P Val	85	0	0	85
TC 07P Wasa	0	0	0	0
TC 08P Arthur	0	0	0	0
TC 09S Alexandra	35	0	0	35
TC 10S Bryna	21	0	0	21
TC 11P Betsy	120	0	0	120
TC 12P Mark	36	0	0	36
TC 13P - - - -	3	0	0	3
TC 14P Cliff	0	0	0	0
TC 15P Celesta	12	0	0	12
TC 16S - - - -	45	0	0	45
TC 17P Daman	70	0	0	70
TC 18P - - - -	19	0	0	19
TC 19S Davilia	6	0	0	6
TC 20S Harriet	137	0	0	137
TC 21P Esau	111	0	0	111
TC 22S Farida	36	0	0	36
TC 23S Ian	79	0	0	79
TC 24S Gerda	15	0	0	15
TC 25P Fran	156	0	0	156
TC 26P Gene	22	0	0	22
TC 27P Hettie	0	0	0	0
TC 28S Neville	115	0	0	115
TC 29S Jane/Irna	130	0	0	130
TC 30P Innis	55	0	0	55
Totals:	1587	0	0	1587
Percentage of Total:	100%	0%	0%	100%

3. SUMMARY OF WESTERN NORTH PACIFIC AND NORTH INDIAN OCEAN TROPICAL CYCLONES

3.1 GENERAL

For the western North Pacific, 1992 was another record-breaking year for the number of warnings issued — 941 (106 more than last year) on 33 tropical cyclones (Table 3-1). This was two more tropical cyclones than the long-term annual mean of 31 (Table 3-2). As in the previous two years, one additional significant tropical cyclone, Ekeka (01C), moved westward across the central North Pacific into JTWC's area of responsibility and was included in the totals. A chronology of the tropical cyclone activity is provided in Figure 3-1. Table 3-3 includes: a climatology of typhoons, tropical storms and typhoons for the period from 1945 to 1959 and 1960 to 1992; and a summary of warning days. JTWC was in warning status 159 days during 1992 compared to 169 in 1991. Although there were less total warning days, an increase in the number of multiple storm days resulted in a greater total number of warnings — 941 compared to 835 the previous year. Of these warnings, 73 were issued by AJTWC when JTWC was incapacitated for 11 days after the destructive passage of Typhoon Omar over Guam. There were 75 warning days for two or more tropical cyclones, 28 days with at least three, and 5 days with four tropical cyclones occurring simultaneously. Thirty-six initial

Tropical Cyclone Formation Alerts were issued on western North Pacific tropical disturbances (Table 3-4). Except for one initial alert that did not develop, alerts preceded warnings on all significant tropical cyclones in the western North Pacific with the exception of Typhoon Gary (07W) and Tropical Storm Val (20W).

For the North Indian Ocean, it was an extremely active year with 13 tropical cyclones which is 7 more than the annual mean of five. Four of these occurred in the Arabian Sea and nine, including Forrest (30W), in the Bay of Bengal. These tropical cyclones required a total of 190 warnings and JTWC was in warning status 48 days during 1992 compared to nine in 1991. Alerts preceded all warnings in the North Indian Ocean.

During the year, a total of 1131 warnings were issued for 45 tropical cyclones in the Northern Hemisphere. When the North Indian Ocean was included with the western North Pacific in the total, there were 182 days with warnings on one cyclone and 90 days with two or more, 41 days with three or more and 9 days with four cyclones occurring at once. There were no days in the Northern Hemisphere when warnings were issued for five or more tropical cyclones at once.

TABLE 3-1

WESTERN NORTH PACIFIC SIGNIFICANT TROPICAL CYCLONES FOR 1992

TROPICAL CYCLONE	PERIOD OF WARNING	NUMBER OF	MAXIMUM	ESTIMATED
		WARNINGS ISSUED	SURFACE WINDS KT (M/SEC)	
(01W) TY AXEL	05 JAN - 15 JAN	38	70 (36)	972
(01C) TS EKEKA	05 FEB - 08 FEB	19	45 (23)	991
(02W) TY BOBBIE	23 JUN - 30 JUN	27	120 (62)	922
(03W) TY CHUCK	25 JUN - 30 JUN	22	80 (41)	964
(04W) TS DEANNA	26 JUN - 03 JUL	24	40 (21)	994
(05W) TY ELI	09 JUN - 14 JUN	18	75 (39)	968
(06W) TS FAYE	16 JUL - 18 JUL	11	55 (28)	984
(07W) TY GARY	19 JUL - 23 JUL	19	65 (33)	976
(08W) TS HELEN	26 JUL - 28 JUL	9	45 (23)	991
(09W) TY IRVING	01 AUG - 05 AUG	17	80 (41)	975
(10W) TY JANIS	03 AUG - 09 AUG	27	115 (59)	927
(11W) STY KENT	05 AUG - 20 AUG	58	130 (67)	910
(12W) TS LOIS	15 AUG - 22 AUG	28	40 (21)	994
(13W) TS MARK	15 AUG - 21 AUG	21	50 (26)	987
(14W) TS NINA	18 AUG - 21 AUG	13	45 (23)	991
(15W) STY OMAR	24 AUG - 05 SEP	50	130 (67)	910
(16W) TS POLLY	25 AUG - 30 AUG	21	50 (26)	987
(17W) TY RYAN	01 SEP - 11 SEP	43	115 (59)	927
(18W) TY SIBYL	07 SEP - 15 SEP	32	110 (57)	933
(19W) TY TED	18 SEP - 24 SEP	27	65 (33)	976
(20W) TS VAL	23 SEP - 27 SEP	15	55 (28)	984
(21W) TY WARD	26 SEP - 06 OCT	40	95 (49)	949
(22W) TS ZACK	07 OCT - 15 OCT	27	40 (21)	993
(23W) STY YVETTE	08 OCT - 17 OCT	40	155 (80)	878
(24W) TY ANGELA	16 OCT - 29 OCT	41	90 (46)	954
(25W) TY BRIAN	17 OCT - 25 OCT	33	95 (49)	949
(26W) TY COLLEEN	18 OCT - 28 OCT	44	80 (41)	963
(27W) TY DAN	24 OCT - 03 NOV	40	110 (57)	927
(28W) STY ELSIE	29 OCT - 07 NOV	36	145 (75)	892
(29W) TD 29W	01 NOV - 02 NOV	3	25 (13)	1002
(30W) TS FORREST	12 NOV - 15 NOV	12	55 (28)	984
(31W) STY GAY	14 NOV - 30 NOV	63	160 (82)	872
(32W) TY HUNT	16 NOV - 21 NOV	23	125 (64)	916

TOTAL: 941

TABLE 3-2 WESTERN NORTH PACIFIC TROPICAL CYCLONE DISTRIBUTION

YEAR	JAN	FEB	MAR	APR	MAY	JUN	JUL	AUG	SEP	OCT	NOV	DEC	TOTALS
1959	0	1	1	1	0	1	3	8	9	3	2	2	31
	000	010	010	100	000	001	111	512	423	210	200	200	17 7 7
1960	1	0	1	1	1	3	3	9	5	4	1	1	30
	001	000	001	100	010	210	210	810	041	400	100	100	19 8 3
1961	1	1	1	1	4	6	5	7	6	7	2	1	42
	010	010	100	010	211	114	320	313	510	322	101	100	20 11 11
1962	0	1	0	1	3	0	8	8	7	5	4	2	39
	000	010	000	100	201	000	512	701	313	311	301	020	24 6 9
1963	0	0	1	1	0	4	5	4	4	6	0	3	28
	000	000	001	100	000	310	311	301	220	510	000	210	19 6 3
1964	0	0	0	0	3	2	8	8	8	7	6	2	44
	000	000	000	000	201	200	611	350	521	331	420	101	26 13 5
1965	2	2	1	1	2	4	6	7	9	3	2	1	40
	110	020	010	100	101	310	411	322	531	201	110	010	21 13 6
1966	0	0	0	1	2	1	4	9	10	4	5	2	38
	000	000	000	100	200	100	310	531	532	112	122	101	20 10 8
1967	1	0	2	1	1	1	8	10	8	4	4	1	41
	010	000	110	100	010	100	332	343	530	211	400	010	20 15 6
1968	0	1	0	1	0	4	3	8	4	6	4	0	31
	000	001	000	100	000	202	120	341	400	510	400	000	20 7 4
1969	1	0	1	1	0	0	3	3	6	5	2	1	23
	100	000	010	100	000	000	210	210	204	410	110	010	13 6 4

TABLE CONTINUED ON TOP OF NEXT PAGE

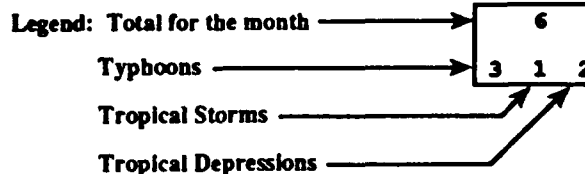
CONTINUED FROM PREVIOUS PAGE

YEAR	JAN	FEB	MAR	APR	MAY	JUN	JUL	AUG	SEP	OCT	NOV	DEC	TOTALS
1970	0	1	0	0	0	2	3	7	4	6	4	0	27
	000	100	000	000	000	110	021	421	220	321	130	000	12 12 3
1971	1	0	1	2	5	2	8	5	7	4	2	0	37
	010	000	010	200	230	200	620	311	511	310	110	000	24 11 2
1972	1	0	1	0	0	4	5	5	6	5	2	3	32
	100	000	001	000	000	220	410	320	411	410	200	210	22 8 2
1973	0	0	0	0	0	0	7	6	3	4	3	0	23
	000	000	000	000	000	000	430	231	201	400	030	000	12 9 2
1974	1	0	1	1	1	4	5	7	5	4	4	2	35
	010	000	010	010	100	121	230	232	320	400	220	020	15 17 3
1975	1	0	0	1	0	0	1	6	5	6	3	2	25
	100	000	000	001	000	000	010	411	410	321	210	002	14 6 5
1976	1	1	0	2	2	2	4	4	5	0	2	2	25
	100	010	000	110	200	200	220	130	410	000	110	020	14 11 0
1977	0	0	1	0	1	1	4	2	5	4	2	1	21
	000	000	010	000	001	010	301	020	230	310	200	100	11 8 2
1978	1	0	0	1	0	3	4	8	4	7	4	0	32
	010	000	000	100	000	030	310	341	310	412	121	000	15 13 4
1979	1	0	1	1	2	0	5	4	6	3	2	3	28
	100	000	100	100	011	000	221	202	330	210	110	111	14 9 5
1980	0	0	1	1	4	1	5	3	7	4	1	1	28
	000	000	001	010	220	010	311	201	511	220	100	010	15 9 4
1981	0	0	1	1	1	2	5	8	4	2	3	2	29
	000	000	100	010	010	200	230	251	400	110	210	200	16 12 1
1982	0	0	3	0	1	3	4	5	6	4	1	1	28
	000	000	210	000	100	120	220	500	321	301	100	100	19 7 2
1983	0	0	0	0	0	1	3	6	3	5	5	2	25
	000	000	000	000	000	010	300	231	111	320	320	020	12 11 2
1984	0	0	0	0	0	2	5	7	4	8	3	1	30
	000	000	000	000	000	020	410	232	130	521	300	100	16 11 3
1985	2	0	0	0	1	3	1	7	5	5	1	2	27
	020	000	000	000	100	201	100	520	320	410	010	110	17 9 1
1986	0	1	0	1	2	2	2	5	2	5	4	3	27
	000	100	000	100	110	110	200	410	200	320	220	210	19 8 0
1987	1	0	0	1	0	2	4	4	7	2	3	1	25
	100	000	000	010	000	110	400	310	511	200	120	100	18 6 1
1988	1	0	0	0	1	3	2	5	8	4	2	1	27
	100	000	000	000	100	111	110	230	260	400	200	010	14 12 1
1989	1	0	0	1	2	2	6	8	4	5	3	2	35
	010	000	000	100	200	110	231	332	220	600	300	101	21 10 4
1990	1	0	0	1	2	4	4	5	5	5	4	1	31
	100	000	000	010	110	211	220	500	410	230	310	100	21 9 1
1991	0	0	2	1	1	1	4	8	6	3	6	0	32
	000	000	110	010	100	100	400	332	420	300	330	000	20 10 2
1992	1	1	0	0	0	3	4	8	5	6	5	0	33
	100	010	000	000	000	210	220	440	410	510	311	000	21 11 1
(1959-1992)													
MEAN:	0.6	0.3	0.6	0.8	1.2	2.2	4.5	6.3	5.7	4.6	3.0	1.4	30.9
CASES:	20	10	20	25	42	73	151	214	192	156	101	46	1049

The criteria used in Table 3-2 are as follows:

1. If a tropical cyclone was first warned on during the last two days of a particular month and continued into the next month for longer than two days, then that system was attributed to the second month.
2. If a tropical cyclone was warned prior to the last two days of a month, it was attributed to the first month, regardless of how long the system lasted.
3. If a tropical cyclone began on the last day of the month and ended on the first day of the next month, that system was attributed to the first month. However, if a tropical cyclone began on the last day of the month and continued into the next month for only two days, then it was attributed to the second month.

TABLE 3-2 LEGEND



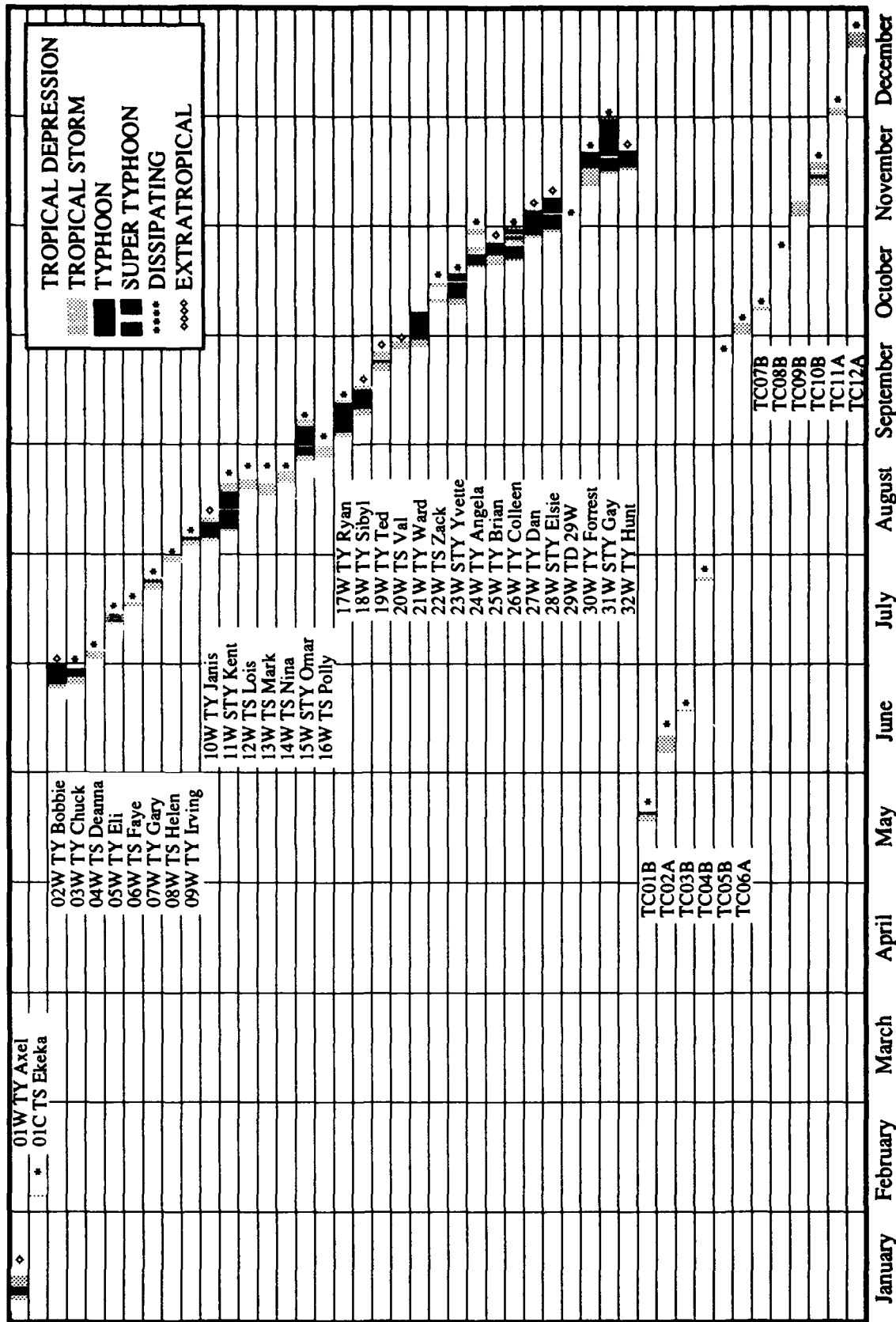


Figure 3-1. Chronology of western North Pacific and North Indian Ocean tropical cyclones for 1992.

TABLE 3-3

WESTERN NORTH PACIFIC TROPICAL CYCLONES

TYPHOONS
(1945 - 1959)

	JAN	FEB	MAR	APR	MAY	JUN	JUL	AUG	SEP	OCT	NOV	DEC	TOTALS
MEAN:	0.3	0.1	0.3	0.4	0.7	1.0	2.9	3.1	3.3	2.4	2.0	0.9	16.4
CASES:	5	1	4	6	10	15	29	46	49	36	30	14	245

(1960 - 1992)

	JAN	FEB	MAR	APR	MAY	JUN	JUL	AUG	SEP	OCT	NOV	DEC	TOTALS
MEAN:	0.3	0.1	0.2	0.5	0.7	1.1	2.7	3.2	3.3	3.2	1.8	0.6	17.7
CASES:	10	2	7	15	24	37	90	106	108	105	60	20	584

TROPICAL STORMS AND TYPHOONS

(1945 - 1959)

	JAN	FEB	MAR	APR	MAY	JUN	JUL	AUG	SEP	OCT	NOV	DEC	TOTALS
MEAN:	0.4	0.1	0.5	0.5	0.8	1.6	2.9	4.0	4.2	3.3	2.7	1.2	22.2
CASES:	6	2	7	8	11	22	44	60	64	49	41	18	332

(1960 - 1992)

	JAN	FEB	MAR	APR	MAY	JUN	JUL	AUG	SEP	OCT	NOV	DEC	TOTALS
MEAN:	0.6	0.3	0.5	0.7	1.1	1.9	4.2	5.4	5.0	4.2	2.8	1.2	27.6
CASES:	19	9	15	22	36	62	137	179	164	139	92	38	912

NUMBER OF CALENDAR WARNING DAYS: 159

NUMBER OF CALENDAR WARNING DAYS WITH TWO TROPICAL CYCLONES: 47

NUMBER OF CALENDAR WARNING DAYS WITH THREE TROPICAL CYCLONES: 23

NUMBER OF CALENDAR WARNING DAYS WITH FOUR TROPICAL CYCLONES: 5

TABLE 3-4

TROPICAL CYCLONE FORMATION ALERTS FOR THE WESTERN NORTH PACIFIC OCEAN

YEAR	INITIAL TCFAS	TROPICAL CYCLONES WITH TCFAS	TOTAL TROPICAL CYCLONES	FALSE ALARM RATE	PROBABILITY OF DETECTION
1976	34	25	25	26%	100%
1977	26	20	21	23%	95%
1978	32	27	32	16%	84%
1979	27	23	28	15%	82%
1980	37	28	28	24%	100%
1981	29	28	29	3%	96%
1982	36	26	28	28%	93%
1983	31	25	25	19%	100%
1984	37	30	30	19%	100%
1985	39	26	27	33%	96%
1986	38	27	27	29%	100%
1987	31	24	25	23%	96%
1988	33	26	27	21%	96%
1989	51	32	35	37%	91%
1990	33	30	31	9%	97%
1991	37	29	31	22%	94%
1992	36	32	32	20%	100%
(1976-1992)					
MEAN:	34.5	26.9	28.2	22%	95%
TOTALS:	587	458	481		

1992 FORMATION ALERTS: 32 OF 34 INITIAL FORMATION ALERTS DEVELOPED INTO SIGNIFICANT TROPICAL CYCLONES.

3.2 WESTERN NORTH PACIFIC TROPICAL CYCLONES

The year of 1992 included five super typhoons, 16 lesser typhoons, 11 tropical storms and one tropical depression. All tropical cyclones with the exception of Helen (08W), which was Tropical Upper Tropospheric Trough (TUTT)-induced, originated in the low-level monsoon trough or near-equatorial trough.

Due to warm sea-surface temperature anomalies in the central equatorial Pacific Ocean, January was a month with westerly low-level wind anomalies that extended from New Guinea eastward into the Central Pacific Ocean (Bureau of Met., 1992). These anomalies aided the development of Axel (01W) in the western North Pacific and a twin tropical cyclone in the Southern Hemisphere, and in late January, the formation of Ekeka (01C), a rare January Hurricane, south of the Hawaiian Islands. After Ekeka, there was a four month break in significant tropical cyclone activity. By mid-June the monsoon trough became established in its normal location across the South China Sea, central Philippine Islands and eastward into the Caroline Islands, and supported the formation of Bobbie (02W), Chuck (03W) and Deanna (04W) in late June (Figure 3-2).

After Deanna recurved on 2 July, the ridging and associated high pressure temporarily built into low latitudes in the Philippine Sea and replaced the monsoon trough. However, low-level southwesterly flow and weak troughing persisted to the east and supported the formation of Eli (05W) the second week of July, followed by Faye (06W), and Gary (07W) (Figure 3-3). After Gary, no significant tropical cyclones originated in the low-level monsoon trough until the end of July. In the interim, Helen (08W), which was a TUTT-induced low-level

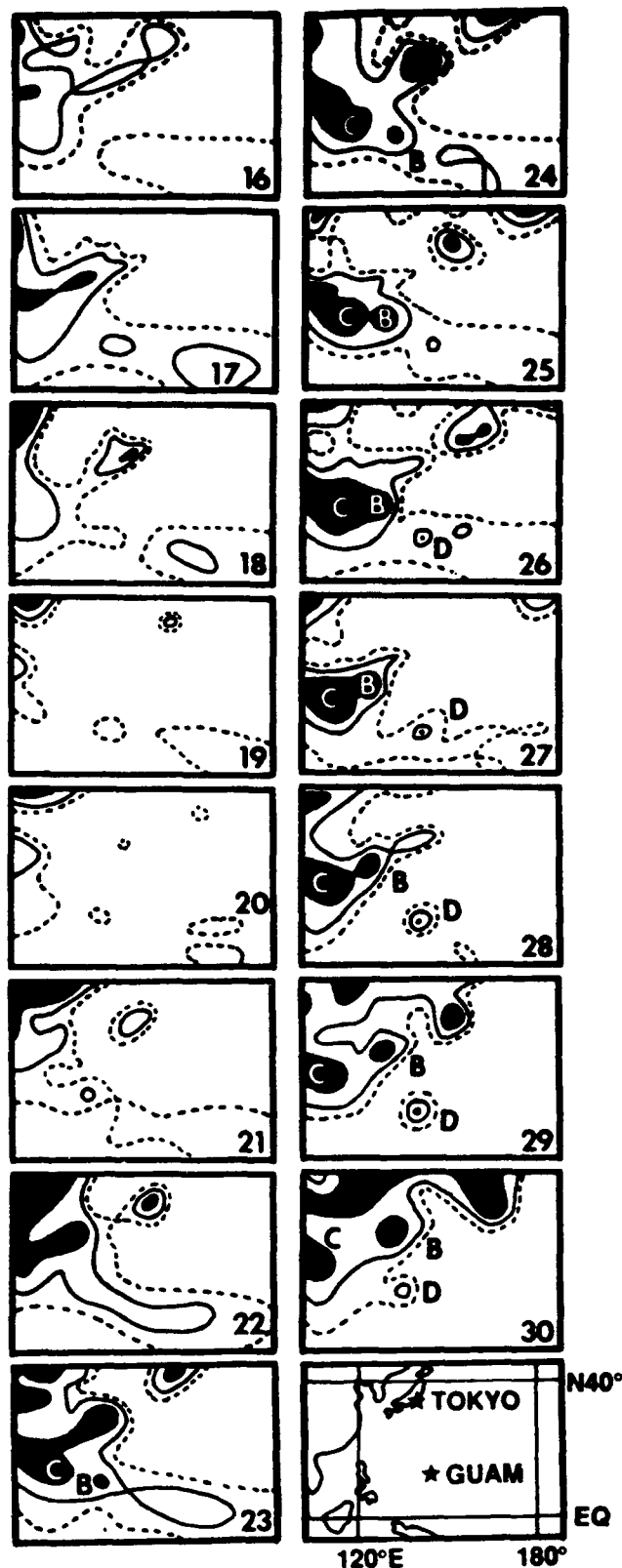


Figure 3-2. Western North Pacific sea-level pressure analyses for 16 to 30 June 1992. Map panels are for 0000Z for the date indicated in the lower right of each panel. A geographical reference appears as the lower right panel. Contours: outer dashed line = 1010 mb; solid line = 1008 mb; and, black area ≤ 1004 mb. Tropical cyclones: B = Bobbie (02W); C = Chuck (03W); and, D = Deanna (04W). (Analyses courtesy of M.A. Lander.)

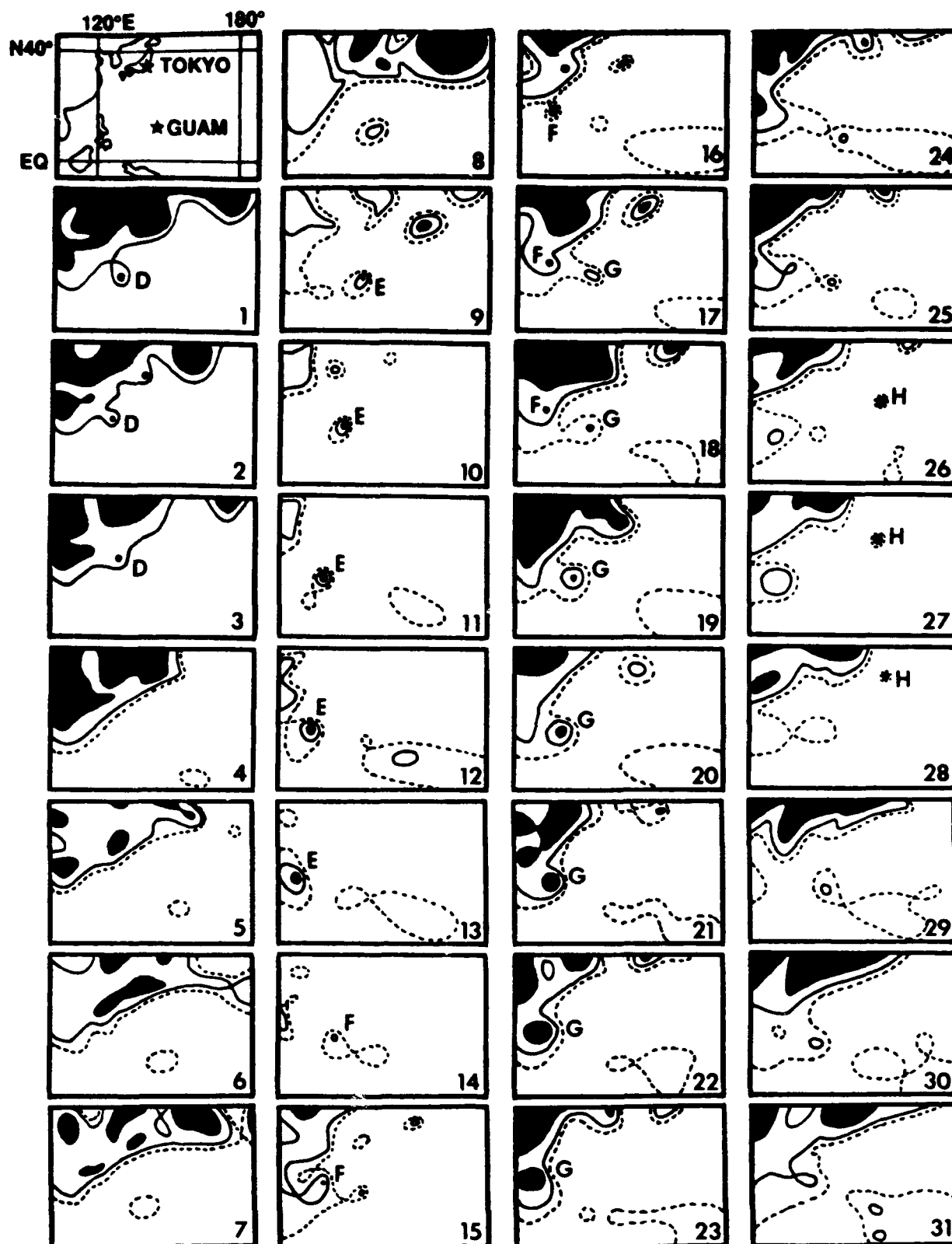


Figure 3-3. Western North Pacific sea-level pressure analyses for July 1992. Map panels are for 0000Z for the date indicated in the lower right of each panel. A geographical reference appears in the upper left panel. Contours: outer dashed line = 1010 mb; solid line = 1008 mb; and, black area ≤ 1004 mb. Tropical cyclones: D = Deanna (04W); E = Eli (05W); F = Faye (06W); G = Gary (07W); and, H = Helen (08W). (Analyses courtesy of M.A. Lander.)

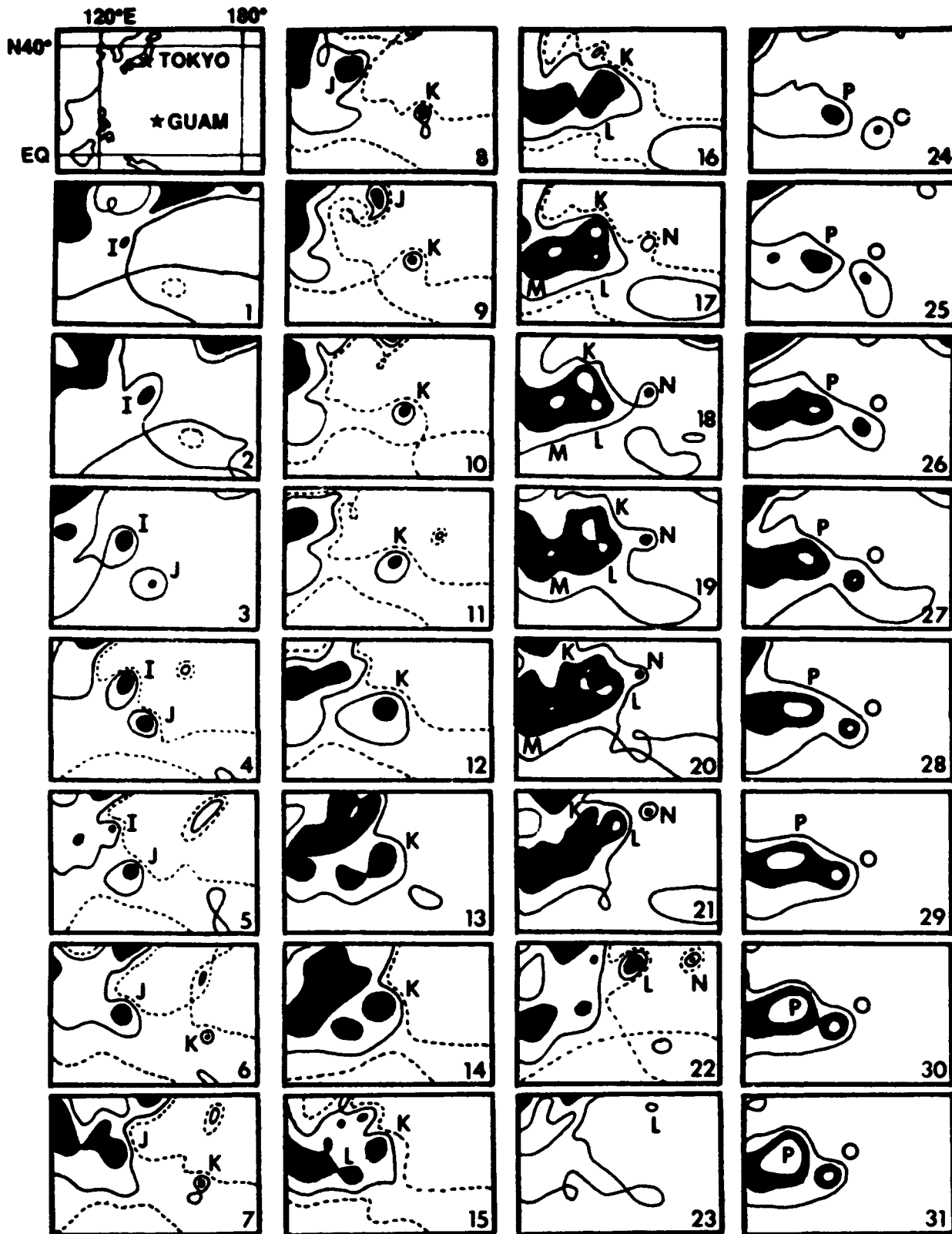


Figure 3-4. Western North Pacific sea-level pressure analyses for August 1992. Map panels are for 0000Z for the date indicated in the lower right of each panel. A geographical reference appears in the upper left panel. Contours: outer dashed line = 1010 mb; solid line = 1008 mb; black area ≤ 1004 mb; and, inner white area ≤ 1000 mb. Tropical cyclones: I = Irving (09W); J = Janis (10W); K = Kent (11W); L = Lois (12W); M = Mark (13W); N = Nina (14W); O = Omar (15W); and, P = Polly (16W). (Analyses courtesy of M.A. Lander.)

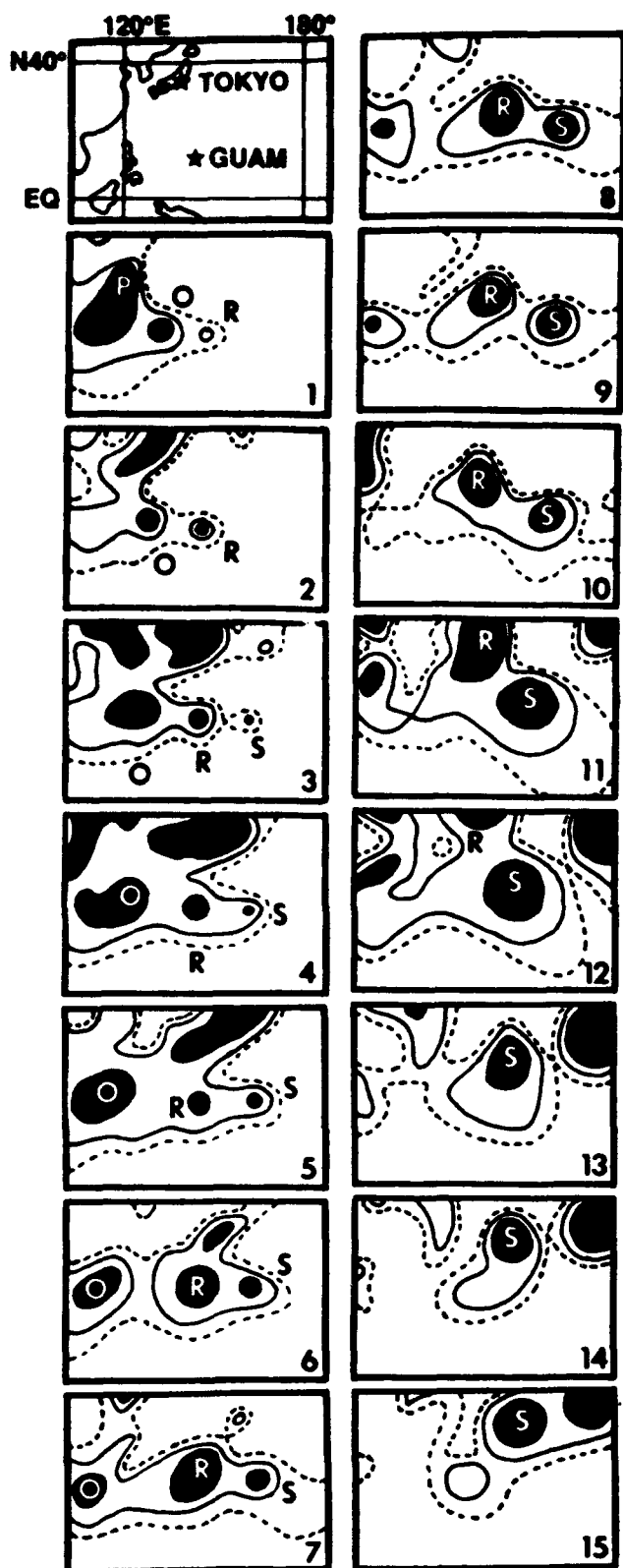


Figure 3-5. Western North Pacific sea-level pressure analyses for 1 to 15 September 1992. Map panels are for 0000Z for the date indicated in the lower right of each panel. A geographical reference appears as the upper left panel. Contours: outer dashed line = 1010 mb; solid line = 1008 mb; and, black area ≤ 1004 mb. Tropical cyclones: O = Omar (15W); P = Polly (16W); R = Ryan (17W); and, S = Sibyl (18W). (Analyses courtesy of M.A. Lander.)

circulation, formed on 24 July at 25° north latitude in an area of relatively high surface pressure and later recurved.

After Irving's (09W) formation on 30 July in the northern Philippine Sea and its subsequent north-oriented track, the axis of the subtropical ridge shifted slowly northward. This was reflected in the higher latitudes of recurvature for Janis (10W) and later, Kent (11W). As Kent intensified, surface pressures dropped across eastern Asia and the Philippine Sea, supporting the multiple storm outbreak which included Lois (12W), Mark (13W) and Nina (14W) (Figure 3-4).

With the demise of Lois and Nina, a major readjustment of the synoptic pattern took place at the end of the third week of August. The orientation of the axis of the monsoon trough, which was southwest-northeast, returned to its more normal northwest-southeast orientation, but extended much farther east than normal. This led to the development of Omar (15W) in the Marshall Islands and Polly (16W) just to the west of Guam. As Omar and Polly tracked west-northwestward along the axis of the trough, Ryan (17W) formed to the southeast in their wake. In its early development, Ryan tracked to the west-northwest for four days before making an abrupt course change to the north. During the first week of September, Sibyl (18W) formed at the eastern end of the low-level trough extending eastward from Omar through Ryan to Sibyl (Figure 3-5). Ryan continued northward on a north-oriented track into the Sea of Okhotsk. Following Sibyl's recurvature, there was a short break before Ted (19W) formed in the monsoon trough which had reestablished at lower latitudes. The development of Val (20W), Ward (21W), Zack (22W) and Yvette (23W) in the monsoon trough followed.

Next came **Angela (24W)** which formed in the monsoon trough in the South China Sea and became the anchor-low for the multiple storm outbreak which contained **Brian (25W)**, **Colleen (26W)** and **Dan (27W)**. As a subset of this event, **Brian's** binary interaction with **Colleen** at the end of the third week of October resulted in **Colleen** slowly executing a broad loop before tracking westward. The last week of October, **Elsie (28W)** and **Tropical Depression 29W** kept the activity going until the short pause before **Forrest (30W)** consolidated the second week of November. **Forrest** became part of another multiple storm outbreak that included **Gay (31W)** and **Hunt (32W)**. As the subtropical ridge strengthened and pushed equatorward, **Forrest** tracked from the Philippine Sea westward across the South China Sea and the Gulf of Thailand, and ultimately recurved in the Bay of Bengal. **Hunt** recurved on 20 November and **Gay**, which was long-lived and required 63, six-hour warnings, recurved on 30 November to close out the year.

JANUARY THROUGH MAY

Typhoon **Axel (01W)**, the first significant tropical cyclone to occur in 1992 in the western North Pacific, developed in the first week of January in conjunction with two other tropical cyclones — **Betsy (11P)** and later **Mark (12P)** — in the Southern Hemisphere in response to an equatorial west wind burst to the east of New Guinea. **Axel's** early intensification at a low latitude proved particularly damaging to the Marshall and eastern Caroline Islands. During the last week of January, **Ekeka (01C)**, which formed south of the Hawaiian Islands, became a rare January central North Pacific hurricane. Due to increasing upper-level wind shear, **Ekeka** had weakened to 40 kt (20 m/sec) when the JTWC assumed warning responsibility on 4 February. The weakening tropical cyclone continued to move westward and passed through the Marshall Islands.

JUNE

After a four month hiatus in tropical cyclone activity in the western North Pacific Ocean, **Bobbie (02W)** developed in the monsoon trough in the central Caroline Islands in late June. **Bobbie's** formation coincided with that of **Chuck's (03W)** over the central Philippine Islands, and the two underwent binary interaction for three days. As Typhoon **Bobbie** passed east of northern Luzon, torrential rains, associated with the deep monsoonal flow into **Bobbie** and enhanced by **Chuck**, caused heavy rains, mudslides, and widespread flooding over the northern half of the Philippines. After, recurving and tracking just to the southeast of Okinawa, **Bobbie** accelerated in forward motion, and underwent extra-tropical transition before passing just south of Tokyo. **Chuck** was the first significant tropical cyclone of the year in the South China Sea. **Deanna (04W)** was the third, and final, significant tropical cyclone to form in June. **Deanna** executed a counter-clockwise loop on 27 and 28 June in the western Caroline Islands before moving out to the northwest on a track parallel to the one taken by **Bobbie** five days earlier.

JULY

After **Deanna** recurved on 2 July, ridging temporarily replaced the monsoon trough across the northern Philippine Islands and Philippine Sea. Weak southwesterlies, however, persisted at low latitudes and **Eli (05W)** formed in the eastern Caroline Islands. Slow to intensify, Typhoon **Eli** tracked rapidly west-northwestward across Luzon, the South China Sea, and into northern Vietnam. Next came **Faye (06W)**, the second of three successive tropical cyclones to pass over northern Luzon and intensify in the South China Sea. Recurving south of Hong Kong on 17 July, **Faye** proceeded north-northeastward into China and dissipated. **Gary (07W)** followed **Faye**, and after presenting

JTWC with early difficulties locating the low-level vortex, the Center correctly predicted that Gary would strike the southern coast of China near Hainan Dao. Gary caused widespread damage across southern China. Typhoon Gary's track paralleled those of Typhoon Eli and Tropical Storm Faye. The fourth of five significant tropical cyclones to develop in July, **Helen (08W)** intensified from a Tropical Upper Tropospheric Trough (TUTT)-induced low-level circulation. The tropical storm began to weaken as it gained latitude and moved into a region of cooler sea-surface temperatures. A few days later, **Irving (09W)** became the first of two successive typhoons to affect southwestern Japan. It formed at the eastern end of the monsoon trough where several low-level vorticity centers were embedded in a broad area of poorly organized convection. Irving slowly intensified and took a north-oriented track into southwestern Japan followed by westward motion toward Korea due to the reestablishment of the mid-level subtropical ridge.

AUGUST

Four days after Irving hammered Shukoku, **Janis (10W)** slammed into Kyushu. Janis began near Pohnpei in the Caroline Islands, took a northwestward track threatening Okinawa, then recurved, passed over Kyushu, and skirted the western coast of Honshu before transitioning to an extratropical low over Hokkaido. The second of eight significant tropical cyclones to develop in August, **Kent (11W)** became the first super typhoon of 1992. During its trek toward Japan, Kent underwent binary interaction with Tropical Storm Lois. Requiring a total of 58 warnings, Kent was second only to Super Typhoon Gay for the highest total number of warnings and longevity for the western North Pacific in 1992. Next came **Lois (12W)**, one of only two tropical cyclones in 1992 which had a persistent eastward component of motion during its period of warning. The storm bedeviled

JTWC forecasters by consistently moving counter to the climatologically expected motion. After escaping the binary interaction with Kent, Lois accelerated northeastward and dissipated over colder water. **Mark (13W)** was part of a multiple storm outbreak with Kent, Lois, and later, Nina. On 15 August, Mark's genesis in the South China Sea in the monsoon trough coincided with Lois' in the Philippine Sea, as deep low-level southwesterly flow surged eastward across the Philippine Islands. Due to strong vertical wind shear, Mark was slow to intensify and spent its short lifetime embedded in the monsoon trough. It dissipated over southern China. **Nina (14W)**, part of the multiple storm outbreak in August with Kent, Lois and Mark, formed as a TUTT-induced tropical cyclone under divergent upper-level flow east of Kent. Nina intensified to a peak intensity of 45 kt (23 m/sec) despite the strongly sheared environment. On 20 August, the second super typhoon of 1992, **Omar (15W)** developed in the southern Marshall Islands, moved steadily west-northwestward and intensified. On 28 August, Omar wreaked havoc on Guam as it rapidly intensified immediately prior to passing directly over the island. Typhoon Omar was the most damaging typhoon to strike Guam since Typhoon Pamela in 1976, causing an estimated \$457 million of damage. After traversing Guam, Omar continued onward into the Philippine Sea where it briefly attained super typhoon intensity. Omar then steadily weakened, passing over Taiwan as a tropical storm, and dissipated over southeastern China. **Polly (16W)**, the eighth and final significant tropical cyclone of August, developed along with Omar as part of a major relocation of the monsoonal trough. Polly was unusual in that throughout most of its life, it maintained the structure of a monsoon depression with a ring of peripheral gales and a broad band of deep convection around a large, relatively cloud free, central area of light-and-variable winds. The outflow aloft from Polly appeared to play an important role in

delaying the intensification of Omar, when Omar was approaching Guam. Although Polly never reached typhoon intensity, it did have quite an impact on eastern Asia.

SEPTEMBER

The first of five significant tropical cyclones to form in September, **Ryan (17W)** became part of a multiple storm outbreak, including Omar and Sibyl, east of 150° east longitude. Although Ryan initially took a west-northwestward course similar to the two preceding tropical cyclones (Polly and Omar), it later stalled, and then acquired a north-orientated track. Two days after transitioning to an extratropical low east of Hokkaido, the remnants of Ryan could still be identified, as an occluded low continuing northward over Siberia, north of the Sea of Okhotsk. **Sibyl (18W)**, like Ryan, formed at the extreme eastern end of the monsoon trough. But unlike Ryan, Sibyl underwent a complex interaction with a cyclonic cell in the TUTT, and later recurved. For five days, Sibyl exhibited erratic motion and slowly intensified near Wake Island, before moving to the northwest and recurving. A short respite ensued for JTWC while the disturbance that was to become Typhoon **Ted (19W)** slowly developed. Ted was marked by moderate to strong upper-level wind shear throughout most of its life. A combination of shearing effects and land interaction prevented Ted from intensifying above minimal typhoon. Ted's tour of Asia included northern Luzon, northeastern Taiwan, eastern China, and finally Korea before the circulation transitioned to a weak extratropical cyclone over the Sea of Japan. The next tropical cyclone, **Val (20W)**, was the only one of five typhoons in September that did not intensify beyond a tropical storm. Like Ted, which formed a day earlier on 18 September, Val was slow to intensify. Next came **Ward (21W)** which formed in the trade wind trough just to the east of the international date line. Ward presented considerable difficul-

ty to JTWC forecasters, as it underwent two major track changes and two significant acceleration episodes.

OCTOBER

The first of eight significant tropical cyclones to form in October, **Zack (22W)** was also the first to threaten the southern Mariana Islands since Omar's devastating passage across Guam in August. Initially its movement was to the west-northwest along the axis of the monsoon trough, but a monsoon surge of deep southwesterly winds resulted in an abrupt track change to the north-northeast for Zack. As the tropical storm weakened, the low-level circulation center became difficult to locate, and JTWC issued a final warning on Zack on 12 October. However, by the following day, the convection and organization of the system had increased, prompting JTWC to issue a "regenerated" warning. Zack briefly reintensified to a tropical storm before transitioning into a subtropical system and dissipating over the ocean. The third Northwest Pacific tropical cyclone of 1992 to achieve super typhoon intensity was **Yvette (23W)**. It formed at the same time as Zack and proved to be an action-packed system which posed many forecast challenges. In the span of two weeks, Yvette developed in a moderately sheared environment, made a run toward Luzon as it intensified to a typhoon, stalled, executed a major, 150-degree track change, weakened, reintensified to a super typhoon, and transitioned to an extratropical cyclone. During the second week of October, **Angela (24W)** developed in the South China Sea, moved east, reversed course and struck southern Vietnam. Angela later crossed southern Indochina and reintensified to a severe tropical storm in the Gulf of Thailand, where it tracked through a clockwise loop, and finally dissipated over the Gulf. While anchoring the western end of a monsoon trough, Angela became part of a multiple storm outbreak along with Brian, Colleen

and Dan. Angela posed a significant threat in the Gulf of Thailand, where manned gas platforms were forced to evacuate as the storm intensified and moved into the area. Forming in the southern Marshall Islands, **Brian (25W)** moved west-northwestward and intensified into a midget typhoon as it passed across Guam. For Guam, it was the second eye passage in less than two months - Omar being the first. Later, Brian underwent binary interaction with Typhoon Colleen, subsequently recurved, and finally transitioned to an extratropical system. **Colleen (26W)** developed from a broad cyclonic circulation in the monsoon trough between Typhoon Angela to the west and Typhoon Brian to the east. Binary interaction occurred between Colleen and Brian, causing Colleen to make a slow anticyclonic loop in the Philippine Sea before turning west. After crossing Luzon, Colleen reintensified into a typhoon before slamming into central Vietnam and dissipating inland. The last significant tropical cyclone to develop in October as part of the four storm outbreak, **Dan (27W)** became the most destructive typhoon to strike Wake Island in the past quarter-century, causing an estimated \$9.0 million in damage. Just as Ekeka and Ward did earlier in 1992, Dan formed east of the international date line, marking the first time that three significant tropical cyclones were observed to cross into the JTWC's area of responsibility from the central North Pacific during a single year. Later, Dan faked a move toward recurvature, took a west-southwesterly course, underwent an episode of reintensification, and finally, underwent a binary interaction with Typhoon Elsie before recurving sharply. Next came the fourth super typhoon of 1992, **Elsie (28W)**, which was the third typhoon to pass within 60 nm (100 km) of Guam in less than three months. After initial movement to the northeast in response to a southwest monsoonal surge, a subsequent turn to the west, and then interaction with Typhoon Dan, which brought Elsie to the north toward the southern Mariana Islands, the

tropical cyclone settled down on a track to the northwest, recurved, and transitioned into a hurricane-force extratropical low.

NOVEMBER AND DECEMBER

Forming in the wake of Typhoon Dan, **Tropical Depression 29W** immediately became a threat to Wake Island which had already been heavily damaged by Dan on 28 October. Fortunately for Wake Island, the Tropical Depression's intensification was severely curtailed by the persistent outflow from Dan. The second of four significant tropical cyclones to get started in November, **Forrest (30W)** became part of a three storm outbreak with Gay and Hunt. Forrest was the only tropical cyclone of 1992 to track from the western North Pacific, across the South China Sea, and into the Bay of Bengal. It reached a maximum intensity of 125 kt (64 m/sec) in the Bay of Bengal over a day after it had recurved. A day after Forrest became a tropical storm, **Hunt (32W)** developed and became the fourth typhoon to pass within 60 nm (110 km) of Guam in less than three months. Hunt was part of a three storm outbreak with Tropical Storm Forrest and Super Typhoon Gay. As Hunt intensified, it brushed by Guam, moved into the Philippine Sea, and later recurved. After recurvature, the typhoon played an important role in the extremely rapid weakening of Super Typhoon Gay which was approaching the southern Mariana Islands. **Gay (31W)** developed at the same time as Hunt. Gay was noteworthy for five reasons: its eye became the record third to pass across Guam in less than three months; it was estimated to be the most intense tropical cyclone to occur in the western North Pacific since Super Typhoon Tip in October of 1979; it went through two intensification periods, which is not rare but is relatively uncommon; it filled an estimated 99 mb in less than 48 hours without moving over land; and, it required the highest number of warnings, 63, for any western North Pacific tropical

cyclone in 1992. Four days after being detected as a tropical disturbance, Gay slammed into several of the Marshall Islands with typhoon force winds. After peaking with sustained winds of 160 kt (82 m/sec) with gusts to 195 kt (100 m/sec), the super typhoon weakened for two days before reaching Guam. Typhoon Gay passed across the center of Guam on 23 November, then reintensified to a second peak before recurving on 30 November, and dissipating over water south of Japan. No significant tropical cyclones occurred in the western North Pacific in December.

Composite best tracks for the western North Pacific tropical cyclones this year are provided in Figures 3-6, 3-7 and 3-8.

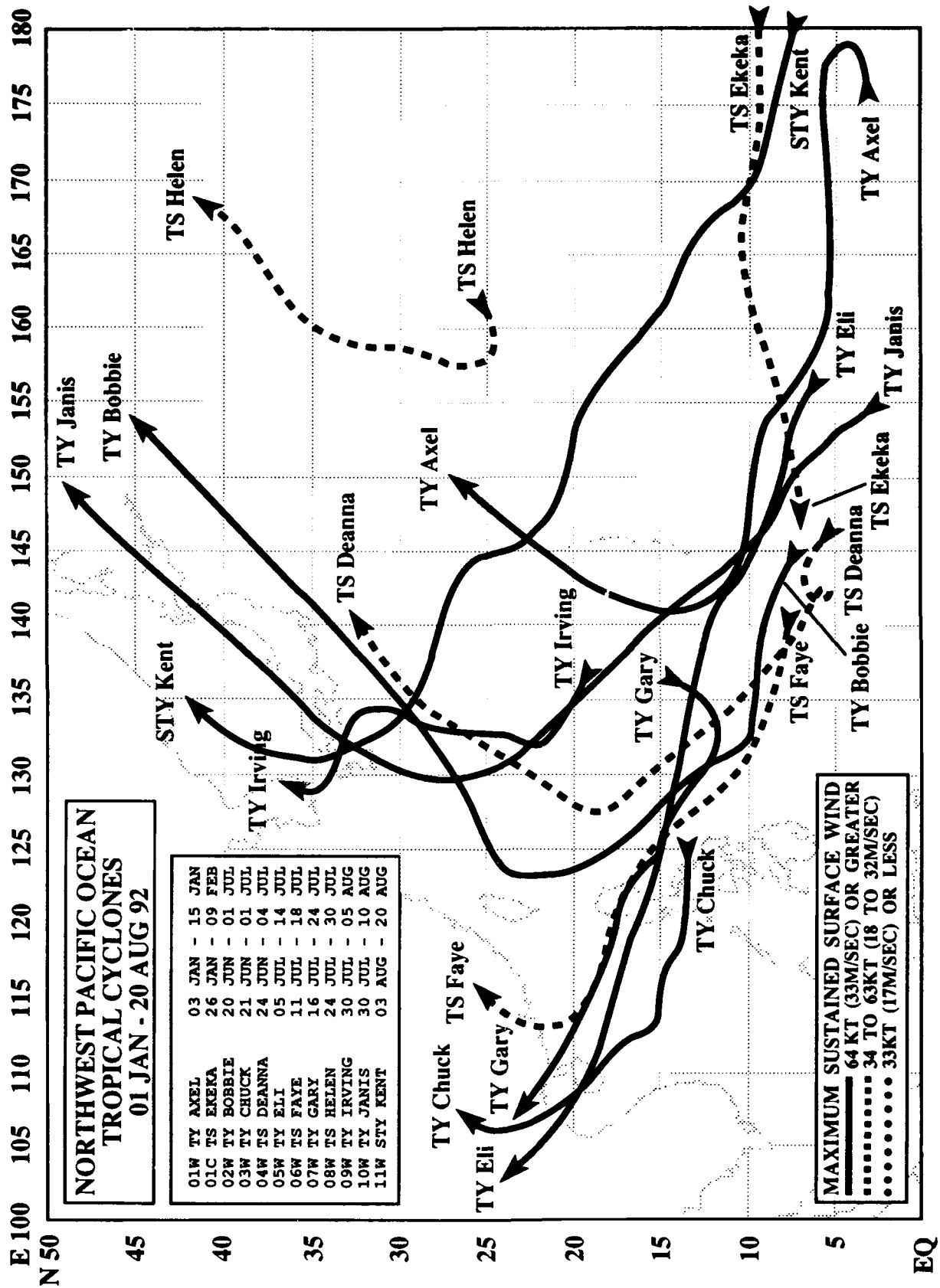


Figure 3-6. Composite best tracks for Northwest Pacific Ocean Tropical cyclones for 01 January to 20 August 1992

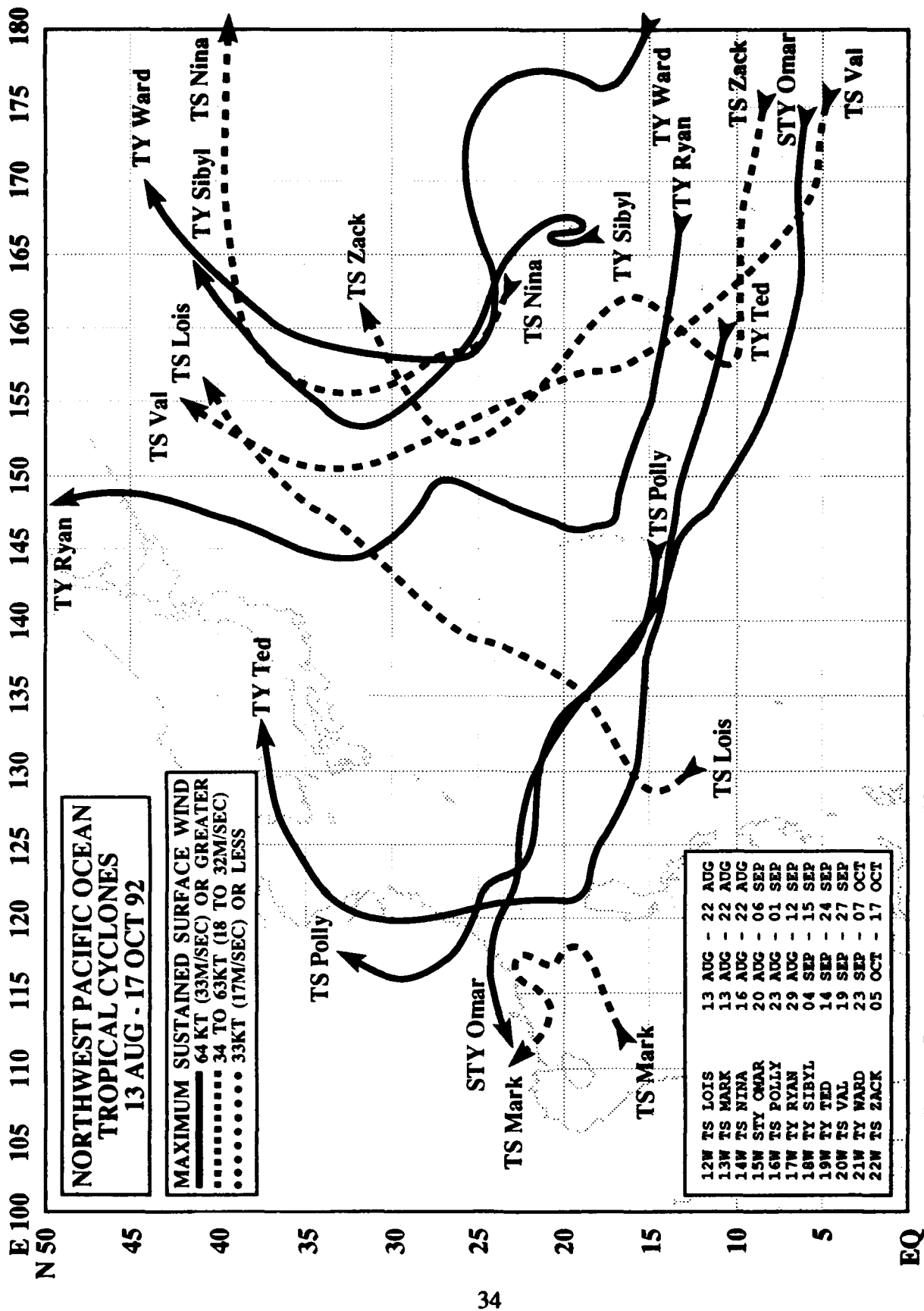


Figure 3-7. Composite best tracks for Northwest Pacific Ocean Tropical cyclones for 13 August to 17 October 1992.

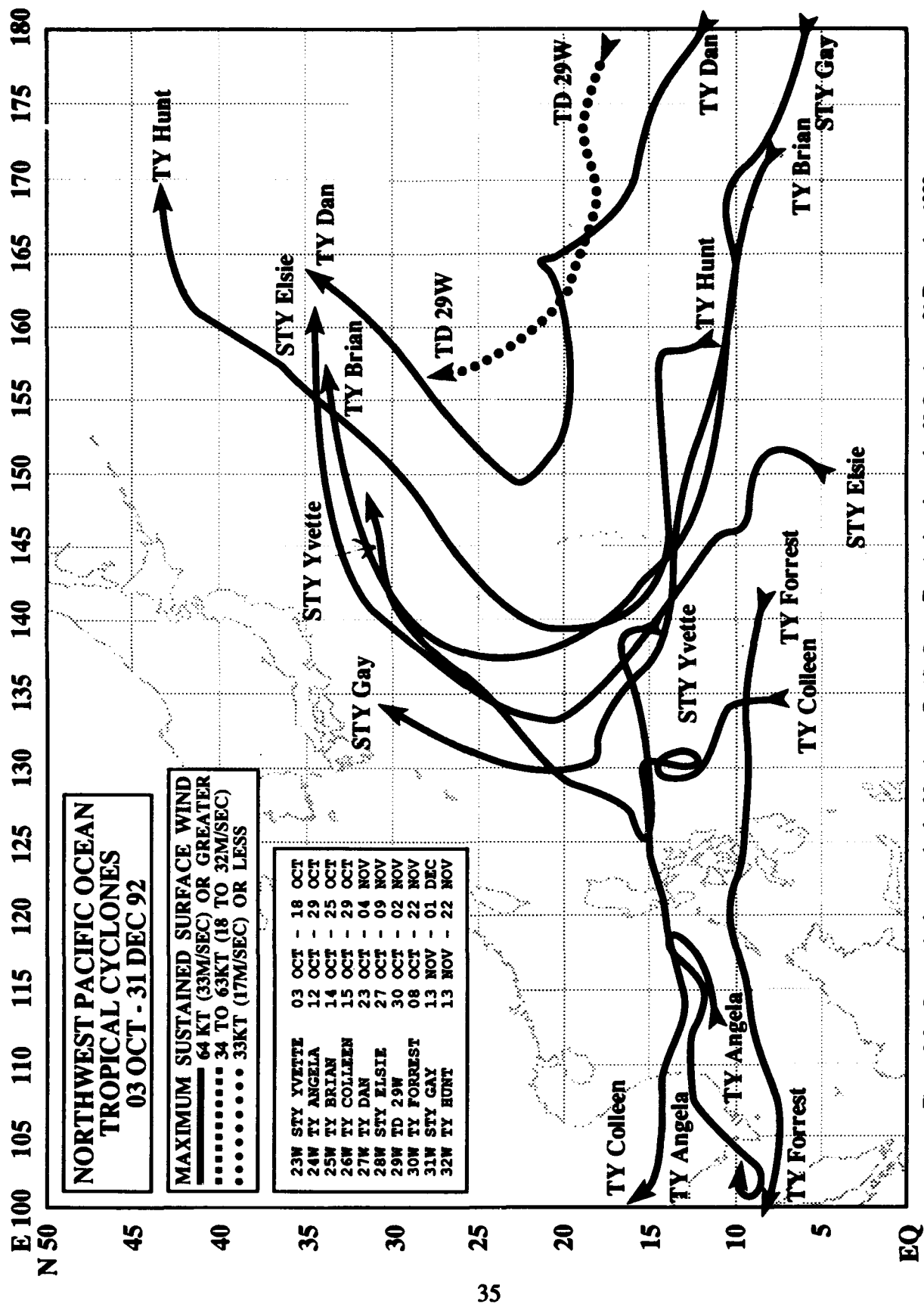
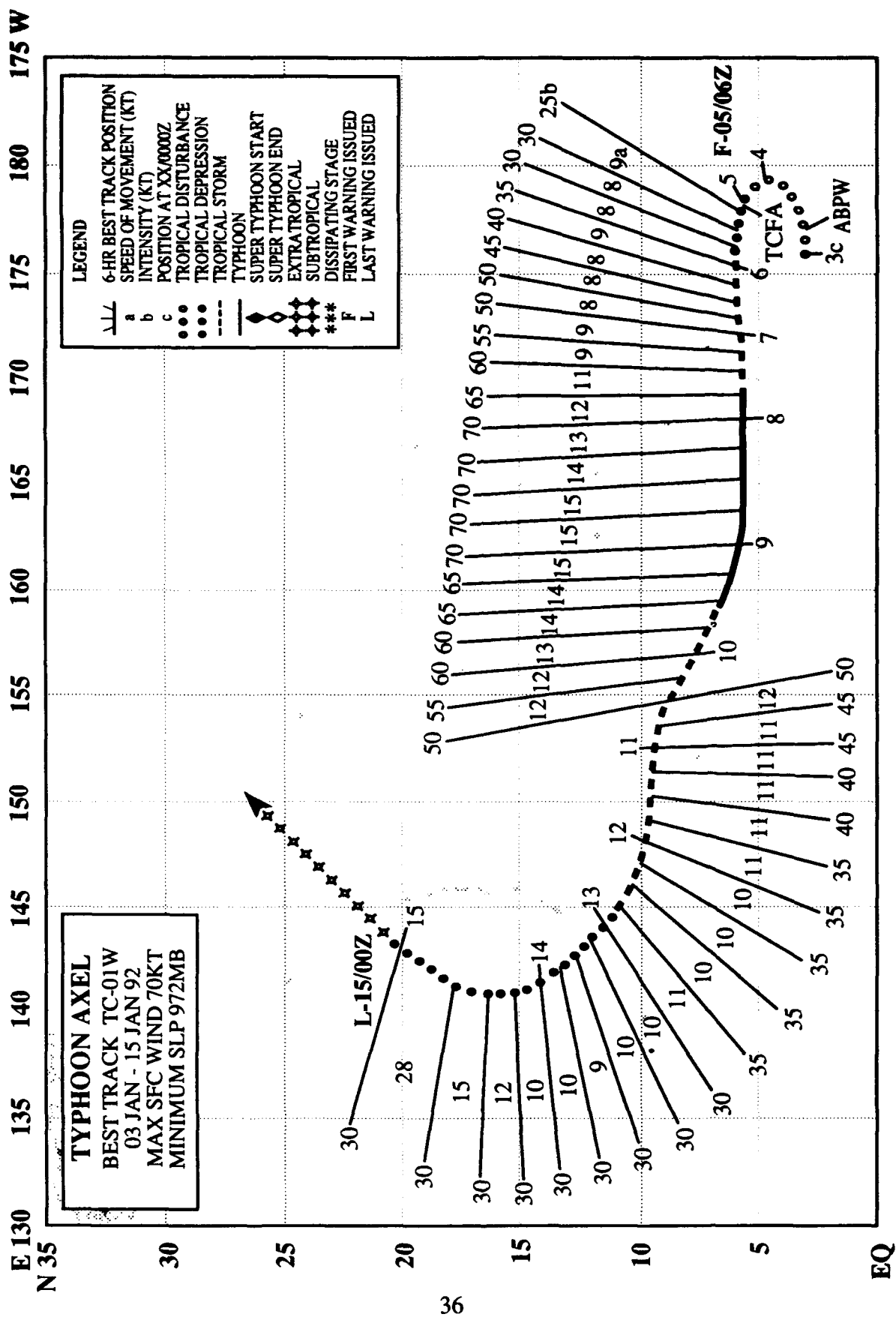


Figure 3-8. Composite best tracks for Northwest Pacific Ocean Tropical cyclones for 03 October to 31 December 1992



TYPHOON AXEL (01W)

I. HIGHLIGHTS

Typhoon Axel was the first significant tropical cyclone to occur in 1992 in the western North Pacific. It developed in January in conjunction with an equatorial west wind burst to the east of New Guinea along with two other tropical cyclones — Betsy (11P) and later Mark (12P) — in the Southern Hemisphere. Axel's early intensification at a low latitude proved particularly damaging to the Marshall Islands.

II. TRACK AND INTENSITY

Stronger than normal low-level westerly winds along the equator were noted east of New Guinea when Tarawa (WMO 91610) in the Gilbert Islands reported 28 kt (14 m/sec) gradient-level winds at 011200Z, 37 kt (19 m/sec) gradient-level winds at 020000Z, and later, at 030000Z, Banaba Island (WMO 91533) 300 nm (555 km) to the southwest of Tarawa reported surface winds of 30 kt (15 m/sec). These increased winds and an area of maximum cloudiness persisted in the area, as twin cyclones began to form. Axel was to the north and Betsy (11P) to the south of the equator. The evolution of these twin cyclones, and later a third, Mark (12P) located to the west of Betsy (11P), is graphically illustrated as cloud silhouettes in Figure 3-01-1. The persistent convection, which was to become Axel, was first mentioned on the Significant Tropical Weather Advisory at 030600Z. As the equatorial westerly winds died down, the convection began to consolidate around the twin disturbances. This prompted the issuance of a Tropical Cyclone Formation Alert on Axel at 050030Z, and the first warning at 050600Z. Strong upper-level divergence over the area enhanced development of the cloud system and Axel (Figure 3-01-2) attained tropical storm intensity based on Dvorak intensity estimates at 060000Z just before slamming into the Marshall Islands. Later, at 070000Z, an 85 kt (44 m/sec) ship report from the SV Cherokee became the basis for an upgrade to typhoon intensity. (In post analysis, comparison of the 85 kt (44 m/sec) report with observations from the nearby islands of Majuro (WMO 91376), Mili (WMO 91378), Jaluit (WMO 91369) and Ailinglapalap (WMO 91367) caused the SV Cherokee's to be questioned.)

By 8 January, Axel and Betsy (11P) were both at typhoon intensity and the distance between the two was steadily increasing with Axel headed west and Betsy (11P) south. After Axel reached a peak intensity of 70 kt (36 m/sec) at 080000Z, the typhoon passed just north of Kosrae and Pingelap (Figure 3-01-3) in the eastern Caroline Islands. Continuing to track south of the subtropical ridge axis and westward towards Guam, the typhoon weakened due to increasing vertical wind shear. As a consequence, JTWC downgraded Axel to a tropical storm at 091800Z, shortly after the cyclone passed 15 nm (30 km) north of Pohnpei (WMO 91348), where a maximum sustained winds of 30 kt (15 m/sec) and a peak gust to 48 kt (25 m/sec) were reported. Six hours after being downgraded to a tropical depression at 130000Z, Axel passed 90 nm (165 km) to the southwest of Guam. The tropical cyclone recurved a day later. As Axel was transitioning to an extratropical low and accelerating into the mid-latitude westerly flow, JTWC issued the final warning on the system at 150000Z.

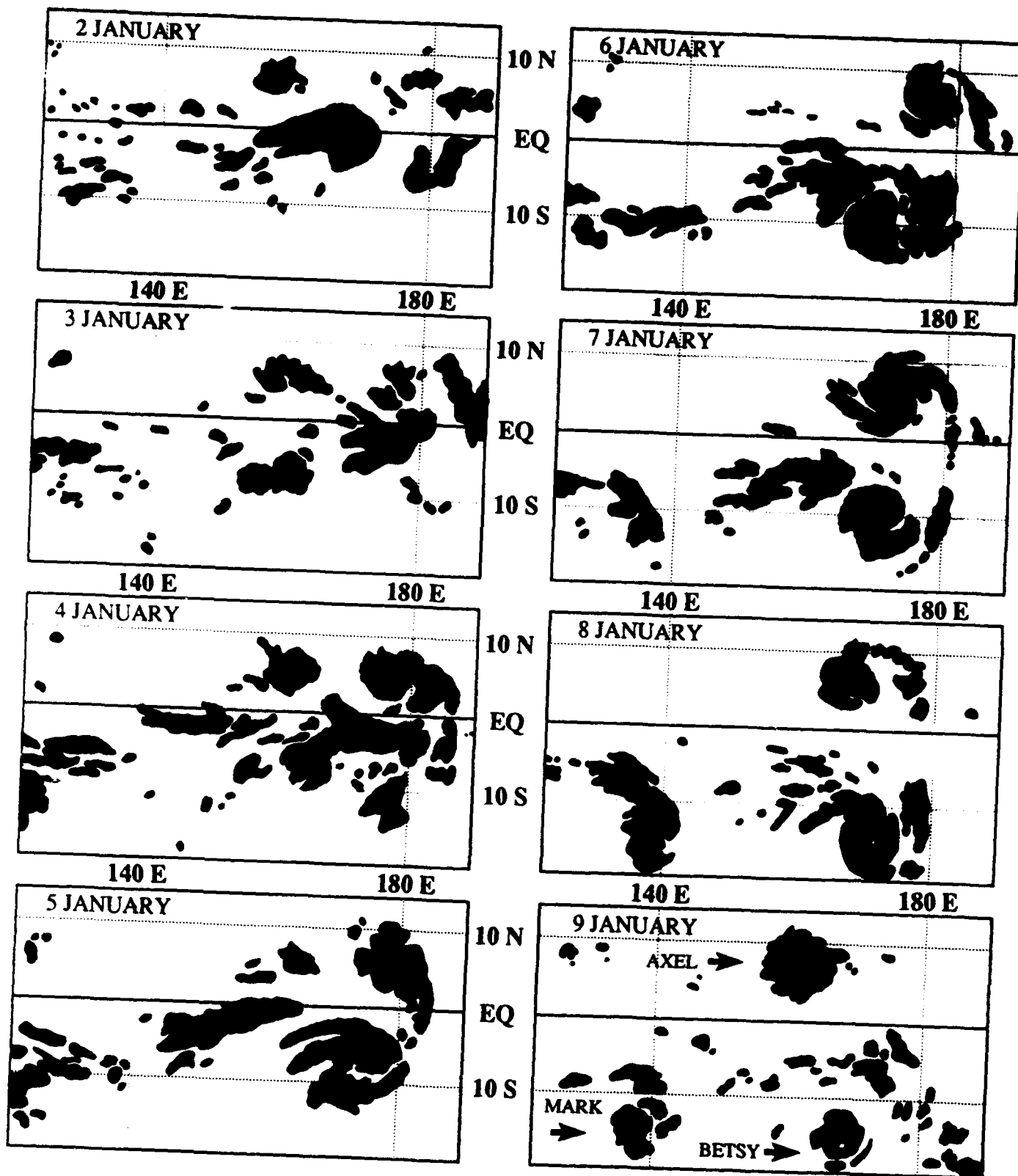


Figure 3-01-1. Cloud silhouettes for the period 2 to 9 January show the development of Axel, Betsy (11P) and later, Mark (12P). As the equatorial convection decreases, the cloudiness consolidates in the twin cyclones in opposite hemispheres.

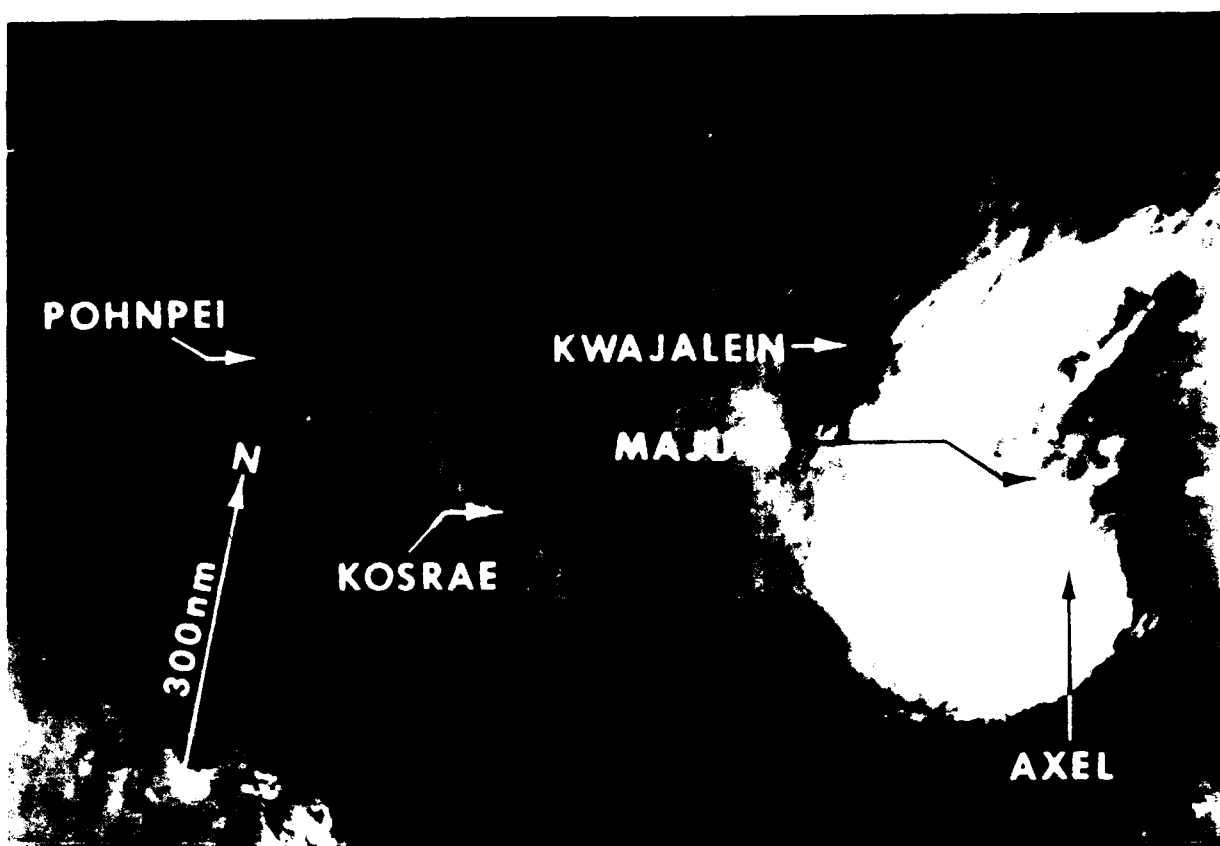


Figure 3-01-2. Axel's convection coils up as the tropical cyclone intensifies over the Marshall Islands (062211Z January DMSP visual imagery).

III. FORECAST PERFORMANCE

The overall mean track errors were 93 nm (172 km), 152 nm (282 km), and 183 nm (339 km) for the 24-, 48-, and 72-hour forecasts respectively. However, JTWC forecasts for a straight runner to the west were longer than needed resulting in larger forecast errors near the point of recurvature where there was a question as to where, or when, a break would appear in the subtropical ridge to allow Axel to track northward.

With regard to the intensity, the initial forecasts based on the development of twin cyclones and strong upper-level divergence, and discussed in the first several prognostic reasoning messages, verified well.

IV. IMPACT

Axel created havoc in the Marshall Islands. In the tropical cyclone's wake, the Federal Emergency Management Agency (FEMA) provided more than two million dollars to over 1300 people requesting assistance on Majuro and four other atolls. Axel washed out airport runways, ruined water reservoir systems, ruined crops and vegetation, and left hundreds of people without roofs over their heads. Mili, the easternmost atoll to be affected, took a direct hit. Houses were blown down and many trees and crops were lost.

Majuro (WMO 91367) experienced peak gusts of 46 kt (24 m/sec) and a low pressure of 997.0 mb as Axel passed 75 nm (139 km) to the south. Unfortunately for Majuro, Axel's closest point of approach coincided with high tide. The high surf, estimated to be in the 13 to 16 foot range on top of the high tide, broke pipes and washed sand, coral rock, and debris onto the island's runway which doubles as a water catchment system and provides almost 90% of the fresh drinking water. Despite the fact that almost 10 inches (254 mm) of rain from Axel fell in a 24-hour period, salt water contaminated most of the water supplies on the island. Sanitation became an immediate problem due to water wells, tanks and toilets being damaged by Axel's passage. The airport was closed for five days while bulldozers were used to clear off the larger debris. The south shore reefs were damaged when huge chunks of coral were ripped out and rolled across the reef. Trees, brush and other debris from the land washed onto the reefs adding to the loss. On land, food crops were ruined by the wind and flooding.

Then, Axel passed across Jaluit Atoll and over four feet of water covered most of the main islands. The strong winds deposited rocks and coral debris on runway and washed away portions of airstrip. Additionally, over one half of the outhouses were destroyed, resulting in serious health concerns for the islanders. Farther north, Kwajalein Atoll, 170 nm (315 km) north of track, experienced maximum sustained winds of only 25 with gusts to 35 kt (10 G 18 m/sec) and reported no damage or injuries.

In the eastern Caroline Islands, Kosrae (WMO 91356) which was 40 nm (75 km) south of track experienced maximum sustained winds of 65 G 80 kt (33 G 41 m/sec) resulting in severe crop losses, trees and vegetation damaged, and some wooden and tin-roofed structures destroyed. Just south of track, Pingelap (Figure 2) and Mokil atolls located east of Pohnpei had their airstrips 60% damaged by the storm surge and the runways were closed for months afterward for repairs. Some wood and tin roofed structures were destroyed. An estimated 50-60% of the small vegetation, such as bananas, was lost, plus some large coconut and breadfruit trees uprooted. As Axel passed 15 nm (30 km) north of the Pohnpei, the island's electrical power was knocked out for 8 hours and houses and building in low-lying areas flooded. Banana and breadfruit trees suffered extensive damage. The storm surge was estimated at 15 feet on the offshore islands and 9.73 inches (247 mm) of rain was recorded in a 24-hour period as the cyclone passed. And finally, Axel was weakening as it passed 90 nm (170 km) southwest of Guam, where no damages or injuries were reported.

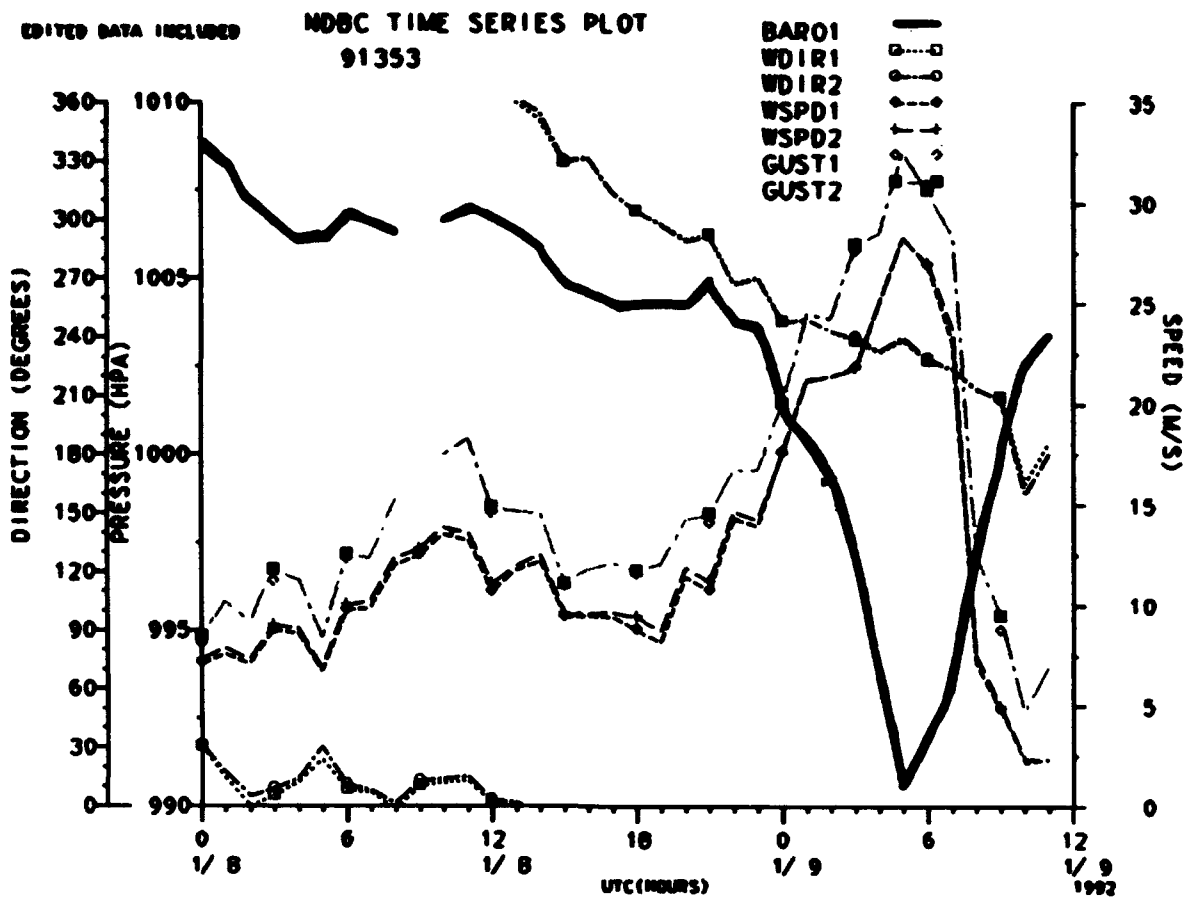
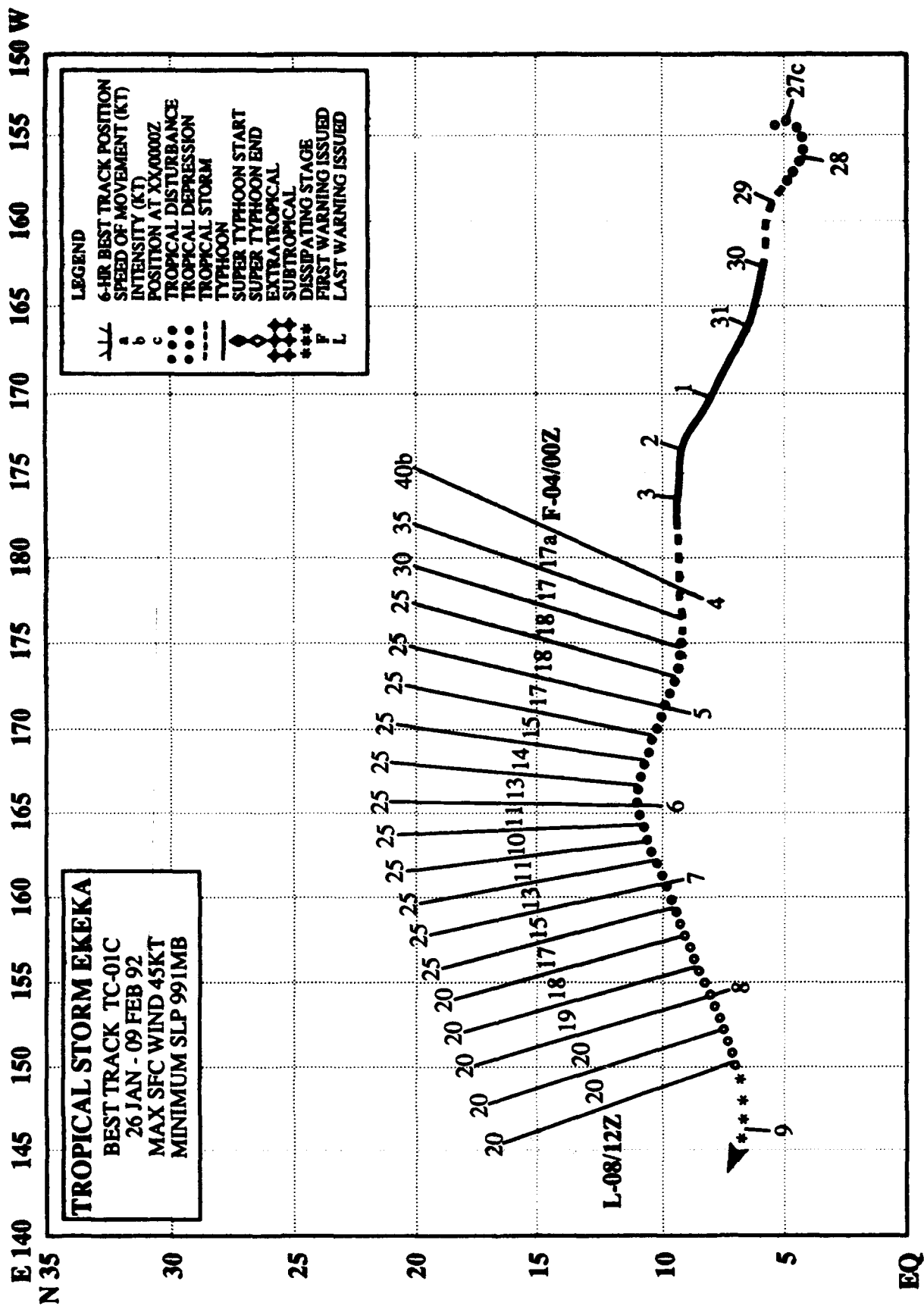


Figure 3-01-3. The Pingelap AMOS (WMO 91353) time series plot courtesy of the National Data Buoy Center shows surface winds gusting to 33 m/sec (64 kt) from the northwest and a minimum pressure of 991 mb at 090500Z as Axel passes by to the north.



TROPICAL STORM EKEKA (01C)



Figure 3-01C-1. Ekeka a day before reaching its peak intensity while east of the international date line. Oahu appears at the top right (312001Z January GOES visual imagery courtesy of the National Weather Service Forecast Office, Honolulu, Hawaii).

After forming south of the Hawaiian Islands, Ekeka became a rare January central North Pacific hurricane which weakened and crossed into JTWC's area of responsibility. The tropical disturbance was initially detected by the Central Pacific Hurricane Center on 26 January, and the first warning was issued at 280600Z on Tropical Depression 01C, when it was 980 nm (1815 km) south of Oahu. On a track to the west-northwest, Ekeka intensified steadily over the next several days, reaching a peak intensity of 95 kt (50 m/sec) on 01 February. Then, the hurricane turned westward and began to accelerate as the subtropical ridge north of the system strengthened. Due to increased upper-level shear, Ekeka began to weaken, so that when the JTWC assumed warning responsibility at 040000Z, the maximum winds had dropped to 40 kt (20 m/sec). Within 12 hours, the tropical storm had further weakened to a tropical depression. Tropical Depression 01C continued to move westward in the deep easterly trade wind flow and passed through the Marshall Islands without causing any significant damage. After the tropical depression

passed over Chuuk (WMO 91334) where maximum winds of 17 kt (9 m/sec) were reported, JTWC issued the final warning at 081200Z. No reports of damage were received.

TYPHOON BOBBIE (02W)

I. HIGHLIGHTS

The second typhoon of the year, Bobbie formed in the monsoon trough in late June after a four month hiatus in tropical cyclone activity in the western North Pacific Ocean. Bobbie's formation in the central Caroline Islands coincided with that of Chuck (03W) over the central Philippine Islands, and the two underwent binary interaction for three days. Bobbie reached typhoon intensity several days prior to recurving. After recurvature, the typhoon accelerated, tracked just to the southeast of Okinawa and underwent extra-tropical transition before passing just south of Tokyo.

II. TRACK AND INTENSITY

By 15 June, the monsoon trough became established in its normal climatological location across the South China Sea, the central Philippine Islands and extended into the Caroline Islands. Bobbie was the first significant cyclone to form in this trough. The tropical disturbance was detected as a poorly organized area of convection south of Guam near Woleai Atoll in the central Caroline Islands and first mentioned on the Significant Tropical Weather Advisory at 200600Z. Development of the circulation continued and JTWC issued a Tropical Cyclone Formation Alert at 221900Z followed by the first warning at 231200Z. At the same time, a second tropical cyclone, Chuck (03W), formed farther to the west in the monsoon trough over the central Philippine Islands. Due to the proximity of the two cyclones, binary interaction occurred during the period between 240600Z and 271200Z. The binary pair remained within 750 nm (1390 km) of each other and appeared to undergo relative cyclonic rotation about a common midpoint for three days (Figure 3-02-1).

Bobbie tracked northwestward and was upgraded to a typhoon at 250600Z. Intensification continued until a peak of 120 kt (62 m/sec) (Figure 3-02-2) was reached at 261800Z. By this time, Bobbie had also reached the western extent of the mid-level subtropical ridge where recurvature began to the east of Taiwan at 271200Z. As gradual acceleration began under increasing southwesterly winds aloft, Bobbie passed over Miyako Jima on 28 June and then just southeast of Okinawa on 29 June. Kadena AB, Okinawa reported the closest point of approach of 24 nm (44 km), a peak wind of 68 kt (35 m/sec), and a minimum sea-level pressure of 978 mb at 290028Z. When Bobbie underwent extratropical transition on 30 June southeast of Kyushu, JTWC issued the final warning on the system at 300000Z. The intense low pressure center with associated gale force winds brushed by the southern tip of Honshu and proceeded out to sea.

III. FORECAST PERFORMANCE

After the fact, Bobbie's best track appears to be a straight forward case of recurvature. At the start however, based on persistent westward movement of Bobbie in the formative stages of development and the guidance provided by the dynamic aids, the forecast philosophy was for a straight running track west-northwestward along the axis of the monsoon trough. It appears that the development of Typhoon Chuck (03W) to the west, and the resulting binary interaction, influenced Bobbie's track change to the northwest. Later, when gradual recurvature was expected to occur, as Bobbie approached the ridge axis situated near 25° North Latitude, the western extension of the subtropical ridge eroded faster than depicted by the dynamic model and the typhoon recurved earlier and at a lower latitude. From the recurvature point, the tropical cyclone was forecast to pass to the west of Okinawa. At 280600Z, the strengthening of the upper-level jet south of Honshu was noted, and at 281800Z the track

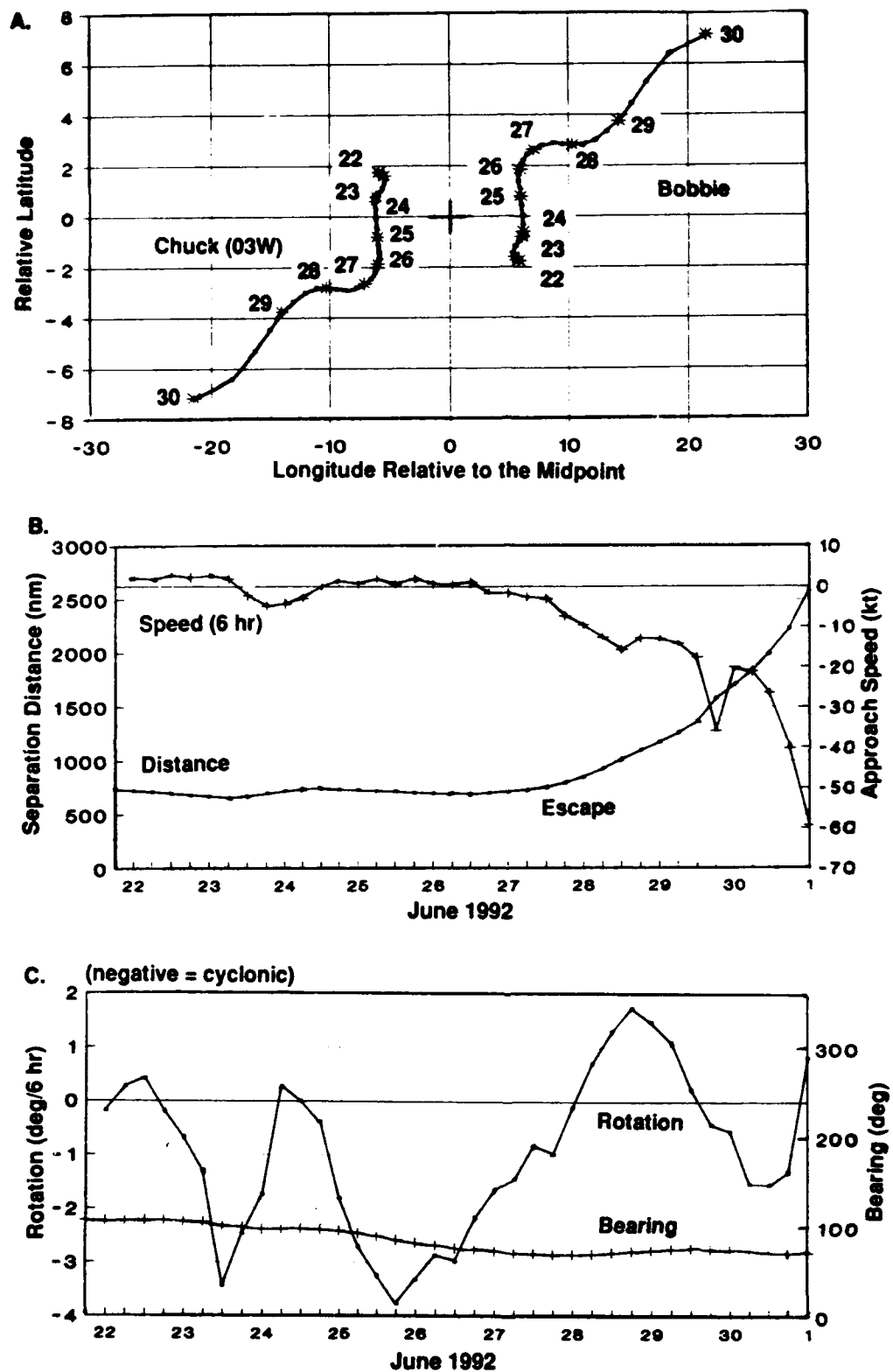


Figure 3-02-1. A set of graphs depict the binary interaction between Bobbie and Chuck (03W). The motion relative to a common midpoint is shown in (A), nearly constant 750 nm (1390 km) separation in (B), and cyclonic rotation in (C).

forecast was adjusted correctly for Bobbie to pass to the east of Okinawa. Despite the shift in the forecast track, ample warnings and detailed prognostic reasoning messages evaluating the potential for alternate scenarios gave Okinawa enough time and information to adequately prepare.

With respect to intensity forecasts, the errors were quite large initially due to the expected interaction with rugged northern Luzon which did not occur. And later, in like fashion, the forecast interaction with Taiwan didn't occur and the typhoon intensified over water.

IV. IMPACT

As the typhoon passed east of the northern Luzon, torrential rains associated with the deep monsoonal flow into Bobbie and enhanced by Chuck (03W) caused heavy rains, mudslides, and widespread flooding over the northern Philippine Islands. These conditions were aggravated in the area of Mount Pinatubo when a "secondary" volcanic explosion occurred on 27 June, triggering flows of lava, mud, ash, and sand up to 5 feet deep down the mountains sides. No deaths or injuries were reported in the towns near the volcano due to timely evacuations of the population. On 28 June, Bobbie passed over Miyako Jima. Okinawa was next. The island boarded up and schools were closed. On 29 June, these preparations paid off and only minor damage to buildings, property and vegetation occurred. Kadena Air Base reporting one trailer overturned and small trees uprooted. One woman received head injuries when she was knocked down by the strong wind.

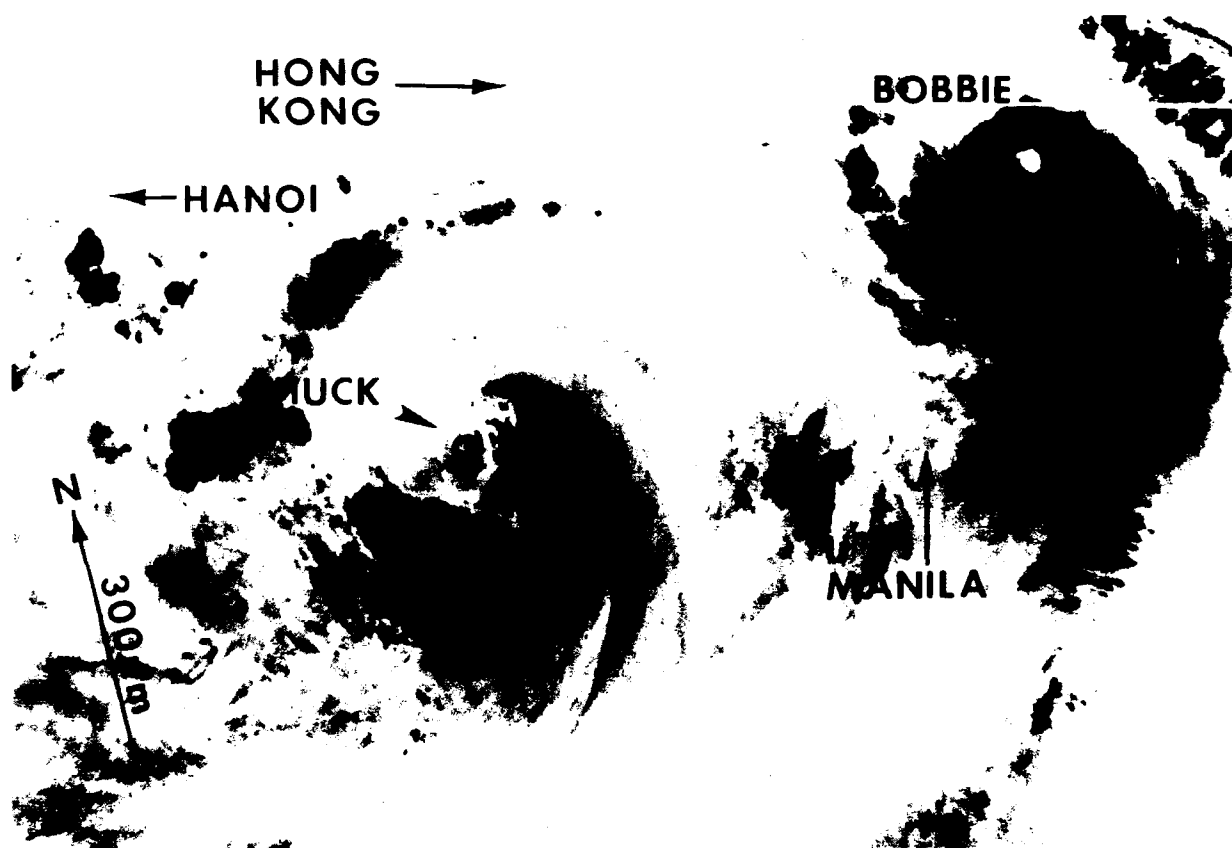
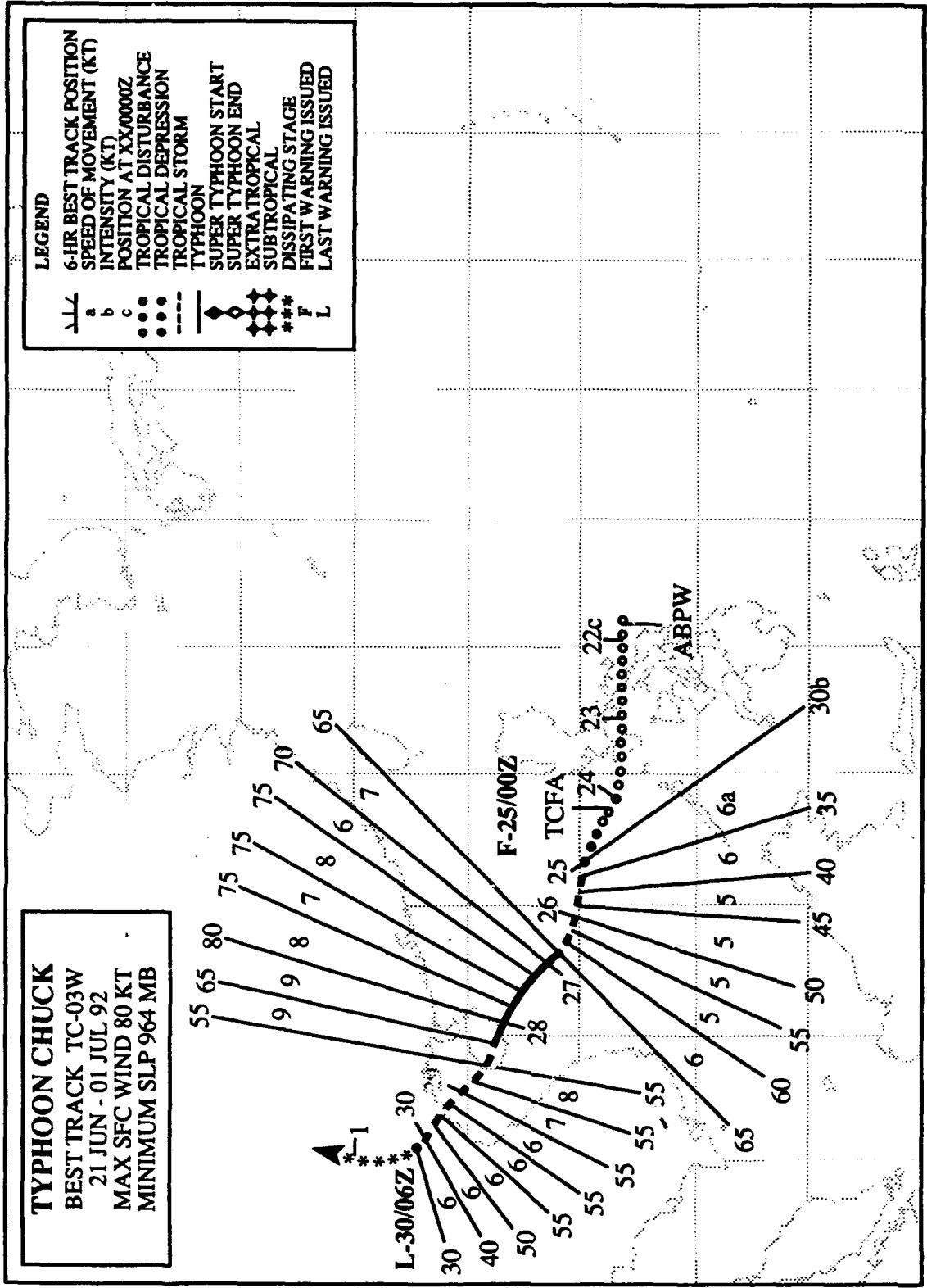


Figure 3-02-2. Typhoon Bobbie at a peak intensity of 120 kt (62 m/sec) and approaching its point of recurvature. Chuck (03W) can be seen over the South China Sea to the southwest of Bobbie (261949Z June NOAA infrared imagery).

E 100 105 110 115 120 125 130 135 140 145 150 E

TYPHOON CHUCK
 BEST TRACK TC-03W
 21 JUN - 01 JUL 92
 MAX SFC WIND 80 KT
 MINIMUM SLP 964 MB

LEGEND
 6-HR BEST TRACK POSITION
 SPEED OF MOVEMENT (KT)
 INTENSITY (KT)
 POSITION AT XX/000Z
 TROPICAL DISTURBANCE
 TROPICAL DEPRESSION
 TROPICAL STORM
 TYPHOON
 SUPER TYPHOON START
 SUPER TYPHOON END
 EXTRA TROPICAL
 SUBTROPICAL
 DISSIPATING STAGE
 FIRST WARNING ISSUED
 LAST WARNING ISSUED



TYPHOON CHUCK (03W)

I. HIGHLIGHTS

Chuck was the first tropical cyclone of the year in the South China Sea. Genesis occurred in the monsoon trough at the same time in late June as Bobbie (02W) and binary interaction took place over the first few days of development.

II. TRACK AND INTENSITY

Chuck developed over the central Philippines as part of a multiple tropical cyclone outbreak, and the Significant Tropical Weather Advisory was reissued at 211900Z to include the event. In conjunction with this development, gradient-level wind reports as far to the west as the Malay Peninsula showed an overall increase of 10 kt (5 m/sec) to the 25-35 kt (13-18 m/sec) range. As the amount and organization of the convection continued to increase, JTWC issued a Tropical Cyclone Formation Alert at 240430Z. The first warning followed at 250000Z, and 12 hours later, Chuck was upgraded to a tropical storm based on satellite and ship synoptic reports. Tracking slowly along the monsoon trough axis, Chuck moved to the west-northwest as it underwent binary interaction with Bobbie (02W) (Figure 3-03-1). Even after 271200Z, when Typhoon Bobbie (02W) began to recurve and the separation distance between the two cyclones started to increase, Chuck showed very little change in track.

A wind report of 60 kt (31 m/sec) and a 981.4 millibar pressure from Xisha Qundao (WMO 59981), was the basis for upgrading Chuck to typhoon intensity at 271200Z. Xisha recorded a minimum sea-level pressure of 966.2 mb (Royal Observatory, June 1992) during the typhoon's passage. Chuck remained a typhoon until it hit the southern tip of Hainan Dao on 28 June. The station at Yaxian (WMO 59948) reported a pressure of 964.1 mb (Royal Observatory, June 1992) when the typhoon made landfall 20 nm (37 km) to the northeast. Chuck weakened slightly as it passed over the southern tip of Hainan Dao, crossed the Gulf of Tonkin and slammed in northern Vietnam on 29 June. The final warning was issued at 300600Z, as Chuck dissipated over land.

III. FORECAST PERFORMANCE

The overall mean errors were 106 nm (196 km), 207 nm (380 km) and 331 nm (610 km) for the 24-, 48-, and 72-hour track forecasts respectively. At the start, larger track errors were associated with forecasts based on a more westerly straight-running track in agreement with the dynamic guidance that turned out to be to the left of track. And later, forecasts based on premature recurvature to the north were to the right of track.

IV. IMPACT

Navy patrol aircraft from Kadena Air Base and Cubi Point NAS, Philippines, searched for two ships in distress and 22 crew members missing after Typhoon Chuck crossed the South China Sea. Only flotsam, oil slicks, and other debris were found. On Hainan Dao, one death and 19 injuries were reported, plus extensive damage to houses and crops. In northern Vietnam, at least 21 people died and 80 were reported missing. In addition, many watercraft were sunk, houses destroyed, and power lines downed.

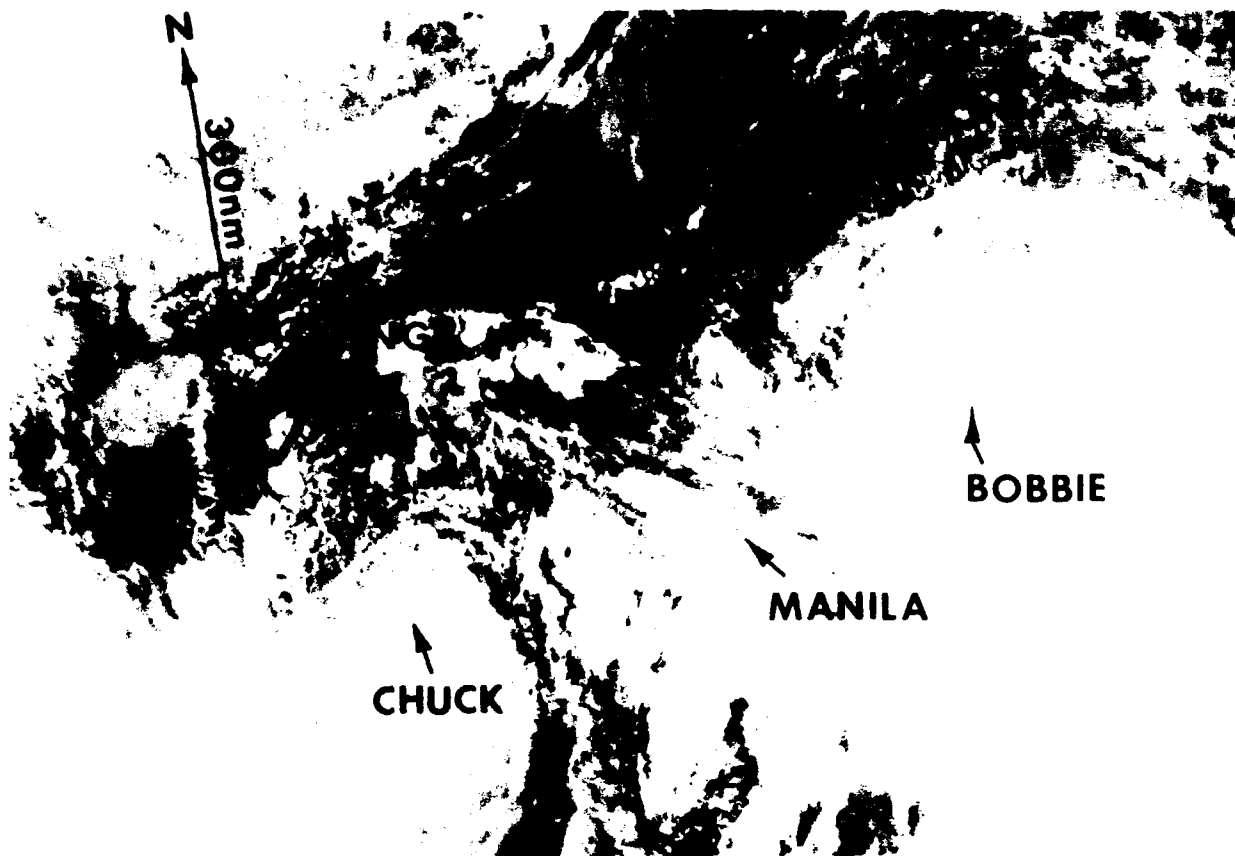
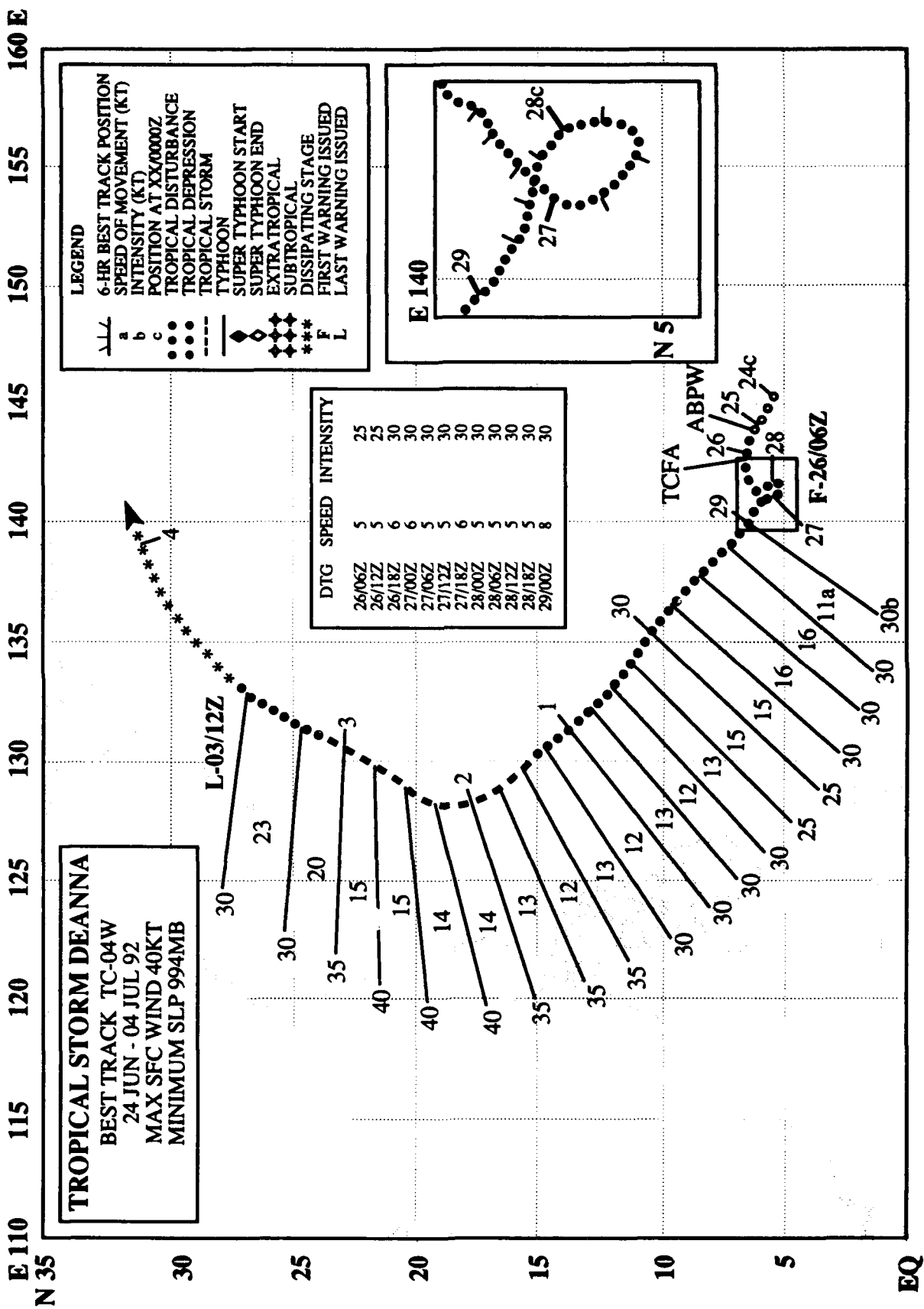


Figure 3-03-1. Chuck at tropical storm intensity churns across the South China Sea and interacts with Typhoon Bobbie (2W) located to the east-northeast (252353Z June NOAA visual imagery).



TROPICAL STORM DEANNA (04W)

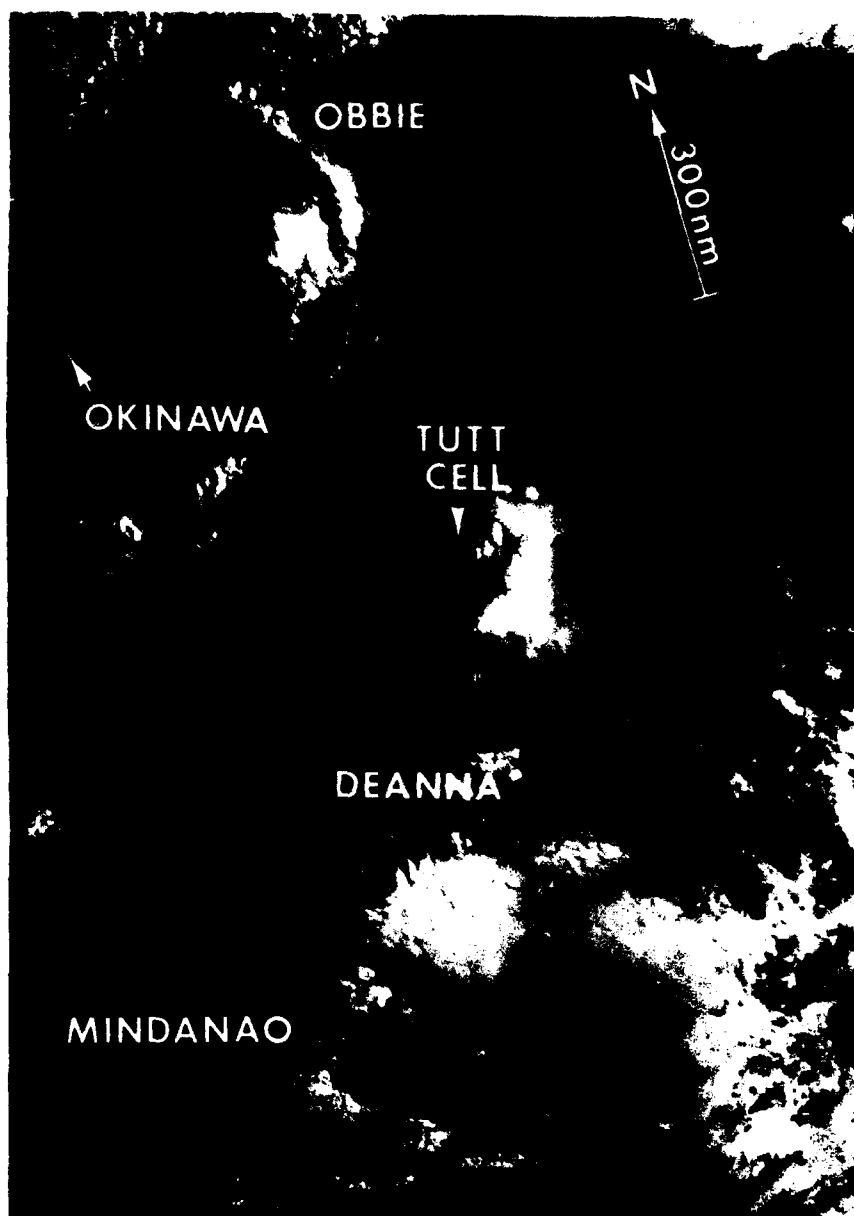
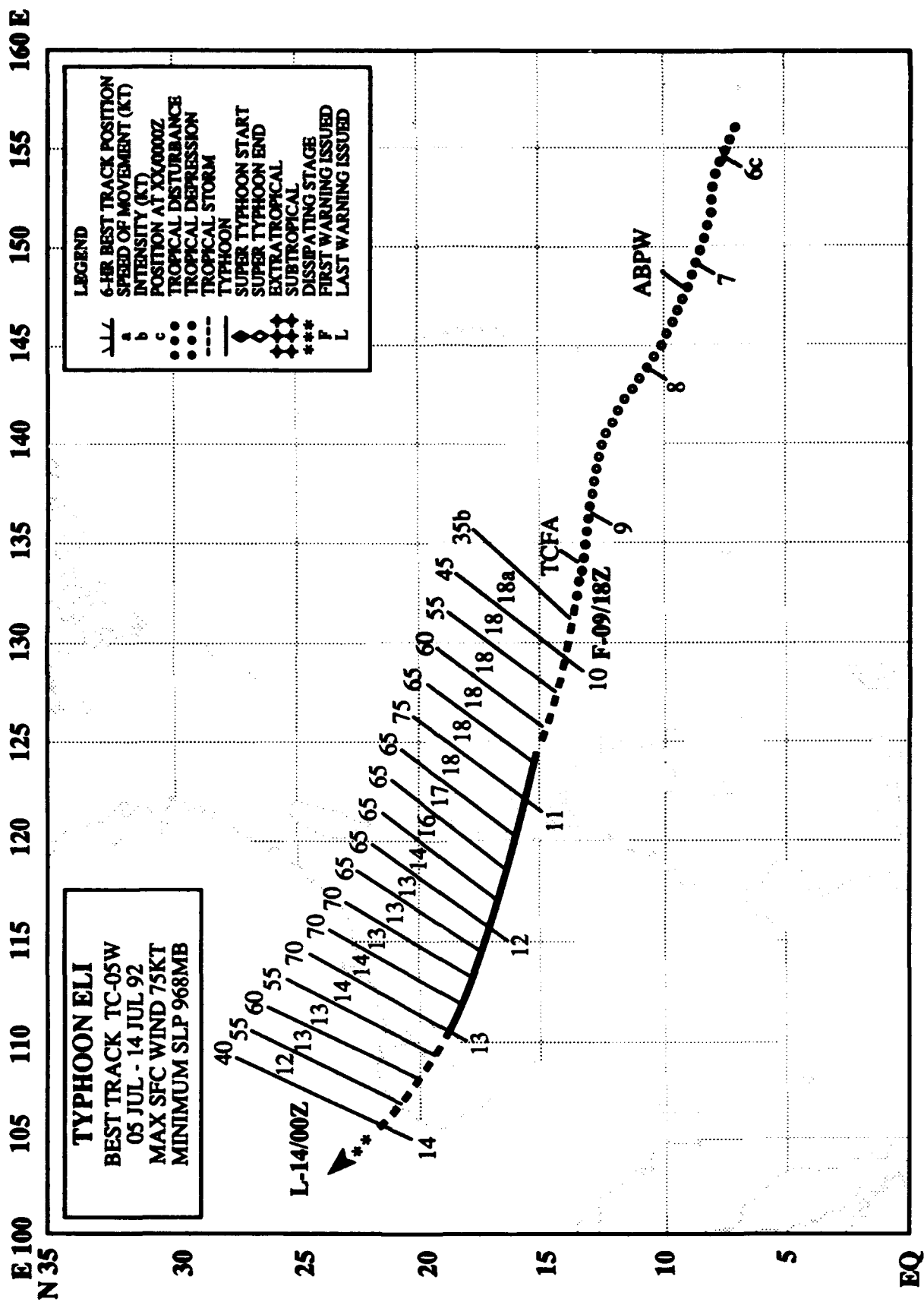


Figure 3-04-1. Deanna's convection was slow to organize due to the vertical wind shear from Bobbie's (02W) outflow and flow around the associated TUTT cell to the north (300945Z June DMSP visual imagery).

Deanna was the third, and final, significant tropical cyclone to form in June. After first mention at 250600Z on the Significant Tropical Weather Advisory, it was the subject of a Tropical Cyclone Formation Alert at 260300Z, and a first warning at 260600Z. Deanna executed a counter-clockwise loop on 27 and 28 June before moving out to the northwest on a track paralleling the one taken by Bobbie (02W) five days earlier. After reaching a peak intensity of 40 kt (21 m/sec) at 020600Z July near the subtropical ridge axis, the tropical storm accelerated to the northeast and dissipated in a frontal band. The final warning was issued at 031200Z.



TYPHOON ELI (05W)

I. HIGHLIGHTS

The first significant tropical cyclone to develop in July, Eli formed in the eastern Caroline Islands, intensified into a typhoon while moving rapidly across the Philippine Sea, and tracked west-northwestward across Luzon, the South China Sea, and into northern Vietnam.

II. TRACK AND INTENSITY

After Deanna (04W) recurved on 2 July, ridging temporarily replaced the monsoon trough across the Philippine Islands and Sea. To the east in the eastern Caroline Islands, however, weak southwesterlies persisted at low latitudes, and a weak cyclonic circulation developed. This circulation and its associated convection was first mentioned in the 070600Z Significant Tropical Weather Advisory. That night, a small mass of convection located in the eastern end of the circulation accelerated westward as a squall line. The squall's brief passage across Guam brought over a half inch of rain and winds gusting to 30 kt (15 m/sec). On 8 July, the tropical disturbance, after tracking to the south of Guam, accelerated to 19 kt (35 km/hr) and increased in organization, prompting JTWC to issue a Tropical Cyclone Formation Alert at 091100Z. The first warning followed at 091800Z as the convection increased throughout the night.

Tropical Depression 05W was upgraded to a tropical storm at 100000Z as Eli's convective buildup continued (Figure 3-05-1). Eli attained typhoon intensity at 101800Z, and peaked at 75 kt (39 m/sec) six hours later, just before making landfall on northern Luzon. Maximum sustained winds of 28 kt (14 m/sec) with gusts to 40 kt (21 m/sec) were reported by Cubi Point Naval Air Station as Eli passed 85 nm (155 km) to the north. After entering the South China Sea, the typhoon's forward motion slowed as the mid-level easterly steering flow weakened near the western end of the subtropical ridge. Eli maintained minimal typhoon intensity until it plowed into Hainan Dao on the night of 13 July. Then, as a tropical storm, Eli moved west-northwestward across the Gulf of Tonkin and dissipated over northern Vietnam on 14 July.

III. FORECAST PERFORMANCE

The overall, mean track forecast errors for JTWC were 80, 138, and 157 nm (148, 256, and 291 km) at 24, 48 and 72 hours, respectively. In comparison with the other aids, these forecasts, plus the guidance provided by OTCM, showed skill when compared to CLIPER, which had mean track errors of 104, 171, and 225 nm (195, 317, and 417 km) at 24, 48 and 72 hours, respectively.

IV. IMPACT

Torrential rains associated with Typhoon Eli caused mudflows in the Mount Pinatubo area on Luzon, where there were reports of three deaths. Regional civil defense authorities reported evacuating 1600 people from their homes in three central Luzon towns to escape avalanches of volcanic debris, or lahars, from Mount Pinatubo. In addition, 25 fishermen were reported missing off the east coast of Luzon.

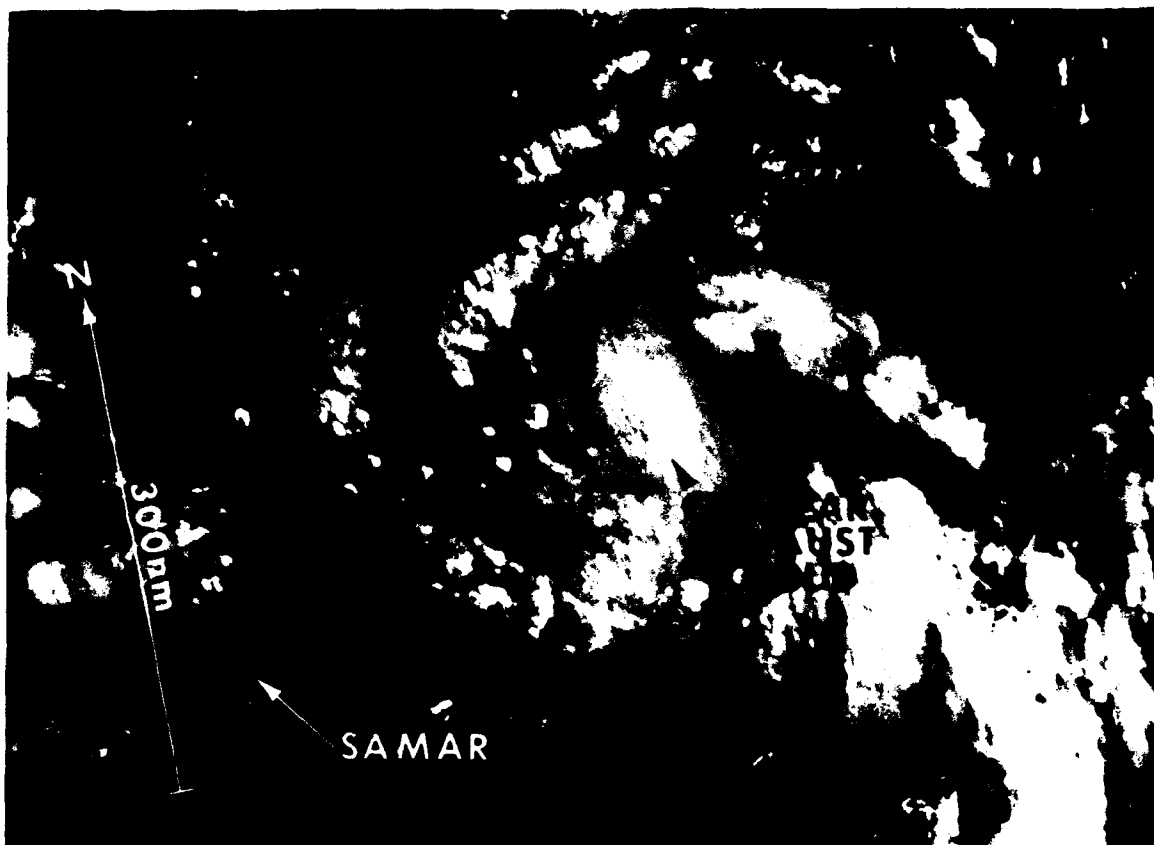
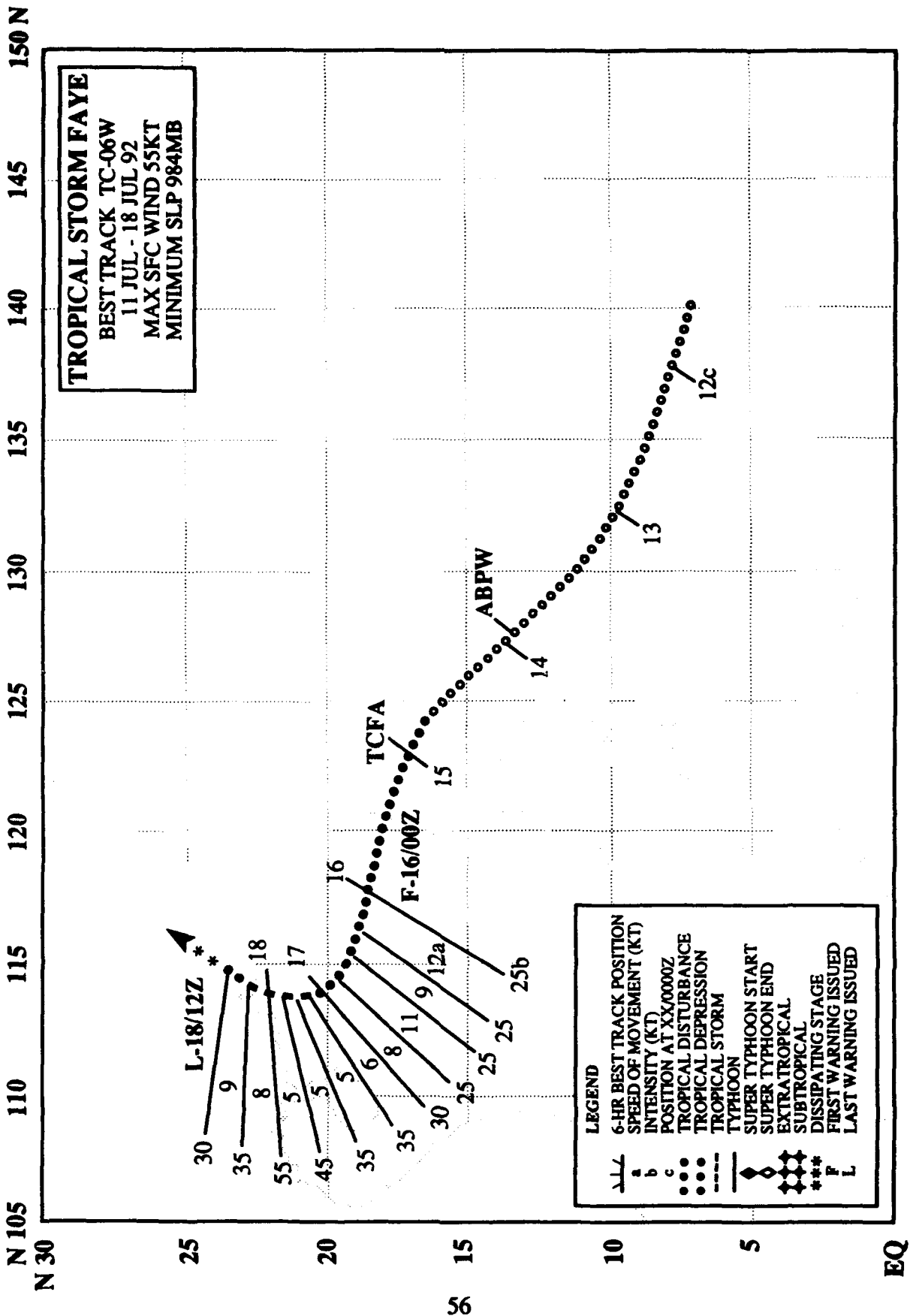


Figure 3-05-1. As Eli intensifies, a circular exhaust cloud (CEC) appears superimposed on the central dense overcast. The low angle of the sun to the east accentuates the cloud-top topography, revealing a concentric, or tree ring-like pattern of gravity waves in the top of the CEC (092354Z, July DMSP visual imagery).



TROPICAL STORM FAYE (06W)

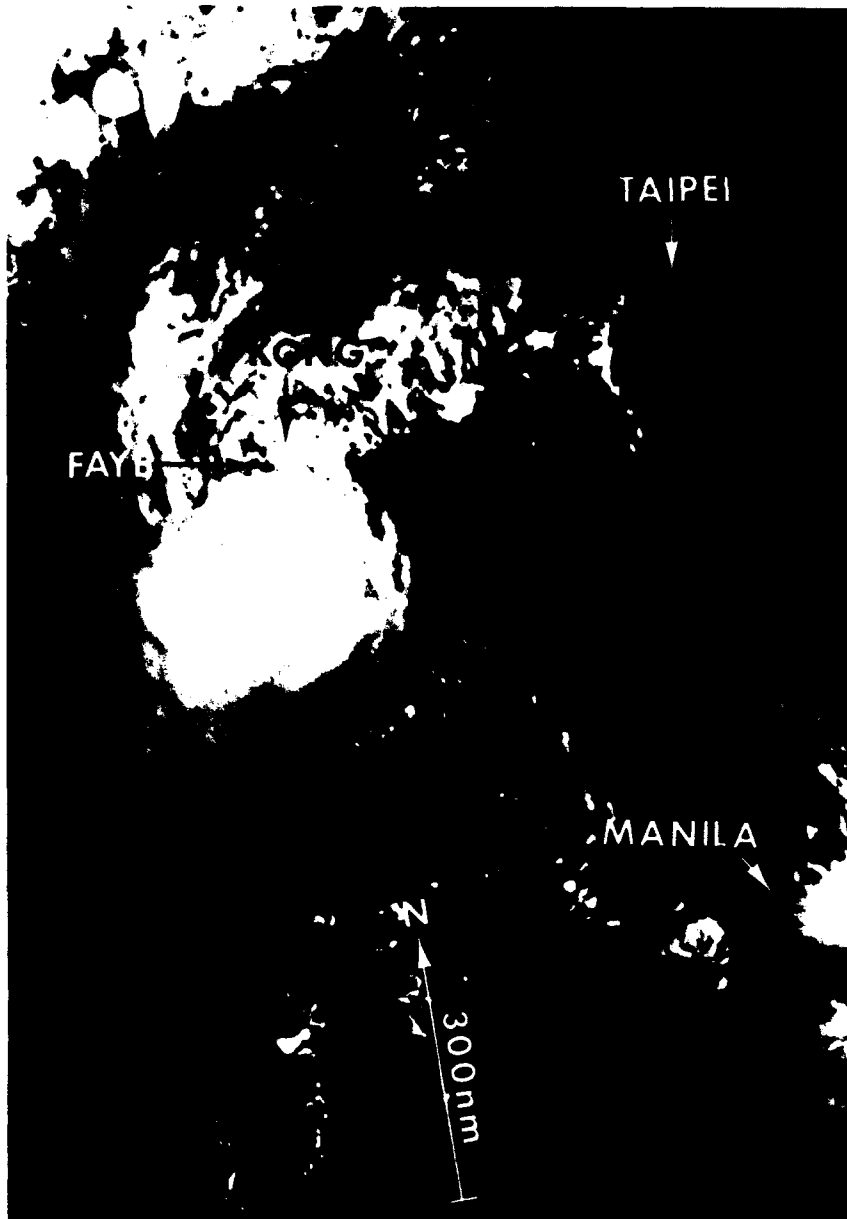
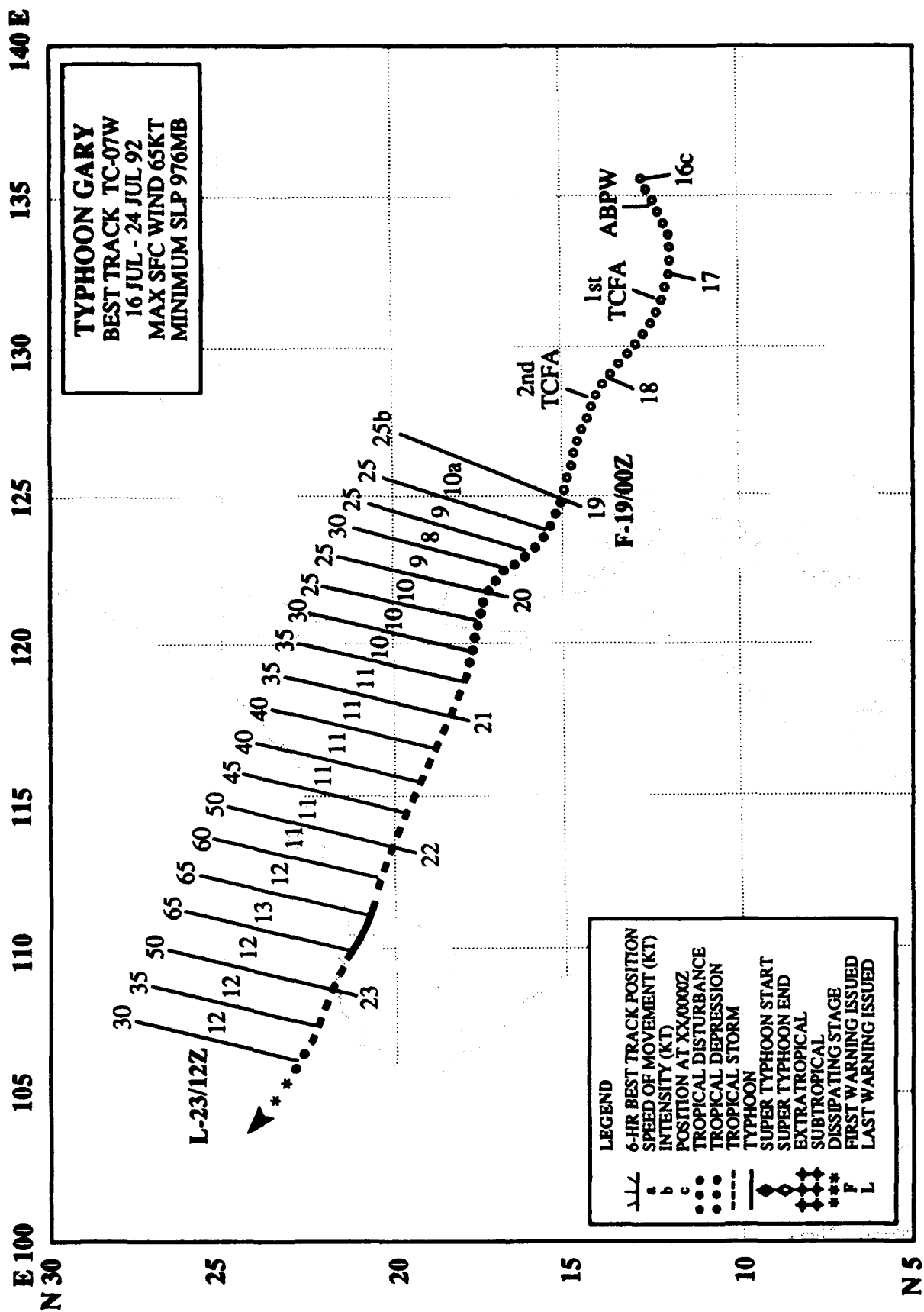


Figure 3-06-1. Tropical Storm Faye's partially exposed low-level circulation center is visible as it moves onshore near Hong Kong (172303Z July NOAA visual imagery).

Faye, the second of three successive tropical cyclones to pass over northern Luzon and intensify in the South China Sea, was first mentioned in the 130600Z July Significant Tropical Weather Advisory after synoptic data in the western Caroline Islands revealed a cyclonic circulation in the low-level wind field. As the circulation crossed the Philippine Sea, its convective organization increased, prompting forecasters to issue a Tropical Cyclone Formation Alert at 150000Z. After the cloud system crossed northern Luzon and the central convection reformed, the first warning was issued at 160000Z. Tropical Depression 06W proceeded west-northwestward until recurving south of Hong Kong on 17 July. At 170600Z, Faye was upgraded to a tropical storm, and shortly thereafter made landfall with an estimated maximum intensity of 55 kt (28 m/sec). Faye proceeded north-northeastward into China and dissipated. The final warning was issued at 181200Z.



TYPHOON GARY (07W)

I. HIGHLIGHTS

Gary was the last of three consecutive tropical cyclones to cross northern Luzon and intensify in the South China Sea during July. After early difficulties locating the low-level vortex, JTWC correctly predicted that the tropical cyclone would strike the southern coast of China near Hainan Dao. Gary caused widespread damage across southern China.

II. TRACK AND INTENSITY

Typhoon Gary's track paralleled those of Typhoon Eli (05W) and Tropical Storm Faye (06W). The genesis mechanism for all three was an active monsoon trough, which extended across the Philippine Sea. On 16 July, mention of an area of vigorous convection was included on the daily Significant Tropical Weather Advisory. Within 24 hours, its organization had improved sufficiently to warrant a Tropical Cyclone Formation Alert, which was issued at 170630Z. The Alert was reissued at 180630Z after the broad low-level circulation, containing multiple vortices, failed to consolidate in the presence of increased upper-level shear. At 190000Z, convective organization had improved to the point that the first warning on Tropical Depression 07W was issued. Because the circulation was large and poorly organized, there were large differences in the satellite fix positions as satellite analysts at network sites attempted to pinpoint the location of the low-level circulation center. The cloud system consolidated and became easier to locate by satellite once it crossed the northern Philippines. After being upgraded to tropical storm intensity at 201800Z, Gary tracked west-northwestward across the South China Sea, and later over the Leizhou Peninsula to the north of Hainan Dao. Shortly before land-fall, Gary developed a large, ragged eye (Figure 3-07-1), which prompted its upgrade to typhoon intensity at 221200Z. After reaching an estimated peak intensity of 65 kt (33 m/sec), the typhoon made land-fall and dissipated. Ship reports near Hainan Dao indicated that winds in excess of 30 kt (15 m/sec) persisted overwater until after the cyclone center was well inland, which necessitated additional tropical cyclone warnings until 231200Z.

III. FORECAST PERFORMANCE

JTWC's track forecasts improved significantly after the low-level circulation center consolidated on 20 July. Initial position errors fell in the 25 nm (45 km) range in contrast to those a day earlier on 19 July, which were in the 125 nm (230 km) range. Early on, JTWC correctly predicted Gary's west-northwestward track across the South China Sea, just as Eli (05W) and Faye (06W) had done less than two weeks earlier.

IV. IMPACT

News reports indicated that Typhoon Gary's passage over southern China resulted in the deaths of 26 people, and injuries to another 63. The southern provinces of Guangdong and Guangxi suffered extensive flood and wind damage with losses estimated at \$148 million (US).

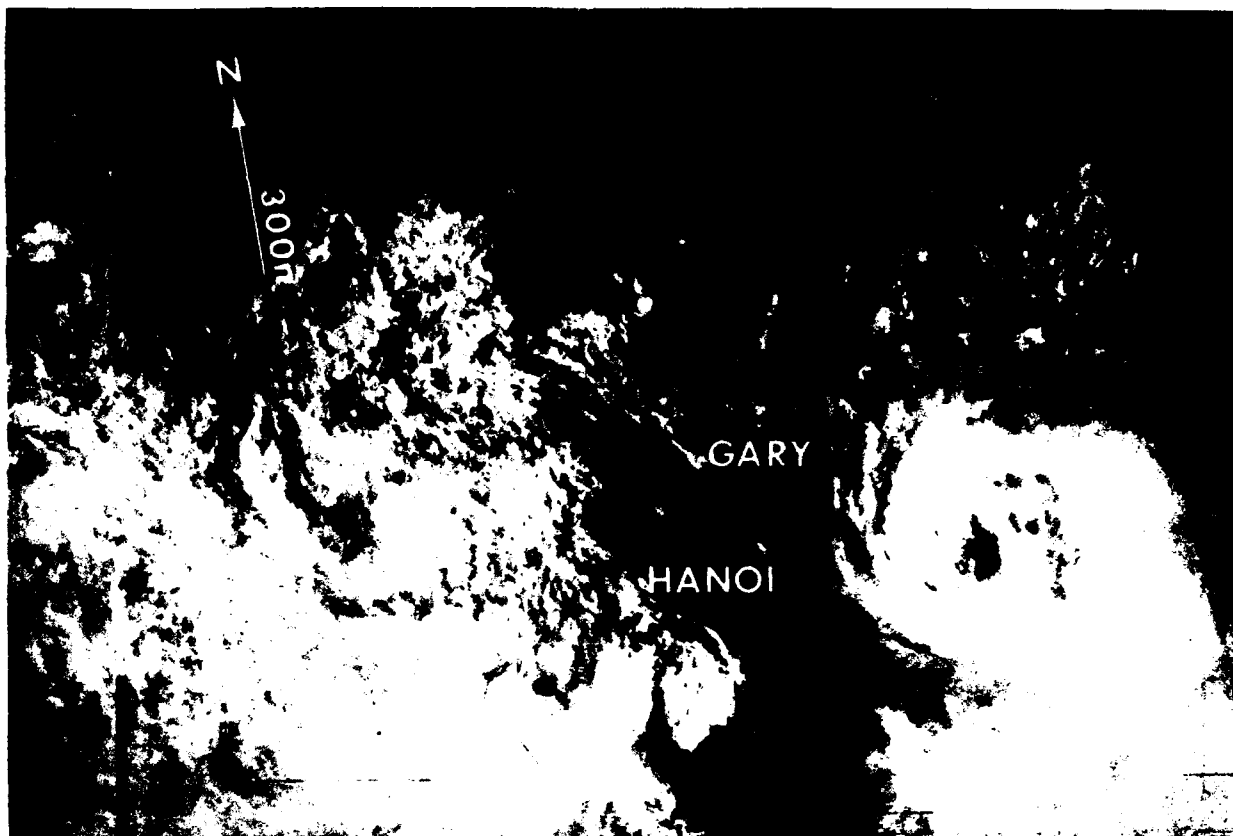


Figure 3-07-1. Gary with a large, ragged eye is intensifying as it approaches the southern coast of China (220200Z July DMSP visual imagery).

E 145

N 45

175 E

170

165

160

155

150

145

140

135

130

125

TROPICAL STORM HELEN

BEST TRACK TC-08W

24 JUL - 30 JUL 92

MAX SFC WIND 45KT

MINIMUM SLP 991MB

40

35

30

25

N 20

L-28/00Z

30

30

35

40

40

40

45

45

45

35b

13

17

19

19

15

8

7

7a

25

30

28

27

26

25

24c

24b

F-26/00Z

TCFA

ABPW

LEGEND

6-HR BEST TRACK POSITION
SPEED OF MOVEMENT (KT)
INTENSITY (KT)
POSITION AT XX/0000Z
TROPICAL DISTURBANCE
TROPICAL DEPRESSION
TROPICAL STORM
TYPHOON
SUPER TYPHOON START
SUPER TYPHOON END
EXTRA TROPICAL
SUBTROPICAL
DISSIPATING STAGE
FIRST WARNING ISSUED
LAST WARNING ISSUED

--- a ---
--- b ---
--- c ---
--- d ---
--- e ---
--- f ---
--- g ---
--- h ---
--- i ---
--- j ---
--- k ---
--- l ---
--- m ---
--- n ---
--- o ---
--- p ---
--- q ---
--- r ---
--- s ---
--- t ---
--- u ---
--- v ---
--- w ---
--- x ---
--- y ---
--- z ---

TROPICAL STORM HELEN (08W)

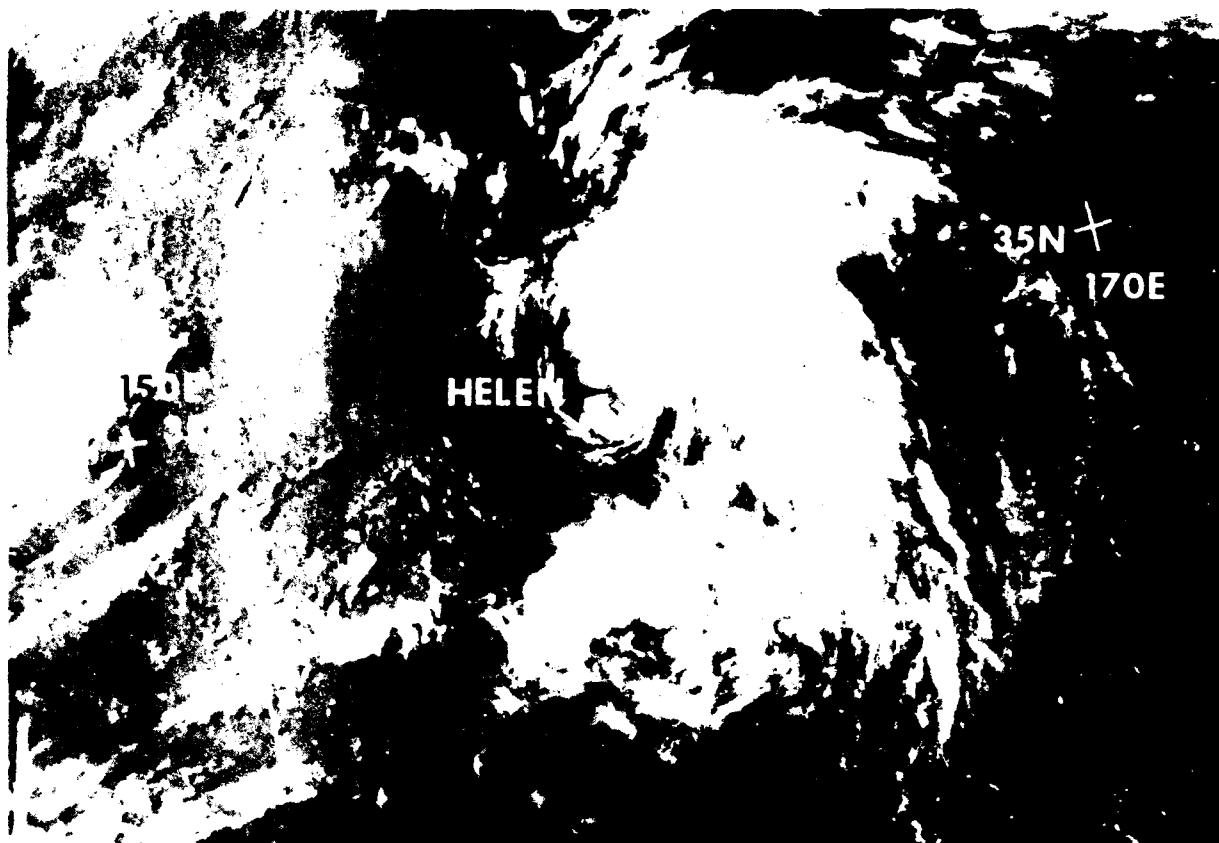
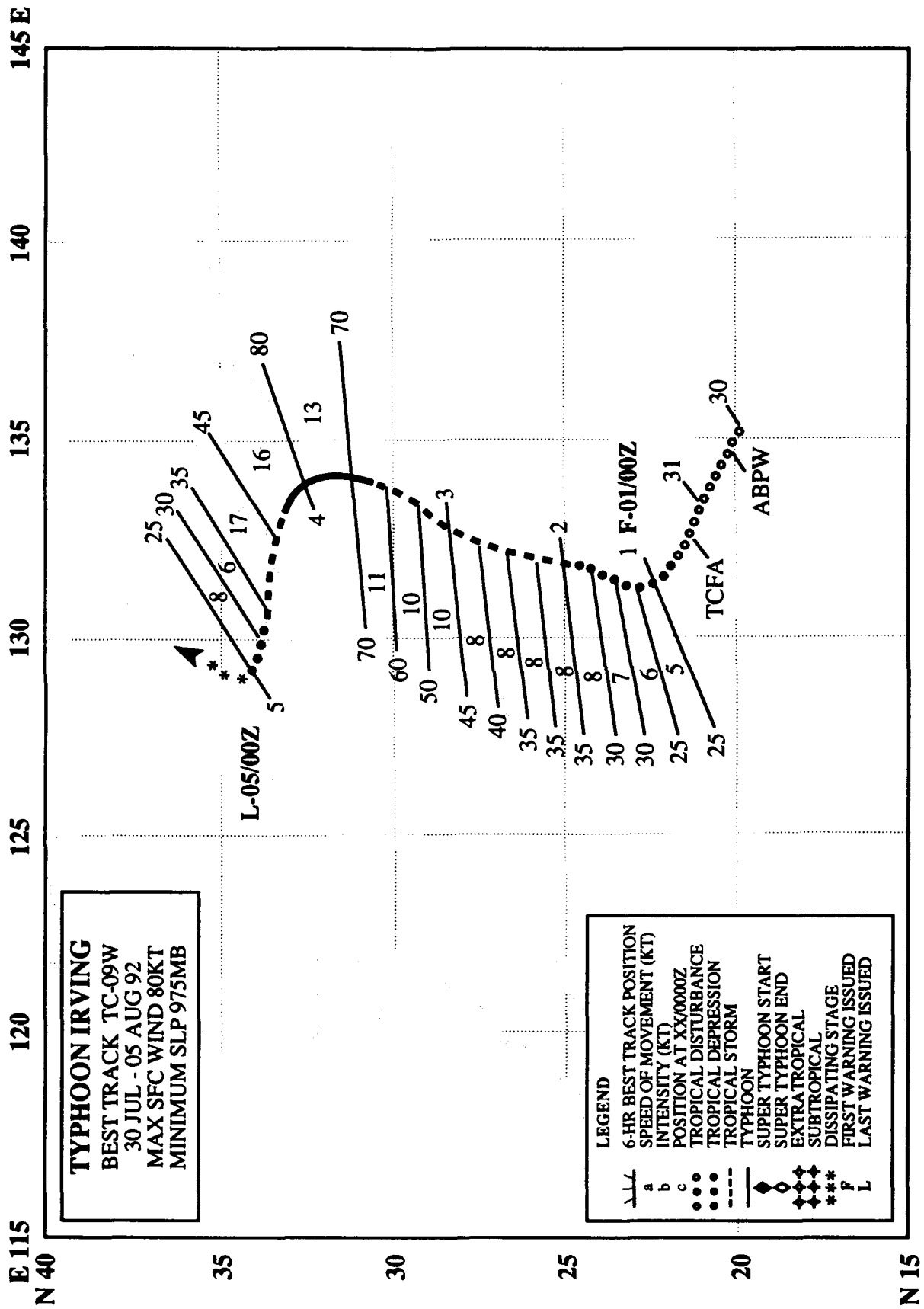


Figure 3-08-1. As Helen weakens, the low-level cloudiness defining its circulation center appears to the south-southwest of the central cloud mass (271401Z July NOAA visual imagery).

The fourth of five significant tropical cyclones to develop in July, Helen intensified from a Tropical Upper Tropospheric Trough (TUTT)-induced low-level circulation. The initial Significant Tropical Weather Advisory issued at 250600Z was reissued at 251900Z to include mention of a persistent area of deep convection. At 252300Z, JTWC issued a Tropical Cyclone Formation Alert when the system showed a steady increase in low-level cloud organization. The first warning followed quickly at 260000Z, based on visual satellite observations of curved low-level cloud lines associated with this midget tropical cyclone and satellite Dvorak intensity estimates of 25 kt (13 m/sec). Helen continued to intensify as it slowly tracked to the north and reached its peak intensity of 45 kt (23 m/sec) at 260600Z. The tropical storm began to weaken as it gained latitude and moved into a region of cooler sea-surface temperatures. The final warning on this system was issued at 280000Z when satellite imagery indicated that Helen no longer maintained any persistent central convection.



TYPHOON IRVING (09W)

I. HIGHLIGHTS

The last of five significant tropical cyclones to develop in July, Irving was the first of two successive typhoons to affect Southwest Japan. It formed at the eastern end of the monsoon trough where several low-level vorticity centers were embedded in a broad area of poorly organized convection, and slowly intensified. Initially, track forecasts suffered due to a difficulty in distinguishing a clear-cut, low-level circulation center. Once an accurate track history was established and the Joint Typhoon Warning Center committed to a north-oriented track followed by westward motion due to the expected reestablishment of the mid-level subtropical ridge north of Irving, forecast errors were significantly reduced. Intensity estimates based solely on satellite imagery proved to be too low as all forecast agencies peaked Irving as a tropical storm. Post-storm analysis has revealed enough synoptic data to justify upgrading Irving to a typhoon.

II. TRACK AND INTENSITY

Initially, synoptic and satellite data indicating a definite, albeit weak, low-level cyclonic circulation within the monsoon trough that extended from the South China Sea to the central Philippine Sea. This circulation was mentioned on the 300600Z July Significant Tropical Weather Advisory. While multiple low-level vorticity centers were present at this early stage of development, JTWC focused on the circulation near a major flare-up of convection occurring in the southwestern portion of the tropical disturbance. The detection of curved low-level cloud lines on the visual satellite imagery resulted in JTWC issuing a Tropical Cyclone Formation Alert at 310800Z. By 01 August at 0000Z, the cloud organization had improved sufficiently to classify this system as a tropical depression, and the first warning was issued. A short time after this warning, a weather reconnaissance aircraft from the Tropical Motion Cyclone Experiment (TCM-92) explored the structure of the tropical depression, and determined that the primary low-level circulation was most probably situated 120 nm (220 km) further to the north than inferred from the satellite data. The circulation proceeded slowly northward over the next two days and gradually intensified. This slow northward motion was attributed to the tropical cyclone being situated near the western periphery of the subtropical ridge. At 020000Z, the amount of centralized deep convection had increased, prompting forecasters to upgrade the tropical depression to a tropical storm.

From the standpoint of satellite intensity estimates, Irving appeared to reach its peak intensity of 55 kt (28 m/sec) at 031200Z based on the curvature of the convection. However, synoptic data indicated that Irving continued to intensify, and attained a peak intensity of 80 kt (41 m/sec) at 040000Z. The surface pressure pattern and key wind reports are depicted in Figure 3-09-1. The figure shows the tight pressure gradient that existed to the north of the typhoon. The visual imagery (Figure 3-09-2) nearest the time of the synoptic data shows Irving with an elliptic eye that was approximately 100 nm (185 km) in diameter. With the ridge established to the north, the tropical cyclone began to track west-northwestward. Upon landfall over southwestern Shikoku, Irving turned sharply to the west, rapidly weakened, and later, dissipated over the Korea Strait near Pusan, Korea.

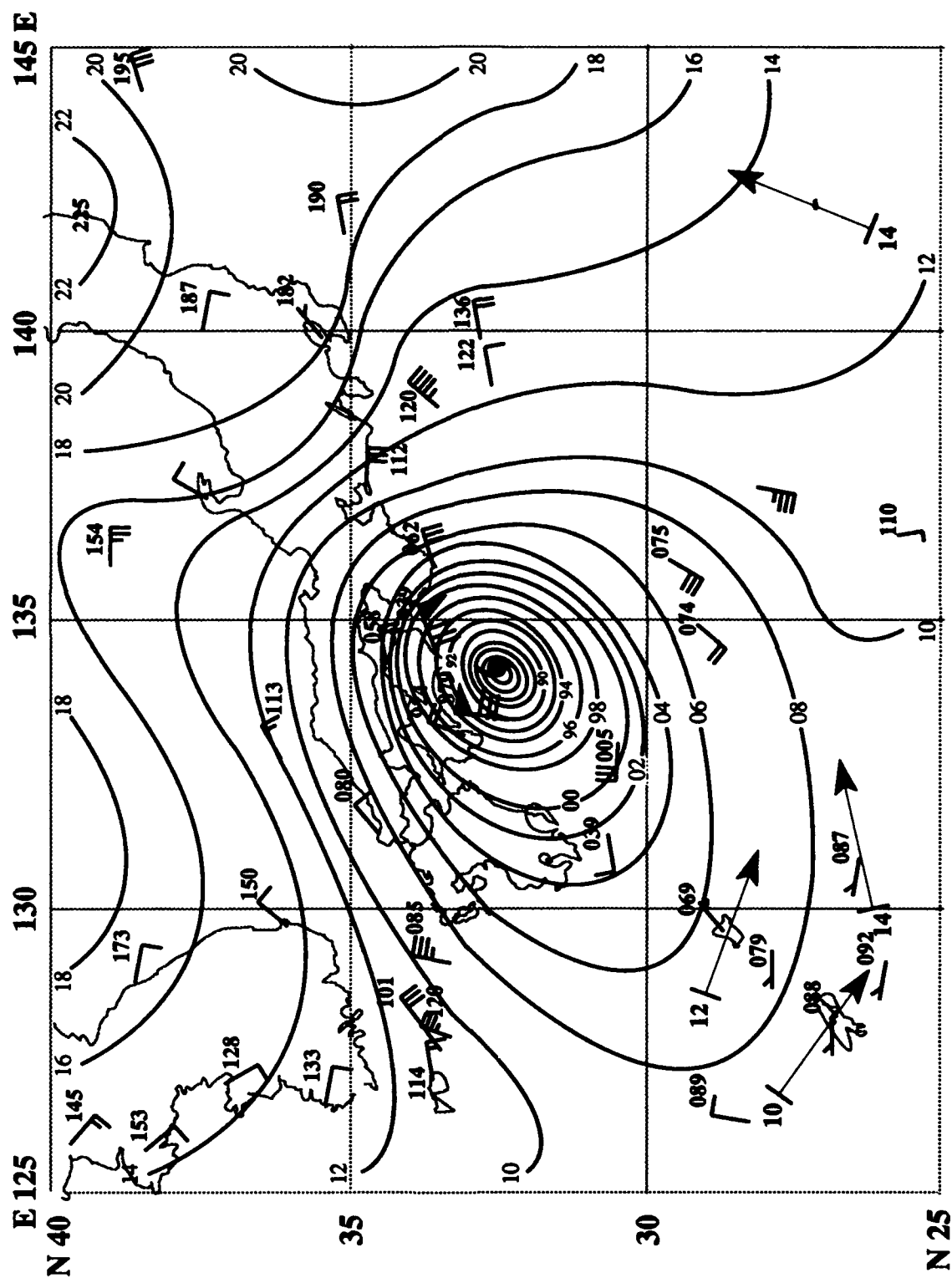


Figure 3-09-1. Synoptic data and analysis for 040000Z August reveals the tight pressure gradient to the north of Irving. The two 80 kt (41 m/sec) reports are located under the wall cloud. (The arrows at the bottom of the analysis indicate gradient-level wind reports.)

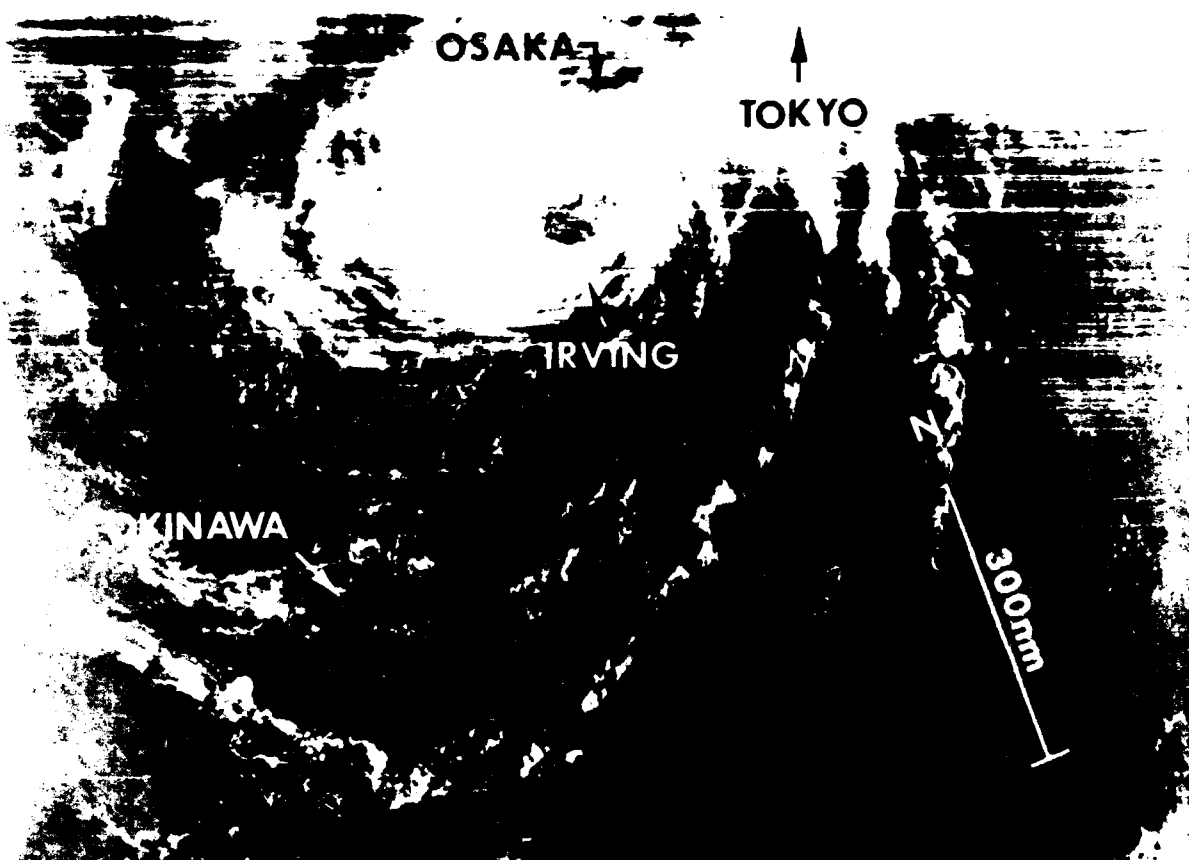


Figure 3-09-2. The satellite data, corresponding to the synoptic analysis in Figure 3-09-1, shows Irving with a large eye just before making landfall on Shikoku (040015Z August DMSP visual imagery).

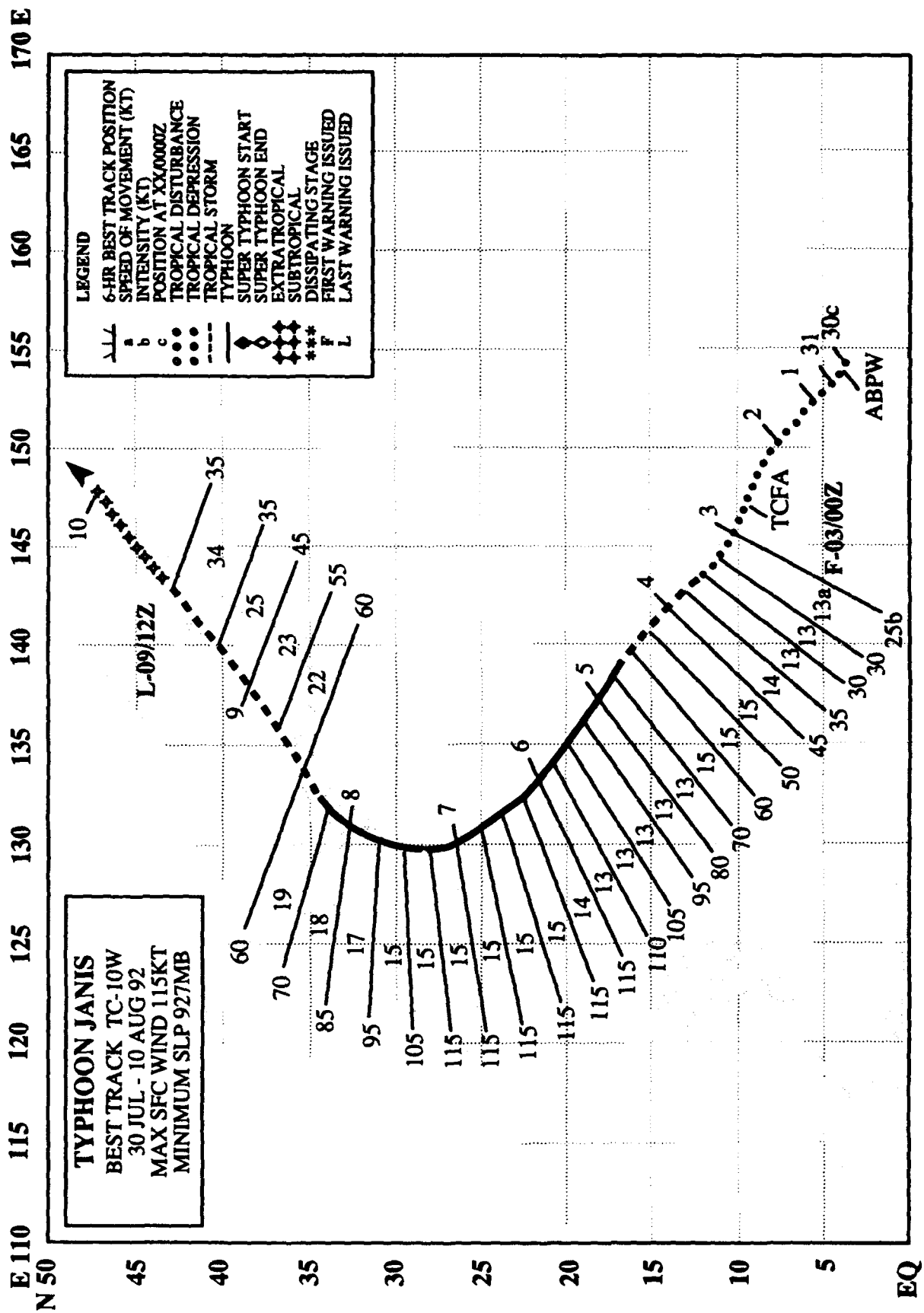
III. FORECAST PERFORMANCE

Forecasting for Irving proved to be quite challenging as climatological and numerical model guidance were in almost total disagreement. To complicate the forecast difficulties, problems with locating the low-level center during the first five warnings led to four relocated warnings. Once the persistent northward motion was established, JTWC placed a heavier reliance on climatological and statistical based models. Then, when Irving was approaching Japan, predictions based on the NOGAPS model provided correct guidance. In retrospect, the Japanese Typhoon Model (JTYM), although biased right-of-track, provided accurate guidance for timing and direction of major track directional changes.

With regard to intensity forecasts, JTWC did not anticipate the further drop in central pressure of the tropical cyclone and building of the pressure gradient to the north as Irving approached Japan, which resulted in underforecasting the winds.

IV. IMPACT

Although some observations from Japan were in excess of 60 kt (31 m/sec) and orographically induced rainfall was heavy, there were no reports of significant damage received.



TYPHOON JANIS (10W)

I. HIGHLIGHTS

Four days after Irving (09W) hammered Shukoku, Janis slammed into Kyushu. Janis began near Pohnpei in the Caroline Islands, took a northwestward track threatening Okinawa, then recurved, passed over Kyushu, and skirted the western coast of Honshu before transitioning to an extratropical low over Hokkaido.

II. TRACK AND INTENSITY

The tropical disturbance, that matured into Janis, formed near Pohnpei in the eastern Caroline Islands, and was first mentioned in the 300600Z July Significant Tropical Weather Advisory. Increased convective development led to the issuance of a Tropical Cyclone Formation Alert at 022130Z August. Intensification continued through the early morning hours, and at 030000Z, JTWC issued the first warning on Tropical Depression 10W. As the depression moved past Guam, it brought winds gusting to 30 kt (15 m/sec) and 2.5 inches (64 mm) of rain in 24 hours to the island, but caused no major damage.

Later that day, at 031439Z, aircraft reconnaissance assigned to the TCM-92 experiment explored the tropical depression and provided a center fix with a minimum 700 mb pressure height of 3081 m, which supported 30 kt (15 m/sec) at the surface. Moving into the Philippine Sea, the depression organized further and was upgraded to a tropical storm at 031800Z and to a typhoon 24 hours later. Janis reached a peak intensity of 115 kt (59 m/sec) at 060000Z, where it posed a major threat to Okinawa (Figure 3-10-1). Fortunately, the typhoon did not directly hit the island, but passed 90 nm (165 km) to the east. On Okinawa, Kadena AB (WMO 47931) reported maximum winds of 30 gusting to 50 kt (15 G 26 m/sec), the Marine Corps Air Station (WMO 47933) at Futenma observed peak winds of 36 gusting to 53 kt (19 G 27 m/sec), and the peak at Naha (WMO 47936) was 34 gusting to 55 kt (18 G 28 m/sec).

Passing near the airport on Amami-O-Shima (WMO 47872) which reported maximum winds of 69 gusting to 94 kt (36 G 48 m/sec), the typhoon began to weaken, recurved, and accelerated toward Kyushu. Over Kyushu, land interaction further weakened Janis to tropical storm intensity at 081500Z. As Janis passed 60 nm (110 km) east-southeast of Sasebo with an estimated intensity of 85 kt (44 m/sec), the base observed maximum winds of 28 gusting to 50 kt (14 G 26 m/sec). The tropical storm moved to the northeast, paralleling the western coast of Honshu. At 091200Z, Janis transitioned into an extratropical low over Hokkaido.

III. FORECAST PERFORMANCE

JTWC correctly forecast the recurvature path of Typhoon Janis. Overall, mean track forecast errors were 92, 182, and 336 nm (170, 337 and 620 km) for 24, 48, and 72 hours, respectively. The largest 72-hour mean position forecast errors occurred after recurvature and were primarily due to the rapid acceleration of Janis to speeds over 30 kt (55 km/hr).

JTWC forecast the intensity trend and period of rapid intensification well. However, with regard to the peak intensity, a procedural difference concerning the application of the Dvorak enhanced infrared technique eye adjustment factor to digital high resolution TIROS-N polar orbiting satellite data led to an overestimation of the raw intensity input to the warning. The analysis procedure was reviewed and adjusted to use the average of the warmest pixels within the eye, instead of the single warmest individual pixel, before determining the eye adjustment factor. This change more closely paralleled the val-

ues derived from the geostationary data , and resulted in the peak intensity being reduced from 125 to 115 kt (64 to 59 m/sec). The largest 72-hour mean intensity forecast errors occurred after recurvature when the system weakened more rapidly than anticipated.

IV. IMPACT

As Janis passed to the east of Taiwan, one fisherman was killed when 26 foot (8 m) waves sank five fishing boats. Only minor damage was reported when the typhoon passed just to the east of Okinawa. The passage of Janis over Kyushu resulted in the death of one person and injuries to at least 25 others. High winds and torrential rains caused the temporary loss of electricity to over 250,000 homes, and disrupted road, rail and air travel in Southwestern Japan.

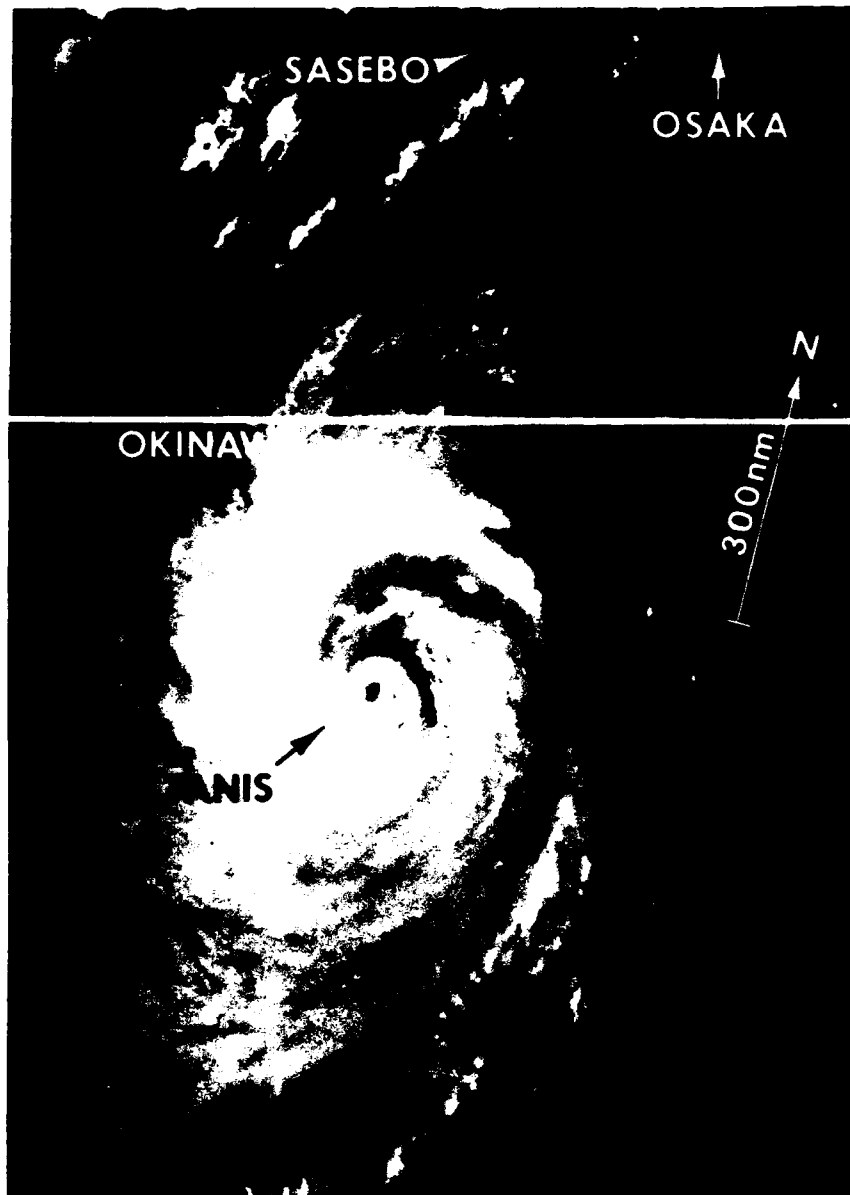
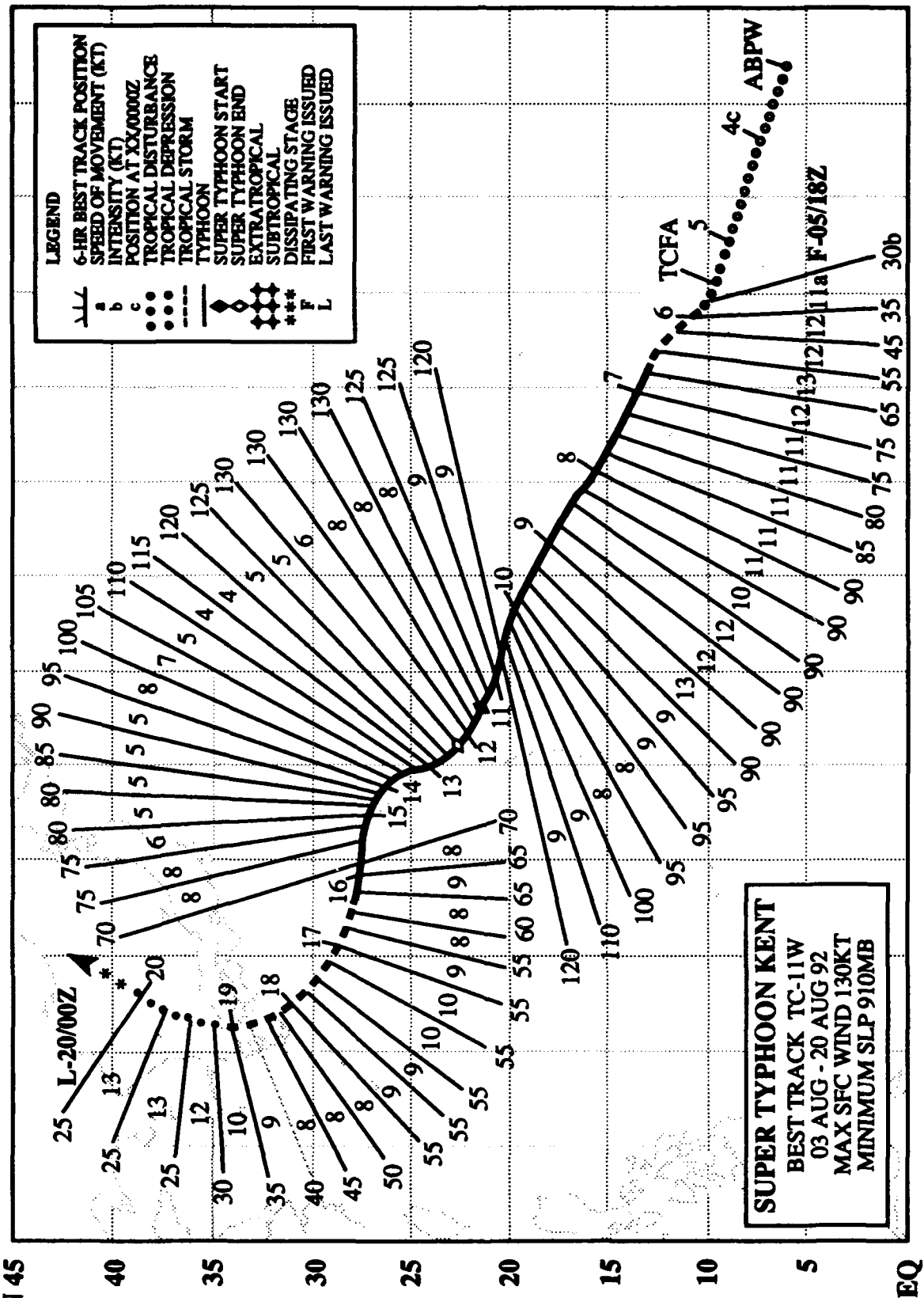


Figure 3-10-1. Typhoon Janis at peak intensity bears down on Okinawa (060533Z August NOAA visual imagery).

E 120 125 130 135 140 145 150 155 160 165 170 175 180 175 W



SUPER TYPHOON KENT (11W)

I. HIGHLIGHTS

The second of eight tropical cyclones to develop in August, Kent became the first super typhoon of 1992. During the trek toward Japan, it underwent binary interaction with Tropical Storm Lois (12W). Requiring a total of 58 warnings, Kent was second only to Super Typhoon Gay (31W) for the total number of warnings and longevity for the western North Pacific in 1992.

II. TRACK AND INTENSITY

As Janis (10W) intensified south of Guam, the tropical disturbance that later became Kent developed east of the international date line. Its persistent convection was first mentioned on the 030600Z August Significant Tropical Weather Advisory. An increase in the amount and organization of the disturbance's deep convection prompted JTWC to issue a Tropical Cyclone Formation Alert at 051500Z. Early intensification was rather rapid. The first warning was issued at 051800Z with an upgrade to tropical storm intensity at 060000Z, and to typhoon intensity at 070000Z. Then the rate of intensification slowed. On 8 August, increased vertical wind shear associated with the passage of a mid-level trough to the north resulted in a reduction in size of Kent's central dense overcast (CDO). Although intensification was arrested, a small core of persistent central convection remained. As the trough passed by, the reappearance of an eye confirmed that intensification was once again underway. At 111200Z, Kent reached super typhoon intensity (Figure 3-11-1).

Under the influence of a subtropical ridge located to the north, the super typhoon continued to move west-northwestward until a short wave trough moved across Honshu on 13 August. Kent, weakened, slowed and its track became more northerly in response to the weakness in the subtropical ridge. Then, the trough passed by and the typhoon, which was weakening due to increasing upper-level winds, headed for Honshu. On 16 August, Kent became involved in a binary interaction with Tropical Storm Lois (12W), which had formed two days earlier. As a consequence, Kent changed its course for Kyushu. By 18 August, the binary interaction between the tropical cyclones had ceased, and Kent was approaching recurvature. After landfall, interaction with the mountainous terrain of Kyushu, along with increased upper-level wind shear, quickly weakened Kent. At 191200Z, the tropical cyclone was downgraded to a tropical depression when it became evident that all deep convection had been completely sheared by upper-level flow. The final warning on Kent was issued on 200000Z.

III. FORECAST PERFORMANCE

Overall JTWC track forecasting was better than average with mean errors of 70, 140, and 235 nm (130, 265, and 435 km) for 24, 48 and 72 hours, respectively, and consistently better than CLIPER's guidance. General guidance provided by the forecast aids for Kent was excellent until the binary interaction with Tropical Storm Lois (12W) commenced and premature recurvature was suggested. Once the binary interaction between both storms ended, however, all forecast aids correctly predicted Kent's track across Kyushu and into the Sea of Japan. Overall JTWC intensity forecasts were handled well with the exception of a number of 72-hours forecasts, which remained 20 to 40 kt (37 to 74 m/sec) too high for three days after Kent's winds reached their maximum.

IV. IMPACT

On 18 August, Kent's high winds and torrential rains struck Kyushu resulting in at least four deaths, disruption of air and ground transportation, and numerous localized power outages.

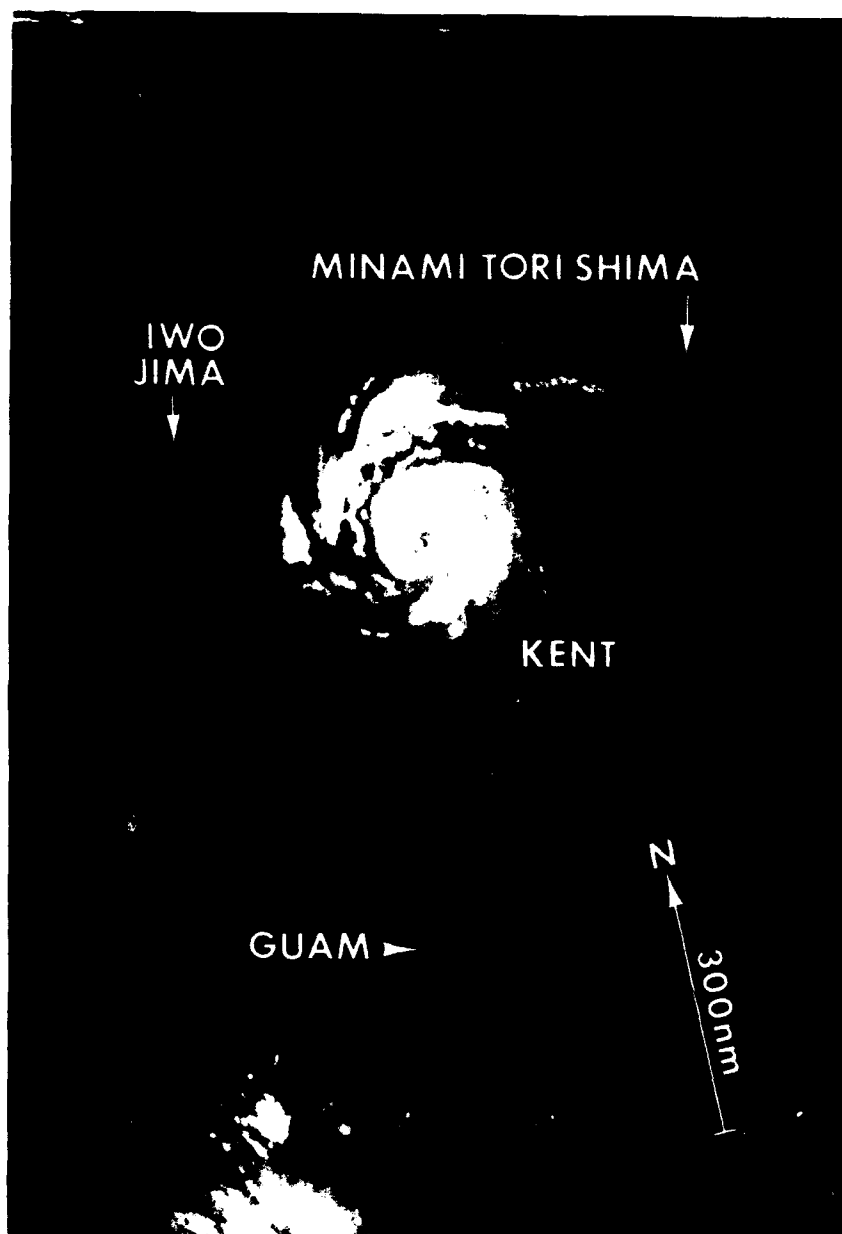
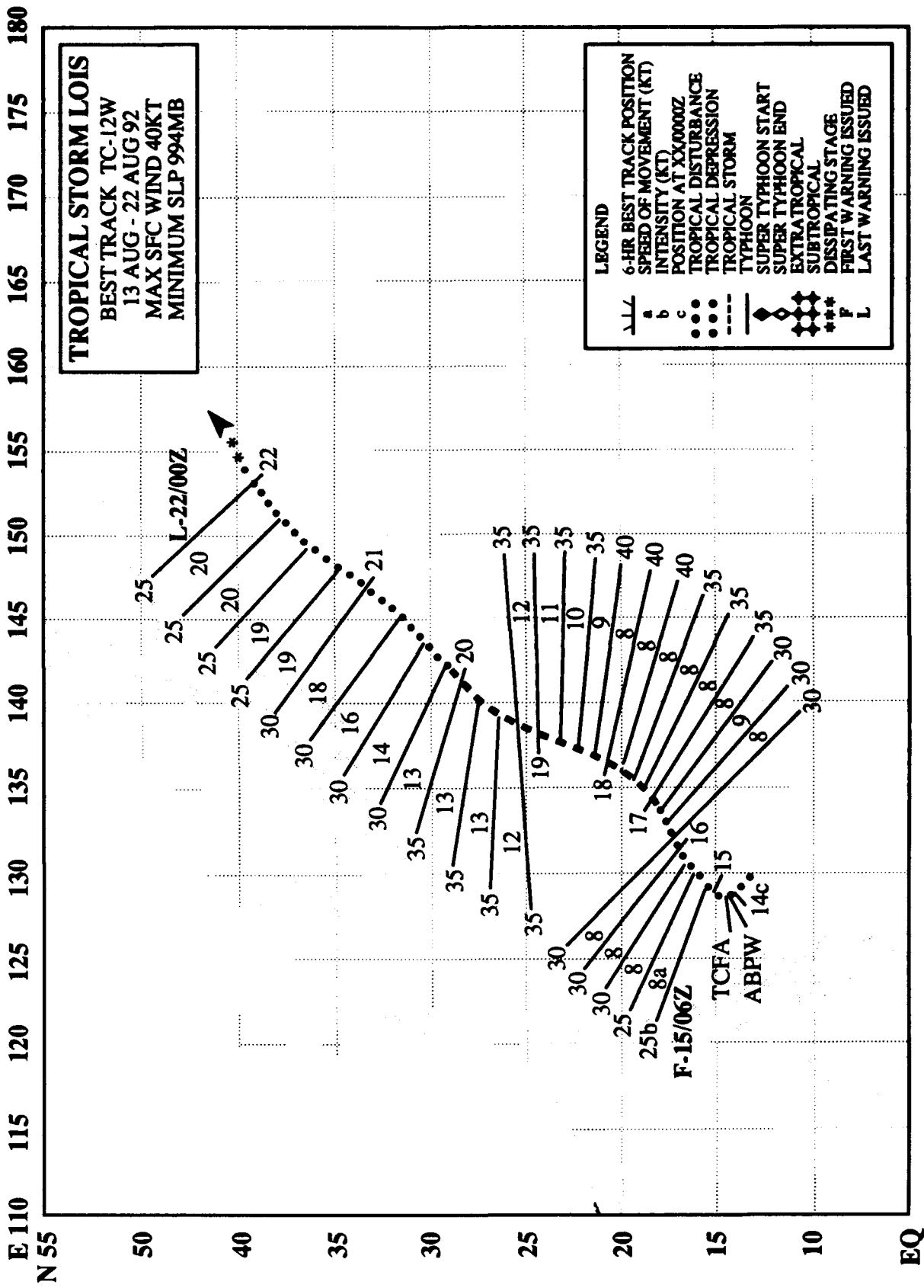


Figure 3-11-1. Kent at super typhoon intensity passes just to the north of the Mariana Islands (112325Z August DMSP visual imagery).



TROPICAL STORM LOIS (12W)

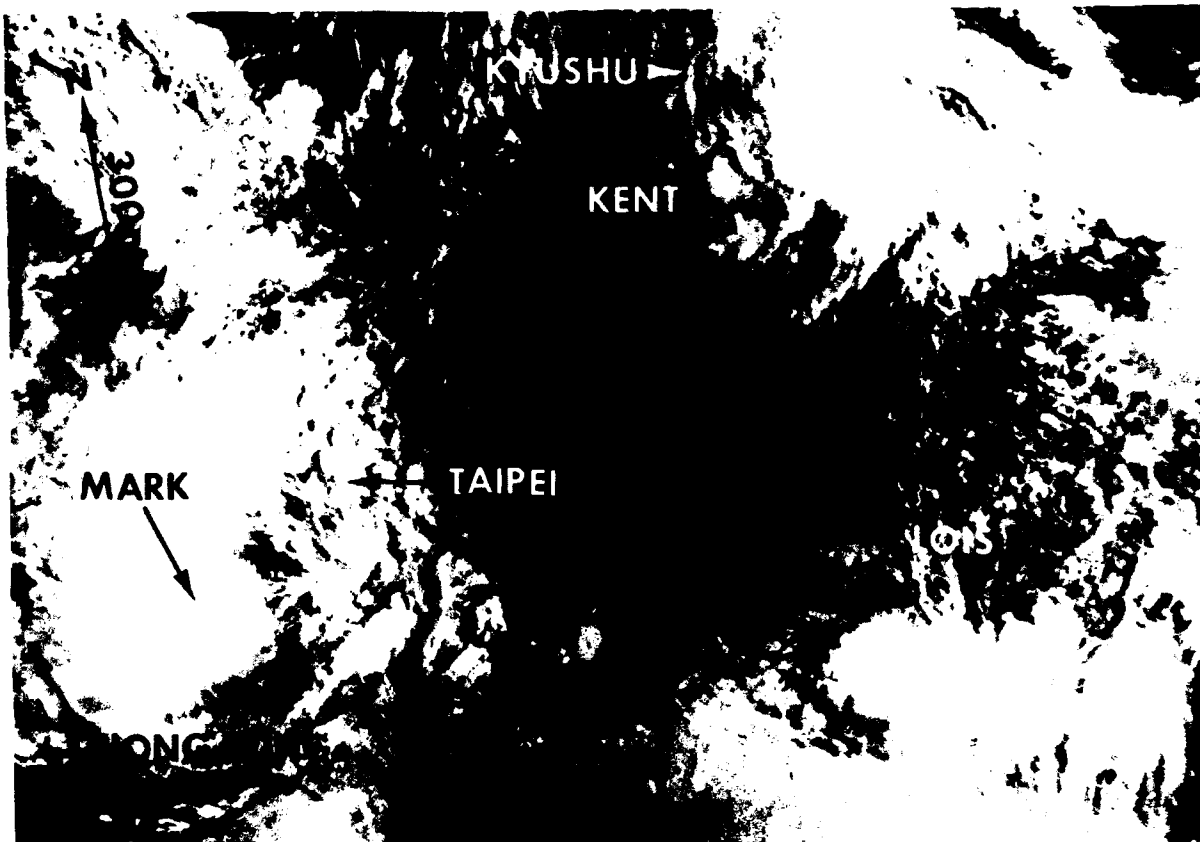
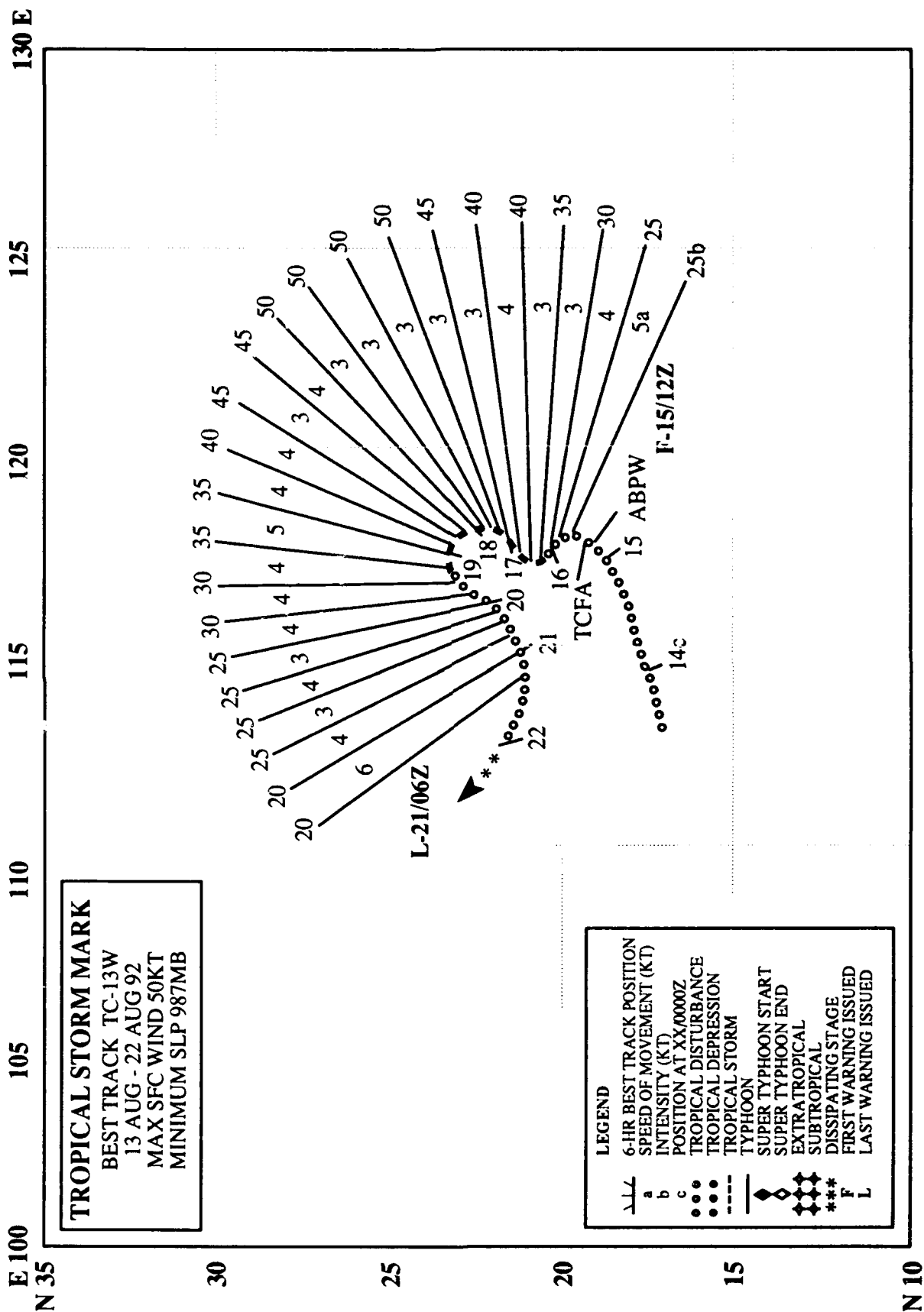


Figure 3-12-1. The partially exposed low-level circulation of Lois is visible to the south of Kent (11W) which is heading for Kyushu. To the west, Mark (13W) is churning up the South China Sea (172325Z August NOAA visual imagery).

Lois, one of only two tropical cyclones in 1992 which had a persistent eastward component of motion during its period of warning, bedeviled JTWC forecasters by consistently moving opposite of the climatologically expected track. During its lifetime, the low-level center of Tropical Storm Lois remained partially exposed, and the system failed to intensify beyond 40 kt (21 m/sec). The apparent binary interaction from 16 to 18 August with Kent (11W) altered Lois' motion and further contributed track forecasting problems. During this period of interaction, the tendency for the NOGAPS to merge nearby tropical cyclones into a single large vortex effectively rendered the model's guidance useless. After escaping the binary interaction, Lois accelerated northeastward and dissipated over colder water. The final warning was issued at 220000Z.



TROPICAL STORM MARK (13W)

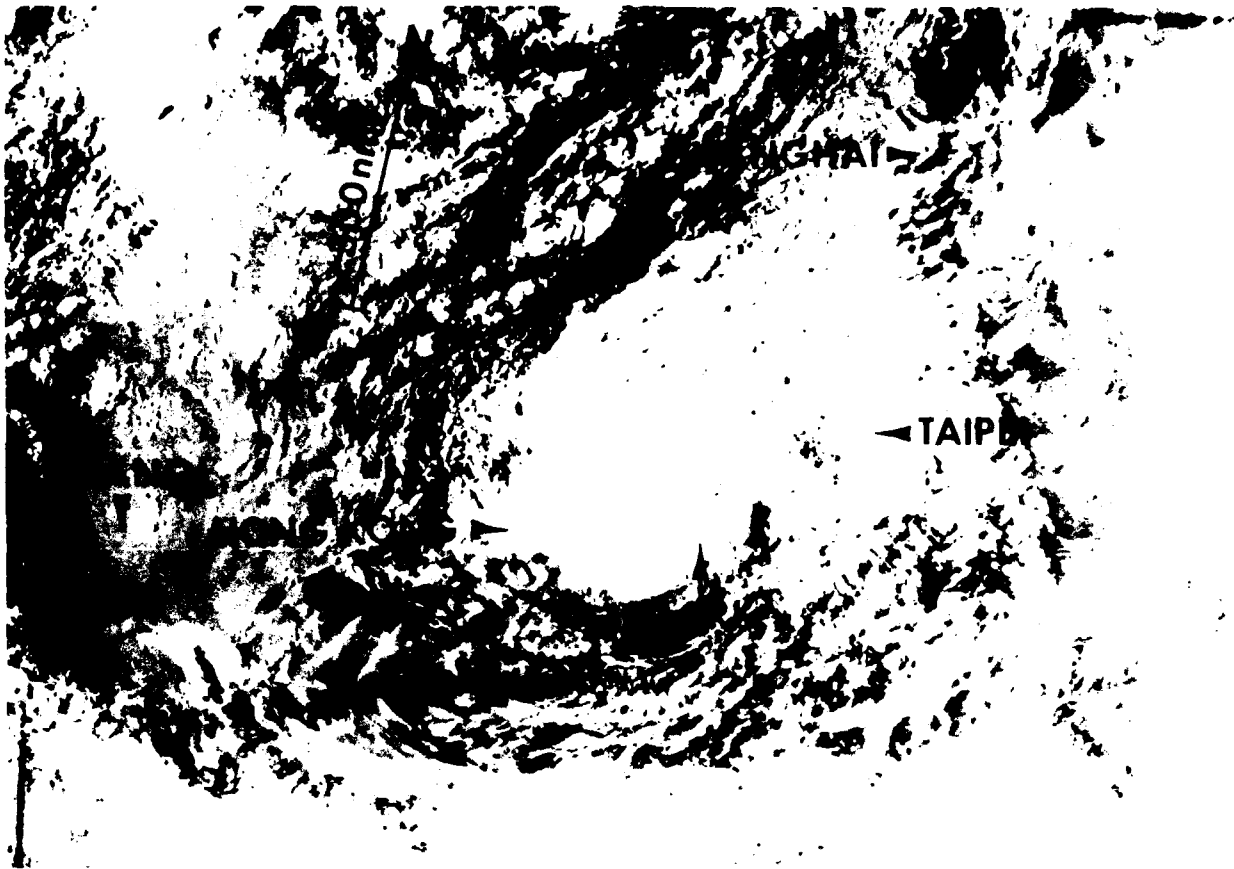
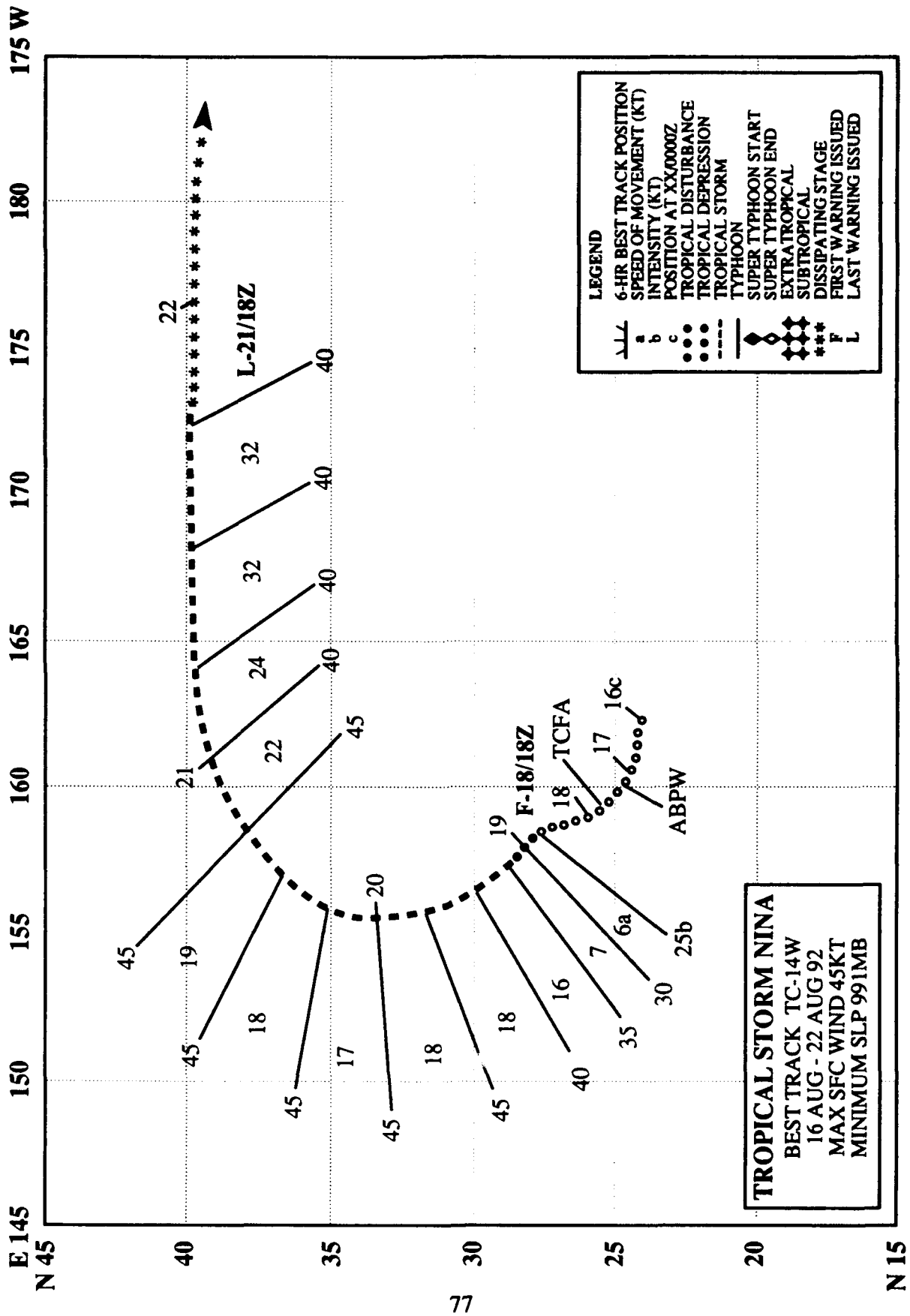


Figure 3-13-1. Mark moves along the southern coast of China (180906Z August DMSP visual imagery).

Mark was part of the three storm outbreak with Kent (11W), Lois (12W), and later, a four storm outbreak when Nina (14W) formed. On 15 August, Mark's genesis in the South China Sea in the monsoon trough coincided with Lois' in the Philippine Sea, as deep low-level southwesterly flow surged eastward across the Philippine Islands. Due to strong vertical shear aloft, the tropical cyclone was slow to intensify, and finally reached a peak intensity of 50 kt (26 m/sec) on 17 August. Mark spent its short lifetime embedded in the monsoon trough and then dissipated over land. The tropical cyclone's passage along the South China coast resulted in at least one death, localized flooding and disruption of transportation.



TROPICAL STORM NINA (14W)

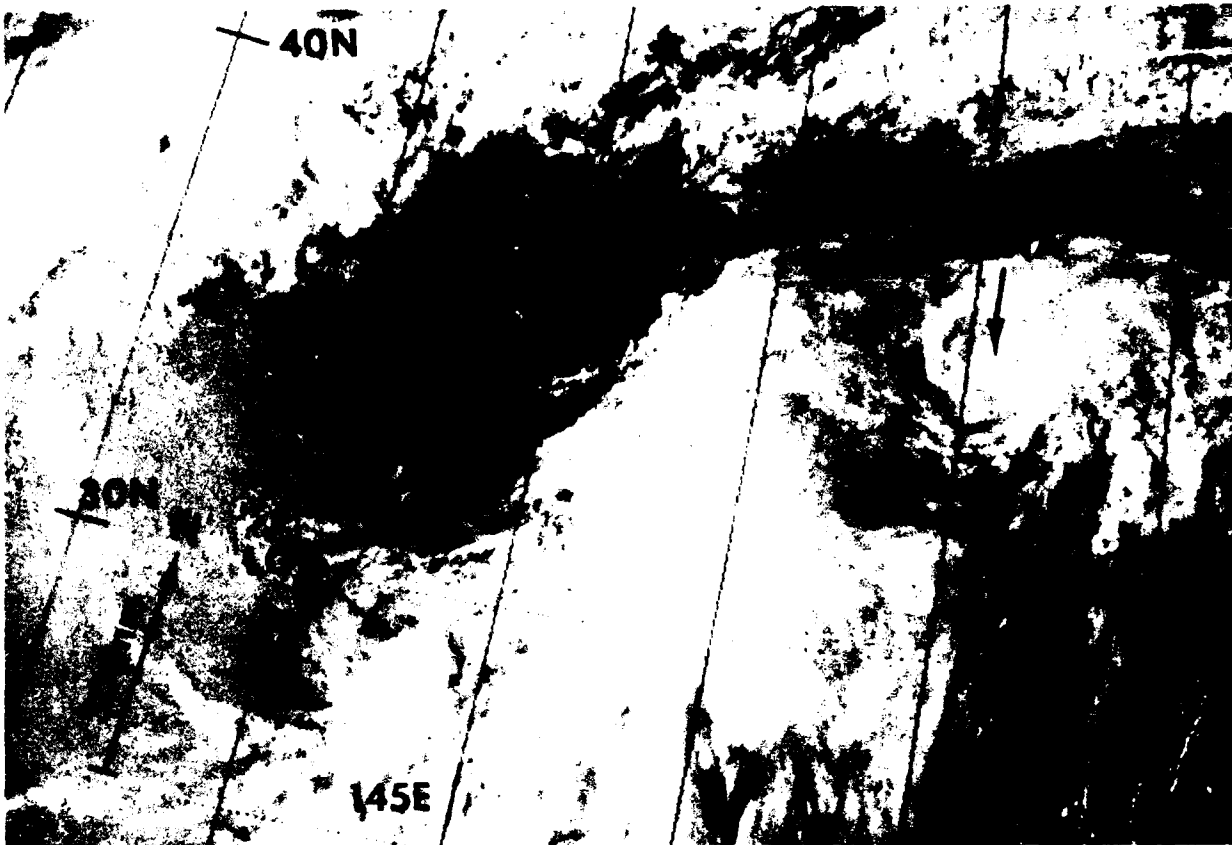
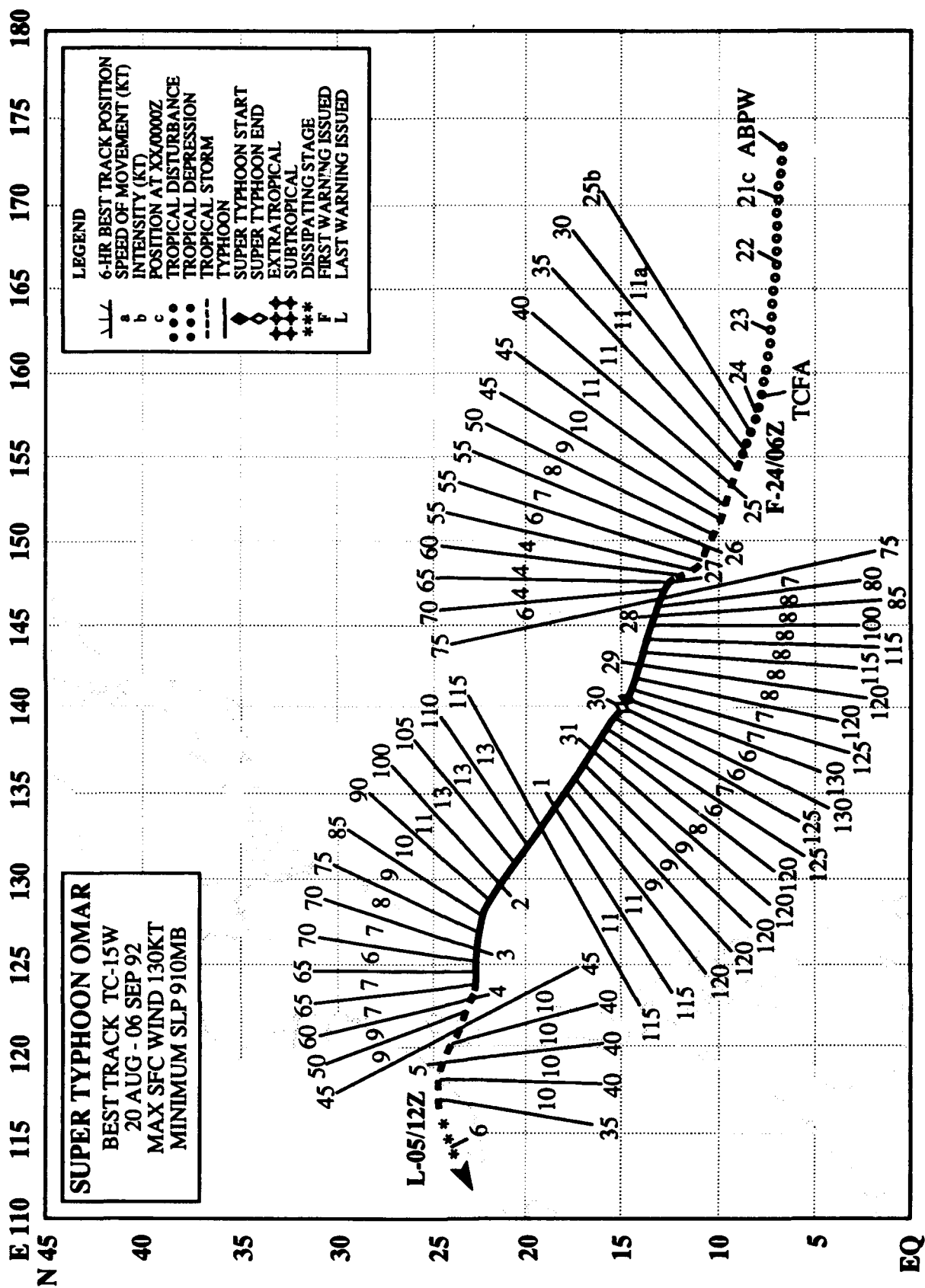


Figure 3-14-1. Tropical Storm Nina at peak intensity is separated from Lois (12W) by a broad band of monsoon cloudiness (200658Z August DMSP visual imagery).

Nina was part of a four storm outbreak in August with Kent (11W), Lois (12W) and Mark (13W). Forming as a TUTT-induced tropical cyclone under the divergent outflow from Kent (11W), Nina intensified to a peak intensity of 45 kt (23 m/sec) despite the strong vertical wind-sheared environment. Later, and most probably due to the persistence of relatively low pressure near its center, Nina became the extreme eastern end of the monsoon trough that extended east-northeastward from the South China Sea. Due to this tropical cyclone's sharp recurvature and unseasonably rapid acceleration, track errors for the three 72-hour forecasts were quite high, ranging from 450 to 880 nm (835 to 1630 km). Lois remained over open ocean for its entire life, threatening only mariners.



SUPER TYPHOON OMAR (15W)

I. HIGHLIGHTS

The second super typhoon of 1992, Omar became the seventh of the eight tropical cyclones to develop in August. The tropical disturbance that became Omar was first noted over the southern Marshall Islands, at a time when Mark (13W) was weakening along the south coast of China, Kent (11W) had dissipated in the Sea of Japan, and Lois (12W) and Nina (14W) were east of Japan. Later, after moving steadily west-northwestward and intensifying, Omar wreaked havoc on Guam as it rapidly intensified immediately prior to passing directly over the island with 105 kt (54 m/sec) sustained winds. After traversing Guam, Omar continued onward into the Philippine Sea where it briefly attained super typhoon intensity. Omar then steadily weakened, passing over Taiwan as a tropical storm, and dissipated over southeastern China.

II. TRACK AND INTENSITY

Based on persistent convection, the tropical disturbance that was to become Omar was first mentioned in the 200600Z August Significant Tropical Weather Advisory. During the next three days, which included the dissipation of Kent (11W) and Mark (13W), and the approaching of the extratropical transitions of Lois (12W) and Nina (14W), the monsoon trough began to reestablish itself in a more normal location, extending across the northern Philippine Islands, east-southeastward into the Caroline Islands. While this major synoptic pattern readjustment was taking place, the tropical disturbance had developed sufficiently to warrant the issuing of a Tropical Cyclone Formation Alert at 232100Z. Intensification continued, and JTWC issued the first warning at 240600Z. Coincident with Omar becoming a tropical depression 750 nm (1390 km) east-southeast of Guam and the southwesterly low-level flow deepening across the western Caroline Islands, Polly (16W) began to develop 200 nm (370 km) to the west of Guam. After Omar was upgraded to a tropical storm on the warning at 250000Z, the rate of intensification decreased due to upper tropospheric wind shear from the extensive outflow of Polly (16W), which was also intensifying. At about the same time, Omar (Figure 3-15-1) began to slow in forward speed. This slowing of development and forward motion continued until early on 27 August when Tropical Storm Omar stalled.

If the strong vertical wind shear created by Polly's proximity continued, or increased, there was a possibility that Omar's upper and lower circulation centers could decouple and further weaken the tropical cyclone. However, the circulation held together, drifted northwestward, and began to intensify. Omar (Figure 3-15-2) was upgraded to typhoon intensity at 270600Z, and 12 hours later at about 271800Z began a period of rapid intensification which lasted for the next 12 to 18 hours. By the evening of 27 August, Omar began to accelerate towards Guam. Gale force sustained winds, began to buffet Guam at 272300Z about the time that a visible eye appeared on satellite imagery. This was followed by the onset of destructive winds, in excess of 50 kt (26 m/sec), which commenced at 280300Z and lasted for 16 hours. These sustained winds rose steadily until they peaked at 105 kt (54 m/sec) with gusts to 130 kt (67 m/sec) in the western half of the eye wall (Figure 3-15-3). As the eye passed across the island, the eastern half of the eye wall followed, battering Guam with torrential rain again and strong winds from the opposite direction (Figure 3-15-4). While Omar's eye passage coincided with one of the highest astronomical tides of August (Figure 3-15-5), the storm surge was not as high as expected. Apparently the rapidly changing wind direction that occurred with eye passage limited the fetch and kept the inundation to a lower level than anticipated. Some low-lying areas on Guam suffered total

wave runup as high as 10 feet on the north shore (Figure 3-15-6). In addition, the typhoon dropped over a foot of rain on the northern half of the island with a maximum of 18 inches (460 mm) measured at the National Weather Service Observatory at Taguac (WMO 91217).

After mauling Guam, Omar continued to intensify as it moved across the Philippine Sea, and, at 291800Z, briefly attained super typhoon intensity (Figure 3-15-7). Then a gradual weakening trend set in. On 4 September, Omar passed across Taiwan as a tropical storm and, on 5 September, it moved into southeastern China and dissipated.

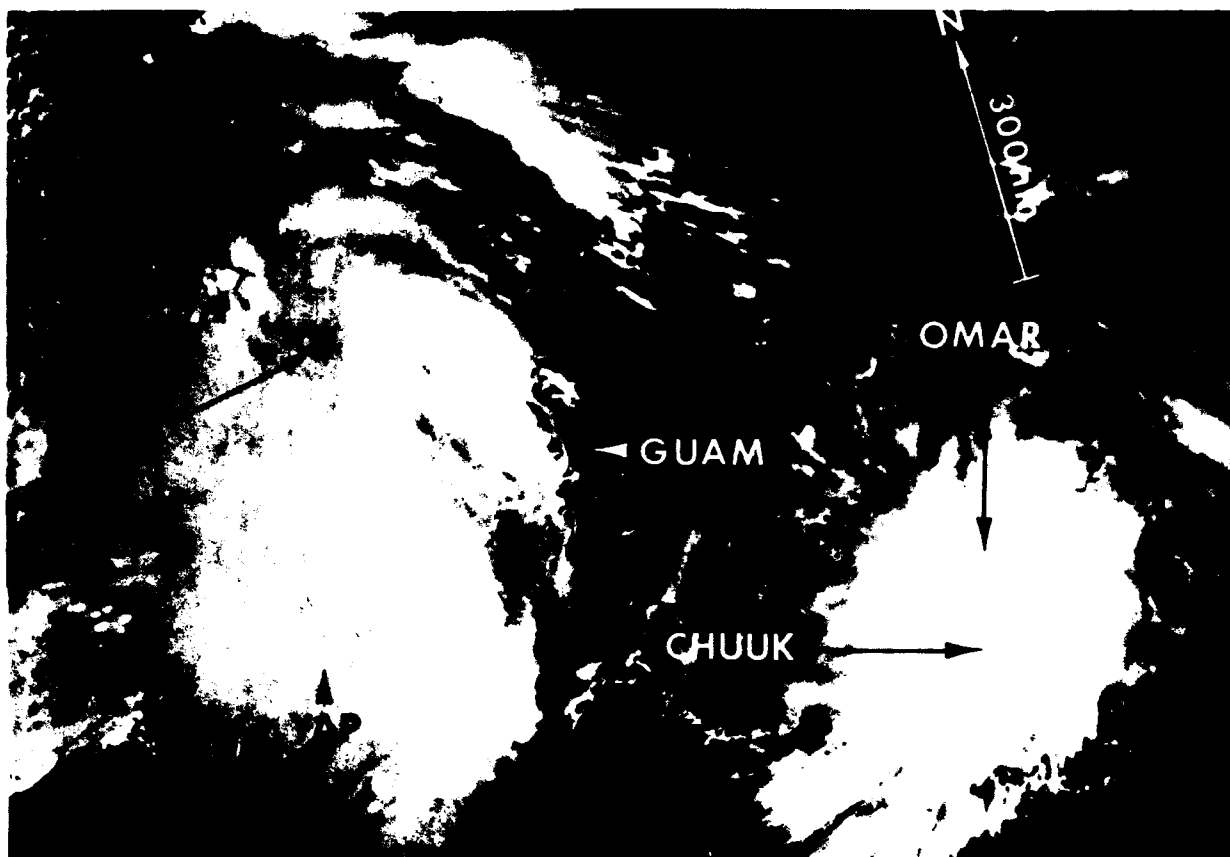


Figure 3-15-1. Omar Passes north of Chuuk as Polly (14W) consolidates to the west of Guam (242320Z August DMSP visual imagery).

III. FORECAST PERFORMANCE

Overall mean errors for the JTWC track forecasts were 75, 160, and 270 nm (135, 300, and 500 km) for 24, 48 and 72 hours, respectively. This was 20% better than the climatology-persistence (CLIPER) baseline for skill at all forecast time intervals. With regard to intensity, the JTWC 24-hour forecasts were representative of events, except for a brief period when they were consistently 20 to 40 kt (37 to 74 m/sec) low for a day and a half before Omar struck Guam.

IV. IMPACT

Typhoon Omar was the most damaging typhoon to strike Guam since Typhoon Pamela in 1976. On Guam, Omar caused an estimated \$457 million of damage, destroyed or severely damaged over 2158 homes leaving nearly 3000 people homeless in temporary shelters until a 200-tent "city" could be erected. Omar almost completely disabled the island-wide power distribution system which in turn caused the water pumping system to fail. Long term mitigation measures such as the erection of concrete power poles limited their damage. Over 400 wooden poles and 20 to 30 concrete poles were destroyed and the damage was limited to approximately \$16 million. Because they could not sortie, two of the Navy's fast supply ships, USS Niagara Falls and USS White Plains, went aground in Apra Harbor after they broke their moorings. Finally, Omar interrupted communications, and ground and air transportation. Although 200 individuals received emergency treatment for typhoon-related injuries, there were no typhoon-inflicted deaths. The efforts of a joint task force, formed to coordinate the civilian and military relief efforts, in addition to airlift and volunteer efforts, both organized and grassroots, were instrumental in getting the debris cleaned up and the island community back on its feet in only a few weeks.

Omar's passage across Taiwan resulted in two deaths, at least 12 people were injured, a major interruption of electrical power, and flooding. Later, as the tropical cyclone dissipated over southeastern China, torrential rains led to localized flooding as far west as the Hong Kong New Territories.

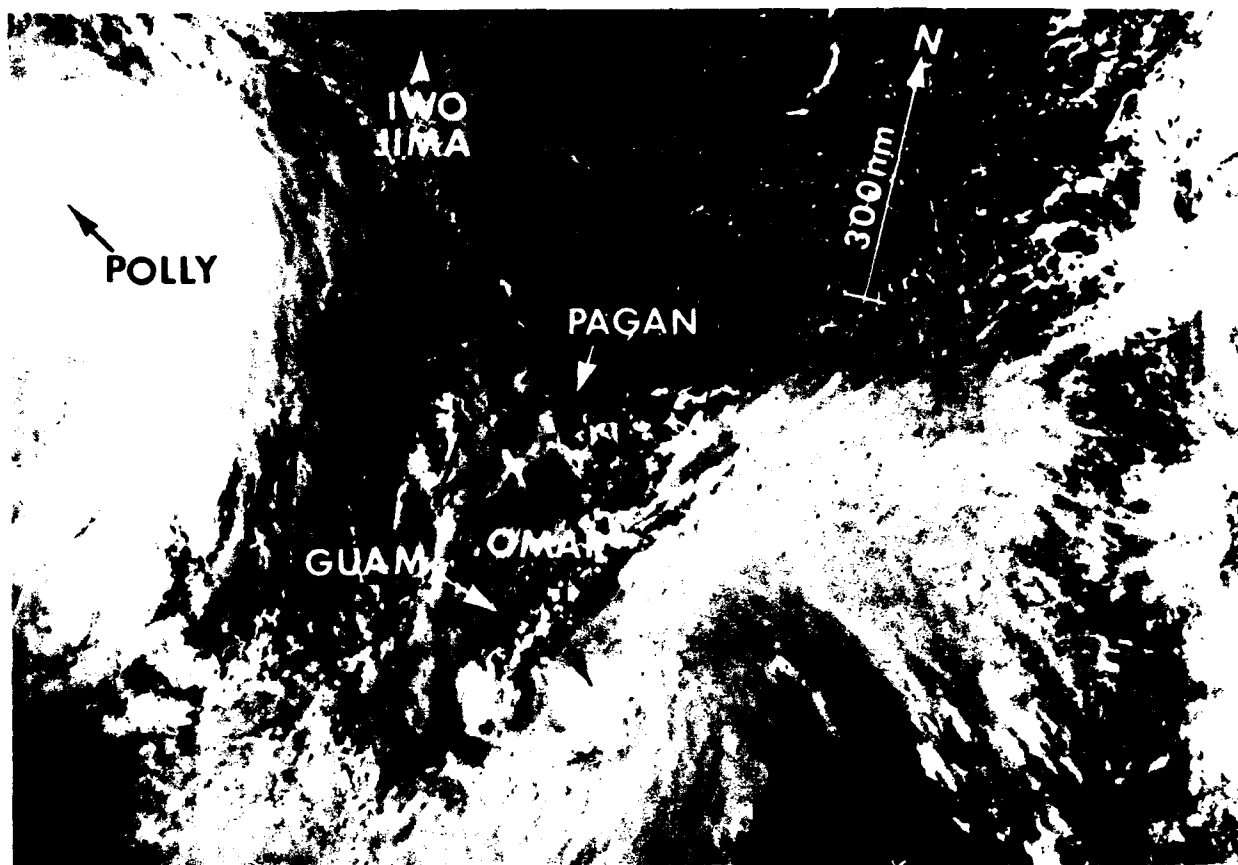


Figure 3-15-2. Omar's convection begins to coil tightly as the typhoon starts to accelerate toward Guam. The outflow across Omar from Polly (16W) to the northwest is starting to weaken (270709Z August DMSP visual imagery).

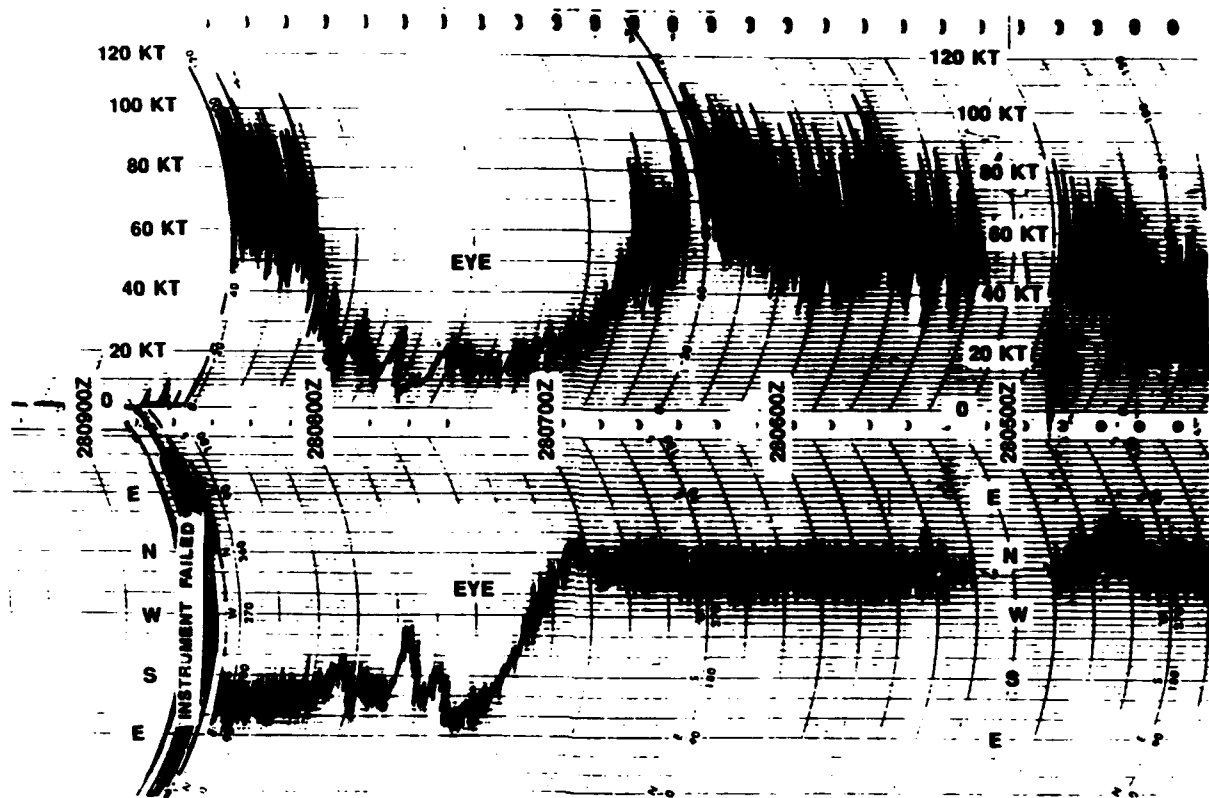


Figure 3-15-3. Wind speed and direction record of Typhoon Omar's passage over NOCD, Agana, Guam on 28 August. Note the wind instrument failed shortly after it entered the eye wall for a second time.

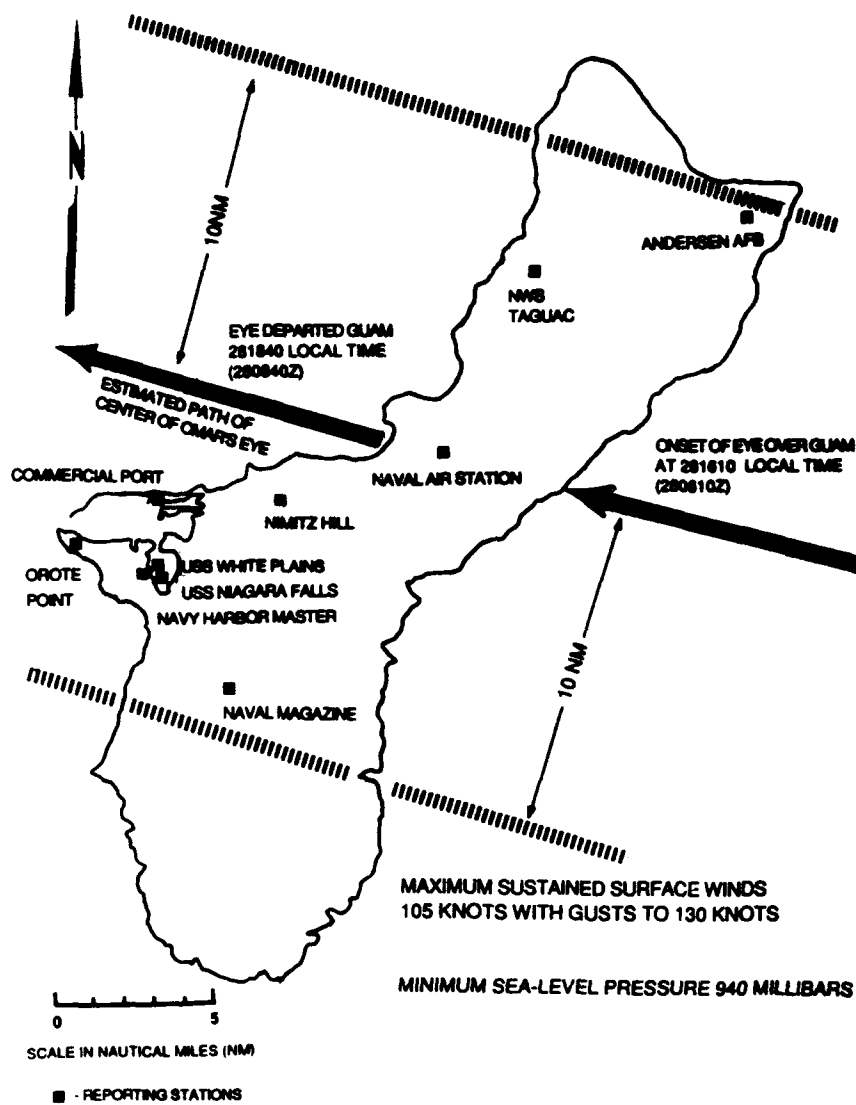


Figure 3-15-4. The geometric center of Omar's 20 nm (37 km) diameter eye with a minimum sea-level pressure of 940 mb tracked across the center of Guam on 28 August.

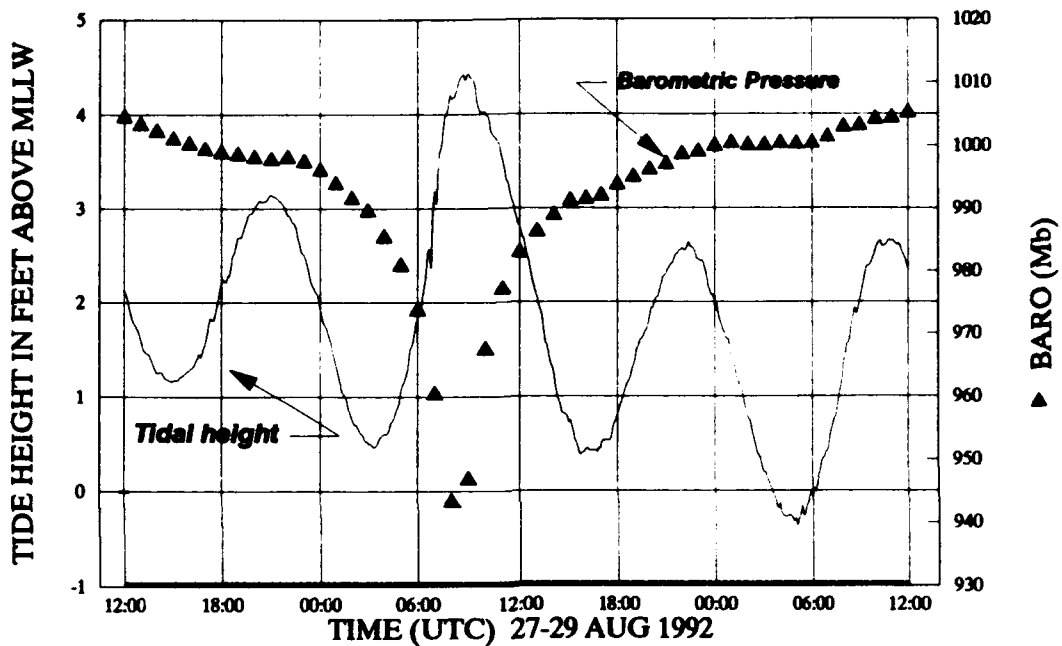


Figure 3-15-5. The NOAA-National Ocean Service (NOS) tide station record of Typhoon Omar's passage over Apra Harbor on the western side of Guam. The eye passage coincided with one of the highest astronomical tides of August (Record courtesy of NOAA/NOS Pacific Operations Section).

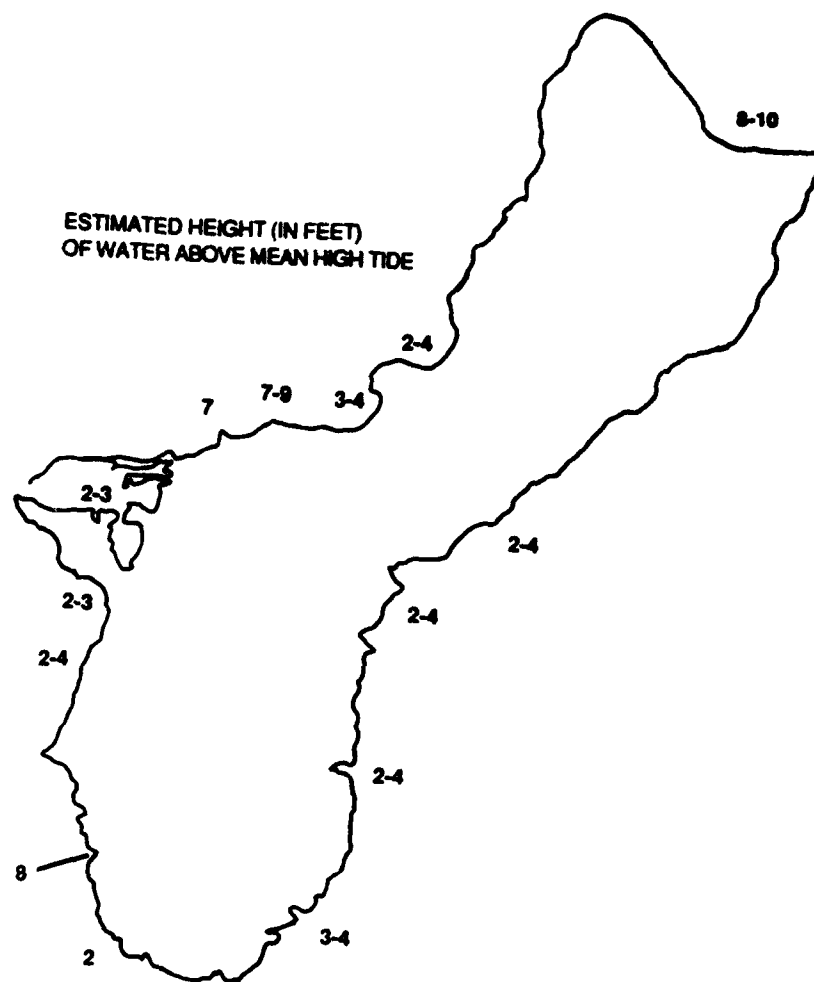


Figure 3-15-6. Maximum "storm surge" heights (which include astronomical tide, hydrostatic effects, and winds driven wave effects) at selected locations on Guam as estimated following Omar's passage.

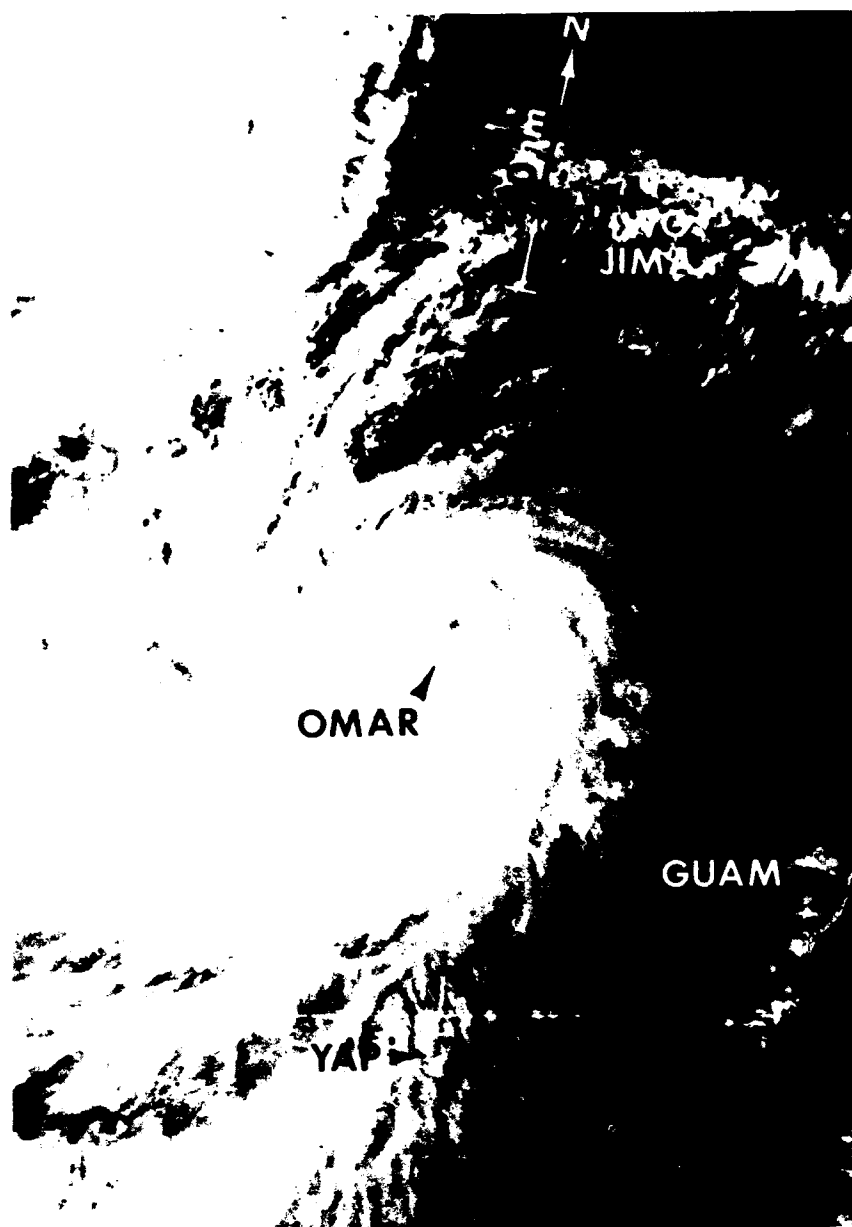
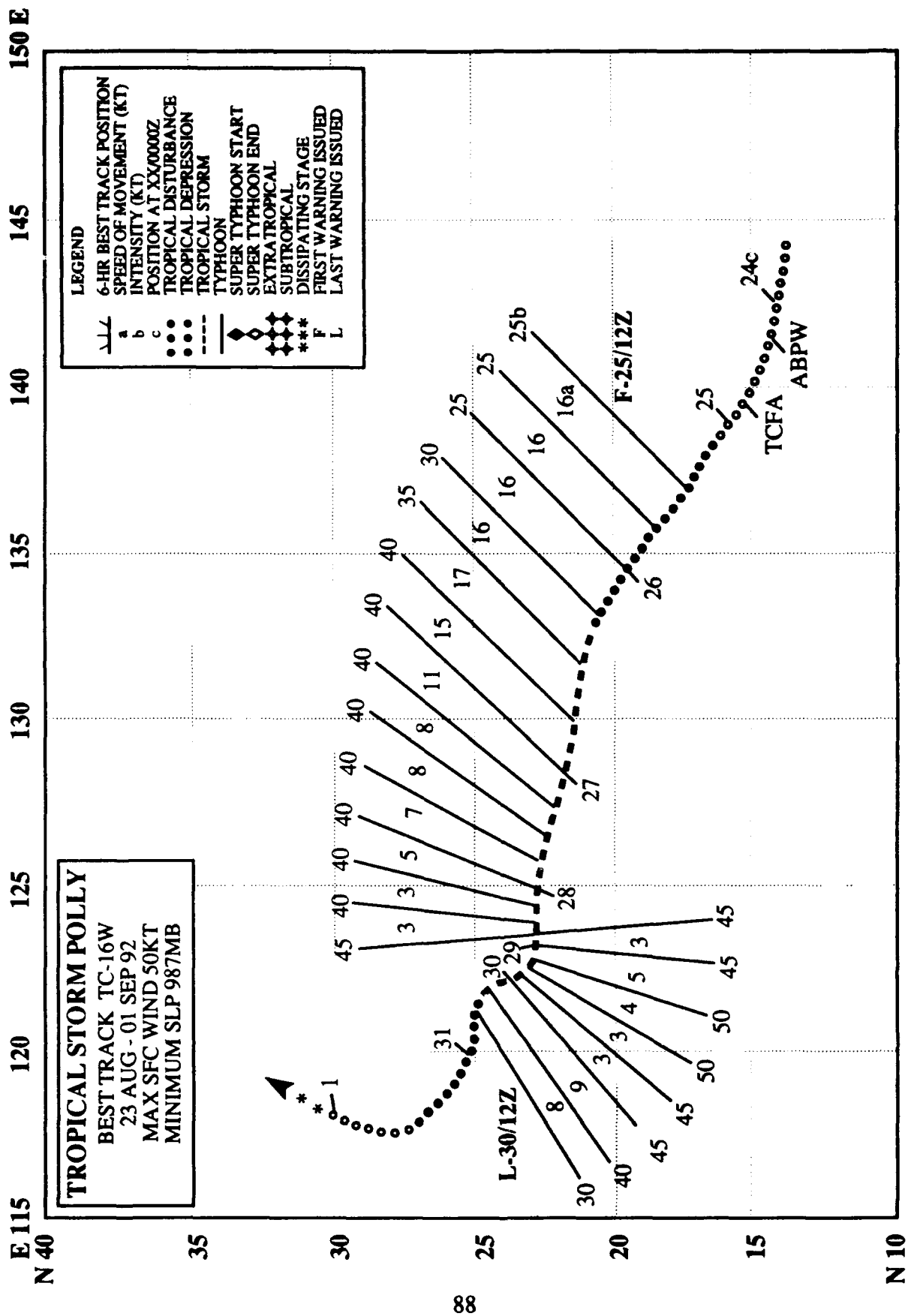


Figure 3-15-7. Omar with an 18 nm (33 km) diameter eye is still packing maximum sustained surface winds of 120 kt (62 m/sec) winds two day after peaking at 130 kt (67 m/sec) (310535Z August NOAA visual imagery).



TROPICAL STORM POLLY (16W)

I. HIGHLIGHTS

The eighth and final significant tropical cyclone of August, Polly developed along with Omar (15W) as part of a major relocation of the monsoonal trough. Polly was unusual in that throughout most of its life, it maintained the pattern of a monsoon depression with a ring of peripheral gales and a broad band of deep convection around a large, relatively cloud free, central area of light-and-variable winds. The outflow aloft from this tropical storm appeared to play an important role in delaying the intensification of Typhoon Omar (15W), when the typhoon was approaching Guam. Although Polly never reached typhoon intensity, it did have quite an impact on eastern Asia.

II. TRACK AND INTENSITY

On 24 August, as the low-level southwesterly flow built westward across the Philippine Sea reestablishing the monsoon trough, the disturbance that developed into Polly appeared as an area of persistent convection just west of Guam. The tropical disturbance was first discussed on the 240600Z Significant Tropical Weather Advisory. A cell in the tropical upper-tropospheric trough (TUTT) dug in west of the disturbance, enhancing the outflow and convective organization through the night. This caused JTWC to issue a Tropical Cyclone Formation Alert at 241900Z. The disturbance continued to increase in organization and began to separate from the general monsoon cloudiness. At 251200Z, JTWC issued the first warning on Tropical Depression 16W. The depression slowly intensified, and was upgraded to a tropical storm at 270000Z. Post analysis indicates that Polly was probably became a tropical storm about 12 hours earlier, at 261200Z.

From 25 to 27 August, the tropical storm moved to the west-northwest at an average speed of 16 kt (30 km/hr). From 27 to 29 August, Polly gradually slowed from 15 to 3 kt (28 to 6 km/hr) of motion, as it approached Taiwan, and became the anchor-low of the major western North Pacific monsoon gyre which was northeast-southwest oriented across the South China Sea. At 290600Z, Polly reached its peak intensity of 50 kt (26 m/sec). During the next 24 hours, it drifted slowly to the northwest, then made landfall on northeastern Taiwan at 300600Z (Figure 3-16-1). The tropical storm weakened to a depression over mountainous Taiwan and accelerated into southeastern China on 31 August where strong upper-level winds from the east Asian upper-level tropical easterly jet sheared the central convection from Polly's center and the tropical cyclone dissipated on 1 September.

During its life, Polly never developed a core of persistent central convection. With a large, poorly defined eye, Polly took on the characteristics of a monsoon depression with a band of strong low-level winds displaced to the east and north some 150-400 nm (280-740 km) from the center and relatively weak winds to the west and southwest (Figure 3-16-2).

From late 26 to late 27 August, Polly's upper-level outflow increased dramatically to the northeast and imposed strong upper-level shear on Typhoon Omar (15W) to the east. The increased subsidence between the two storms build a mid-level ridge between them which temporarily blocked the westward motion of Omar. The shear also slowed Omar's intensification. However, once the distance between the two storms increased and the shear abruptly decreased on the morning of 28 August Omar began to rapidly intensify. Thus, Polly greatly affected the behavior of Omar.

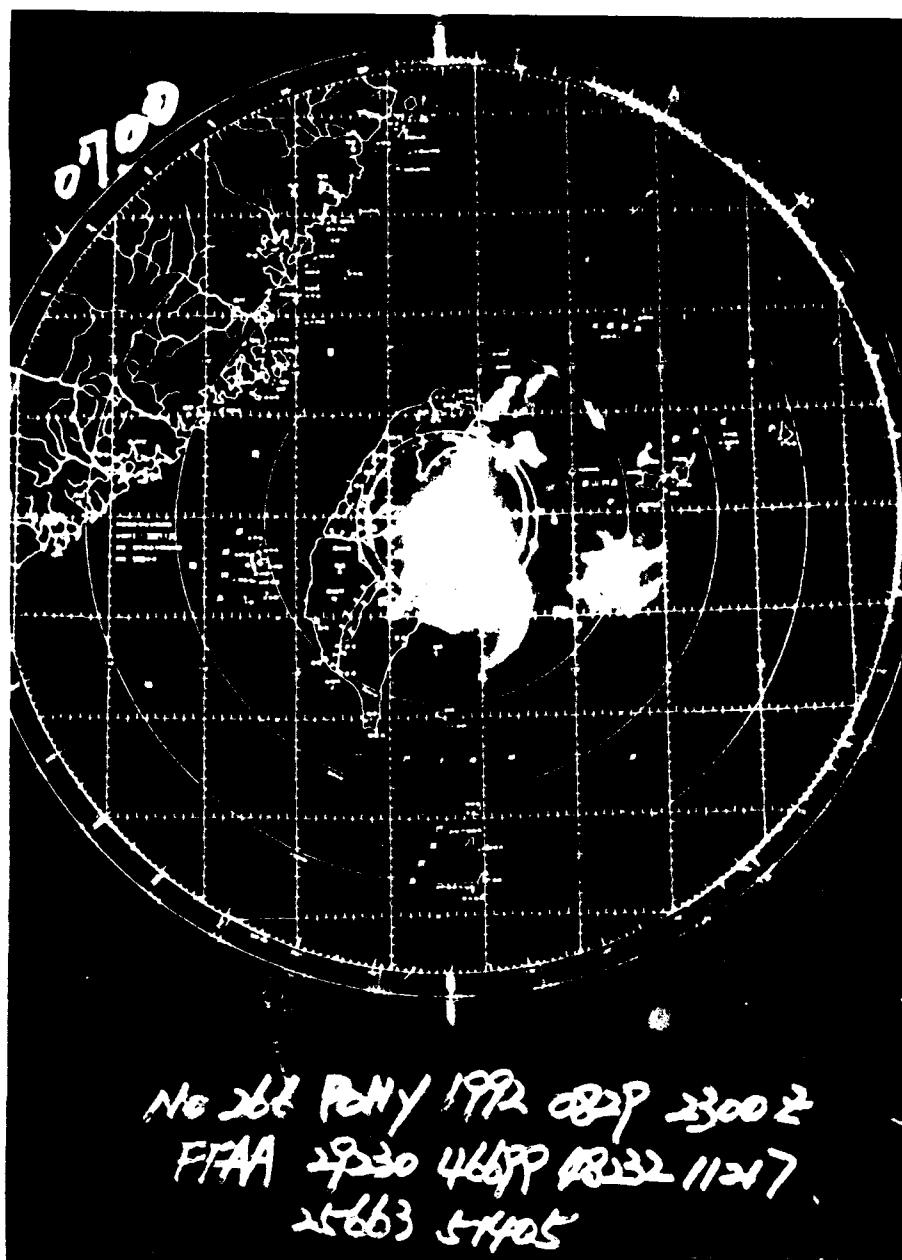


Figure 3-16-1. Although Polly is weakening, its eye remain's visible on the radar at Hualcin (WMO 46699) (292300Z August radar photo courtesy of the Central weather Bureau, Taipei, Taiwan).

III. FORECAST PERFORMANCE

Overall JTWC mean track forecast errors were worse than normal at 12 to 24 hours, but better at 48 and 72 hours. This was primarily the result of relatively large along-track or speed errors for the short range forecasts, but relatively low cross-track or pointing errors for all of the forecasts. Forecasters did not expect the anchor-low of the monsoon trough to immediately accelerate to the west-northwest in the early stages. They did not anticipate the slow down that began on 28 August. As Polly moved westward, forecasters slowed the tropical cyclone's motion to more climatological speeds. This allowed the longer range forecasts to benefit from Polly's slow speed near Taiwan.

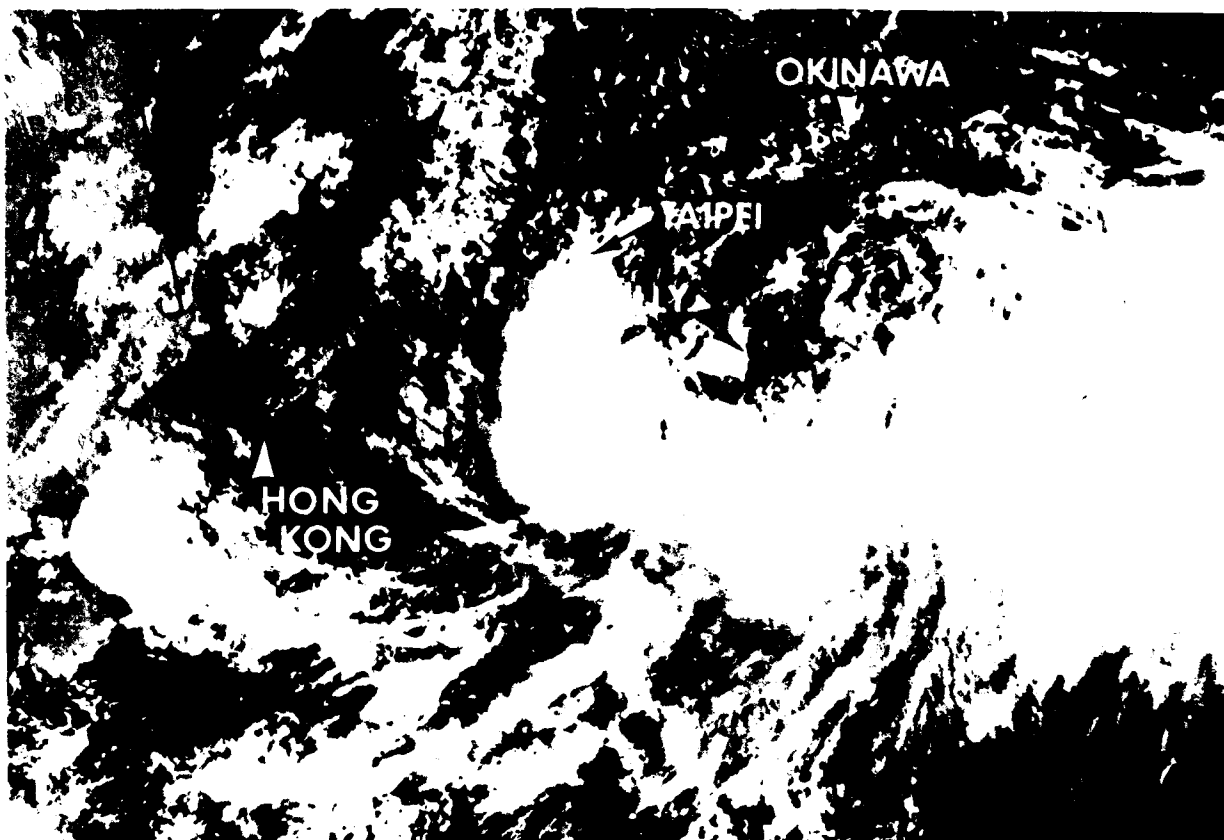


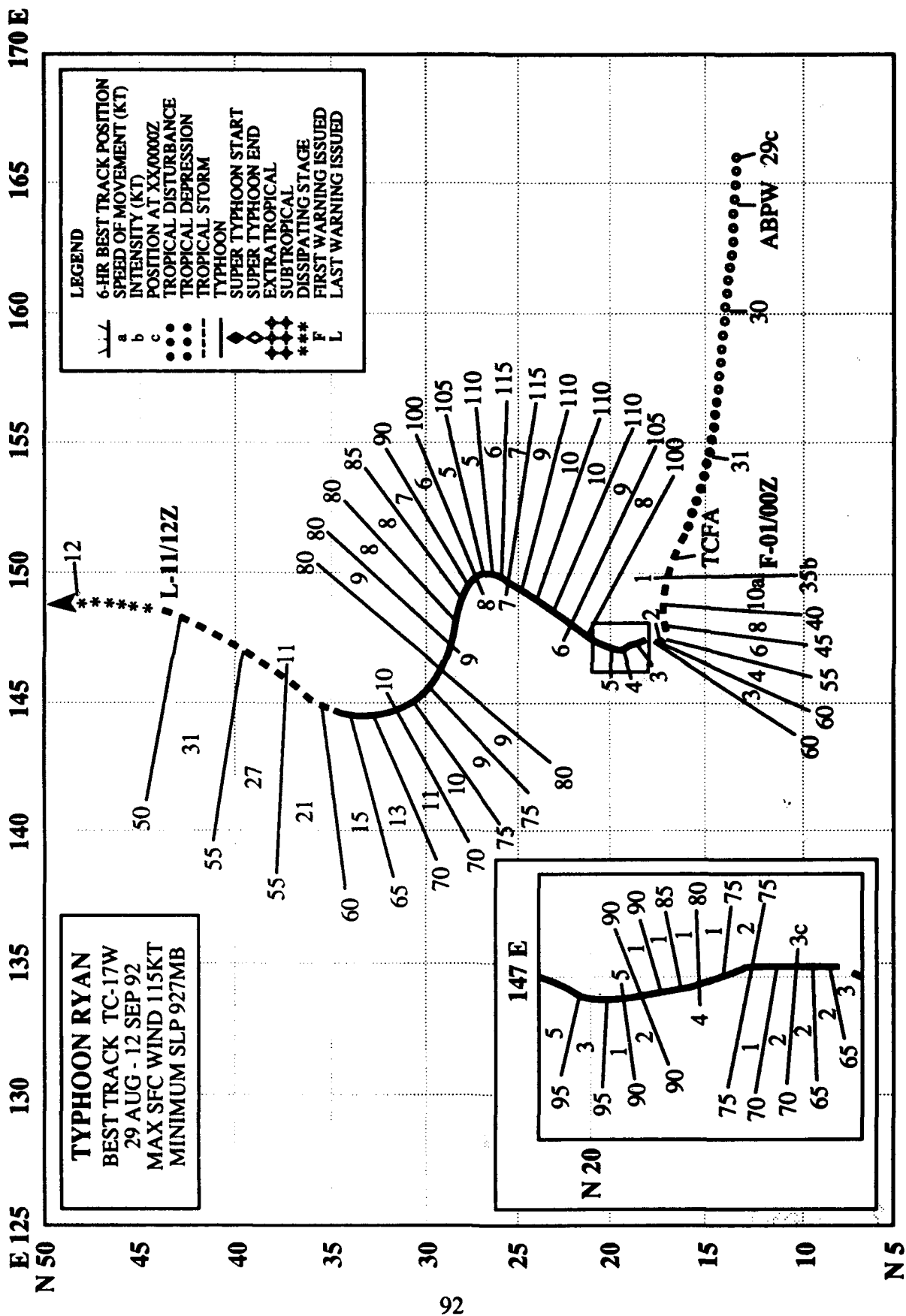
Figure 3-16-2. Polly's large, relatively cloud free, circulation center is supported by a deep band of convection to the south (280107Z August DMSP visual imagery).

JTWC accurately anticipated slow development and only development to minimum typhoon intensity. As a result, average intensity forecast errors for the first 48 hours were 10 kt (5 m/sec) or less. Seventy-two hour forecast errors were 19 kt (10 m/sec), primarily as a result of early forecasts anticipating peaking in three days instead of the observed five days.

In general, the dynamic models performed poorly on Polly. However, the FNOC Beta Advection Model (FBAM) in the mean out performed all of the forecast guidance. This model seems to do well with the motion of cyclones associated with large monsoon gyres. JTWC forecasts were superior to CLIPER at 24 hours, but nearly identical at 48 and 72 hours.

IV. IMPACT

Polly's greatest impact to forecasters was its effect on Typhoon Omar's (15W) motion and intensity. Polly created more than three days of gale- or near gale-force winds over Okinawa and the north Ryukyu Islands. The strong cross winds hampered flying operations on Okinawa, even though Polly never got closer than 300 nm (555 km). In northern Luzon, the torrential rains, associated with Polly's passage to the north, caused lahars, or steaming mudflows, on the slopes of Mount Pinatubo that claimed five lives. On Taiwan, Polly's rain and wind were responsible for at least eight fatalities, widespread flooding that inundated thousands of homes and acres of farmland, and electrical power outages. As the remnants of the tropical storm slammed into southeastern China, heavy rains and flooding led to at least 165 deaths, the loss of 11,000 homes, 1400 fishing boats, and thousands of livestock.



TYPHOON RYAN (17W)

I. HIGHLIGHTS

The first of five significant tropical cyclones to form in September, Ryan became part of a three storm outbreak east of 150° E longitude along with Typhoons Omar (15W) and Sibyl (18W). Although Ryan initially took a west-northwestward course similar to the two preceding tropical cyclones, it later stalled, and then changed to a north-orientated track. Two days after transitioning to an extratropical low east of Hokkaido, the remnants of Ryan could still be identified, as an occluded low continuing northward over Siberia, north of the Sea of Okhotsk.

II. TRACK and INTENSITY

On 29 August, one day after Typhoon Omar (15W) roared across Guam knocking the Joint Typhoon Warning Center out of commission, the Alternate JTWC (AJTWC) noticed a persistent area of convection east of the Mariana Islands and included it on the 290600Z Significant Tropical Weather Advisory. As this persistent area of convection at the extreme eastern end of the monsoon trough moved west-northwestward, the tropical disturbance steadily increased in convective organization, prompting AJTWC to issue a Tropical Cyclone Formation Alert at 312100Z, and the first warning shortly afterward at 010000Z September.

Instead of continuing along the axis of the monsoon trough to the west-northwest, as Omar (15W) and Polly (16W) had done, Ryan stalled on 2 September, and abruptly changed course in response to a weakening of the subtropical ridge to the north caused by the passage of a deep mid-level trough. As the tropical cyclone drifted northward in a weak steering environment, it gradually intensified and became a typhoon at 021200Z.

On 5 September, a second mid-level trough began to deepen near Honshu and effect the subtropical ridge. As a consequence, the typhoon (Figure 3-17-1) changed to a north-northeast track, and reached a peak intensity of 115 kt (59 m/sec) at 070000Z. When the ridge reestablished itself after the trough's passage on 8 September, the typhoon began to move northwestward. Then, on 10 September, the cyclone turned east of north again, and began to accelerate ahead of a third mid-latitude trough. At 111200Z, Ryan transitioned into an extratropical low east of Hokkaido and JTWC, which had resumed primary warning responsibility on 8 September, released a final warning. The extratropical remnants of Ryan continued northward across the Sea of Okhotsk and was still evident as a large occluded low over Siberia two days later.

III. FORECAST PERFORMANCE

Ryan's first 28 warnings were issued by AJTWC and the last 15 by JTWC. Early track forecasts predicted that Ryan would be a straight-runner to the west, however, after it became apparent that the track would become north-oriented, the errors were noticeably reduced. Overall mean JTWC track forecast errors were 97, 238 and 360 nm (180, 445, and 665 km) for 24, 48 and 72 hours, respectively. Although the mean errors at 48 and 72 hours were larger than average, JTWC and AJTWC did show skill by bettering CLIPER by 70% on this harder-than-average typhoon. However, for 72-hour forecasts, the best overall guidance was provided by OTCM, which in the mean, was considerably better than JTWC/AJTWC by 139 nm (255 km). With regard to intensity, the short range forecasts verified well. Nevertheless, for the 36-hour period beginning at 021800Z, the 72-hour intensity forecasts were low by 20 to 50 kt (10 to 26 m/sec) due to anticipated weakening that did not occur.

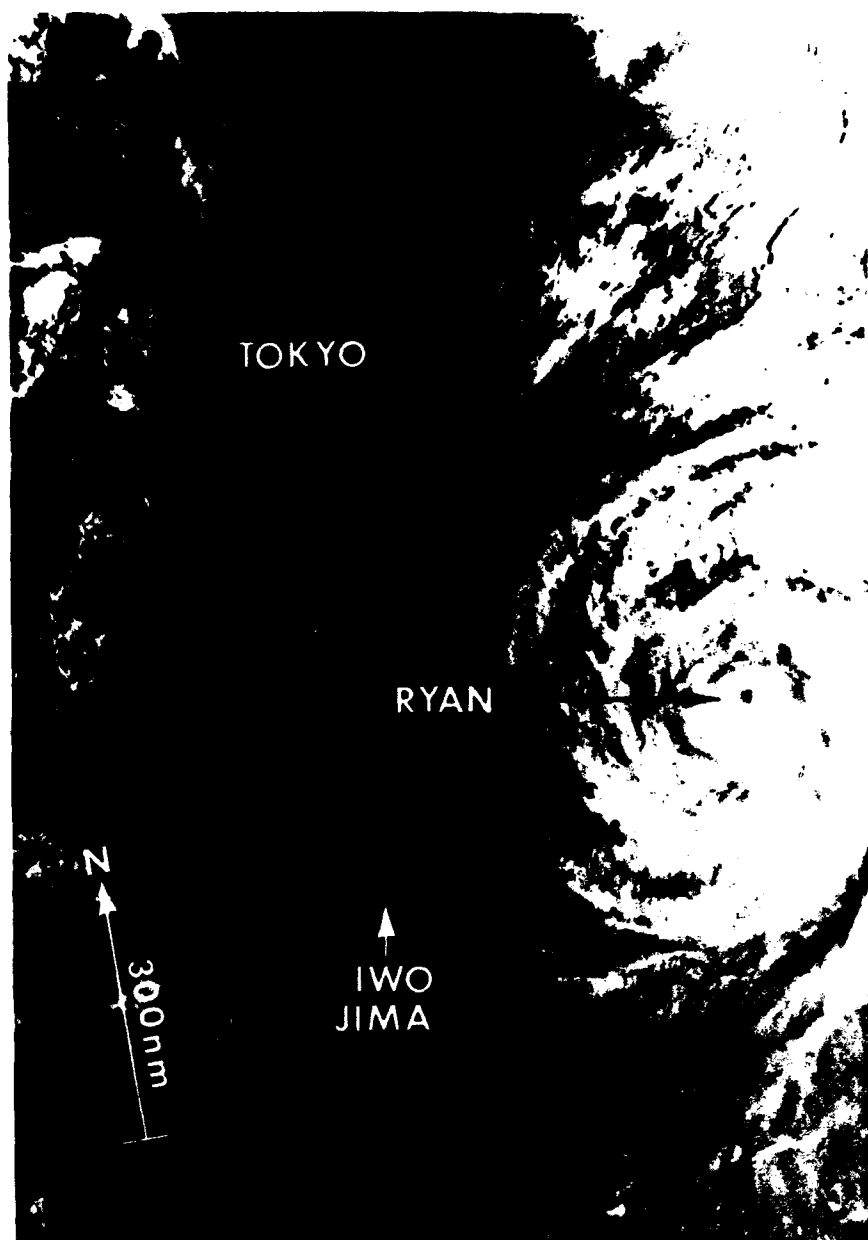
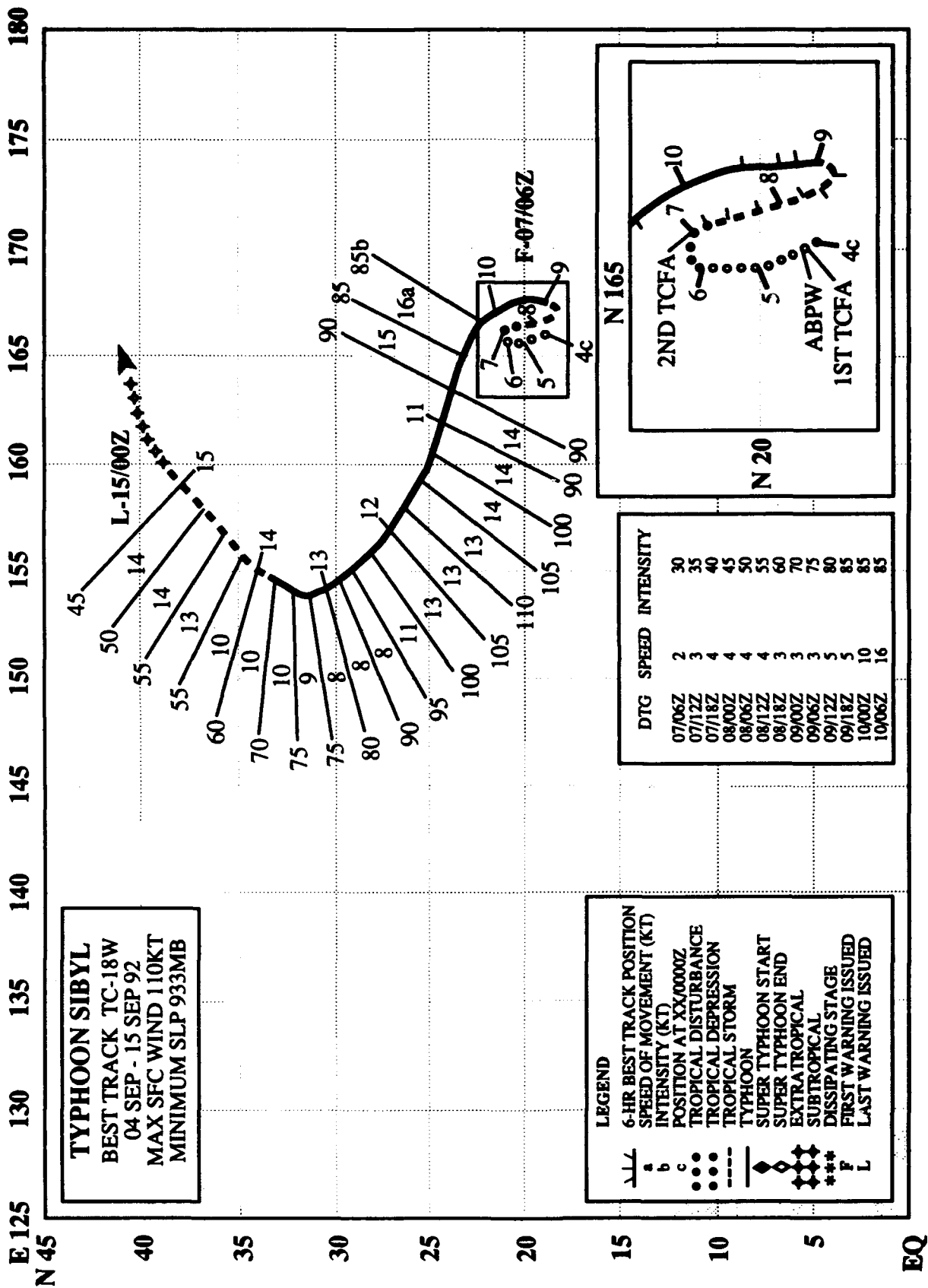


Figure 3-17-1. Just after reaching its peak intensity, Typhoon Ryan is located southeast of Tokyo (072238Z September NOAA visual imagery).

IV. IMPACT

Typhoon Ryan remained over open ocean and no reports of property damage or loss of life were received. While Ryan was developing northeast of Saipan, and moving erratically, it threatened the sparsely populated islands of Pagan and Agrihan which were in Condition of Readiness One for nearly two days. The system also enhanced the southwest monsoon between Guam and Saipan, delaying the arrival of barges carrying bucket trucks and line crews from Saipan to help restore power on Guam.

This was the first time in recent history that the AJTWC had to activate in the middle of the western North Pacific tropical cyclone season for JTWC and keep the Pacific Command's warning system running for a long period, 11 days. AJTWC rose to the challenge and the excellent statistics bear this out.



TYPHOON SIBYL (18W)

I. HIGHLIGHTS

The second of five significant tropical cyclones to form in September, Sibyl, like Ryan (17W), formed at the extreme eastern end of the monsoon trough. But unlike Ryan, Sibyl underwent a complex interaction with a cyclonic cell in the Tropical Upper-Tropospheric Trough (TUTT), and later recurved. For five days Sibyl exhibited erratic motion and slowly intensified near Wake Island, before moving to the northwest and recurving.

II. TRACK AND INTENSITY

The tropical disturbance that became Sibyl formed at the eastern end of the monsoon trough that included both Typhoon Omar (15W) and Typhoon Ryan (17W). As Ryan (17W) intensified, the falling surface pressures along the monsoon trough extended eastward into the Wake Island area. In response, the surface pressure at Wake Island (WMO 91245) had been slowly, but steadily falling since 1 September (Figure 3-18-1). The combination of the falling surface pressures, soundings from Wake Island (WMO 91245) showing strengthening southwesterlies, and the appearance of an exposed low-level circulation center on the satellite imagery, prompted the Alternate JTWC (AJTWC) to issue a Tropical Cyclone Formation Alert (TCFA) at 040400Z.

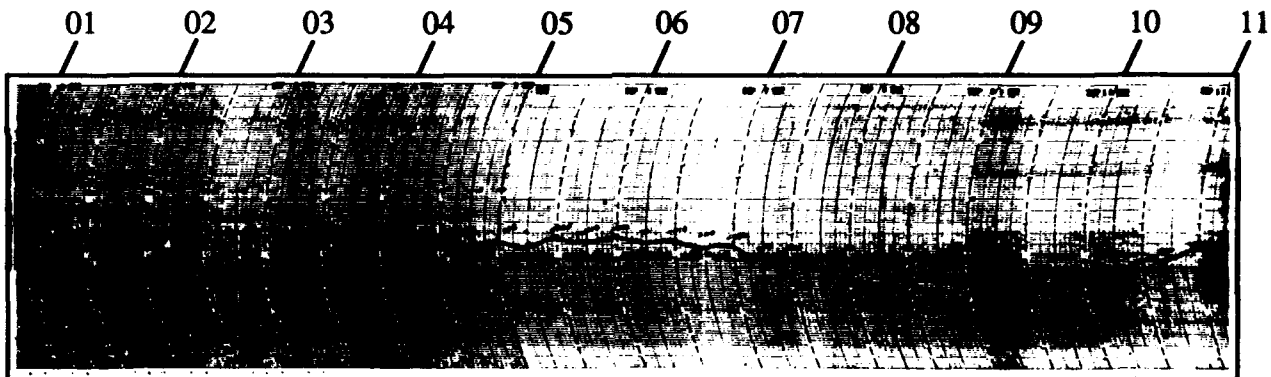


Figure 3-18-1. Barograph trace for the period 01-11 September for Wake Island (WMO 91245) showing the steadily falling pressures from 010000Z to 091445Z associated with the extension of the monsoon trough into the area, and the formation and intensification of Sibyl near the island. (Microbarograph trace courtesy of the National Weather Service Office, Wake Island).

In the TUTT over the alert area, in conjunction with the increasing outflow from Ryan (15W), a cyclonic cell developed. As the complex interaction between the tropical disturbance and the TUTT-cell progressed, the deep convection was sheared from the low-level circulation center by strong 35- to 45-kt (18- to 23-m/sec) winds around the TUTT-cell at 200 mb. As a result, the TCFA was canceled at 050400Z. Though the strong vertical wind shear remained over the area, the stronger than normal low-level winds remained. The ambient surface pressure near Wake Island continued to fall, and the tropical disturbance persisted in the form of a monsoon depression. A second TCFA, issued at 070000Z, discussed the gales, and the presence of a low-level circulation center evident in the synoptic and satellite data. The reappearance of central convection resulted in AJTWC issuing the first warning at 070600Z. Subsequently, Sibyl was upgraded to tropical storm intensity at 071800Z as the central convection expanded displacing the TUTT-cell aloft farther to the north. The tropical storm continued to intensify,

and a visible eye developed in the central dense overcast. The resulting satellite intensity estimate of 65 kt (33 m/sec) was the basis for Sibyl's upgrade to typhoon on the 090000Z warning issued by JTWC. At 091445Z, Wake Island recorded its lowest pressure, 984.5 mb, and northwest winds of 35 gusting to 48 kt (18 G 25 m/sec) at 091500Z, as Typhoon Sibyl finally began moving away.

Until 9 September, Sibyl's erratic track appeared to be the consequence the southwest flow associated with the interaction of the monsoon flow and with the easterlies of the subtropical ridge to the north and east of Wake Island. The TUTT may have played a role in the erratic movement as well. This complex synoptic pattern changed on 9 September, and Sibyl made an abrupt track change to the north. By 10 September the typhoon had accelerated and had settled into a more normal northwestward course under the influence of the subtropical ridge (Figure 3-18-2). Sibyl continued tracking toward the northwest until 13 September, when it passed through a break in the mid-tropospheric subtropical ridge and recurved. The final warning was issued by JTWC at 150000Z as Sibyl became extratropical and accelerated to the northeast.

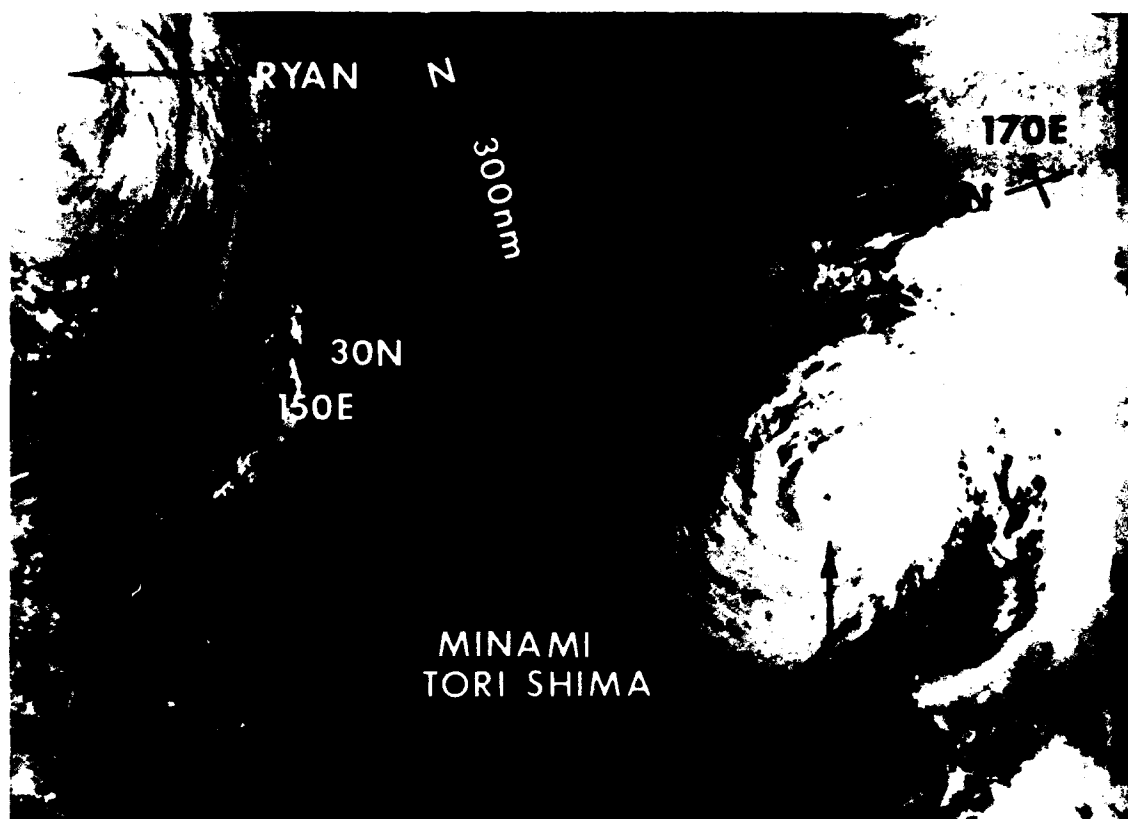


Figure 3-18-2. Typhoon Sibyl finally moves away from Wake Island. Typhoon Ryan (17W) is visible at the top left of the picture (102133Z September NOAA visual imagery).

III. FORECAST PERFORMANCE

Sibyl proved to a difficult system for AJTWC/JTWC to forecast. The overall mean track errors were 100, 194 and 305 nm (185, 360 and 565 km) for the 24-, 48 and 72-hour forecasts, respectively. While these are below average, they would have been much larger had Sibyl not moved so slowly. Although AJTWC/JTWC showed skill overall on the 24-hour forecasts, CLIPER, which provides the performance baseline, was superior at the 48- and 72-hour points with 10% and 30% better performance, respectively.

With regard to intensity, the short term forecasts were good, however, the extended outlooks for 72-hours were low by 20 to 45 kt (10 to 23 m/sec) for the first day and a half, and high by 40 to 55 kt (21 to 28 m/sec) for a day after 110600Z.

IV. IMPACT

Although Wake Island was buffeted by gales for days, no major damage or injuries were reported. Some minor water damage occurred, and Wake Island was in Condition of Readiness 1 for a day.

As with Typhoon Ryan (17W), AJTWC warned on Sibyl while JTWC was incapacitated. However, many of the direct telephone discussions with customers in Micronesia, including Wake Island, were handled by the JTWC, Guam forecasters. JTWC was able to resume its full service on 8 September.

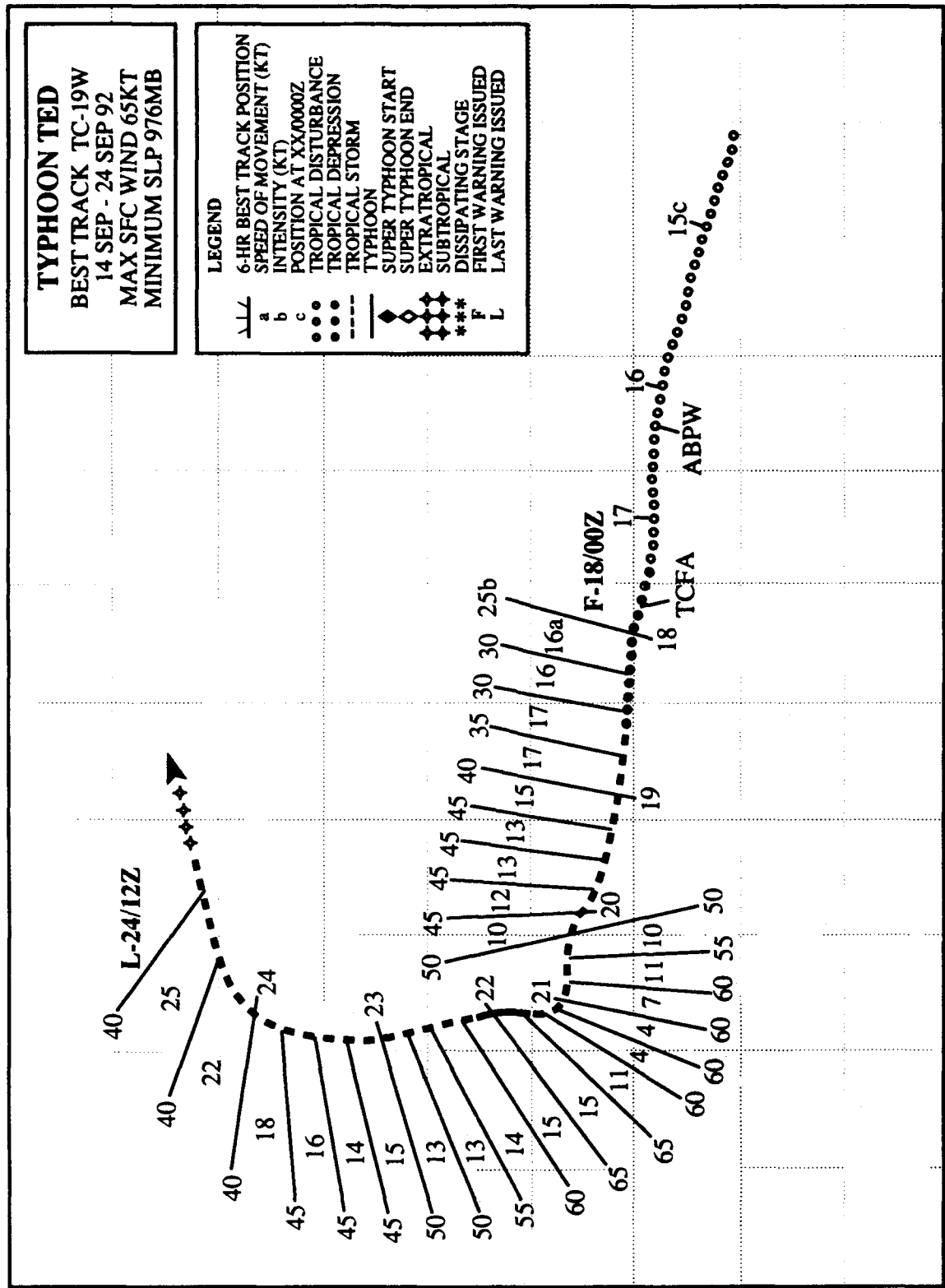
E 110 115 120 125 130 135 140 145 150 155 160 165 E

TYPHOON TED

BEST TRACK TC-19W
14 SEP - 24 SEP 92
MAX SFC WIND 65KT
MINIMUM SLP 976MB

LEGEND

- 6-HR BEST TRACK POSITION
- SPEED OF MOVEMENT (KT)
- POSITION AT XX0000Z
- TROPICAL DISTURBANCE
- TROPICAL DEPRESSION
- TROPICAL STORM
- TYPHOON
- SUPER TYPHOON START
- SUPER TYPHOON END
- EXTRATROPICAL
- SUBTROPICAL
- DISSIPATING STAGE
- FIRST WARNING ISSUED
- LAST WARNING ISSUED



TYPHOON TED (19W)

I. HIGHLIGHTS

As Typhoon Sibyl (18W) transitioned to an extratropical system and proceeded northeastward, a weak monsoon trough was becoming established to the north of the Caroline Island chain. A few days of respite ensued for JTWC while the disturbance that was to become Typhoon Ted slowly developed. Ted was marked by moderate to strong upper-level shear throughout most of its life, creating a cloud pattern which obscured the low-level circulation center rather frequently. A combination of shearing effects and land interaction prevented Ted from intensifying above minimal typhoon. Ted's tour of Asia included northern Luzon, northeastern Taiwan, eastern China, and finally Korea before the circulation transitioned to a weak extratropical cyclone over the Sea of Japan.

II. TRACK and INTENSITY

On the 13 September Significant Tropical Weather Advisory, forecasters first noted the monsoon trough which would produce the circulation of Typhoon Ted. But, it was not until 16 September that a circulation became apparent. By 17 September, a TUTT-cell had become positioned to the northwest of the disturbance, enhancing its outflow, and organization began to significantly improve. A Tropical Cyclone Formation Alert was issued at 172030Z in response to an increase in convective curvature and a flare-up of convection coincidental with the convectional diurnal maximum. In retrospect, the alert was about 18 hours behind the power curve. The first warning was issued by JTWC at 180000Z, and the depression initially proceeded west-northwestward. But, at 180600Z, the mid-level subtropical ridge became stronger and the system accelerated on a more westward course. Convective banding and organization continued to improve, and the system was upgraded to tropical storm intensity at 181800Z. Shortly thereafter, the first indication of significant shear over Ted was observed as the low-level circulation was consistently located under the eastern portion of the deepest convection (Figure 3-19-1). Between 191800Z and 201200Z, Ted slowed, and proceeded generally northwestward as a deepening low pressure system near Hokkaido, Japan temporarily weakened the low- to mid-level subtropical ridge. Ted resumed its westward track, and continued to slow as the system approached the westernmost extent of the ridge. At the surface, a high pressure system was building behind the low pressure system over Hokkaido and this wave pattern proceeded eastward rapidly. By 210000Z, all of the pieces were in place for Ted to proceed northward: 1) satellite imagery revealed a coupling between outflow from Ted and the mid-latitude frontal system; 2) as the high pressure system to the north of Ted moved eastward, pressures immediately north of Ted were falling; and, 3) synoptic data revealed that a weakness in the mid-level subtropical ridge became situated to the north of Taiwan. The reduced upper-level winds Ted encountered in the vicinity of the Luzon Strait enabled the system to briefly attain typhoon intensity (Figure 3-19-2), but at 220600Z, land interaction and increased upper-level wind flow caused Ted to revert back to tropical storm status where it remained until transformation to an extratropical low several days later. Ted accelerated during its northward transit until reaching 25 kt (46 km/hr) after recurvature. At 241200, Ted became extratropical and JTWC issued the final warning on the system.

III. FORECAST PERFORMANCE

Systems which are consistently difficult to accurately locate generally produce the largest track forecast errors, and Ted was no exception. The initial acceleration of Ted south of the subtropical ridge was not forecast, but the acceleration was a relatively short-term phenomenon and did not severely

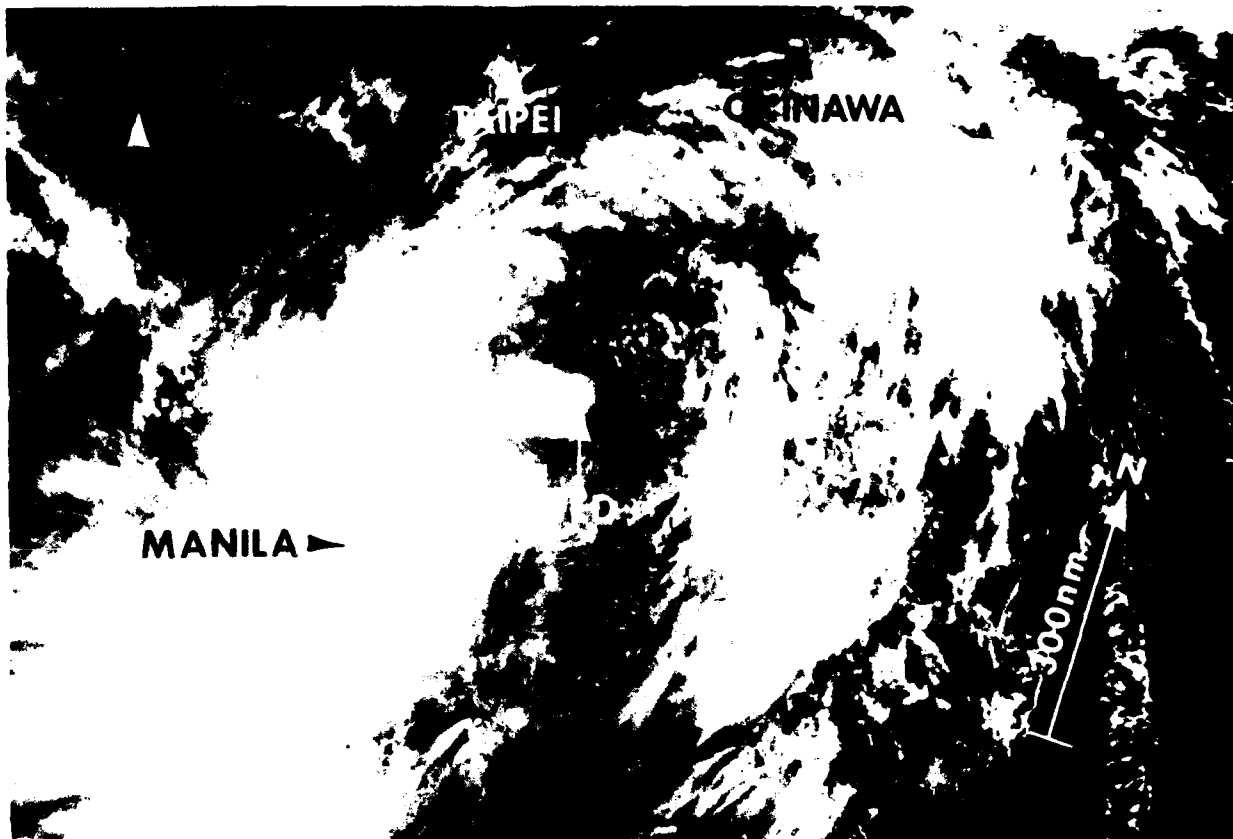


Figure 3-19-1. Tropical Storm Ted's low-level circulation is partially exposed as it approaches northern Luzon (200637Z September NOAA visual imagery).

impact the longer range forecast errors. JTWC forecasters lost faith in the NOGAPS numerical model early on as the model predicted slow northwestward to northward motion at the time Ted was transiting rapidly westward. As a result, forecasters relied heavily on persistence-and-climatological-based aids. After Ted turned north near Luzon, NOGAPS performed well, accurately predicting wave patterns in the mid-latitudes and the breakdown of the mid-level subtropical ridge near Taiwan. The premature lifting of a tropical cyclone to the north through a break in the subtropical ridge is typical of the NOGAPS or any model in general due to the coarse resolution. Once Ted entered the Luzon Strait, NOGAPS locked on to Ted's track (Figure 3-19-3). Tropical Storm Wendy in 1974 exhibited remarkably similar track characteristics, and was initially used by forecasters as an analog. It was recognized as an analog by forecasters only after northward movement in the Luzon Strait became apparent. The following forecast weaknesses were noted:

- 1) Over reliance on persistence and inadequate interpretation of flow patterns observed in satellite imagery and predicted by numerical models. For example: once Ted slowed to 4 kt (7 km/hr) in the Luzon Strait, forecasters hesitated in showing northward acceleration. The weakness in the subtropical ridge to the north was suggested by the linkage of convection between Ted and the mid-latitude frontal boundary on satellite images. Only when the speed had apparently increased to above 10 kt (19 km/hr), did JTWC forecasts indicated significant acceleration.

- 2) Failure to modify longer range intensity forecasts once it became apparent that upper-level shear would increase and remain persistent, and land interaction became inevitable. Some of the difficulty in this area could be attributed to the uncertainty in initial position of Ted at the various warning times, which inaccurately reflected the true motion over the previous 6- to 12-hour period.

IV. IMPACT

On northern Luzon, torrential rains from Ted caused landslides and flooding which resulted in at least 8 fatalities. The impact on Taiwan and eastern China was similar with heavy rains, flooding and landslides. However, the losses were much greater in eastern China where at least 53 lives were lost and as many people were reported as missing; over 30,000 houses collapsed; and extensive damage to agricultural land occurred. No loss of life or significant damage reports were received from Korea.

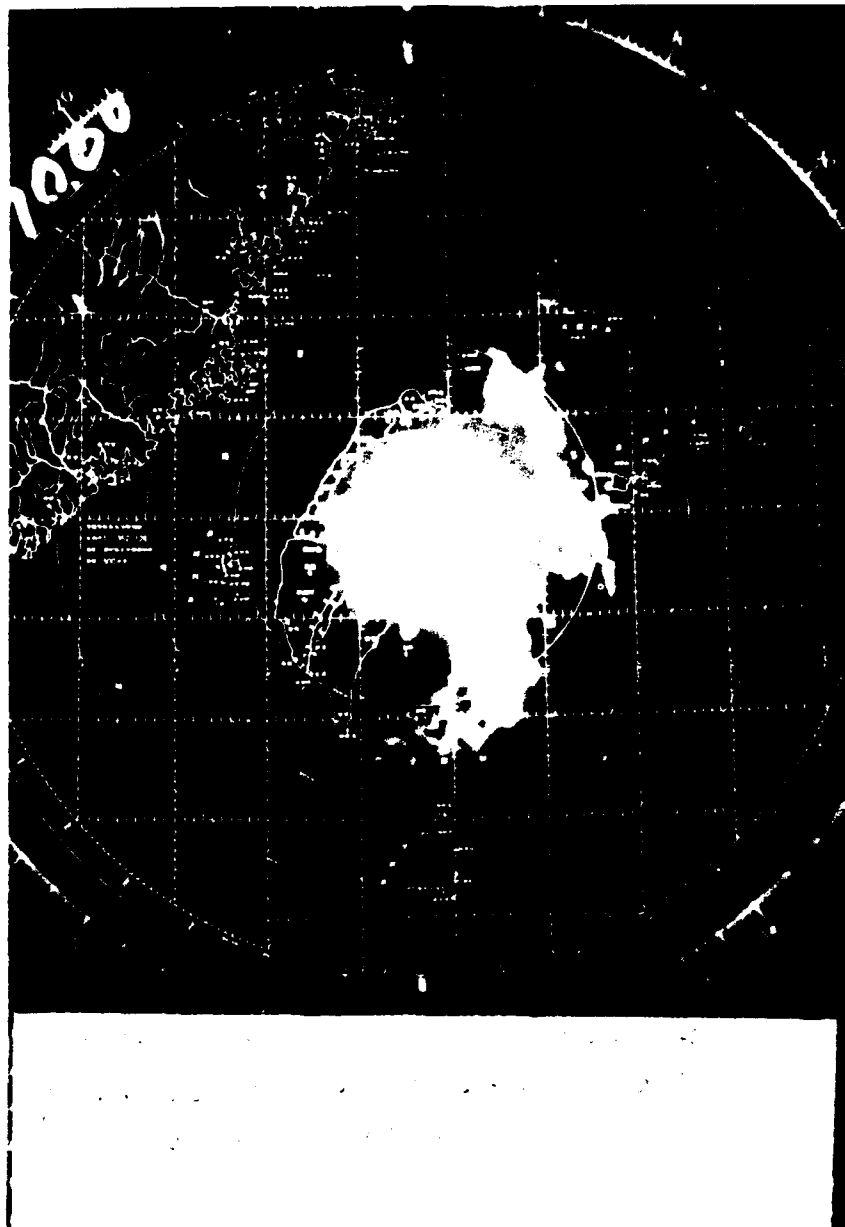


Figure 3-19-2. The 220200Z September radar image from Haulien (WMO 46699) of Ted at peak intensity (radar photo courtesy of the Central Weather Bureau, Taipei, Taiwan).

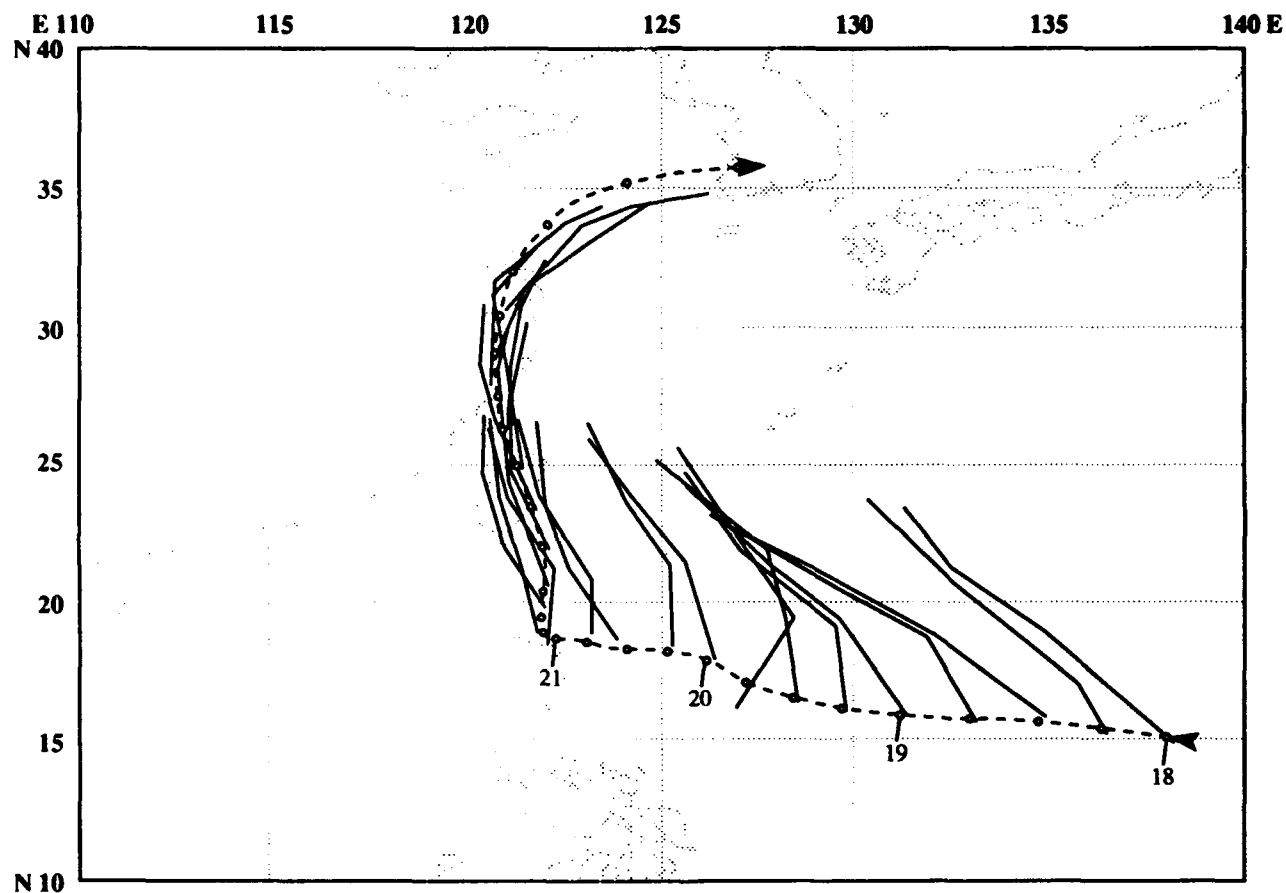
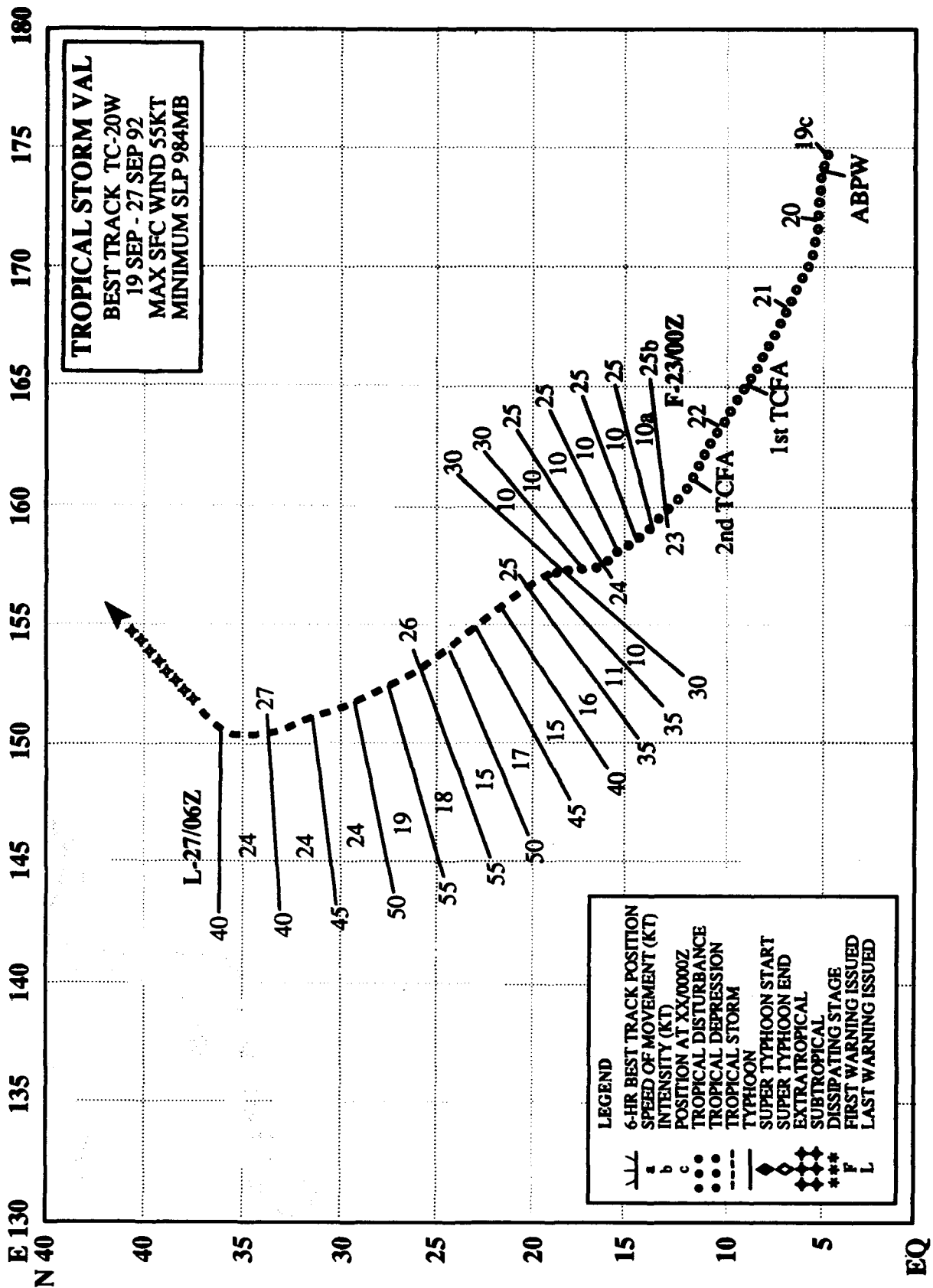


Figure 3-19-3. NOGAPS guidance for Ted is consistently north of track until the tropical storm enters the Luzon Strait, then the model locks on.



TROPICAL STORM VAL (20W)

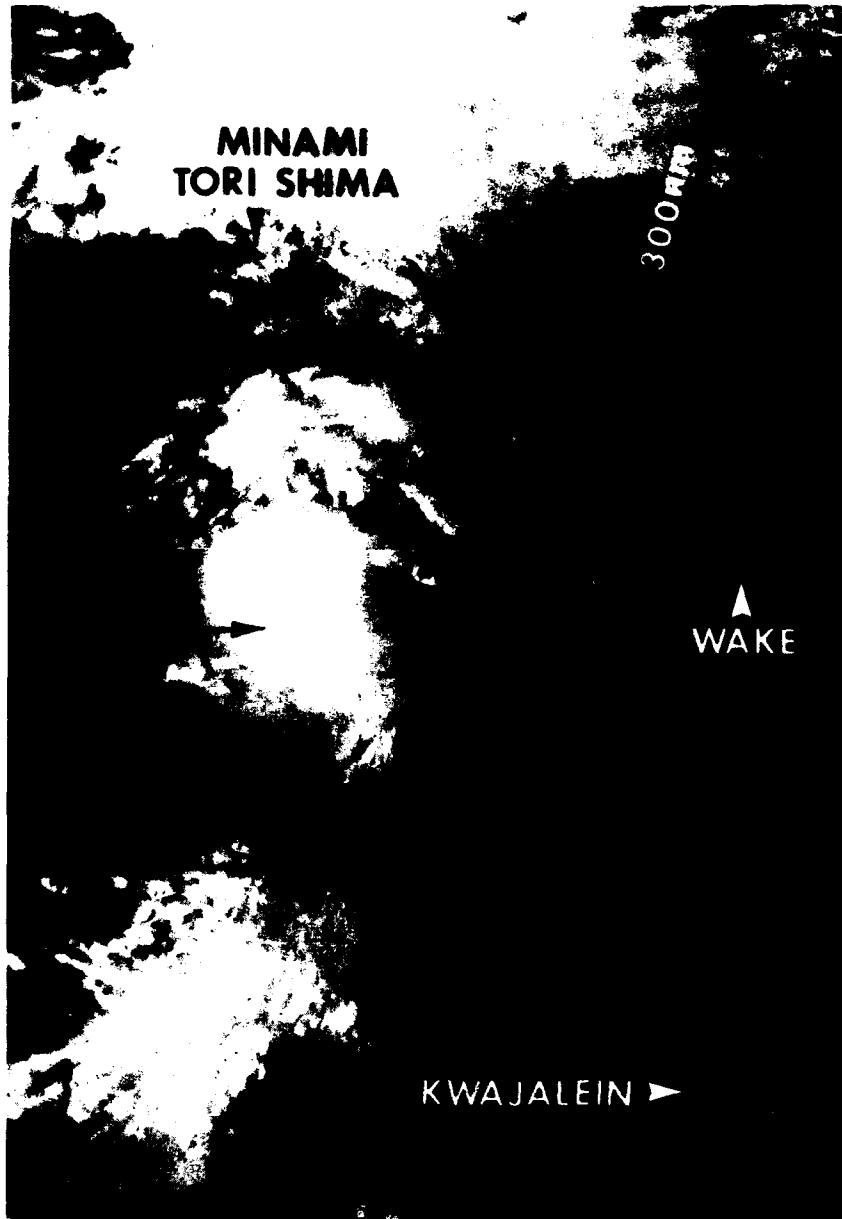
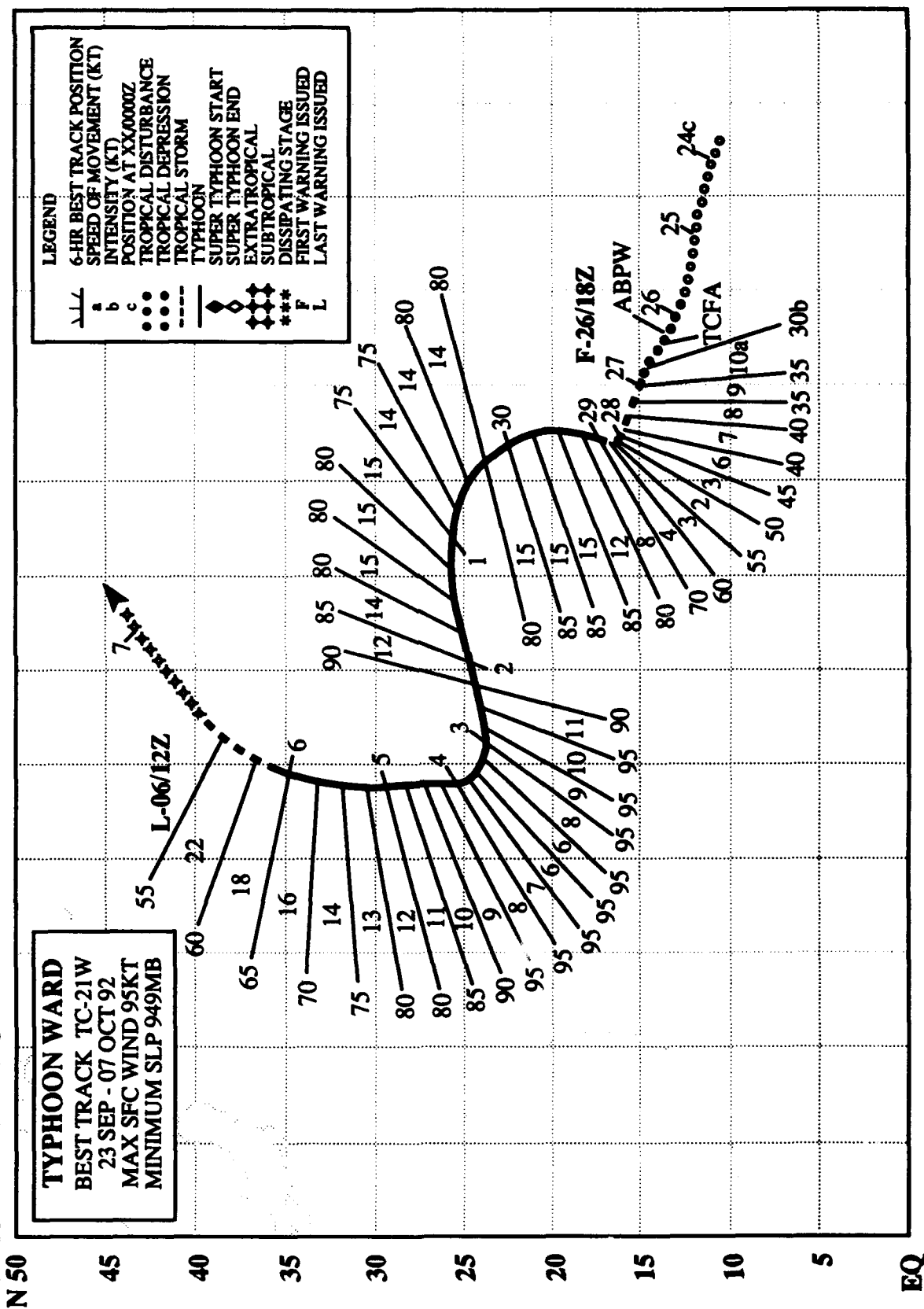


Figure 3-20-1. Poorly organized, but persistent convection defines Val 12 hours before it reaches tropical storm intensity (240406Z September NOAA visual imagery).

The fourth of five significant tropical cyclones to form in September, Val was the only one not to intensify beyond a tropical storm. Like Ted (19W), which formed a day earlier on 18 September, Val was slow to intensify. After first being mentioned as a broad area of convection on the 190600Z September Significant Tropical Weather Advisory, Val became the subject of two Tropical Cyclone Formation Alerts before the first warning. The tropical storm passed to the west of Minami Tori Shima, weakened, and on 27 September recurved. Val's transition to an extratropical low prompted JTWC to issue the final warning at 270600Z.

E 135 140 145 150 155 160 165 170 175 180 185 190 195 200 205 210 215 220 225 230 235 240 245 250 255 260 265 270 275 280 285 290 295 300 305 310 315 320 325 330 335 340 345 350 355 360 365 370 375 380 385 390 395 400 405 410 415 420 425 430 435 440 445 450 455 460 465 470 475 480 485 490 495 500 505 510 515 520 525 530 535 540 545 550 555 560 565 570 575 580 585 590 595 600 605 610 615 620 625 630 635 640 645 650 655 660 665 670 675 680 685 690 695 700 705 710 715 720 725 730 735 740 745 750 755 760 765 770 775 780 785 790 795 800 805 810 815 820 825 830 835 840 845 850 855 860 865 870 875 880 885 890 895 900 905 910 915 920 925 930 935 940 945 950 955 960 965 970 975 980 985 990 995 1000



TYPHOON WARD (21W)

I. HIGHLIGHTS

The last of five significant tropical cyclones to form in September, Ward was unusual in that it underwent two major track changes and two significant acceleration episodes. As a result, it presented considerable difficulty to JTWC forecasters. Ward remained over open ocean its entire life and only posed a threat to maritime interests.

II. TRACK and INTENSITY

Ward developed from a tropical disturbance that formed in the trade wind trough just to the east of the international date line. This disturbance was initially detected on 24 September when its persistent convection attracted the attention of satellite analysts collocated with JTWC. Even though the circulation was located east of the international date line, it was mentioned on the 260600Z September Significant Tropical Weather Advisory because it was anticipated to become a significant tropical cyclone as it crossed into JTWC's area of responsibility. At 261100Z, JTWC issued a Tropical Cyclone Formation Alert. Seven hours later, the first warning was issued at 261800Z, based on a satellite-derived intensity estimate of 30 kt (15 m/sec) and the presence of a well-defined low-level circulation center on the animated satellite imagery, near the area of deep convection. After being upgraded to a tropical storm, at 270000Z, Ward continued to track west-northwestward, gradually slowing down as it approached a weakness in the subtropical ridge which had developed in response to an approaching mid-tropospheric short-wave trough. On 28 September, the tropical storm turned sharply to the north and accelerated as the trough to the north swept past. Then, as the subtropical ridge strengthened to the north, Ward again made a sharp turn, this time to a more westward track. The appearance of a visible eye on 01 October indicated that the typhoon had begun to intensify a second time, reaching a maximum intensity of 95 kt (49 m/sec) at 021200Z. During the following 24 hours, the diameter of the eye expanded from 20 to 70 nm (37 to 130 km) (Figure 3-21-1).

On 5 October, a break in the subtropical ridge developed near 155°E longitude, allowing Ward to recurve and accelerate northward. Extratropical transition ensued on 6 October as the system moved over colder waters north of the Kuroshio current. JTWC issued its final warning at 061200Z.

III. FORECAST PERFORMANCE

Ward's track proved to be difficult for JTWC forecasters to predict. Changes in the strength and orientation of the subtropical ridge led to two abrupt track changes, a series of deceleration and acceleration episodes, and a wide, arcing path as Ward's heading backed 130° from north-northeastward to west-southwestward between 29 September and 01 October. Typically, such a complex track would lead to larger than normal forecast errors, and this case was no exception. JTWC's overall mean track errors were 120, 255 and 360 nm (220, 470 and 665 km) for 24-, 48- and 72-hour forecasts, respectively. These results on average were 15% better than those of CLIPER, which provides the performance baseline for demonstrating skill. The primary reason for JTWC's acceptable performance was the guidance provided by the NOGAPS model which for Ward was impressive. However, this was not really appreciated until after the fact, when the overall mean track error for NOGAPS guidance was tabulated. It showed that NOGAPS bettered JTWC track forecasts at all time intervals except 12-hour forecasts. At 72-hours, the overall mean track errors for NOGAPS were 40% lower than JTWCs.

Overall intensity forecast errors were average; however, for a 2-day period starting at 300600Z, the 72-hour intensity forecasts were low by 15 to 30 kt (8 to 15 m/sec), as anticipated vertical shear did not occur to arrest intensification.

IV. IMPACT

Because Ward remained over open ocean during its lifetime, it only threatened maritime interests. No reports of any damage or loss of life were received.

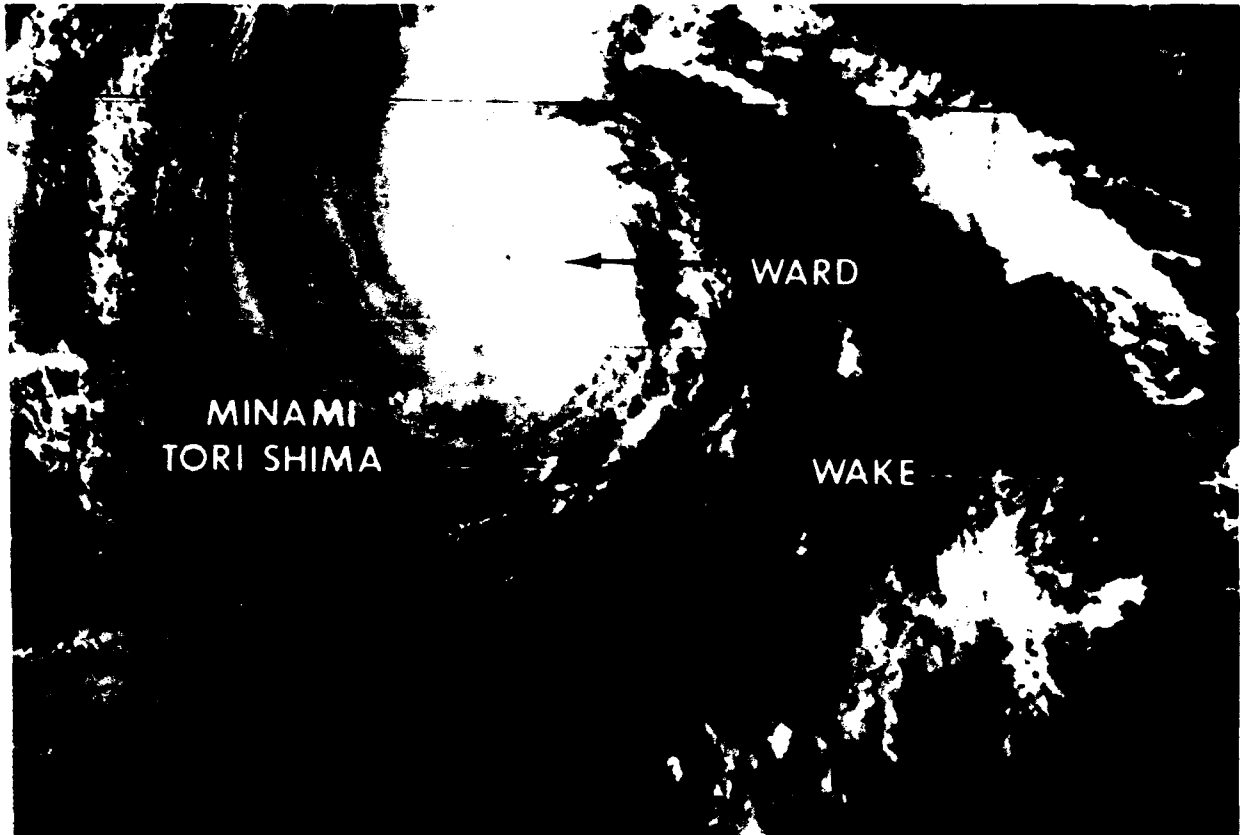
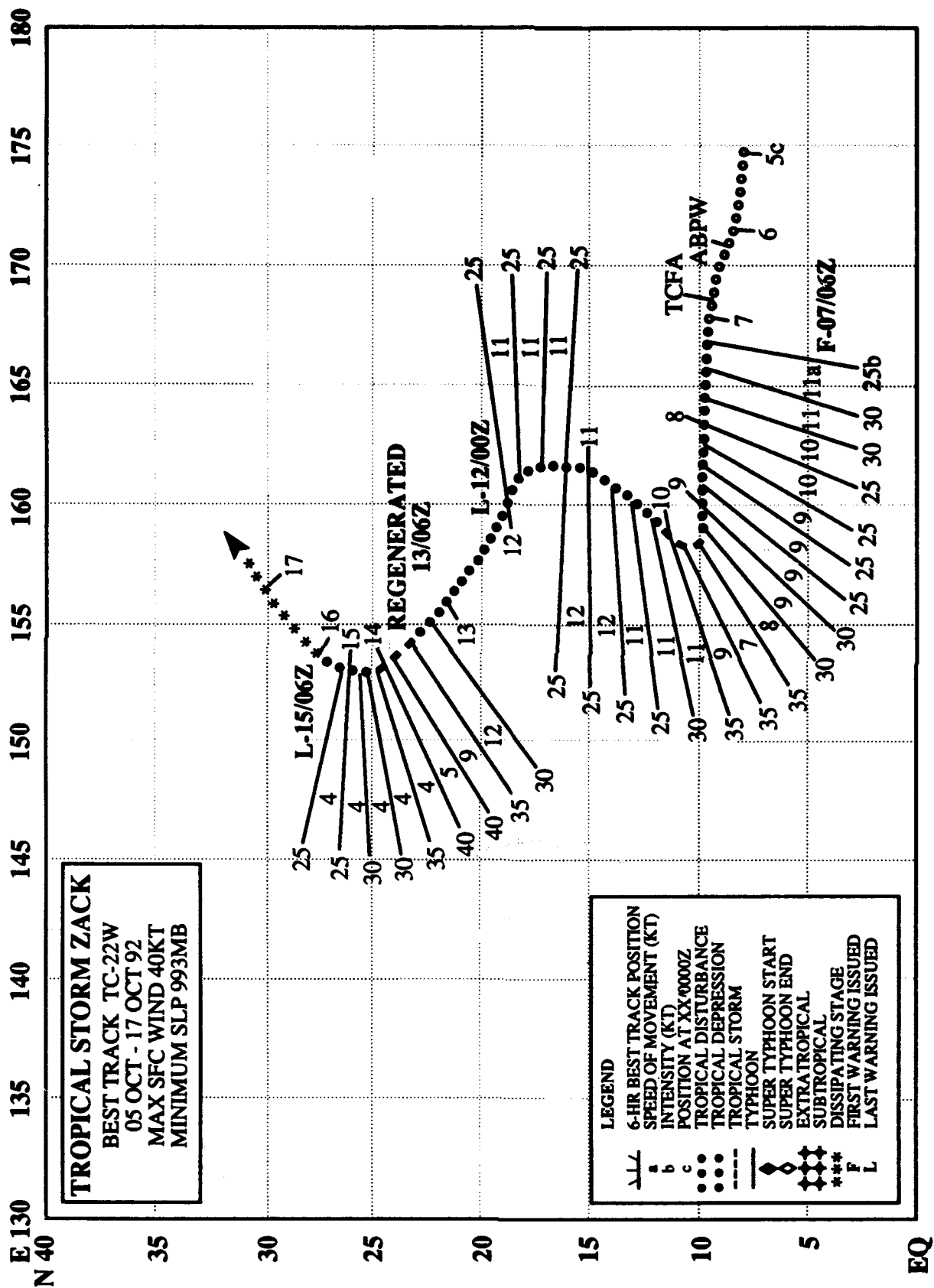


Figure 3-21-1. Ward's 55 nm (100 km) diameter eye is visible to the east of Minami Tori Shima (032232Z October DMSP visual imagery).



TROPICAL STORM ZACK (22W)

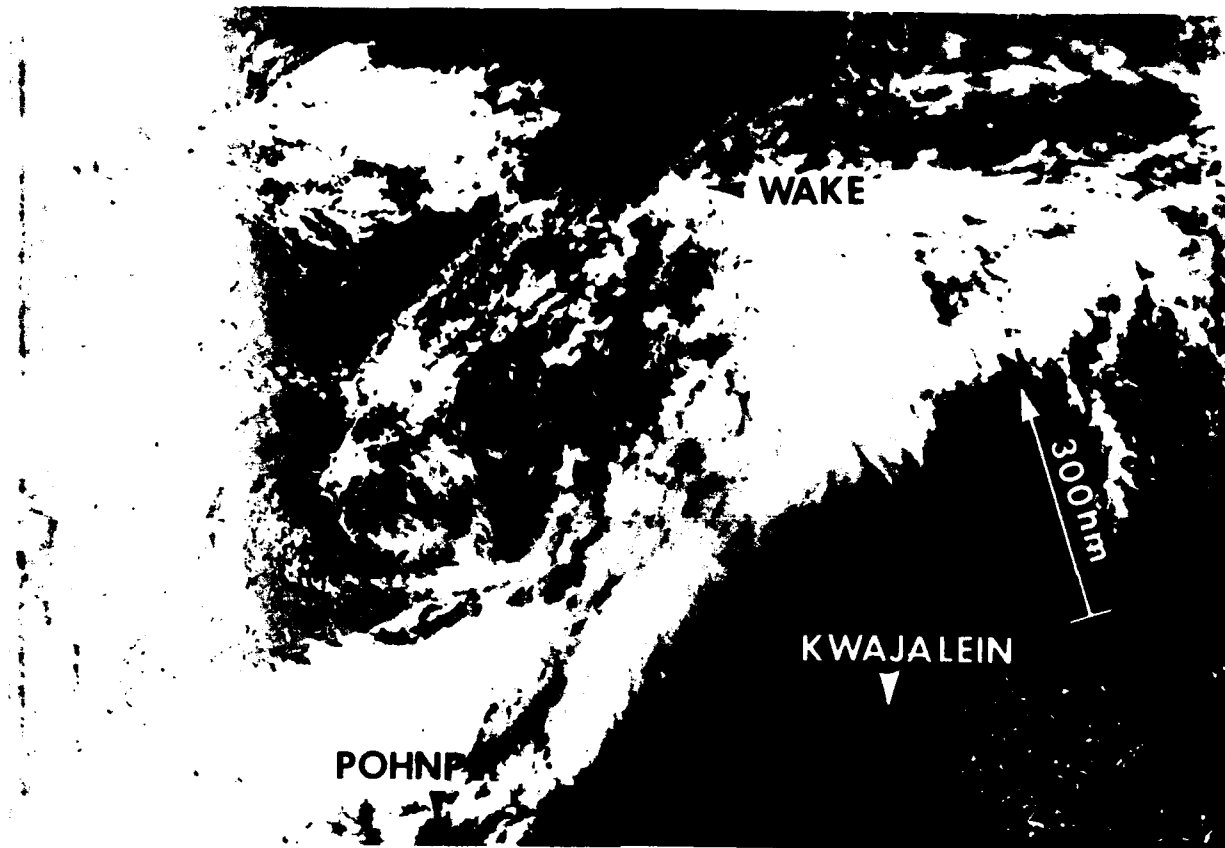
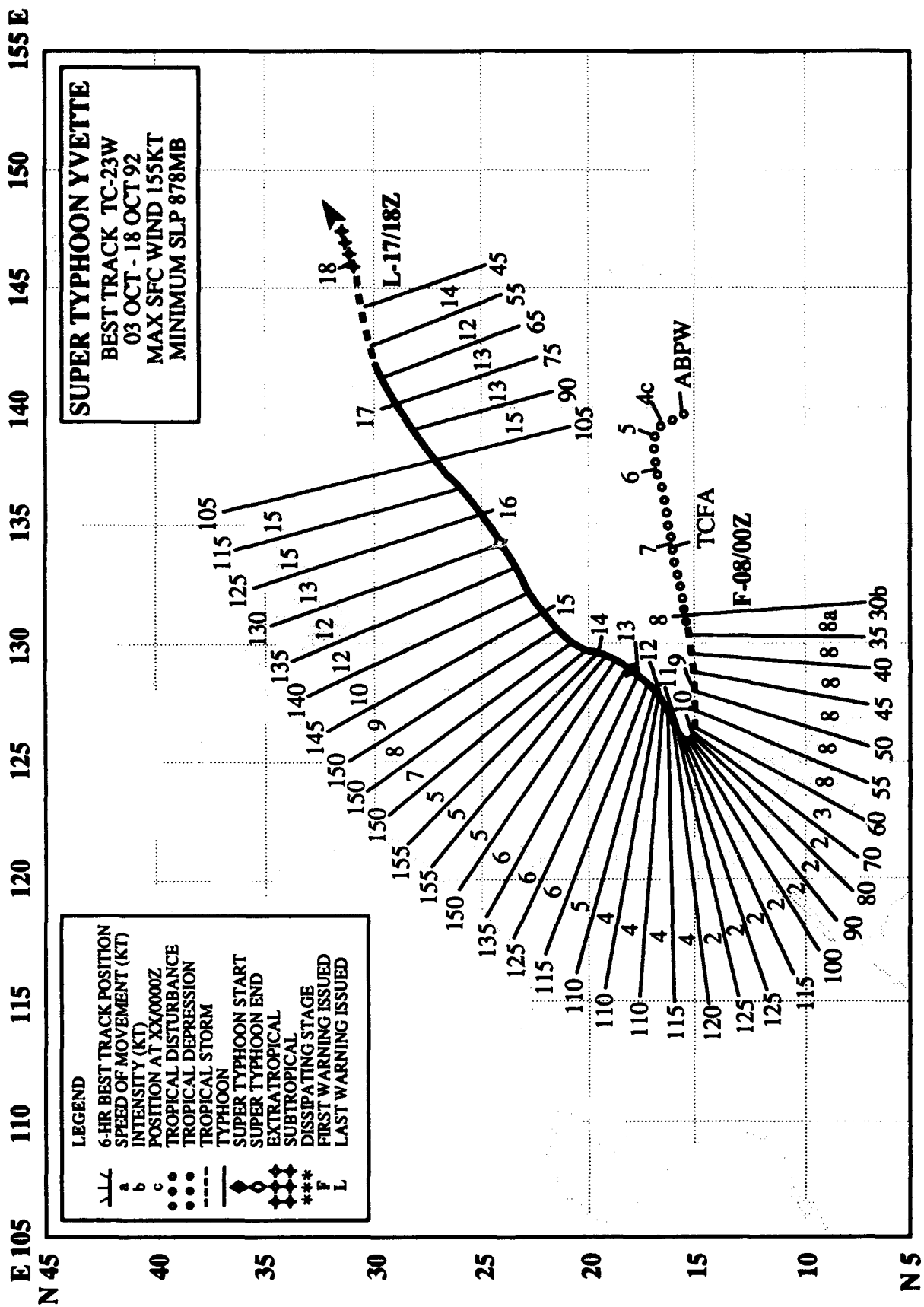


Figure 3-22-1. Cirrus cloud partially obscures Zack's exposed low-level circulation center, which appears at the western edge of a band of deep convective cloudiness associated with enhanced low-level southwesterly flow.

The first of eight significant tropical cyclones to form in October, Zack was also the first to threaten the southern Mariana Islands since Omar's (15W) devastating passage across Guam in August. Initial JTWC track forecasts towards the southern Mariana Islands and Guam were based on continued west-northwestward movement along the axis of the monsoon trough. On 9 October, however, a monsoon surge of deep southwesterly winds resulted in an abrupt track change to the north-northeast for Zack. As the tropical storm weakened, the low-level circulation center became difficult to locate, and JTWC issued a final warning on Zack at 120000Z. However, by the following day, the convection and organization of the system had increased, prompting JTWC to issue a "regenerated" warning at 130600Z. Zack briefly reintensified to a tropical storm before transitioning into a subtropical system and dissipating over the ocean. No reports of damage or injury were received.



SUPER TYPHOON YVETTE (23W)

I. HIGHLIGHTS

The third Northwest Pacific tropical cyclone of 1992 to achieve super typhoon intensity, Yvette was an action-packed system which posed many forecast challenges. In the span of two weeks, Yvette developed in a moderately sheared environment, made a run toward Luzon as it intensified to a typhoon, stalled, executed a major, 150-degree track change, weakened, reintensified to a super typhoon, and transitioned to an extratropical cyclone. This tropical cyclone marked the beginning of the 1992 super typhoon season - October being the month of most frequent super typhoon occurrence.

II. TRACK AND INTENSITY

On 3 October, the monsoon trough extended from the South China Sea eastward across the southern Philippine Islands and Philippine Sea, through the southern Mariana Islands, and northeastward to Typhoon Ward (21W), located 1080 nm (2000 km) northeast of Guam. The persistence of convective activity along the trough in the Philippine Sea prompted JTWC forecasters to mention a broad tropical disturbance on the 030600Z Significant Tropical Weather Advisory. Due to moderate vertical wind shear, the low-level circulation center of this tropical disturbance, which was to become Yvette, remained poorly defined. On 5 October, the amount of convection started to increase around the center. At 070600Z, a Tropical Cyclone Formation Alert was released as the convective organization was rapidly improving. When a comma-shaped cloud mass developed in association with the center, JTWC issued the first warning for Tropical Depression 23W at 080000Z. With the rapid appearance of a central dense overcast, the system was upgraded to a tropical storm at 080600Z.

As Yvette tracked westward under the steering influence of the mid-level subtropical ridge to the north, it steadily intensified. At 091200Z, rapid intensification commenced with Yvette reaching typhoon intensity at 091800Z. The intensification process continued until the typhoon peaked at 125 kt (64 m/sec) at 110000Z (Figure 3-23-1). Coincident with the onset of rapid intensification, the typhoon virtually stalled and slowly executed a major track change to the northeast in conjunction with the subtropical ridge being weakened by the deepening and retrogression of the mid-level East Asian trough. After peaking, Yvette weakened slightly until 121200Z, when rapid intensification again started. This process of premature, low latitude recurvature and subsequent intensification has been described by Guard (1983). At the same time, a large plume of cirrus appeared, extending from the typhoon's central dense overcast to the frontal cloudiness to the north and northeast over Japan. By the time that Yvette had reached its maximum intensity of 155 kt (80 m/sec), at 131800Z, the extensive plume of cirrus to the northeast had almost disappeared, suggesting some relationship between the rapid intensification and the cirrus plume.

At 140600Z, the super typhoon (Figure 3-23-2) reached a position where it could proceed around the western end of the mid-level subtropical ridge. As vertical wind shear from southwesterlies aloft increased, Yvette's intensity decreased slowly until 16 October, then decreased more rapidly. At 171800Z, just before Yvette completed its transition to an extratropical low pressure system, JTWC issued the final warning.

III. FORECAST PERFORMANCE

The overall mean errors for the track forecasts were 85, 190 and 340 nm (155, 355 and 630 km) for 24, 48 and 72 hours, respectively. These errors were essentially the same as those for CLIPER, which is used as a performance baseline. Problems that prevented JTWC from outperforming CLIPER were: 1) the stall and major track change from west to northeast when Yvette was approaching Luzon.

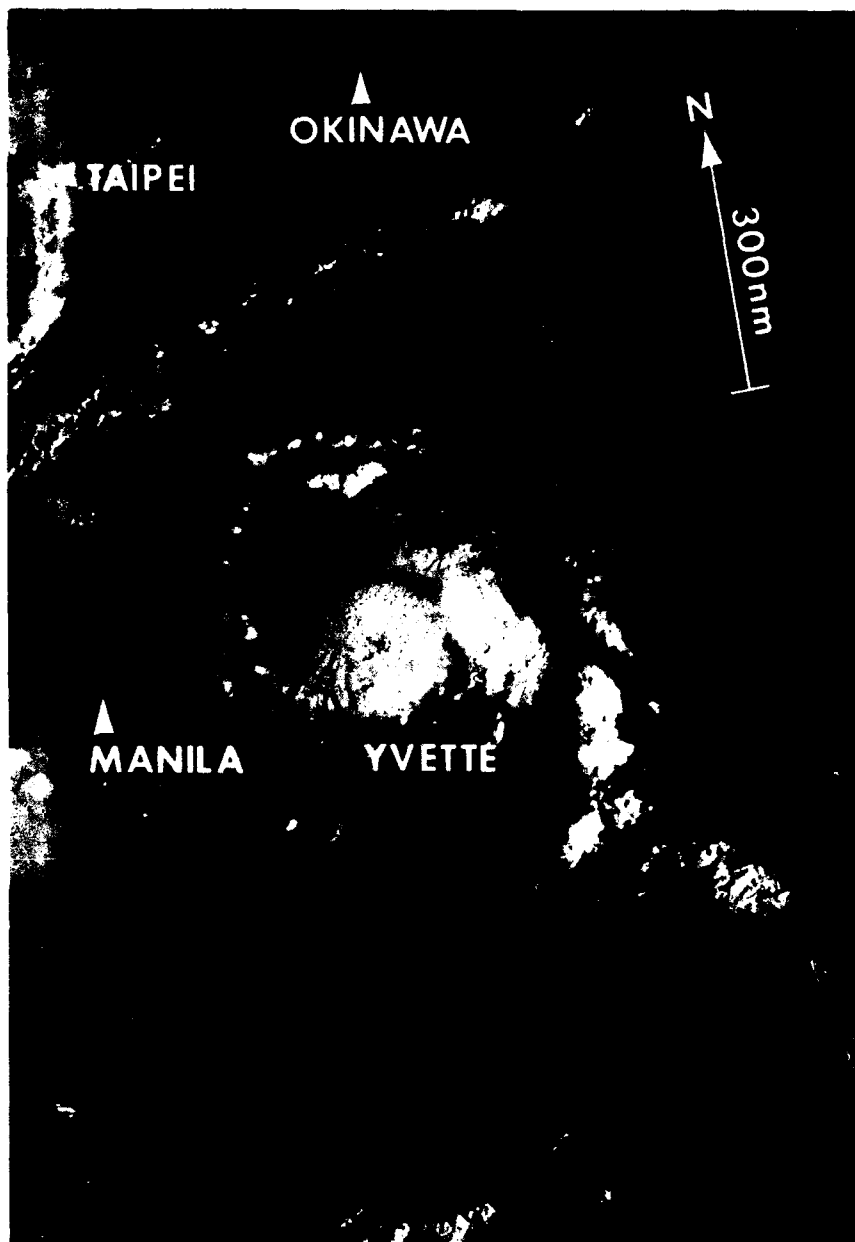


Figure 3-23-1. The tops of cumulonimbus embedded in Yvette's eye wall penetrate the cirrus overcast (100025Z October DMSP visual imagery).

The northeastward drift of Yvette was mentioned as an alternate scenario and then abandoned as the system appeared to be accelerating westward shortly before it stalled. This acceleration was not real, but resulted from differences between the raw satellite data based on poorly defined upper-level cloud top fixes and the location of the low-level circulation center, which was totally obscured by the high cloud shield; 2) the reintensification-to-super-typhoon episode was not considered as a possibility until six hours before it occurred. This was due primarily to an over-reliance on extrapolating the ongoing intensity trend into the future without any reliable intensity guidance from the numerical models to contradict that assumption; 3) the rapid rate of weakening, starting on 16 October, was under forecast again based on extrapolation of the earlier trend. In this case, numerical models did predict strong shear over Yvette but, it appeared to be a system that could remain intact much longer than it did in the presence of moderate-to-strong upper-level winds; and, 4) acceleration was over forecast during the period Yvette was becoming extratropical. This was caused by the slowing of the low-level circulation center after its decoupling from the from the mid- to upper-level center has occurred.

In retrospect and with regard to intensity forecasting, the first rapid intensification episode was successfully identified, before it occurred, based on the results of a study of tropical cyclone intensity climatology and application of a satellite pixel counting technique (Zehr, 1987).

The numerical model, NOGAPS, performed very well, identifying the exact longitude where Yvette would stall, and then its subsequent motion until it moved under strong mid- to upper-level wind flow on 11 October.

VI. IMPACT

Super Typhoon Yvette remained over open ocean its entire life, and no reports of fatalities or damage were received at JTWC.

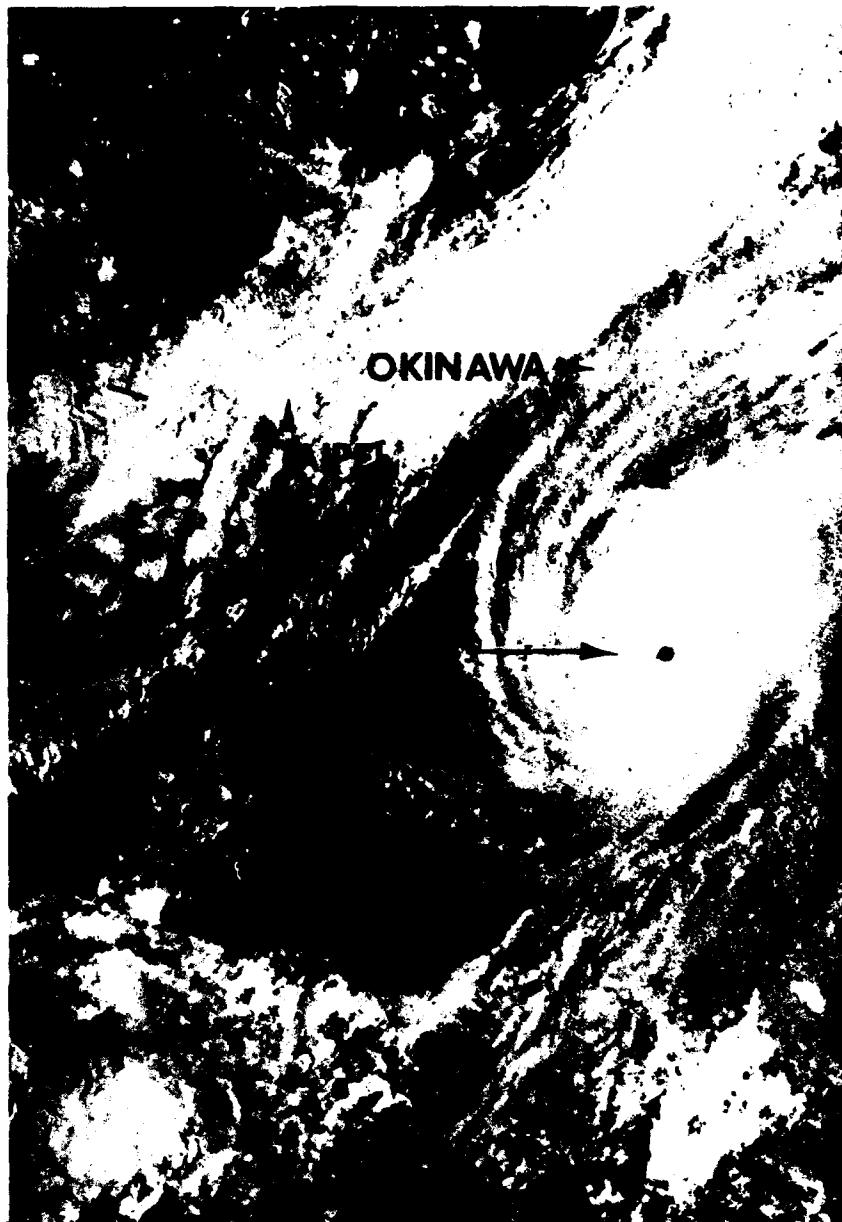
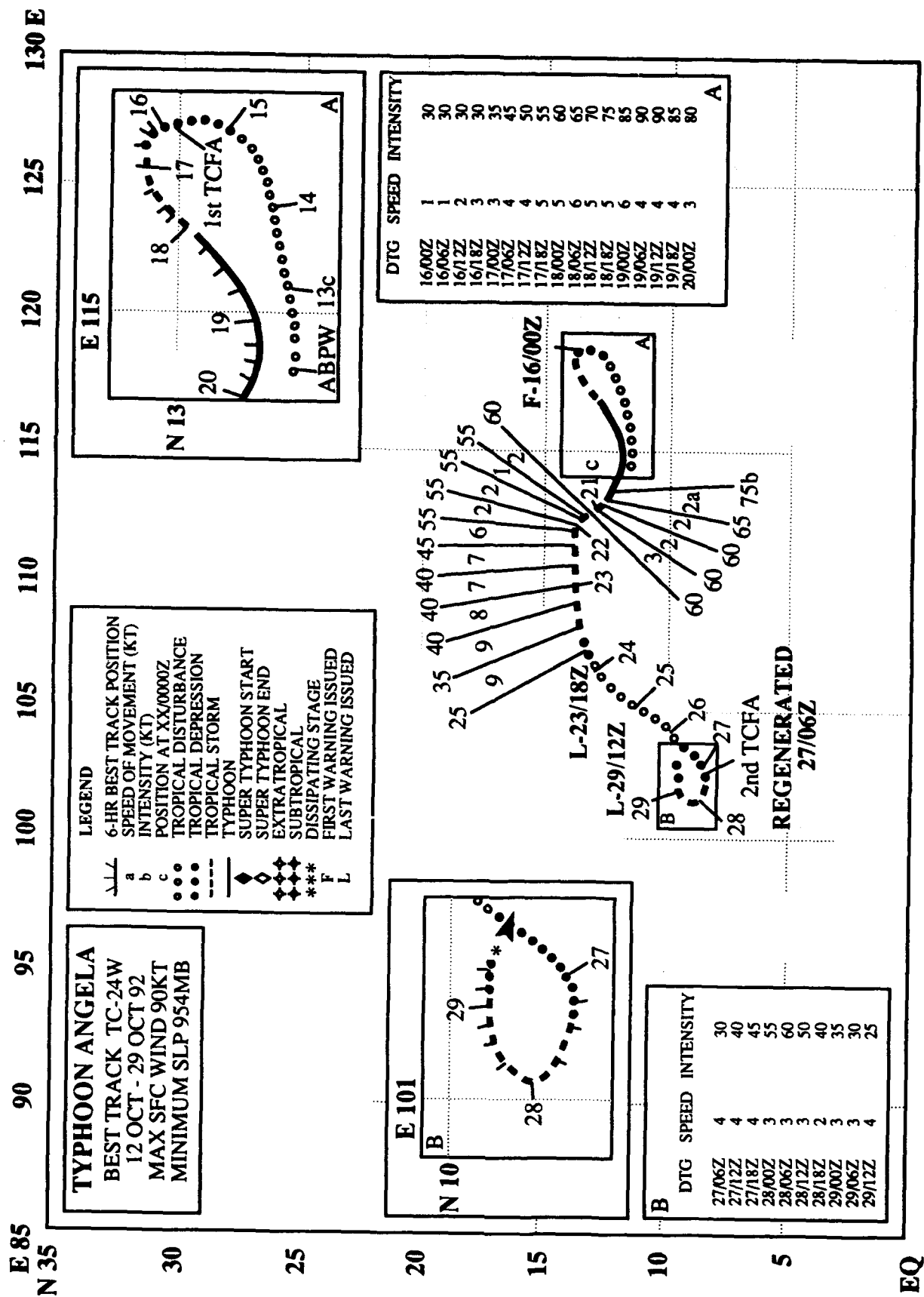


Figure 3-23-2. A moonlight image of Super Typhoon Yvette near peak intensity. Note the city lights of Shanghai, Taipei, Manila and of cities on Okinawa (141235Z October DMSP nighttime visual imagery).



TYPHOON ANGELA (24W)

I. HIGHLIGHTS

The third of eight significant tropical cyclones to form in October, Angela developed in the South China Sea, moved east, reversed course and struck southern Vietnam, crossed southern Indochina, reintensified to a severe tropical storm in the Gulf of Thailand, tracked through a clockwise loop, and finally dissipated over water. While anchoring the western end of a monsoon trough, Angela became part of a four storm outbreak along with Brian (25W), Colleen (26W) and Dan (27W).

II. TRACK AND INTENSITY

Developing in the South China Sea in the monsoon trough that trailed southwestward from Super Typhoon Yvette (23W), the tropical disturbance, which became Angela, was first mentioned on the 120600Z October Significant Tropical Weather Advisory as an area of persistent convection. The tropical disturbance drifted slowly eastward along the edge of the deep southwesterly flow on the south side of the trough. On 15 October, as Yvette (23W) reached the axis of the subtropical ridge and began recurving to the northeast, the vertical wind shear over the disturbance weakened. As a consequence, the disturbance began to intensify, prompting JTWC to issue a Tropical Cyclone Formation Alert (TCFA) at 151830Z, and the first warning at 160000Z.

With Yvette's (23W) departure from the tropics, the monsoon trough moved south to reestablish itself east-southeastward across the central Philippines and into the Caroline Islands. As this shift occurred, the orientation of the trough axis changed from southwest/northeast to east-southeast/west-northwest, and Tropical Depression 24W reversed course and slowly headed westward. Angela's further consolidation required JTWC to upgrade the 170000Z warning to tropical storm intensity, and later typhoon intensity at 180000Z.

By 18 October, Angela also became the anchor-low for the western end of the monsoon trough that extended eastward through Colleen (26W), Brian (25W), and into the southern Marshall Islands. As the northeasterly winds aloft increased, Angela's low-level circulation became partially exposed to the east of the deep central convection, and forecasters downgraded the typhoon to a tropical storm at 201800Z. Further weakening ensued as the tropical cyclone moved westward into southern Vietnam (3-24-1). This necessitated another downgrade to a tropical depression and, six hours later, a final warning at 231800Z, as the low-level center dissipated over land.

For the next four days the mid-level remnants of Angela persisted without central convection and moved southwestward across southern Indochina. Upon entering the Gulf of Thailand on 27 October, the cyclonic circulation slowly regained its convection and deepened through the lower troposphere. Another TCFA was issued by JTWC at 270330Z, and immediately followed by a regenerated warning on 270600Z. As the compact circulation of Angela intensified and began to execute a clockwise loop in the central Gulf of Thailand, it moved through a group of manned gas platforms which provided invaluable surface and radar reports. The reports from the Satun Station gas platform (9.3°N 101.4°E) proved to be important for describing the passage of this midget tropical cyclone. The 280240Z depiction of the Satun Station radar display in Figure 3-24-2 and the wind reports (Figure 3-24-3), which included the 70 kt (36 m/sec) peak at 280440Z, prompted JTWC forecasters to upgrade the 280600Z warning to typhoon intensity. Later, during post analysis, this 6-hour maximum at typhoon intensity was reduced to a severe tropical storm intensity of 60 kt (31 m/sec) based on the relatively high surface pressures near 1000 mb, other wind reports in the area, and the determination that the 70-kt

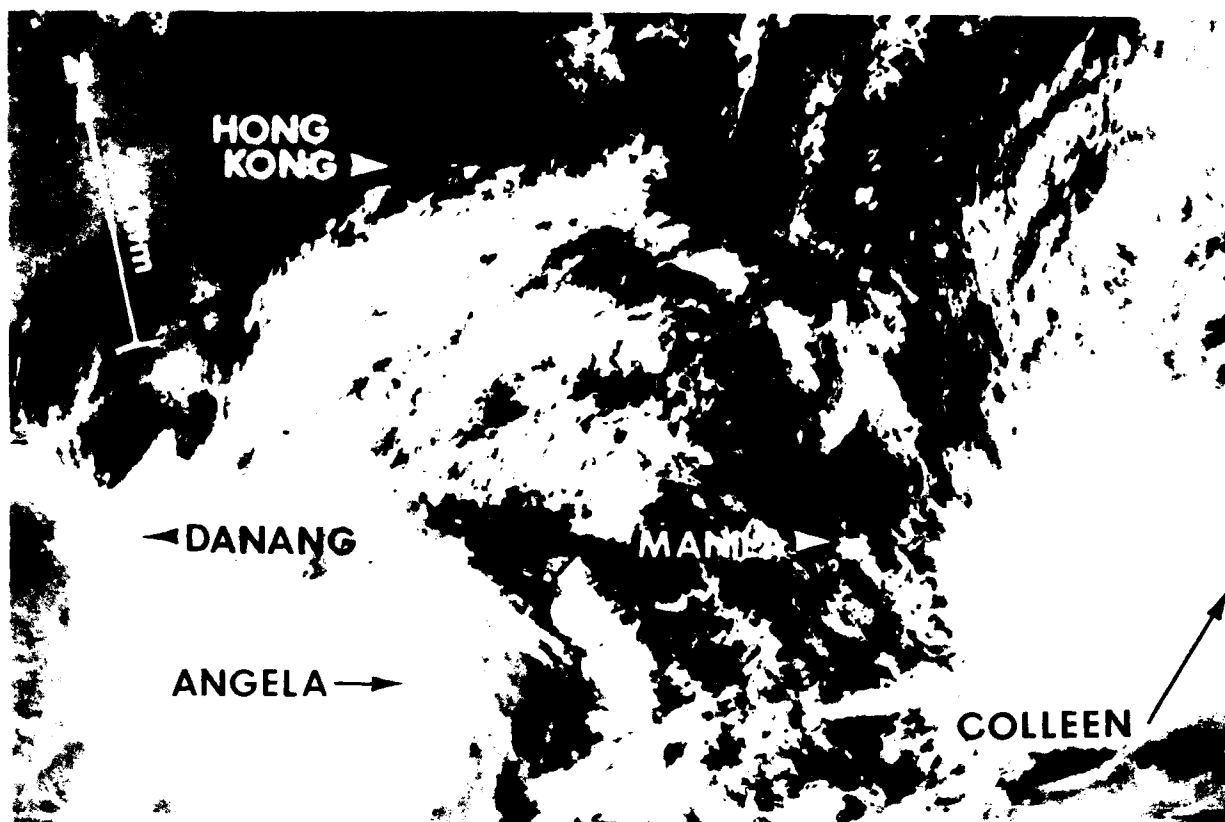


Figure 3-24-1. Twelve hours after being downgraded to a tropical storm, Angela churns westward across the South China Sea towards southern Vietnam. Part of Colleen's (26W) dense overcast is visible at the lower right of the picture (210122Z October DMSP visual imagery).

wind report was averaged over a period of less than one minute. After this peak, Angela's organization and intensity rapidly weakened due to upper-level wind shear until the "second" final warning was issued by JTWC at 291200Z as the tropical cyclone dissipated over the Gulf.

III. FORECAST PERFORMANCE

The overall mean track forecasting errors showed that JTWC's performance was better than average and showed skill in comparison with CLIPER, which is used as the baseline for performance. With overall errors of 80, 145 and 180 nm (145, 265 and 330 km) at 24, 48 and 72 hours, respectively, JTWC bettered CLIPER's performance by 30%. Initially, due to the relatively weak steering flow affecting Angela, track forecast guidance was poor. However, once Angela began to move westward toward the Vietnamese coast, most forecast aids did well. Later, in the Gulf of Thailand, the track guidance tended to track Angela across the Malay Peninsula and into the Bay of Bengal.

IV. IMPACT

In southern Vietnam, at least seven people were reported missing and 17 others injured. Angela's torrential rains caused extensive flooding, loss of crops, livestock and fishing boats, and damage to rail lines and roads. In Thailand, there were two fatalities and seven people were reported missing. Heavy rains and flooding resulted in at least 600 houses being destroyed. Angela posed a significant threat in the Gulf of Thailand, where manned gas platforms were forced to evacuate as Angela intensified and moved into the area. All platform evacuations proceeded smoothly and no reports of damage or injuries were received.

The weather and radar reports from the manned gas platforms in the Gulf of Thailand presented forecasters at JTWC a unique opportunity to gather data on the rainbands and compact wind field associated with a very small tropical cyclone.

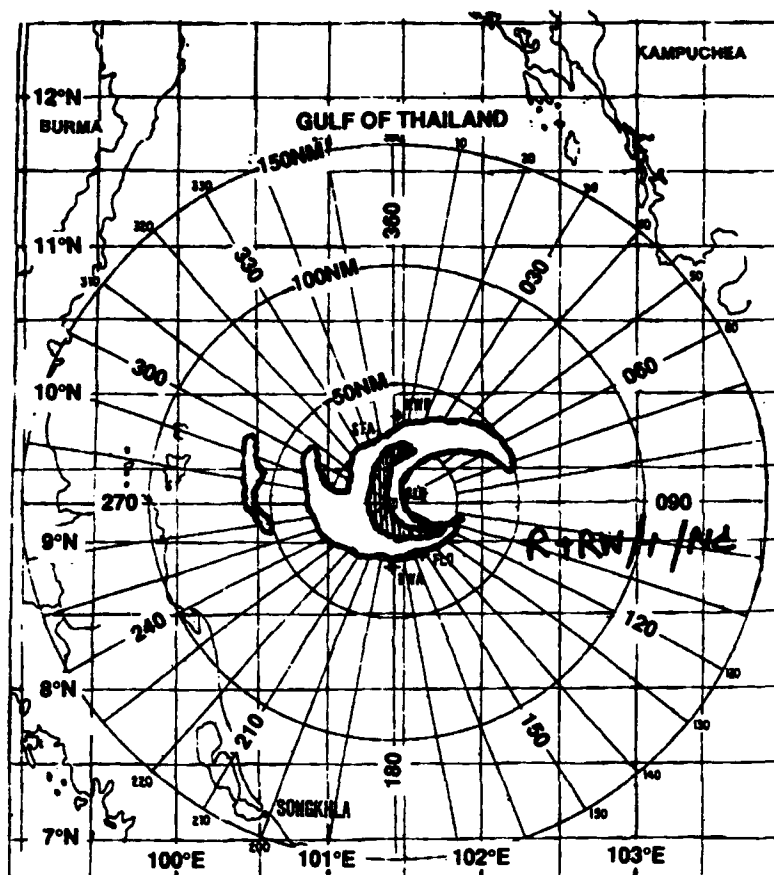
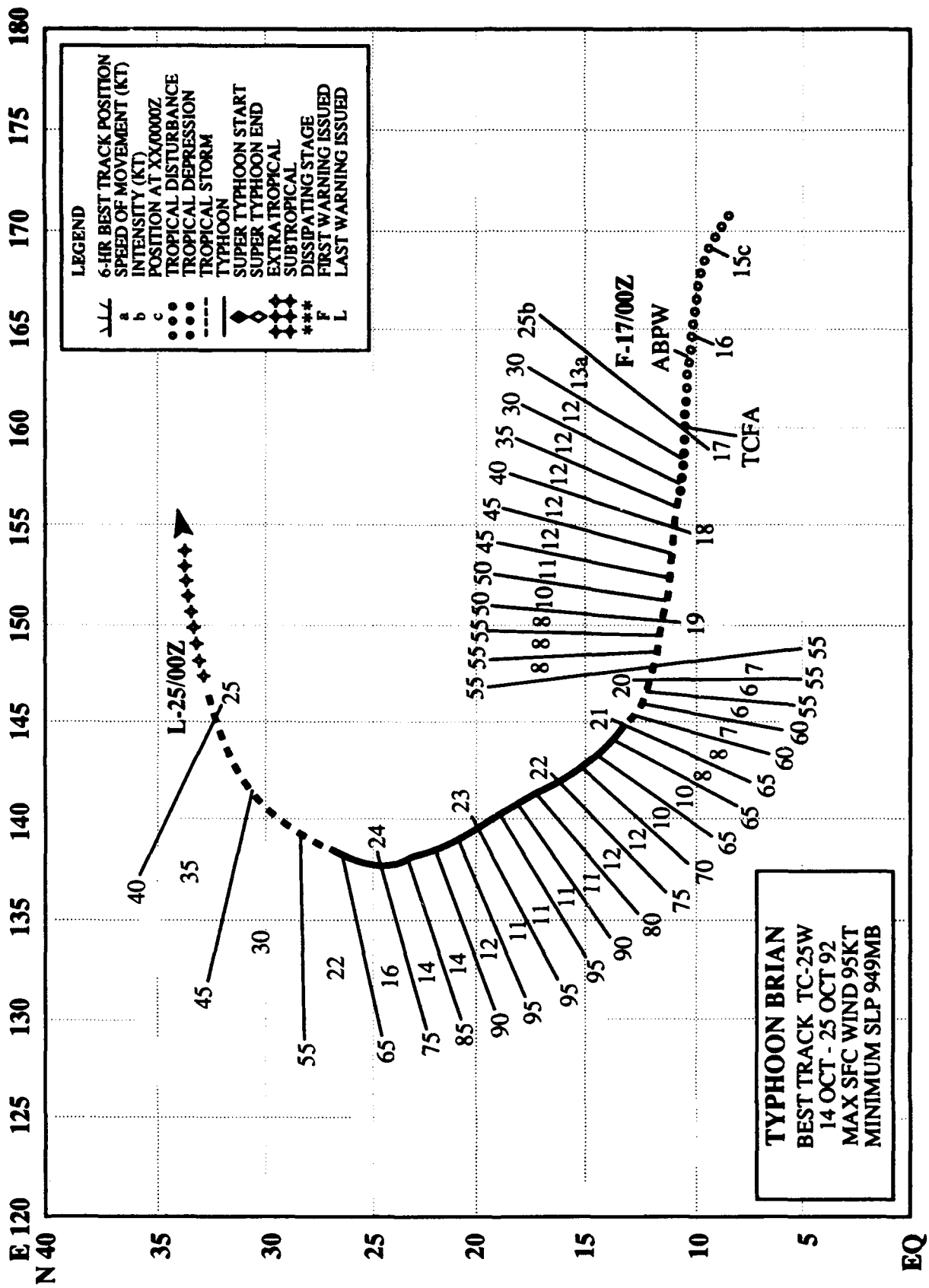


Figure 3-24-2. Angela's tightly curved rainbands as seen on radar from the Satun Station gas platform located at 9.3°N and 101.4°E (radar depiction courtesy of UNOCAL Thailand, Ltd.).

28 OCTOBER 1993							
Time (Z)	00	01	02	03	04	05	06 07
Pressure (mb)	1002.3	1001.5	m	m	998.1	1000.1	1001.9 1000.9
Wind (kt)							
Wave Height (m)	5.2	5.3	m	m	6.2	5.0	5.0 3.9

Figure 3-24-3. Wind reports which are plotted to the nearest hour for the Satun Station gas platform (9.3°N, 101.4°E) for the 24-hour period commencing 270900Z. Angela's passage close by the platform is reflected by the storm force winds, wind shift, and lower pressures from 280300Z to 280600Z. The lowest pressure reported was 998.1 mb at 280400Z, however, the pressure an hour earlier, which was missing from the data set, could have been considerably lower (data courtesy of Uncope Thailand, Ltd.).



TYPHOON BRIAN (25W)

I. HIGHLIGHTS

Brian was part of the four storm outbreak in October that included Angela (24W), Colleen (26W) and Dan (27W). Forming in the southern Marshall Islands, Brian moved west-northwestward and intensified to a typhoon as it passed across Guam. For Guam, it was the second eye passage in less than two months - Omar (15W) was the first. Later, Brian underwent binary interaction with Typhoon Colleen (26W), subsequently recurved, and finally transitioned to an extratropical system.

II. TRACK AND INTENSITY

JTWC began monitoring the tropical disturbance, that would become Typhoon Brian, in the southern Marshall Islands on 14 October. After an increase in the amount and organization of the cloudiness, the tropical disturbance was mentioned on the 161600Z Significant Tropical Weather Advisory. Initially the potential for development was considered to be poor. However, a rapid increase in convection prompted JTWC to reissue the Advisory at 161800Z, and the area's potential for development was upgraded to fair. A Tropical Cyclone Formation Alert followed at 162223Z as organization continued to improve. Anticipating continued consolidation within the small compact cloud system, and assessing the potential for subsequent rapid intensification as good, JTWC issued the first warning at 170300Z.

The tropical cyclone was upgraded to Tropical Storm Brian at 171800Z. As it approached Guam, Brian's convection increased markedly during the nighttime hours. With no synoptic data reports near the center of the small circulation and impressive convective flare-ups for two nights running on the satellite imagery, there was a question on the second night: "Was rapid intensification taking place or not?" When satellite data gave conflicting information concerning the intensity of the storm, JTWC elected to go with the higher intensity that indicated that rapid intensification was occurring. Subsequently, Brian was upgraded to typhoon intensity at 190600Z based on the higher satellite intensity estimates. As the tropical cyclone approached Guam on the morning of 21 October, it became apparent that Brian was a smaller than expected system, and that its intensity and area affected by the high surface winds were significantly less than forecast. Brian was, in fact, a midget typhoon with 65-kt (33-m/sec) sustained winds.

The extended outlook for the track was more straight forward. For two days prior to Brian hitting Guam, JTWC predicted a direct hit. As Brian approached Guam, fixes from satellite imagery and the Federal Aviation Administration flight control radar at Mount Santa Rosa showed that as the tropical cyclone slowed, it began to exhibit erratic motion. Despite the erratic motion, JTWC continued to predict a direct hit, and actually pin-pointed the southern half of the island as the target. The leading edge of the small, 10 nm (19 km) diameter eye came ashore just northeast of DanDan at 202350Z, and later exited near Orote Point at 210300Z (Figure 3-25-1).

As Brian's eye came across Guam, an interesting phenomena was observed by residents on the west side of the island from Orote Point northward to Taguac. Preceding the onset of the primary area of light-and-variable winds within the eye, there was another low pressure area — a precursor — where the winds lessened prematurely and the sky lightened. This precursor event was followed by a band of heavy rain and wind. Figure 3-25-2 illustrates the merge of the leeside low with the eye of Brian. The event appears on the Nimitz Hill microbarograph trace (Figure 3-25-3) as a drop in pressure (at Point A) followed by a rise in pressure associated with the squall, and then another drop in pressure (at Point B).

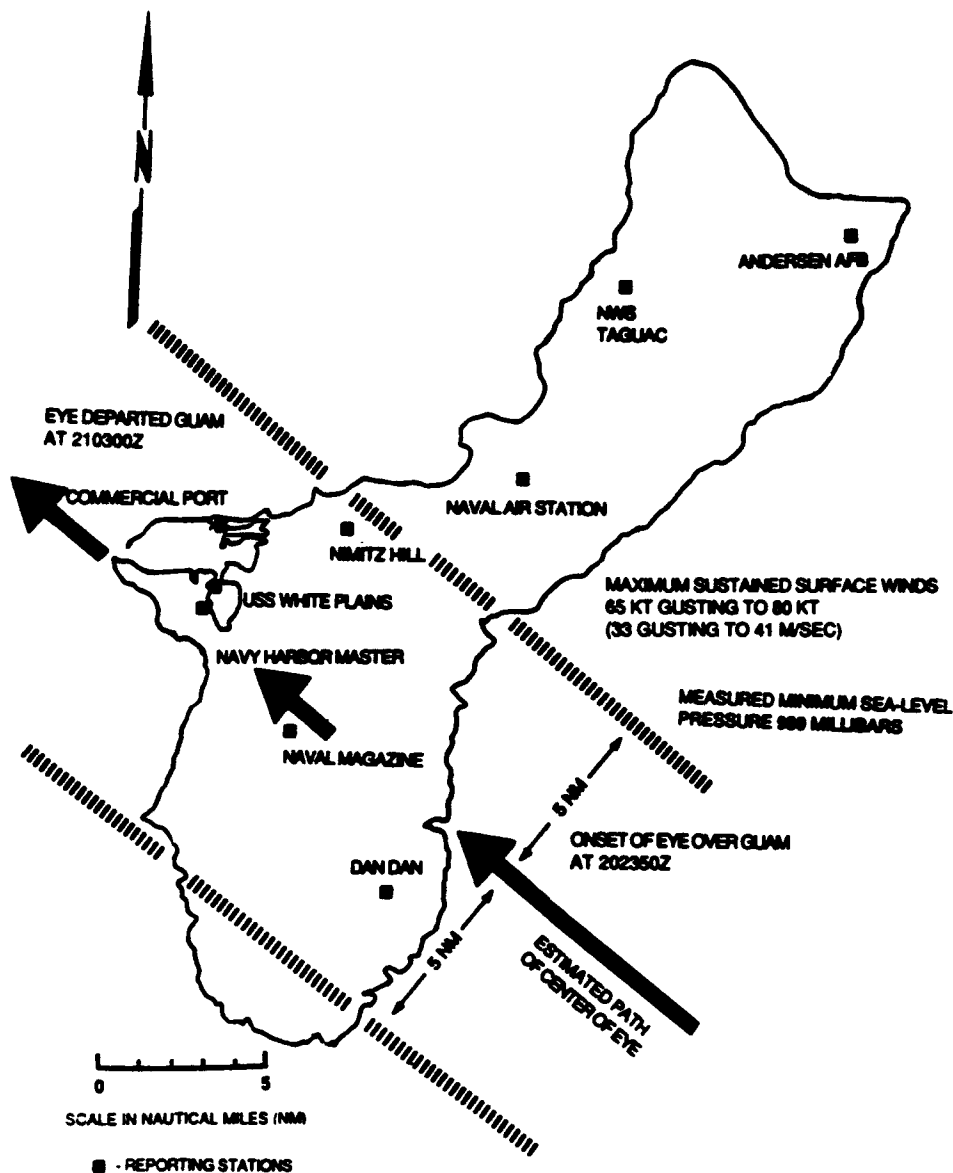


Figure 3-25-1. Graphic of Brian's 10 nm (19 km) diameter eye passage across Guam on 21 October.

What is suggested was that Brian, which was small and at minimal typhoon intensity, encountered a barrier, the island of Guam, in its path. The wind field within the core region adjusted to the barrier and a lee side low, or secondary circulation, formed ahead, and to the west of, the primary circulation center. As the eye approached, the lee side low shrunk in size, consolidating over the northwest portion of Guam. Once the eye moved to the west side of the island, strong low-level winds trying to flow toward the low pressure of the eye quickly returned to normal, and Brian regained its more normal form and intensified. During this time, Guam's maximum sustained 1-minute winds of 65 kt (33 m/sec) gusting to 80 kt (41 m/sec) were recorded at Nimitz Hill, which is 650 feet (200 m) above sea level. Typhoon force winds may also have occurred in the east coastal areas, but the no wind recording were available at these locations. The minimum sea-level pressure reading of 989 mb was recorded in the eye by the

fast supply ship **U.S.S White Plains**, which was moored in Apra Harbor. While this pressure is too high to support typhoon-force winds for a normal sized tropical cyclone, computations indicate that it was sufficient to support typhoon-force winds for a cyclone the size of Brian

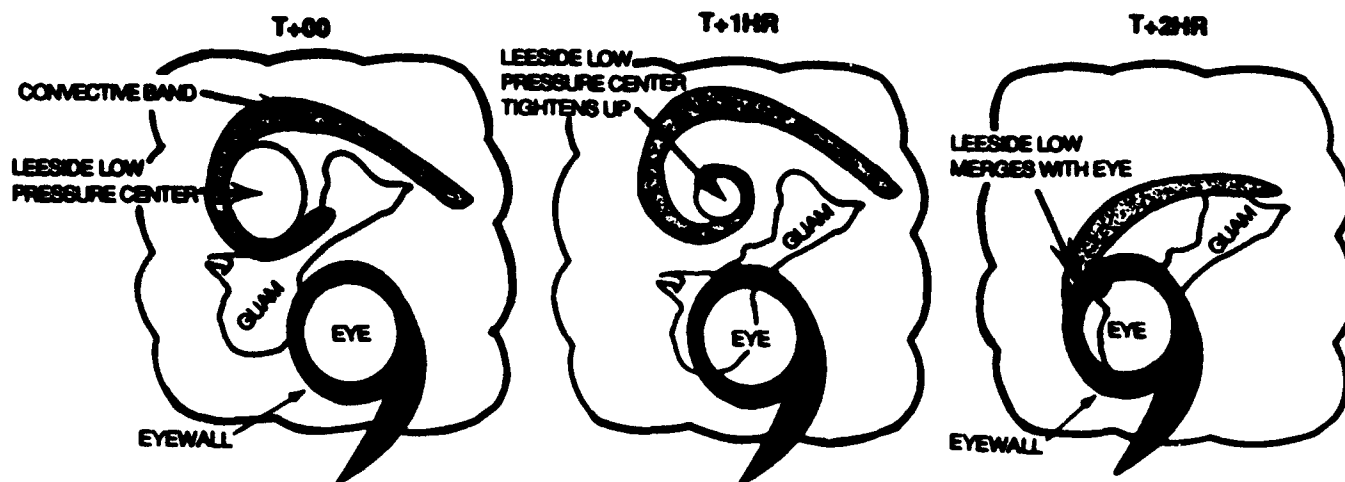


Figure 3-25-2. Sequence of events illustrating the merger of a low on the leeward side of Guam with the eye of Brian.

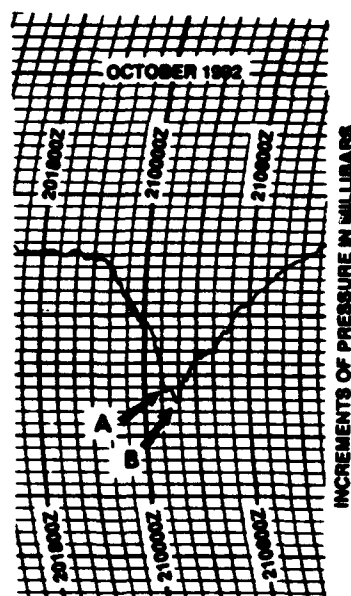


Figure 3-25-3. Microbarograph trace from the Nimitz Hill, Guam during the passage of Typhoon Brian. Point A is the passage of the leeward low that preceded the passage of the eye at point B.

On 21 October, as Brian moved into the Philippine Sea, it became involved in a binary interaction for the next three days with Typhoon Colleen (26W) which was located to the west (Figure 3-25-4). Brian peaked at 95 kt (49 m/sec) at 221800Z, and on 24 October, the typhoon recurved south of Japan, accelerated, and transitioned to an extratropical low. The final warning was issued by JTWC at 250000Z.

III. FORECAST PERFORMANCE

The overall mean track errors for JTWC were 90, 140 and 225 nm (170, 255 and 415 km) for the 24-, 48- and 72-hour forecasts, respectively. These were 25-42% lower than JTWC's long term average and approximately 25% better than those of CLIPER, which is used as a baseline for determining skill. Typhoon Colleen (26W), which was about 1000 nm (1850 km) to the west of Brian, added a measure of difficulty and uncertainty to both the intensity and track forecasts for Brian. Colleen's outflow aloft blew eastward across Brian and impeded the formation of Brian's upper level anticyclone, which may have slowed the intensification of Brian's midlevel circulation. Also, the induced ridging between the two cyclones probably contributed to the slowing and erratic motion of Brian's track as it neared Guam. Finally, the binary interaction between the typhoons was of significant concern until Brian recurved.

In contrast to the track forecasts, the intensity forecasts were poor. For a four day period starting at 171800Z, the 72-hour outlooks were consistently 25 to 55 kt (13 to 28 m/sec) too high. And for two days before Brian crossed Guam, the initial warning intensities were determined to be 25 to 35 kt (13 to 18 m/sec) high. The high intensity forecasts for four days resulted from anticipation of rapid intensification that did not occur, and were compounded, for two of the four days, by high values for intensity on the initial warnings.

IV. IMPACT

Damage on Guam was much less than would have occurred had Typhoon Omar not hit less than 2 months earlier. Omar destroyed most structures that a weaker storm might have damaged or destroyed. Schools and businesses were closed for two days as the typhoon passed. Some power lines were blown down, and there were isolated reports of damage in the central portion of the island. The agriculture industry suffered the most, as the coastal regions received considerable salt water spray damage.

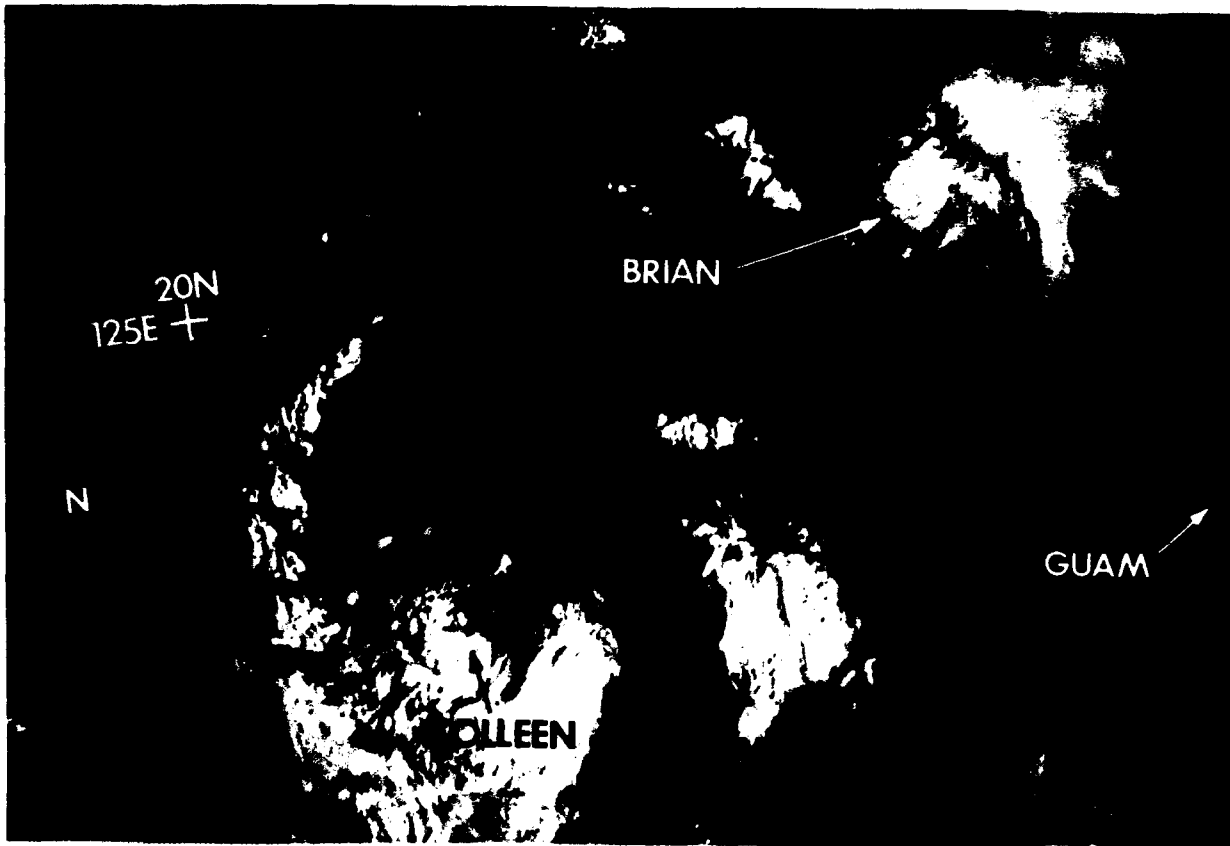
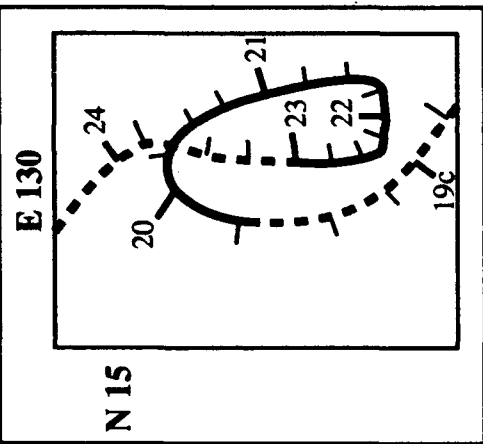


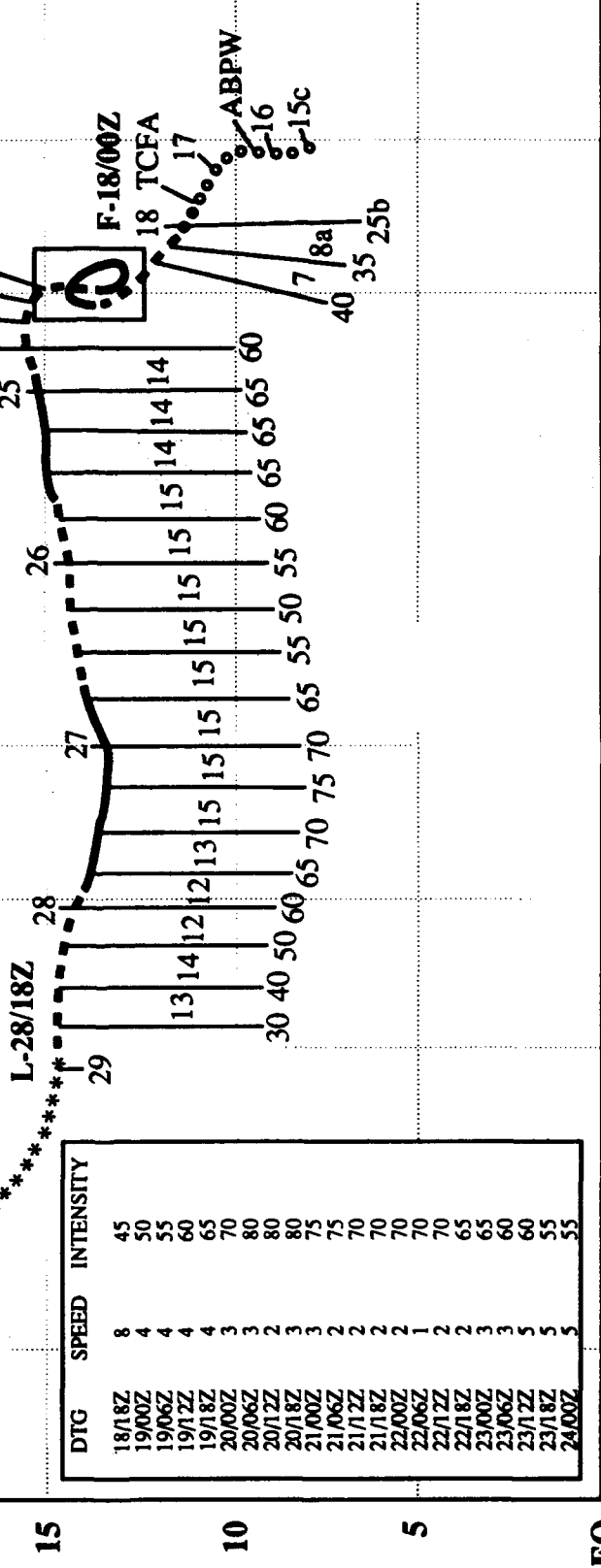
Figure 3-25-4. Brian undergoes binary interaction with Typhoon Colleen (26W) (230019Z October DMSP visual imagery).

N 30 E 90 95 100 105 110 115 120 125 130 135 140 E

TYPHOON COLLEEN
 BEST TRACK TC-26W
 15 OCT - 29 OCT 92
 MAX SFC WIND 80KT
 MINIMUM SLP 963MB



LEGEND
 6-HR BEST TRACK POSITION
 SPEED OF MOVEMENT (KT)
 INTENSITY (KT)
 POSITION AT XX/0000Z
 TROPICAL DISTURBANCE
 TROPICAL DEPRESSION
 TROPICAL STORM
 TYPHOON
 SUPER TYPHOON START
 SUPER TYPHOON END
 EXTRATROPICAL
 SUBTROPICAL
 DISSIPATING STAGE
 FIRST WARNING ISSUED
 LAST WARNING ISSUED



TYPHOON COLLEEN (26W)

I. HIGHLIGHTS

The third significant tropical cyclone to form as part of the four storm outbreak in mid-October, Colleen developed from a broad cyclonic circulation in the monsoon trough between Typhoon Angela (24W) to the west and Typhoon Brian (25W) to the east. Binary interaction occurred between Colleen and Brian (25W), causing Colleen to make a slow anticyclonic loop in the Philippine Sea before turning west. After crossing Luzon, Colleen reintensified to a typhoon before slamming into central Vietnam and dissipating inland.

II. TRACK AND INTENSITY

Anchored by what was to become Typhoon Angela (24W) in the South China Sea, the monsoon trough extended eastward into the southern Marshall Islands where Typhoon Brian (25W) was developing. The weak low-level circulation, that was to become Colleen, formed in the monsoon trough in the Philippine Sea and was first mentioned on the Significant Tropical Weather Advisory at 160600Z. A Tropical Cyclone Formation Alert was issued by JTWC at 171600Z based on the increased cloud organization in satellite imagery of the disturbance and increasing gradient-level winds at Koror (WMO 91408). Continued intensification during the morning prompted JTWC to issue the first warning at 180000Z. Only six hours later, JTWC upgraded Tropical Depression 26W to Tropical Storm Colleen. But, Tropical Storm Colleen went through several reorganization periods over the first few days as its broad circulation became more vertically aligned. The upper-level flow was shearing the convection to the west while the southwesterly surface flow associated with the monsoon trough forced the low-level to track and reorganize to the east. Despite the strong shear, the cyclone continued to consolidate, and JTWC upgraded Colleen to typhoon intensity on the 191800Z warning.

With regard to the episode of binary interaction, Colleen and Brian (25W) had been, in a relative sense, approaching each other since 15 October (Figure 3-26-1). It became apparent that capture of the two circulations had occurred at 201200Z when they began to orbit around a common point, or centroid (Figures 3-26-2 and 3-26-3). On 22 October, the binary pair reached a minimum separation distance of 680 nm (1260 km). During the binary interaction, Colleen, the larger of the two cyclones, slowed and made an anticyclonic loop as Typhoon Brian accelerated northwestward. On 24 October, Brian escaped to the northeast and recurved. Colleen, which had initially intensified then weakened during the period of interaction, moved westward toward Luzon. Ship reports confirmed that Colleen, with a large ragged eye, had its strongest winds in a ring displaced approximately 40 to 80 nm (75 to 150 km) from the center of the circulation.

While weakening, Colleen passed over central Luzon and then reintensified as it moved into the South China Sea. After peaking at 75 kt (39 m/sec) in the central South China Sea, at 270600Z, Colleen slowly weakened until it made landfall in central Vietnam on the morning of 28 October (Figure 3-26-4). When it was evident that the circulation was dissipating overland, the final warning was issued by JTWC at 281800Z.

III. FORECAST PERFORMANCE

Forecasters at JTWC recognized early on that Colleen was going to be a challenge, and that's exactly how it turned out. Overall the mean track errors were significantly larger than the long term average errors with values of 130, 290 and 500 nm (240, 535 and 925 km) for the 24-, 48- and 72-hour

forecasts, respectively. In addition, JTWC tied at 24 and 48 hours with CLIPER, which is used as a baseline for determining skill, but lost to CLIPER by 10% at the 72-hour point. JTWC forecasters anticipated that interaction could occur with both Angela (24W) to the west and Brian (25W) to the east, but the question was "when, where and how much?" The forecast aids for this cyclone were in poor agreement with each other from the start. In addition, the numerical model, NOGAPS, had a difficult time resolving all three circulations and consistently tried to merge Colleen and Brian (25W). Nevertheless, once Brian (25W) escaped from its interaction with Colleen, JTWC forecasts correctly predicted that Colleen would move to the west.

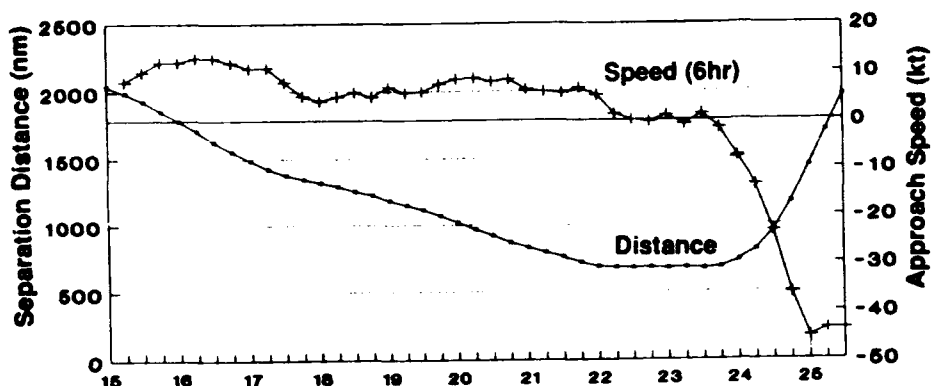


Figure 3-26-1. Graph of the relative separation distances (nm) and speeds of approach (kt) for Colleen and Brian (25W). The closest points of approach between the two typhoons occur on 22 through 24 October.

Figure 3-26-2. Graph of binary interaction between Colleen and Brian (25W). The positions, which are relative to a midpoint, show capture at 201200Z, orbit from 201200Z to 240000Z, and escape at 240000Z October.

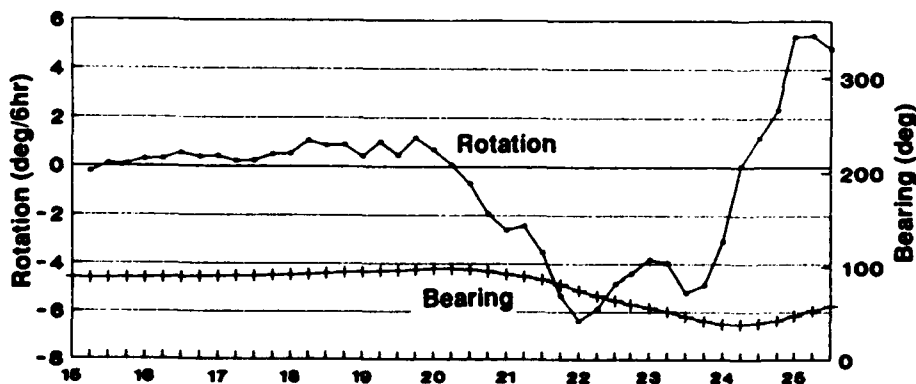
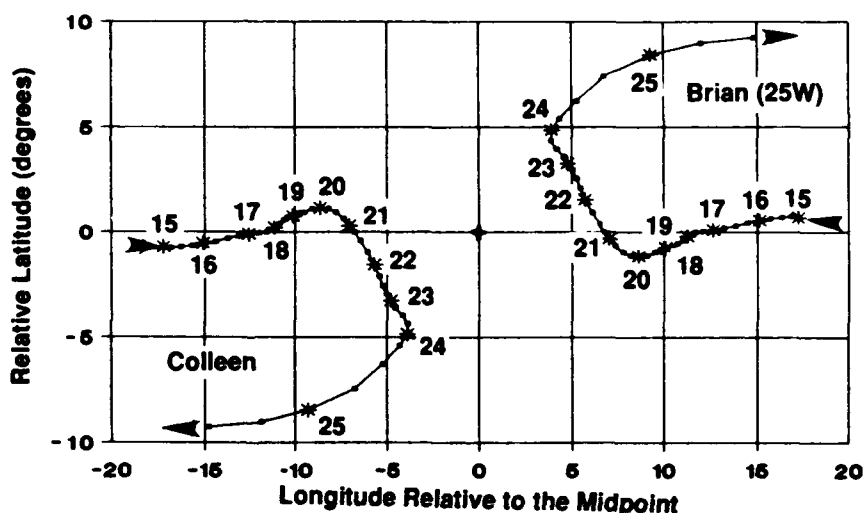
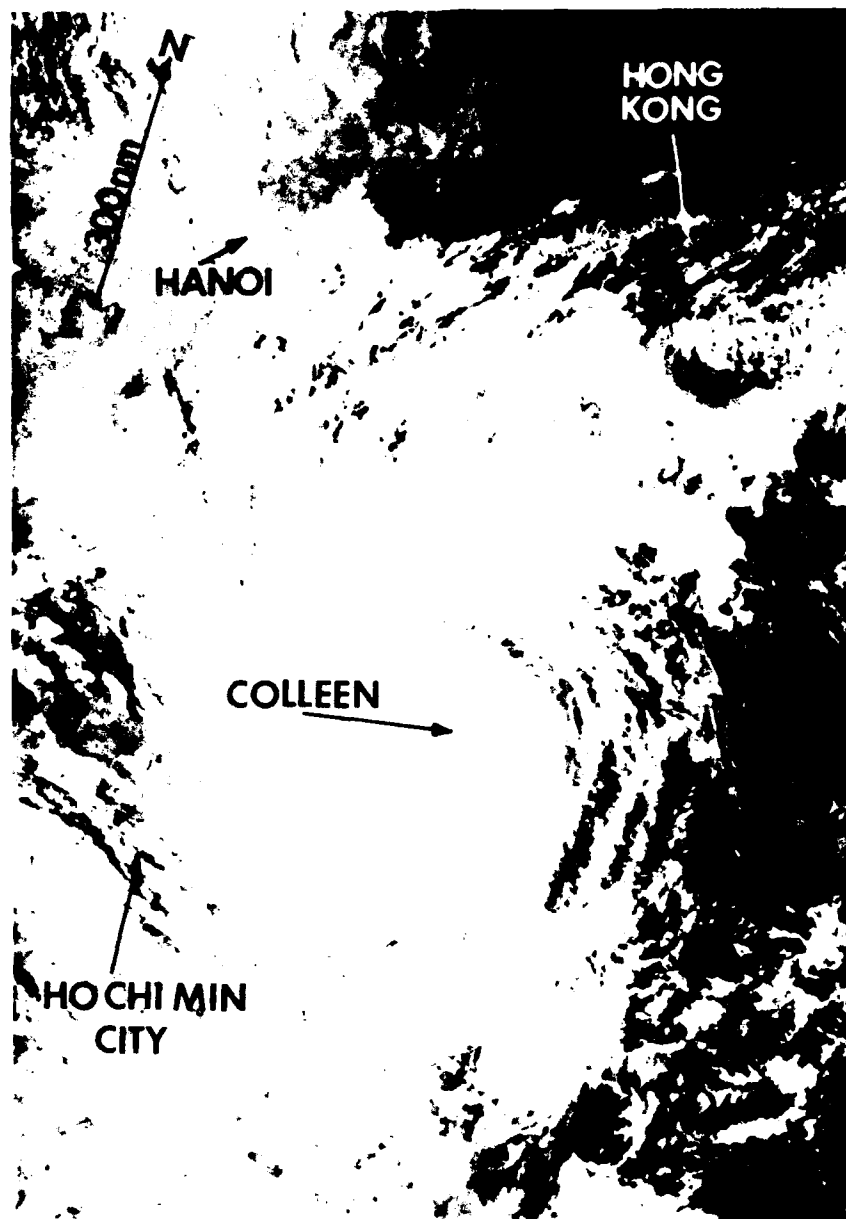


Figure 3-26-3. Graph of Colleen and Brian's rotation (degrees/6 hours) and bearing (degrees) shows that cyclonic rotation (negative values) commenced around 201200Z and ended shortly after 240000Z October.

Figure 3-26-4. Typhoon Colleen, at its peak intensity in the South China Sea, is less than a day from making landfall in Vietnam (270915Z October DMSP visual imagery).



IV. IMPACT

On October 21, the Korean iron ore bulk carrier, **Daeyang Honey**, was reported missing in the Philippine Sea. A nine day search effort, involving aircraft from the Navy's VQ-1 Squadron on Guam and VP-6 Squadron from Okinawa, Japan, was coordinated by the U.S. Coast Guard's Marianas Rescue Coordination Center (Guam), Japan Maritime Safety Agency, and Pan Ocean Shipping. Floating debris was ultimately found by rescue personnel, but there was no sign of the 28 crew members.

On 26 October, Colleen's torrential rains and high winds struck central Luzon. Manila experienced widespread flooding. Government offices, schools, and businesses had to close in the metropolitan area. Water was chest-high in many of the communities surrounding Manila, and over 1,300 residents had to be evacuated. One death was reported due to drowning. Farther to the north, the heavy rains triggered landslides which blocked the roads to Baguio.

No reports of fatalities or damage from Colleen's passage were received from Vietnam.

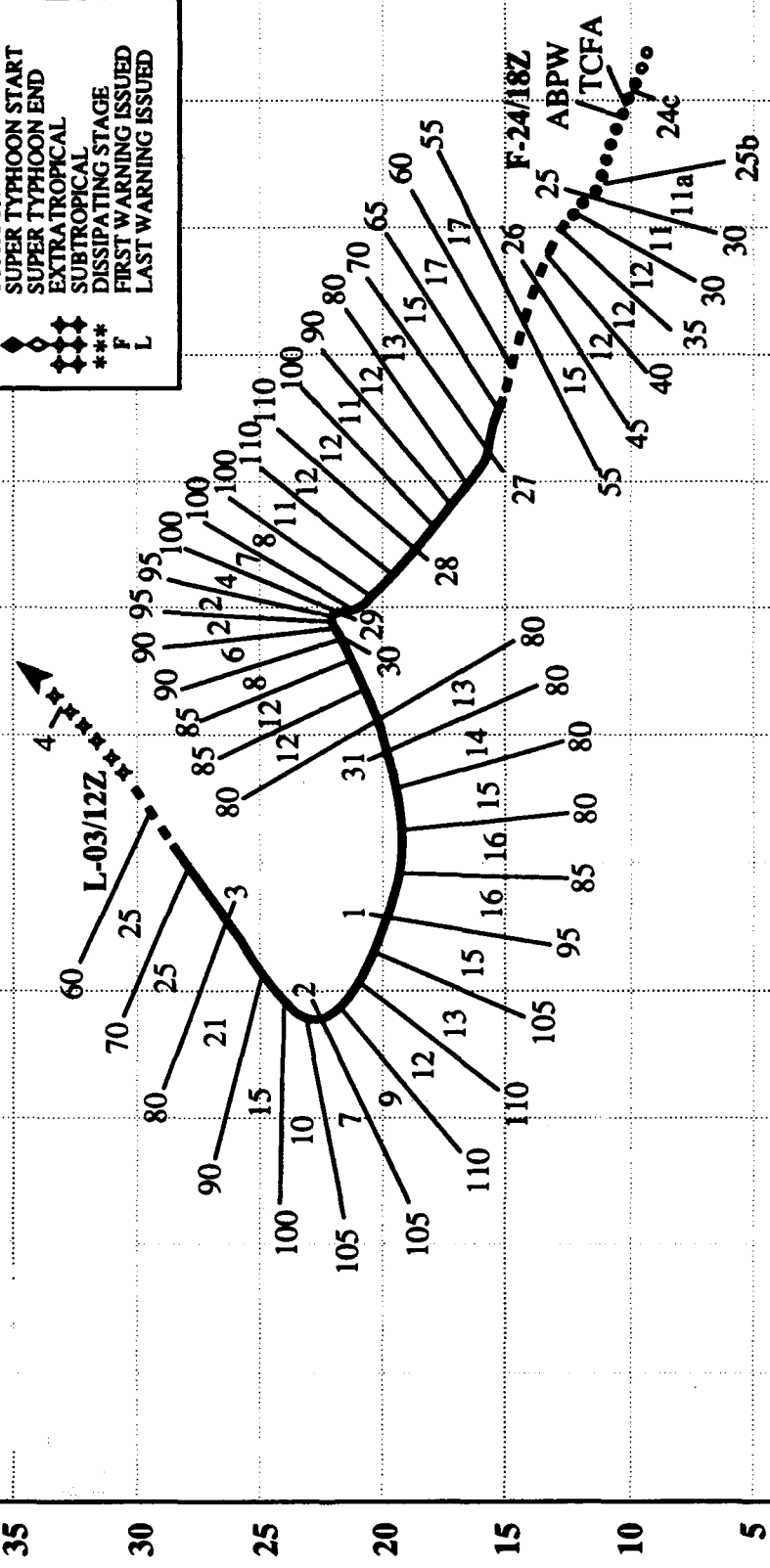
E 130 135 140 145 150 155 160 165 170 175 180 185 190 W

LEGEND

6-HR BEST TRACK POSITION
SPEED OF MOVEMENT (KT)
INTENSITY (KT)
POSITION AT XX/0000Z
TROPICAL DISTURBANCE
TROPICAL DEPRESSION
TROPICAL STORM
TYPHOON
SUPER TYPHOON START
SUPER TYPHOON END
EXTRA TROPICAL
DISSIPATING STAGE
FIRST WARNING ISSUED
LAST WARNING ISSUED

--- a
--- b
--- c
--- d
--- e
--- f
--- g
--- h
--- i
--- j
--- k
--- l
--- m
--- n
--- o
--- p
--- q
--- r
--- s
--- t
--- u
--- v
--- w
--- x
--- y
--- z

TYPHOON DAN
BEST TRACK TC-27W
23 OCT - 04 NOV 92
MAX SFC WIND 110KT
MINIMUM SLP 933MB



TYPHOON DAN (27W)

I. HIGHLIGHTS

The last significant tropical cyclone to develop in October as part of the four storm outbreak including Angela (24W), Brian (25W) and Colleen (26W), Dan became the most destructive typhoon to strike Wake Island in the past quarter-century, causing an estimated \$9.0 million in damage. Just as Ekeka (01C) and Ward (21W) did earlier in 1992, Dan formed east of the international date line, marking the first time that three significant tropical cyclones crossed into the JTWC's area of responsibility from the central North Pacific during a single year. Later, Dan faked a move toward recurvature, took a west-southwesterly course, underwent an episode of reintensification, and finally, underwent a binary interaction with Typhoon Elsie (28W) before recurving sharply.

II. TRACK and INTENSITY

On 23 October, the Naval Western Oceanography Center (NWOC) initially detected the tropical disturbance that developed into Dan in the trade-wind trough 450 nm (830 km) south of Johnston Island in the central North Pacific. At 240000Z, a Tropical Cyclone Formation Alert was issued by NWOC based on an increase in convection around a well-defined low-level circulation. Because of the large field-of-view geostationary images available on the MIDDAS system, satellite analysts at Detachment 1, 633 OSS (collocated with JTWC) were able to continuously monitor the ongoing development of the tropical disturbance as it tracked toward the international date line. Based on these data, which showed that the tropical disturbance was intensifying and the close proximity of the system to JTWC's area of responsibility, JTWC forecasters, in coordination with the Central Pacific Hurricane Center, elected to issue the first warning on Tropical Depression 27W at 241800Z.

As the tropical depression moved west-northwestward, normal development brought it to tropical storm intensity shortly after crossing into the western North Pacific at 251200Z. The next day, JTWC upgraded Dan to a typhoon at 261800Z. Intensification continued, and Dan began to close in on Wake Island, where it would become the most intense tropical cyclone to affect Wake since Typhoon Sarah in September, 1967. On 28 October, at the typhoon's closest point of approach (CPA) to Wake — approximately 15 nm (28 km) to the southwest — Dan had estimated maximum sustained surface winds of 110 kt (57 m/sec). The National Weather Service Office at Wake Island recorded peak wind gusts of 90 kt (46 m/sec) in the eye wall before losing electrical power (Figure 3-27-1), and a minimum sea-level pressure of 980.8 mb (Figure 3-27-2). Later reports from Wake Island indicated that the strongest winds occurred after the CPA at 280315Z.

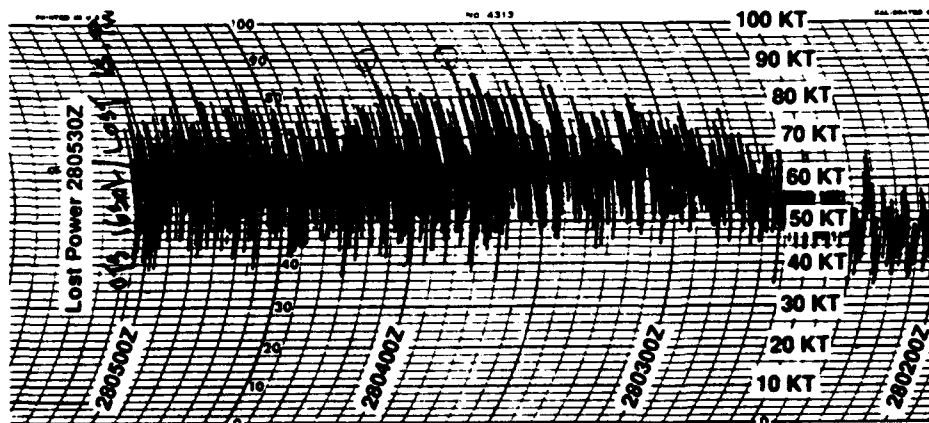


Figure 3-27-1. Wake Island's anemometer trace shows two peak wind gust to 90 kt (46 m/sec) before power was lost at 280403Z (Data courtesy of National Weather Service Office, Wake Island).

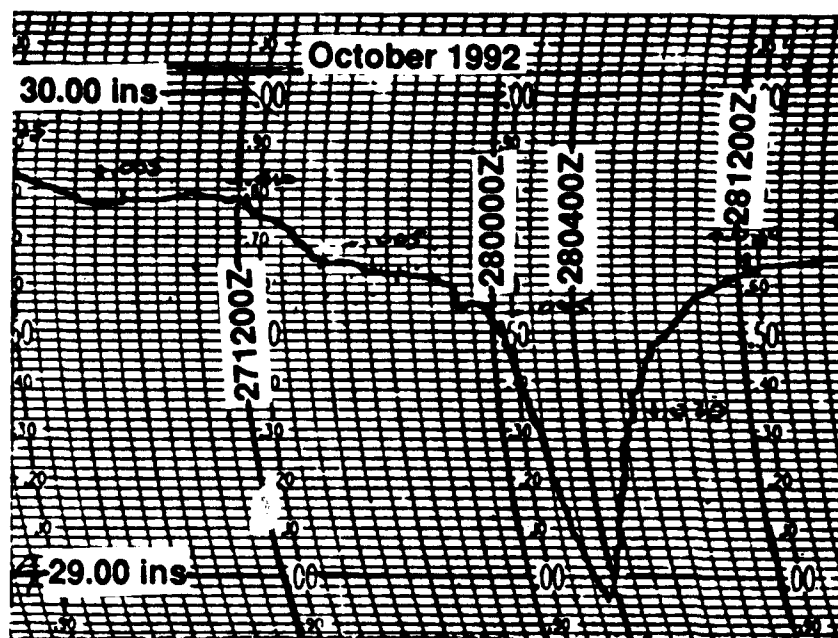


Figure 3-27-2. Microbarograph record for the period 27 through 28 October at Wake Island showing a minimum pressure of 28.95 inches (980.8 mb), at 280315Z, at Typhoon Dan's closest point of approach (Data courtesy of the National Weather Service Office, Wake Island).

On 29 October, one day after hammering Wake Island, the typhoon made a northward motion towards recurvature, stalled, and then made an abrupt track change to the west-southwest in response to the subtropical ridge strengthening after the passage of a mid-latitude trough to the north. At the same time, Dan weakened as upper-level westerlies increased aloft. As a consequence, the typhoon's eye disappeared from the satellite imagery and the typhoon's intensity dropped to 80 kt (41 m/sec). On 31 October, binary interaction commenced with Typhoon Elsie (28W), which was located to the southwest near the Mariana Islands (Figure 3-27-3).

At one point, the two cyclones closed to within 630 nm (1170 km) of each other. The upper-level shear diminished during the binary interaction event, allowing Typhoon Dan to intensify again to a peak of 110 kt (57 m/sec) at 011200Z November. Twelve hours later, Dan recurved sharply and accelerated northeastward when an approaching mid-latitude trough moving eastward from Japan created a large break in the subtropical ridge. The final warning was issued by JTWC at 031200Z, when satellite imagery indicated the system was rapidly transitioning into an extratropical cyclone.

III. FORECAST PERFORMANCE

For JTWC, the overall mean track forecast errors were 130, 245 and 330 nm (240, 455 and 610 km) for 24, 48 and 72 hours, respectively. Although these values were larger than the long term mean, JTWC's extended outlooks for track were 30% and 60% better at 48 and 72 hours, respectively, than CLIPER. JTWC's track forecasting performance is summarized graphically in Figure 3-27-4. The four areas of concern were: the approach to Wake Island, possible recurvature after passing Wake, the effects of binary interaction with Typhoon Elsie (28W), and recurvature revisited. JTWC addressed these challenges by shifting to a northwest forecast track on 26 October, and indicated in its 260600Z Prognostic Reasoning message that the tropical cyclone would "pass near Wake Island within the next 36 to 60 hours at a peak intensity of close to 105 knots." The track and intensity forecasts made on the 26 October proved to be accurate, allowing Wake Island to make sufficient preparations two days prior to the onset of destructive winds. After Dan passed Wake Island, the forecast aids gave conflicting guidance. The climatological and statistical aids hinted at recurvature, while the numerical models and dynamic forecast aids indicated a sharp westward turn was going to occur (Figure 3-27-5). JTWC adopted a "stairstep" forecast, but at 291200Z changed its track scenario to a west-southwest track, when the track change occurred. The effects of binary interaction with Elsie (28W) on Typhoon Dan were also over-estimated by the JTWC. It was believed that the interaction would keep Dan on a nearly

westward course and preclude short-term recurvature, thus the sharpness of recurvature caught the forecasters by surprise.

On the short term, intensity forecasts were average, however, the failure of track scenario and Dan's reintensification after passing Wake Island had a definite impact on the intensity outlooks. Starting on 281200Z and for two-and-one-half days, the 72-hour intensity forecasts errors ranged from 30 to 80 kt (20 to 41 m/sec) too low, resulting in the largest intensity errors of 1992.

IV. IMPACT

Although the eye did not pass directly over Wake Island, Typhoon Dan devastated the tiny island which was still recovering from a near-miss by Typhoon Sybil (18W). Damage was officially estimated to be \$9.0 million. High surf surged over the surrounding coral reef, inundating most of the permanent structures. All residents sought safety in concrete shelters. For the rest of Dan's life, it threatened only maritime interests. There were no reports of any loss of life.

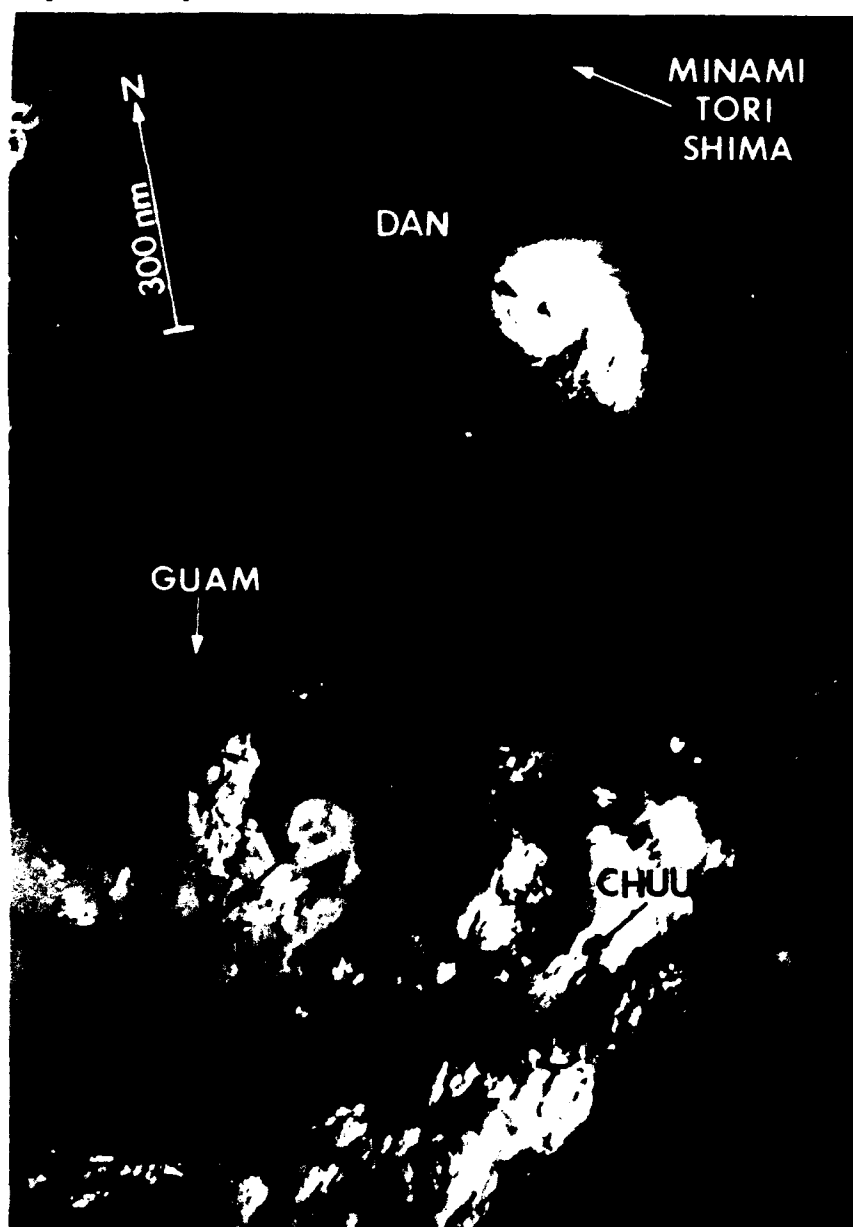


Figure 3-27-3. Near its second peak intensity, Typhoon Dan is involved in a binary interaction with Typhoon Elsie (28W), which is visible to the southwest (312258Z October DMSP visual imagery).

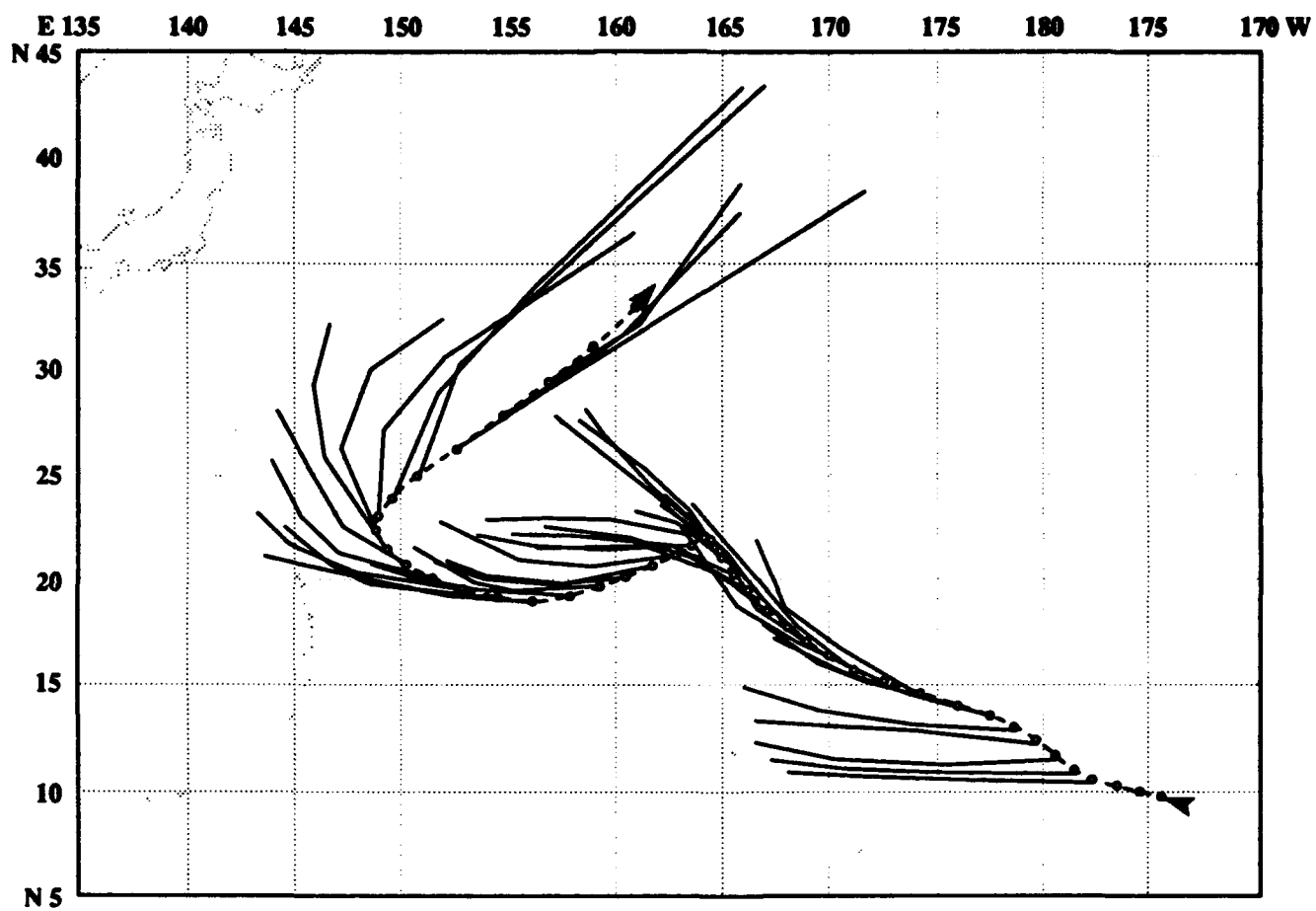


Figure 3-27-4. JTWC forecasts for Dan relative to the official best track.

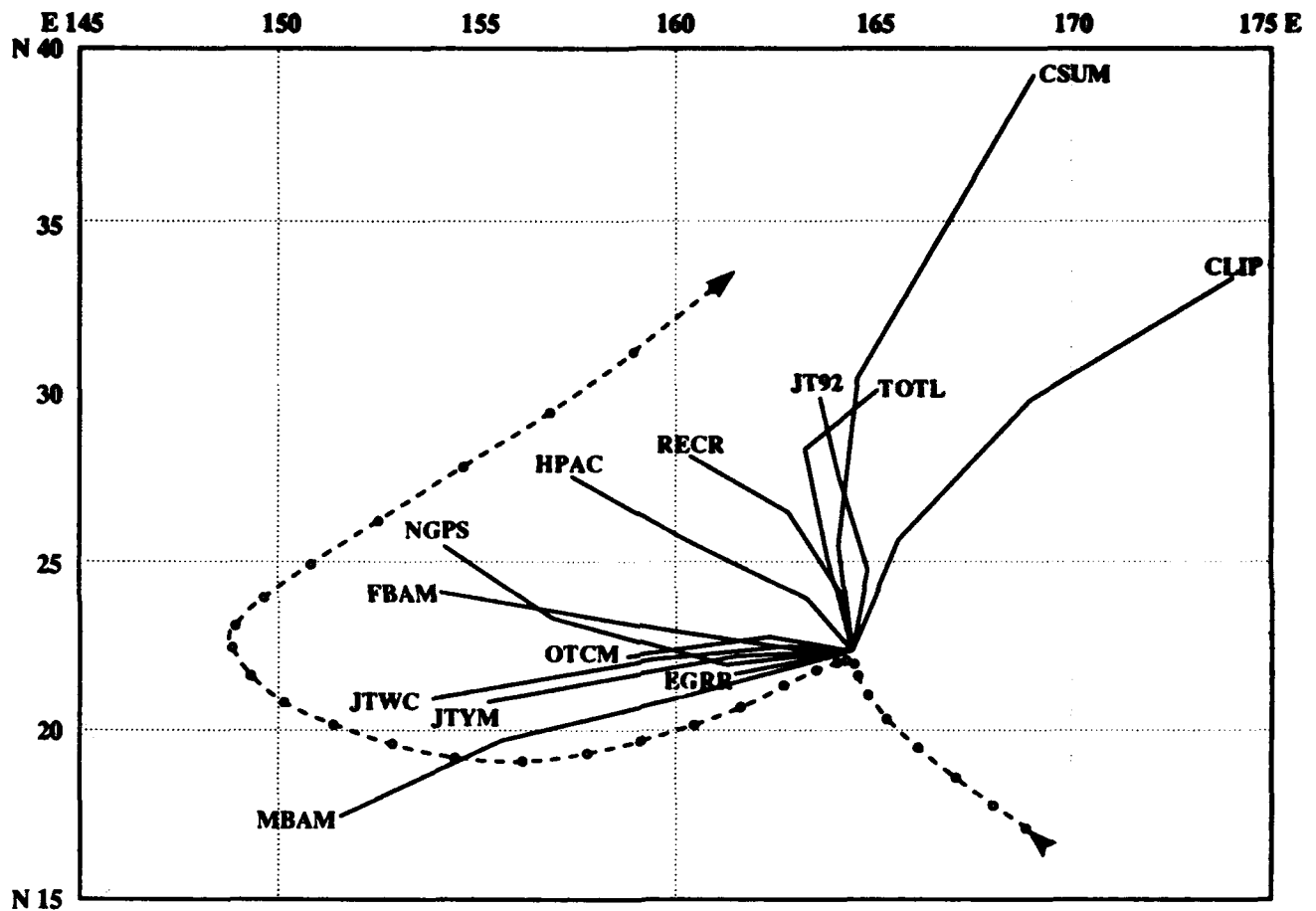


Figure 3-27-5. Forecast aids at 291200Z October for the major track change. Shown are the climatological/statistical forecast aids HPAC, CLIP, TOTL, RECR, JT92 and CSUM along with the dynamic aids OTCM, FBAM, MBAM, JTYM and the numerical models, NGPS and EGRR.

SUPER TYPHOON ELSIE (28W)

I. HIGHLIGHTS

The fourth super typhoon of 1992, Elsie was the third typhoon to pass within 60 nm (100 km) of Guam in less than three months. After initial movement to the northeast in response to a southwest monsoonal surge, a subsequent turn to the west, and then interaction with Typhoon Dan (27W), Elsie settled down on a track to the northwest, recurved, and transitioned into a hurricane-force extratropical low.

II. TRACK AND INTENSITY

The tropical disturbance that became Elsie formed in the monsoon trough near Chuuk in the central Caroline Islands, and was first described on the 280600Z October Significant Tropical Weather Advisory as an area of poorly organized, persistent convection. The combination of increasing deep convection near the cloud system center and falling pressure in excess of 3 mb in 24 hours at Chuuk (WMO 91344) led forecasters at JTWC to issue a Tropical Cyclone Formation Alert at 291200Z. A short time later, the appearance of deep cyclonically curved spiral convective bands around the system center prompted JTWC to issue the first warning for Tropical Depression 28W at 291800Z.

The tropical cyclone initially moved to the northeast in response to a deep southwest monsoonal surge. The northward component of this movement, plus the depression's early intensification, brought the tropical cyclone under the influence of the mid-level steering flow of the subtropical ridge to the north, causing the track to become more westward. As intensification continued at a rate of 1.25 mb/hour, JTWC upgraded Elsie to a tropical storm six hours later on the 300000Z warning, and to a typhoon at 301200Z. Meanwhile, the separation distance between Elsie and Typhoon Dan (27W) was steadily decreasing. During the period 311800Z October through 020600Z November, binary interaction between the two typhoons caused Elsie to slow, undergo erratic motion, and again take a more northward track toward the southern Mariana Islands. At the same time, the outflow from Dan (27W) was causing moderate upper-level shear from the east across Elsie's cloud shield, and retarding intensification. At its closest point of approach to Guam on 2 November, Elsie was located 55 nm (100 km) to the south-southwest of the island. Peak wind gusts to 62 kt (32 m/sec) were recorded at the Naval Air Station, Guam (WMO 91212), but recordings were not available for the southern portion of the island.

After Dan (27W) recurved, ending the binary interaction on 2 November, Elsie resumed development at a rate of 5 kt (3 m/sec) per six hours, reaching super typhoon intensity at 040600Z and a peak of 145 kt (75 m/sec) at 050600Z (Figure 3-28-1). Elsie's intensification kept Guam in gale-force winds for two days after its passage and movement away from the southern Mariana Islands. After Elsie's recurvature at 060000Z, increasing southwesterly winds aloft weakened the super typhoon to typhoon intensity at 060600Z. As Elsie was transitioning into an intense extratropical low with hurricane-force winds, the final warning was issued by JTWC at 071200Z.

III. FORECAST PERFORMANCE

Although Elsie's track is basically one of recurvature, the initial monsoon surge from the southwest, binary interaction, recurvature and the subsequent acceleration into midlatitudes proved difficult to handle. With mean track errors of 110, 250 and 340 nm (205, 465 and 630 km) for the 24-, 48- and 72-hour forecasts, respectively, JTWC's performance overall was below average and tied with CLIPER. The specific forecasting successes were accurately predicting Typhoon Dan's (27W) influ-

ence on Elsie's track change to the north and anticipating Elsie's intensification to a super typhoon. With respect to Guam, JWC predicted that intensification would take place a little early and that the typhoon would pass 30 nm (55 km) closer than actually occurred. For Okinawa, JWC forecasts were used to prevent the unnecessary preparations for destructive winds at DOD installations there.

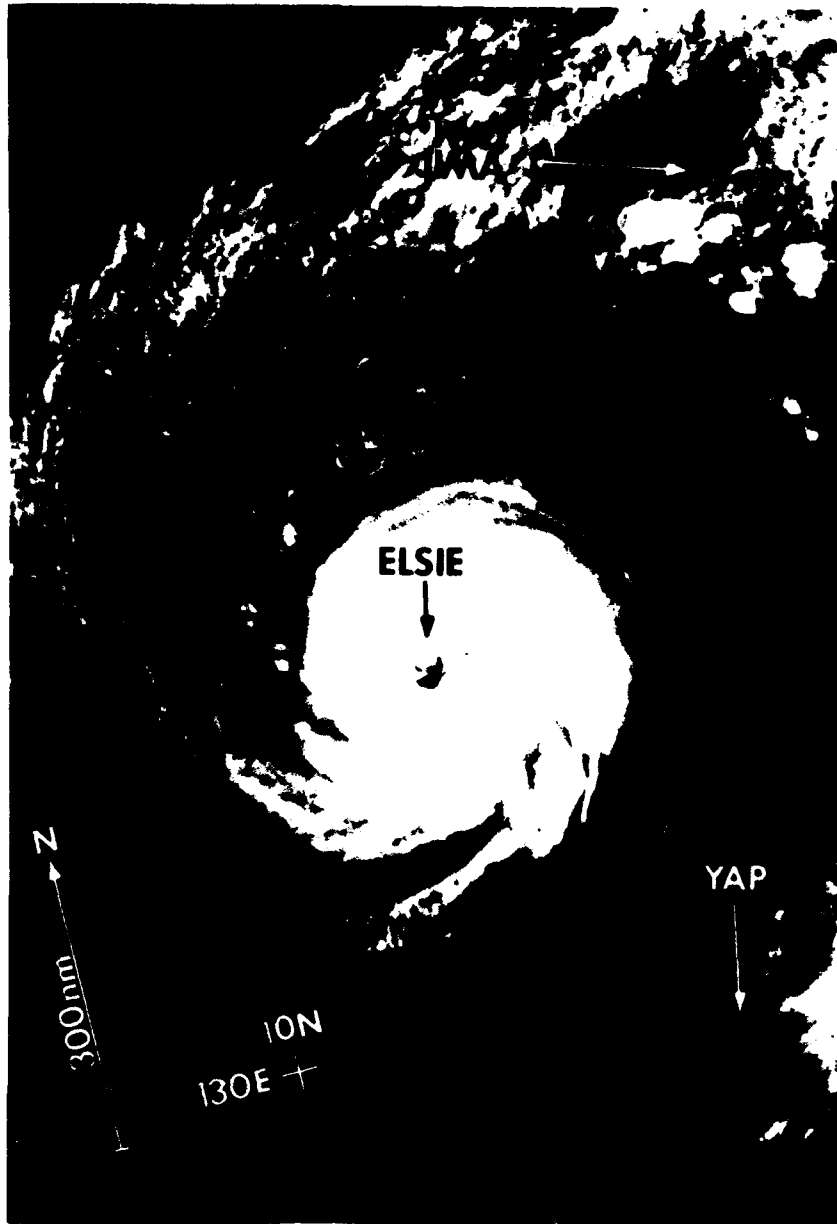
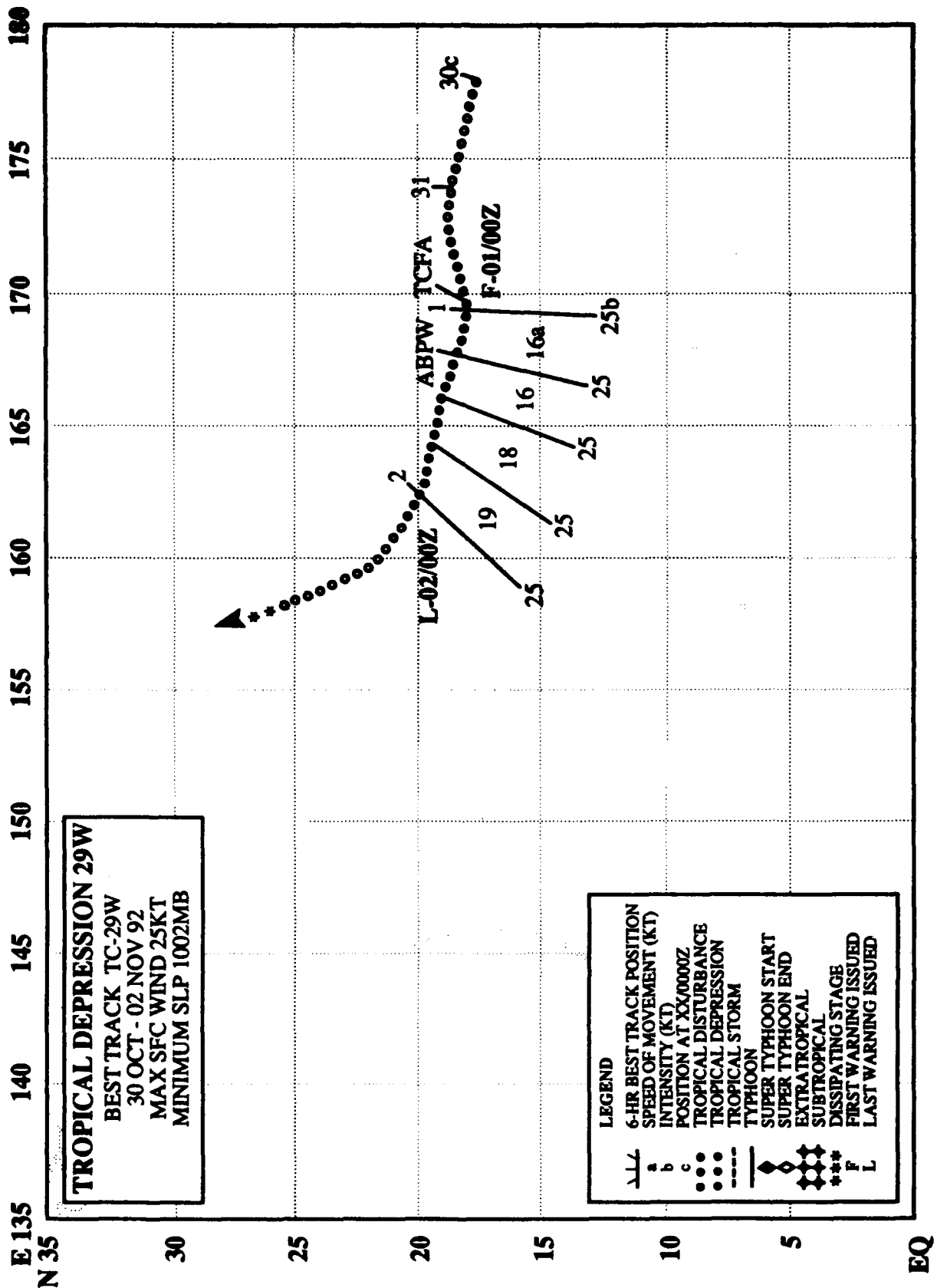


Figure 3-28-1. Elsie at super typhoon intensity in the central Philippine Sea (042342Z November DMSP visual imagery).

IV. IMPACT

On Guam, no deaths, injuries, or significant property damage occurred. As a precaution, military aircraft from the Navy's VQ-1, VQ-5 and VRC-50 squadrons were temporarily relocated from Guam to Japan, and all ships in port at Guam were sent to sea. Residents of Guam and Rota spent a day in typhoon Condition of Readiness 1, and the Guam general election had to be postponed for the first time in its history.

Later on, as Elsie moved northward in the Philippine Sea, the prepositioning of some support units for the military exercise, ANNUAL-EX 92, had to be delayed.



TROPICAL DEPRESSION 29W

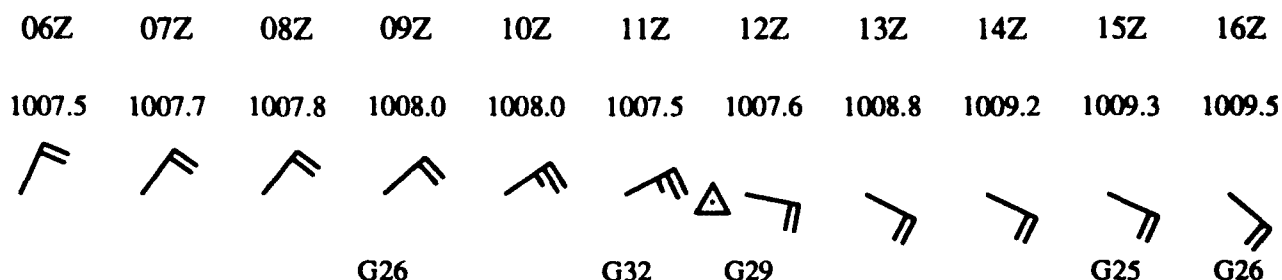


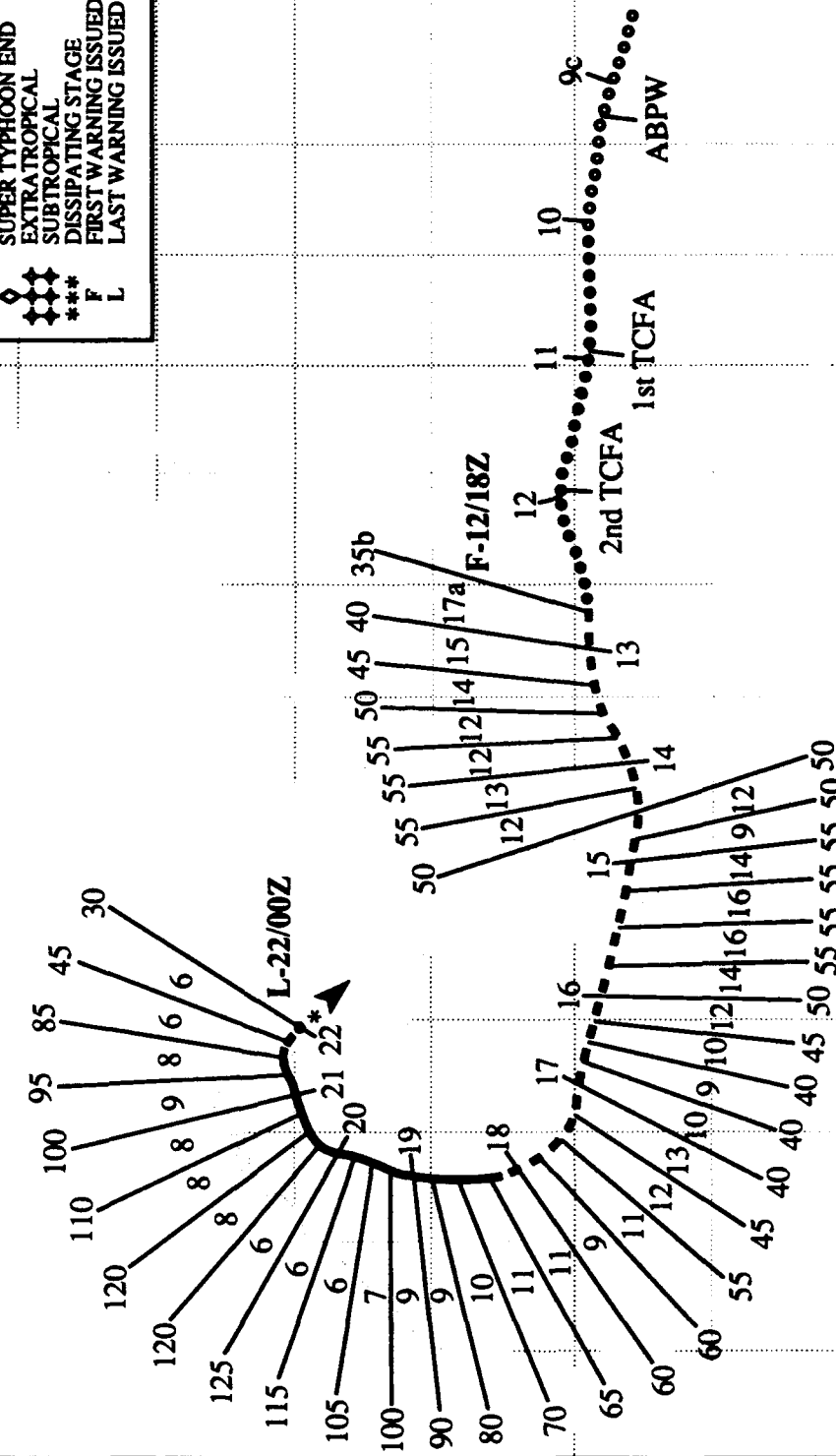
Figure 3-29-1. Surface reports from Wake Island (WMO 91245) for the period 010600Z through 011600Z November reflect the passage of Tropical Depression 29W at 011100Z with the winds shifting from the northeast to the southeast.

Forming in the wake of Typhoon Dan (27W), Tropical Depression 29W immediately become a threat to Wake Island which had already been heavily damaged by Dan (27W) on 28 October. Fortunately for Wake, the Tropical Depression's intensification was severely curtailed by the persistent outflow from Dan (27W). When Tropical Depression 29W reached its closest point of approach, 30 nm (55 km) to the south-southwest of Wake, at 011200Z, the island experienced surface winds gusting to 32 kt (16 m/sec).

N 40 E 75 80 85 90 95 100 105 110 115 120 125 130 135 140 145 E

TYPHOON FORREST
 BEST TRACK TC-30W
 08 NOV - 22 NOV 92
 MAX SFC WIND 125KT
 MINIMUM SLP 916MB

LEGEND
 6-HR BEST TRACK POSITION
 SPEED OF MOVEMENT (KT)
 POSITION AT XX/0000Z
 TROPICAL DISTURBANCE
 TROPICAL DEPRESSION
 TROPICAL STORM
 TYPHOON
 SUPER TYPHOON START
 SUPER TYPHOON END
 EXTRATROPICAL
 SUBTROPICAL
 DISSIPATING STAGE
 FIRST WARNING ISSUED
 LAST WARNING ISSUED



TYPHOON FORREST (30W)

I. HIGHLIGHTS

The second of four significant tropical cyclones to start in November, Forrest became part of a three storm outbreak with Gay (31W) and Hunt (32W). Forrest was the only tropical cyclone of 1992 to track from the western North Pacific, across the South China Sea, and into the Bay of Bengal. It reached a maximum intensity of 125 kt (64 m/sec) in the Bay of Bengal over a day after it had started recurvature.

II. TRACK AND INTENSITY

On 9 November, the tropical disturbance that became Forrest was detected as a persistent area of convection in the western Caroline Islands, and was first mentioned on the 090600Z Significant Tropical Weather Advisory. As the tropical disturbance was approaching the southern Philippine Islands, an increase in its convective organization prompted JTWC to issue a Tropical Cyclone Formation Alert on 102300Z, forecasting for further development once the disturbance exited the Islands. The cloud system was slow to intensify and required the alert to be reissued at 112300Z. Once past Palawan Island and over open water in the South China Sea, the disturbance's organization and convection increased rapidly. JTWC issued the first warning on Tropical Depression 30W at 121800Z. The upgrade to Tropical Storm Forrest followed at 130000Z, which in post analysis appeared to be six hours slow.

As Forrest continued westward, disruptive land interactions with southern Vietnam and the Malay Peninsula temporarily prevented it from developing into a typhoon. On 15 November, the tropical storm crossed the Malay Peninsula and lost most of its central convection (Figure 3-30-1). Although a low-level circulation center remained, Forrest continued to slowly weaken for the next two days. Its central convection rebuilt and again became persistent on 17 November. Coincident with the tropical storm's intensification came a gradual track change to the north in response to the steering provided by the subtropical ridge over Southeastern Asia. At 180600Z, Forrest reached typhoon intensity and passed through the axis of the mid-tropospheric subtropical ridge to begin its recurvature. Despite the recurvature, upper-level winds were from the south-southwest, and provided enhanced outflow. As a result, Forrest reached its peak intensity of 125 kt (64 m/sec) 36 hours after it commenced recurvature. As Forrest proceeded to the north, sharper recurvature commenced, and increasing upper-level wind shear from the southwest started to weaken the typhoon. On 21 November, Forrest underwent rapid weakening as it made landfall on the coast of Burma. At landfall, the maximum surface winds gusting to 56 kt (29 m/sec) were recorded at Cox's Bazar (WMO 41992), Bangladesh, 75 nm (140 km) north of the cyclone's center. Based on Forrest's rapid dissipation over Burma's rugged terrain the final warning was issued by JTWC at 220000Z (Figure 3-30-2).

III. FORECAST PERFORMANCE

The sample of mean track forecast errors for the South China Sea area was small and the errors of 75 and 105 nm (135 and 195 km) for 24 and 48 hours, respectively, were roughly equal to CLIPER. The mean forecasting errors for track in the Bay of Bengal were considerably larger at 100, 220 and 415 nm (185, 405 and 770 km) for 24, 48 and 72 hours, respectively. This performance, which again matched CLIPER's performance, was average for the short range, and less than average for the extended outlooks. JTWC did correctly forecast Forrest's track change to the north in the Bay of Bengal, but did

not anticipate the sharpness of the typhoon's turn towards the coast of Burma three days later.

The intensity forecasts were good, except for a two-and-one-half-day period starting on 160600Z where the 72-hour extended outlooks were 35 to 80 kt (18 to 41 m/sec) too low when forecast weakening in the central Bay of Bengal did not occur, and unforecast intensification did occur.



Figure 3-30-1. Forrest's cloud pattern remains tightly coiled as the tropical cyclone crosses the Malay Peninsula (151419Z November DMSP infrared imagery).

IV. IMPACT

In the Gulf of Thailand, Forrest threatened the numerous manned gas platforms. All platforms were evacuated in advance of the tropical storm's approach and no injuries were reported. Afterward, Forrest swept across the Malay Peninsula. No fatalities were reported, most probably due to the evacuation of approximately 10,000 people from the coastal areas. More than 1000 houses and many roads were seriously damaged or destroyed.

As the typhoon turned in the direction of the northern Bay of Bengal, authorities in the region had not forgotten the effect of Tropical Cyclone 02B, which struck Bangladesh in April 1991 killing an estimated 138,000 people. Disaster preparedness officials in Bangladesh successfully evacuated of an estimated 500,000 people in response. Fortunately, the center of Forrest went ashore in a relatively sparsely populated region of Burma and spared Cox's Bazar where over 250,000 Burmese refugees were housed in tents. U.S. agencies had activated plans for a massive relief effort, but the sharper recurvature and small size of Forrest allowed the plans to be canceled. Only two fatalities in Bangladesh were reported.

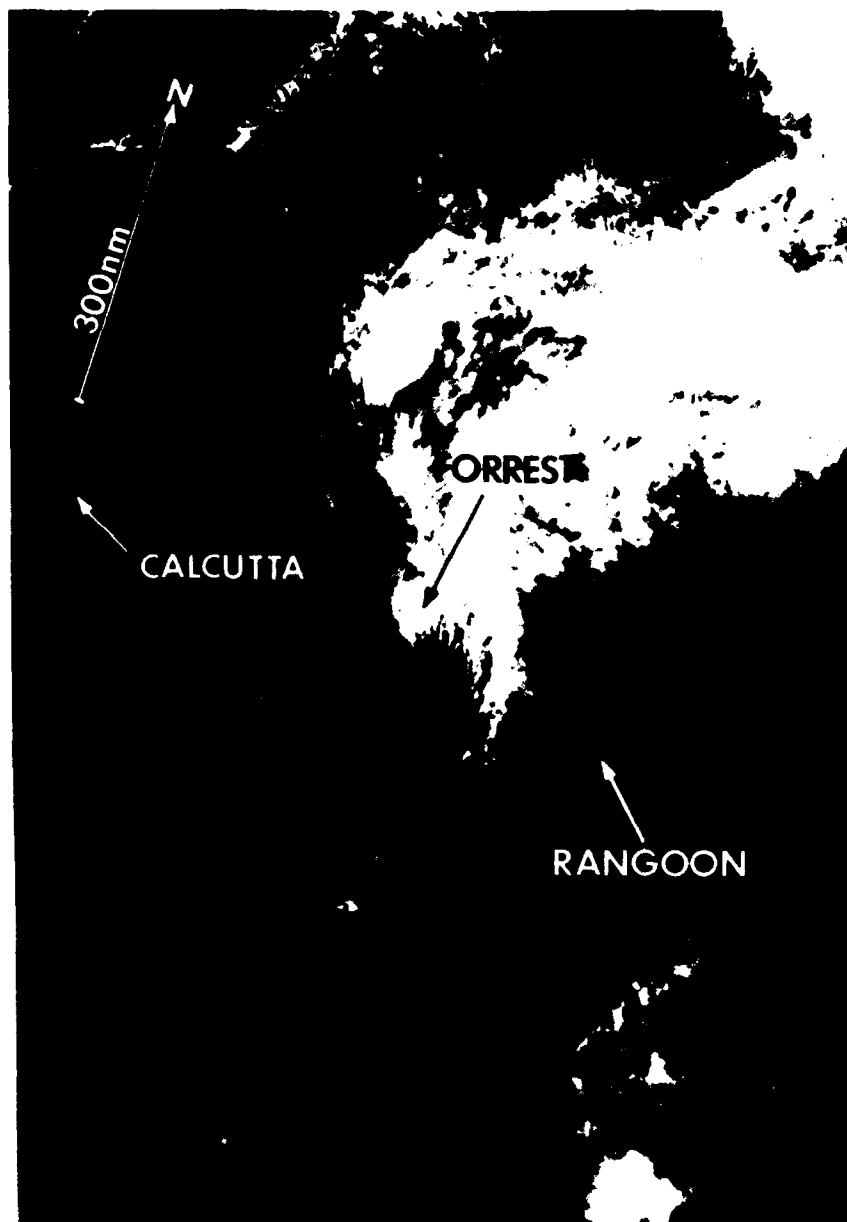
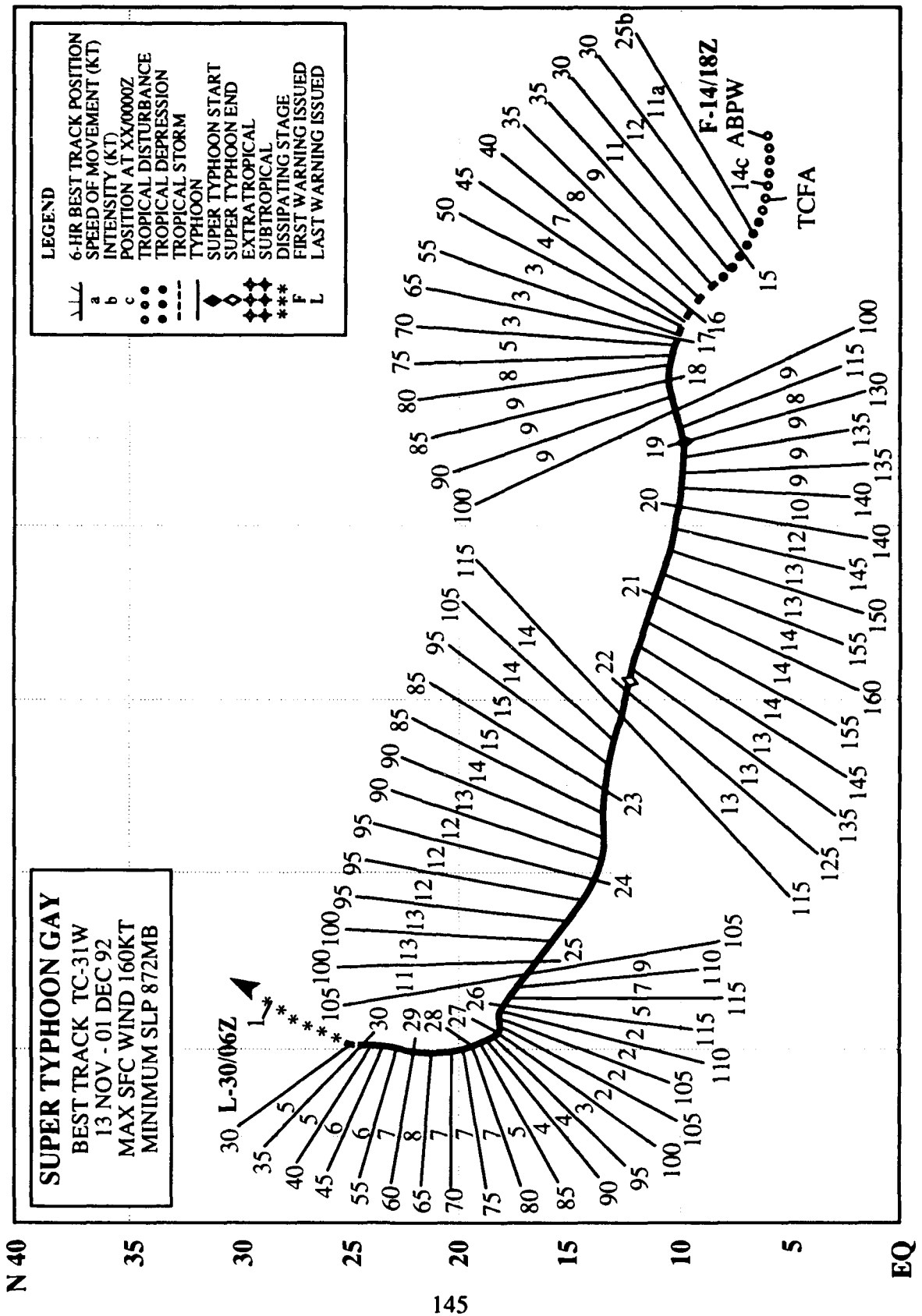


Figure 3-30-2. After being overland for 12 hours, all that remains of Forrest is a low-level cloud vortex (220255Z November DMSP visual imagery).

E 120 125 130 135 140 145 150 155 160 165 170 175 180 185 190 195 200



SUPER TYPHOON GAY (31W)

I. HIGHLIGHTS

Gay was noteworthy for five reasons: its eye became the record third to pass across Guam in less than three months; it was estimated to be the most intense tropical cyclone to occur in the western North Pacific since Super Typhoon Tip in October of 1979; it went through two intensification periods, which is not rare but is relatively uncommon; it filled an estimated 99 mb in less than 48 hours without moving over land; and, it required the highest number of warnings, 63, for any western North Pacific tropical cyclone in 1992. Four days after being detected as a tropical disturbance, Gay slammed into several of the Marshall Islands with typhoon force winds. After peaking with sustained winds of 160 kt (82 m/sec) with gusts to 195 kt (100 m/sec), the super typhoon weakened for two days before reaching Guam. Typhoon Gay passed across the center of Guam on 23 November, then reintensified to a second peak before recurving, and dissipating over water south of Japan.

II. TRACK AND INTENSITY

On 13 November, the tropical disturbance that became Super Typhoon Gay was detected just east of the international date line in the monsoon trough which extended westward through the southern Marshall Islands, where Hunt (32W) was forming, to Tropical Storm Forrest (30W) in the South China Sea. JTWC first mentioned the disturbance as a convective area with fair potential for development on the 130600Z November Significant Tropical Weather Advisory. As the disturbance moved westward, the overall area of cloudiness decreased, but there was a marked increase in central convection and organization. To address this development, the Center issued a Tropical Cyclone Formation Alert at 140500Z. Intensification continued and the first warning followed at 141800Z with an upgrade to Tropical Storm Gay at 150000Z.

As Gay approached the Marshall Islands and slowed, it intensified reaching typhoon intensity at 170000Z. Mejit Island and the atolls of Ailuk and Wotje, just east-northeast of Kwajalein Atoll, were the first to be buffeted by the typhoon which inflicted considerable damage. Then Typhoon Gay swept westward, passing 60 nm (110 km) north of Kwajalein, and later over Wotho Atoll, where all the homes and crops were destroyed, fortunately without any loss of life. At 190600Z, JTWC upgraded Gay to a super typhoon, the peak intensity of 160 kt (82 m/sec) based on estimates from satellite imagery was not reached until 210000Z. This peak intensity, although estimated, established Gay as the most intense typhoon to occur in the western North Pacific since Typhoon Tip peaked in October 1979 with sustained winds of 165 kt (85 m/sec).

In the meantime, Typhoon Hunt (32W) had brushed by Guam, intensified, recurved, and was located, on 21 November, on the north side of the subtropical ridge, north of Guam, and north-northwest of Super Typhoon Gay. From this position, Hunt's strong upper-level outflow combined with a massive upper-level anticyclone to the north-northeast of Gay brought strong northeasterly flow to bear on Gay, decapitating the north side of its well organized thunderstorm structure. As a consequence, sea-level pressures began to rapidly rise within the typhoon's eye, the torrential rains abated, and the winds within the core region spun down faster than forecast by JTWC.

Fortunately, for the southern Mariana Islands, the weakening trend continued at a phenomenal rate of 10 kt (5 m/sec) per 6 hours, and JTWC downgraded the super typhoon to typhoon status at 221200Z. Twelve hours later, Gay crossed Guam (Figure 3-31-1) packing sustained winds of 85 kt (44 m/sec) gusting to 105 kt (54 m/sec). Post analysis indicates that during the rapid weakening event,

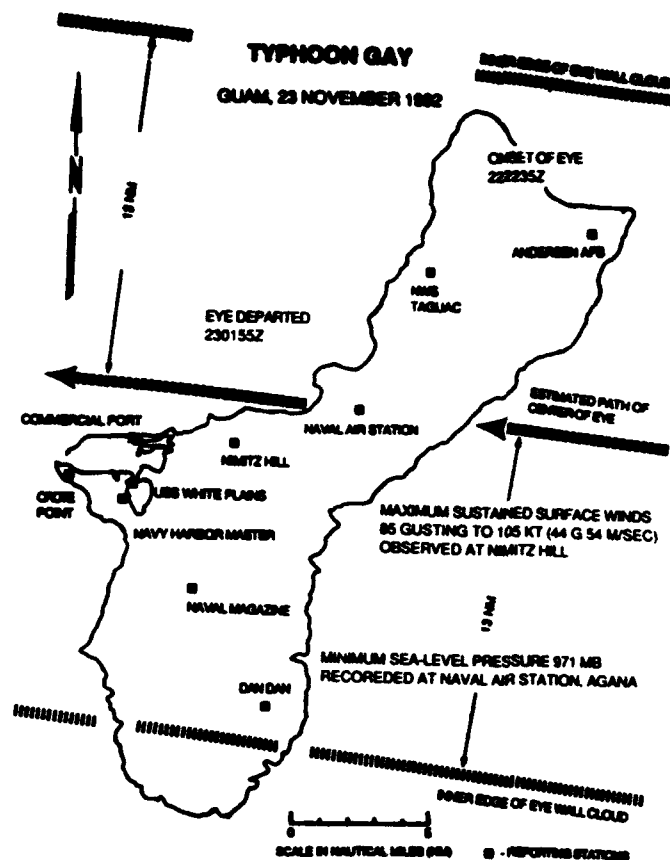


Figure 3-31-1. Graphic depicting the passage of the eye of Typhoon Gay across the island of Guam on 23 November.

JTWC's intensity estimates lagged the actual intensities by about 12 hours. The eye passage at Nimitz Hill is graphically shown on the pressure trace in Figure 3-31-2. The minimum sea-level pressure of 971 mb was recorded at the Naval Air Station. In Figure 3-31-3, the Nimitz Hill wind speed and direction record shows the light winds during the eye passage and that the wind direction gradually shifted in a clockwise direction. The wind record also shows that before the eye passed, the north-northwest winds were more uniform or stable, while in contrast, after the eye passed, the flow across Nimitz Hill was southerly, more turbulent and stronger. In terms of strength and size, Gay was large, nearly 800 nm (1480 km) across. As a result, the winds at Andersen AFB (WMO 91218), Guam gusted to gale force (33 kt (17 m/sec)), or higher, for 24 hours. Even with the duration and strength of these winds, the structural damage on Guam and Rota was relatively light. Damage would have been much greater, probably in the tens of millions of dollars, had Typhoon Omar (15W) not hit Guam less than three months earlier and destroyed the weaker structures. Nevertheless, due to surprisingly light 24-hour rainfall amounts from 1.5 to 3.5 inches (40 to 90 mm), the winds of this "dry" typhoon were laden with salt and left the island's new growth of vegetation and crops as if scorched or seared from intense heat. The maximum storm surge and wave runup were generally from 5 to 7 feet (2 m) on northern exposed reefs and beaches with a maximum near the Cabras port/container area of 9 to 11 feet (3 m) (Figure 3-31-4).

On 23 November, the effect of Hunt's (32W) outflow on Gay lessened. The environment allowed the deep thunderstorm structure to redevelop, and Typhoon Gay reintensified, reaching a second peak of 115 kt (59 m/sec) at 251800Z (Figure 3-31-5). The typhoon stalled for two days and weakened south-southeast of Okinawa, Japan before tracking to the north on 27 November. As Gay recurved

Figure 3-31-2. The microbarograph trace for Nimitz Hill, Guam shows the passage of Typhoon Gay's center on 23 November. The instrument, which was corrected to sea level, recorded a minimum pressure of 972 mb.

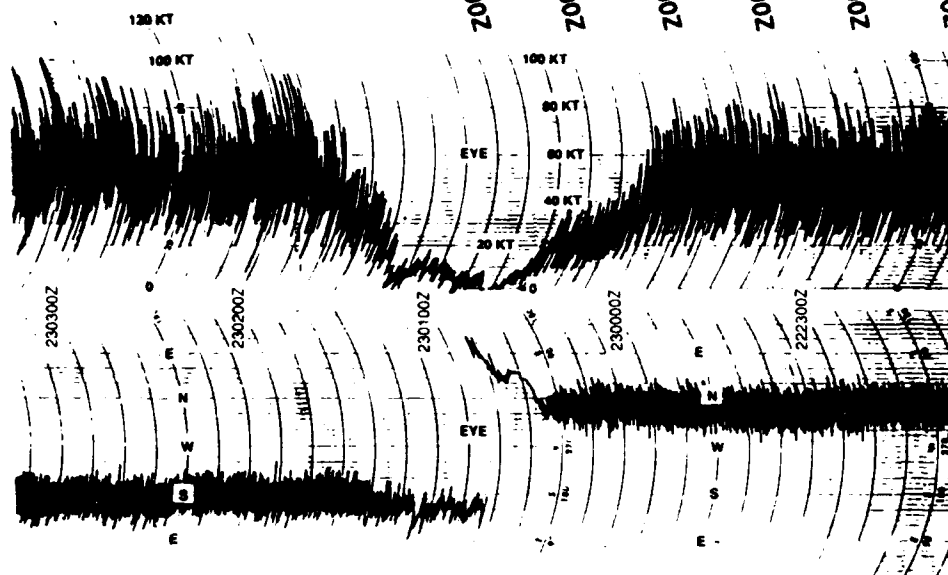
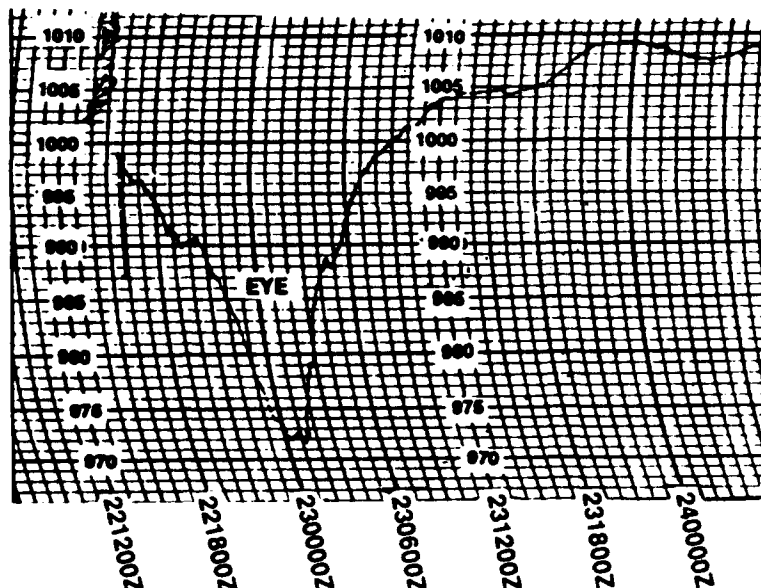


Figure 3-31-3. The passage of the eye of Typhoon Gay as measured by the anemometer at Nimitz Hill, Guam on 23 November.

southeast of Okinawa on 30 November, JTWC downgraded the typhoon to a tropical storm. The following day, the last of 63 warnings, the most for any 1992 tropical cyclone, was issued at 300600Z as the system dissipated over water south of Japan.

III. FORECAST PERFORMANCE

The overall mean track forecasting errors were 85, 155 and 200 nm (155, 285 and 370 km) for 24, 48 and 72 hours, respectively. JTWC's performance was 60-70% better than average, and provided an overall 70, 60 and 55% improvement over CLIPER for the 24-, 48- and 72-hour forecasts, respectively. JTWC got a head start on the aids on the very first warning by correctly anticipating Gay's track toward Guam. While JTWC had a fairly good handle on the tropical cyclone's motion, the dynamic guidance consistently recurved Gay well east of Guam. The numerical model guidance provided by NOGAPS actually got worse as the typhoon approached Guam, even depicting movement to the north as Gay passed directly overhead. NOGAPS predicted that Typhoon Hunt (32W) would stall east of Guam and that Gay would take a more northerly course, recurving prior to Hunt. OTCM, FBAM,

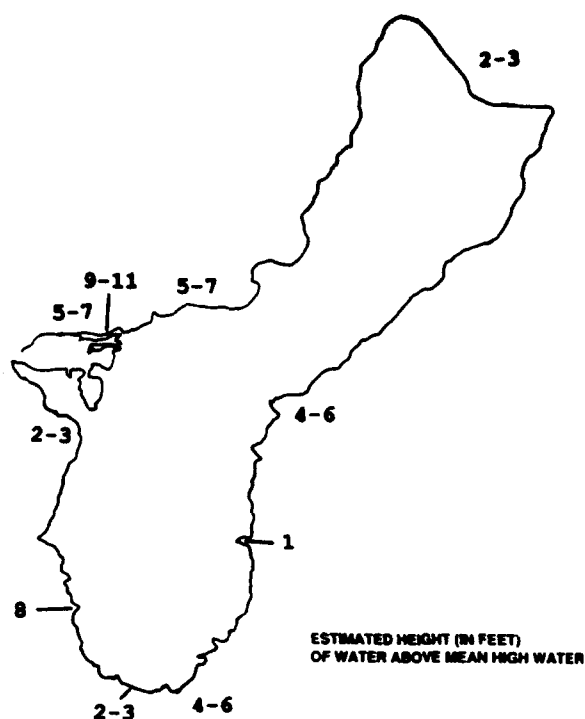


Figure 3-31-4. Estimates of the storm surge and wave runup experienced on Guam from the passage of Typhoon Gay on 23 November.

JTYM, EGRR, and CSUM all followed suit. Once Hunt recurved, the models, which had had trouble handling the two vortices, provided better guidance for Gay's track. By 26 November, as Gay approached the western extent of the mid-tropospheric subtropical ridge axis, most of the dynamic objective aids were back on track providing good guidance about the recurvature point and subsequent motion.

Gay was estimated to be the most intense tropical cyclone in the western North Pacific since Typhoon Tip in October 1979, and was identified early on as a probable rapid intensifier based on the tropical cyclone climatology for the location, time of year, sea surface temperature distribution and upper-tropospheric wind patterns. Prior to Gay's landfall on Guam, the Center also correctly predicted a decrease in intensity, due to the strong vertical wind shear from Typhoon Hunt (32W) to the north, but not nearly as fast as the weakening occurred. As Gay weakened, JTWC correctly anticipated the expansion of the typhoon's surface wind distribution and recommended that Conditions of Readiness 1 be set for the southern Mariana Islands of Guam, Rota, Tinian and Saipan. Reintensification after Gay passed to the west of Guam was also predicted based on the decreasing vertical wind shear from Hunt (32W).

IV. IMPACT

Gay bulldozed a path of destruction through most of the northern Marshall Islands, where the typhoon left over 5,000 people homeless, and knocked out power, water, and radio communications in Majuro. Miraculously, only one islander in the entire republic was injured, which reflects positively on the quality of the warning and disaster preparedness. President Amata Kabua declared Mejit Island and eight other northern atolls disaster areas. The hardest hit island was Wotho Atoll, population 160, where all trees and houses "fell down!" Amazingly, no one was injured as Gay ripped through the small atoll. Mejit Island fared only slightly better. They lost all wooden structures on the island, leaving almost all of the 445 people on that island homeless. The winds were so strong that most of the coconut trees

were blown down and 75% of the crops were lost. Ailuk Atoll suffered about the same crop losses as Mejit, but only had minor house damage. Utirik and Likiep Atolls suffered 50% crop and tree losses, and experienced damage to half of their houses. Maloelop and Aur Atolls were on the fringes of the damaging winds and only suffered 20 - 30% crop and house damage. Most of the atolls were without fresh drinking water for weeks or months after the typhoon, as catchment basins were destroyed or contaminated with salt water.

Majuro, the capital of the Marshall Islands, suffered from island-wide power outages due to lightning strikes. Another lightning strike hit the Outer Island Dispensary and knocked out the radio link to 67 of the outer island hospitals. One boat smashed into the seawall and sank as it broke loose in Majuro Harbor. For two days after Gay's passage, Air Marshall Island flights were canceled until the debris could be cleared from the runways.

Gay's next target was Guam. Passing over the center of the island, Gay became the fifth typhoon to pass within 60 nm (110 km) in less than three months, and everyone in the Marianas Islands took Gay's threat extremely seriously. Just to the north, Saipan recorded a record 1639 people in shelters as Gay passed, and twelve families had to be evacuated from their homes by emergency crews as the storm surge threatened to sweep away their houses. One house was destroyed by the storm surge and another was damaged by a fire caused by burning candles and kerosene lamps used after the power was out. On Tinian, four houses lost their sheet iron-roofs to Gay.

On Guam, it was difficult to isolate the damage from Gay alone because Typhoon Omar (15W) had already destroyed most of the weaker structures. The most visible result of Gay's passage over Guam was to the crops and vegetation on the island. Gay was a "dry" cyclone, and airborne salt whipped up from the ocean as the typhoon passed burnt the vegetation. Farmers suffered the most losses due to Typhoon Gay. The typhoon disrupted everyday life for the fifth time during the year: ships were sent to sea; 4,300 residents sought typhoon shelters; the port and airports were shut down; schools and other government and civilian offices were closed, and the power plant was placed in standby operation. The storm surge brought sand, coral rubble and water ashore, especially in the area of the Cabras Island port access road. Some wharf damage occurred when a fishing vessel broke loose from its mooring, and a fuel storage tank that was under construction collapsed. It must be remembered that it could have been worse, had it not been for the incredible timing of Typhoon Hunt's (32W) interaction with Gay, Guam would have had to face the devastation of a super typhoon.

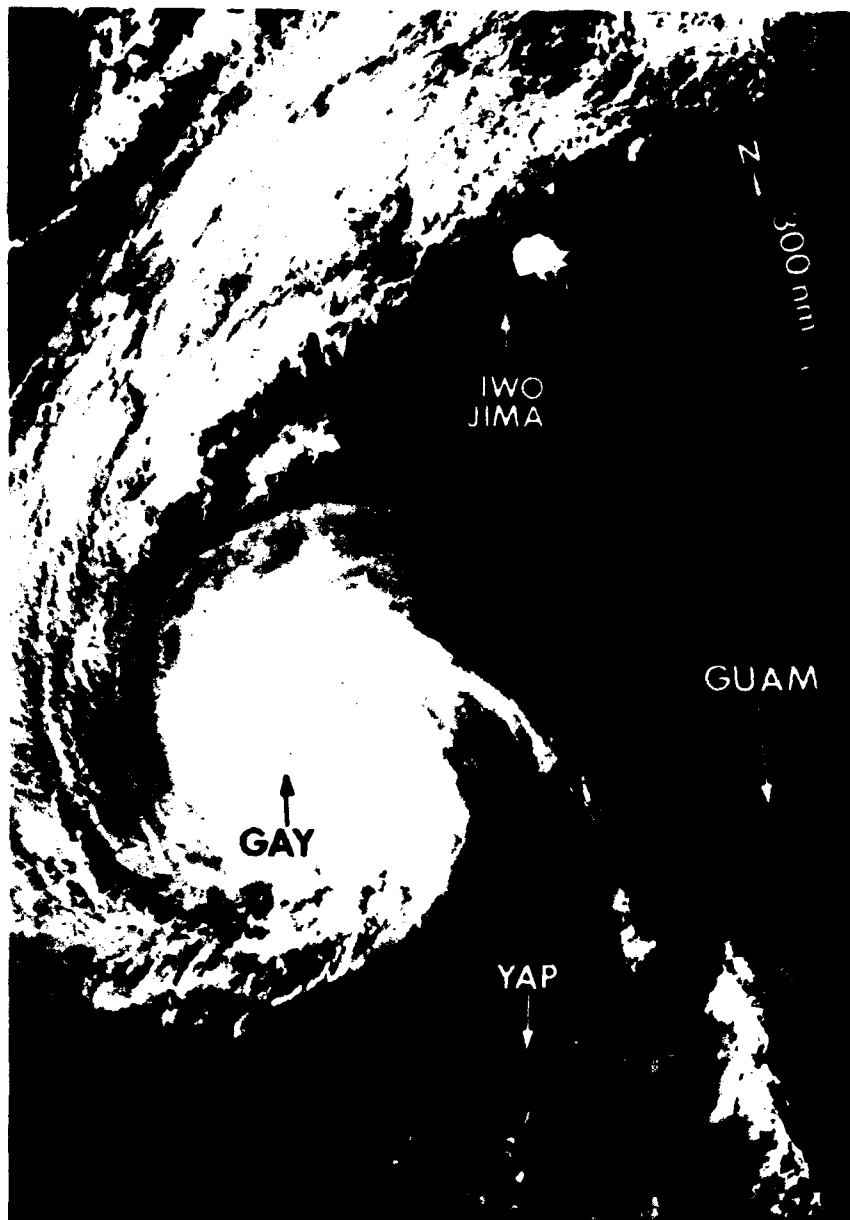
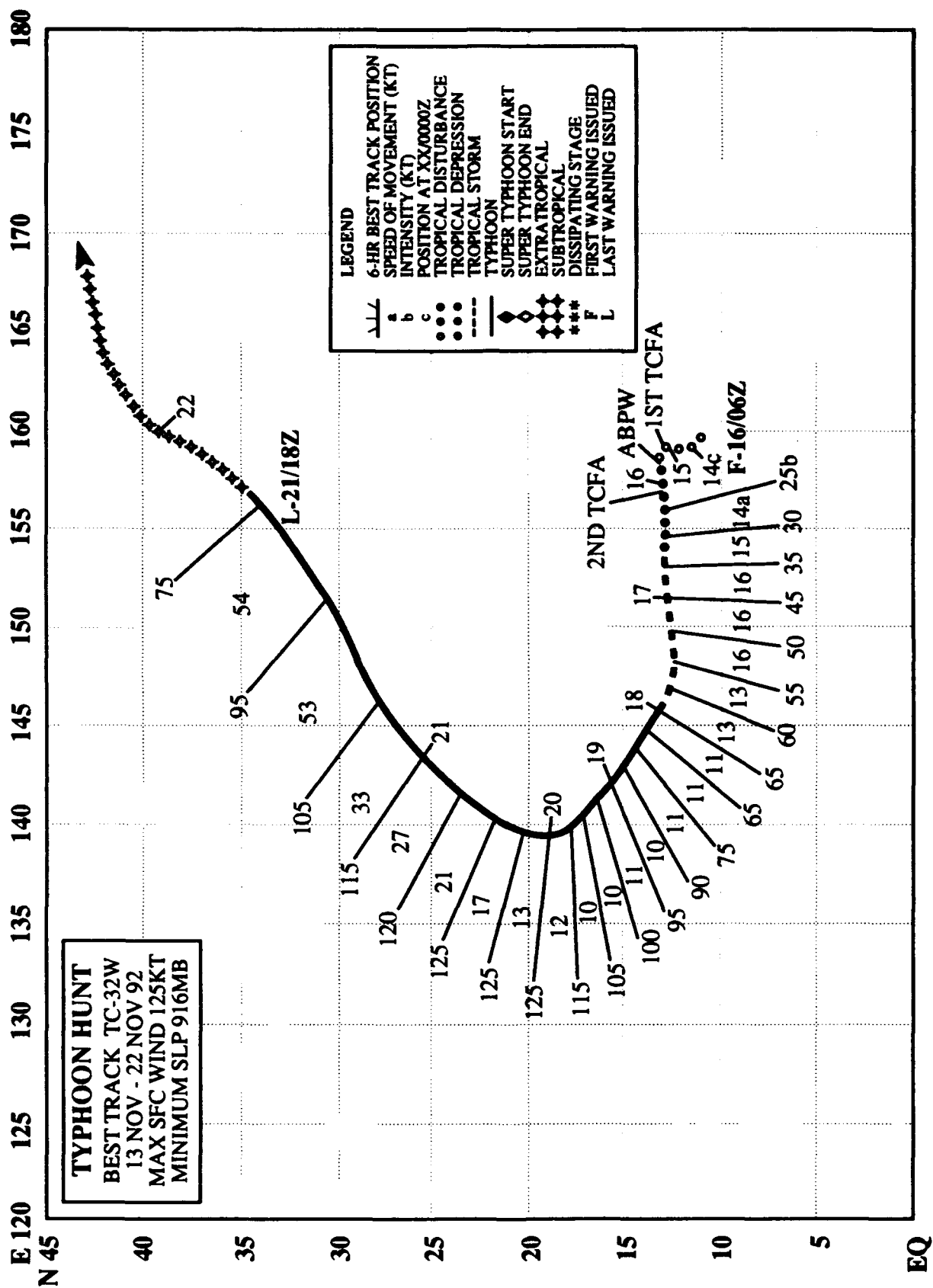


Figure 3-31-5. Gay's cloud filled eye is visible as the typhoon approaches its second peak intensity. The circulation is large which is typical of November typhoons (242348Z November DMSP visual imagery).



TYPHOON HUNT (32W)

I. HIGHLIGHTS

The fourth typhoon to pass within 60 nm (110 km) of Guam in less than three months, Hunt was part of a three storm outbreak with Tropical Storm Forrest (30W) and Gay (31W). As Hunt intensified, it brushed by Guam, moved into the Philippine Sea, and later recurved. After recurvature, the typhoon played an important role in the extremely rapid weakening of Super Typhoon Gay (31W) which was approaching the southern Mariana Islands.

II. TRACK AND INTENSITY

On 13 November, the monsoon trough extended eastward from Tropical Storm Forrest (30W) in the South China Sea, across the southern Philippines, through the Caroline Islands to a tropical disturbance in the southern Marshall Islands, and on further to the another tropical disturbance forming just to the east of the international dateline that would become Gay (31W). The tropical disturbance in the southern Marshall Islands that became Hunt was first mentioned by JTWC on the 140600Z November Significant Tropical Weather Advisory. As the cloud system associated with this disturbance slowly drifted northward, increasing convection prompted JTWC to issue the first Tropical Cyclone Formation Alert at 150400Z. Because the disturbance was slow to consolidate, the alert was reissued at 160400Z. The first warning followed at 160600Z based on the appearance of a poorly defined low-level circulation center with improved convective organization on the animated visual and infrared satellite imagery.

Tropical Depression 32W tracked westward under the steering influence of the mid-tropospheric subtropical ridge. Intensifying at an average rate of one Dvorak T-number per day, the depression was upgraded by JTWC to Tropical Storm Hunt at 170000Z. Twenty-four hours later, Hunt was further upgraded to a typhoon based on an Dvorak intensity estimate of 65 kt (33 m/sec), and convective organization that had continued to improve.

As Hunt approached Guam, it was expected to pass close to, or over, the southern portion of the island. However, to the east of the island, the typhoon changed course and began to track northwestward toward a break in the subtropical ridge. The typhoon passed 10 nm (20 km) east-northeast of Andersen AFB (WMO 91218) where a minimum sea-level pressure of 987.2 mb was recorded at 180455Z. After Hunt churned through the channel between the islands of Guam and Rota, a strong convective band crossed Guam producing two to three hours of 60 kt (31 m/sec) winds with gusts to 75 kt (39 m/sec), and heavy rain.

Continuing to intensify on its northwestward track, Hunt reached a peak of 125 kt (64 m/sec) near its point of recurvature at 200000Z (Figure 3-32-1). The typhoon's acceleration into the mid-latitude westerlies was one of the fastest noted in 1992 or any year, reaching an average 6-hour track speed of 54 kt (100 km/hr) as it transitioned into an extratropical low. (See the Super Typhoon Gay (31W) synopsis for a more complete description of Hunt's affect on Gay (31W).) The final warning for Hunt was issued by JTWC at 211800Z when Hunt became extratropical.

III. FORECAST PERFORMANCE

The overall mean track errors for JTWC were 145, 300 and 545 nm (265, 556 and 1010 km) for the 24-, 48- and 72-hour forecasts. This performance was much worse than average and was beaten by CLIPER at 48 and 72 hours. The poor overall performance resulted from several factors. First, over estimation of the strength of the subtropical ridge led to steady westward track forecasts, even after

Hunt began to move northwestward. Second, forecasters were heavily influenced by the NOGAPS guidance which had a difficult time resolving both the circulations of Typhoon Hunt and Super Typhoon Gay (31W), and erroneously indicated that Hunt would stall as Gay (31W) recurved first and accelerated into the westerlies. Finally, the greatest errors at 48 and 72 hours were due to under forecasting Hunt's unusually rapid acceleration after recurvature.

Overall intensity forecasts were good with the exception of the 72-hour extended outlooks for the first four warnings. These proved to be 45 to 50 kt (23 to 26 m/sec) too low when an anticipated increase in vertical shear did not occur, and Hunt intensified more rapidly than expected.

IV. IMPACT

In preparation for Hunt's passage on 18 November, Guam boarded up, closed schools and other government offices, evacuated aircraft, and sent ships to sea. The disaster preparations paid off. No fatalities or injuries were reported and damage appeared to minimal, however, the quantitative assessments of the minor damage caused by Hunt were not completed before Super Typhoon Gay (31W) slammed into the island five days later. As with Brian (25W) and Elsie (28W), more damage would have occurred had not Omar (15W) destroyed most of the island's weaker structures earlier on 28 August.

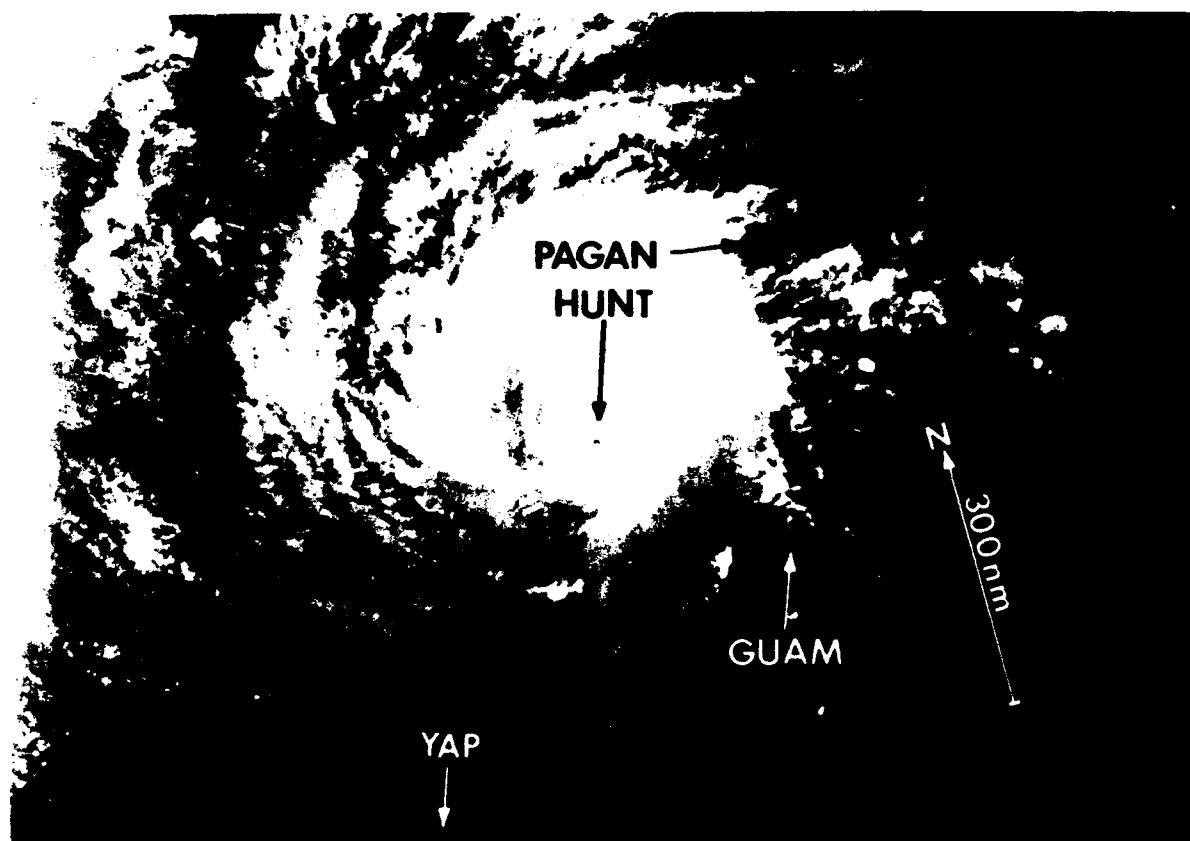


Figure 3-32-1. As Hunt intensifies, the diameter of its cloud-filled eye, which had been 14 nm (26 km) nine hours earlier, decreases to 7 nm (13 km) (182336Z November DMSP visual imagery).

3.3 NORTH INDIAN OCEAN TROPICAL CYCLONES

Spring and fall in the North Indian Ocean are periods of transition between major climatic controls and the most favorable seasons for tropical cyclone activity (Tables 3-5 and 3-6). This year was the most active North Indian Ocean tropical cyclone season since JTWC started issuing warnings for the region in 1971. A record 12 tropical cyclones formed in the North Indian Ocean, 4 in the Arabian Sea and 8 in the Bay of Bengal. A total of 13 cyclones transited the North Indian Ocean if you count Typhoon Forrest (30W) that crossed from the Gulf of Thailand into the Bay of Bengal. This was well above the 5 per year average, and 4 more than the previous record of 8 tropical cyclones in 1987.

The JTWC was in warning status a total of 53 days, 34 more days than last year. Also, JTWC was in warning status on 2 tropical cyclones simultaneously, Tropical Cyclone 10B and Typhoon 30W (Forrest), for a 3-day period in November. For the 22-year period of record, Tropical Cyclone 04B became the first tropical cyclone to occur in July, leaving March as the only month without a recorded tropical cyclone. Also, a record-breaking 3 tropical cyclones occurred in October and then again in November. Tropical Cyclone 12A was the last cyclone of the year and caused delays for ships transiting the Arabian Sea in support of OPERATION RESTORE HOPE. Composite best tracks for the North Indian Ocean tropical cyclones for 1992 are shown in Figure 3-9.

TABLE 3-5.

**1992 SIGNIFICANT TROPICAL CYCLONES
NORTH INDIAN OCEAN**

TROPICAL CYCLONE	PERIOD OF WARNING	NUMBER OF WARNINGS ISSUED	MAXIMUM SURFACE WINDS-KT (M/SEC)	ESTIMATED MSLP (MB)
TC 01B	16 MAY - 20 MAY	15	65 (33)	976
TC 02A	05 JUN - 12 JUN	29	35 (18)	997
TC 03B	17 JUN - 18 JUN	6	45 (23)	991
TC 04B	26 JUL - 27 JUL	4	40 (21)	994
TC 05B	22 SEP - 24 SEP	7	30 (15)	1000
TC 06A	01 OCT - 03 OCT	10	55 (28)	984
TC 07B	07 OCT - 09 OCT	10	45 (23)	991
TC 08B	21 OCT - 21 OCT	3	30 (15)	1000
TC 09B	03 NOV - 07 NOV	20	55 (28)	984
TC 10B	11 NOV - 17 NOV	28	70 (36)	972
TC 30W	15 NOV - 22 NOV	26	125 (64)	916
TC 11A	30 NOV - 03 DEC	14	50 (26)	987
TC 12A	20 DEC - 24 DEC	18	50 (26)	987

TOTAL: 190

TABLE 3-6. NORTH INDIAN OCEAN TROPICAL CYCLONES DISTRIBUTION

YEAR	JAN	FEB	MAR	APR	MAY	JUN	JUL	AUG	SEP	OCT	NOV	DEC	TOTAL
1971*	-	-	-	-	-	0	0	0	0	1	1	0	2
1972*	0	0	0	1	0	0	0	0	2	0	1	0	4
1973*	0	0	0	0	0	0	0	0	0	1	2	1	4
1974*	0	0	0	0	0	0	0	0	0	0	1	0	1
1975	1	0	0	0	2	0	0	0	0	1	2	0	6
1976	0	0	0	1	0	1	0	0	1	1	0	1	5
1977	0	0	0	0	1	1	0	0	0	1	2	0	5
1978	0	0	0	0	1	0	0	0	0	1	2	0	4
1979	0	0	0	0	1	1	0	0	2	1	2	0	7
1980	0	0	0	0	0	0	0	0	0	0	1	1	2
1981	0	0	0	0	0	0	0	0	0	1	1	1	3
1982	0	0	0	0	1	1	0	0	0	2	1	0	5
1983	0	0	0	0	0	0	0	1	0	1	1	0	3
1984	0	0	0	0	1	0	0	0	0	1	2	0	4
1985	0	0	0	0	2	0	0	0	0	2	1	1	6
1986	1	0	0	0	0	0	0	0	0	0	2	0	3
1987	0	1	0	0	0	2	0	0	0	1	2	2	8
1988	0	0	0	0	0	1	0	0	0	1	2	1	5
1989	0	0	0	0	1	1	0	0	0	0	1	0	3
1990	0	0	0	1	1	0	0	0	0	0	1	1	4
1991	1	0	0	1	0	1	0	0	0	0	1	0	4
1992	0	0	0	0	1	2	1	0	1	3	3	2	13

(1975-1992)

AVERAGE: 0.2 0.1 0.0 0.2 0.7 0.6 0.0 0.0 0.3 0.9 1.5 0.6 5.0
 TOTAL: 3 1 0 3 12 11 1 1 4 17 27 10 90

* JTWC WARNING RESPONSIBILITY BEGAN ON 4 JUNE 1971 FOR THE BAY OF BENGAL, EAST OF 90° EAST LONGITUDE. AS DIRECTED BY CINCPAC, JTWC ISSUED WARNINGS ONLY FOR THOSE TROPICAL CYCLONES THAT DEVELOPED OR TRACKED THROUGH THAT PART OF THE BAY OF BENGAL. IN 1975, JTWC'S AREA OF RESPONSIBILITY WAS EXTENDED WESTWARD TO INCLUDE THE WESTERN PART OF THE BAY OF BENGAL AND THE ENTIRE ARABIAN SEA.

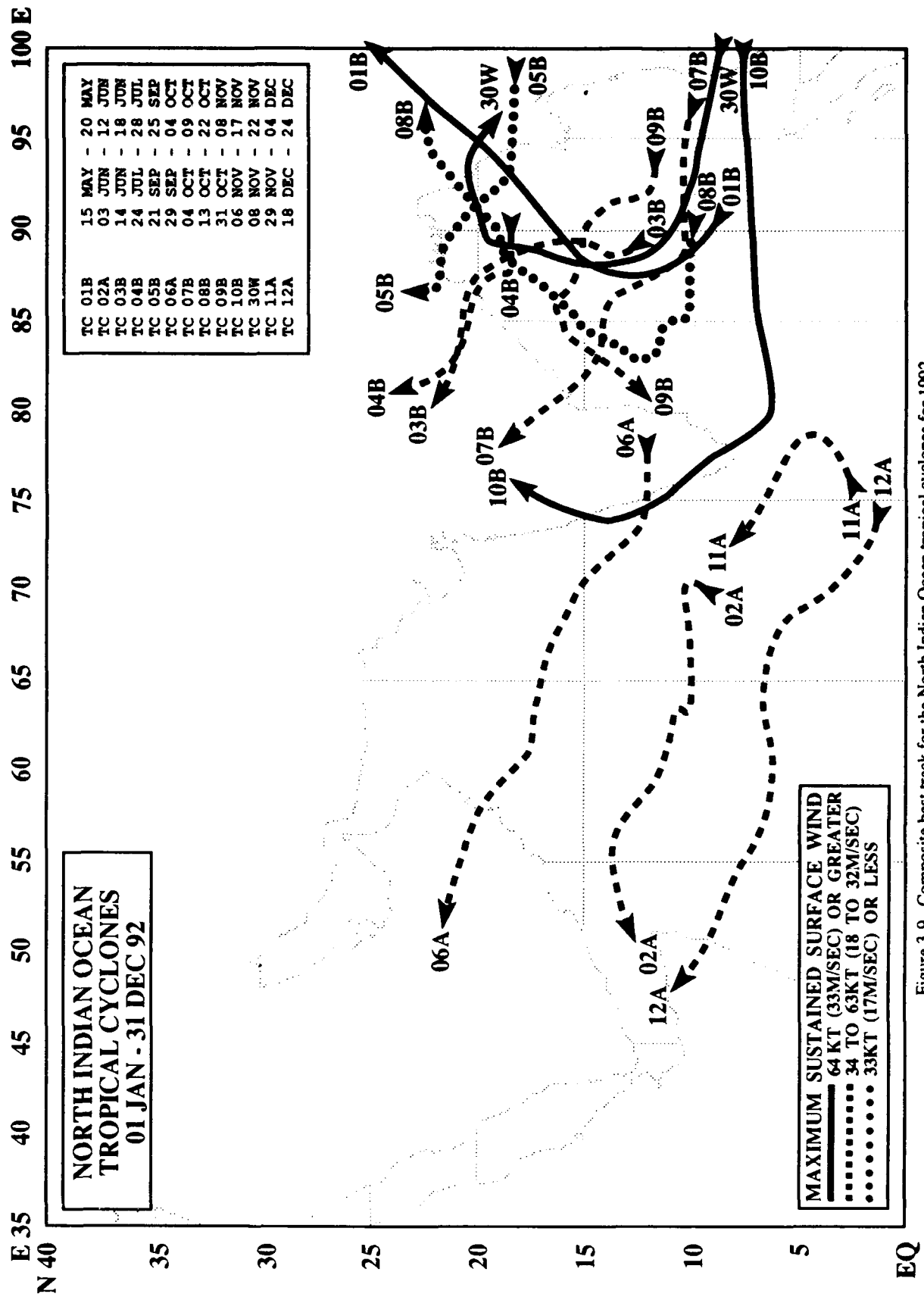
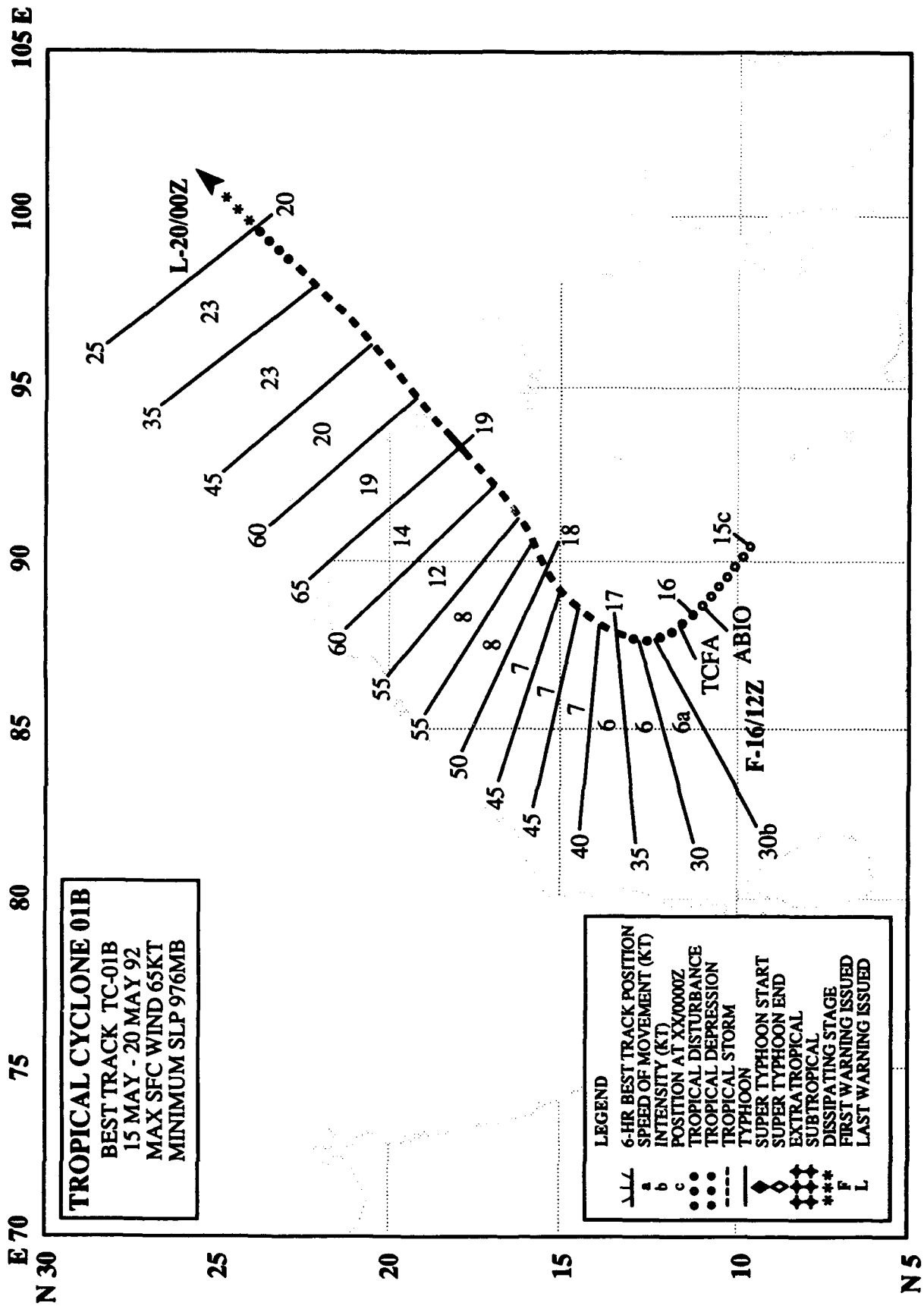


Figure 3-9. Composite best track for the North Indian Ocean tropical cyclones for 1992.



TROPICAL CYCLONE 01B

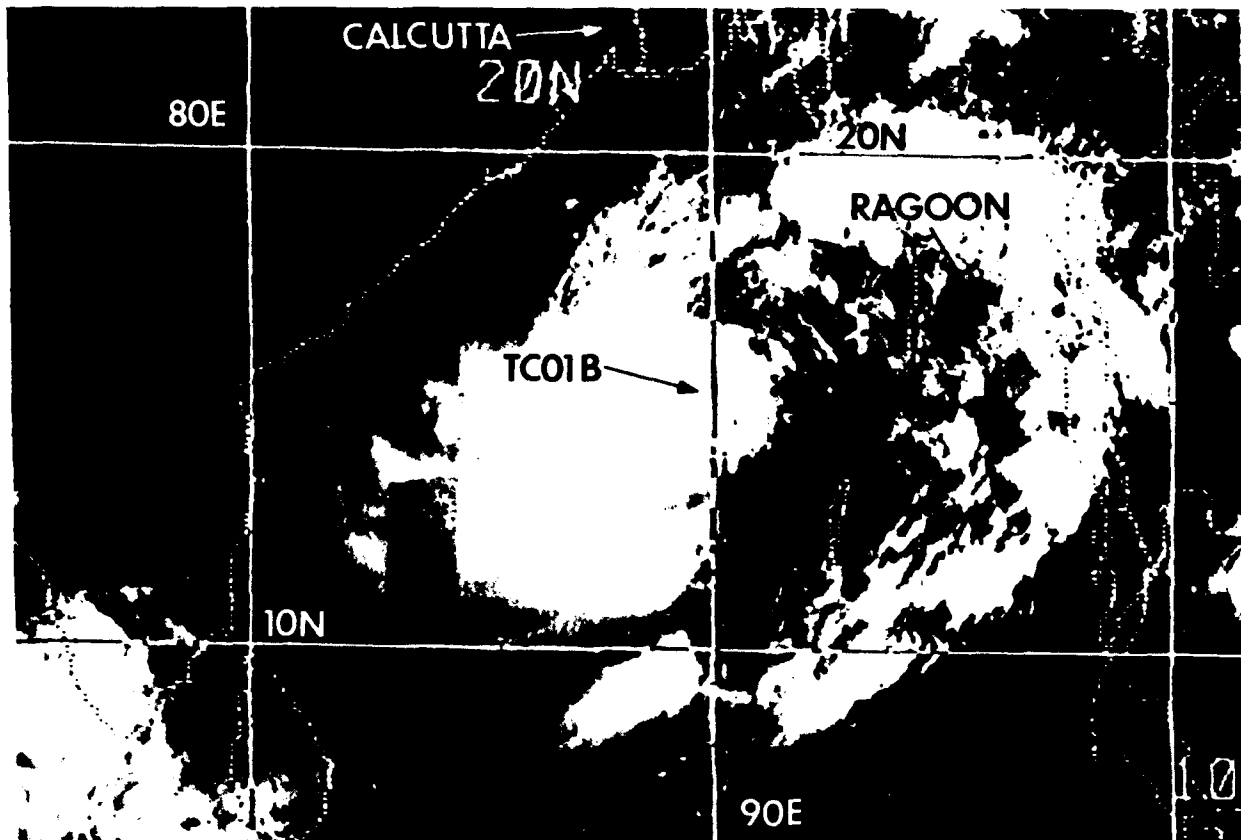
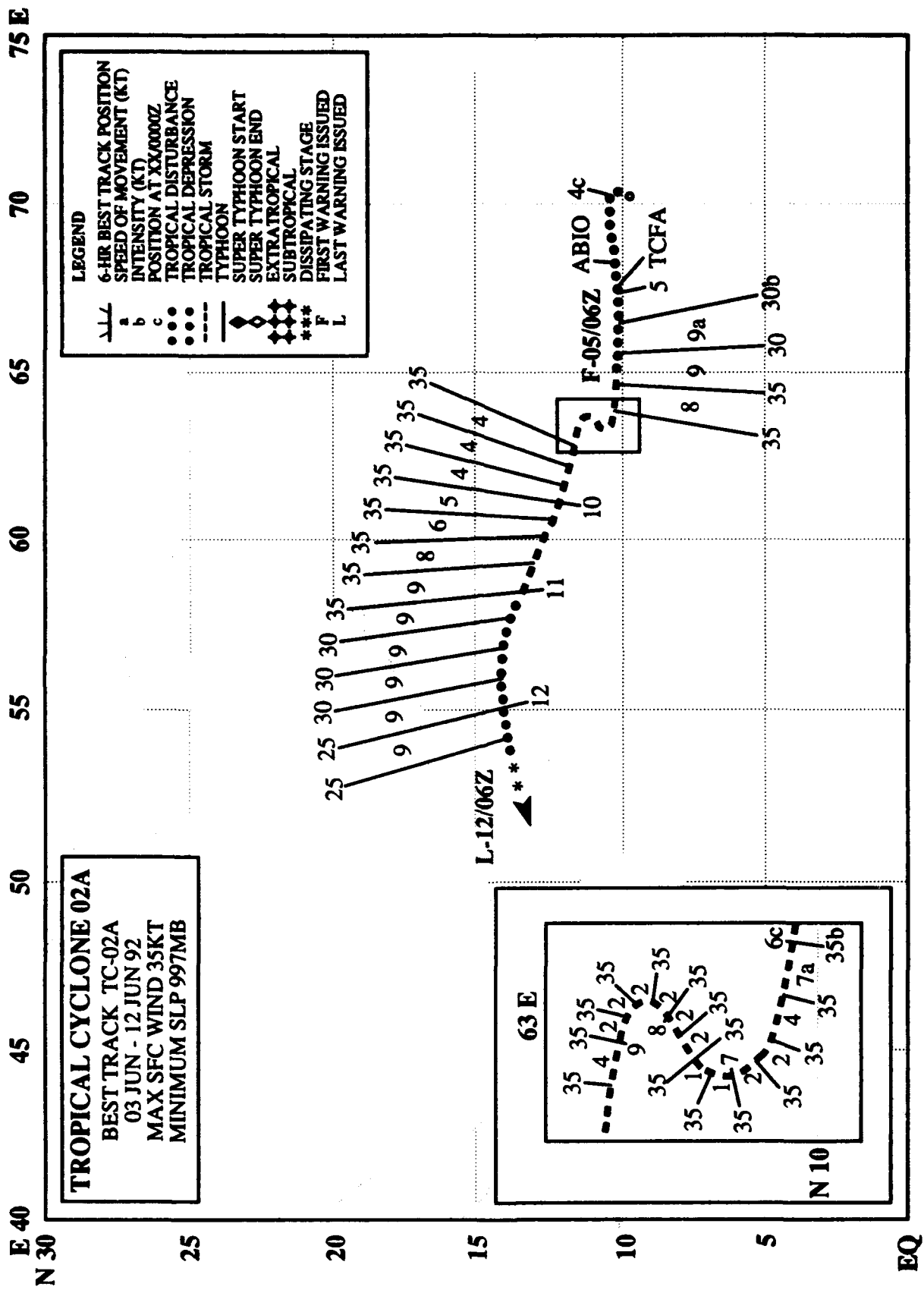


Figure 3-01B-1. Although TC01B's central dense overcast is located near the center of the Bay of Bengal, a broad band of enhanced cloudiness associated with the tropical cyclone is already affecting Burma (180200Z - 180400Z May DMSP visual digitized mosaic).

After an absence of tropical cyclone activity in the North Indian Ocean for six months, TC01B developed in the Bay of Bengal with the onset of the summer monsoon. It was first mentioned on the 151800Z May Significant Tropical Weather Advisory and was the subject of a Tropical Cyclone Formation Alert at 160451Z, which was followed by the first warning at 161200Z. Because of the slow intensification and poorly defined cloud system center of TC01B, JTWC had to relocate the initial position on the second warning. The system recurved on 16 May, and continued to intensify afterward, reaching minimal typhoon intensity for a short period prior to landfall in Burma on 19 May. The final warning was issued by JTWC at 200000Z.



TROPICAL CYCLONE 02A

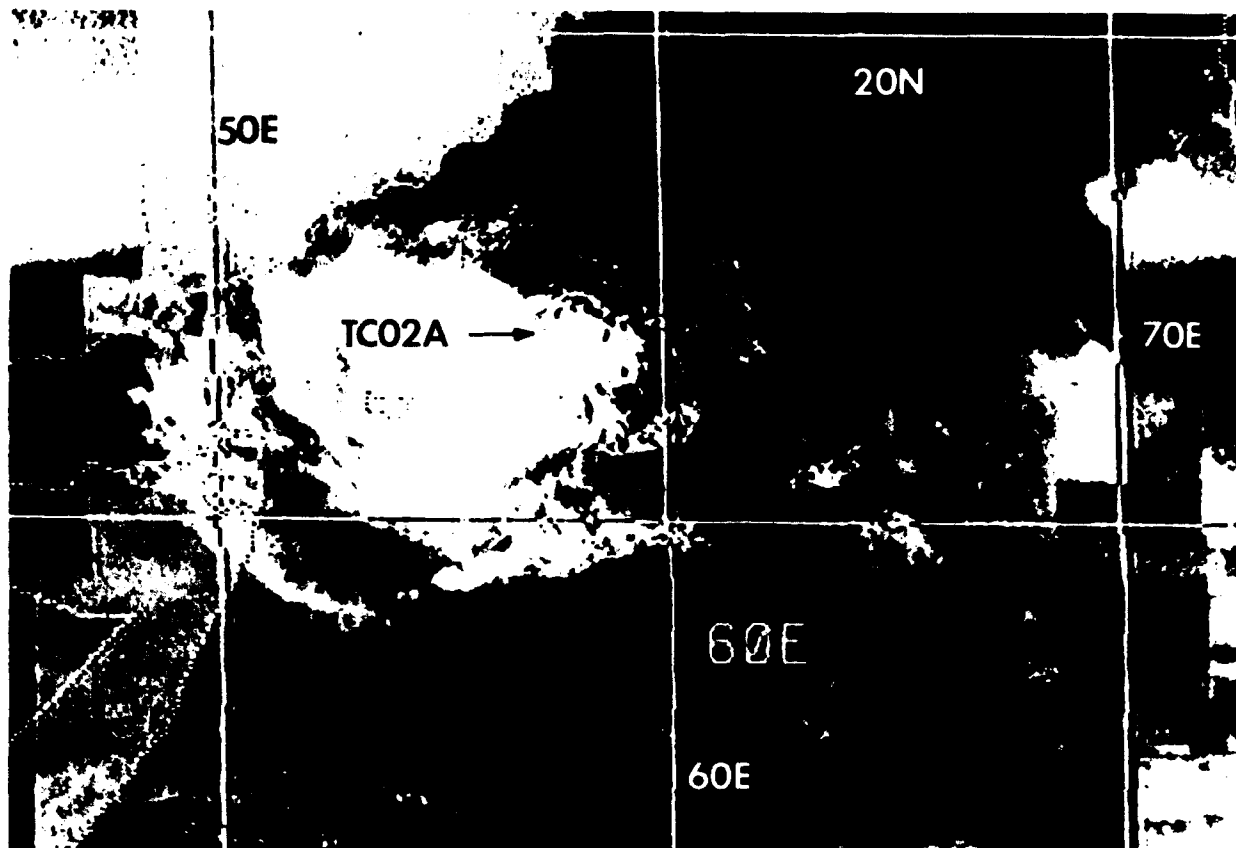
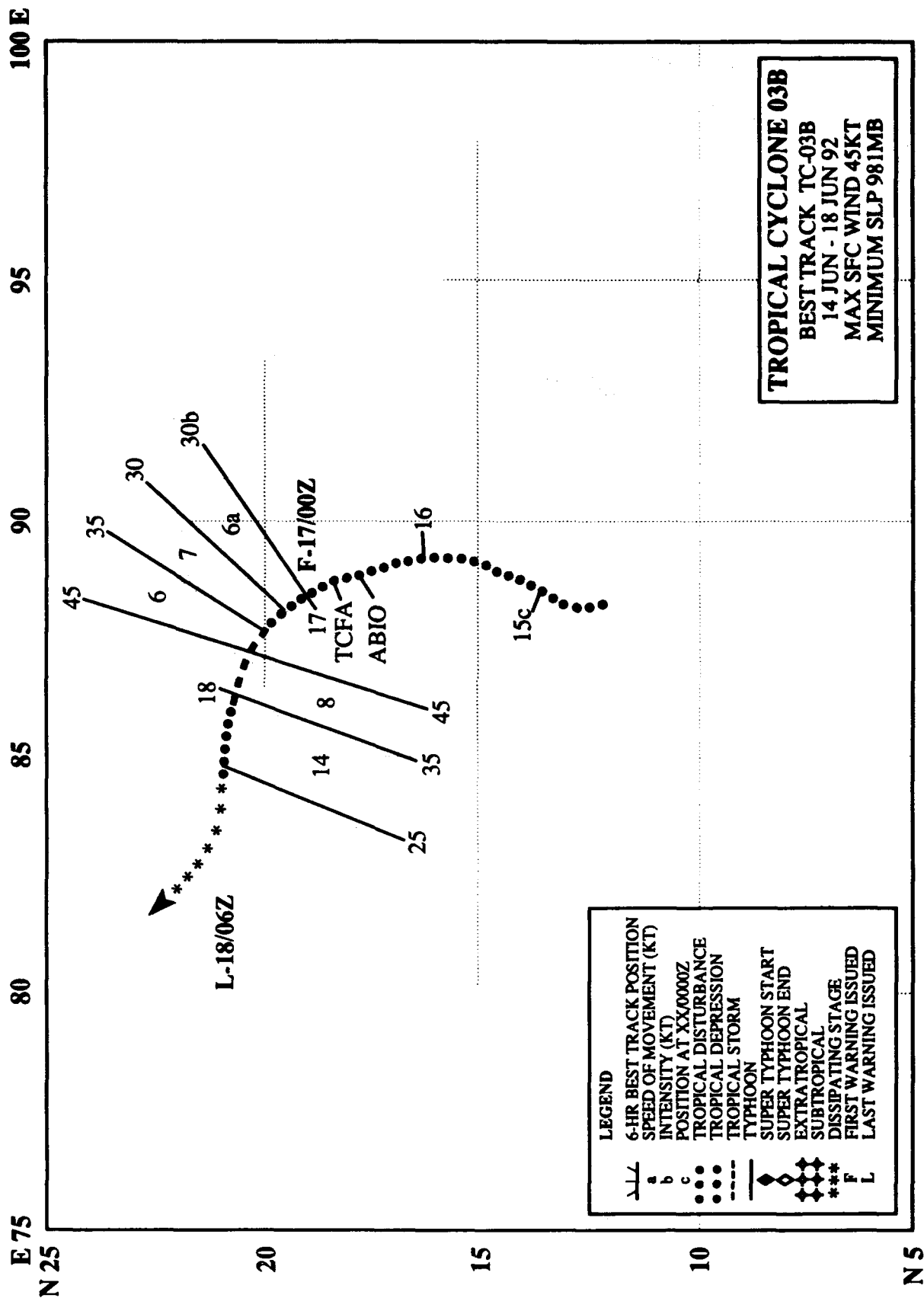


Figure 3-02A-1. A partially exposed low-level circulation is visible to the east of TC02A's central cloud mass (110300Z - 110400Z June DMSP visual digitized mosaic).

Two weeks after TC01B formed in the Bay of Bengal, a small low-level circulation center developed in the monsoon trough in the Arabian Sea. Increasing convection prompted JTWC to mention it on the 041800Z June Significant Tropical Weather Advisory. As convective organization rapidly improved, this was followed by a Tropical Cyclone Formation Alert at 042300Z, and the first warning at 050600Z. However, strong upper-level easterly winds restricted the outflow aloft, keeping the cyclone at minimum tropical storm intensity over the next five days as it tracked slowly westward across the Arabian Sea. Interpretation of DMSP microwave imagery on 7 June indicated that the low-level circulation was further east than analyzed from infrared data, resulting in a relocated position and an amended forecast at 072100Z. As the presence of upper-level shear persisted, TC02A gradually weakened. The final warning was issued by JTWC at 120600Z as the cyclone dissipated over the open ocean just north of the island of Socotra. TC02A was the first of four tropical cyclones to develop during 1992 in the Arabian Sea, a basin that averages only one per year.



TROPICAL CYCLONE 03B

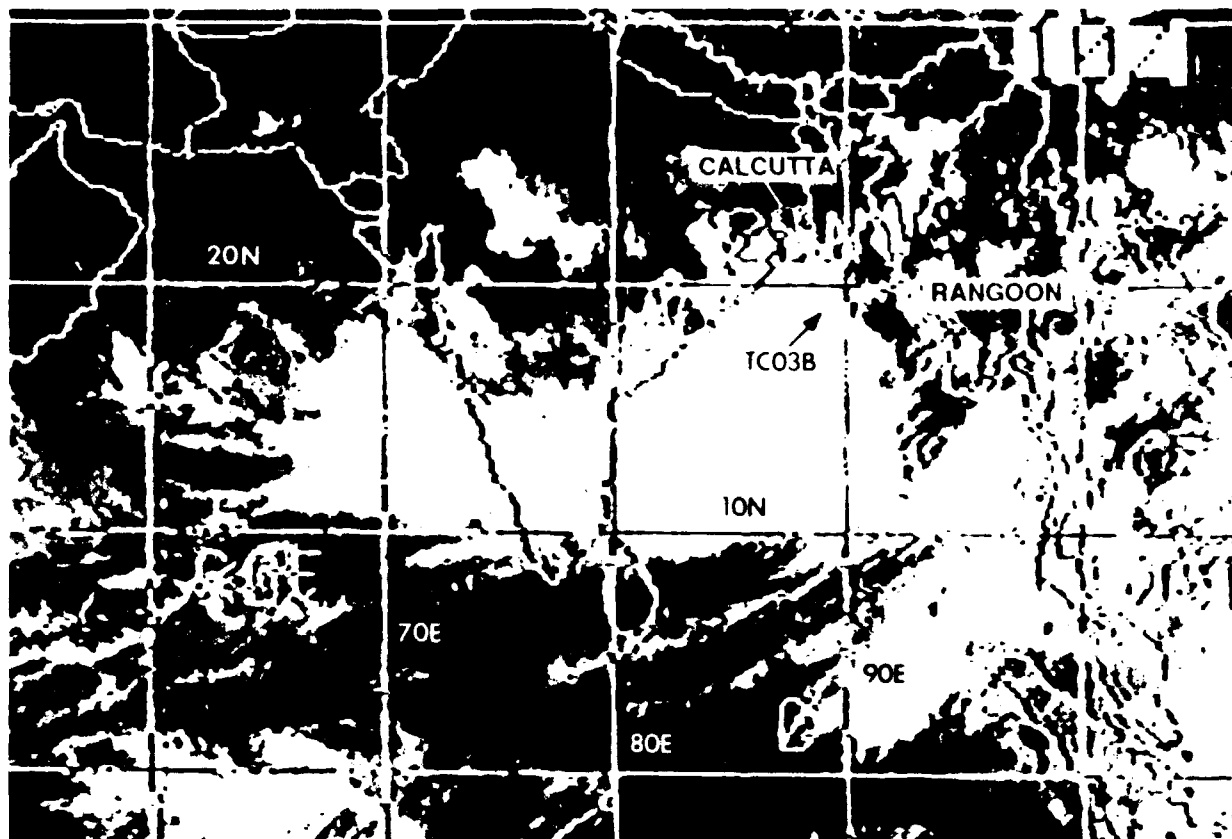
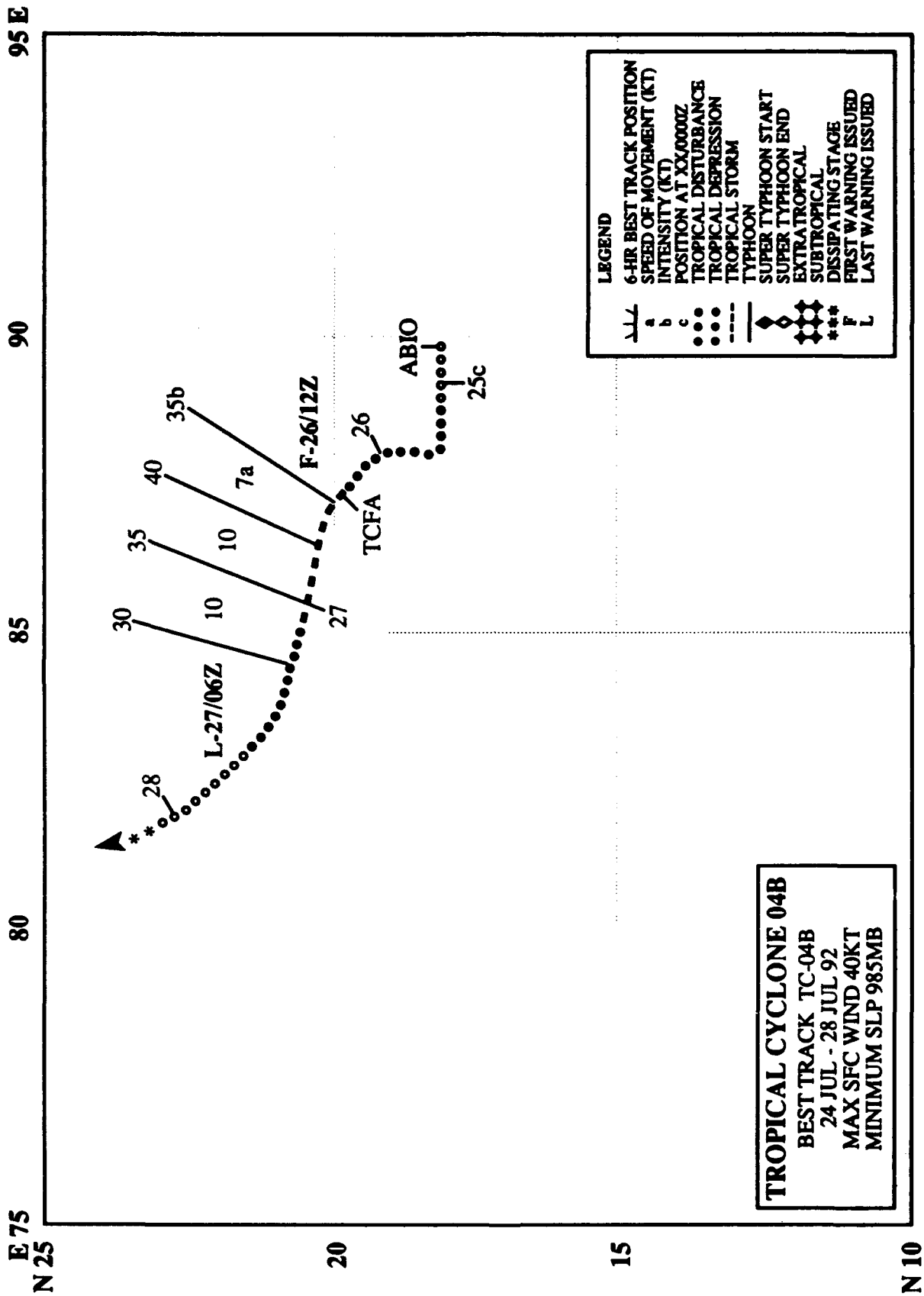


Figure 3-03B-1. TC03B a day before making landfall in India (161000Z - 161200Z June DMSP infrared digitized mosaic).

In response to a surge in the monsoon the second week of June, a tropical disturbance developed in the Bay of Bengal which prompted JTWC to reissue the Significant Tropical Weather Advisory for the Indian Ocean at 161300Z June to include mention of the disturbance's consolidation. A Tropical Cyclone Formation Alert followed at 161800Z, and the first warning was issued by JTWC at 170000Z as the cyclone turned northwestward towards India. Due to its nearness to the coast of India, TC03B had little time to intensify. The tropical cyclone struck the coast with a peak intensity of 45 kt (23 m/sec) at 172000Z, and slowly dissipated overland. JTWC issued the final warning at 180600Z.



TROPICAL CYCLONE 04B

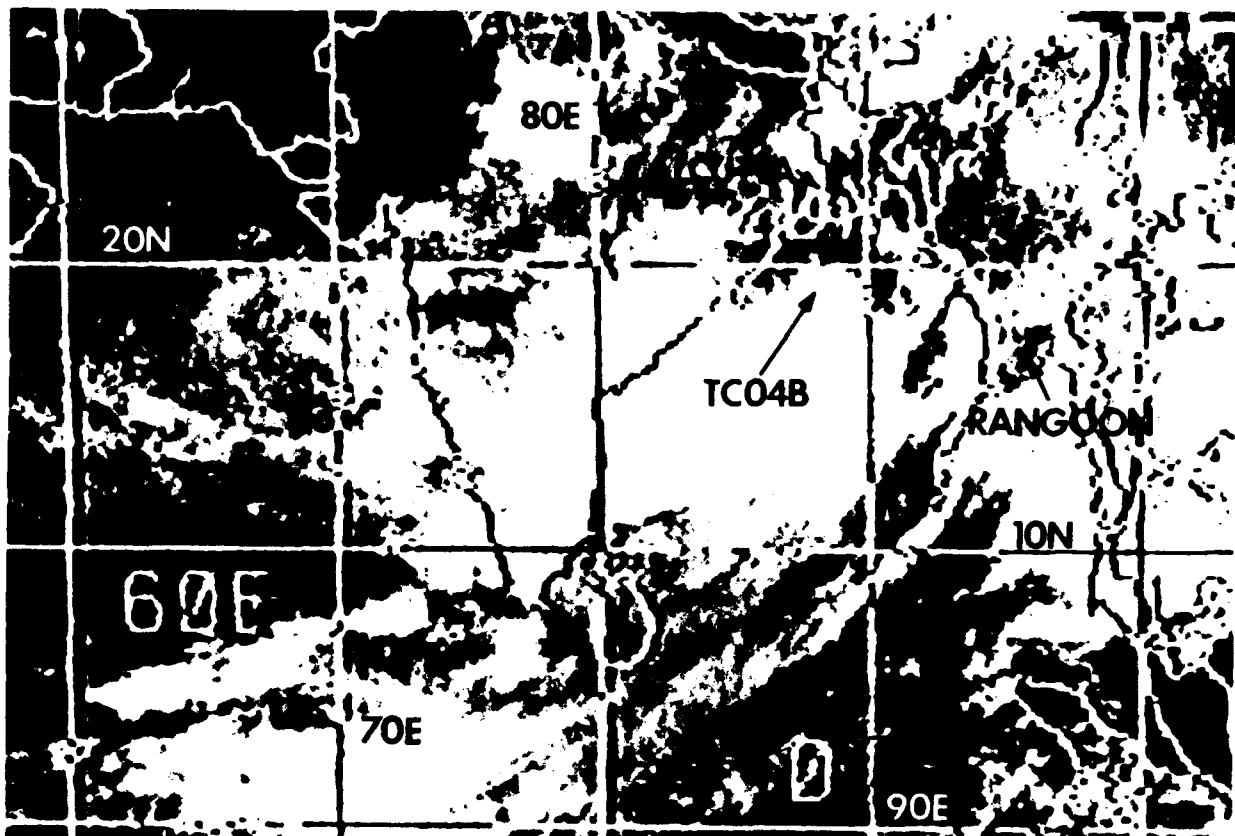


Figure 3-04B-1. The deep convection and torrential rains associated with TC04B are located to the south of the circulation center, a result of strong vertical wind shear between low-level convergent and high-level divergent winds (252300Z - 260100Z July DMSP infrared digitized mosaic).

A rare July cyclone in the Bay of Bengal, TC04B followed a track very similar to Tropical Cyclone 03B in June. The tropical disturbance was first mentioned by JTWC on the 241800Z July Significant Tropical Weather Advisory. As the southwesterly monsoonal surge increased in strength, TC04B intensified, prompting JTWC to issue a Tropical Cyclone Formation Alert at 261000Z. The first warning followed almost immediately at 261200Z based on the extent of the surge and surface pressure falls on the coast of India. TC04B reached a peak intensity of 40 kt (21 m/sec) at landfall. As the tropical cyclone slowly weakened overland, JTWC issued the final warning at 270600Z.

TROPICAL CYCLONE 05B

After a two month hiatus of tropical cyclone activity in the North Indian Ocean, the tropical disturbance that became TC05B moved into the Bay of Bengal and developed on 21 September. As the broad monsoon depression moved over open water in the Bay of Bengal and its convection increased, JTWC went directly to a Tropical Cyclone Formation Alert at 220525Z. Within the next six hours, the increased convection had organized and the Center issued the first warning at 221200Z. TC05B remained close to the shoreline of Bangladesh and India and did not intensify above 30 kt (15 m/sec). The final warning was issued by JTWC at 240000Z as the tropical cyclone dissipated over land.

TROPICAL CYCLONE 06A

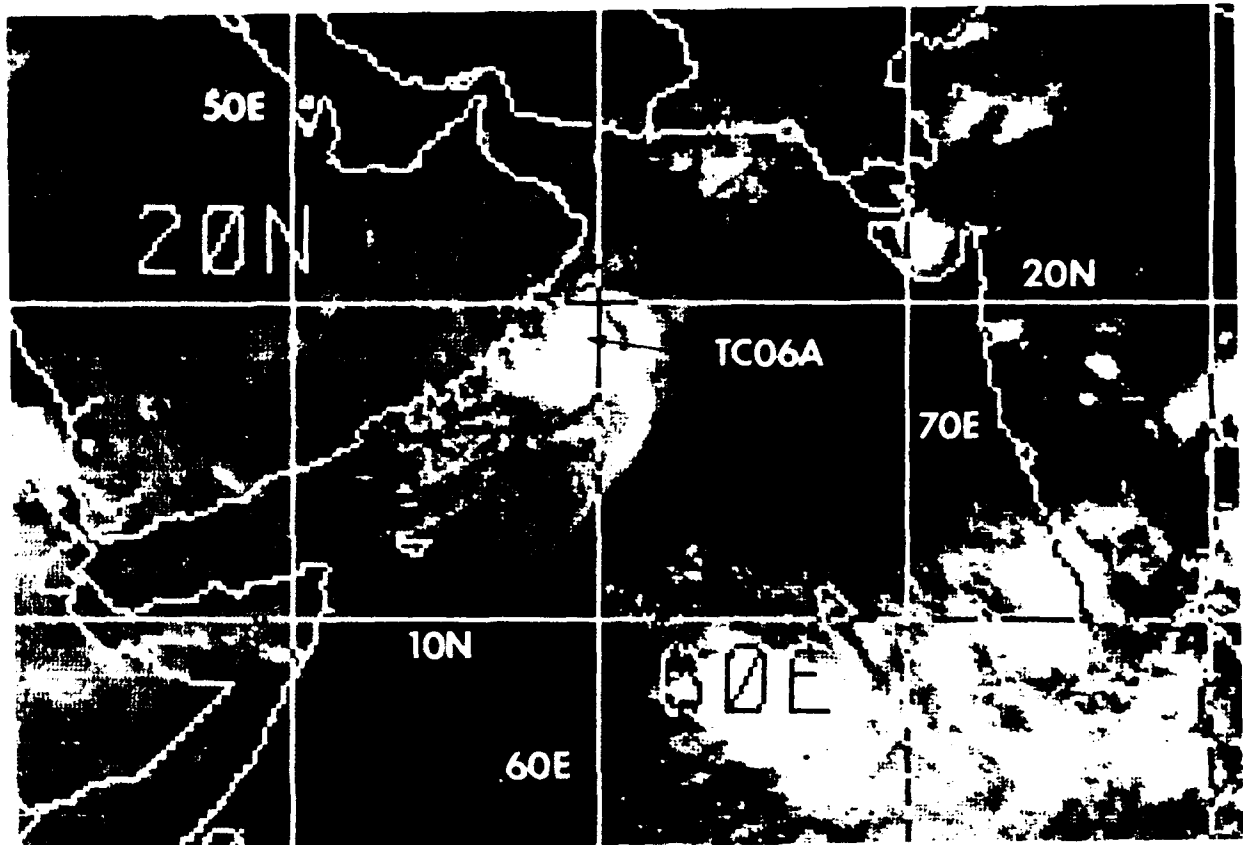
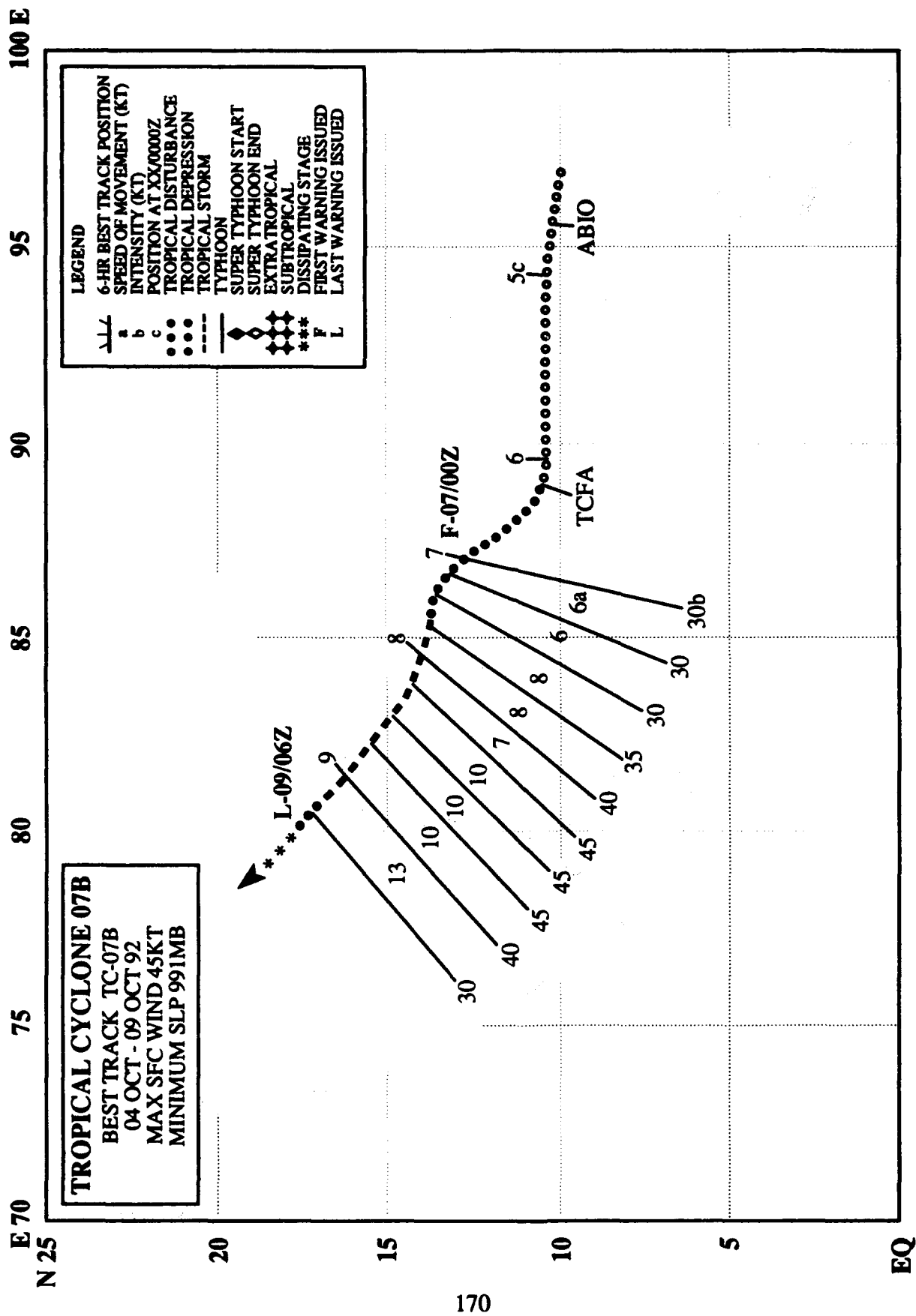


Figure 3 06A-1. Near peak intensity, TC06A approaches landfall on Oman (021600Z - 021800Z October DMSP infrared digitized mosaic).

An area of low pressure which developed over southern India moved offshore, tracking west-northwestward across the Arabian Sea. Because of strong easterly winds aloft, most of the deep convection associated with the tropical disturbance was displaced west of its poorly defined surface circulation center. As a consequence, the tropical cyclone developed slowly. Eventually, increased organization in the low-level circulation center required JTWC to issue a 301800Z September Tropical Cyclone Formation Alert. The first warning followed at 010600Z. TC06A continued to intensify as it tracked west-northwestward reaching a peak intensity of 55 kt (28 m/sec) approximately 250 nm (465 km) off the coast of Oman. Land interaction and vertical wind shear increased as it tracked closer to the Arabian Peninsula, shearing the low level away from the upper-level circulation center. As TC06A dissipated over Oman, the last warning by JTWC was issued at 031200Z.



TROPICAL CYCLONE 07B

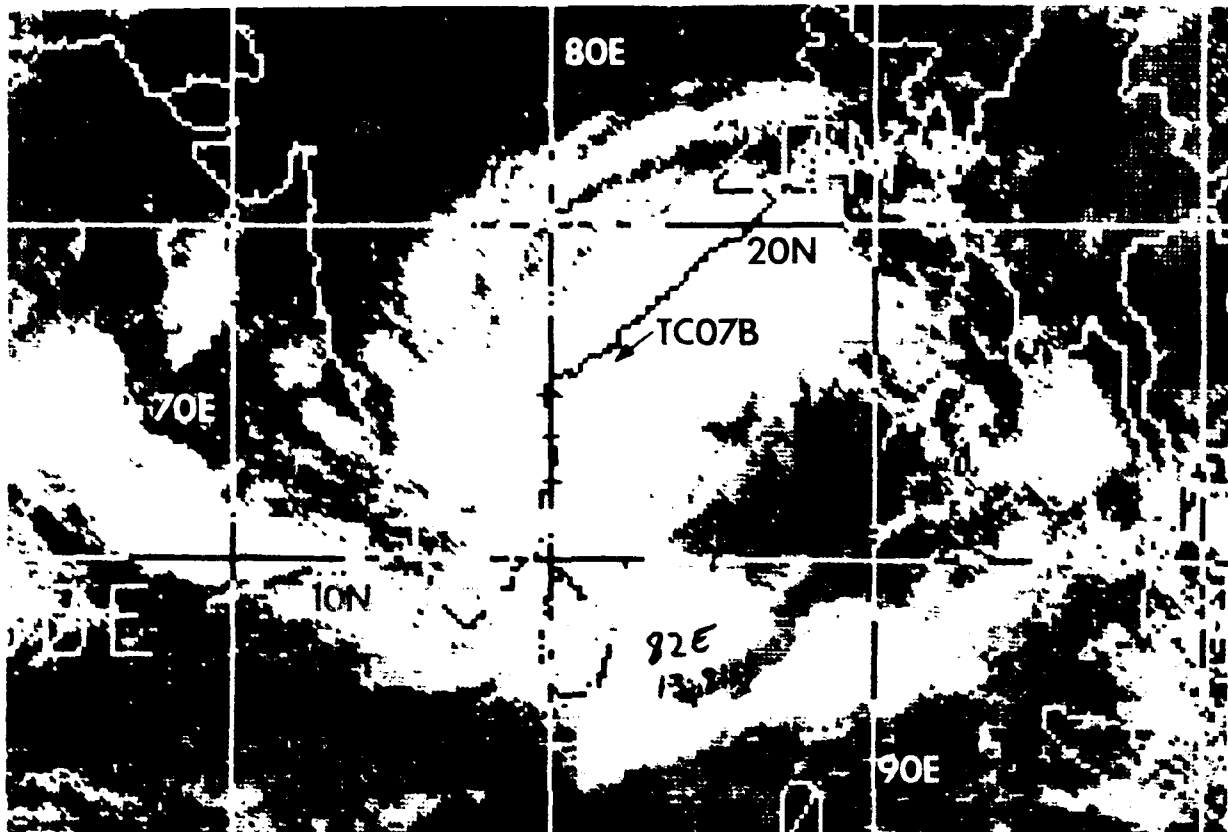
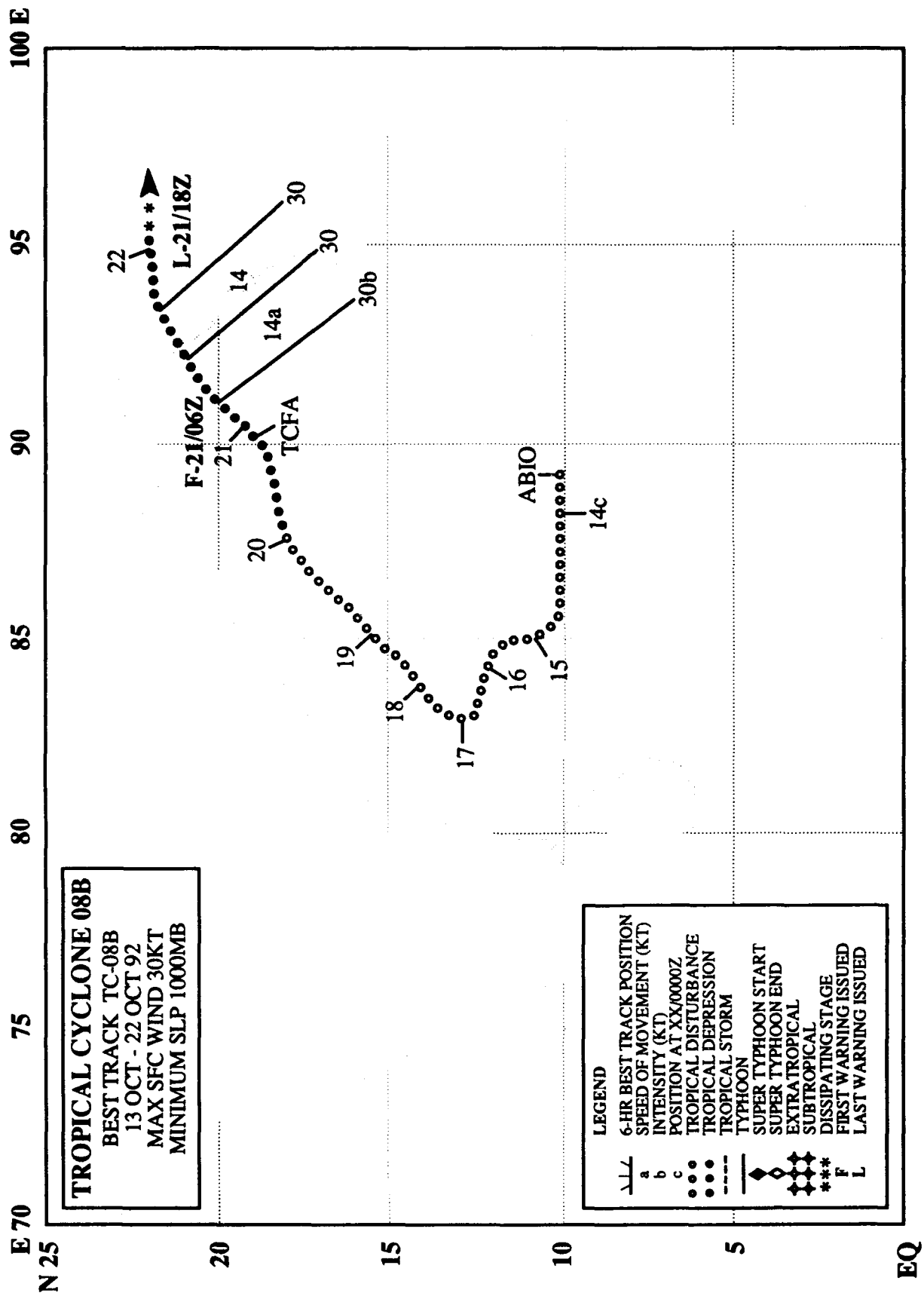


Figure 3 07B 1. At peak intensity, TC07B nears the coast of India (082200Z October DMSP infrared digitized mosaic).

A southwesterly surge into the Andaman Sea resulted in the development of the tropical disturbance that became TC07B. Continued support from a receding southwesterly monsoonal flow led to intensification of the disturbance which was first mentioned by JTWC on the 041800Z October Significant Tropical Weather Advisory. Some 10 hours later, a Tropical Cyclone Formation Alert (TCFA) was issued at 060400Z. Following the TCFA and an abrupt change to its westward track, TC07B moved in a general northwestward direction, reaching a peak intensity of 45 kt (23 m/sec). However, increased vertical shear hindered further development and TC07B weakened. After the tropical cyclone moved over land, it weakened, JTWC issued the final warning at 090600Z.



TROPICAL CYCLONE 08B

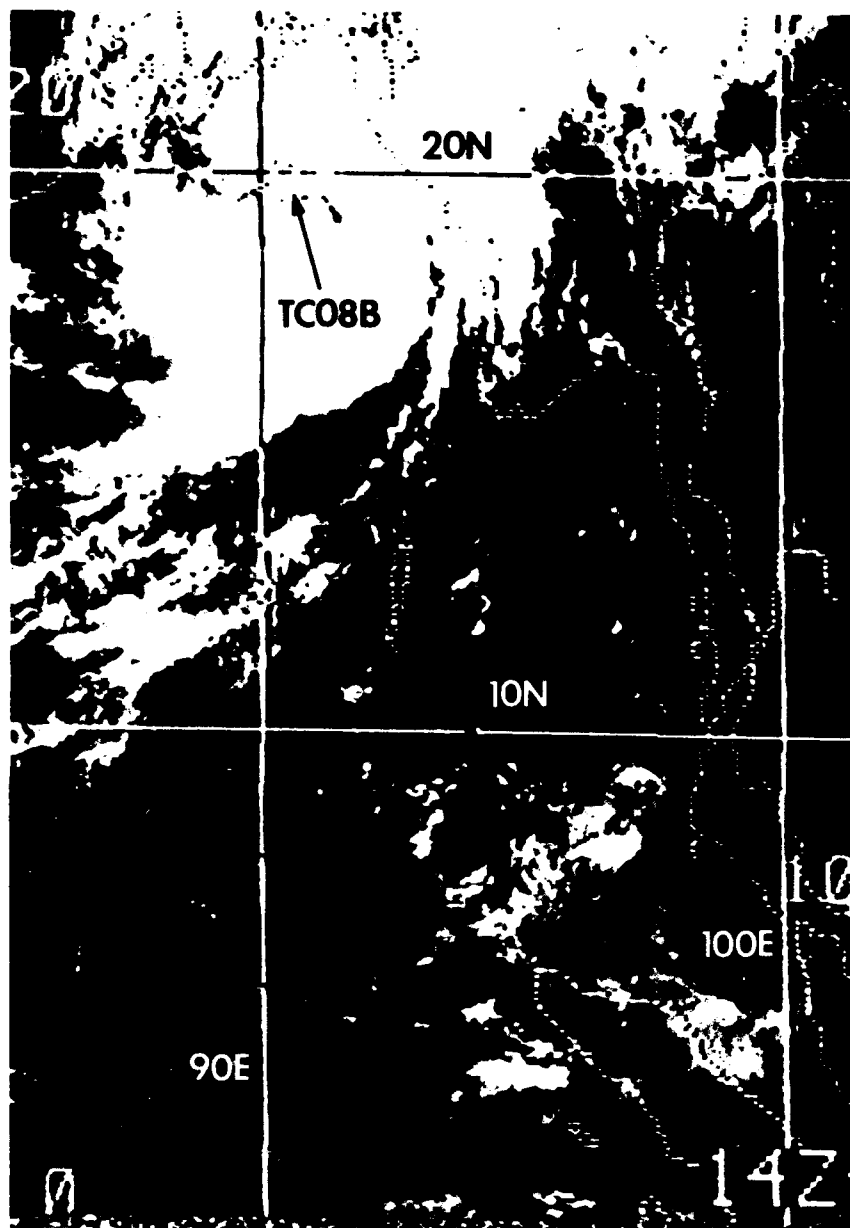


Figure 3-08B-1. Deep convection and heavy rains accompany TC08B as it nears landfall in Bangladesh (210200Z October DMSP infrared digitized mosaic).

Although the tropical disturbance that became TC08B was first mentioned on the 131800Z October Significant Tropical Weather Advisory, noticeable development did not occur until a week later, at which time a Tropical Cyclone Formation Alert was issued by JTWC at 202215Z. The first warning followed at 210600Z when satellite imagery indicated an increase in the amount of cold cloud tops near the cloud system center and improved overall convective organization. TC08B made landfall shortly thereafter on the southern coast of Bangladesh on 21 October. The final warning was issued by JTWC at 211800Z as the weak tropical cyclone dissipated over land.

100 E

95

90

85

80

75

70

N 25

TROPICAL CYCLONE 09B
 BEST TRACK TC-09B
 31 OCT - 08 NOV 92
 MAX SFC WIND 55KT
 MINIMUM SLP 984MB

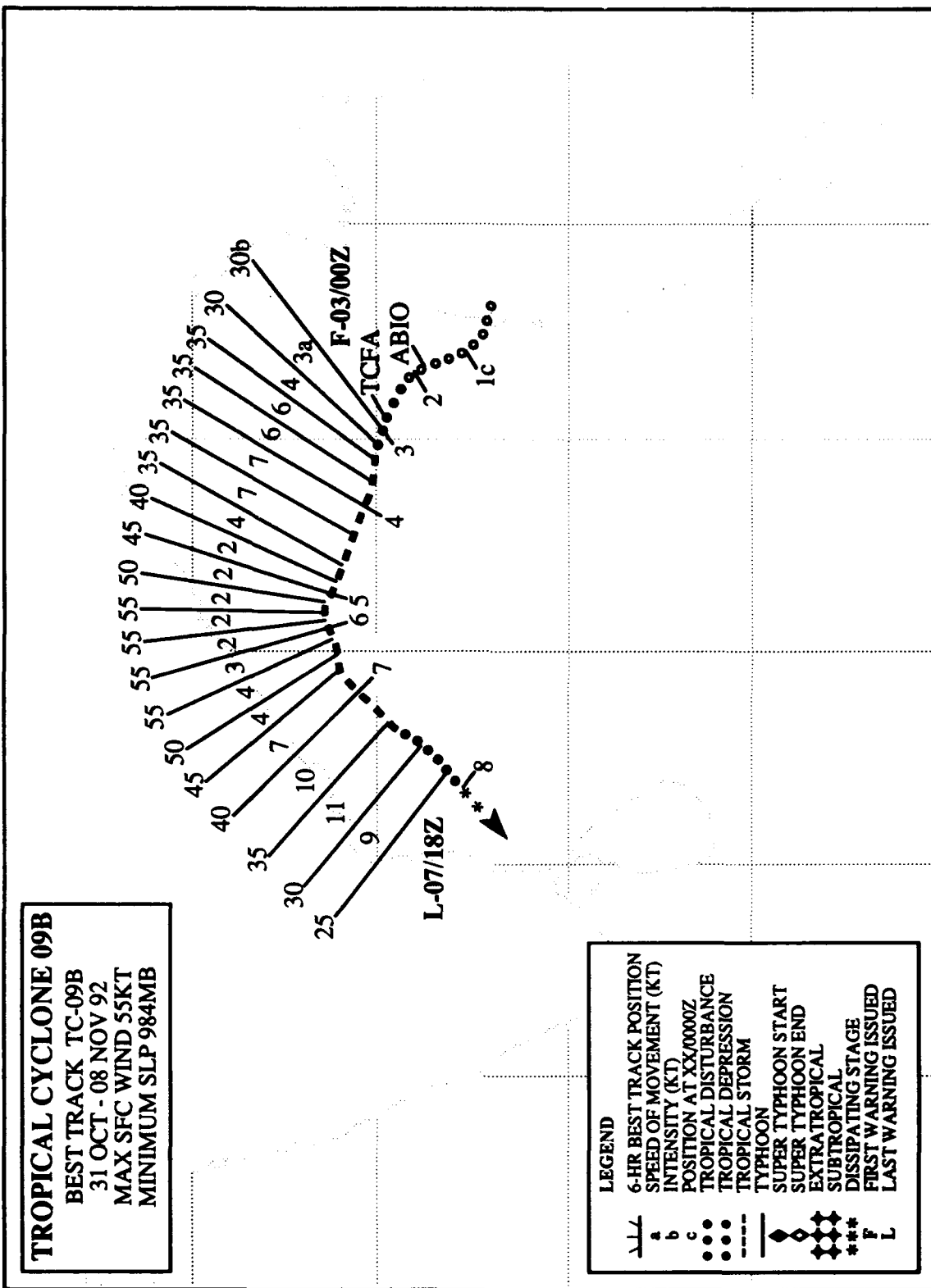
20

15

10

5

EQ



LEGEND

▲▲▲	6-HR BEST TRACK POSITION
a	SPEED OF MOVEMENT (KT)
b	INTENSITY (KT)
c	POSITION AT XX/0000Z
•••	TROPICAL DISTURBANCE
•••	TROPICAL DEPRESSION
•••	TROPICAL STORM
—	TYPHOON
◆	SUPER TYPHOON START
◆	SUPER TYPHOON END
◆	EXTRATROPICAL
◆	SUBTROPICAL
***	DISSIPATING STAGE
F	FIRST WARNING ISSUED
L	LAST WARNING ISSUED

TROPICAL CYCLONE 09B

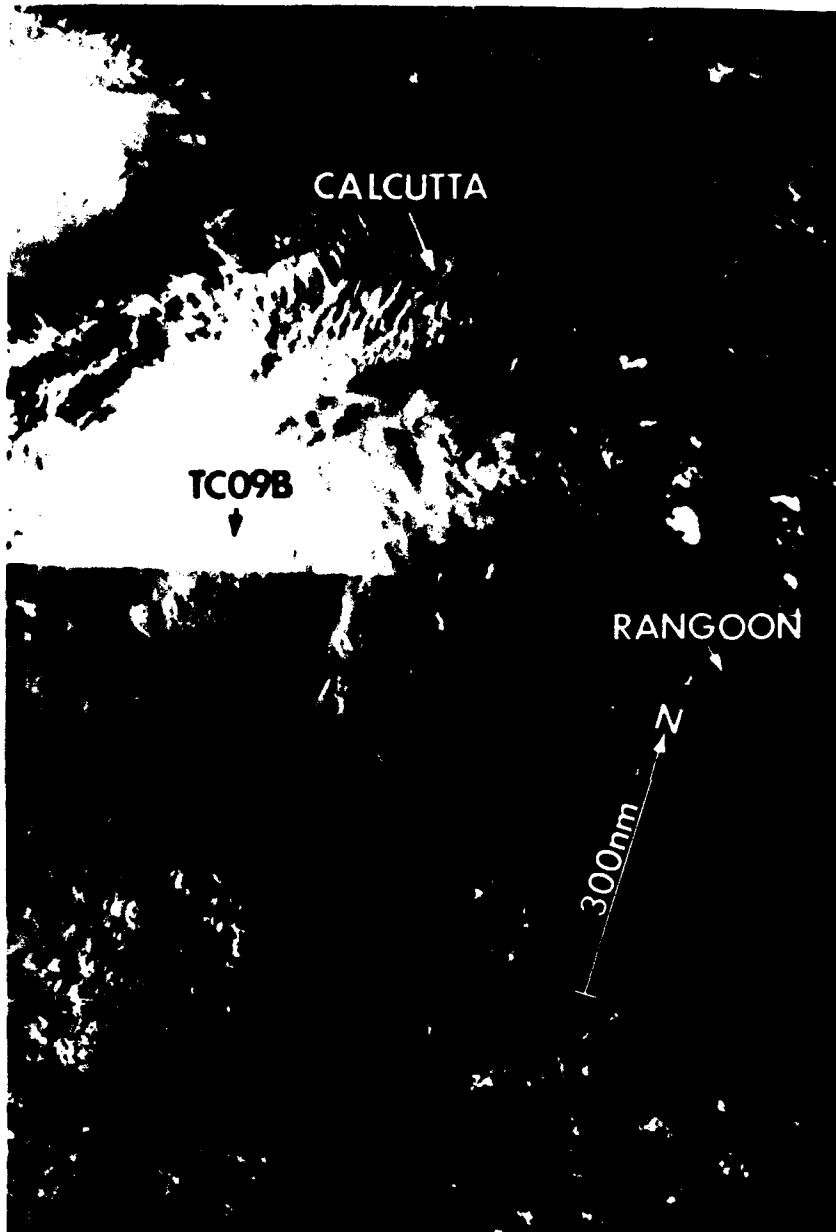
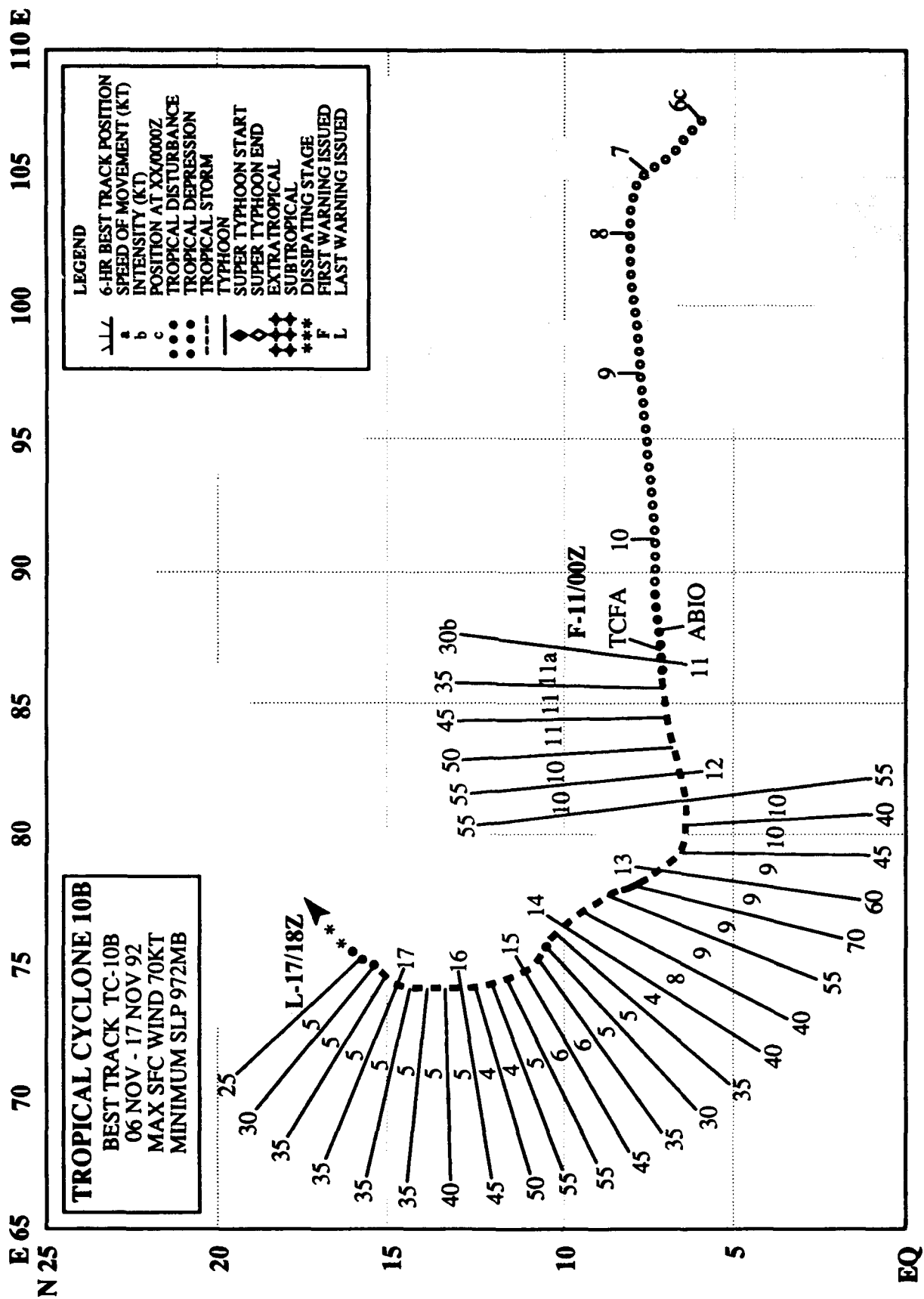


Figure 3-09B-1. TC09B at peak intensity (051048Z November DMSP visual imagery).

The tropical disturbance that became TC09B was first identified on the 011800Z November Significant Tropical Weather Advisory by JTWC as a broad area of convection in the Bay of Bengal. As the tropical disturbance tracked north-northwestward, its convection increased in amount and organization. JTWC issued a Tropical Cyclone Formation Alert at 022100Z, and the first warning at 030000Z. Intensification continued until the tropical cyclone stalled on 5 November. With increasing wind shear aloft over the cyclone, a weakening trend set in on 6 November which continued until TC09B dissipated over water two days later. The final warning was issued by JTWC at 071800Z.



TROPICAL CYCLONE 10B

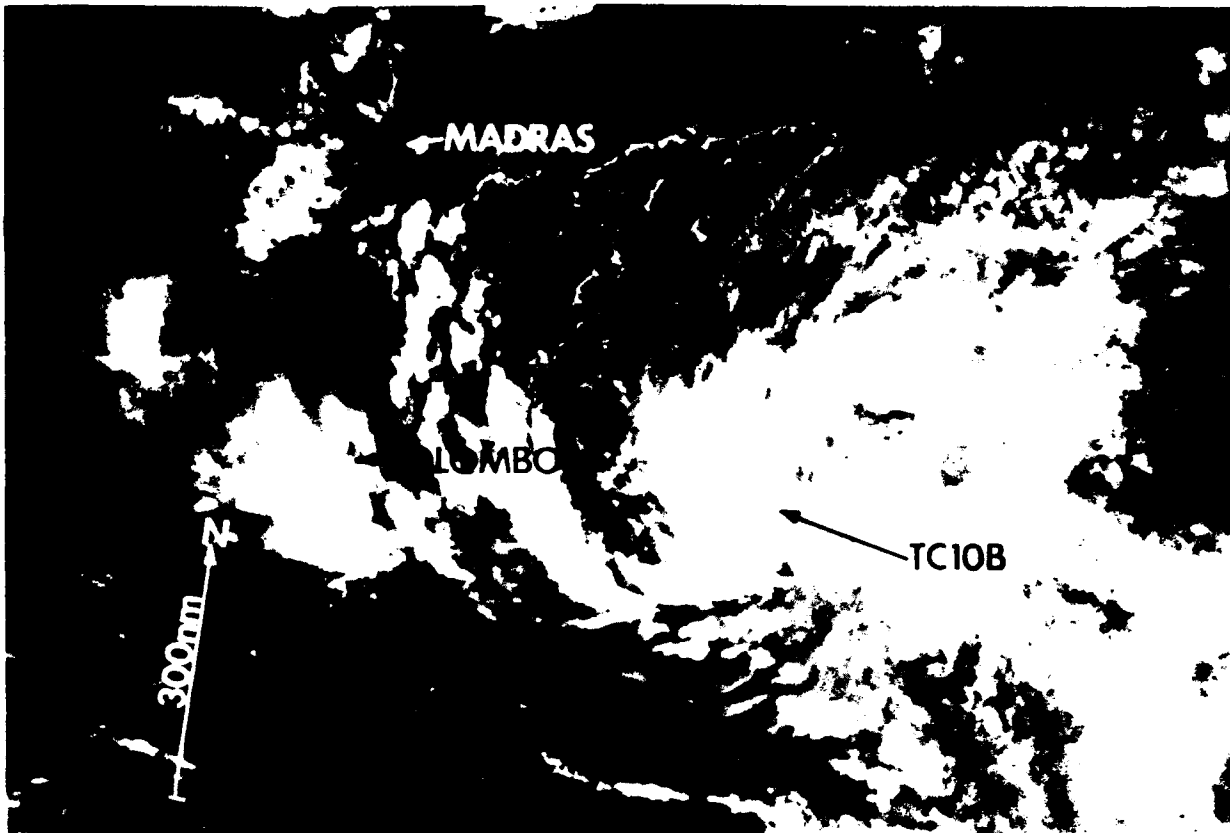


Figure 3-10B-1. TC10B consolidates its convection east of Sri Lanka (101516Z November DMSP moonlight visual imagery).

Forming in the South China Sea on 6 November, the tropical disturbance that became TC10B tracked westward across the Gulf of Thailand, Malay Peninsula, and into the Bay of Bengal on 8 November. Intensification was arrested by strong upper-level winds until the tropical disturbance was halfway across the Bay of Bengal. The cloud system was first mentioned on the 101800Z November Significant Tropical Weather Advisory and was rapidly followed by a Tropical Cyclone Formation Alert at 102200Z, and the first warning at 110000Z. TC10B intensified rapidly, reaching 55 kt (28 m/sec) prior to striking the southern tip of Sri Lanka, and then intensified again to 70 kt (36 m/sec) six hours prior to making landfall on the tip of India. The tropical cyclone tracked northwestward across India, weakened, and moved back offshore into the Arabian Sea where a slight reintensification occurred. As TC10B tracked further north, upper-level westerlies weakened it, and on 17 November it moved over India again. The final warning was issued by JTWC at 171800Z as the cyclonic circulation dissipated over land.

85 E

80

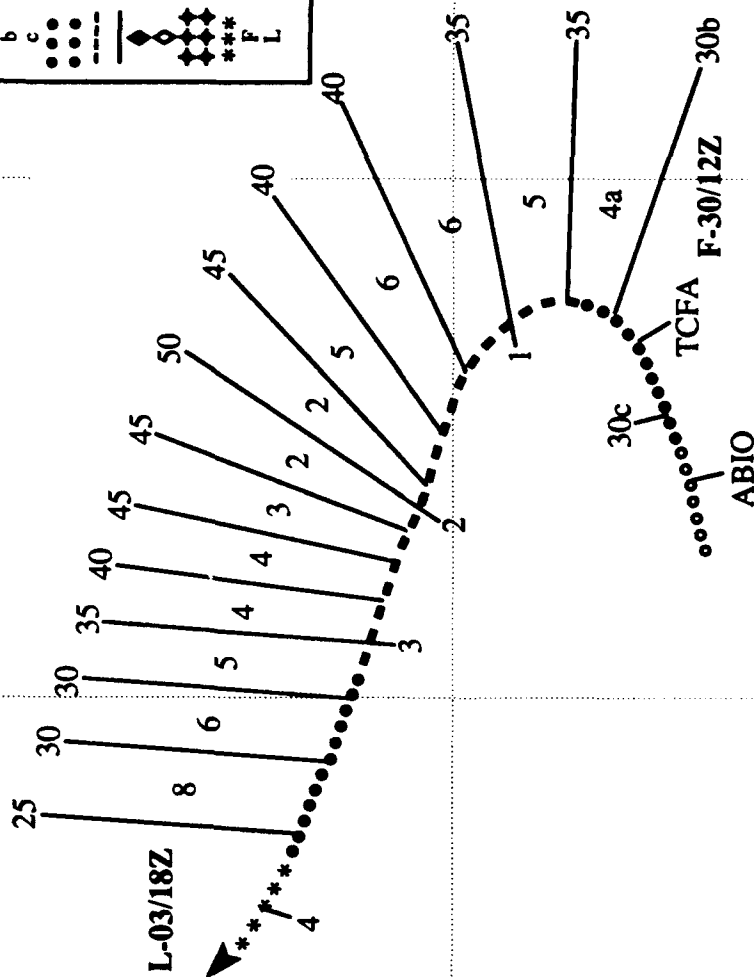
75

E 70

N 10

LEGEND

---	6-HR BEST TRACK POSITION
a	SPEED OF MOVEMENT (KT)
b	INTENSITY (KT)
c	POSITION AT XX/0000Z
...	TROPICAL DISTURBANCE
...	TROPICAL DEPRESSION
---	TROPICAL STORM
---	TYPHOON
---	SUPER TYPHOON START
---	SUPER TYPHOON END
---	SUBTROPICAL
---	DISSIPATING STAGE
***	FIRST WARNING ISSUED
F	LAST WARNING ISSUED
L	



TROPICAL CYCLONE 11A
BEST TRACK TC-11A
29 NOV - 04 DEC 92
MAX SFC WIND 50KT
MINIMUM SLP 987MB

TROPICAL CYCLONE 11A

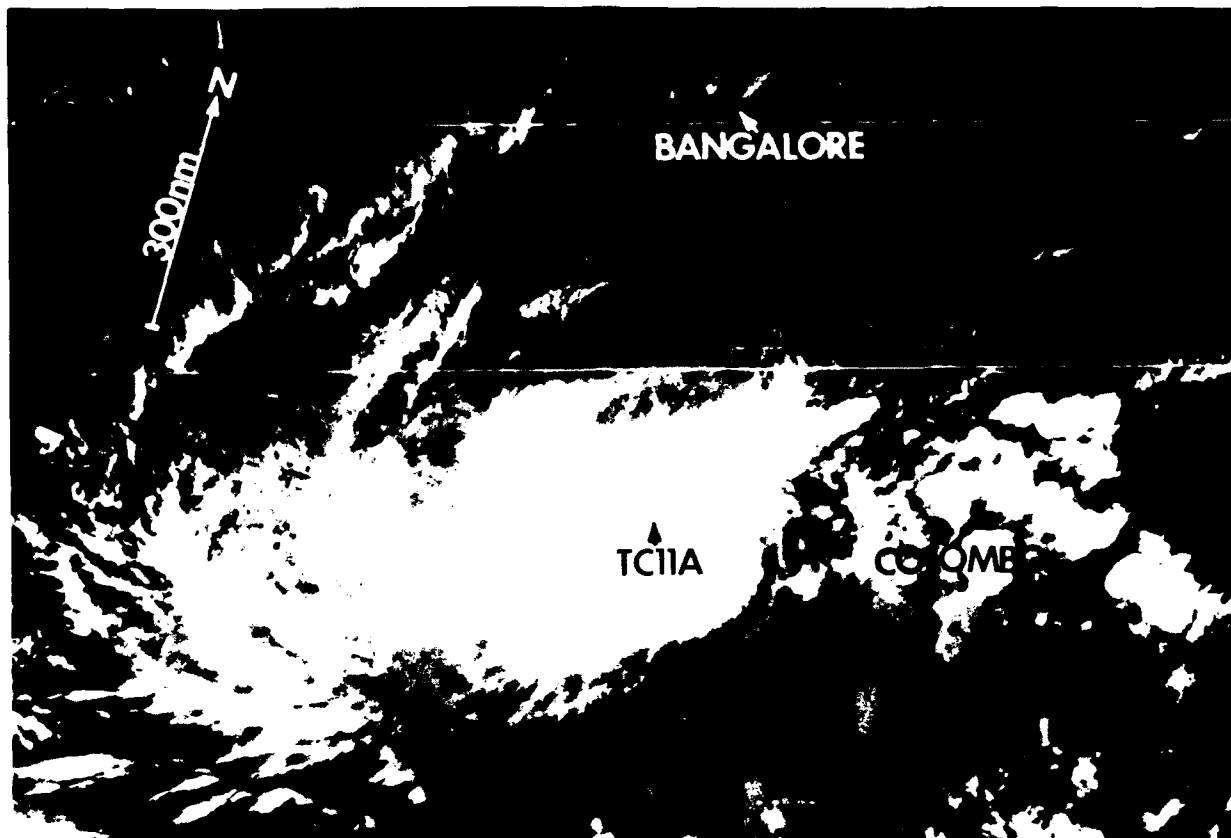
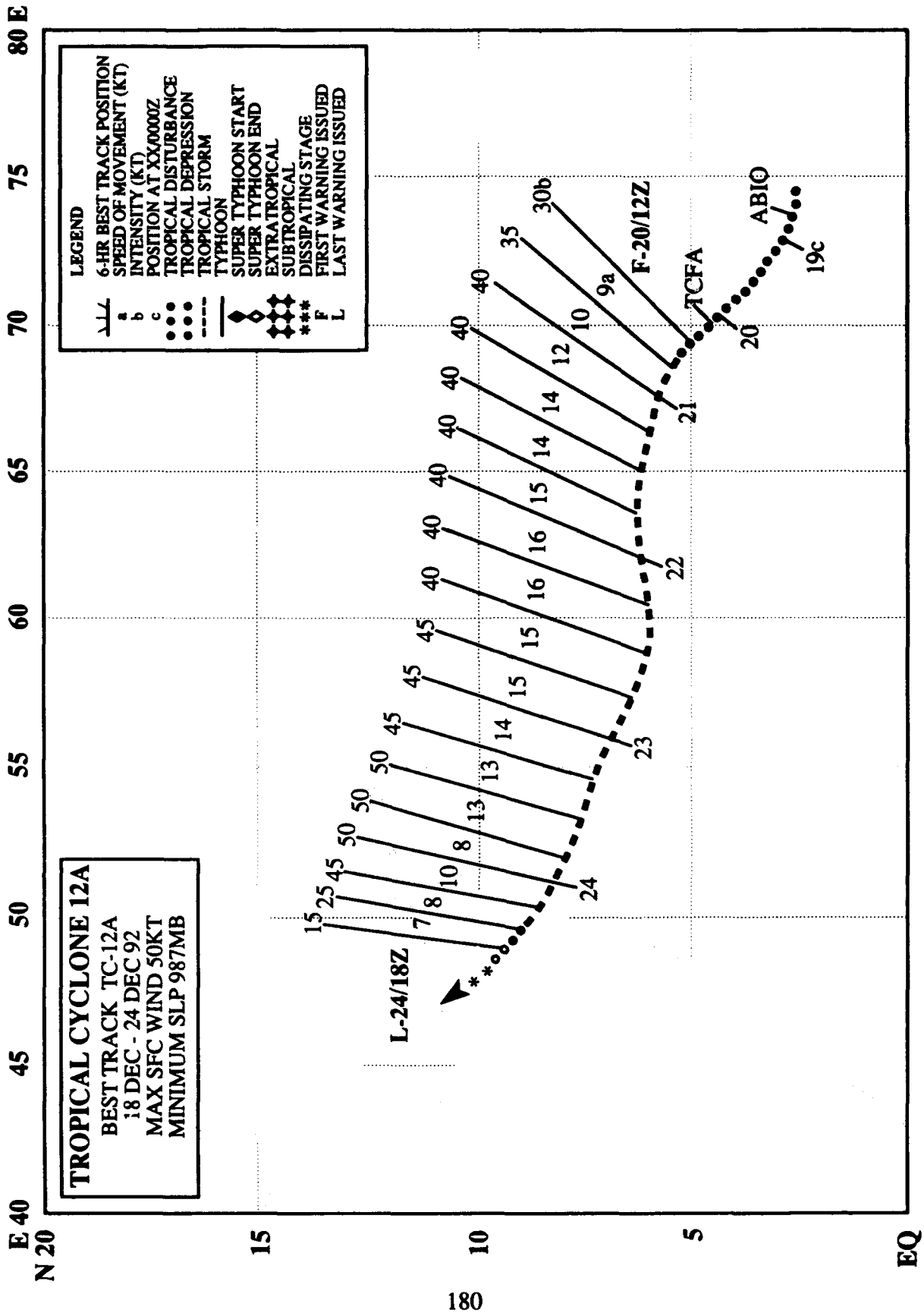


Figure 3-11A-1. TC11A at peak intensity (011559Z December infrared imagery).

The third Arabian Sea tropical cyclone of 1992 developed in the near equatorial trough southwest of Sri Lanka. The tropical disturbance that eventually became TC11A was first mentioned by JTWC on the 291800Z December Significant Tropical Weather Advisory. Increasing convective curvature prompted JTWC to issue a Tropical Cyclone Formation Alert at 300800Z followed by the first warning at 301200Z. As TC11A intensified, it turned to the northwest under the steering of the mid-level subtropical ridge. The tropical cyclone reached a maximum intensity of 50 kt (26 m/sec) briefly at 020000Z before the onset of increasing upper-level wind shear. TC11A gradually weakened until it dissipated over water on 3 December. The final warning was issued by JTWC at 031800Z.



TROPICAL CYCLONE 12A

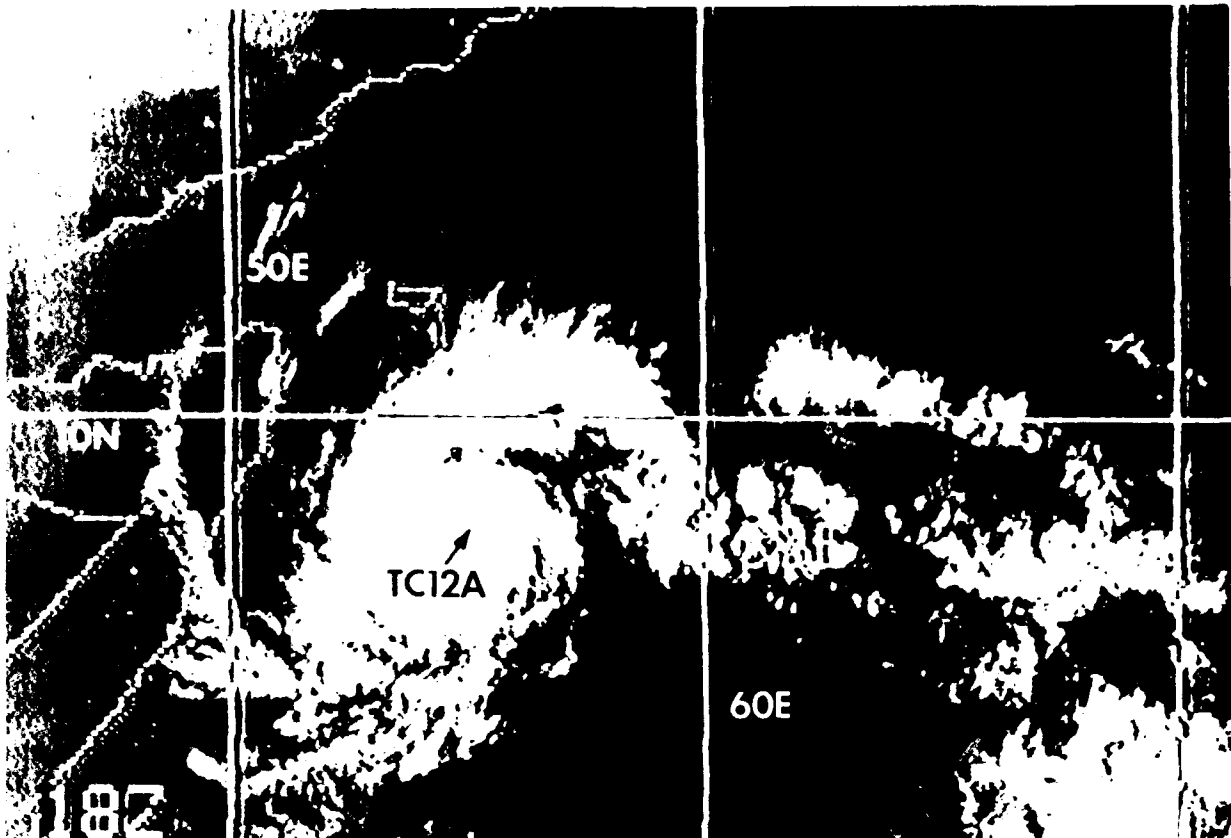


Figure 3-12A-1. At peak intensity, TC12A approaches the coast of Somalia (230500Z December DMSP infrared imagery).

Tropical cyclone 12A was the fourth cyclone in the Arabian Sea and the twelfth cyclone in the North Indian Ocean in 1992. For JTWC, this set an all-time record for the number of significant North Indian Ocean tropical cyclones. The previous record was eight significant tropical cyclones in 1987. The tropical disturbance that became TC12A formed in the Maldives in the near equatorial trough and was initially mentioned by JTWC on the 181800Z December Significant Tropical Weather Advisory. A Tropical Cyclone Formation Alert was issued at 200400Z followed by the first warning at 201200Z. TC12A tracked quickly westward across the central Arabian Sea towards the coast of Somalia. Accurate warnings allowed ships supporting Operation RESTORE HOPE to transit the Arabian Sea without any damage, diversions or delays. Warnings were sent out with expanded prognostic reasoning messages to keep operational commanders and their weather personnel informed on JTWC's rationale for the tropical cyclone's movement and intensity forecasts. Reaching a peak intensity of 50 kt (26 m/sec) just prior to landfall, TC12A weakened rapidly after making landfall in Somalia, bringing much needed rain to a dry country. JTWC issued the final warning at 241800Z as TC12A dissipated over land.

Intentionally left blank

4. SUMMARY OF SOUTH PACIFIC AND SOUTH INDIAN TROPICAL CYCLONES

4.1 GENERAL

On 1 October 1980, JTWC's area of responsibility (AOR) was expanded to include the Southern Hemisphere from 180° east longitude westward to the coast of Africa. Details on Southern Hemisphere tropical cyclones and JTWC warnings from July 1980 through June 1982 are contained in Diercks et al. (1982) and from July 1982 through June 1984, in Wirfel and Sandgathe (1986). Information on Southern Hemisphere tropical cyclones after June 1984 can be found in the applicable Annual Tropical Cyclone Report. The Naval Western Oceanography Center (NWOC) Pearl Harbor, HI issues warnings on tropical cyclones in the South Pacific east of 180° east longitude.

In accordance with CINCPACINST 3140.1V, Southern Hemisphere tropical cyclones are numbered sequentially from 1 July through 30 June. This convention is established to encompass the Southern Hemisphere tropical cyclone season, which primarily occurs from January through April. There are two ocean basins for warning purposes - the South Indian (west of 135° east longitude) and the South Pacific (east of 135° east longitude) - which are identified by appending the suffixes "S" and "P" respectively to the tropical cyclone number.

Intensity estimates for Southern Hemisphere tropical cyclones are derived from the interpretation of satellite imagery using the Dvorak technique (Dvorak, 1984) and in rare instances from surface observations. The Dvorak technique relates specific cloud signatures to maximum sustained one-minute average wind speeds. The conversion from maximum sustained winds to minimum sea-level pressure is obtained from the Atkinson and Holliday (1977) relationship (Table 4-1).

4.2 SOUTH PACIFIC AND SOUTH INDIAN OCEAN TROPICAL CYCLONES

Tropical cyclone activity in 1992 (Table 4-2) which includes the period of 1 July 1991 to 30 June 1992 was three above the climatological mean of 27 storms, and the third highest seasonal total since 1981 (Table 4-3). The above-average number of cyclones was a reflection of very high activity in the Southeast Pacific. A record thirteen cyclones developed east of 165° east longitude, 12 more than last year and 7

TABLE 4-1 MAXIMUM SUSTAINED SURFACE WINDS AND EQUIVALENT MINIMUM SEA-LEVEL PRESSURE (ATKINSON AND HOLLIDAY, 1977)

MAXIMUM SUSTAINED SURFACE WIND (KT)	MINIMUM SEA-LEVEL PRESSURE (MB)
30	1000
35	997
40	994
45	991
50	987
55	984
60	980
65	976
70	972
75	967
80	963
85	958
90	954
95	948
100	943
105	938
110	933
115	927
120	922
125	916
130	910
135	906
140	898
145	892
150	885
155	879
160	872
165	865
170	858
175	851
180	844

above the 1981-1992 average (Table 4-4). Tropical cyclones started in mid-September and ended in early May. An unusually active February resulted in a record 11 cyclones forming that month, with the JTWC warning on 5 cyclones for a 2-day period late in the month (Figure 4-1). Composites of the best tracks are provided in Figures 4-2 and 4-3.

The JTWC was in warning status a total of 98 days, which includes 25 days when the JTWC issued warnings on two or more Southern Hemisphere cyclones, 13 days with three or more, 6 days with four or more, and 2 days with five cyclones occurring simultaneously. For the record, if the number of Southeast Pacific warning days were added to those of the Southwest Pacific and South Indian Oceans, the total would increase from 98 to 120 days. All tropical cyclones warnings with the exception of those for Tropical Cyclone 18P were preceded by Tropical Cyclone Formation Alerts. Tropical cyclones 06P (Val), 21P (Esau), and 25P (Fran) all made it to super typhoon intensity in contrast to only one during the 1991 year.

**TABLE 4-2 SOUTH PACIFIC AND SOUTH INDIAN OCEAN 1992 SIGNIFICANT TROPICAL CYCLONES
(1 July 1991 - 30 June 1992)**

<u>TROPICAL CYCLONE</u>	<u>PERIOD OF WARNING</u>	<u>NUMBER WARNINGS ISSUED</u>	<u>MAXIMUM SURFACE WINDS-KT (M/SEC)</u>	<u>ESTIMATED MSLP (MB)</u>
01S ----	11 Sep - 13 Sep	5	40 (21)	994
02S ----	17 Oct - 21 Oct	8	35 (18)	997
03P Tia	15 Nov - 21 Nov	17	95 (49)	949
04S ----	22 Nov - 26 Nov	10	45 (23)	991
05S Graham	02 Dec - 10 Dec	19	120 (62)	922
06P Val	05 Dec - 13 Dec	17	140 (72)	898
07P Wasa	05 Dec - 13 Dec	16	105 (54)	938
08P Arthur	15 Dec - 17 Dec	4	45 (23)	991
09S Alexandra	20 Dec - 25 Dec	12	105 (54)	938
10S Bryna	30 Dec - 02 Jan	7	45 (23)	991
11P Betsy	06 Jan - 15 Jan	19	95 (49)	949
12P Mark	08 Jan - 10 Jan	6	55 (28)	984
13P ----	17 Jan - 18 Jan	4	35 (18)	997
14P Cliff	06 Feb - 09 Feb	7	60 (31)	980
15S Celesta	11 Feb - 13 Feb	5	45 (23)	991
16S ----	12 Feb - 14 Feb	4	25 (13)	1003
17P Daman	14 Feb - 19 Feb	11	85 (44)	958
18P ----	19 Feb - 20 Feb	4	35 (18)	997
19S Davilia	23 Feb - 24 Feb	3	35 (18)	997
20S Harriet	26 Feb - 08 Mar	23	120 (62)	922
21P Esau	26 Feb - 06 Mar	20	130 (67)	910
22S Farida	26 Feb - 03 Mar	15	120 (62)	922
23S Ian	26 Feb - 03 Mar	13	115 (60)	927
24S Gerda	27 Feb - 28 Feb	3	35 (18)	997
25P Fran*	06 Mar - 17 Mar	23	140 (72)	898
26P Gene	15 Mar - 19 Mar	9	65 (33)	976
27P Hettie	25 Mar - 29 Mar	9	50 (26)	987
28S Neville	06 Apr - 14 Apr	18	120 (62)	922
29S Jane/Irna	08 Apr - 18 Apr	23	120 (62)	922
30P Innis	28 Apr - 02 May	8	65 (33)	976
Total:		340		

* First 2 Warnings Issued by NWOC

NOTE: Names of Southern Hemisphere Tropical Cyclones are given by the Regional Warning Centers (Nadi, Brisbane, Darwin, Perth, Reunion and Mauritius) and are appended to JTWC Warnings, when available.

TABLE 4-3

MONTHLY DISTRIBUTION OF SOUTH PACIFIC AND
SOUTH INDIAN OCEAN TROPICAL CYCLONES

YEAR (1959-1978)	JUL	AUG	SEP	OCT	NOV	DEC	JAN	FEB	MAR	APR	MAY	JUN	TOTAL
AVERAGE*	-	-	-	0.4	1.5	3.6	6.1	5.8	4.7	2.1	0.5	-	24.7
1981	0	0	0	1	3	2	6	5	3	3	1	0	24
1982	1	0	0	1	1	3	9	4	2	3	1	0	25
1983	1	0	0	1	1	3	5	6	3	5	0	0	25
1984	1	0	0	1	2	5	5	10	4	2	0	0	30
1985	0	0	0	0	1	7	9	9	6	3	0	0	35
1986	0	0	1	0	1	1	9	9	6	4	2	0	33
1987	0	1	0	0	1	3	6	8	3	4	1	1	28
1988	0	0	0	0	2	3	5	5	3	1	2	0	21
1989	0	0	0	0	2	1	5	8	6	4	2	0	28
1990	2	0	1	1	2	2	4	4	10	2	1	0	29
1991	0	0	1	1	1	3	2	5	5	2	1	1	22
1992	0	0	1	1	2	5	4	11	3	2	1	0	30
TOTAL:	5	1	4	7	19	38	69	84	54	35	12	2	330
(1981-1992)													
AVERAGE:	0.4	0.1	0.3	0.6	1.6	3.2	5.8	7.0	4.5	2.9	1.0	0.2	27.5

* (Gray, 1979)

TABLE 4-4

ANNUAL VARIATION OF SOUTHERN HEMISPHERE
TROPICAL CYCLONES BY OCEAN BASIN

YEAR (1959-1978)	SOUTH INDIAN (WEST OF 105°E)	AUSTRALIAN (105°E - 165°E)	SOUTH PACIFIC (EAST OF 165°E)	TOTAL
AVERAGE*	8.4	10.3	5.9	24.7
1981	13	8	3	24
1982	12	11	2	25
1983	7	6	12	25
1984	14	14	2	30
1985	14	15	6	35
1986	14	16	3	33
1987	9	8	11	28
1988	14	2	5	21
1989	12	9	7	28
1990	18	8	3	29
1991	11	10	1	22
1992	11	6	13	30
TOTAL:	149	113	68	330
(1981-1992)				
AVERAGE:	12.4	9.4	5.7	27.5

* (Gray, 1979)

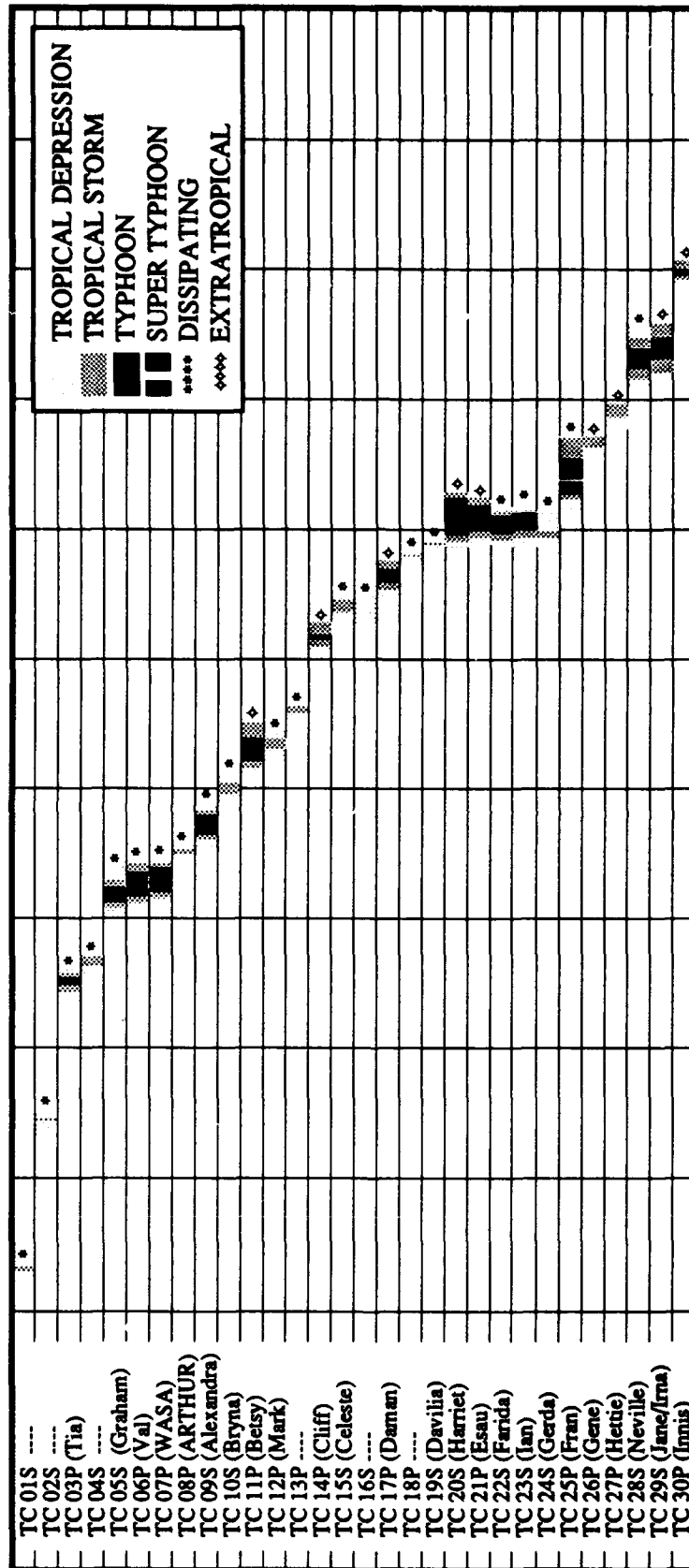


Figure 4-1. Chronology of South Pacific and South Indian Ocean tropical cyclones for 1992.

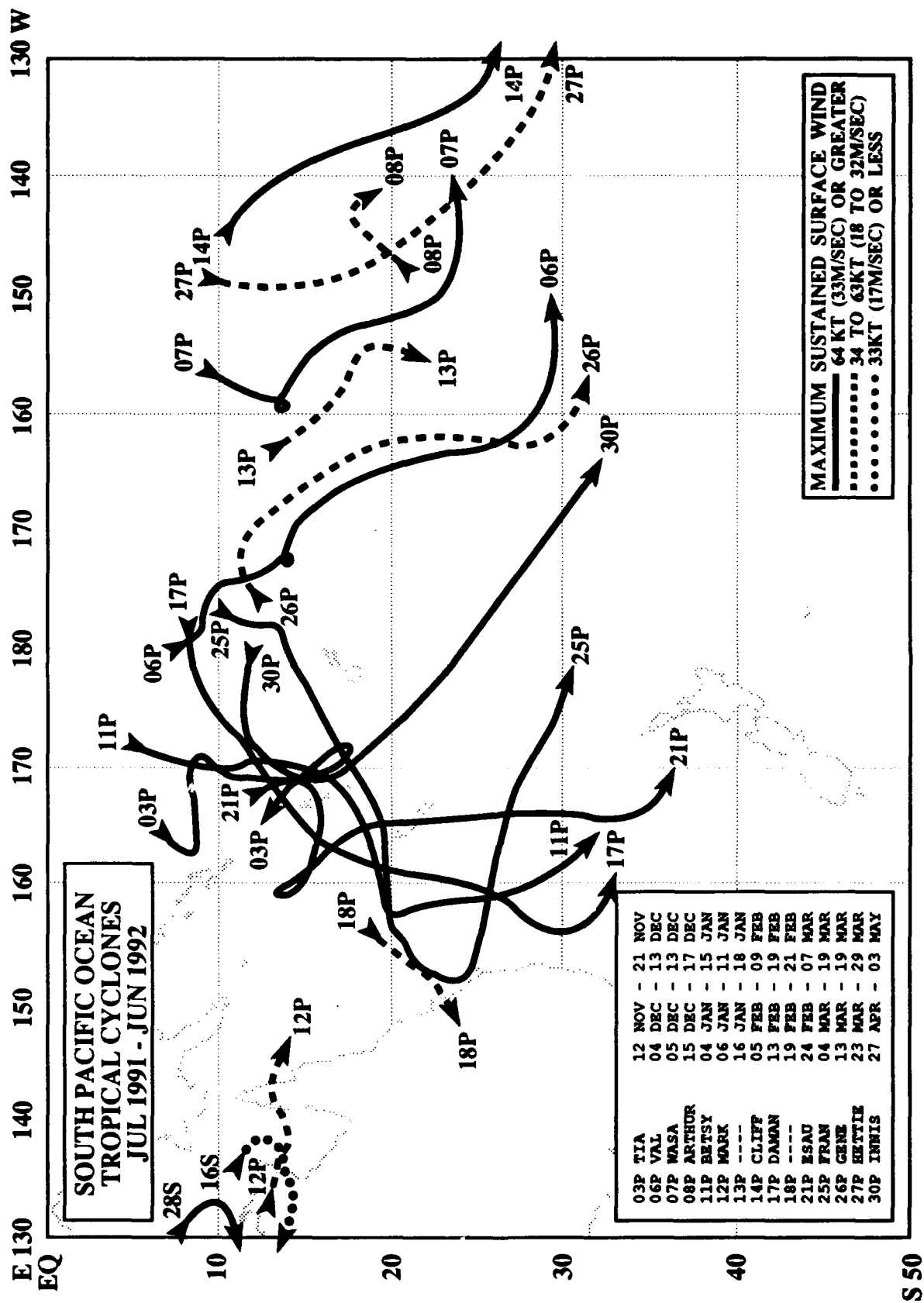


Figure 4-2. Tropical cyclone best tracks east of 130° east longitude.

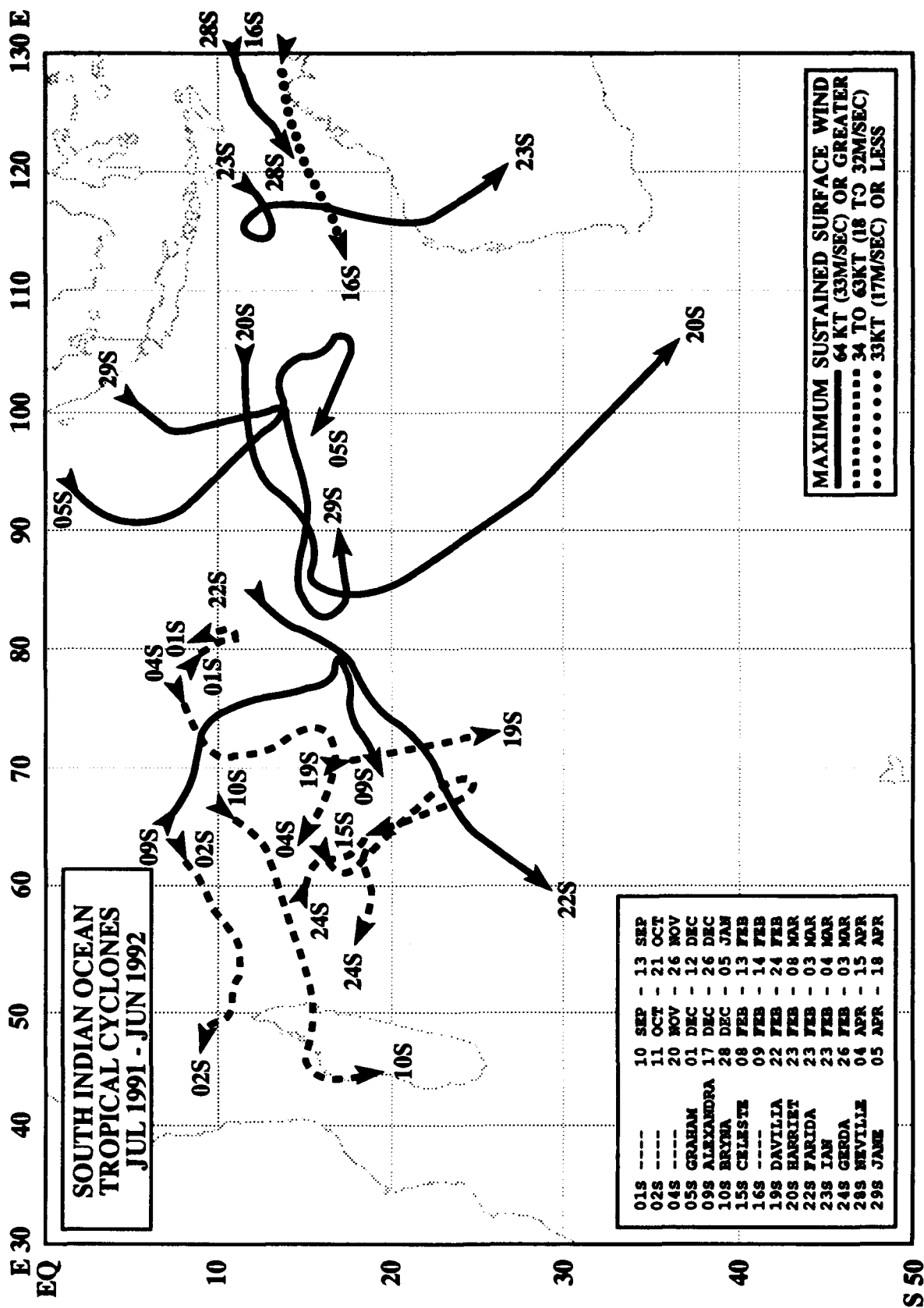


Figure 4-3. Tropical cyclone best tracks west of 130° east longitude.

Intentionally left blank

5. SUMMARY OF FORECAST VERIFICATION

5.1 ANNUAL FORECAST VERIFICATION

Verification of warning positions and intensities at initial, 24-, 48- and 72-hour forecast periods was made against the final best track. The (scalar) track forecast, along-track and cross-track errors (illustrated in Figure 5-1) were calculated for each verifying JTWC forecast. These data, in addition to a detailed summary for each tropical cyclone, is included as Chapter 6 (formerly Annex A). This section summarizes verification data for 1992 and contrasts it with annual verification statistics from previous years.

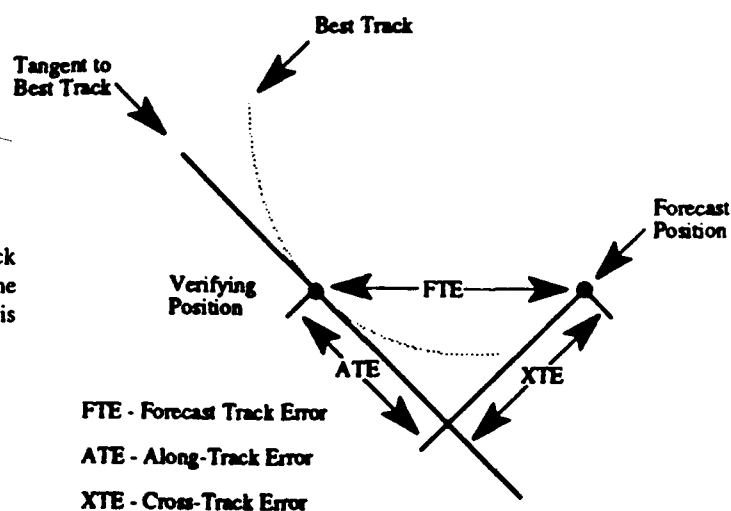
5.1.1 NORTH WEST PACIFIC OCEAN — The frequency distributions of errors for initial warning positions and 12-, 24-, 36-, 48- and 72-hour forecasts are presented in Figures 5-2a through 5-2f, respectively. Table 5-1 includes mean track, along-track and cross-track errors for 1978-1992. Figure 5-3 shows mean track errors and a 5-year moving average of track errors at 24-, 48- and 72-hours for the past 23 years. Table 5-2 lists annual mean track errors from 1959, when the JTWC was founded, until

the present. Figure 5-4 illustrates JTWC intensity forecast errors at 24-, 48- and 72-hours for the past 22 years.

5.1.2 NORTH INDIAN OCEAN — The frequency distributions of errors for warning positions and 12-, 24-, 36-, 48- and 72-hour forecasts are presented in Figures 5-5a through 5-5f, respectively. Table 5-3 includes mean track, along-track and cross-track errors for 1978-1992. Figure 5-6 shows mean track errors and a 5-year moving average of track errors at 24-, 48- and 72-hours for the 21 years that the JTWC has issued warnings in the region.

5.1.3 SOUTH PACIFIC AND SOUTH INDIAN OCEANS — The frequency distributions of errors for warning positions and 24- and 48-hour forecasts are presented in Figures 5-7A through 5-7C, respectively. Table 5-4 includes mean track, along-track and cross-track errors for 1981-1992. Figure 5-8 shows mean track errors and a 5-year moving average of track errors at 24- and 48-hours for the 12 years that the JTWC has issued warnings in the region.

Figure 5-1. Definition of cross-track error (XTE), along-track error (ATE) and forecast track error (FTE). In this example, the XTE is positive (to the right of the best track) and the ATE is negative (behind or slower than the best track).



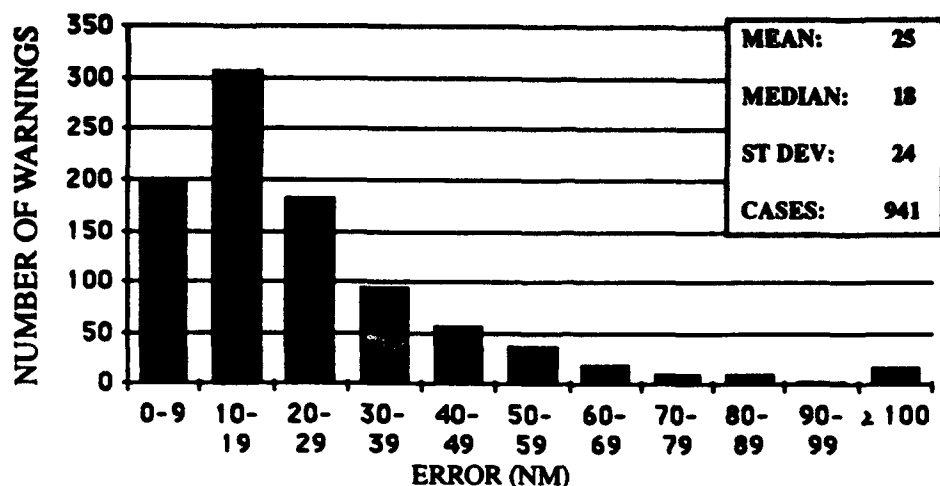


Figure 5-2a. Frequency distribution of initial warning position errors (10 nm increments) for the western North Pacific Ocean in 1992. The largest error, 249 nm, occurred on Typhoon Ward (22W).

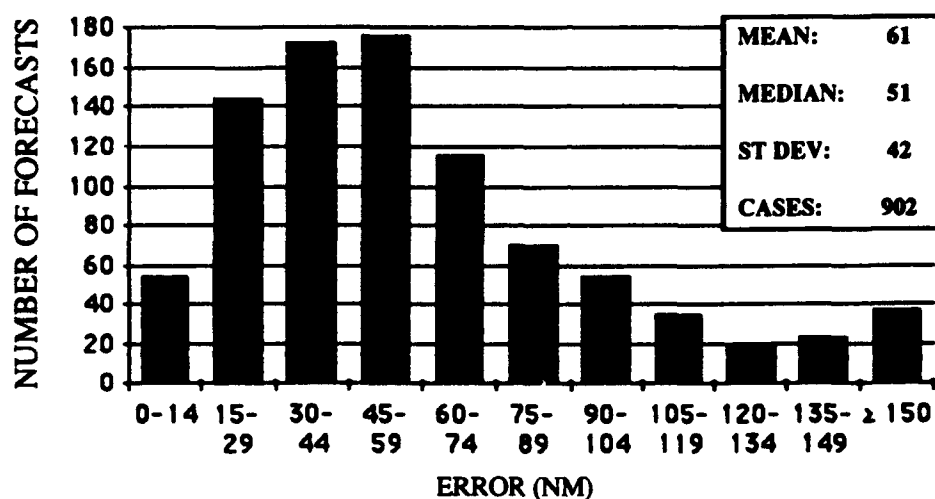


Figure 5-2b. Frequency distribution of 12-hour forecast errors (15 nm increments) for the western North Pacific Ocean in 1992. The largest error, 307 nm, occurred on Typhoon Ward (22W).

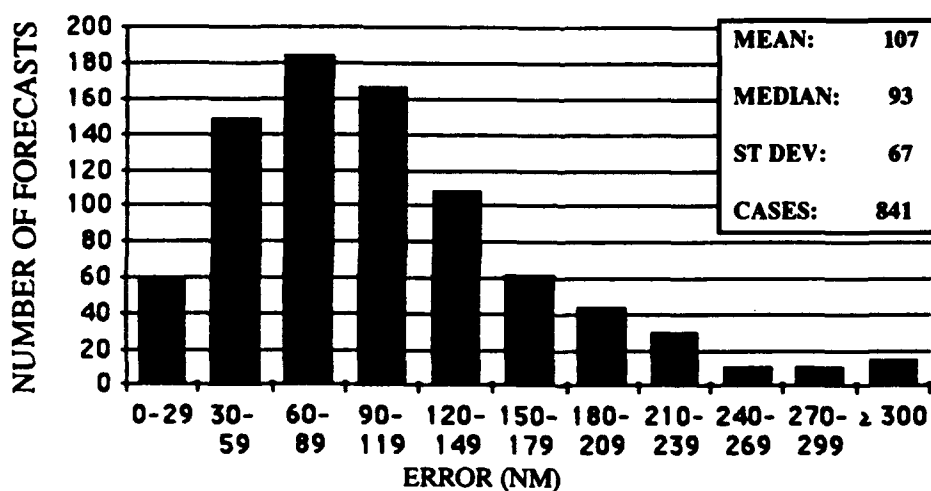


Figure 5-2c. Frequency distribution of 24-hour forecast errors (30 nm increments) for the western North Pacific Ocean in 1992. The largest error, 442 nm, occurred on Typhoon Hunt (32W).

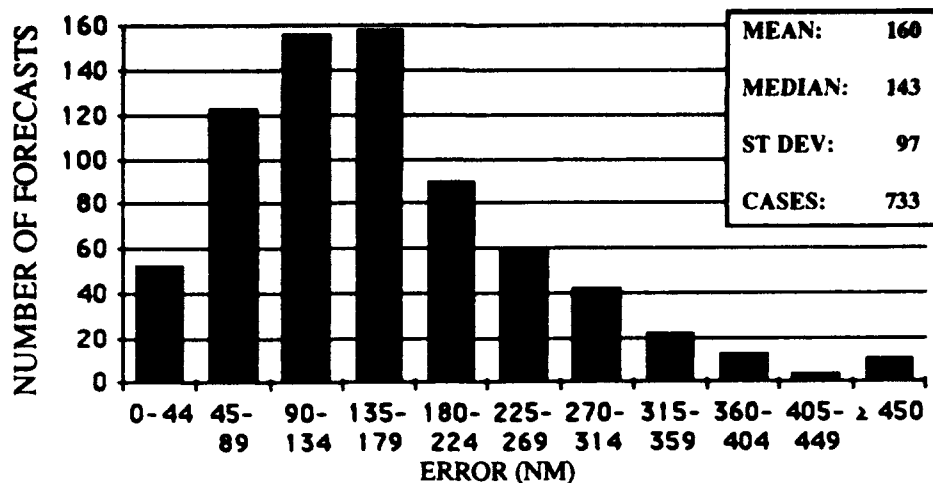


Figure 5-2d. Frequency distribution of 36-hour forecast errors (45 nm increments) for the western North Pacific Ocean in 1992. The largest error, 707 nm, occurred on Typhoon Hunt (32W).

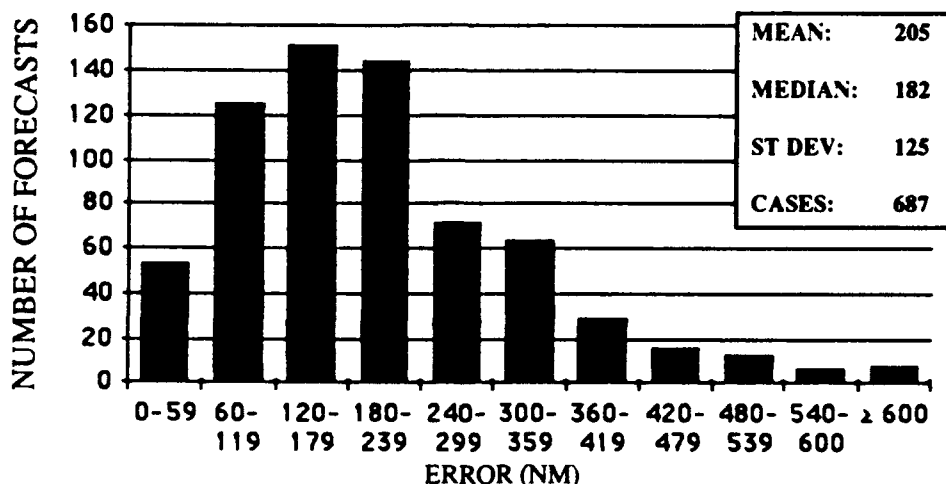


Figure 5-2e. Frequency distribution of 48-hour forecast errors (60 nm increments) for the western North Pacific Ocean in 1992. The largest error, 714 nm, occurred on Typhoon Colleen (26W).

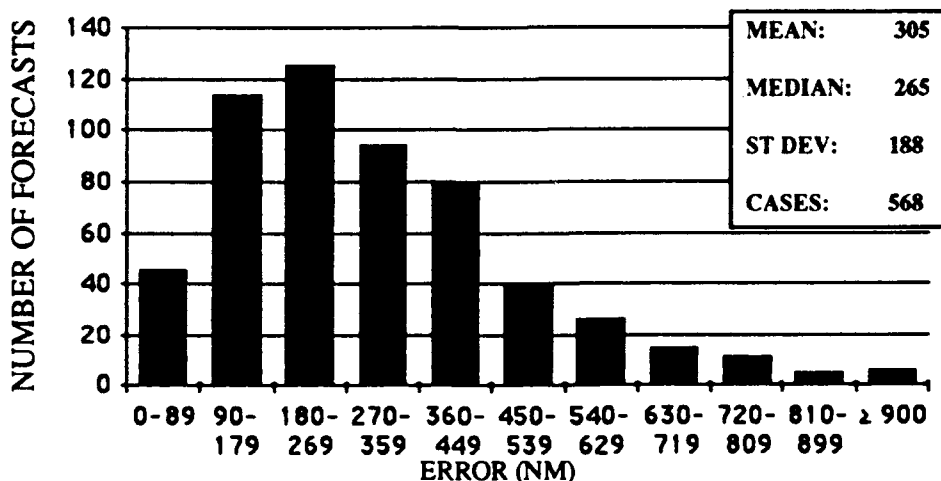


Figure 5-2f. Frequency distribution of 72-hour forecast errors (90 nm increments) for the western North Pacific Ocean in 1992. The largest error, 1014 nm, occurred on Typhoon Colleen (26W).

TABLE 5-1. INITIAL WARNING POSITION AND FORECAST ERRORS (NM) FOR THE WESTERN NORTH PACIFIC 1978-1992.

YEAR	NUMBER OF INITIAL WARNINGS POSITION		24-HOUR		48-HOUR		72-HOUR							
			NUMBER OF FORECASTS	TRACK ALONG CROSS	NUMBER OF FORECASTS	TRACK ALONG CROSS	NUMBER OF FORECASTS	TRACK ALONG CROSS						
1978	696	21	556	126	87	71	420	274	194	151	295	411	296	218
1979	695	25	589	125	81	76	469	227	146	138	366	316	214	182
1980	590	28	491	127	86	76	369	244	165	147	267	391	266	230
1981	584	25	466	124	80	77	348	221	146	131	246	334	206	219
1982	786	19	666	113	74	70	532	238	162	142	425	342	223	211
1983	445	16	342	117	76	73	253	260	169	164	184	407	259	263
1984	611	22	492	117	84	64	378	232	163	131	286	363	238	216
1985	592	18	477	117	80	68	336	231	153	138	241	367	230	227
1986	743	21	645	126	85	70	535	261	183	151	412	394	276	227
1987	657	18	563	107	71	64	465	204	134	127	389	303	198	186
1988	465	23	373	114	85	58	262	216	170	103	183	315	244	159
1989	710	20	625	120	83	69	481	231	162	127	363	350	265	177
1990	794	21	658	120	81	70	404	237	162	138	305	355	242	211
1991	835	22	733	96	69	53	599	185	137	97	484	287	229	146
1992	941	25	841	107	77	59	687	205	143	116	568	305	210	172
AVERAGE 78-92:	676	22	568	116	79	67	436	229	158	131	334	343	237	198

NOTE: Cross-track and along-track errors were adopted by the JTWC in 1986. Right-angle errors (used prior to 1986) were recomputed as cross-track and along-track errors after the fact to extend the data base. See Figure 5-1 for the definitions of cross-track and along-track errors.

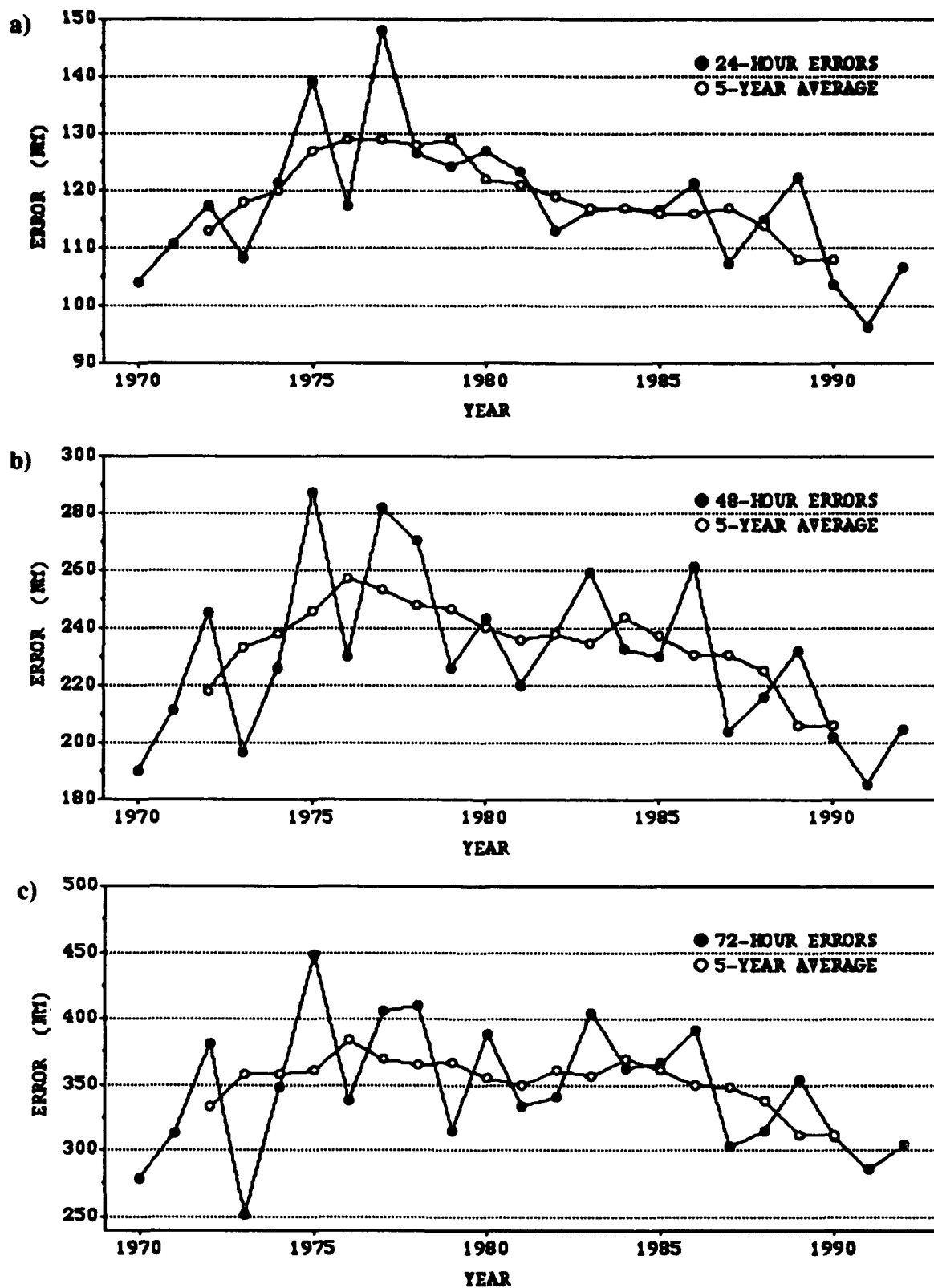


Figure 5-3. Mean track forecast error (nm) and 5-year running mean for a) 24 hours, b) 48 hours and c) 72 hours for the western North Pacific Ocean in 1992.

TABLE 5-2 MEAN FORECAST ERRORS (NM) WESTERN NORTH PACIFIC

YEAR	24-HOUR		48-HOUR		72-HOUR	
	ALL	TYPHOONS*	ALL	TYPHOONS*	ALL	TYPHOONS*
1959		117**		267**		
1960		177**		354**		
1961		136		274		
1962		144		287		476
1963		127		246		374
1964		133		284		429
1965		151		303		418
1966		136		280		432
1967		125		276		414
1968		105		229		337
1969		111		237		349
1970	104	98	190	181	279	272
1971	111	99	212	203	317	308
1972	117	116	245	245	381	382
1973	108	102	197	193	253	245
1974	120	114	226	218	348	357
1975	138	129	288	279	450	442
1976	117	117	230	232	338	336
1977	148	140	283	266	407	390
1978	127	120	271	241	410	459
1979	124	113	226	219	316	319
1980	126	116	243	221	389	362
1981	123	117	220	215	334	342
1982	113	114	237	229	341	337
1983	117	110	259	247	405	384
1984	117	110	233	228	363	361
1985	117	112	231	228	367	355
1986	121	117	261	261	394	403
1987	107	101	204	211	303	318
1988	114	107	216	222	315	327
1989	120	107	231	214	350	325
1990	103	98	203	191	310	299
1991	96	93	185	187	286	298
1992	107	97	205	194	305	295

* Forecasts were verified when the tropical cyclone intensities were at least 35 kt (18 m/sec).

** Forecast positions north of 35° north latitude were not verified.

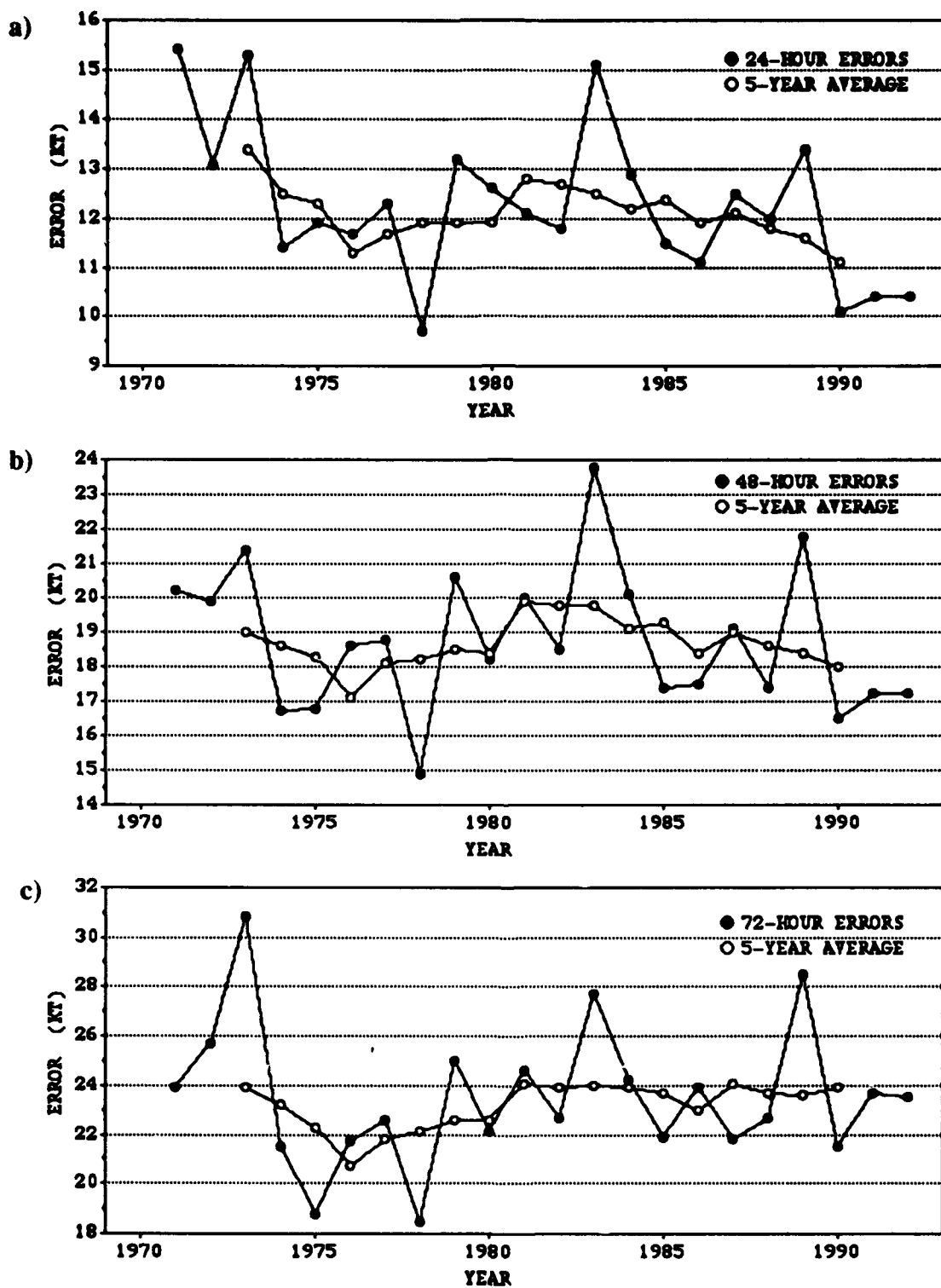


Figure 5-4. Mean intensity forecast errors (kt) and 5-year running mean for a) 24 hours, b) 48 hours and c) 72 hours for the western North Pacific Ocean in 1992.

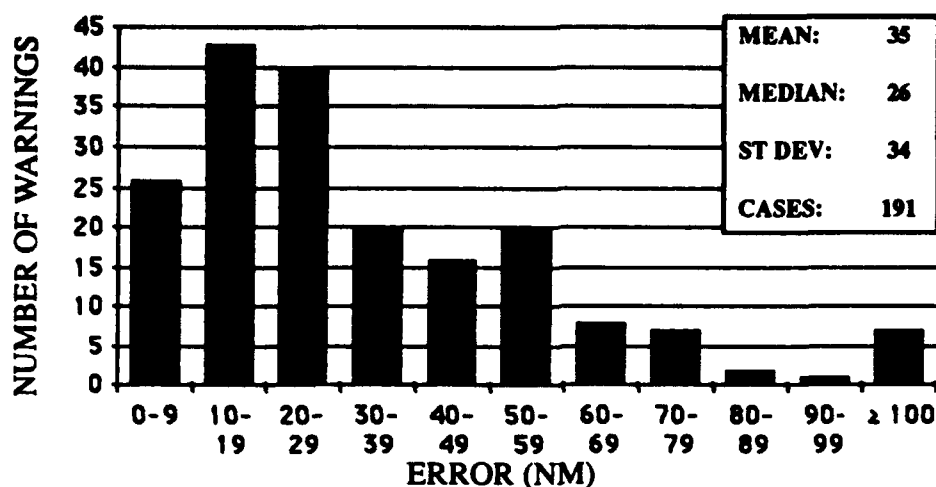


Figure 5-5a. Frequency distribution of initial warning position errors (10 nm increments) for the North Indian Ocean in 1992. The largest error, 306 nm, was on TC02A.

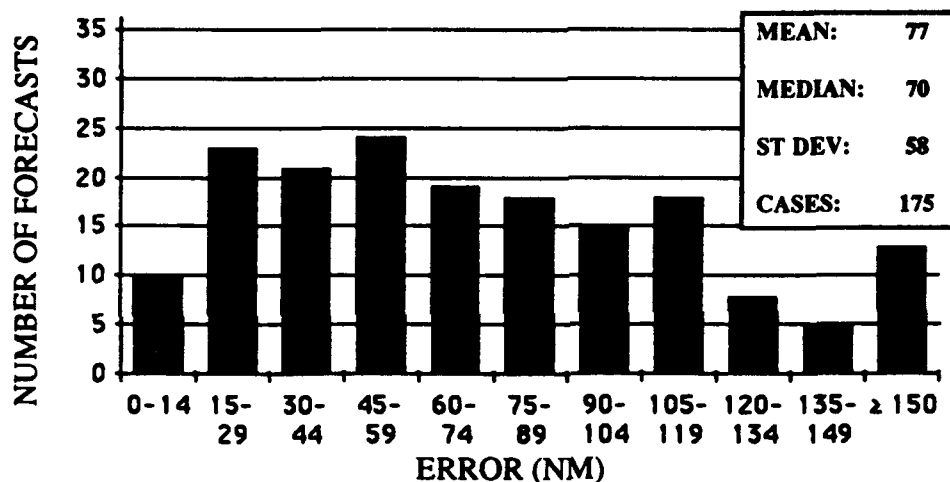


Figure 5-5b. Frequency distribution of 12-hour forecast errors (15 nm increments) for the North Indian Ocean in 1992. The largest error, 460 nm, was on TC02A.

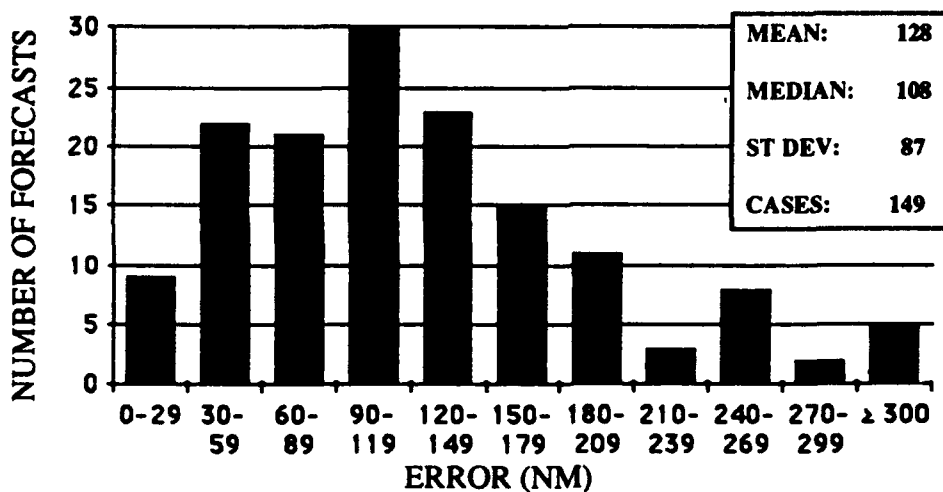


Figure 5-5c. Frequency distribution of 24-hour forecast errors (30 nm increments) for the North Indian Ocean in 1992. The largest error, 592 nm, was on TC02A.

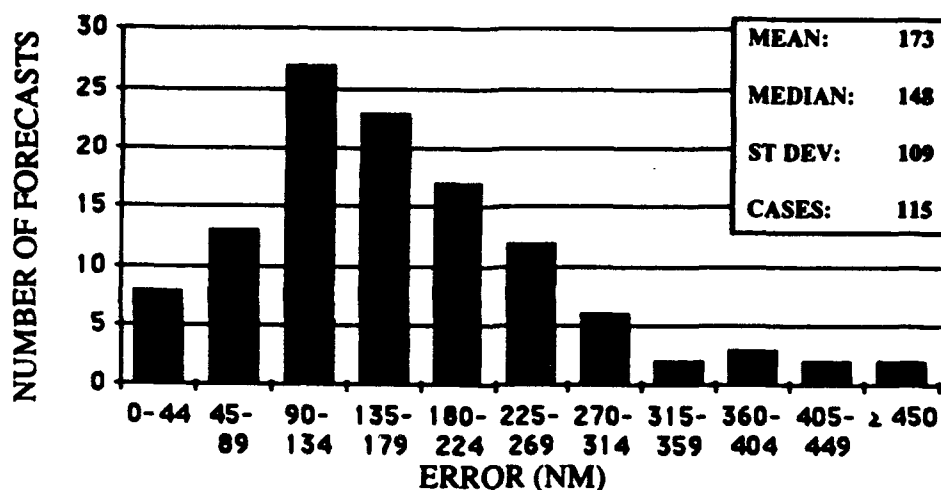


Figure 5-5d. Frequency distribution of 36-hour forecast errors (45 nm increments) for the North Indian Ocean in 1992. The largest error, 683 nm, was on TC02A.

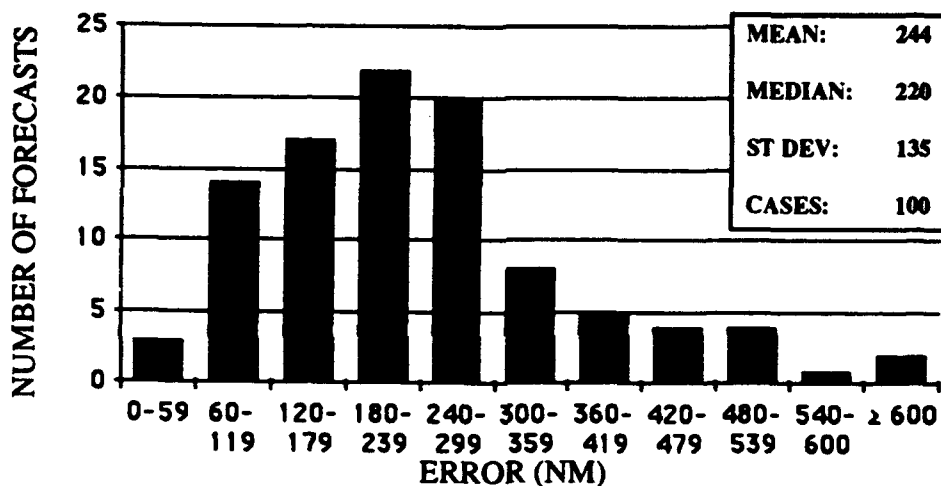


Figure 5-5e. Frequency distribution of 48-hour forecast errors (60 nm increments) for the North Indian Ocean in 1992. The largest error, 733 nm, was on TC02A.

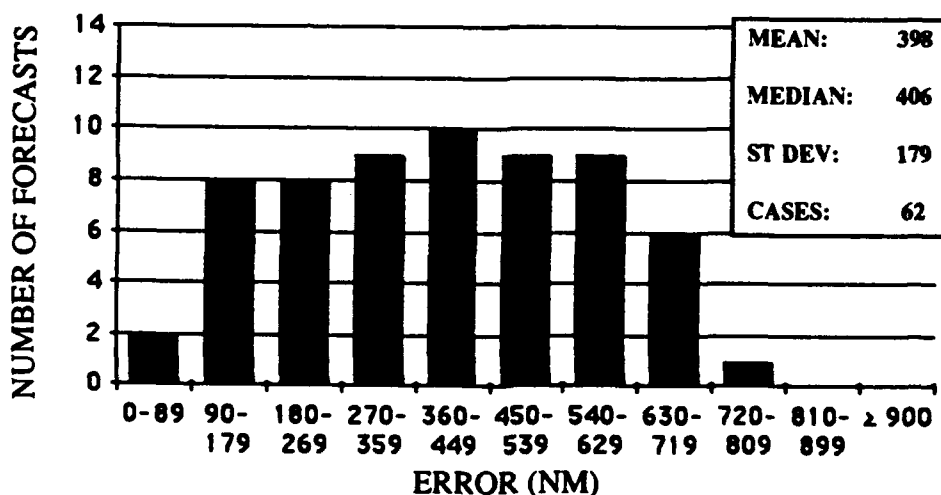


Figure 5-5f. Frequency distribution of 72-hour forecast errors (90 nm increments) for the North Indian Ocean in 1992. The largest error, 723 nm, was on TC02A.

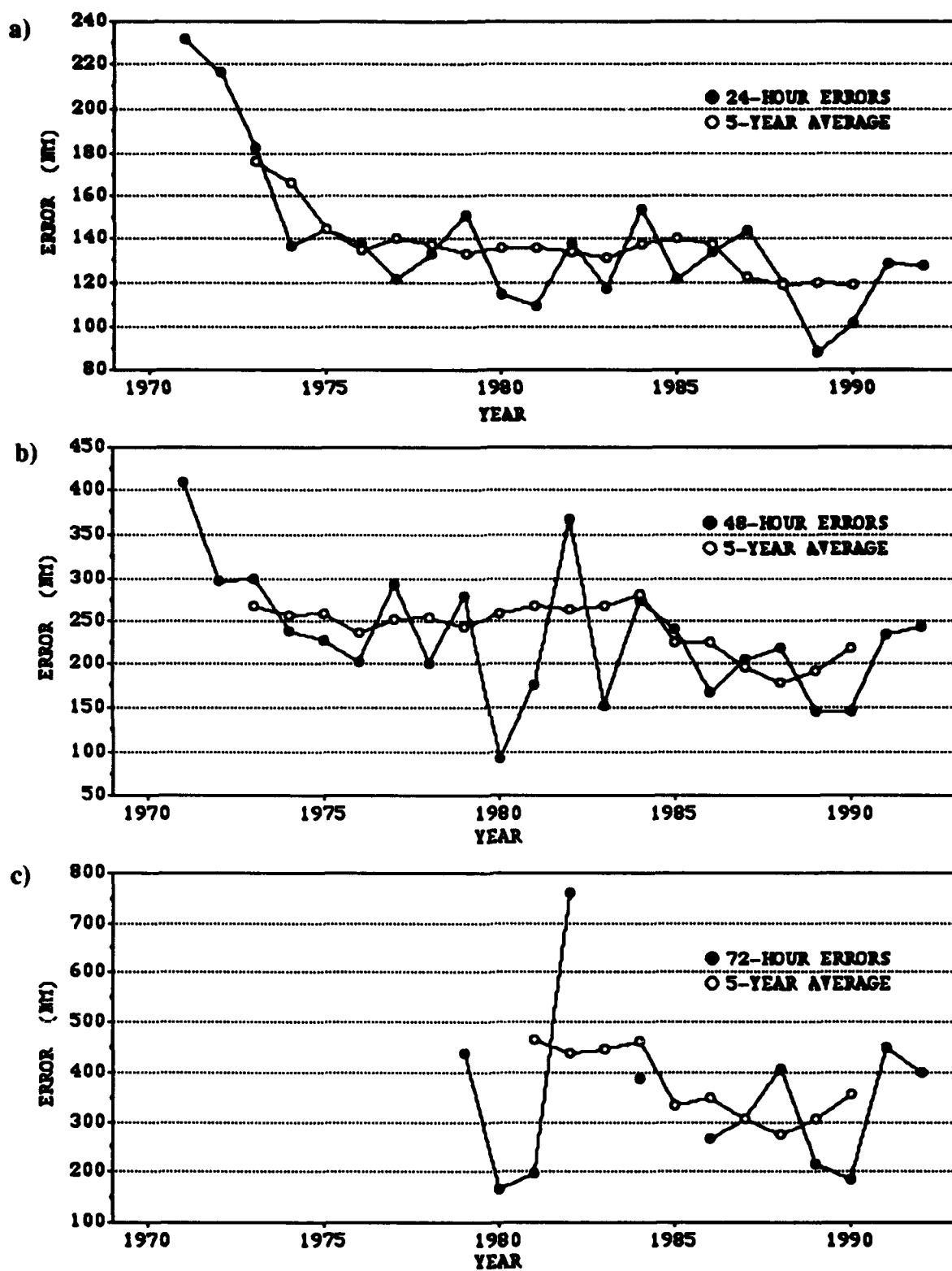


Figure 5-6. Mean track errors (nm) and 5-year running mean for a) 24 hours, b) 48 hours and c) 72 hours in the North Indian Ocean. Note: no 72-hour forecasts verified prior to 1979, in 1983 and 1985.

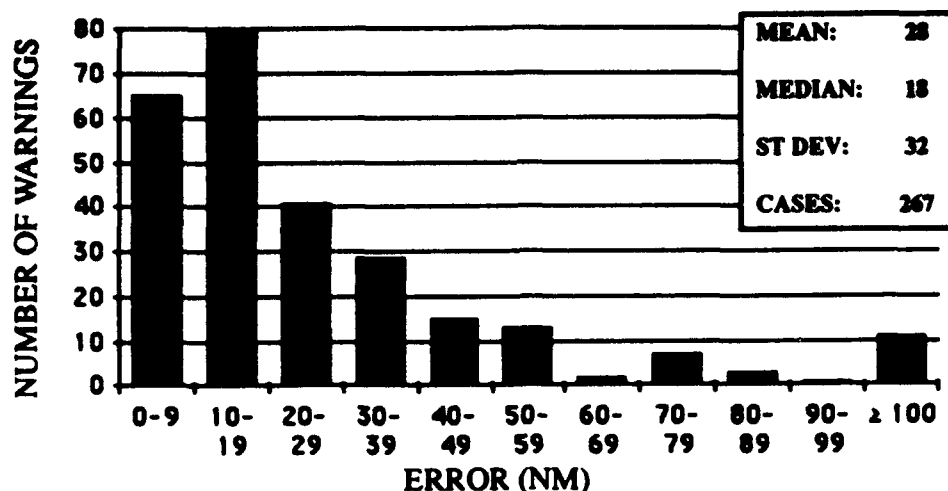


Figure 5-7a. Frequency distribution of initial warning position errors (10 nm increments) for the South Pacific and South Indian Oceans. The largest error, 297 nm, occurred on Tropical Cyclone 15P (Celesta).

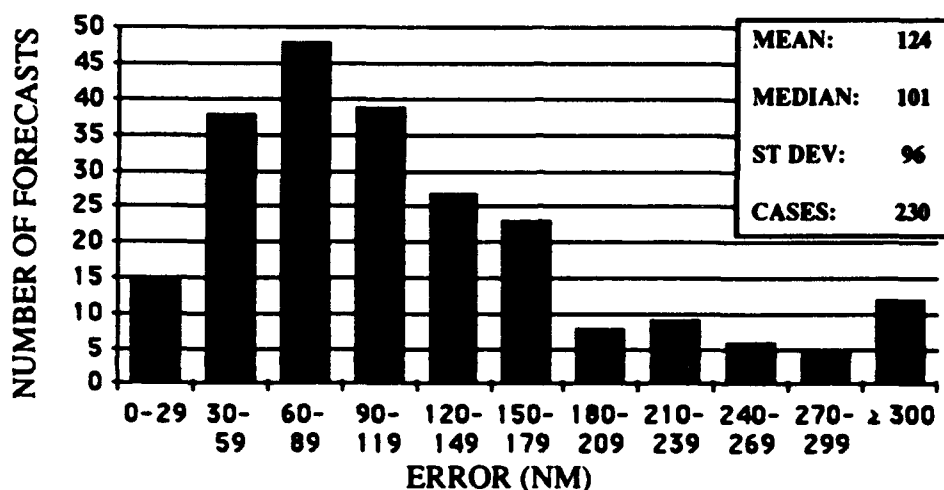


Figure 5-7b. Frequency distribution of 24-hour forecast errors (30 nm increments) for the South Pacific and South Indian Oceans. The largest error, 620 nm, occurred on Tropical Cyclone 15P (Celesta).

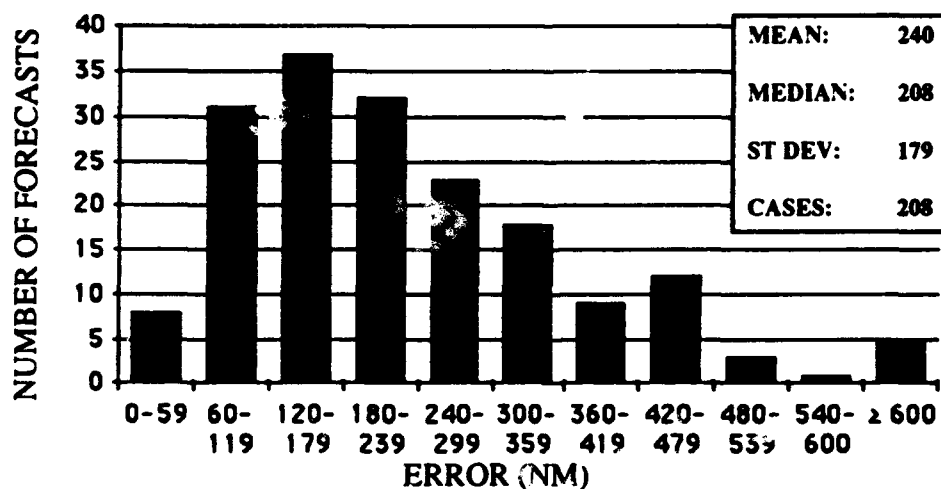


Figure 5-7c. Frequency distribution of 48-hour forecast errors (60 nm increments) for the South Pacific and South Indian Oceans. The largest error, 1281 nm, occurred on Tropical Cyclone 03P (Tia).

TABLE 5-4. JTWC ANNUAL INITIAL POSITION AND FORECAST POSITION ERRORS (NM) 1981-1992 FOR THE SOUTHERN HEMISPHERE

YEAR	NUMBER OF INITIAL WARNINGS POSITION		NUMBER OF FORECASTS TRACK		24-HOUR ALONG CROSS		NUMBER OF FORECASTS TRACK		48-HOUR ALONG CROSS	
1981	226	48	190	165	103	106	140	315	204	201
1982	275	38	238	144	98	86	176	274	188	164
1983*	191	35	163	130	88	77	126	241	158	145
1984	301	36	252	133	90	79	191	231	159	134
1985*	306	36	257	134	92	79	193	236	169	132
1986*	279	40	227	129	86	77	171	262	169	164
1987*	189	46	138	145	94	90	101	280	153	138
1988*	204	34	99	146	98	83	48	290	246	144
1989*	287	31	242	124	84	73	186	240	166	136
1990*	272	27	228	143	105	74	177	263	178	152
1991*	264	24	231	115	75	69	185	220	152	129
1992*	267	28	230	124	91	64	208	240	177	129
AVERAGE 81-92:	255	35	208	135	91	79	156	246	168	141

NOTE: Cross-track and along-track errors were adopted by the JTWC in 1986. Right-angle errors (used prior to 1986) were recomputed as cross-track and along-track errors after the fact to extend the data base.

See Figure 5-1 for the definitions of cross-track and along-track errors.

* These statistics are for JTWC forecasts only. NWOC statistics are not included.

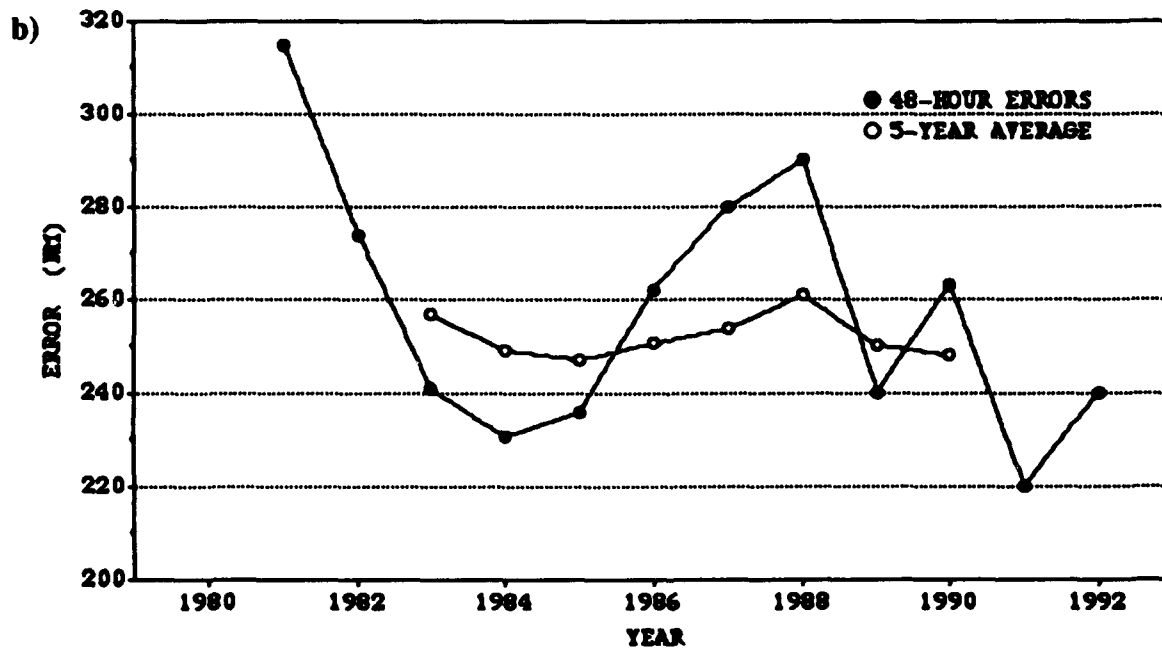
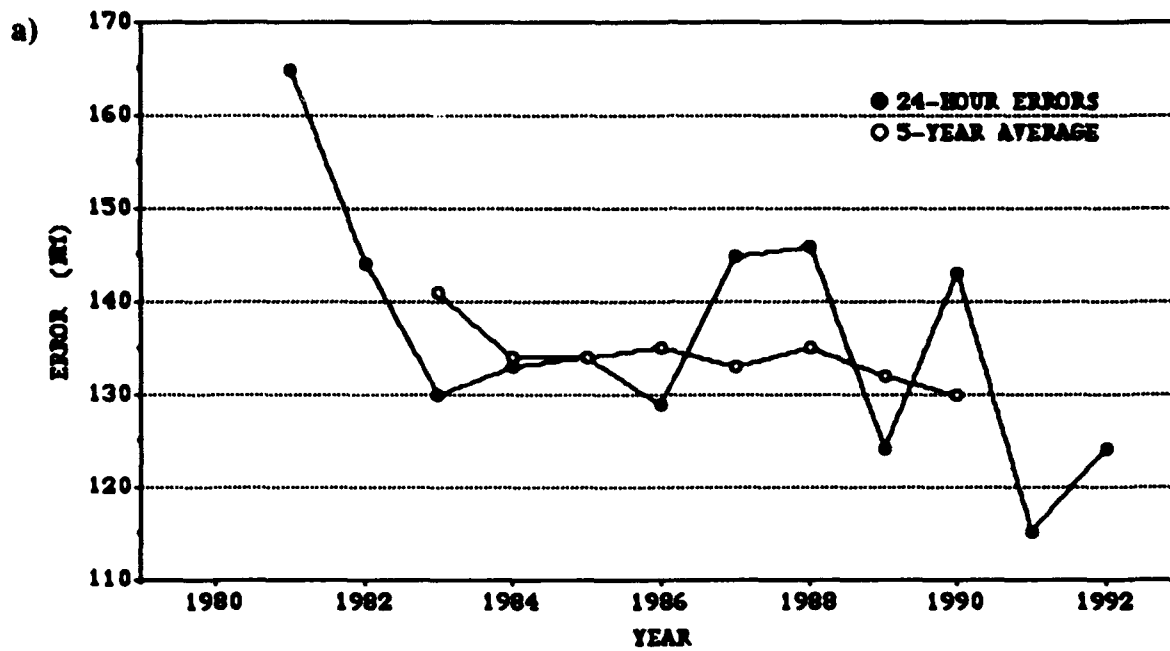


Figure 5-8. Mean track forecast errors (nm) and 5-year running mean for a) 24 hours and b) 48 hours for the South Pacific and South Indian Oceans.

5.2 COMPARISON OF OBJECTIVE TECHNIQUES

JTWC uses a variety of objective techniques for guidance in the warning development process. Multiple techniques are required, because each technique has particular strengths and weaknesses which vary by basin, numerical model initialization, time of year, synoptic situation and forecast period. The accuracy of objective aid forecasts depends on both the specified position and the past motion of the tropical cyclone as determined by the working best track. JTWC initializes its objective techniques using the extrapolated warning position.

An initiative is presently underway to convert most of the objective techniques that currently run on mainframe computers at FNOC to desktop computer versions that run on ATCF workstations. These will eventually replace the FNOC-generated techniques. Three of these new aids have been received and are under evaluation.

Unless stated otherwise, all the objective techniques discussed below run in all basins covered by JTWC's AOR and provide forecast positions at 24-, 48-, and 72-hours unless the technique aborts prematurely during computations. The techniques can be divided into six general categories: extrapolation, climatology and analogs, statistical, dynamic, hybrids, and empirical or analytical.

5.2.1 EXTRAPOLATION (XTRP) — Past speed and direction are computed using the rhumb line distance between the current and 12-hour old positions of the tropical cyclone. Extrapolation from the current warning position is used to compute forecast positions.

5.2.2 CLIMATOLOGY and ANALOGS

5.2.2.1 CLIMATOLOGY (CLIM) — Employs time and location windows relative to the current position of the storm to determine which historical storms will be used to compute the forecast. The historical data base is 1945-1981 for the Northwest Pacific, and 1900 to 1990 for the rest of JTWC's AOR. A second climatology-based technique exists on JTWC's Macintosh[®] II computers. It employs data bases from 1945 to 1992 and from 1970 to 1992. The latter is referred to as the satellite-era data base. Objective intensity forecasts are available from these data bases. Scatter diagrams of expected tropical cyclone motion at bifurcation points are also available from these data bases.

5.2.2.2 ANALOGS — JTWC's analog and climatology techniques use the same historical data base, except that the analog approach imposes more restrictions on which storms will be used to compute the forecast positions. Analogs in all basins must satisfy time, location, speed, and direction windows, although the window definitions are distinctly different in the Northwest Pacific. In this basin, acceptable analogs are also ranked in terms of a similarity index that includes the above parameters and: storm size and size change, intensity and intensity change, and heights and locations of the 700-mb subtropical ridge and upstream midlatitude trough. In other basins, all acceptable analogs receive equal weighting and a persistence bias is explicitly added to the forecast. Inside the Northwest Pacific, analog weighting is varied using the similarity index, and a persistence bias is implicitly incorporated by rotating the analog tracks so that they initially match the 12-hr old motion of the current storm. In the Northwest Pacific, a forecast based on all acceptable analogs called TOTL, as well as a forecast based only on historical recurvers called RECR are available. Outside this basin, only the TOTL technique is available.

5.2.3 STATISTICAL

5.2.3.1 CLIMATOLOGY AND PERSISTENCE

(CLIP) — A statistical regression technique that is based on climatology, current position and 12-hour and 24-hour past movement. This technique is used as a crude baseline against which to measure the forecast skill of other more sophisticated techniques. CLIP in the Northwest Pacific uses third-order regression equations and is based on the work of Xu and Neumann (1985). CLIP has been available outside this basin since mid-1990, with regression coefficients recently recomputed by FNOC based on the updated 1900-1989 data base.

5.2.3.2 COLORADO STATE UNIVERSITY

MODEL (CSUM) — A statistical-dynamical technique based on the work of Matsumoto (1984). Predictor parameters include the current and 24-hr old position of the storm, heights from the current and 24-hr old NOGAPS 500-mb analyses, and heights from the 24-hr and 48-hr NOGAPS 500 mb prognoses. Height values from 200-mb fields are substituted for storms that have an intensity exceeding 90 knots and are located north of the subtropical ridge. Three distinct sets of regression equations are used depending on whether the storm's direction of motion falls into "below," "on," or "above" the subtropical ridge categories. During the development of the regression equation coefficients for CSUM, the so-called "perfect prog" approach was used, in which verifying analyses were substituted for the numerical prognoses that are used when CSUM is run operationally. Thus, CSUM was not "tuned" to any particular version of NOGAPS, and in fact, the performance of CSUM should presumably improve as new versions of NOGAPS improve. CSUM runs only in the Northwest Pacific, South China Sea, and North Indian Ocean basins.

5.2.3.3 JTWC92 (JT92) - JTWC92 is a statistical-dynamical model for the Northwest Pacific Ocean basin which forecasts tropical cyclone positions at 12-hour intervals to 72 hours. The model uses the deep-layer mean height field derived from the NOGAPS forecast fields. These deep-layer mean height fields are spectrally truncated to wave numbers 0 through 18 prior to use in JT92. Separate forecasts are made for each position. That is, the forecast 24 hour position is not a 12-hour forecast from the forecasted 12-hour position.

JT92 uses five internal sub-models which are blended and iterated to produce the final forecasts. The first sub-model is a statistical blend of climatology and persistence, known as CLIPER. The second sub-model is an analysis mode predictor, which only uses the "analysis" field. The third sub-model is the forecast mode predictor, which uses only the forecast fields. The fourth sub-model is a combination of 1 and 2 to produce a "first guess" of the 12-hourly forecast positions. The fifth sub-model uses the output of the "first guess" combined with 1, 2, and 3 to produce the forecasts. The iteration is accomplished by using the output of sub-model 5 as though it were the output from sub-model 4. The optimum number of iterations has been determined to be three.

When JT92 is used in the operational mode, all the NOGAPS fields are forecast fields. The 00Z and 12Z tropical forecasts are based upon the previous 12-hour old synoptic time NOGAPS forecasts. The 06Z and 18Z tropical forecasts are based on the previous 00Z and 12Z NOGAPS forecasts, respectively. Therefore, the second sub-model uses forecast fields and not analysis fields operationally.

5.2.4 DYNAMIC

5.2.4.1 NOGAPS VORTEX TRACKING ROUTINE (NGPS) —

This objective technique follows the movement of the point of minimum height on the 1000 mb pressure surface ana-

lyzed and predicted by NOGAPS. A search in the expected vicinity of the storm is conducted every six hours through 72 hours, even if the tracking routine temporarily fails to discern a minimum height point. Explicit insertion of a tropical cyclone bogus via data provided over TYMNET by JTWC began in mid-1990, and should improve the ability of the NOGAPS technique to track the vortex.

5.2.4.2 ONE-WAY INFLUENCE TROPICAL CYCLONE MODEL (OTCM) — This technique is a coarse resolution (205 km grid), three layer, primitive equation model with a horizontal domain of 6400 x 4700 km. OTCM is initialized using 6-hour or 12-hour prognostic fields from the latest NOGAPS run, and the initial fields are smoothed and adjusted in the vicinity of the storm to induce a persistence bias into OTCM's forecast. A symmetric bogus vortex is then inserted, and the boundaries updated every 12 hours by NOGAPS fields as the integration proceeds. The bogus vortex is maintained against frictional dissipation by an analytical heating function. The forecast positions are based on the movement of the vortex in the lowest layer of the model (effectively 850-mb).

5.2.4.3 FNOC BETA AND ADVECTION MODEL (FBAM) — This model is an adaptation of the Beta and Advection model used by NMC. The forecast motion results from a calculation of environmental steering and an empirical correction for the observed vector difference between that steering and the 12-hour old storm motion. The steering is computed from the NOGAPS Deep Layer Mean (DLM) wind fields which are a weighted average of the wind fields computed for the 1000-mb to 100-mb levels. The difference between past storm motion and the DLM steering is treated as if the storm were a Rossby wave with an "effective radius" propagating in response to the horizontal gradient of the coriolis parameter, Beta. The forecast proceeds in one-hour steps, recomputing the effective

radius as Beta changes with storm latitude, and blending in a persistence bias for the first 12 hours.

5.2.5 HYBRIDS

5.2.5.1 HALF PERSISTENCE AND CLIMATOLOGY (HPAC) — Forecast positions are generated by equally weighting the forecasts given by XTRP and CLIM.

5.2.5.2 COMBINED CONFIDENCE WEIGHTED FORECASTS (CCWF) — An optimal blend of objective techniques produced by the ATCF. The ATCF blends the selected techniques (currently OTCM, CSUM and HPAC) by using the inverse of the covariance matrices computed from historical and real-time cross-track and along-track errors as the weighting function.

5.2.6 EMPIRICAL OR ANALYTICAL

5.2.6.1 DVORAK — An estimation of a tropical cyclone's current and 24-hour forecast intensity is made from the interpretation of satellite imagery (Dvorak, 1984). These intensity estimates are used with other intensity related data and trends to forecast short-term tropical cyclone intensity.

5.2.6.2 MARTIN/HOLLAND — The technique adapts an earlier work (Holland, 1980) and specifically addresses the need for realistic 30-, 50- and 100-kt (15-, 26- and 51-m/sec) wind radii around tropical cyclones. It solves equations for basic gradient wind relations within the tropical cyclone area, using input parameters obtained from enhanced infrared satellite imagery. The diagnosis also includes an asymmetric area of winds caused by tropical cyclone movement. Satellite-derived size and intensity parameters are also used to diagnose internal steering components of tropical cyclone motion known collectively as "beta-drift".

5.2.6.3 TYPHOON ACCELERATION PREDICTION TECHNIQUE (TAPT) — This technique (Weir, 1982) utilizes upper-tropospheric and surface wind fields to estimate acceleration associated with the tropical cyclone's interaction with the mid-latitude westerlies. It includes guidelines for the duration of acceleration, upper limits and probable path of the cyclone.

5.3 TESTING AND RESULTS

A comparison of selected techniques is included in Table 5-5 for all Northwest Pacific tropical cyclones; Table 5-6 for all North Indian Ocean tropical cyclones and Table 5-7 for the Southern Hemisphere. In these tables, "x-axis" refers to techniques listed vertically. For example (Table 5-5) in the 861 cases available for a (homogeneous) comparison, the average forecast error at 24 hours was 137 nm (254 km) for CSUM and 139 nm (257 km) for FBAM. The difference of 2 nm (4 km) is shown in the lower right. (Differences are not always exact, due to computational round-off which occurs for each of the cases available for comparison).

TABLE 5-5

**1992 ERROR STATISTICS FOR SELECTED OBJECTIVE TECHNIQUES
IN THE NORTHWEST PACIFIC (1 JAN 1992 - 31 DEC 1992)**

24-HOUR MEAN FORECAST ERROR (NM)

	JTWC		NGPS		OTCM		CSUM		FBAM		CLIP		HPAC	
JTWC	841	107												
	107	0												
NGPS	427	99	428	146										
	146	47	146	0										
OTCM	795	105	421	145	881	129								
	126	21	117	-28	129	0								
CSUM	793	107	419	144	846	127	872	146						
	129	22	121	-23	145	18	146	0						
FBAM	804	107	416	145	866	128	861	137	891	140				
	138	31	138	-7	140	12	139	2	140	0				
CLIP	814	107	422	146	876	128	868	137	888	140	905	140		
	134	27	121	-25	139	11	133	-4	140	0	140	0		
HPAC	809	107	422	145	862	128	866	137	874	139	887	135	888	139
	136	29	126	-19	136	8	139	2	139	0	139	4	139	0

Number of Cases	X-Axis Technique Error
Y-Axis Technique Error	Error Difference (Y-X)

48-HOUR MEAN FORECAST ERROR (NM)

	JTWC		NGPS		OTCM		CSUM		FBAM		CLIP		HPAC	
JTWC	685	205												
	205	0												
NGPS	360	201	364	238										
	237	36	238	0										
OTCM	641	202	356	233	756	229								
	226	24	219	-14	229	0								
CSUM	651	204	355	234	723	228	755	252						
	235	31	236	2	251	23	252	0						
FBAM	658	204	353	235	743	228	745	241	775	257				
	253	49	258	23	256	28	255	14	257	0				
CLIP	665	204	358	237	751	229	751	242	772	257	788	277		
	261	57	246	9	276	47	262	20	277	20	277	0		
HPAC	661	204	358	236	739	229	750	242	759	256	771	264	772	255
	247	43	247	11	253	24	256	14	255	-1	256	-8	255	0

72-HOUR MEAN FORECAST ERROR (NM)

	JTWC		NGPS		OTCM		CSUM		FBAM		CLIP		HPAC	
JTWC	565	305												
	305	0												
NGPS	271	297	280	319										
	313	16	319	0										
OTCM	521	300	265	315	629	326								
	326	26	314	-1	326	0								
CSUM	544	302	273	313	601	327	645	340						
	330	28	338	25	332	5	340	0						
FBAM	549	303	274	316	619	325	638	339	664	373				
	363	60	364	48	367	42	369	30	373	0				
CLIP	553	303	276	319	626	326	642	340	661	374	675	402		
	386	83	374	55	392	66	385	45	400	26	402	0		
HPAC	548	302	276	318	612	326	638	340	645	370	655	387	556	355
	348	46	343	25	349	23	356	16	354	-16	355	-32	355	0

JTWC - JTWC Forecast

OTCM - One-Way Tropical Cyclone Model

FBAM - FVOC Beta and Advection Model

HPAC - Half Persistence and Climatology

NGPS - Navy-Operational Global-Atmospheric Prediction System

CSUM - Colorado State University Model

CLIP - Climatology/Persistence

TABLE 5-6

**1992 ERROR STATISTICS FOR SELECTED OBJECTIVE TECHNIQUES
IN THE NORTH INDIAN OCEAN (1 JAN 1992 - 31 DEC 1992)**

24-HOUR MEAN FORECAST ERROR (NM)

	JTWC		OTCM		FBAM		CLIP		HPAC		TOTL		CLIM	
JTWC	147	128												
	128	0												
OTCM	140	128	155	146										
	141	13	146	0										
FBAM	141	129	155	146	156	144								
	144	15	145	-1	144	0								
CLIP	141	129	155	146	156	144	156	146						
	141	12	146	0	146	2	146	0						
HPAC	141	129	155	146	156	144	156	146	156	148				
	145	16	148	2	148	4	148	2	148	0				
TOTL	126	133	135	147	136	146	136	146	136	152	136	153		
	152	19	153	6	153	7	153	7	153	1	153	0		
CLIM	141	129	155	146	156	144	156	146	156	148	136	153	156	157
	157	28	158	12	157	13	157	11	157	9	164	11	157	0

Number of Cases	X-Axis Technique Error
Y-Axis Technique Error	Error Difference (Y-X)

48-HOUR MEAN FORECAST ERROR (NM)

	JTWC		OTCM		FBAM		CLIP		HPAC		TOTL		CLIM	
JTWC	99	245												
	245	0												
OTCM	82	240	95	277										
	275	35	277	0										
FBAM	95	247	95	277	111	256								
	267	20	259	-18	256	0								
CLIP	95	247	95	277	111	256	111	259						
	268	21	254	-23	259	3	259	0						
HPAC	94	247	94	279	110	257	110	260	110	262				
	271	24	258	-21	262	5	262	2	262	0				
TOTL	76	254	69	287	85	258	85	253	85	256	85	276		
	284	30	267	-20	276	18	276	23	276	20	276	0		
CLIM	94	247	94	279	110	257	110	260	110	262	85	276	110	262
	280	33	265	-14	262	5	262	2	262	0	260	-16	262	0

72-HOUR MEAN FORECAST ERROR (NM)

	JTWC		OTCM		FBAM		CLIP		HPAC		TOTL		CLIM	
JTWC	61	402												
	402	0												
OTCM	42	386	56	486										
	499	113	486	0										
FBAM	58	406	56	486	75	408								
	423	17	394	-92	408	0								
CLIP	58	406	56	486	75	408	75	404						
	423	17	387	-99	404	-4	404	0						
HPAC	58	406	56	486	75	408	75	404	75	398				
	409	3	361	-125	398	-10	398	-6	398	0				
TOTL	44	428	38	501	52	432	52	387	52	390	52	435		
	449	21	383	-118	435	3	435	48	435	45	435	0		
CLIM	58	406	56	486	75	408	75	404	75	398	52	435	75	342
	371	-35	317	-169	342	-66	342	-62	342	-56	353	-82	342	0

JTWC - JTWC Forecast

FBAM - FVOC Beta and Advection Model

HPAC - Half Persistence and Climatology

CLIM - Climatology

OTCM - One-Way Tropical Cyclone Model

CLIP - Climatology/Persistence

TOTL - Total Analog

TABLE 5-7

**1992 ERROR STATISTICS FOR SELECTED OBJECTIVE TECHNIQUES
IN THE SOUTHERN HEMISPHERE (1 JUL 1991 - 30 JUN 1992)**

24-HOUR MEAN FORECAST ERROR (NM)

	<u>JTWC</u>	<u>OTCM</u>	<u>FBAM</u>	<u>CLIP</u>	<u>HPAC</u>	<u>TOTL</u>	<u>CLIM</u>	<u>XTRP</u>
JTWC	234 125							
	125 0							
OTCM	213 117	368 133						
	123 6	133 0						
FBAM	210 123	350 134	357 181					
	179 56	178 44	181 0					
CLIP	219 124	365 132	355 180	373 169				
	166 42	167 35	171 -9	169 0				
HPAC	219 124	365 132	355 180	373 169	373 150			
	144 20	148 16	152 -28	150 -19	150 0			
TOTL	117 125	175 125	175 184	182 160	182 139	182 141		
	150 25	134 9	138 -46	141 -19	141 2	141 0		
CLIM	219 124	367 132	356 180	373 169	373 150	182 141	375 197	
	187 63	195 63	198 18	196 27	196 46	179 38	197 0	
XTRP	219 124	366 132	356 180	373 169	373 150	182 141	374 196	374 151
	146 22	147 15	152 -28	151 -18	151 1	141 0	151 -45	151 0

Number of Cases	X-Axis Technique Error
Y-Axis Technique Error	Error Difference (Y-X)

48-HOUR MEAN FORECAST ERROR (NM)

	<u>JTWC</u>	<u>OTCM</u>	<u>FBAM</u>	<u>CLIP</u>	<u>HPAC</u>	<u>TOTL</u>	<u>CLIM</u>	<u>XTRP</u>
JTWC	154 242							
	242 0							
OTCM	165 238	307 243						
	236 -2	243 0						
FBAM	168 242	290 243	304 315					
	306 64	317 74	315 0					
CLIP	175 240	305 243	303 316	320 283				
	285 45	280 37	288 -28	283 0				
HPAC	175 240	305 243	303 316	320 283	320 256			
	246 6	254 11	260 -56	256 -27	256 0			
TOTL	88 229	135 224	137 304	143 260	143 232	143 259		
	265 36	257 33	258 -46	259 -1	259 27	259 0		
CLIM	175 240	307 243	304 315	320 283	320 256	143 259	322 335	
	322 82	328 85	339 24	333 50	333 77	301 42	335 0	
XTRP	175 240	306 243	304 315	320 283	320 256	143 259	321 334	321 285
	276 36	284 41	287 -28	285 2	285 29	264 5	285 -49	285 0

JTWC - JTWC Forecast
CLIP - Climatology/Persistence
TOTL - Total Analog
XTRP - Extrapolation

OTCM - One-Way Tropical Cyclone Model
HPAC - Half Persistence and Climatology
CLIM - Climatology

Intentionally left blank

6. TROPICAL CYCLONE WARNING VERIFICATION STATISTICS

6.1 GENERAL

Due to the rapid growth of micro-computers in the meteorological community and to save publishing costs, tropical cyclone track data (with best track, initial warning, 12-, 24-, 36-, 48-, and 72-hour JTWC forecasts) and fix data (satellite, aircraft, radar and synoptic) are now available separately upon request. Pre- and post-warning best track positions are not printed in this chapter, but are available on floppy diskettes upon request. The data will be in ASCII format on 5.25 inch "floppy" or 3.5 inch diskettes and will fill two diskettes (or one high density diskette). These data include the western North Pacific Ocean (1 January - 31 December 1992) on one and North Indian Ocean (1 January - 31 December 1992), and

South Western Pacific and South Indian Oceans (1 July 1991 - 30 June 1992) on the other. Agencies or individuals desiring these data sets should send the appropriate number of diskettes to NAVOCEANCOMCEN/JTWC Guam with their request. When the request and your diskettes are received, the data will be copied onto your diskettes and returned with an explanation of the data formats.

6.2 WARNING VERIFICATION STATISTICS

6.2.1 WESTERN NORTH PACIFIC

This section includes verification statistics for each warning in the western North Pacific during 1992.

JTWC FORECAST TRACK AND INTENSITY ERRORS BY WARNING

TYPHOON AXEL (01W)																
DTG	WRN NO.	BEST TRACK			POSITION ERRORS							WIND ERRORS				
		LAT	LONG	WIND	00	12	24	36	48	72	00	12	24	36	48	72
92010506	1	5.9N	177.7E	25	43	65	78		59	69	0	0	-5		0	5
92010512	2	6.0N	176.8E	30	42	48	48		76	141	0	0	0		5	15
92010518	3	6.1N	176.0E	30	58	97	108		144	230	0	-5	-5		0	15
92010600	4	6.2N	175.2E	35	59	85	117		152	200	0	0	5		5	15
92010606	5	6.2N	174.3E	40	26	59	91		106	114	0	0	5		10	20
92010612	6	6.2N	173.5E	45	21	59	103		105	73	0	5	5		15	25
92010618	7	6.0N	172.7E	50	32	72	88		77	43	0	5	5		15	25
92010700	8	5.9N	171.9E	50	18	24	29		115	157	15	20	20		30	40
92010706	9	5.8N	171.0E	55	16	8	21		130	169	15	20	25		35	45
92010712	10	5.8N	170.1E	60	110	123	119		90	29	10	0	5		20	45
92010718	11	5.8N	169.0E	65	94	107	126		139	125	5	0	-5		10	30
92010800	12	5.9N	167.8E	70	30	66	126		171	155	0	0	-5		10	30
92010806	13	6.0N	166.5E	70	59	137	202		226	211	0	0	0		15	35
92010812	14	6.0N	165.1E	70	75	139	167		185	219	0	0	10		30	45
92010818	15	6.0N	163.6E	70	29	33	34		47	143	5	15	25		45	60
92010900	16	6.2N	162.1E	70	17	34	49		56	84	10	15	25		45	60
92010906	17	6.5N	160.6E	65	25	71	112		127	159	10	10	20		40	45
92010912	18	6.9N	159.3E	65	5	24	45		69	118	10	5	20		35	40
92010918	19	7.3N	158.0E	60	18	40	55		23	47	-5	5	20		35	40
92011000	20	7.7N	156.7E	60	11	48	13		72	65	0	10	20		35	45
92011006	21	8.3N	155.6E	55	34	41	53		71	85	0	5	10		20	30
92011012	22	8.9N	154.5E	50	43	67	96		116	218	0	0	5		15	25
92011018	23	9.3N	153.4E	45	13	48	84		60	126	0	0	5		15	25
92011100	24	9.5N	152.3E	45	17	64	101		83	174	0	0	5		10	5
92011106	25	9.6N	151.2E	40	23	53	61		99	253	0	5	0		5	0
92011112	26	9.7N	150.1E	40	11	26	34		186	439	-5	0	-5		-5	-10

TYPHOON AXEL (01W) (CONTINUED)

92011118	27	9.8N	149.0E	35	8	6	42	223	552	0	0	0	0	-10
92011200	28	9.9N	147.9E	35	42	56	97	241	727	5	5	10	5	-5
92011206	29	10.1N	146.9E	35	50	59	119	327		5	5	10	5	
92011212	30	10.4N	145.9E	35	71	134	220	504		0	5	5	5	
92011218	31	10.9N	145.0E	35	95	166	262	622		0	5	5	5	
92011300	32	11.6N	144.2E	30	31	54	97	228		0	0	-5	-10	
92011306	33	12.2N	143.4E	30	6	34	66	228		0	0	0	-5	
92011312	34	12.8N	142.6E	30	21	36	64	144		0	0	0	-5	
92011318	35	13.5N	142.0E	30	24	21	63			0	0	0		
92011400	36	14.3N	141.3E	30	8	53	166			0	0	0		
92011412	37	16.4N	140.8E	30	24	81				0	0			
92011500	38	20.2N	142.8E	30	5					0				

AVERAGE	35	64	94	200	152	184	3	4	8	7	17	28
# CASES	38	37	36	3	31	28	38	37	36	3	31	28

TROPICAL STORM EKEKA (01C)

DTG	WRN NO.	BEST TRACK				POSITION ERRORS					WIND ERRORS					
		LAT	LONG	WIND	00	12	24	36	48	72	00	12	24	36	48	72
92020400	1	9.2N	178.2E	40	6	41	103		206	217	0	5	10		10	15
92020406	2	9.1N	176.5E	35	29	97	172		217	236	5	15	15		25	35
92020412	3	9.2N	174.8E	30	0	54	114		111	187	10	15	15		20	35
92020418	4	9.4N	173.0E	25	18	68	93		34		10	5	0		-5	
92020500	5	9.9N	171.2E	25	8	48	93		124		10	10	5		-5	
92020506	6	10.3N	169.5E	25	13	55	102				10	5	0			
92020512	7	10.6N	168.0E	25	30	30	16				5	5	0			
92020518	8	10.9N	166.6E	25	16	45	97				5	5	0			
92020600	9	11.0N	165.3E	25	11	80	108		114		5	5	5		10	
92020606	10	10.8N	164.2E	25	13	43	93		247		5	5	5		10	
92020612	11	10.5N	163.2E	25	8	21	64		259		5	5	10		10	
92020618	12	10.2N	162.1E	25	11	59	116				5	5	10			
92020700	13	9.8N	160.8E	25	5	24	71				5	10	15			
92020706	14	9.5N	159.3E	25	13	51	110				5	10	15			
92020712	15	9.0N	157.7E	20	36	96	173				5	10	15			
92020718	16	8.5N	156.0E	20	18	64					5	10				
92020800	17	8.0N	154.1E	20	18	5					5	5				
92020806	18	7.4N	152.2E	20	17						5					
92020812	19	7.0N	150.2E	20	11						5					

AVERAGE	15	52	102	0	165	214	6	8	8	5	12	28
# CASES	19	17	15	0	8	3	19	17	15	1	8	3

TYPHOON BOBBIE (02W)

DTG	WRN NO.	BEST TRACK				POSITION ERRORS					WIND ERRORS					
		LAT	LONG	WIND	00	12	24	36	48	72	00	12	24	36	48	72
92062312	1	10.7N	131.6E	30	35	100	136	147	188	302	0	0	0	-10	-15	-50
92062318	2	11.2N	131.4E	30	43	104	139	134	120	109	5	5	5	-5	-10	-50
92062400	3	11.6N	131.2E	35	32	53	75	84	86	58	0	0	-5	-10	-20	-50
92062406	4	11.9N	130.9E	35	21	74	148	212	263	332	0	-5	-20	-25	-40	-60
92062412	5	12.3N	130.3E	40	16	42	97	138	185	264	0	-10	-20	-30	-50	-45
92062418	6	12.7N	129.6E	45	18	37	69	102	145	240	0	-10	-15	-30	-50	-30
92062500	7	13.4N	128.9E	55	11	34	58	91	155	323	0	-10	-20	-35	-40	-30
92062506	8	14.2N	128.2E	65	18	36	61	101	178	379	0	-5	-15	-35	-35	-25
92062512	9	15.0N	127.6E	70	21	29	39	86	151	357	0	-5	-25	-30	-25	-25
92062518	10	15.8N	126.9E	75	13	11	29	73	138	352	0	-15	-35	-35	-30	-35
92062600	11	16.6N	126.3E	85	5	11	41	91	155	379	-5	-30	-35	-30	-30	-30
92062606	12	17.4N	125.7E	95	11	28	68	117	197	457	0	-15	-5	5	-15	-15
92062612	13	18.2N	125.0E	110	6	25	68	137	228	477	-5	0	5	5	-15	-10

TYPHOON BOBBIE (02W) (CONTINUED)

92062618	14	19.1N	124.6E	120	16	46	88	168	277	473	-5	0	10	0	-10	-5
92062700	15	20.0N	124.2E	120	6	34	105	191	300	441	0	5	10	0	-5	5
92062706	16	20.9N	124.0E	120	16	44	55	129	234		0	5	0	0	0	
92062712	17	21.8N	123.8E	115	8	21	101	217	311		0	0	-10	-15	-20	
92062718	18	22.7N	123.9E	110	6	34	128	216	259		0	0	-5	-15	-15	
92062800	19	23.6N	124.2E	110	6	57	138	230	310		0	0	0	-15	-5	
92062806	20	24.3N	124.8E	105	8	72	136	175			0	5	5	-5		
92062812	21	24.8N	125.7E	105	5	61	107	166			0	10	10	0		
92062818	22	25.3N	126.7E	95	12	36	50				0	5	15			
92062900	23	25.8N	127.9E	90	5	8	59				0	5	15			
92062906	24	26.3N	129.2E	85	10	39					0	5				
92062912	25	27.0N	130.7E	80	20	73					0	10				
92062918	26	28.0N	132.2E	70	36						5					
92063000	27	29.2N	133.7E	60	24						0					

AVERAGE	16	45	87	144	205	330	1	6	12	16	23	31
# CASES	27	25	23	21	19	15	27	25	23	21	19	15

TYPHOON CHUCK (03W)

DTG	WRN NO.	BEST TRACK			00	POSITION ERRORS					00	WIND ERRORS				
		LAT	LONG	WIND		12	24	36	48	72		12	24	36	48	72
92062500	1	14.6N	116.4E	30	13	23	31	40	59	104	-5	-15	-20	-25	-30	-35
92062506	2	14.8N	115.8E	35	64	78	86	63	78	150	-10	-20	-20	-25	-30	-20
92062512	3	14.9N	115.2E	40	0	64	104	121	138	238	-5	-10	-15	-25	-30	-15
92062518	4	14.9N	114.7E	45	16	58	86	95	140	237	-5	-10	-20	-30	-35	-20
92062600	5	15.0N	114.2E	50	29	66	129	190	259	406	-10	-20	-30	-30	-35	-10
92062606	6	15.2N	113.7E	55	42	74	127	183	257	395	-15	-25	-35	-30	-20	-10
92062612	7	15.4N	113.2E	60	37	72	128	186	234	306	-20	-25	-25	-25	0	-5
92062618	8	15.8N	112.7E	65	11	23	45	82	133	225	-10	-15	-15	-10	-5	-15
92062700	9	16.3N	112.2E	70	5	58	46	46	98	206	-10	-15	-20	0	-5	-5
92062706	10	16.8N	111.8E	75	5	5	51	107	130	189	-15	-15	-25	-15	-15	5
92062712	11	17.4N	111.3E	75	8	36	92	97	110		-10	-20	-10	-15	-20	
92062718	12	17.8N	110.7E	75	12	62	119	151	211		-10	-10	-15	-20	-20	
92062800	13	18.3N	110.0E	80	17	85	113	152	208		-15	0	-15	-20	-15	
92062806	14	18.7N	109.2E	65	17	48	62	89	124		-10	-5	-15	-15	-5	
92062812	15	19.0N	108.3E	55	5	12	11	70			-10	-15	-20	-15		
92062818	16	19.6N	107.7E	55	8	30	32	75			-10	-15	-15	-5		
92062900	17	20.2N	107.3E	55	18	35	63	75			0	5	0	0		
92062906	18	20.7N	106.9E	55	21	43	85	102			5	0	5	5		
92062912	19	21.0N	106.4E	55	28	72	72				0	0	-5			
92062918	20	21.3N	105.9E	50	5	40	53				0	10	0			
92063000	21	21.7N	105.4E	40	12	40					0	0				
92063006	22	22.2N	105.1E	30	17	72					0	0				

AVERAGE	18	50	77	107	156	246	8	11	16	17	19	14
# CASES	22	22	20	18	14	10	22	22	20	18	14	10

TROPICAL STORM DEANNA (04W)

DTG	WRN NO.	BEST TRACK			00	POSITION ERRORS					00	WIND ERRORS				
		LAT	LONG	WIND		12	24	36	48	72		12	24	36	48	72
92062606	1	6.9N	142.4E	25	21	64	182	291			0	-5	0	0		
92062612	2	6.8N	141.9E	25	23	89	198	288	334	357	0	-5	0	5	20	35
92062618	3	6.5N	141.4E	30	18	113	217	238	275	249	0	0	5	15	25	40
92062700	4	5.9N	141.2E	30	66	177	253	295	329	290	0	0	5	5	10	25
92062706	5	5.4N	141.2E	30	17	115	137	162	180	250	0	0	0	5	10	20
92062712	6	5.1N	141.6E	30	18	77	97	117	159	278	0	0	0	5	10	15
92062718	7	5.3N	142.2E	30	68	83	97	97	164	306	0	0	0	5	10	15
92062800	8	5.7N	141.9E	30	121	160	206	347			0	0	0	-5		

TROPICAL STORM DEANNA (04W) (CONTINUED)

92062812	9	6.2N	141.0E	30	126	179	322	486			0	0	-5	0		
92062900	10	6.9N	139.9E	30	30	123	246	329			0	0	5	0		
92062912	11	8.7N	137.8E	30	122	248	357	453			0	5	0	0		
92063000	12	10.7N	135.4E	25	84	123	159	169	211	554	5	0	5	0	5	20
92063006	13	11.4N	134.1E	25	64	72	155	238			0	0	0	-5		
92063018	14	13.0N	132.2E	30	47	41	55	134			-5	-5	-10	-15		
92070106	15	14.8N	130.5E	30	24	26	74	224	387		0	-5	-5	0	15	
92070112	16	15.7N	129.6E	35	16	18	132	315	498		0	0	0	10	15	
92070118	17	16.6N	128.8E	35	16	54	216	385			0	0	5	15		
92070200	18	17.7N	128.1E	35	43	140	297	500			0	0	10	15		
92070206	19	19.1N	128.1E	40	34	163	267				0	0	15			
92070212	20	20.3N	128.8E	40	28	55	145				0	5	5			
92070218	21	21.5N	129.7E	40	12	85					0	10				
92070300	22	22.8N	130.5E	35	37	146					0	5				
92070306	23	24.6N	131.4E	30	30						5					
92070312	24	26.5N	132.8E	30	26						0					
AVERAGE					46	107	191	282	282	327	1	2	4	6	13	24
# CASES					24	22	20	18	9	7	24	22	20	18	9	7

TYPHOON ELI (05W)

DTG	WRN NO.	BEST TRACK			00	POSITION ERRORS					00	WIND ERRORS				
		LAT	LONG	WIND		12	24	36	48	72		12	24	36	48	72
92070918	1	13.9N	131.3E	35	5	21	50	89	121	125	-10	-20	-20	-5	-10	5
92071000	2	14.2N	129.5E	45	21	62	104	141	158	178	-10	-15	-25	-5	-10	5
92071006	3	14.6N	127.7E	55	29	75	125	187	205	213	0	-5	0	-15	-10	20
92071012	4	15.1N	125.9E	60	28	69	133	160	155	148	0	-5	-5	-5	0	15
92071018	5	15.5N	124.1E	65	40	86	143	148	161	240	0	10	-5	0	0	5
92071100	6	15.9N	122.3E	75	13	16	22	61	55	50	0	-5	5	5	10	20
92071106	7	16.2N	120.5E	65	16	12	66	86	78	32	10	15	25	20	15	30
92071112	8	16.6N	118.8E	65	16	60	92	94	104	134	0	5	0	-5	-10	5
92071118	9	16.9N	117.2E	65	34	92	130	160	191		0	0	-5	5	-20	
92071200	10	17.2N	115.8E	65	45	82	122	139	153		0	-5	-5	0	5	
92071206	11	17.5N	114.5E	65	37	61	97	132	180		0	-5	5	0	10	
92071212	12	17.9N	113.2E	70	6	18	30	54	83		0	5	0	5	0	
92071218	13	18.4N	111.9E	70	8	22	39	45			0	5	0	5		
92071300	14	19.0N	110.6E	70	28	23	20	48			0	5	5	5		
92071306	15	19.6N	109.3E	55	25	38	53				10	0	15			
92071312	16	20.2N	108.1E	60	13	24	21				0	0	0			
92071318	17	20.9N	106.9E	55	16	24					0	0				
92071400	18	21.7N	105.9E	40	12	29					0	-5				
AVERAGE					22	46	78	111	138	140	2	6	7	5	8	13
# CASES					18	18	16	14	12	8	18	18	16	14	12	8

TROPICAL STORM FAYE (06W)

DTG	WRN NO.	BEST TRACK			00	POSITION ERRORS					00	WIND ERRORS				
		LAT	LONG	WIND		12	24	36	48	72		12	24	36	48	72
92071600	1	18.9N	117.6E	25	23	55	105	161			0	5	5	-10		
92071606	2	19.2N	116.4E	25	26	72	87	143			0	5	0	-20		
92071612	3	19.5N	115.5E	25	60	120	165	188			0	0	-15	-35		
92071618	4	19.7N	114.4E	25	39	96	167				0	-10	-25			
92071700	5	20.2N	113.8E	30	16	45	95	176			0	0	-25	-10		
92071706	6	20.8N	113.8E	35	11	29	56	60			0	-10	-10	-5		
92071712	7	21.3N	113.8E	35	17	24	35				0	-25	-10			
92071718	8	21.8N	113.8E	45	17	18	76				-10	-5	-5			
92071800	9	22.3N	113.8E	55	5	50					-10	0				
92071806	10	23.0N	114.3E	35	22	67					0	0				

TROPICAL STORM FAYE (06W) (CONTINUED)

92071812	11	23.7N	114.9E	30	6						0				
				AVERAGE	23	58	99	146			2	6	12	16	
				# CASES	11	10	8	5			11	10	8	5	

TYPHOON GARY (07W)

DTG	WRN NO.	BEST TRACK			POSITION ERRORS							WIND ERRORS						
		LAT	LONG	WIND	00	12	24	36	48	72	00	12	24	36	48	72		
92071900	1	14.9N	124.8E	25	81	115	181	180			0	0	0	0				
92071906	2	15.3N	123.9E	25	58	97	113	125			0	-5	5	-10				
92071912	3	15.9N	123.2E	25	161	192	233	297	379	547	0	5	5	0	-10 -40			
92071918	4	16.6N	122.7E	30	112	137	184	258	326	483	-5	10	-15	-15	-20 -35			
92072000	5	17.1N	121.9E	25	125	153	190	218	254	341	5	5	-10	-15	-20 -15			
92072006	6	17.3N	120.9E	25	58	58	66	57	82	231	5	-10	-15	-15	-20 -5			
92072012	7	17.5N	119.9E	30	23	39	41	26	46	194	-5	-10	-10	-15	-25 -10			
92072018	8	17.7N	118.9E	35	26	45	49	39	39	217	0	0	0	-10	-20 -5			
92072100	9	18.1N	117.8E	35	24	30	48	70	122		0	0	-5	-10	5			
92072106	10	18.5N	116.7E	40	6	8	30	68	102		0	0	-10	-15	-5			
92072112	11	18.9N	115.6E	40	0	5	46	78	155		0	-5	-15	-10	-10			
92072118	12	19.4N	114.6E	45	8	28	67	138	215		-5	-15	-15	0	-5			
92072200	13	19.9N	113.6E	50	5	49	94	168			0	-10	-5	-5				
92072206	14	20.2N	112.5E	60	6	39	74	119			0	-5	5	-5				
92072212	15	20.5N	111.3E	65	13	37	57				0	10	10					
92072218	16	21.1N	110.1E	65	24	48	74				0	15	5					
92072300	17	21.6N	108.9E	50	0	30					0	5						
92072306	18	22.1N	107.7E	35	12	17					0	0						
92072312	19	22.5N	106.5E	30	13						0							
				AVERAGE	40	63	97	132	173	336	1	6	8	9	14	18		
				# CASES	19	18	16	14	10	6	19	18	16	14	10	6		

TROPICAL STORM HELEN (08W)

DTG	WRN NO.	BEST TRACK			POSITION ERRORS							WIND ERRORS						
		LAT	LONG	WIND	00	12	24	36	48	72	00	12	24	36	48	72		
92072600	1	26.5N	157.2E	35	81	180	283	428	556		-10	-5	5	10	15			
92072606	2	27.2N	157.4E	45	12	33	173	325	384		0	10	15	25	25			
92072612	3	27.8N	157.7E	45	12	36	165	209	189		0	10	15	15	10			
92072618	4	28.6N	157.9E	40	10	97	206	224	155		0	0	5	0	0			
92072700	5	30.0N	158.4E	40	16	72	104	60			0	5	5	0				
92072706	6	31.9N	158.8E	40	20	63	92				0	5	0					
92072712	7	33.7N	159.4E	35	11	71	170				0	0	0					
92072718	8	35.3N	160.1E	30	18	51					0	-5						
92072800	9	36.5N	160.8E	30	11	60					0	5						
				AVERAGE	22	74	171	250	321		1	5	6	10	13			
				# CASES	9	9	7	5	4		9	9	7	5	4			

TYPHOON IRVING (09W)

DTG	WRN NO.	BEST TRACK			POSITION ERRORS							WIND ERRORS						
		LAT	LONG	WIND	00	12	24	36	48	72	00	12	24	36	48	72		
92080100	1	22.8N	131.2E	25	86	127	200	288	389	656	0	-5	-5	0	0 -20			
92080106	2	23.3N	131.0E	25	50	80	137	230	359	563	0	-5	-5	-5	-5 20			
92080112	3	23.9N	131.2E	30	56	105	185	285	429	532	0	-5	0	-10	-15 30			
92080118	4	24.5N	131.5E	30	106	173	259	352	477	523	0	-5	-5	-15	-25 35			
92080200	5	25.3N	131.6E	35	58	99	156	248	361	303	0	5	0	-5	-20 35			
92080206	6	26.1N	131.7E	35	6	5	58	154	160	86	0	0	-5	-20	5 20			
92080212	7	26.9N	131.9E	35	8	31	89	145	114		0	-5	-15	-30	5			

TYPHOON IRVING (09W) (CONTINUED)

92080218	8	27.7N	132.1E	40	12	47	128	127	84	0	-10	-25	0	10		
92080300	9	28.5N	132.4E	45	12	76	136	117	99	0	-10	-30	10	15		
92080306	10	29.3N	133.1E	50	21	47	87	140	142	-5	-20	5	15	15		
92080312	11	30.2N	133.7E	60	15	36	210	258		-10	-30	10	15			
92080318	12	31.2N	134.1E	70	24	151	283	321		-20	0	10	10			
92080400	13	32.5N	134.0E	80	30	144	208			-30	5	5				
92080406	14	33.3N	132.3E	45	25	7	111			-5	5	0				
92080412	15	33.8N	130.4E	35	11	39				0	5					
92080418	16	33.9N	129.7E	30	34	105				0	0					
92080500	17	34.1N	128.8E	25	18					0						
AVERAGE					34	80	161	222	262	444	4	7	9	11	12	27
# CASES					17	16	14	12	10	6	17	16	14	12	10	6

TYPHOON JANIS (10W)

DTG	WRN NO.	BEST TRACK			00	POSITION ERRORS					00	WIND ERRORS				
		LAT	LONG	WIND		12	24	36	48	72		12	24	36	48	72
92080300	1	11.1N	145.7E	25	12	48	98	166	219	279	0	0	-5	-5	-15	-25
92080306	2	11.9N	144.6E	30	13	56	119	183	192	268	0	0	-5	-10	-25	-20
92080312	3	12.8N	143.7E	30	18	53	113	161	162	264	0	-10	-15	-20	-35	-20
92080318	4	13.7N	142.7E	35	24	61	110	117	138	252	0	-10	-20	-30	-35	-15
92080400	5	14.7N	141.7E	45	18	17	26	35	22	110	0	0	-5	-20	-15	0
92080406	6	15.8N	140.6E	50	29	53	90	92	63	102	5	-5	-15	-15	-10	0
92080412	7	16.9N	139.6E	60	24	22	39	32	28	97	-5	-15	-25	-20	-10	10
92080418	8	18.0N	138.5E	70	26	36	45	32	37	177	-5	-20	-25	-20	-5	30
92080500	9	18.8N	137.4E	80	20	34	18	21	62	234	-5	-10	0	15	15	35
92080506	10	19.3N	136.1E	95	32	50	82	120	186	372	-10	-10	5	20	20	55
92080512	11	20.0N	135.0E	105	26	50	101	156	239	496	-10	-10	5	20	30	65
92080518	12	20.9N	134.0E	110	16	50	92	158	233	575	0	0	5	15	30	60
92080600	13	21.9N	133.1E	115	18	36	97	180	282	591	0	0	0	5	20	45
92080606	14	22.9N	132.1E	115	13	47	121	220	340	612	0	0	0	15	30	50
92080612	15	24.1N	131.2E	115	5	16	91	214	335	624	10	15	20	25	40	50
92080618	16	25.3N	130.3E	115	8	63	128	222	321		10	15	30	40	45	
92080700	17	26.7N	129.6E	115	18	63	157	257	332		0	5	15	30	30	
92080706	18	28.2N	129.3E	115	12	39	92	130	90		0	10	25	30	35	
92080712	19	29.7N	129.2E	105	24	69	122	173	191		0	10	25	25	25	
92080718	20	31.1N	129.7E	95	26	55	81	69			0	10	15	25		
92080800	21	32.7N	130.4E	85	24	52	107	204			5	20	25	25		
92080806	22	34.1N	131.7E	70	15	38	73				0	5	15			
92080812	23	35.5N	133.3E	60	12	63	88				0	5	10			
92080818	24	36.9N	135.4E	55	24	51					0	10				
92080900	25	38.5N	137.5E	45	30	125					0	5				
92080906	26	40.2N	139.9E	35	27						0					
92080912	27	42.8N	142.8E	35	26						0					
AVERAGE					20	50	91	141	183	337	2	8	13	20	25	32
# CASES					27	25	23	21	19	15	27	25	23	21	19	15

SUPER TYPHOON KENT (11W)

DTG	WRN NO.	BEST TRACK			00	POSITION ERRORS					00	WIND ERRORS				
		LAT	LONG	WIND		12	24	36	48	72		12	24	36	48	72
92080518	1	9.8N	169.4E	30	11	93	130	171	196	287	0	-5	-15	-15	-10	10
92080600	2	10.5N	168.6E	35	26	63	71	75	95	217	0	-10	-20	-15	-10	15
92080606	3	11.5N	167.9E	45	18	56	93	104	90	101	0	-10	-10	-5	5	20
92080612	4	12.1N	166.8E	55	26	72	109	130	96	82	-5	-20	-15	-10	5	15
92080618	5	12.8N	165.7E	65	0	18	48	55	57	108	-5	-10	-15	-10	5	15
92080700	6	13.4N	164.6E	75	16	29	49	103	126	222	-5	5	10	25	35	30
92080706	7	14.0N	163.6E	75	21	23	69	125	156	297	0	0	10	25	35	25

SUPER TYPHOON KENT (11W) (CONTINUED)

92080712	8	14.6N	162.6E	80	12	5	50	54	72	231	-5	-10	-5	5	10	15
92080718	9	15.0N	161.5E	85	6	24	53	62	97	192	-5	0	10	20	20	5
92080800	10	15.5N	160.5E	90	8	46	51	59	85	153	-5	0	10	15	20	0
92080806	11	16.2N	159.6E	90	13	17	29	5	53	139	0	5	15	20	20	0
92080812	12	17.0N	158.9E	90	36	66	91	70	32	63	0	0	0	10	5	-5
92080818	13	17.5N	157.8E	90	38	73	72	71	78	111	-5	0	0	5	-5	-10
92080900	14	18.0N	156.7E	90	16	25	42	72	92	118	-5	-5	0	-5	-10	-10
92080906	15	18.5N	155.4E	90	16	25	74	90	111	222	0	-5	-5	-15	-10	-10
92080912	16	18.9N	154.5E	95	11	46	87	129	171	315	0	5	-5	-15	-15	-5
92080918	17	19.2N	153.6E	95	12	17	26	57	108	267	0	0	-15	-15	-15	0
92081000	18	19.4N	152.8E	95	0	21	29	50	90	275	5	-5	-15	-15	-10	10
92081006	19	19.6N	152.0E	100	6	18	30	53	86	238	0	-15	-15	-15	-10	15
92081012	20	19.9N	151.1E	110	16	22	34	27	30	161	-10	-20	-20	-15	-10	0
92081018	21	20.2N	150.2E	120	8	28	20	31	85	219	-5	5	0	0	5	15
92081100	22	20.5N	149.3E	125	6	12	28	82	162	267	-5	0	0	5	10	20
92081106	23	20.9N	148.4E	125	11	22	50	100	181	272	-5	0	0	10	15	30
92081112	24	21.3N	147.7E	130	13	16	50	123	193	264	-5	0	5	15	20	35
92081118	25	21.7N	147.0E	130	8	33	82	141	203	270	0	0	10	20	25	40
92081200	26	22.1N	146.3E	130	11	34	93	156	179	257	0	5	10	20	25	35
92081206	27	22.5N	145.8E	130	13	61	127	172	191	251	0	10	15	20	25	35
92081212	28	22.8N	145.4E	125	12	44	76	84	97	130	0	5	10	20	25	35
92081218	29	23.2N	145.1E	120	0	20	56	51	66	120	-5	-5	0	5	10	20
92081300	30	23.6N	145.0E	115	17	38	49	43	53	101	0	0	5	10	10	20
92081306	31	24.0N	144.8E	110	12	42	42	26	27	145	0	0	5	15	15	20
92081312	32	24.5N	144.7E	105	5	20	17	60	138	278	-5	-5	5	10	20	35
92081318	33	25.2N	144.5E	100	17	50	108	168	250	424	-5	0	10	15	25	40
92081400	34	25.8N	144.0E	95	17	135	72	143	249	441	0	5	10	15	30	40
92081406	35	26.1N	143.6E	90	16	41	84	187	296	502	0	10	15	15	20	5
92081412	36	26.4N	143.2E	85	6	24	68	135	220	426	0	5	10	25	35	40
92081418	37	26.7N	142.7E	80	11	48	102	175	267	445	0	10	15	25	40	15
92081500	38	27.0N	142.3E	80	18	58	117	187	267	402	0	5	20	30	35	10
92081506	39	27.2N	141.7E	75	5	63	120	197	262	345	0	5	5	15	15	15
92081512	40	27.4N	140.8E	75	28	71	127	173	230	303	0	5	10	15	15	25
92081518	41	27.5N	139.9E	70	16	42	80	120	161	210	0	0	5	5	10	30
92081600	42	27.7N	139.0E	65	27	72	119	171	186	184	0	5	10	15	20	25
92081606	43	27.9N	138.0E	65	16	57	91	99	79	79	0	10	5	0	0	15
92081612	44	28.1N	137.1E	60	16	37	41	20	0	159	0	0	-5	0	10	20
92081618	45	28.3N	136.2E	55	28	49	64	58	46	189	0	0	5	5	5	15
92081700	46	28.7N	135.3E	55	28	57	83	107	145	379	0	-5	-5	0	5	10
92081706	47	29.1N	134.3E	55	21	54	106	139	199		0	5	5	10	10	
92081712	48	29.7N	133.4E	55	13	44	70	121	211		0	5	10	15	15	
92081718	49	30.3N	132.7E	55	23	66	105	175	303		0	10	15	20	15	
92081800	50	31.0N	132.1E	55	13	39	80	144	225		0	10	15	20	15	
92081806	51	31.7N	131.6E	50	23	65	103	175			5	15	20	20		
92081812	52	32.4N	131.2E	45	23	24	53	111			5	10	15	15		
92081818	53	33.2N	131.0E	40	30	38	54				5	10	10			
92081900	54	34.1N	130.9E	35	26	50	90				5	15	10			
92081906	55	35.1N	130.9E	30	41	90					0	5				
92081912	56	36.3N	131.2E	25	43	35					0	0				
92081918	57	37.5N	131.9E	25	48						0					
92082000	58	38.6N	132.8E	25	35						0					

AVERAGE	18	44	72	105	142	237	2	6	9	14	16	19
# CASES	58	56	54	52	50	46	58	56	54	52	50	46

TROPICAL STORM LOIS (12W)

DTG	WRN	BEST TRACK			POSITION ERRORS							WIND ERRORS						
	NO.	LAT	LONG	WIND	00	12	24	36	48	72	00	12	24	36	48	72		
92081506	1	15.8N	129.3E	25	34	97	195	315	423	629	0	-5	-5	0	-5	-5		
92081512	2	16.3N	130.0E	25	45	142	257	349	407	457	0	-5	-5	-5	-5	0		
92081518	3	16.7N	130.7E	30	83	183	280	370	420	480	0	5	10	10	10	20		
92081600	4	17.1N	131.4E	30	37	139	220	297	364	468	5	10	15	20	25	40		
92081606	5	17.3N	132.2E	30	8	67	128	176	225	362	5	5	5	5	10	30		
92081612	6	17.6N	133.0E	30	16	43	80	106	154	329	5	0	5	5	15	30		
92081618	7	18.0N	133.8E	30	24	75	122	157	200	371	5	0	0	5	15	30		
92081700	8	18.4N	134.5E	35	12	12	17	24	52	258	0	0	0	10	20	35		
92081706	9	18.8N	135.2E	35	13	42	94	134	187	367	0	-5	0	10	20	40		
92081712	10	19.4N	135.7E	35	36	96	142	172	213	432	0	-5	5	10	20	40		
92081718	11	20.0N	136.2E	40	62	119	186	231	289	522	-5	-5	5	10	20	40		
92081800	12	20.7N	136.6E	40	58	90	153	225	294	555	0	10	20	30	40	55		
92081806	13	21.4N	137.0E	40	49	95	124	163	231	561	0	10	20	30	45	60		
92081812	14	22.2N	137.4E	35	55	100	116	182	279	622	5	5	10	15	30	40		
92081818	15	23.1N	137.8E	35	69	82	114	167	311	697	5	5	10	20	30	40		
92081900	16	24.1N	138.3E	35	16	43	123	247	410	789	0	0	5	15	20	35		
92081906	17	25.1N	139.0E	35	5	51	150	297	456	817	5	10	20	25	30	20		
92081912	18	26.1N	139.7E	35	17	80	210	359	503		5	10	20	25	30			
92081918	19	27.2N	140.5E	35	16	52	135	205	285		5	10	10	15	15			
92082000	20	28.1N	141.5E	35	32	90	177	271	369		5	10	10	15	15			
92082006	21	29.0N	142.7E	30	24	74	134	219	283		10	10	15	15	10			
92082012	22	30.0N	144.1E	30	26	54	114	132			10	10	15	15				
92082018	23	31.2N	145.7E	30	54	130	180	197			10	15	15	15				
92082100	24	32.7N	147.1E	30	31	72	96				5	10	5					
92082106	25	34.3N	148.4E	25	14	39	18				5	5	-5					
92082112	26	35.9N	149.8E	25	49	147					0	0						
92082118	27	37.3N	151.6E	25	100	212					0	-5						
92082200	28	38.5N	153.7E	25	30						0							
AVERAGE					37	90	143	218	303	513	3	6	9	14	20	33		
# CASES					28	27	25	23	21	17	28	27	25	23	21	17		

TROPICAL STORM MARK (13W)

DTG	WRN	BEST TRACK				POSITION ERRORS						WIND ERRORS					
	NO.	LAT	LONG	WIND	00	12	24	36	48	72	00	12	24	36	48	72	
92081512	1	19.7N	117.5E	25	101	197	289	339			0	-5	-10	-15			
92081600	2	20.6N	117.2E	30	45	81	126	155			-5	-10	-10	-25			
92081606	3	20.8N	116.9E	35	26	60	110	155			5	0	-15	-25			
92081612	4	21.1N	116.9E	40	8	55	83	90	72		0	-5	-15	-25	-20		
92081618	5	21.4N	117.2E	40	13	44	65	65	68		0	-10	-15	-15	-15		
92081700	6	21.6N	117.5E	45	26	53	54	42	42		0	0	5	5	-5		
92081706	7	21.9N	117.6E	50	30	45	68	72	73	105	-5	0	5	15	20	20	
92081712	8	22.1N	117.8E	50	26	36	53	69	82	158	-5	-5	5	20	25	20	
92081718	9	22.4N	117.9E	50	37	61	84	105	121	224	-5	0	10	20	25	30	
92081800	10	22.7N	117.9E	50	8	20	71	140	212	345	0	10	20	25	25	30	
92081806	11	23.1N	117.9E	45	18	42	104	172	229	394	5	15	20	25	25	30	
92081812	12	23.4N	117.8E	45	12	49	122	174	235		0	10	20	20	15		
92081818	13	23.7N	117.6E	40	11	73	147	221	294		5	5	5	5	-5		
92081900	14	23.8N	117.2E	35	22	85	154	216			0	0	0	-5			
92081906	15	23.8N	116.7E	35	13	37	89	129			0	0	0	-5			
92081912	16	23.6N	116.3E	30	11	58	90				-5	0	-5				
92081918	17	23.2N	116.1E	30	24	66					-5	0					
92082000	18	22.9N	115.9E	25	45	45	36				0	0	5				
92082006	19	22.6N	115.8E	25	40	58	115				0	0	5				
92082018	20	22.1N	115.3E	25	8	37					0	5					
92082106	21	21.6N	114.3E	20	6						0						

TROPICAL STORM MARK (13W) (CONTINUED)

AVERAGE	26	61	104	143	143	246	2	4	9	17	18	26
# CASES	21	20	18	15	10	5	21	20	18	15	10	5

TROPICAL STORM NINA (14W)

WRN		BEST TRACK			POSITION ERRORS						WIND ERRORS					
DTG	NO.	LAT	LONG	WIND	00	12	24	36	48	72	00	12	24	36	48	72
92081818	1	27.6N	158.3E	25	23	27	153	288	406	881	0	-10	-20	-15	-15	-5
92081900	2	28.0N	157.8E	30	31	86	132	165	211	493	-5	-5	-5	-5	-5	-10
92081906	3	28.5N	157.2E	35	13	98	200	310	424	799	0	-5	0	-5	-5	-5
92081912	4	29.9N	156.3E	40	7	86	179	309	467		0	0	0	0	-5	
92081918	5	31.6N	155.6E	45	15	50	113	186	333		0	-5	-15	-15	-20	
92082000	6	33.4N	155.4E	45	31	98	180	312			0	-5	-10	-15		
92082006	7	35.1N	155.8E	45	11	25	46	239			0	-5	-10	-15		
92082012	8	36.7N	156.9E	45	0	23	45				-5	0	-10			
92082018	9	38.1N	158.5E	45	15	18	83				-5	-10	-20			
92082100	10	39.2N	161.0E	40	30	119	268				0	-10	-15			
92082106	11	39.8N	164.0E	40	5	95					-5	-15				
92082112	12	39.8N	168.2E	40	17	79					-10	-15				
92082118	13	39.8N	172.4E	40	5						-15					
AVERAGE					16	67	140	259	369	725	3	7	11	10	10	7
# CASES					13	12	10	7	5	3	13	12	10	7	5	3

SUPER TYPHOON OMAR (15W)

WRN		BEST TRACK			POSITION ERRORS						WIND ERRORS					
DTG	NO.	LAT	LONG	WIND	00	12	24	36	48	72	00	12	24	36	48	72
92082406	1	8.3N	156.5E	25	30	17	24	34	77	231	0	-5	-10	-5	0	5
92082412	2	8.6N	155.4E	30	24	17	24	29	63	186	-5	-10	-5	-5	5	5
92082418	3	8.9N	154.3E	35	18	25	18	8	59	153	-5	-10	-5	0	5	5
92082500	4	9.2N	153.2E	40	5	6	33	88	176	289	-5	0	0	10	10	10
92082506	5	9.6N	152.2E	45	54	89	130	205	290	358	-5	-5	0	5	5	-5
92082512	6	9.9N	151.2E	45	63	101	144	216	294	402	-5	-10	-5	-5	-5	-20
92082518	7	10.2N	150.3E	50	55	95	150	246	304	379	-5	-5	-5	-10	-10	-25
92082600	8	10.6N	149.6E	55	29	85	179	263	282	331	-5	0	-5	0	5	-15
92082606	9	10.8N	148.9E	55	16	68	133	174	193	262	0	5	0	0	-10	-10
92082612	10	11.1N	148.4E	55	5	47	94	114	155	229	0	0	-5	-5	-25	-15
92082618	11	11.4N	148.1E	60	8	59	76	95	147	255	-5	-10	-20	-35	-45	-40
92082700	12	11.8N	148.0E	65	34	36	34	31	34	60	-5	-15	-20	-45	-40	-40
92082706	13	12.2N	147.8E	70	18	39	68	65	66	43	-5	-15	-30	-40	-40	-35
92082712	14	12.5N	147.3E	75	17	11	26	46	69	95	-10	-15	-40	-40	-35	-35
92082718	15	12.8N	146.6E	80	13	35	48	45	66	109	-5	-25	-35	-35	-40	-30
92082800	16	13.1N	145.8E	85	12	8	13	34	48	74	-5	-30	-30	-30	-30	-20
92082806	17	13.4N	145.0E	100	13	34	62	70	79	108	10	0	0	-5	5	10
92082812	18	13.6N	144.2E	115	0	30	62	91	122	207	0	0	0	0	10	20
92082818	19	13.8N	143.4E	115	8	29	62	99	160	203	0	5	-5	5	10	15
92082900	20	14.0N	142.6E	120	8	37	81	127	178	222	5	5	5	10	20	30
92082906	21	14.2N	141.8E	120	13	42	26	124	160	227	10	0	10	15	20	30
92082912	22	14.4N	141.1E	125	24	61	98	120	138	184	5	0	10	15	20	35
92082918	23	14.7N	140.5E	130	30	66	90	122	141	234	0	5	15	15	20	35
92083000	24	15.0N	140.0E	130	0	5	0	18	58	170	0	5	5	5	5	20
92083006	25	15.4N	139.5E	125	13	16	36	65	118	227	5	0	-10	-15	-15	0
92083012	26	15.8N	138.9E	125	17	25	33	24	13	63	-10	-10	-20	-20	-20	0
92083018	27	16.0N	138.3E	120	29	20	13	0	46	82	-5	-15	-10	0	10	40
92083100	28	16.5N	137.6E	120	18	40	62	88	117	126	-5	-10	0	5	15	45
92083106	29	16.9N	136.8E	120	22	8	41	94	141	194	-5	-5	-5	0	10	30
92083112	30	17.3N	136.0E	120	6	17	35	87	127	210	0	0	0	5	15	25
92083118	31	17.8N	135.2E	120	0	25	73	113	147	255	0	5	10	15	25	25
92090100	32	18.4N	134.2E	115	12	45	107	139	185	305	5	5	10	20	30	30

SUPER TYPHOON OMAR (15W) (CONTINUED)

92090106	33	19.1N	133.3E	115	11	17	27	71	161	380	0	0	15	30	30	40
92090112	34	19.8N	132.2E	110	8	20	33	88	195	434	0	5	20	35	35	45
92090118	35	20.5N	131.0E	105	23	91	180	298	441	713	10	5	10	10	10	30
92090200	36	21.2N	129.8E	100	58	39	115	216	342	614	0	0	10	10	10	25
92090206	37	21.7N	128.8E	90	16	37	108	202	302	614	5	10	10	10	20	20
92090212	38	22.1N	127.8E	85	30	44	45	73	115	312	0	10	10	10	20	25
92090218	39	22.3N	126.9E	75	38	73	121	176	229	503	5	5	5	15	20	30
92090300	40	22.4N	126.0E	70	55	98	158	220	310	663	5	5	5	20	15	25
92090306	41	22.5N	125.2E	70	37	63	81	107	166		0	0	10	15	5	
92090312	42	22.5N	124.5E	65	22	28	55	101	176		-5	-10	-5	-5	-5	
92090318	43	22.6N	123.8E	65	20	30	55	117	175		-10	0	0	-5	0	
92090400	44	22.7N	123.1E	60	5	30	97	153	180		-5	5	0	0	5	
92090406	45	23.0N	122.2E	50	5	61	115	148			5	10	0	5		
92090412	46	23.4N	121.3E	45	44	26	11	34			0	-5	-5	0		
92090418	47	23.8N	120.3E	40	13	13	55				5	5	0			
92090500	48	24.2N	119.3E	40	21	108	210				5	-5	0			
92090506	49	24.4N	118.2E	40	48	141					5	0				
92090512	50	24.4N	117.1E	35	36	68					-5	0				

AVERAGE	23	45	74	111	161	268	4	6	9	13	17	24
# CASES	50	50	48	46	44	40	50	50	48	46	44	40

TROPICAL STORM POLLY (16W)

DTG	WRN NO.	BEST TRACK			POSITION ERRORS						WIND ERRORS					
		LAT	LONG	WIND	00	12	24	36	48	72	00	12	24	36	48	72
92082512	1	17.4N	136.9E	25	33	115	199	269	268	166	0	5	5	10	20	40
92082518	2	18.5N	135.7E	25	45	104	162	206	197	50	0	0	-5	5	15	25
92082600	3	19.6N	134.4E	25	78	137	217	227	204	72	0	-5	-5	5	15	30
92082606	4	20.5N	133.0E	30	50	151	176	150	168	338	-5	-10	-5	5	15	0
92082612	5	21.1N	131.4E	35	20	49	43	81	190	375	-5	-5	0	5	0	-20
92082618	6	21.3N	129.6E	40	22	26	48	105	216	414	-10	-5	0	5	-5	-15
92082700	7	21.7N	128.1E	40	90	77	93	144	197	365	-5	-5	0	5	-5	-15
92082706	8	22.0N	127.0E	40	47	81	146	221	300	427	-5	-5	0	0	-10	-10
92082712	9	22.3N	126.2E	40	57	93	182	277	341		-5	-5	0	-5	-15	
92082718	10	22.6N	125.4E	40	75	127	206	253	311		-5	-5	-5	-10	-10	
92082800	11	22.7N	124.6E	40	89	172	242	284	343		0	0	-15	-20	-20	
92082806	12	22.7N	124.1E	40	112	180	230	271	331		0	-10	-15	-15	-15	
92082812	13	22.7N	123.8E	40	94	127	143	211			-5	-15	-20	-20		
92082818	14	22.7N	123.5E	45	66	55	37	102	126		-10	-10	-15	-15	-5	
92082900	15	22.7N	123.2E	45	39	28	80	137	126		-5	-10	-15	-5	-5	
92082906	16	22.8N	122.7E	50	20	31	92	157	215		-10	-5	-5	0	0	
92082912	17	22.9N	122.3E	50	13	36	124	146			-10	-5	5	0		
92082918	18	23.1N	122.0E	45	48	32	79	128			0	5	5	5		
92083000	19	23.4N	122.0E	45	39	32	54				0	10	0			
92083006	20	24.2N	121.6E	40	100	32	40				0	5	5			
92083012	21	24.8N	121.0E	30	52	49					0	-5				

AVERAGE	57	83	130	188	236	276	4	6	6	8	10	19
# CASES	21	21	20	18	15	8	21	21	20	18	15	8

TYPHOON RYAN (17W)

DTG	WRN NO.	BEST TRACK			POSITION ERRORS						WIND ERRORS					
		LAT	LONG	WIND	00	12	24	36	48	72	00	12	24	36	48	72
92090100	1	17.1N	149.6E	35	82	139	191	259	333	499	-10	-10	-20	-20	-20	-25
92090106	2	17.3N	148.6E	40	49	59	172	300	416	633	-5	-10	-5	-5	-5	-15
92090112	3	17.2N	147.8E	45	49	114	225	336	453	657	0	-5	-5	-5	-5	-15
92090118	4	17.3N	147.2E	55	64	88	165	255	335	527	-5	5	5	10	15	15
92090200	5	17.6N	147.0E	60	54	119	185	259	317	468	5	0	0	5	10	15

TYPHOON RYAN (17W) (CONTINUED)

92090206	6	17.9N	147.0E	60	12	59	141	218	279	441	5	5	10	15	15	15
92090212	7	18.2N	147.1E	65	20	18	48	78	126	210	0	-5	-5	0	0	5
92090218	8	18.4N	147.1E	65	18	12	16	24	32	58	0	-5	-5	-25	-35	-50
92090300	9	18.6N	147.1E	70	17	11	16	42	53	96	-5	-5	-5	-20	-25	-45
92090306	10	18.8N	147.1E	70	5	16	39	62	72	78	-5	-5	-10	-20	-30	-50
92090312	11	18.9N	147.1E	75	8	20	37	45	47	108	-5	-5	-10	-5	-10	-25
92090318	12	19.1N	147.0E	75	13	32	53	84	139	367	0	-5	-5	-10	-15	-25
92090400	13	19.2N	146.9E	80	5	12	16	39	110	318	-5	-10	-5	-10	-20	-30
92090406	14	19.3N	146.8E	85	12	23	34	73	170	374	-10	0	0	0	-10	-20
92090412	15	19.4N	146.8E	90	20	30	50	115	228	431	-5	0	0	-5	-5	-5
92090418	16	19.5N	146.7E	90	21	24	66	154	261	385	-5	-5	-10	-20	-25	-20
92090500	17	19.7N	146.7E	90	18	30	96	203	306	402	-5	-5	-15	-20	-30	-15
92090506	18	19.8N	146.7E	95	11	39	124	235	333	438	-5	-10	-20	-20	-30	-5
92090512	19	20.1N	146.8E	95	6	63	162	268	343	407	-10	-15	-20	-25	-25	0
92090518	20	20.6N	147.0E	100	16	73	167	263	327	326	-10	-20	-20	-25	-20	5
92090600	21	21.4N	147.3E	105	32	92	162	207	226	145	-15	-20	-25	-25	-15	5
92090606	22	22.3N	147.6E	110	32	45	97	117	93	89	-10	-20	-25	-20	-5	5
92090612	23	23.2N	148.1E	110	12	60	86	75	34	121	-5	-10	-10	-10	0	5
92090618	24	24.1N	148.6E	110	24	64	70	32	53	214	-5	-15	-10	0	5	5
92090700	25	24.8N	149.2E	115	40	50	16	59	157	256	-15	-10	-5	5	5	10
92090706	26	25.4N	149.6E	115	0	16	70	150	229	309	-15	-5	5	10	5	10
92090712	27	25.9N	149.9E	110	12	68	159	266	345	388	-10	-5	5	5	5	10
92090718	28	26.4N	150.0E	105	13	17	79	159	242	362	-5	0	5	5	5	5
92090800	29	26.9N	149.8E	100	16	48	105	142	163	307	-5	5	5	10	10	10
92090806	30	27.4N	149.4E	90	12	53	99	127	158	403	5	10	5	5	5	5
92090812	31	27.8N	148.8E	85	8	36	76	113	182	590	5	10	10	10	10	10
92090818	32	28.2N	148.0E	80	7	31	65	115	198		5	0	0	0	0	
92090900	33	28.6N	147.2E	80	13	24	54	128	250		0	0	0	0	5	
92090906	34	29.2N	146.4E	80	7	19	54	126	302		-5	0	0	0	-5	
92090912	35	29.8N	145.6E	75	5	17	67	171	388		-5	-5	-5	-5	-5	
92090918	36	30.5N	145.0E	75	19	27	77	259			-10	-10	-5	-5		
92091000	37	31.4N	144.6E	70	11	60	164	381			-5	-5	0	0		
92091006	38	32.5N	144.3E	70	30	63	167				-5	0	0			
92091012	39	33.8N	144.3E	65	20	50	73				5	10	5			
92091018	40	35.2N	144.8E	60	20	83					10	10				
92091100	41	37.1N	145.8E	55	41	98					5	5				
92091106	42	39.6N	147.0E	55	34						0					
92091112	43	42.6N	148.1E	50	37						5					

AVERAGE	22	49	96	161	220	336	6	7	8	10	12	15
# CASES	43	41	39	37	35	31	43	41	39	37	35	31

TYPHOON SIBYL (18W)

DTG	WRN NO.	BEST TRACK			POSITION ERRORS						WIND ERRORS					
		LAT	LONG	WIND	00	12	24	36	48	72	00	12	24	36	48	72
92090706	1	20.7N	166.4E	30	36	75	144	207								
92090712	2	20.4N	166.5E	35	61	113	166	188	187	265	-10	-10	-15	-30	-40	-45
92090718	3	20.0N	166.7E	40	34	33	37	56	82	303	-5	-10	-15	-25	-35	-40
92090800	4	19.6N	166.8E	45	16	47	45	52	45	236	0	0	-10	-15	-20	-15
92090806	5	19.2N	167.0E	50	16	33	51	39	113	283	-5	-5	-10	-15	-5	-20
92090812	6	18.8N	167.2E	55	20	36	43	64	180	344	-5	-10	-10	-10	-5	-25
92090818	7	18.7N	167.5E	60	13	37	47	137	236	399	-5	-10	-10	-5	-10	-30
92090900	8	18.9N	167.7E	70	11	28	82	162	246	395	0	0	5	10	5	-10
92090906	9	19.2N	167.6E	75	18	60	157	249	316	371	0	0	5	5	-5	-5
92090912	10	19.7N	167.6E	80	42	108	217	277	328	380	-5	0	5	5	-10	0
92090918	11	20.2N	167.6E	85	18	88	175	251	309	329	0	5	5	-5	-15	5
92091000	12	21.2N	167.5E	85	13	118	208	266	302	273	0	5	5	-10	-10	10
92091006	13	22.5N	166.5E	85	24	54	114	156	191	195	0	0	-10	-20	-10	10

TYPHOON SIBYL (18W) (CONTINUED)

92091012	14	23.3N	165.0E	85	8	52	62	66	120	265	0	0	-15	-15	-5	10
92091018	15	23.9N	163.5E	90	11	30	42	72	144	276	-5	-10	-20	-10	-5	10
92091100	16	24.3N	162.0E	90	16	45	60	99	188	316	-5	-15	-15	-5	5	15
92091106	17	24.8N	160.6E	100	8	34	31	98	172	285	-10	-20	-10	0	10	20
92091112	18	25.5N	159.3E	105	8	36	73	106	160	380	-5	5	20	35	30	40
92091118	19	26.3N	158.1E	110	13	18	48	102	145	295	5	25	35	45	40	45
92091200	20	27.1N	157.0E	105	5	26	111	158	201	277	20	30	45	45	50	50
92091206	21	28.1N	156.0E	100	13	70	133	188	231	247	20	30	40	45	55	55
92091212	22	29.0N	155.2E	95	13	72	112	154	222	285	15	20	15	15	10	20
92091218	23	29.7N	154.7E	90	7	16	76	128	202	290	10	15	10	15	10	5
92091300	24	30.4N	154.3E	80	11	39	88	156	204		10	5	10	5	5	
92091306	25	31.2N	154.1E	75	6	40	84	149	200		10	5	10	5	5	
92091312	26	32.1N	154.2E	75	5	39	90	108	128		5	10	5	10	5	
92091318	27	33.0N	154.6E	70	16	53	96	109	140		0	5	5	10	5	
92091400	28	33.9N	155.1E	60	18	37	61	77			0	-10	-5	0		
92091406	29	34.7N	155.8E	55	15	35	103	128			0	5	10	5		
92091412	30	35.6N	156.9E	55	22	81	132				0	10	10			
92091418	31	36.7N	158.0E	50	60	129	146				5	10	5			
92091500	32	37.8N	159.1E	45	26	37					0	-5				

AVERAGE	19	54	98	138	192	304	5	10	13	16	16	22
# CASES	32	32	31	29	26	22	32	32	31	29	26	22

TYPHOON TED (19W)

DTG	WRN NO.	BEST TRACK			POSITION ERRORS						WIND ERRORS					
		LAT	LONG	WIND	00	12	24	36	48	72	00	12	24	36	48	72
92091800	1	15.1N	137.9E	25	16	58	124	160	154	189	0	0	-5	0	10	10
92091806	2	15.5N	136.3E	30	44	110	175	196	193	166	0	0	0	10	15	15
92091812	3	15.7N	134.7E	30	29	75	111	90	97	58	0	0	0	10	10	15
92091818	4	15.8N	132.9E	35	11	8	34	80	86	298	0	-5	5	10	5	10
92091900	5	16.0N	131.1E	40	21	31	85	126	177	271	0	0	5	5	10	10
92091906	6	16.2N	129.6E	45	24	75	123	147	232	552	-5	0	0	-10	0	15
92091912	7	16.5N	128.3E	45	64	161	214	250	367	655	10	20	5	5		25
92091918	8	17.1N	127.1E	45	12	25	102	160	168	175	0	5	10	25	30	65
92092000	9	17.9N	126.1E	45	41	79	159	191	139	196	0	0	10	25	30	65
92092006	10	18.2N	125.1E	50	21	108	189	183	86	117	0	0	10	20	30	45
92092012	11	18.4N	124.1E	55	21	66	136	90	32	196	0	0	10	20	30	40
92092018	12	18.5N	122.9E	60	18	66	120	150	173	330	0	5	5	25	35	40
92092100	13	18.7N	122.2E	60	41	95	150	168	225	439	0	5	5	30	35	45
92092106	14	19.0N	121.9E	60	34	143	293	416	541	869	0	0	10	30	40	45
92092112	15	19.4N	121.8E	60	26	147	282	378	482	731	5	0	15	30	40	45
92092118	16	20.5N	121.9E	65	54	174	276	378	498		5	10	25	25	25	
92092200	17	22.0N	121.9E	65	60	152	230	322	452		0	5	0	5	5	
92092206	18	23.5N	121.6E	60	18	52	97	142	205		0	0	5	5	5	
92092212	19	24.9N	121.2E	55	12	58	88	135	103		0	0	5	10	5	
92092218	20	26.2N	120.9E	50	28	52	87	139			-5	0	0	0		
92092300	21	27.5N	120.8E	50	22	38	65	23			0	0	5	0		
92092306	22	29.0N	120.7E	45	12	58	79				0	0	5			
92092312	23	30.4N	120.8E	45	50	141	181				5	5	5			
92092318	24	32.0N	121.2E	45	23	50					0	5				
92092400	25	33.7N	122.0E	40	12	86					0	0				
92092406	26	35.2N	124.0E	40	35						0					
92092412	27	35.7N	127.0E	40	6						-10					

AVERAGE	28	85	148	187	233	350	2	3	6	14	20	33
# CASES	27	25	23	21	19	15	27	25	23	21	19	15

TROPICAL STORM VAL (20W)

DTG	WRN	BEST TRACK			POSITION ERRORS						WIND ERRORS					
	NO.	LAT	LONG	WIND	00	12	24	36	48	72	00	12	24	36	48	72
92092300	1	12.8N	159.6E	25	11	67	146	264			-5	0	0	0		
92092312	2	14.4N	158.4E	25	53	87	150	243			0	0	-5	-5		
92092400	3	16.2N	157.4E	25	37	114	195	263			0	-5	-10	-15		
92092412	4	18.2N	157.1E	30	71	124	237	351	485		5	0	-5	-10	0	
92092418	5	19.2N	156.9E	35	128	227	350	439	567		0	-5	-10	-10	5	
92092500	6	20.2N	156.5E	35	54	114	180	302	495		0	0	-5	5	20	
92092506	7	21.6N	155.7E	40	45	129	181	299	446		0	-5	-5	10	20	
92092512	8	22.9N	154.8E	45	66	117	180	316			-5	-10	0	15		
92092518	9	24.3N	153.8E	50	104	148	247	379			-5	-10	5	15		
92092600	10	25.7N	153.1E	55	42	120	277				-5	0	15			
92092606	11	27.4N	152.4E	55	56	155	311				0	10	10			
92092612	12	29.2N	151.8E	50	26	140					0	5				
92092618	13	31.5N	151.1E	45	51	200					0	0				
92092700	14	33.8N	150.3E	40	7						0					
92092706	15	36.2N	150.4E	40	20						0					
AVERAGE					52	135	224	318	499		2	4	6	9	11	
# CASES					15	13	11	9	4		15	13	11	9	4	

TYPHOON WARD (21W)

DTG	WRN	BEST TRACK			POSITION ERRORS							WIND ERRORS						
	NO.	LAT	LONG	WIND	00	12	24	36	48	72	00	12	24	36	48	72		
92092618	1	14.7N	179.0W	30	23	29	87	196	349	554	0	5	10	10	10	5		
92092700	2	15.1N	180.0W	35	13	42	91	195	307	515	0	0	5	5	0	5		
92092706	3	15.4N	179.1E	35	0	29	107	222	341	513	0	5	0	0	-10	10		
92092712	4	15.8N	178.4E	40	6	34	127	252	375	435	0	5	5	0	-5	10		
92092718	5	16.1N	177.7E	40	31	87	190	313	427	401	5	5	5	-5	0	15		
92092800	6	16.5N	177.2E	45	33	104	201	299	372	276	0	0	-5	-10	0	15		
92092806	7	16.7N	177.0E	50	41	106	186	274	304	174	-5	-5	-15	-10	5	10		
92092812	8	16.9N	177.0E	55	24	66	178	300	372	369	-10	-15	-20	-10	5	10		
92092818	9	17.2N	177.1E	60	30	87	213	318	376	410	-5	-15	-10	0	10	20		
92092900	10	17.6N	177.3E	70	21	116	229	306	330	377	0	-5	5	15	25	15		
92092906	11	18.4N	177.5E	80	18	97	210	295	327	382	-5	-5	10	20	20	10		
92092912	12	19.6N	177.7E	85	42	129	216	281	332	432	0	5	15	25	20	0		
92092918	13	21.1N	177.5E	85	84	153	219	260	315	413	0	10	20	15	20	5		
92093000	14	22.5N	176.9E	85	12	55	110	195	271	316	0	5	5	0	-5	-15		
92093006	15	23.7N	175.9E	80	42	84	129	202	242	162	5	5	0	0	-15	-20		
92093012	16	24.7N	174.9E	80	24	55	101	146	156	170	0	5	-5	-10	-25	-30		
92093018	17	25.4N	173.5E	75	20	69	144	165	195	188	0	-5	-5	-20	-25	-30		
92100100	18	25.7N	172.0E	75	13	62	130	186	219	236	0	-5	-10	-25	-25	-30		
92100106	19	25.7N	170.3E	80	16	69	121	150	171	264	0	5	0	-10	-15	-15		
92100112	20	25.5N	168.6E	80	8	26	69	95	113	169	0	-5	-20	-20	-20	-25		
92100118	21	25.1N	167.0E	80	0	30	65	90	128	202	0	-10	-20	-20	-25	-25		
92100200	22	24.7N	165.5E	85	5	52	106	138	182	255	0	-10	-15	-20	-25	-20		
92100206	23	24.3N	164.2E	90	16	50	104	180	254	331	0	-5	-10	-15	-20	-10		
92100212	24	24.0N	163.0E	95	18	30	90	174	274	409	0	-5	-10	-15	-15	-5		
92100218	25	23.8N	161.9E	95	21	50	124	221	295	458	5	0	-5	-10	-5	5		
92100300	26	23.7N	160.9E	95	13	52	134	228	301	480	0	0	0	0	5	10		
92100306	27	23.9N	160.1E	95	6	21	76	125	175	338	0	0	0	5	0	10		
92100312	28	24.3N	159.6E	95	0	12	49	99	170	418	0	0	5	10	5	15		
92100318	29	24.8N	159.2E	95	16	56	105	146	225		0	0	10	10	10			
92100400	30	25.5N	159.0E	95	12	36	67	119	206		0	5	10	10	10			
92100406	31	26.3N	159.0E	95	5	18	49	90	141		0	5	0	0	0			
92100412	32	27.2N	159.0E	90	16	44	77	128	194		0	5	5	5	5			
92100418	33	28.2N	159.0E	85	12	63	113	144			0	0	0	0				
92100500	34	29.3N	158.9E	80	0	7	30	52			0	0	0	0				

TYPHOON WARD (21W) (CONTINUED)

92100506	35	30.5N	158.8E	80	6	5	58	0	0	0						
92100512	36	31.8N	158.9E	75	11	47	90	0	5	5						
92100518	37	33.2N	159.1E	70	24	43		0	0							
92100600	38	34.8N	159.5E	65	15	24		0	0							
92100606	39	36.5N	160.2E	60	5			0								
92100612	40	38.4N	161.5E	55	15			0								
AVERAGE				18	57	123	194	264	345	1	4	7	10	12	14	
# CASES				40	38	36	34	32	28	40	38	36	34	32	28	

TROPICAL STORM ZACK (22W)

DTG	WRN NO.	BEST TRACK			00	POSITION ERRORS					00	WIND ERRORS				
		LAT	LONG	WIND		12	24	36	48	72		12	24	36	48	72
92100706	1	9.5N	166.9E	25	249	307	325	325	320	106	0	0	15	25	30	50
92100712	2	9.5N	165.8E	30	38	55	58	72	97	323	-5	5	15	20	25	55
92100718	3	9.6N	164.7E	30	42	50	58	91	81	421	0	10	15	20	25	55
92100800	4	9.7N	163.7E	25	41	60	93	124	270	692	5	10	10	15	25	55
92100806	5	9.8N	162.7E	25	50	90	138	216	411	789	0	5	5	5	20	45
92100812	6	9.9N	161.8E	25	21	43	60	153	367	745	0	0	0	5	25	45
92100818	7	9.9N	160.9E	25	13	43	83	274	482	786	0	0	0	10	25	45
92100900	8	9.9N	160.0E	30	34	58	101	297	494	672	0	0	5	20	30	50
92100906	9	9.7N	159.1E	30	67	41	137	331	512	614	5	0	10	20	30	50
92100912	10	9.9N	158.3E	35	29	156	337	520	649	650	0	5	20	25	35	50
92100918	11	10.6N	158.3E	35	71	221	407	571	666	656	0	5	15	25	35	50
92101000	12	11.4N	158.8E	35	76	8	115	237	292	345	0	10	15	25	35	45
92101006	13	12.2N	159.5E	30	37	59	175	278	285	332	5	10	10	15	20	25
92101012	14	13.1N	160.2E	25	37	91	183	185	143	195	10	10	10	10	15	15
92101018	15	14.0N	160.8E	25	59	96	147	135	139	217	10	10	10	10	10	-5
92101100	16	15.0N	161.4E	25	126	216	277	340			0	0	0	0		
92101112	17	17.3N	161.6E	25	189	181	156	186			0	0	0	-5		
92101200	18	18.9N	160.1E	25	202	227					-5	-5				
92101306*	19	22.5N	155.2E	30	88	121	133	160	211	303	0	-10	0	5	10	5
92101312	20	23.3N	154.2E	35	8	59	136	196	231		-5	-10	5	10	10	
92101318	21	24.0N	153.5E	40	29	84	131	191	250		-10	-5	0	10	10	
92101400	22	24.4N	153.2E	40	23	80	165	227	298		-10	0	5	5	5	
92101406	23	24.8N	153.0E	35	21	76	120	186	246		-5	0	5	5	5	
92101412	24	25.2N	152.9E	30	18	45	81	124			0	5	0	0		
92101418	25	25.6N	152.9E	30	34	86	142	231			0	0	0	0		
92101500	26	26.0N	152.9E	25	32	35					0	0				
92101506	27	26.4N	152.9E	25	40	52					0	-5				
AVERAGE				62	98	157	236	323	491	3	4	7	12	21	40	
# CASES				27	27	24	24	20	16	27	27	24	24	20	16	

* Regenerated Warning

SUPER TYPHOON YVETTE (23W)

DTG	WRN NO.	BEST TRACK			00	POSITION ERRORS					00	WIND ERRORS				
		LAT	LONG	WIND		12	24	36	48	72		12	24	36	48	72
92100800	1	15.4N	131.1E	30	62	116	166	224	309	533	-5	-5	-5	-5	-20	-55
92100806	2	15.3N	130.3E	35	35	70	99	138	225	408	-5	0	0	-5	-15	-55
92100812	3	15.2N	129.5E	40	36	58	79	156	266	472	0	0	0	-15	-35	-50
92100818	4	15.1N	128.7E	45	25	34	63	136	226	461	10	10	5	0	-20	-25
92100900	5	15.0N	127.9E	50	16	16	66	139	226	437	10	15	10	0	-15	-20
92100906	6	15.0N	127.1E	55	13	41	117	205	314	519	5	0	-5	-15	-25	-20
92100912	7	15.0N	126.3E	60	18	92	186	279	371	580	0	-10	-15	-25	-45	-25
92100918	8	15.0N	126.0E	70	41	116	193	296	406	615	-5	-15	-25	-35	-40	-30
92101000	9	15.1N	125.8E	80	8	21	49	93	150	274	-5	-10	-20	0	15	-5
92101006	10	15.3N	125.8E	90	16	36	81	132	189	313	-5	-15	-10	10	15	-15

SUPER TYPHOON YVETTE (23W) (CONTINUED)

92101012	11	15.5N	125.8E	100	6	39	70	130	190	309	0	0	15	25	20	-25
92101018	12	15.7N	125.8E	115	6	47	83	125	176	250	0	10	20	25	15	-30
92101100	13	15.8N	126.0E	125	8	39	90	158	220	330	5	20	25	20	5	-30
92101106	14	15.9N	126.2E	125	24	68	114	171	246	352	10	25	25	15	-5	-25
92101112	15	16.0N	126.4E	120	6	23	57	103	148	153	15	25	20	-5	-40	-55
92101118	16	16.2N	126.8E	115	0	23	42	80	87	96	15	5	-15	-45	-65	-75
92101200	17	16.4N	127.2E	110	8	26	54	95	114	262	10	0	-25	-60	-75	-75
92101206	18	16.7N	127.5E	110	8	12	33	49	58	230	0	-10	-35	-65	-70	-70
92101212	19	17.0N	127.8E	110	8	11	18	18	26	116	5	-15	-45	-55	-60	-60
92101218	20	17.3N	128.2E	115	0	11	12	18	32	153	0	-25	-50	-50	-60	-55
92101300	21	17.7N	128.6E	125	6	24	53	58	60	211	0	-20	-35	-40	-45	-35
92101306	22	18.2N	129.0E	135	13	26	53	56	74	257	-5	-20	-30	-40	-40	-25
92101312	23	18.7N	129.3E	150	6	22	30	13	72	243	-10	-5	0	-5	-10	0
92101318	24	19.2N	129.4E	155	6	16	16	56	131	294	-10	-5	-10	-10	-10	15
92101400	25	19.7N	129.4E	155	8	11	63	142	218	390	0	10	0	-5	-5	35
92101406	26	20.2N	129.6E	150	6	40	114	195	292	441	5	10	0	0	5	45
92101412	27	20.8N	130.0E	150	11	53	118	203	306	431	5	10	5	5	15	55
92101418	28	21.5N	130.5E	150	13	55	126	219	320	404	0	5	0	5	20	45
92101500	29	22.1N	131.2E	145	13	18	50	140	178		5	10	5	15	35	
92101506	30	22.7N	132.1E	140	8	49	126	208	200		5	15	15	30	45	
92101512	31	23.4N	133.1E	135	16	65	129	157	166		5	5	15	35	45	
92101518	32	24.1N	134.1E	130	5	38	76	89	127		5	10	25	40	45	
92101600	33	25.0N	135.2E	125	8	32	41	28			5	20	40	50		
92101606	34	26.1N	136.4E	115	17	48	134	248			5	20	35	45		
92101612	35	27.0N	137.7E	105	10	60	138				5	20	25			
92101618	36	28.0N	139.0E	90	22	73	147				10	25	30			
92101700	37	28.8N	140.1E	75	5	18					-5	-5				
92101706	38	29.5N	141.3E	65	0	33					0	5				
92101712	39	30.0N	142.6E	55	15						0					
92101718	40	30.3N	144.2E	45	27						5					

AVERAGE	14	42	86	135	192	341	5	11	18	24	31	38
# CASES	40	38	36	34	32	28	40	38	36	34	32	28

TYPHOON ANGELA (24W)

DTG	WRN NO.	BEST TRACK			00	POSITION ERRORS					WIND ERRORS					
		LAT	LONG	WIND		12	24	36	48	72	00	12	24	36	48	72
92101600	1	13.7N	118.6E	30	0	18	40	101			-5	-5	-5	-20		
92101612	2	13.9N	118.5E	30	11	18	61	107	155	190	0	-5	-20	-25	-35	-45
92101618	3	14.0N	118.3E	30	30	71	114	158	200	200	0	-15	-20	-30	-35	-40
92101700	4	13.9N	118.0E	35	38	58	111	149	179	217	0	-10	-15	-20	-30	-15
92101706	5	13.7N	117.8E	45	8	48	79	168	218	219	-5	-5	-10	-15	-25	5
92101712	6	13.4N	117.5E	50	8	8	41	72	85	54	5	5	0	-10	-10	10
92101718	7	13.2N	117.1E	55	5	21	46	55	54	21	0	0	-5	-15	-5	15
92101800	8	12.9N	116.7E	60	16	13	18	16	11	71	5	5	0	0	10	25
92101806	9	12.6N	116.3E	65	21	13	11	8	24	96	5	5	-5	5	15	25
92101812	10	12.3N	115.8E	70	5	30	32	8	0	71	0	-5	-5	10	25	30
92101818	11	12.1N	115.3E	75	17	34	26	17	11	60	-5	-15	-5	10	20	20
92101900	12	12.0N	114.8E	85	13	34	81	121	185	306	0	5	30	45	50	-15
92101906	13	12.0N	114.2E	90	29	64	104	162	226	313	0	15	35	50	40	-25
92101912	14	12.1N	113.8E	90	18	40	67	119	168	200	0	10	25	20	15	-15
92101918	15	12.3N	113.4E	85	24	46	78	107	140	131	5	10	15	5	0	-10
92102000	16	12.5N	113.1E	80	41	78	117	146	174	136	0	10	5	0	-20	-15
92102006	17	12.6N	112.8E	75	37	72	118	152	157	71	0	5	-5	-5	-20	-15
92102012	18	12.7N	112.6E	65	16	34	66	77	72	105	0	0	0	-5	5	10
92102018	19	12.9N	112.5E	60	24	55	85	90	47	105	0	0	0	-5	10	15
92102100	20	13.1N	112.5E	60	8	16	21	13	41	144	0	5	0	10	10	25
92102106	21	13.4N	112.4E	60	18	26	24	69	128	246	0	5	0	15	10	25

TYPHOON ANGELA (24W) (CONTINUED)

92102112	22	13.6N	112.3E	55	18	18	35	87	169	278	0	0	10	10	15	30
92102118	23	13.7N	112.2E	55	5	11	62	131	211	305	0	0	10	10	20	25
92102200	24	13.8N	112.0E	55	6	24	82	159	235	295	0	10	10	15	25	25
92102206	25	13.8N	111.8E	55	5	58	123	202	259	307	0	10	10	20	25	25
92102212	26	13.8N	111.2E	45	24	81	157	244	282	324	0	5	10	20	25	20
92102218	27	13.8N	110.5E	40	6	35	120	176	229		0	0	10	10	10	
92102300	28	13.8N	109.8E	40	8	64	129	152	184		0	5	15	15	10	
92102306	29	13.7N	109.0E	40	18	53	80	115			0	5	5	5		
92102312	30	13.6N	108.1E	35	35	87	113				0	10	5			
92102318	31	13.3N	107.2E	25	44	85					5	0				
92102706*	32	8.4N	102.3E	30	45	72	126	151	150		0	-10	-20	10	35	
92102712	33	8.4N	101.9E	40	26	83	122	145	163		-10	-20	-10	10	25	
92102718	34	8.6N	101.5E	45	8	32	68	107			10	5	30	45		
92102800	35	8.9N	101.4E	55	11	46	72	120			0	15	35	50		
92102806	36	9.2N	101.5E	60	5	37	77				5	30	45			
92102812	37	9.4N	101.7E	50	18	61	124				0	10	15			
92102818	38	9.5N	101.9E	40	36	96					0	10				
92102900	39	9.5N	102.2E	35	34	65					0	5				
92102906	40	9.5N	102.5E	30	48						0					
92102912	41	9.5N	102.9E	25	8						0					

AVERAGE	20	47	79	113	144	179	2	7	12	16	20	21
# CASES	41	39	36	33	29	25	41	39	36	33	29	25

* Regenerated Warning

TYPHOON BRIAN (25W)

WRN		BEST TRACK				POSITION ERRORS					WIND ERRORS					
DTG	NO.	LAT	LONG	WIND	00	12	24	36	48	72	00	12	24	36	48	72
92101700	1	10.5N	159.7E	25	11	13	24	37	63	186	0	0	0	5	10	25
92101706	2	10.6N	158.4E	30	8	18	31	52	95	187	-5	-5	-5	0	5	25
92101712	3	10.7N	157.2E	30	24	21	23	30	43	120	0	-5	-5	-5	0	15
92101718	4	10.8N	156.0E	35	36	26	35	47	50	92	0	0	5	10	25	45
92101800	5	10.9N	154.8E	40	5	11	26	63	105	121	0	5	10	15	30	45
92101806	6	11.0N	153.6E	45	6	13	54	92	138	172	0	5	10	25	40	55
92101812	7	11.1N	152.4E	45	6	21	65	114	169	226	5	10	15	30	40	55
92101818	8	11.3N	151.3E	50	6	26	55	96	127	128	5	10	20	35	45	55
92101900	9	11.5N	150.3E	50	13	41	73	116	133	138	10	15	30	40	50	55
92101906	10	11.6N	149.5E	55	35	79	124	163	177	172	10	25	40	50	55	50
92101912	11	11.8N	148.7E	55	54	90	122	144	139	150	25	40	55	60	65	40
92101918	12	11.9N	147.9E	55	5	26	29	55	81	165	35	50	55	60	65	40
92102000	13	12.0N	147.2E	55	48	46	24	23	72	180	35	40	45	55	50	40
92102006	14	12.2N	146.6E	55	13	18	18	34	92	196	30	35	40	45	40	25
92102012	15	12.4N	146.0E	60	6	17	33	75	128	237	30	35	45	40	30	30
92102018	16	12.8N	145.4E	60	8	24	55	120	167	306	35	40	45	35	25	35
92102100	17	13.3N	144.8E	65	8	26	83	142	178	347	25	35	30	20	20	40
92102106	18	13.8N	144.2E	65	5	36	95	152	191	325	25	20	15	5	15	45
92102112	19	14.5N	143.5E	65	16	58	103	136	176	334	25	20	5	5	20	55
92102118	20	15.2N	142.8E	70	26	69	106	139	213	450	20	15	0	5	25	50
92102200	21	16.2N	142.1E	75	21	23	47	85	143	440	15	5	0	0	0	10
92102206	22	17.2N	141.5E	80	5	34	71	128	172		10	0	0	-5	0	
92102212	23	18.1N	140.9E	90	25	71	106	147	97		0	0	5	5	10	
92102218	24	19.0N	140.3E	95	6	53	87	109	24		5	0	10	15	20	
92102300	25	19.9N	139.7E	95	20	44	103	212	492		0	-10	-15	-10	-5	
92102306	26	20.9N	139.2E	95	41	86	146	326			-10	-10	-10	-5		
92102312	27	22.0N	138.7E	90	53	93	127	281			-10	-5	-5	-5		
92102318	28	23.3N	138.2E	85	30	110	360				-10	0	5			
92102400	29	24.7N	137.9E	75	72	221	421				-5	0	0			
92102406	30	26.3N	138.3E	65	40	166					-5	0				

TYPHOON BRIAN (25W) (CONTINUED)

92102412	31	28.2N	139.5E	55	65	137						0	5						
92102418	32	30.5N	141.7E	45	54							5							
92102500	33	32.1N	145.3E	40	10							0							
AVERAGE						24	56	92	116	139	223	12	14	18	22	28	40		
# CASES						33	31	29	27	25	21	33	31	29	27	25	21		

TYPHOON COLLEEN (26W)

DTG	WRN	BEST TRACK				POSITION ERRORS						WIND ERRORS					
	NO.	LAT	LONG	WIND	00	12	24	36	48	72	00	12	24	36	48	72	
92101800	1	11.3N	132.3E	25	30	65	97	120	171	288	0	-10	-15	-20	-20	-15	
92101806	2	11.8N	131.6E	35	11	25	68	121	205	353	-5	-10	-15	-20	-25	-10	
92101812	3	12.2N	131.0E	40	18	29	73	157	239	393	-5	-10	-15	-20	-20	0	
92101818	4	12.7N	130.4E	45	30	54	123	228	337	524	-5	-5	-5	-10	0	25	
92101900	5	13.0N	130.1E	50	13	54	132	245	338	494	-10	-10	-10	-10	5	25	
92101906	6	13.4N	129.9E	55	29	82	174	266	370	534	-5	0	-5	5	15	20	
92101912	7	13.7N	129.7E	60	26	93	163	248	319	384	0	-5	-5	10	20	20	
92101918	8	14.1N	129.7E	65	53	139	215	293	355	389	-5	0	15	25	30	35	
92102000	9	14.3N	129.9E	70	82	158	222	293	349	405	-5	-10	0	15	15	20	
92102006	10	14.4N	130.2E	80	48	107	165	217	254	275	-15	-15	0	15	15	25	
92102012	11	14.3N	130.4E	80	24	46	83	135	188	222	-15	-10	-5	-5	-5	5	
92102018	12	14.1N	130.6E	80	11	46	83	132	181	215	-15	-10	-5	-5	0	10	
92102100	13	13.8N	130.7E	75	13	18	89	169	262	388	-5	0	0	0	0	5	
92102106	14	13.6N	130.8E	75	13	47	89	167	252	387	-5	0	0	5	5	5	
92102112	15	13.4N	130.9E	70	12	53	88	129	174	392	0	0	0	5	5	0	
92102118	16	13.2N	130.8E	70	32	56	80	107	140	387	0	0	5	5	10	0	
92102200	17	13.0N	130.7E	70	8	24	70	113	184	426	0	0	5	5	10	-5	
92102206	18	13.0N	130.6E	70	13	50	93	130	223	486	0	5	10	10	10	-5	
92102212	19	13.0N	130.4E	70	25	58	107	171	267	573	0	5	10	10	5	0	
92102218	20	13.1N	130.2E	65	37	79	114	187	279	656	5	20	25	20	10	10	
92102300	21	13.4N	130.1E	65	13	37	62	90	180	547	15	20	25	15	5	10	
92102306	22	13.7N	130.0E	60	18	54	66	96	250	608	20	25	25	15	5	15	
92102312	23	14.1N	130.3E	60	33	39	66	191	374	761	20	25	15	5	0	5	
92102318	24	14.6N	130.4E	55	96	116	99	122	222	519	20	15	5	-5	-5	-15	
92102400	25	15.0N	130.1E	55	13	55	218	392	568	929	15	5	0	-5	0	-20	
92102406	26	15.5N	129.6E	55	8	93	257	428	593	949	10	0	-10	-10	0	-30	
92102412	27	15.7N	129.0E	60	36	174	337	505	663	993	0	-10	-15	-5	-10	-25	
92102418	28	15.6N	128.1E	60	78	236	392	547	714	1014	-5	-10	-10	0	-20	-25	
92102500	29	15.2N	126.7E	65	25	102	200	311	406	503	0	0	10	15	0	-5	
92102506	30	15.0N	125.3E	65	42	111	198	287	363	458	0	5	20	0	-20	10	
92102512	31	15.0N	123.9E	65	8	41	95	159	223	263	5	20	10	-5	0	35	
92102518	32	14.8N	122.4E	60	26	52	116	178	210	290	15	15	5	0	10	50	
92102600	33	14.6N	120.9E	55	26	33	64	105	134	208	0	0	-10	-5	5	15	
92102606	34	14.5N	119.4E	50	21	35	79	116	138		0	-20	-30	-15	5		
92102612	35	14.3N	117.9E	55	24	75	110	127	157		-5	-15	-5	5	25		
92102618	36	14.0N	116.4E	65	24	60	93	121	177		0	0	10	15	20		
92102700	37	13.5N	114.9E	70	18	33	101	160	177		0	5	5	-5	5		
92102706	38	13.5N	113.4E	75	21	70	135	156			0	10	5	5			
92102712	39	13.7N	111.9E	70	13	45	88	98			0	0	-5	0			
92102718	40	13.9N	110.6E	65	16	48	61				-5	-5	0				
92102800	41	14.3N	109.4E	60	32	53	54				0	5	5				
92102806	42	14.7N	108.2E	50	26	64					0	5					
92102812	43	14.8N	106.8E	40	5	55					0	0					
92102818	44	14.8N	105.5E	30	5						0						
AVERAGE					27	69	128	201	288	492	5	8	9	9	10	15	
# CASES					44	43	41	39	37	33	44	43	41	39	37	33	

TYPHOON DAN (27W)

DTG	WRN NO.	BEST TRACK			00	POSITION ERRORS					00	WIND ERRORS				
		LAT	LONG	WIND		12	24	36	48	72		12	24	36	48	72
92102418	1	10.7N	177.6W	25	25	89	173	200	234	377	0	0	-5	-10	-10	-25
92102500	2	11.0N	178.7W	30	21	117	174	210	259	391	0	0	0	-5	-5	-25
92102506	3	11.7N	179.5W	30	56	143	180	231	273	393	0	0	-5	-5	-10	-20
92102512	4	12.6N	179.7E	35	17	51	107	170	225	373	5	5	-5	-10	-20	-10
92102518	5	13.3N	178.7E	40	24	75	154	205	231	330	0	-5	-5	-15	-25	-5
92102600	6	13.7N	177.5E	45	29	70	112	108	100	108	0	-5	-5	-15	-20	0
92102606	7	14.2N	176.0E	55	26	76	81	47	22	83	-5	-5	-5	-10	-5	0
92102612	8	14.7N	174.3E	60	13	35	12	8	48	68	-5	-5	-15	-20	5	0
92102618	9	15.2N	172.6E	65	13	5	24	55	87	149	0	-5	-10	-5	5	5
92102700	10	15.7N	171.1E	70	0	31	74	117	169	192	0	-15	-20	5	5	5
92102706	11	16.4N	169.9E	80	17	75	129	197	285	329	-5	-15	-10	5	10	10
92102712	12	17.1N	168.9E	90	20	54	99	155	220	248	-5	-15	5	15	20	15
92102718	13	17.8N	168.0E	100	13	42	82	143	182	180	-5	-5	15	20	25	20
92102800	14	18.6N	167.1E	110	8	34	18	50	108	210	5	25	25	25	25	20
92102806	15	19.5N	166.2E	110	20	35	8	62	174	461	5	10	5	0	-5	-10
92102812	16	20.3N	165.4E	100	5	39	83	130	205	508	10	5	5	-5	-15	-30
92102818	17	21.0N	164.9E	100	12	21	72	151	263	535	5	5	5	-5	-15	-40
92102900	18	21.6N	164.6E	100	5	77	161	250	357	533	0	0	0	-10	-20	-45
92102906	19	22.0N	164.5E	95	24	113	199	302	409	553	0	0	0	-5	-20	-55
92102912	20	22.1N	164.3E	95	21	69	152	226	256	193	-10	-20	-25	-30	-35	-80
92102918	21	22.0N	164.1E	90	26	95	187	243	260	156	-10	-15	-20	-30	-40	-80
92103000	22	21.7N	163.6E	90	29	99	172	246	265	163	-10	-20	-25	-30	-50	-75
92103006	23	21.3N	162.8E	85	33	98	178	257	311	224	-10	-15	-25	-35	-60	-75
92103012	24	20.7N	161.7E	85	23	28	84	147	187	168	-15	-15	-25	-40	-65	-70
92103018	25	20.2N	160.5E	80	8	32	37	63	116	342	-5	-5	-15	-40	-50	-40
92103100	26	19.7N	159.2E	80	20	36	28	71	138	519	-5	-5	-25	-45	-45	-30
92103106	27	19.3N	157.8E	80	8	52	107	153	186	648	-5	-10	-35	-45	-45	-20
92103112	28	19.1N	156.2E	80	18	76	139	169	212	730	-5	-20	-35	-35	-35	-5
92103118	29	19.2N	154.5E	85	16	50	96	148	315		-10	-30	-35	-35	-25	
92110100	30	19.6N	152.9E	95	29	53	103	207	455		-20	-35	-30	-30	-15	
92110106	31	20.1N	151.4E	105	42	103	200	390	713		-30	-15	-15	-5	15	
92110112	32	20.8N	150.2E	110	5	24	127	361	640		-5	10	15	25	30	
92110118	33	21.6N	149.3E	110	8	77	235	506			0	0	10	25		
92110200	34	22.4N	148.8E	105	11	115	319	544			-5	0	20	35		
92110206	35	23.1N	148.9E	105	22	142	343				-10	-5	0			
92110212	36	23.9N	149.6E	100	12	64	193				-5	0	5			
92110218	37	24.9N	150.8E	90	24	136					0	5				
92110300	38	26.2N	152.6E	80	28	68					0	5				
92110306	39	27.8N	154.7E	70	30						0					
92110312	40	29.4N	156.9E	60	75						-10					
AVERAGE					21	69	129	192	248	328	6	9	14	20	24	29
# CASES					40	38	36	34	32	28	40	38	36	34	32	28

SUPER TYPHOON ELSIE (28W)

DTG	WRN NO.	BEST TRACK			00	POSITION ERRORS					00	WIND ERRORS				
		LAT	LONG	WIND		12	24	36	48	72		12	24	36	48	72
92102918	1	8.6N	151.1E	30	66	67	41	105	182	230	-5	-10	-15	-15	-10	-5
92103000	2	8.9N	151.0E	35	24	71	149	236	282	242	0	0	-5	-5	0	10
92103006	3	9.0N	150.6E	40	36	116	198	267	245	177	0	-5	-5	0	5	10
92103012	4	9.2N	150.1E	45	24	50	112	174	163	126	0	-5	-5	0	5	15
92103018	5	9.3N	149.5E	50	16	78	143	153	168	150	0	0	5	10	20	20
92103100	6	9.4N	148.9E	55	0	51	85	87	97	201	10	10	15	25	40	35
92103106	7	9.5N	148.2E	60	13	62	86	98	130	113	15	20	25	30	35	30
92103112	8	9.5N	147.6E	65	8	30	40	66	100	107	15	20	25	35	35	20
92103118	9	9.4N	147.0E	65	8	47	50	84	81	66	20	20	25	30	30	10

SUPER TYPHOON ELSIE (28W) (CONTINUED)

92110100	10	9.6N	146.7E	70	23	53	60	85	71	109	15	15	25	25	25	5
92110106	11	10.0N	146.6E	70	18	46	54	36	64	154	15	15	20	20	20	0
92110112	12	10.3N	146.2E	75	18	55	60	118	185	323	10	10	10	15	10	0
92110118	13	10.6N	145.7E	75	23	21	71	141	212	346	10	5	5	10	0	-5
92110200	14	11.0N	145.5E	75	11	36	96	187	289	480	10	5	0	0	-5	-10
92110206	15	11.5N	145.5E	80	5	46	132	221	332	533	5	0	-5	-10	-15	-30
92110212	16	11.9N	145.1E	85	13	71	151	238	318	425	-5	-10	-20	-30	-25	-30
92110218	17	12.3N	144.5E	90	11	52	96	132	168	197	-10	-15	-30	-35	-30	-25
92110300	18	12.7N	143.8E	95	8	29	72	117	187	384	-5	-10	-15	-10	-15	-5
92110306	19	13.1N	143.0E	100	5	13	18	76	145	378	-5	-15	-10	-5	-10	15
92110312	20	13.5N	142.1E	110	11	52	99	142	195	406	-5	-10	0	-5	-15	5
92110318	21	14.0N	141.2E	120	29	69	120	186	243	518	0	5	5	-10	-10	15
92110400	22	14.4N	140.2E	125	18	39	83	154	251	762	5	15	10	0	0	20
92110406	23	14.9N	139.3E	130	16	46	96	186	355	921	0	5	-5	0	5	25
92110412	24	15.5N	138.2E	130	13	36	90	189	396	839	0	-10	-20	-15	-5	20
92110418	25	16.2N	137.2E	135	18	48	126	272	514		0	-15	-15	-5	5	
92110500	26	17.0N	136.2E	140	18	42	153	364	560		0	0	0	5	10	
92110506	27	17.9N	135.2E	145	12	41	168	378	562		5	5	10	15	20	
92110512	28	19.0N	134.4E	145	16	66	224	385	475		5	5	15	20	25	
92110518	29	20.3N	133.9E	140	16	97	260	393			10	15	25	30		
92110600	30	21.8N	133.8E	135	5	102	179	193			0	10	15	20		
92110606	31	23.5N	134.6E	125	26	91	131				0	5	10			
92110612	32	25.6N	135.6E	115	42	60	51				5	15	20			
92110618	33	27.6N	136.9E	105	32	67					-5	5				
92110700	34	29.4N	138.5E	95	6	50					0	10				
92110706	35	30.8N	140.3E	85	19						0					
92110712	36	32.0N	142.2E	75	36						0					

AVERAGE	19	56	110	183	249	342	5	9	13	15	15	15
# CASES	36	34	32	30	28	24	36	34	32	30	28	24

TROPICAL DEPRESSION 29W

DTG	WRN	BEST TRACK				POSITION ERRORS						WIND ERRORS					
	NO.	LAT	LONG	WIND	00	12	24	36	48	72	00	12	24	36	48	72	
92110100	1	18.2N	169.4E	25	13	109	217				0	0	0				
92110112	2	19.1N	166.1E	25	24	85					0	5					
92110200	3	20.0N	162.2E	25	21						0						
AVERAGE					20	97	218				0	3	0				
# CASES					3	2	1				3	2	1				

TROPICAL STORM FORREST (30W)

	WRN	BEST TRACK			POSITION ERRORS						WIND ERRORS					
DTG	NO.	LAT	LONG	WIND	00	12	24	36	48	72	00	12	24	36	48	72
92111218	1	9.5N	113.5E	35	56	59	71	104	103	69	-5	-5	-5	0	5	0
92111300	2	9.4N	111.8E	40	21	8	58	74	61	130	0	-5	-5	5	10	15
92111306	3	9.2N	110.3E	45	8	48	90	89	81	142	0	-5	0	10	10	20
92111312	4	8.9N	108.9E	50	37	120	141	177	167	208	0	-5	10	5	5	25
92111318	5	8.4N	107.8E	55	30	41	50	82	78	88	0	5	15	5	5	25
92111400	6	8.0N	106.7E	55	16	32	81	91	108	79	0	10	10	5	10	25
92111406	7	7.7N	105.4E	55	18	55	84	149	165	59	0	5	5	-5	10	20
92111412	8	7.7N	104.2E	50	5	26	26	71	48	11	0	0	-10	0	15	10
92111418	9	7.8N	103.0E	50	42	71	47	53	95	55	0	-15	-10	5	15	5
92111500	10	7.9N	102.1E	55	29	8	67	50	11	39	-5	-15	-5	10	15	5
92111506	11	8.1N	100.7E	55	0	71	106	103	114	43	5	-15	0	10	10	0
92111512	12	8.4N	99.1E	55	13	37	33	38	69	143	-5	-5	10	15	10	-5
92111518	13	8.7N	97.5E	55	30	48	36	59	66	79	-15	0	15	20	5	-15
92111600	14	9.0N	96.1E	50	29	8	26	33	42	232	-10	5	15	10	5	-25

TROPICAL STORM FORREST (30W) (CONTINUED)

92111606	15	9.3N	94.9E	45	8	67	89	79	122	359	-5	5	10	5	0	-35
92111612	16	9.5N	93.9E	40	8	18	38	30	143	429	5	10	5	5	-5	-40
92111618	17	9.6N	93.0E	40	17	60	91	114	201	416	5	10	0	0	-15	-50
92111700	18	9.8N	92.0E	40	29	70	88	161	264	491	5	0	0	-5	-25	-60
92111706	19	10.0N	90.7E	45	61	84	132	246	367	604	0	-5	-5	-15	-35	-55
92111712	20	10.4N	89.6E	55	24	92	222	363	503	726	-5	-5	-10	-25	-40	-80
92111718	21	11.1N	88.7E	60	54	125	246	372	473	719	-5	-10	-20	-35	-45	-70
92111800	22	11.9N	88.2E	60	25	94	187	309	437	713	-5	-15	-30	-40	-55	-60
92111806	23	12.9N	87.8E	65	11	68	145	225	335		-10	-25	-40	-50	-50	
92111812	24	14.0N	87.7E	70	23	54	119	170	221	369	-5	-20	-30	-50	-55	-45
92111818	25	15.0N	87.8E	80	17	46	57	66	116	290	-5	-15	-35	-45	-45	-20
92111900	26	15.9N	88.0E	90	13	58	85	126	186	288	0	-5	-20	-20	-30	5
92111906	27	16.7N	88.3E	100	6	55	102	162	192		0	-5	-5	5	-15	
92111912	28	17.3N	88.6E	105	8	40	49	96	126		-5	-10	-5	5	-10	
92111918	29	17.9N	88.8E	115	23	52	53	61	133		0	-5	0	10	30	
92112000	30	18.5N	89.0E	125	0	32	95	148	221		0	5	25	30	55	
92112006	31	19.0N	89.3E	120	6	70	130	200			5	15	25	65		
92112012	32	19.4N	90.0E	120	28	24	71	160			0	20	25	65		
92112018	33	19.6N	90.8E	110	5	49	119				5	20	45			
92112100	34	19.9N	91.6E	100	12	49	137				0	5	45			
92112106	35	20.3N	92.5E	95	11	34					0	30				
92112112	36	20.4N	93.3E	85	30	146					0	30				
92112118	37	20.2N	93.9E	45	16						0					
92112200	38	19.9N	94.5E	30	20						0					

AVERAGE	21	57	94	134	175	272	3	10	15	18	21	29
# CASES	38	36	34	32	30	25	38	36	34	32	30	25

SUPER TYPHOON GAY (31W)

	WRN	BEST TRACK				POSITION ERRORS						WIND ERRORS					
DTG	NO.	LAT	LONG	WIND	00	12	24	36	48	72	00	12	24	36	48	72	
92111418	1	6.7N	176.7E	25	49	98	106	88	42	130	0	0	0	0	0	0	
92111500	2	7.2N	175.7E	30	11	45	84	138	214	300	5	5	10	5	0	0	
92111506	3	7.8N	174.6E	30	64	135	211	321	442	577	5	5	5	0	-5	-5	
92111512	4	8.5N	173.7E	35	18	24	78	159	229	257	0	5	5	0	0	-10	
92111518	5	9.1N	173.0E	35	18	39	125	226	279	343	5	0	0	-5	-5	-25	
92111600	6	9.5N	172.3E	40	5	59	138	200	234	342	5	0	-5	-5	-5	-35	
92111606	7	9.8N	171.7E	45	11	79	169	203	219	279	5	0	-5	-5	-5	-40	
92111612	8	10.0N	171.3E	50	5	29	61	63	88	168	5	-5	-10	-15	-20	-35	
92111618	9	10.1N	171.0E	55	13	55	64	63	91	147	0	-10	-15	-20	-35	-40	
92111700	10	10.1N	170.7E	65	29	33	61	74	88	88	5	5	5	0	-20	-20	
92111706	11	10.2N	170.4E	70	5	11	29	70	102	114	10	10	10	-5	-15	-15	
92111712	12	10.4N	169.9E	75	26	48	76	125	174	174	5	5	0	-25	-20	-20	
92111718	13	10.5N	169.1E	80	18	64	122	163	180	186	-5	-5	-20	-30	-25	-25	
92111800	14	10.6N	168.2E	85	17	69	117	157	169	175	-5	-10	-30	-25	-20	-30	
92111806	15	10.5N	167.3E	90	11	53	84	108	122	185	-10	-25	-35	-30	-25	-25	
92111812	16	10.3N	166.4E	100	13	52	82	102	88	91	-15	-35	-30	-25	-25	-15	
92111818	17	10.1N	165.5E	115	5	24	30	40	50	102	-5	-5	0	-5	-20	-10	
92111900	18	10.0N	164.7E	130	11	37	54	94	135	158	-10	-5	0	-10	-25	0	
92111906	19	9.9N	163.8E	135	13	13	16	41	67	71	-5	-5	-5	-15	-20	10	
92111912	20	9.9N	162.9E	135	12	8	5	31	70	138	5	0	-10	-25	-10	20	
92111918	21	10.0N	162.0E	140	8	5	48	93	114	160	0	0	-15	-20	-35	30	
92112000	22	10.1N	161.0E	140	13	39	82	124	104	122	15	5	-10	-5	5	40	
92112006	23	10.3N	159.8E	145	13	30	55	77	76	166	10	0	-5	5	15	45	
92112012	24	10.5N	158.5E	150	16	37	65	71	88	201	10	-5	5	15	25	35	
92112018	25	10.8N	157.2E	155	16	31	35	52	79	250	5	0	15	25	35	35	
92112100	26	11.2N	155.8E	160	13	18	29	56	114	275	0	15	30	40	45	30	
92112106	27	11.6N	154.4E	155	17	49	78	90	139	197	5	20	35	50	45	25	

SUPER TYPHOON GAY (31W) (CONTINUED)

92112112	28	11.9N	153.0E	145	6	32	41	74	130	170	10	25	35	45	35	20
92112118	29	12.2N	151.7E	135	5	18	18	71	110	144	15	25	40	40	30	5
92112200	30	12.4N	150.4E	125	11	21	52	110	152	170	15	25	35	30	20	5
92112206	31	12.6N	149.1E	115	17	64	118	170	187	219	15	30	35	20	10	-10
92112212	32	13.0N	147.7E	105	18	52	114	158	173	270	20	30	25	15	10	-15
92112218	33	13.3N	146.3E	95	11	56	113	166	205	324	30	40	30	25	15	-10
92112300	34	13.4N	144.8E	90	24	55	73	75	99	101	15	10	5	0	-5	-25
92112306	35	13.4N	143.3E	85	8	11	31	56	72	200	15	10	0	-5	-15	-20
92112312	36	13.5N	141.9E	90	16	29	68	120	145	227	10	5	5	-5	-20	-15
92112318	37	13.7N	140.6E	90	33	61	120	182	223	349	10	5	0	-10	-25	-15
92112400	38	13.9N	139.4E	95	8	45	91	123	147	278	5	5	-5	-20	-25	-15
92112406	39	14.5N	138.3E	95	30	68	110	135	183	344	0	-5	-15	-25	-25	-10
92112412	40	15.1N	137.2E	95	42	78	104	137	225	418	0	-5	-20	-25	-20	-5
92112418	41	15.8N	136.1E	100	5	12	58	146	246	329	-5	-5	-10	5	5	15
92112500	42	16.5N	135.0E	100	23	31	49	124	192	226	5	0	0	5	0	15
92112506	43	17.1N	134.0E	105	21	33	80	156	201	196	5	-5	5	5	5	20
92112512	44	17.5N	133.2E	110	11	54	119	197	220	191	10	10	20	15	15	25
92112518	45	17.9N	132.6E	115	13	79	149	197	229	211	10	15	15	20	20	30
92112600	46	18.1N	132.1E	115	0	26	48	67	92	133	-5	0	0	0	0	5
92112606	47	18.2N	131.9E	110	8	37	62	75	81	121	0	0	5	5	5	10
92112612	48	18.2N	131.7E	105	8	32	58	78	79	116	5	5	10	10	10	20
92112618	49	18.2N	131.5E	105	11	24	43	57	81	119	0	5	5	5	10	25
92112700	50	18.2N	131.3E	100	6	25	54	97	144	110	-5	0	5	10	10	20
92112706	51	18.3N	131.0E	95	13	30	72	113	125	76	-5	-5	0	0	5	15
92112712	52	18.5N	130.6E	90	13	32	72	120	139	91	-5	0	5	5	15	15
92112718	53	18.8N	130.4E	85	17	49	102	150	150	120	0	0	5	5	15	20
92112800	54	19.2N	130.1E	80	16	47	86	109	111	144	5	5	10	15	20	20
92112806	55	19.9N	130.0E	75	18	23	36	24	81		0	0	0	10	10	
92112812	56	20.6N	129.9E	70	8	23	37	94	142		0	5	10	15	10	
92112818	57	21.3N	129.8E	65	50	126	218	343	376		0	5	15	20	15	
92112900	58	22.1N	129.9E	60	49	93	201	322	347		0	10	15	15	15	
92112906	59	22.8N	130.1E	55	52	122	233	281			0	5	10	10		
92112912	60	23.4N	130.2E	45	0	21	40	42			0	5	5	10		
92112918	61	24.0N	130.3E	40	24	94	99				0	10	10			
92113000	62	24.5N	130.3E	35	39	78	77				-5	0	5			
92113006	63	25.0N	130.3E	30	29	112					0	5				

AVERAGE	18	48	84	124	154	200	6	8	12	14	16	19
# CASES	63	63	62	60	58	54	63	63	62	60	58	54

TYPHOON HUNT (32W)

DTG	WRN NO.	BEST TRACK			00	POSITION ERRORS					00	WIND ERRORS				
		LAT	LONG	WIND		12	24	36	48	72		12	24	36	48	72
92111606	1	13.0N	155.9E	25	8	87	161	226	221	220	0	-10	-20	-25	-25	-50
92111612	2	13.0N	154.5E	30	34	13	35	59	100	230	-5	-15	-20	-25	-30	-45
92111618	3	13.0N	153.0E	35	24	46	77	85	126	262	-5	-15	-20	-20	-40	-50
92111700	4	12.7N	151.4E	45	40	100	120	138	168	323	-5	-10	-15	-20	-30	-50
92111706	5	12.6N	149.8E	50	18	41	75	120	196	403	0	0	5	-15	-15	-25
92111712	6	12.5N	148.2E	55	0	55	147	225	287	554	0	0	5	-5	0	-10
92111718	7	12.7N	146.9E	60	5	79	155	252	337	671	0	5	-5	0	0	0
92111800	8	13.2N	145.7E	65	5	35	91	152	224	706	5	5	-5	-5	-10	5
92111806	9	13.9N	144.8E	65	18	52	89	130	253	819	5	-10	-10	-15	-10	15
92111812	10	14.4N	143.8E	75	0	13	62	125	256	806	-5	-10	-5	-10	-5	20
92111818	11	15.0N	142.9E	90	6	6	30	129	298	974	-10	-5	-5	-5	-5	15
92111900	12	15.7N	142.1E	95	24	49	98	207	377		5	5	-5	-5	0	
92111906	13	16.5N	141.3E	100	24	20	71	228	474		0	-5	-10	-5	0	
92111912	14	17.2N	140.5E	105	5	29	101	196	481		0	-15	-20	-15	-5	
92111918	15	17.8N	139.7E	115	34	42	105	282	706		0	-15	-15	-5	15	

TYPHOON HUNT (32W) (CONTINUED)

92112000	16	19.0N	139.4E	125	12	82	230	569		0	-5	-10	5			
92112006	17	20.3N	139.5E	125	23	100	278	707		0	-5	-5	20			
92112012	18	21.8N	140.3E	125	21	84	357			0	0	5				
92112018	19	23.6N	141.5E	120	29	111	442			0	10	25				
92112100	20	25.7N	143.3E	115	26	229				-15	-10					
92112106	21	27.8N	146.2E	105	10	210				-10	10					
92112112	22	30.5N	151.4E	95	20					-10						
92112118	23	34.0N	156.2E	75	54					-5						
AVERAGE					20	71	144	226	301	543	4	8	11	12	13	26
# CASES					23	21	19	17	15	11	23	21	19	17	15	11

6.2.2 NORTH INDIAN OCEAN

This section includes verification

statistics for each warning in the North Indian Ocean during 1992.

JTWC FORECAST TRACK AND INTENSITY ERRORS BY WARNING

TROPICAL CYCLONE 01B

DTG	WRN NO.	BEST TRACK			POSITION ERRORS						WIND ERRORS					
		LAT	LONG	WIND	00	12	24	36	48	72	00	12	24	36	48	72
92051612	1	12.3N	87.6E	30	26	74	142		293	593	0	0	0		0	20
92051618	2	12.9N	87.6E	30	13	53	110		260	593	0	-5	-5		-10	25
92051700	3	13.5N	87.8E	35	13	24	58		152	456	0	-5	-5		-5	35
92051706	4	14.0N	88.1E	40	11	29	63		205		0	5	5		5	
92051712	5	14.5N	88.6E	45	46	97	149		320		0	0	5		20	
92051718	6	15.0N	89.1E	45	70	128	190		449		0	-5	0		30	
92051800	7	15.3N	89.7E	50	101	171	258		561		-5	-5	-5		40	
92051806	8	15.8N	90.4E	55	55	117	257				-5	0	5			
92051812	9	16.3N	91.1E	55	43	130	293				0	-10	20			
92051818	10	17.1N	92.1E	60	37	137	336				0	0	30			
92051900	11	18.0N	93.2E	65	16	162	348				0	25	20			
92051906	12	19.3N	94.7E	60	12	93					15	15				
92051912	13	20.6N	96.3E	45	17	108					15	20				
92051918	14	22.2N	98.0E	35	5						10					
92052000	15	23.9N	99.7E	25	11						5					
AVERAGE					32	102	201		321	548	4	7	9		16	27
# CASES					15	13	11		7	3	15	13	11		7	3

TROPICAL CYCLONE 02A

DTG	WRN NO.	BEST TRACK			POSITION ERRORS						WIND ERRORS					
		LAT	LONG	WIND	00	12	24	36	48	72	00	12	24	36	48	72
92060506	1	10.1N	66.5E	30	5	24	38	48	113	291	0	0	0	5	10	0
92060512	2	10.1N	65.6E	30	24	37	45	103	210	424	0	-5	0	5	10	10
92060518	3	10.2N	64.7E	30	5	0	58	141	247	453	0	-5	0	0	5	5
92060600	4	10.3N	63.9E	35	8	30	106	195	296	452	5	-5	0	5	5	-5
92060606	5	10.4N	63.2E	35	30	110	204	311	429	564	0	0	5	5	5	-5
92060612	6	10.5N	62.8E	35	54	138	244	380	498	599	0	0	5	5	5	-5
92060618	7	10.6N	62.6E	35	84	180	299	418	518	632	0	0	0	5	5	-5
92060700	8	10.8N	62.5E	35	130	233	346	445	517	636	0	0	0	5	5	-5
92060706	9	10.9N	62.5E	35	201	363	521	618	676	678	0	0	0	0	-5	-5
92060712	10	11.0N	62.6E	35	306	460	592	683	733		-5	-5	-5	-5	-5	
92060718	11	11.1N	62.8E	35	70	117	129	113	107	77	0	0	5	5	5	5
92060800	12	11.2N	63.0E	35	18	47	111	158	176	215	0	0	0	-5	-10	-10
92060806	13	11.3N	63.2E	35	18	76	140				0	-5	-10			
92060812	14	11.5N	63.2E	35	25	42	65	61	68		0	0	-5	-10	-15	
92060818	15	11.6N	63.0E	35	26	47	58	47			0	-5	-5	-10		
92060900	16	11.7N	62.8E	35	24	46	82	131			-5	-5	-10	-10		
92060906	17	11.8N	62.4E	35	21	29	29				-5	-5	-10			
92060912	18	11.9N	62.0E	35	21	42	81	113	127		5	5	0	-5	-5	
92060918	19	12.0N	61.6E	35	16	17	45	99			5	0	-5	-5		
92061000	20	12.2N	61.2E	35	18	30	77	129	176		0	0	0	0	0	
92061006	21	12.4N	60.7E	35	11	37	94	139			0	0	0	0		
92061012	22	12.7N	60.2E	35	16	73	120	155			0	0	0	0		
92061018	23	13.0N	59.4E	35	29	75	126				0	0	0			
92061100	24	13.5N	58.6E	35	58	93	129				0	0	5			
92061106	25	13.9N	57.8E	30	11	29	53				5	0	0			
92061112	26	14.1N	56.9E	30	13	48					5	5				

TROPICAL CYCLONE 06A (CONTINUED)

AVERAGE	37	73	108	129	142	164	3	5	8	6	5	0
# CASES	10	10	8	7	6	2	10	10	8	7	6	2

TROPICAL CYCLONE 07B

DTG	WRN NO.	BEST TRACK			POSITION ERRORS							WIND ERRORS						
		LAT	LONG	WIND	00	12	24	36	48	72	00	12	24	36	48	72		
92100700	1	12.8N	86.9E	30	37	87	175	220	232		0	5	5	10	20			
92100706	2	13.2N	86.5E	30	64	130	203	237	236		0	0	0	10	20			
92100712	3	13.6N	86.0E	30	93	193	245	277	295		0	-5	0	15	25			
92100718	4	13.8N	85.2E	35	73	136	188	246			0	-10	0	25				
92100800	5	14.0N	84.4E	40	108	159	195	286			-5	-5	5	30				
92100806	6	14.3N	83.7E	45	55	116	199				0	0	5					
92100812	7	14.9N	82.9E	45	70	96	165				0	0	5					
92100818	8	15.5N	82.1E	45	16	39					0	5						
92100900	9	16.2N	81.3E	40	66	154					5	15						
92100906	10	17.2N	80.4E	30	33						0							
AVERAGE					62	124	196	254	255		1	5	3	18	22			
# CASES					10	9	7	5	3		10	9	7	5	3			

TROPICAL CYCLONE 08B

DTG	WRN NO.	BEST TRACK			POSITION ERRORS							WIND ERRORS						
		LAT	LONG	WIND	00	12	24	36	48	72	00	12	24	36	48	72		
92102106	1	20.0N	91.0E	30	50	145					0	5						
92102112	2	20.9N	92.1E	30	37	113					0	5						
92102118	3	21.7N	93.3E	30	23						0							
AVERAGE					37	129					0	5						
# CASES					3	2					3	2						

TROPICAL CYCLONE 09B

DTG	WRN NO.	BEST TRACK			POSITION ERRORS							WIND ERRORS						
		LAT	LONG	WIND	00	12	24	36	48	72	00	12	24	36	48	72		
92110300	1	14.9N	90.2E	30	11	47	120	194	243	324	0	0	10	20	20	20		
92110306	2	15.0N	89.9E	30	17	69	133	178	201	275	5	5	10	10	10	15		
92110312	3	15.1N	89.5E	35	34	82	126	121	102	156	0	5	10	5	5	20		
92110318	4	15.2N	88.9E	35	57	92	121	115	106	197	0	5	5	0	5	25		
92110400	5	15.4N	88.3E	35	5	0	33	87	146	300	0	5	0	-5	5	-15		
92110406	6	15.7N	87.7E	35	21	18	34	77	141	336	0	5	0	5	10	-10		
92110412	7	16.0N	87.0E	35	52	36	17	53	109	374	0	0	-5	5	15	-5		
92110418	8	16.2N	86.6E	40	26	23	49	113	180	442	-5	-5	-5	5	20	0		
92110500	9	16.3N	86.4E	45	21	51	93	131	203		0	0	5	10	-10			
92110506	10	16.4N	86.2E	50	42	89	124	164	290		0	5	5	-15	-10			
92110512	11	16.5N	86.0E	55	21	33	69	144	313		0	5	10	5	-5			
92110518	12	16.5N	85.8E	55	8	33	91	205	335		0	5	20	30	30			
92110600	13	16.4N	85.6E	55	21	6	18	106	139		-5	-5	0	10	10			
92110606	14	16.3N	85.3E	55	18	8	77	147			0	10	15	20				
92110612	15	16.2N	84.9E	50	18	21	109	147			5	15	20	20				
92110618	16	16.1N	84.5E	45	5	90	186				10	20	25					
92110700	17	15.6N	84.0E	40	21	113	159				5	10	15					
92110706	18	14.8N	83.3E	35	59	130					0	5						
92110712	19	13.9N	82.7E	30	104	158					0	0						
92110718	20	13.2N	82.1E	25	145						0							
AVERAGE					36	58	92	133	193	301	2	6	9	10	11	14		
# CASES					20	19	17	15	13	8	20	19	17	15	13	8		

TROPICAL CYCLONE 10B

DTG	WRN NO.	BEST TRACK			00	POSITION ERRORS					00	WIND ERRORS				
		LAT	LONG	WIND		12	24	36	48	72		12	24	36	48	72
92111100	1	7.1N	86.6E	30	11	21	107	182	250	439	0	-5	-20	-5	-20	5
92111106	2	7.0N	85.5E	35	8	69	150	218	314	528	0	-5	-20	-5	-25	10
92111112	3	6.9N	84.4E	45	11	48	66	109	201	395	-5	-5	-5	-20	-10	15
92111118	4	6.7N	83.3E	50	11	46	67	148	247	459	0	-15	-5	-25	5	10
92111200	5	6.5N	82.3E	55	5	21	18	122	206	362	0	10	-15	-10	5	0
92111206	6	6.3N	81.3E	55	62	84	66	142	219	355	0	5	-25	5	10	-10
92111212	7	6.4N	80.3E	40	34	17	131	207	273	431	-10	-25	-10	5	15	-10
92111218	8	6.5N	79.3E	45	5	106	207	288	368	588	0	-15	20	25	25	10
92111300	9	7.1N	78.6E	60	42	156	257	336	408	613	0	15	35	55	45	45
92111306	10	7.8N	78.1E	70	78	181	259	334	410	638	0	40	55	50	20	25
92111312	11	8.6N	77.7E	55	45	77	107	180	273	526	0	15	30	20	10	25
92111318	12	9.3N	77.1E	40	36	51	106	189	294	573	0	10	20	10	15	25
92111400	13	9.9N	76.5E	40	6	71	122	189	294	527	0	15	10	10	20	25
92111406	14	10.2N	76.2E	35	52	100	139	199	304	574	10	10	0	15	25	25
92111412	15	10.5N	75.8E	30	29	16	59	122	209	388	5	-5	-5	10	20	25
92111418	16	10.7N	75.3E	35	21	34	91	170	249	474	-5	-15	0	15	20	30
92111500	17	11.1N	74.8E	45	18	29	82	168	261		-10	-15	5	20	20	
92111506	18	11.6N	74.5E	55	34	30	63	120	224		-20	-10	10	20	20	
92111512	19	12.1N	74.3E	55	33	88	169	255	358		-15	5	20	20	25	
92111518	20	12.5N	74.2E	50	71	144	215	306	397		-5	10	20	20	30	
92111600	21	12.9N	74.1E	45	55	108	152	251			0	15	20	20	25	
92111606	22	13.4N	74.1E	40	13	31	104	184			5	10	15	30		
92111612	23	13.9N	74.1E	35	21	55	132				10	10	20			
92111618	24	14.4N	74.1E	35	21	63	127				5	5	10			
92111700	25	14.9N	74.2E	35	29	98					5	5				
92111706	26	15.2N	74.6E	35	52	105					0	10				
92111712	27	15.5N	75.0E	30	40						0					
92111718	28	15.9N	75.3E	25	37						0					
AVERAGE					32	72	125	201	289	492	4	12	16	19	19	18
# CASES					28	26	24	22	20	16	28	26	24	22	20	16

TROPICAL CYCLONE 11A

DTG	WRN NO.	BEST TRACK			00	POSITION ERRORS					00	WIND ERRORS				
		LAT	LONG	WIND		12	24	36	48	72		12	24	36	48	72
92113012	1	3.6N	78.7E	30	16	72	102	62	8	104	0	0	0	-10	-10	-5
92113018	2	4.0N	78.8E	35	29	51	69	13	53	173	0	0	0	-5	-5	0
92120100	3	4.5N	78.6E	35	51	79	55	5	71		5	5	-5	-5	0	
92120106	4	4.9N	78.1E	40	36	79	174	252	323		0	0	-5	0	5	
92120112	5	5.1N	77.5E	40	43	109	179	226	251		5	5	20	35	40	
92120118	6	5.2N	77.0E	45	64	151	201	245	247		5	15	30	40	40	
92120200	7	5.3N	76.8E	50	102	166	213	232			0	0	5	5		
92120206	8	5.4N	76.6E	45	18	8	18	23			0	0	10	10		
92120212	9	5.5N	76.3E	45	13	13	18				-5	5	10			
92120218	10	5.6N	75.9E	40	13	11	23				0	15	25			
92120300	11	5.7N	75.5E	35	13	18					5	15				
92120306	12	5.9N	75.0E	30	0	17					10	10				
92120312	13	6.1N	74.4E	30	29						0					
92120318	14	6.4N	73.7E	25	42						0					
AVERAGE					34	65	106	133	160	139	3	6	11	14	17	3
# CASES					14	12	10	8	6	2	14	12	10	8	6	2

TROPICAL CYCLONE 12A

DTG	WRN NO.	BEST TRACK			POSITION ERRORS						WIND ERRORS					
		LAT	LONG	WIND	00	12	24	36	48	72	00	12	24	36	48	72
92122012	1	5.0N	69.4E	30	45	73	45	32	86	150	0	-10	-5	-5	-5	-20
92122018	2	5.5N	68.6E	35	43	63	89	131	173	219	0	0	5	5	-5	-15
92122100	3	5.8N	67.6E	40	24	73	134	208	232	244	0	0	5	5	-5	-15
92122106	4	6.0N	66.4E	40	32	95	175	239	274	262	0	0	5	0	-5	-10
92122112	5	6.2N	65.0E	40	62	125	199	256	291	237	0	0	5	-5	-10	10
92122118	6	6.3N	63.6E	40	40	97	161	203	223	167	0	0	-10	-10	-20	15
92122200	7	6.2N	62.1E	40	56	125	166	191	178		0	0	-10	-15	-20	
92122206	8	6.0N	60.5E	40	5	40	64	77	85		0	-5	-10	-15	-15	
92122212	9	6.1N	58.9E	40	21	62	103	129	179		0	-5	-15	-15	5	
92122218	10	6.4N	57.4E	45	59	111	155	175	216		-5	-5	-15	-10	15	
92122300	11	6.9N	56.0E	45	26	24	26	132			0	0	0	0		
92122306	12	7.3N	54.6E	45	8	25	79	160			0	0	-10	10		
92122312	13	7.6N	53.3E	50	13	56	107				0	0	10			
92122318	14	8.0N	52.0E	50	13	39	101				0	-5	10			
92122400	15	8.2N	51.2E	50	29	42					0	15				
92122406	16	8.6N	50.3E	45	32	77					0	15				
92122412	17	9.0N	49.6E	25	24						10					
92122418	18	9.4N	49.0E	15	34						15					
AVERAGE					32	71	115	162	194	214	2	4	8	8	11	14
# CASES					18	16	14	12	10	6	18	16	14	12	10	6

TROPICAL STORM FORREST (30W)

NOTE: THE NORTH INDIAN OCEAN PORTION OF THIS BEST TRACK IS INCLUDED IN WESTERN NORTH PACIFIC WARNING VERIFICATION STATISTICS FOR TROPICAL STORM FORREST(30W) ON PAGES 231 AND 232.

6.2.3 SOUTHERN HEMISPHERE

This section includes verification statistics for each warning in the South Indian

and western South Pacific Oceans from 1 July 1991 to 30 June 1992.

JTWC FORECAST TRACK AND INTENSITY ERRORS BY WARNING

TROPICAL CYCLONE 01S

DTG	WRN NO.	BEST TRACK			POSITION ERRORS				WIND ERRORS			
		LAT	LONG	WIND	00	24	48	72	00	24	48	72
91091100	1	10.1S	80.6E	30	111	280	530		0	-5	10	
91091112	2	10.7S	80.4E	35	142	388			0	0		
91091200	3	11.2S	80.6E	40	130	340			-5	-5		
91091212	4	11.0S	81.3E	40	114				0			
91091300	5	10.1S	81.3E	30	104				-5			
AVERAGE					120	336	530		2	3	10	
# CASES					5	3	1		5	3	1	

TROPICAL CYCLONE 02S

DTG	WRN NO.	BEST TRACK			POSITION ERRORS				WIND ERRORS			
		LAT	LONG	WIND	00	24	48	72	00	24	48	72
91101706	1	11.4S	53.9E	30	17	40	72		0	5	0	
91101718	2	11.3S	52.9E	30	5	30	96		0	5	5	
91101806	3	11.0S	51.9E	35	8	70	213		0	0	5	
91101818	4	10.9S	51.1E	35	17	53	151		0	5	10	
91101906	5	10.8S	50.3E	35	29	101	166		0	5	10	
91101918	6	10.5S	49.7E	30	53	151			0	10		
91102006	7	10.0S	49.4E	30	85	142			0	5		
91102018	8	9.5S	49.2E	25	119				0			
AVERAGE					42	84	140		0	5	6	
# CASES					8	7	5		8	7	5	

TROPICAL CYCLONE 03P (TIA)

DTG	WRN NO.	BEST TRACK			POSITION ERRORS				WIND ERRORS			
		LAT	LONG	WIND	00	24	48	72	00	24	48	72
91111500	1	8.6S	167.0E	40	37	78	67		-5	-5	-15	
91111512	2	8.4S	168.8E	50	16	84	307		-10	-10	-15	
91111600	3	8.6S	170.2E	60	13	173	415		0	0	-10	
91111612	4	8.8S	170.9E	70	31	241	434		0	-5	-15	
91111700	5	9.3S	170.7E	80	13	168	235		-10	-10	0	
91111706	6	9.8S	170.2E	85	13	154	240		0	0	25	
91111712	7	10.4S	169.6E	85	16	108	162		0	5	40	
91111800	8	12.7S	169.1E	90	16	159	422		0	-5	5	
91111812	9	14.0S	169.0E	95	5	84	460		0	25	30	
91111900	10	15.9S	169.5E	80	29	297	1120		-5	5	5	
91111912	11	16.8S	170.5E	60	136	540	1281		0	10	10	
91112000	12	17.7S	171.7E	50	20	504			0	-5		
91112012	13	16.0S	170.7E	35	21	84			0	-5		
91112100	14	14.6S	168.9E	35	0				0			
91112112	15	13.7S	167.6E	30	21				0			
AVERAGE					26	206	468		2	7	15	
# CASES					15	13	11		15	13	11	

TROPICAL CYCLONE 04S

DTG	WRN NO.	BEST TRACK			POSITION ERRORS				WIND ERRORS			
		LAT	LONG	WIND	00	24	48	72	00	24	48	72
91112200	1	10.5S	70.6E	25	78	288	570		0	0	5	
91112212	2	11.3S	70.7E	30	31	139	287		0	0	5	
91112218	3	11.8S	70.7E	35	31	134	187		10	15	30	
91112300	4	12.4S	70.8E	35	8	166	196		0	15	30	
91112312	5	13.6S	71.4E	40	18	70	72		0	5	5	
91112400	6	14.9S	72.3E	45	18	167	279		0	10	10	
91112412	7	16.2S	71.7E	45	54	223	388		0	10	15	
91112500	8	16.4S	70.3E	40	24	133			5	5		
91112512	9	16.2S	68.9E	35	13	100			0	0		
91112600	10	15.8S	67.6E	30	5				0			
AVERAGE					28	158	283		2	7	14	
# CASES					10	9	7		10	9	7	

TROPICAL CYCLONE 05S (GRAHAM)

DTG	WRN NO.	BEST TRACK			POSITION ERRORS				WIND ERRORS			
		LAT	LONG	WIND	00	24	48	72	00	24	48	72
91120212	1	5.7S	93.5E	30	17	45	131		0	-10	-20	
91120300	2	6.5S	93.1E	40	33	102	271		-5	-15	-30	
91120306	3	6.9S	92.9E	45	55	151	351		0	-10	-30	
91120312	4	7.2S	92.8E	50	51	138	348		0	-10	-35	
91120400	5	7.9S	92.9E	65	0	90	303		0	-5	-20	
91120412	6	8.5S	93.5E	75	5	127	317		0	-10	10	
91120500	7	9.2S	94.7E	95	11	148	311		0	-5	30	
91120512	8	10.0S	96.1E	110	21	136	281		0	10	40	
91120518	9	10.6S	96.9E	115	8	48	143		0	20	45	
91120600	10	11.1S	97.7E	120	12	94	250		0	30	55	
91120612	11	12.0S	98.9E	105	26	228	396		0	0	15	
91120700	12	12.6S	100.0E	85	35	114	221		5	15	10	
91120712	13	12.5S	101.4E	65	52	43			5	10		
91120800	14	12.6S	102.8E	45	11	116	176		5	0	-10	
91120812	15	13.3S	103.5E	35	24	135			5	-5		
91120900	16	13.9S	103.8E	35	17	56			5	0		
91120912	17	14.4S	104.3E	30	0	130			0	0		
91121000	18	14.7S	104.8E	30	18				0			
91121012	19	15.2S	104.6E	25	8				0			
AVERAGE					21	112	269		2	9	27	
# CASES					19	17	13		19	17	13	

TROPICAL CYCLONE 09S (ALEXANDRA)

DTG	WRN NO.	BEST TRACK			POSITION ERRORS				WIND ERRORS			
		LAT	LONG	WIND	00	24	48	72	00	24	48	72
91122006	1	11.5S	75.6E	40	16	48	57		-5	-10	-10	
91122018	2	13.4S	76.4E	60	23	29	108		5	-5	5	
91122106	3	15.1S	77.0E	85	13	135	252		-5	0	15	
91122118	4	16.3S	77.7E	95	30	192	370		0	-5	5	
91122206	5	16.7S	78.8E	100	61	204	475		0	5	15	
91122218	6	16.8S	79.4E	100	41	200	528		5	15	30	
91122306	7	17.1S	79.6E	85	17	92	259		15	20	30	
91122318	8	17.4S	78.8E	75	31	203	296		15	20	15	
91122406	9	17.6S	77.3E	60	20	62	105		15	15	5	
91122418	10	17.6S	75.5E	45	22	45			10	5		
91122506	11	17.9S	74.0E	35	30	64			0	-5		
91122518	12	18.5S	72.6E	30	11				0			

TROPICAL CYCLONE 09S (ALEXANDRA) (CONTINUED)

AVERAGE	26	116	272	6	10	14
# CASES	12	11	9	12	11	9

TROPICAL CYCLONE 10S (BRYNA)

DTG	WRN NO.	BEST TRACK			POSITION ERRORS				WIND ERRORS			
		LAT	LONG	WIND	00	24	48	72	00	24	48	72
91123018	1	13.6S	59.4E	30	50	115	139		10	20	25	
91123106	2	14.0S	57.4E	35	23	87	83		0	5	15	
91123118	3	14.5S	55.4E	40	5	42	34		5	10	20	
92010106	4	14.9S	53.6E	45	0	23	72		0	10	15	
92010118	5	15.2S	52.3E	40	13	70			5	10		
92010206	6	15.4S	50.8E	35	8	89			5	-5		
92010218	7	15.4S	49.2E	30	0				0			
AVERAGE					14	71	82		4	10	19	
# CASES					7	6	4		7	6	4	

TROPICAL CYCLONE 11S (BETSY)

DTG	WRN NO.	BEST TRACK			POSITION ERRORS				WIND ERRORS			
		LAT	LONG	WIND	00	24	48	72	00	24	48	72
92010600	1	8.7S	170.3E	25	30	204	431		0	-5	-5	
92010612	2	9.5S	169.9E	35	80	302	439		-5	-5	-15	
92010700	3	10.8S	170.1E	45	55	151	216		0	0	-15	
92010712	4	12.4S	170.5E	55	13	11	147		0	-5	-5	
92010800	5	13.9S	170.5E	65	42	233	448		5	-5	0	
92010812	6	15.2S	169.7E	80	8	155	453		0	-5	10	
92010900	7	16.4S	167.9E	90	33	176	375		0	10	15	
92010912	8	17.3S	165.5E	95	20	122	238		0	5	15	
92011000	9	18.2S	162.6E	90	12	162	284		-5	-15	0	
92011012	10	19.0S	160.3E	85	23	211	414		-10	-10	-15	
92011100	11	19.6S	158.3E	85	23	132			-15	0		
92011112	12	20.1S	157.4E	70	16	60			0	-10		
92011200	13	20.9S	157.5E	60	28	169			5	-15		
92011212	14	21.8S	157.8E	60	26	147	281		-10	-15	-20	
92011300	15	22.8S	157.9E	60	47	26	83		-15	-15	-15	
92011312	16	24.3S	158.1E	55	16	24			-15	-20		
92011400	17	26.2S	158.6E	55	36	187			-10	-10		
92011412	18	28.3S	160.0E	55	16				-15			
92011500	19	30.1S	161.9E	50	0				-10			
AVERAGE					28	145	318		6	9	11	
# CASES					19	17	12		19	17	12	

TROPICAL CYCLONE 12P (MARK)

DTG	WRN NO.	BEST TRACK			POSITION ERRORS				WIND ERRORS			
		LAT	LONG	WIND	00	24	48	72	00	24	48	72
92010806	1	14.0S	138.0E	30	31	44	90		5	-5	10	
92010818	2	14.1S	138.9E	35	11	120	202		5	-5	25	
92010906	3	13.9S	139.9E	45	17	89	153		-5	0	10	
92010918	4	13.4S	141.0E	55	16	46			-15	10		
92011006	5	13.1S	142.3E	45	13	54			-5	-5		
92011018	6	13.2S	143.5E	25	24				5			
AVERAGE					19	70	148		7	5	15	
# CASES					6	5	3		6	5	3	

TROPICAL CYCLONE 15P (CELESTA)

DTG	WRN NO.	BEST TRACK			POSITION ERRORS				WIND ERRORS			
		LAT	LONG	WIND	00	24	48	72	00	24	48	72
92021100	1	22.0S	67.5E	35	72	389	1144		0	5	20	
92021112	2	23.6S	69.1E	45	131	481			-5	-10		
92021200	3	24.3S	67.8E	45	163	620			0	0		
92021212	4	22.2S	66.4E	40	154				-5			
92021300	5	19.9S	65.1E	30	297				0			
AVERAGE					164	497	1144		2	5	20	
# CASES					5	3	1		5	3	1	

TROPICAL CYCLONE 16S

DTG	WRN NO.	BEST TRACK			POSITION ERRORS				WIND ERRORS			
		LAT	LONG	WIND	00	24	48	72	00	24	48	72
92021218	1	13.7S	128.1E	20	35	241			15	35		
92021306	2	14.1S	124.8E	25	21	242			20	40		
92021318	3	14.9S	120.8E	20	79				20			
92021406	4	16.4S	116.6E	15	11				20			
AVERAGE					37	242			19	38		
# CASES					4	2			4	2		

TROPICAL CYCLONE 17P (DAMAN)

DTG	WRN NO.	BEST TRACK			POSITION ERRORS				WIND ERRORS			
		LAT	LONG	WIND	00	24	48	72	00	24	48	72
92021412	1	11.5S	172.6E	35	90	112	130		-5	-5	-5	
92021500	2	12.7S	169.9E	40	24	60	123		-5	-10	-10	
92021512	3	13.7S	167.2E	55	13	88	218		-5	5	10	
92021600	4	15.2S	164.7E	65	13	108	336		0	5	20	
92021612	5	17.2S	162.6E	75	18	102	223		5	10	15	
92021700	6	19.6S	161.4E	85	30	240	318		5	30	40	
92021712	7	22.8S	160.4E	80	17	238	293		10	10	0	
92021800	8	26.3S	158.9E	70	28	70			0	0		
92021812	9	28.4S	156.6E	55	26	342			5	-10		
92021900	10	30.2S	155.5E	45	23				5			
92021912	11	32.0S	157.6E	40	20				0			
AVERAGE					27	151	234		4	9	14	
# CASES					11	9	7		11	9	7	

TROPICAL CYCLONE 18P

DTG	WRN NO.	BEST TRACK			POSITION ERRORS				WIND ERRORS			
		LAT	LONG	WIND	00	24	48	72	00	24	48	72
92021918	1	21.2S	153.1E	25	11	102			10	0		
92022000	2	21.8S	152.6E	30	45				10			
92022006	3	22.3S	151.9E	35	33				5			
92022018	4	22.9S	150.5E	25	0				5			
AVERAGE					22	102			8	0		
# CASES					4	1			4	1		

TROPICAL CYCLONE 19S (DAVILIA)

DTG	WRN NO.	BEST TRACK			POSITION ERRORS				WIND ERRORS			
		LAT	LONG	WIND	00	24	48	72	00	24	48	72
92022318	1	21.4S	72.2E	35	74	103			0	15		
92022406	2	22.2S	72.6E	30	21				5			
92022418	3	23.0S	73.0E	25	12				5			

TROPICAL CYCLONE 19S (DAVILIA) (CONTINUED)

AVERAGE	36	103	3	15
# CASES	3	1	3	1

TROPICAL CYCLONE 20S (HARRIET)

DTG	WRN NO.	BEST TRACK			POSITION ERRORS				WIND ERRORS			
		LAT	LONG	WIND	00	24	48	72	00	24	48	72
92022600	1	11.4S	98.2E	35	6	46	113		0	-10	-5	
92022612	2	11.5S	97.1E	45	11	63	90		-10	0	-10	
92022700	3	11.7S	96.1E	55	39	55	69		0	10	0	
92022712	4	11.9S	95.2E	55	29	92	140		5	-5	-10	
92022800	5	12.2S	94.4E	65	13	96	125		0	-5	-20	
92022812	6	12.9S	93.5E	80	0	18	74		0	-5	-40	
92022900	7	13.5S	92.6E	90	8	36	139		0	-15	-40	
92022912	8	14.2S	91.7E	100	5	53	174		5	-20	-25	
92030100	9	14.9S	90.6E	110	16	138	264		-10	-30	-30	
92030112	10	15.1S	89.4E	120	5	102	217		0	-10	-5	
92030200	11	15.1S	88.4E	120	0	51	88		0	-5	5	
92030212	12	14.9S	87.5E	115	5	58	108		5	-5	0	
92030300	13	14.8S	86.8E	110	13	55	154		0	0	-20	
92030312	14	15.0S	86.2E	95	8	95	215		-5	-5	-30	
92030400	15	15.5S	85.6E	85	8	53	82		-10	-30	-40	
92030412	16	16.5S	85.1E	80	12	33	140		-15	-30	-50	
92030500	17	17.6S	85.0E	90	6	64	290		-30	-20	-30	
92030512	18	18.7S	85.2E	90	16	73	368		0	-5	-10	
92030600	19	20.0S	85.8E	90	11	140	465		0	-5	0	
92030612	20	21.7S	87.2E	90	16	166			0	-10		
92030700	21	24.4S	89.5E	85	48	380			-5	-10		
92030712	22	28.2S	93.1E	75	41				-10			
92030800	23	32.4S	98.4E	60	11				-5			

AVERAGE	14	89	175	5	11	19
# CASES	23	21	19	23	21	19

TROPICAL CYCLONE 21P (ESAU)

DTG	WRN NO.	BEST TRACK			POSITION ERRORS				WIND ERRORS			
		LAT	LONG	WIND	00	24	48	72	00	24	48	72
92022600	1	15.7S	167.5E	30	29	76	182		0	0	-5	
92022612	2	15.9S	166.8E	40	26	124	240		0	0	-20	
92022700	3	15.8S	165.4E	45	8	42	141		0	0	-35	
92022712	4	15.4S	163.8E	55	59	73	158		0	-20	-45	
92022800	5	15.2S	162.2E	70	13	42	208		0	-40	-25	
92022812	6	14.7S	160.6E	95	8	92	342		-5	-20	-5	
92022900	7	13.9S	159.6E	125	5	114	275		-5	-5	-5	
92022912	8	13.4S	159.4E	130	13	135	265		-5	15	-10	
92030100	9	13.6S	160.1E	115	5	89	210		0	5	-10	
92030112	10	14.4S	160.8E	95	6	63	131		0	-20	-30	
92030200	11	15.3S	161.6E	95	25	75	167		0	-20	-25	
92030212	12	16.1S	162.7E	100	0	52	90		0	-5	0	
92030300	13	16.9S	163.7E	100	6	55	108		-5	-10	10	
92030312	14	18.0S	164.8E	95	0	62	153		0	-5	5	
92030400	15	19.6S	165.3E	90	12	60	257		-5	0	0	
92030412	16	21.2S	165.5E	80	12	85	366		-5	0	-5	
92030500	17	22.8S	165.5E	65	35	169	336		-10	-10	-10	
92030512	18	24.8S	165.9E	60	36	283	372		-15	-10	-15	
92030600	19	28.4S	166.1E	50	20	147			-5	-10		
92030612	20	31.8S	165.7E	45	39				-5			

AVERAGE	18	97	222	3	10	14
# CASES	20	19	18	20	19	18

TROPICAL CYCLONE 22S (FARIDA)

DTG	WRN NO.	BEST TRACK			POSITION ERRORS				WIND ERRORS			
		LAT	LONG	WIND	00	24	48	72	00	24	48	72
92022600	1	15.5S	81.1E	45	29	80	126		-5	-10	-15	
92022606	2	15.9S	80.8E	55	13	18	143		0	10	-15	
92022618	3	16.7S	80.2E	65	30	136	265		0	5	-30	
92022706	4	17.5S	79.3E	80	18	18	37		10	-15	-40	
92022718	5	18.0S	78.0E	85	33	79	145		0	-50	-65	
92022806	6	18.3S	76.8E	105	18	23	49		5	-10	-15	
92022818	7	18.9S	75.7E	120	5	41	127		-5	-20	-25	
92022906	8	19.5S	74.7E	120	8	66	196		5	-10	5	
92022918	9	20.4S	73.7E	115	38	157	386		5	0	10	
92030106	10	21.5S	72.3E	110	34	143	334		5	15	25	
92030118	11	22.4S	70.4E	100	86	285	480		-5	15	30	
92030206	12	23.2S	68.0E	80	11	101			0	10		
92030218	13	24.3S	65.5E	65	5	154			-10	10		
92030306	14	26.1S	63.2E	50	0				-5			
92030318	15	28.3S	61.0E	30	27				0			
AVERAGE					24	100	208		4	14	25	
# CASES					15	13	11		15	13	11	

TROPICAL CYCLONE 23S (IAN)

DTG	WRN NO.	BEST TRACK			POSITION ERRORS				WIND ERRORS			
		LAT	LONG	WIND	00	24	48	72	00	24	48	72
92022618	1	12.4S	114.5E	30	47	241	458		0	0	-20	
92022706	2	12.0S	114.8E	35	41	229	405		0	0	-25	
92022718	3	11.7S	115.4E	40	29	179			-5	-35		
92022806	4	11.7S	116.4E	50	26	120	233		-5	-5	-25	
92022818	5	12.3S	117.0E	70	11	66	196		0	-15	-35	
92022906	6	13.4S	117.3E	90	5	66	174		5	-5	-15	
92022918	7	14.6S	117.3E	100	16	87	155		0	-20	-10	
92030106	8	16.1S	117.2E	105	12	113	171		0	-10	30	
92030118	9	17.8S	116.7E	115	17	24	227		0	-10	40	
92030206	10	19.3S	116.0E	105	11	151			10	35		
92030218	11	20.8S	115.8E	100	12	175			5	50		
92030306	12	22.5S	116.3E	55	16				20			
92030318	13	24.3S	117.8E	25	30				20			
AVERAGE					21	132	252		5	17	25	
# CASES					13	11	8		13	11	8	

TROPICAL CYCLONE 24S (GERDA)

DTG	WRN NO.	BEST TRACK			POSITION ERRORS				WIND ERRORS			
		LAT	LONG	WIND	00	24	48	72	00	24	48	72
92022718	1	15.9S	61.7E	35	8	67	160		0	20	35	
92022806	2	16.9S	61.8E	30	77	225			5	-5		
92022818	3	17.8S	62.3E	30	36				-5			
AVERAGE					40	146	160		3	13	35	
# CASES					3	2	1		3	2	1	

TROPICAL CYCLONE 25P (FRAN)

DTG	WRN NO.	BEST TRACK			POSITION ERRORS				WIND ERRORS			
		LAT	LONG	WIND	00	24	48	72	00	24	48	72
92030706*	3	14.6S	178.4E	90	17	194	345		0	-5	-30	
92030718	4	15.4S	176.1E	100	16	153	308		-10	-40	-10	
92030806	5	16.4S	173.4E	115	6	98	170		-10	-15	0	
92030818	6	17.3S	170.7E	140	5	91	211		0	20	30	

92030818	6	17.3S	170.7E	140	5	91	211	0	20	30
TROPICAL CYCLONE 25P (FRAN) (CONTINUED)										
92030906	7	18.4S	168.4E	130	6	115	319	5	-20	-10
92030918	8	19.2S	166.0E	120	11	69	89	0	-10	5
92031006	9	19.6S	163.7E	110	8	25	61	0	0	0
92031018	10	19.6S	161.4E	100	13	45	158	5	5	-15
92031106	11	19.8S	159.3E	90	8	33	151	0	-20	-25
92031118	12	19.9S	157.6E	85	5	84	214	5	-15	-20
92031206	13	19.9S	156.3E	90	0	120	202	0	0	5
92031218	14	20.0S	155.5E	90	12	127	180	0	5	15
92031306	15	20.6S	155.3E	85	12	16	53	0	5	15
92031318	16	20.8S	154.7E	80	33	110	125	0	10	15
92031406	17	21.0S	153.8E	70	46	49	190	-5	5	5
92031418	18	21.4S	152.8E	60	65	97	313	0	5	0
92031506	19	22.5S	151.9E	50	6	150		-5	-10	
92031518	20	23.8S	151.4E	45	36	239		-5	-20	
92031606	21	24.7S	152.9E	45	0	45		-5	-20	
92031618	22	24.9S	154.6E	45	6			-10		
92031706	23	25.3S	156.2E	45	0			-15		

AVERAGE	15	98	193	4	12	13
# CASES	21	19	16	21	19	16

*Two warnings issued by NWOC

TROPICAL CYCLONE 28S (NEVILLE)

DTG	WRN NO.	BEST TRACK			POSITION ERRORS				WIND ERRORS			
		LAT	LONG	WIND	00	24	48	72	00	24	48	72
92040606	1	9.8S	133.6E	35	18	107	208		0	-5	-50	
92040618	2	10.3S	133.2E	40	35	106	139		0	-15	-65	
92040706	3	10.6S	132.3E	50	29	94	77		-5	-50	-70	
92040718	4	11.0S	131.0E	65	18	79	202		0	-30	-20	
92040806	5	11.1S	129.7E	95	8	89	224		-15	-35	-25	
92040818	6	11.3S	128.8E	115	11	118	228		-5	5	20	
92040906	7	11.5S	128.3E	120	8	46	84		-5	0	10	
92040918	8	11.6S	128.1E	115	8	5	11		10	10	20	
92041006	9	11.6S	127.8E	110	0	17	18		5	20	20	
92041018	10	11.8S	127.2E	100	50	89	104		10	15	25	
92041100	11	11.9S	127.0E	95	41	146	252		10	20	25	
92041106	12	12.0S	126.7E	90	59	169	272		10	15	15	
92041118	13	12.2S	126.2E	80	50	83	135		5	5	5	
92041206	14	12.3S	125.7E	70	8	37	89		5	15	15	
92041218	15	12.5S	125.3E	60	18	58	105		-5	-5	-5	
92041306	16	12.9S	124.9E	50	18	65			-10	-5		
92041318	17	13.1S	124.5E	40	29	58			0	5		
92041406	18	13.5S	124.3E	30	13	66			0	0		

AVERAGE	23	80	143	6	14	26
# CASES	18	18	15	18	18	15

TROPICAL CYCLONE 29S (JANE/IRNA)

DTG	WRN NO.	BEST TRACK			POSITION ERRORS				WIND ERRORS			
		LAT	LONG	WIND	00	24	48	72	00	24	48	72
92040806	1	8.1S	98.6E	35	43	111	184		0	0	15	
92040818	2	8.9S	98.8E	45	32	60	122		5	25	15	
92040906	3	9.8S	99.1E	55	13	74	113		5	20	15	
92040918	4	11.0S	99.6E	55	24	50	79		5	20	20	
92041006	5	12.3S	99.9E	60	18	75	83		0	-20	-35	
92041018	6	13.2S	100.3E	70	71	283	670		5	-15	-25	
92041100	7	13.5S	100.4E	75	21	97	278		-10	-15	-25	

TROPICAL CYCLONE 29S (JANE/IRNA) (CONTINUED)

92041118	9	14.0S	99.8E	80	42	231	464	0	-10	-40
92041206	10	14.2S	98.2E	80	41	202	422	5	-15	-60
92041218	11	14.6S	95.9E	80	26	111	250	0	-20	-55
92041306	12	15.0S	93.3E	85	47	68	123	-10	-45	-60
92041318	13	15.0S	90.7E	95	18	79	69	-5	-40	-45
92041400	14	14.8S	89.5E	105	8	42	52	5	0	0
92041406	15	14.7S	88.4E	115	0	26	85	0	0	10
92041418	16	14.5S	86.3E	120	8	107	314	5	5	35
92041506	17	14.7S	84.6E	120	11	50	191	0	10	30
92041518	18	15.2S	83.4E	115	25	149	320	-5	20	15
92041606	19	15.7S	82.8E	100	50	175	350	5	25	15
92041618	20	16.4S	83.1E	75	5	115		0	-10	
92041706	21	17.2S	84.1E	55	16	246		0	-10	
92041718	22	17.2S	85.8E	50	23			-5		
92041806	23	17.0S	87.7E	45	8			-15		

AVERAGE	24	117	236	4	16	28
# CASES	23	21	19	23	21	19

TROPICAL CYCLONE 30P (INNIS)

DTG	WRN NO.	BEST TRACK			POSITION ERRORS				WIND ERRORS			
		LAT	LONG	WIND	00	24	48	72	00	24	48	72
92042818	1	11.3S	172.2E	35	16	115	294		0	-15	5	
92042906	2	12.3S	170.6E	50	8	34	263		5	10	30	
92042918	3	13.5S	169.5E	65	32	66	231		0	20	35	
92043006	4	14.6S	168.8E	65	18	159	646		-10	-10	-10	
92043018	5	16.2S	169.0E	65	44	345			-15	-10		
92050106	6	18.0S	170.7E	55	77	416			-15	-10		
92050118	7	20.4S	173.9E	50	28				-15			
92050206	8	23.6S	178.7E	40	56				-5			

AVERAGE	35	189	359	8	13	20
# CASES	8	6	4	8	6	4

Intentionally left blank

7. TROPICAL CYCLONE SUPPORT SUMMARY

7.1 AN UPDATED VALUE ANALYSIS OF JTWC WARNING SUPPORT

Lt Col Chip Guard
Joint Typhoon Warning Center, Guam

A comprehensive analysis of the costs of western North Pacific DOD typhoon preparations, the value of JTWC support, and the cost effectiveness of the USPACOM Tropical Cyclone Warning System was accomplished. The study analyzes the warning process at JTWC, describes various typhoon strike scenarios, explains the value of credibility, considers both tangible and intangible costs and benefits, ascertains port/facility costs for typhoon preparation, illustrates the value of resources at risk, and finally computes the cost-benefit ratio of the Warning System. The analysis provides a baseline for future assessments whenever support requirements change. (It will be published as a NOCC/JTWC Technical Note.)

7.2 A TROPICAL CYCLONE WIND SPEED VERSUS DAMAGE SCALE FOR THE TROPICAL WESTERN PACIFIC

Lt Col Chip Guard
Joint Typhoon Warning Center, Guam
and

Dr. Mark A. Lander
University of Guam

A scale that relates tropical cyclone wind speed to potential structural, agricultural, and coastal damage has been developed for use in the tropical western Pacific Ocean. The scale employs the basic model of the Saffir-Simpson Hurricane Scale which has been used for many years along the Atlantic and Gulf of Mexico coastal areas of the United States. It incorporates construction materials and plant life that

are common to the tropical Pacific region, and considers the structural weakening of wood from termites and wet and dry wood rot. The scale also modifies expected storm surge values of the Saffir-Simpson Hurricane Scale to account for the effects of island near-shore bottom topography (such as fringing coral reefs) on storm surge, wind-driven waves, and near-coastal surf action. Because many of the islands of the tropical Pacific contain crops and shelters that are highly susceptible to damage by sub-hurricane-force winds, the scale addresses the potential damage from the winds and seas associated with tropical depressions and tropical storms as well as with typhoons. The scale has good potential for application in other tropical cyclone-prone areas in the global tropical belt. The paper will be submitted to a meteorological journal, and a User's Manual has been completed and will be published as an NOCC/JTWC Technical Note.

7.3 MIDGET TROPICAL CYCLONES: A SURVEY AND DESCRIPTION

Dr. Mark A. Lander
University of Guam
and

Lt Col Chip Guard
Joint Typhoon Warning Center, Guam

This paper attempts to distill from historical accounts, technical studies, and recent observations, a descriptive climatology of midget tropical cyclones (MTCs). A definition of the MTC is presented. Several examples of MTCs are provided to illustrate the special diagnostic and forecast problems associated with these storms. An argument is presented that the MTC is a unique subset of tropical cyclones possessing a unique set of characteristics, and not merely a continuum of smaller than normal tropical

cyclones based solely on size. These unique characteristics are identified and a physical model is presented. Foremost among these are the presence of inner core winds only (no significant outer core winds), rapid intensity changes, and preferred areas for genesis under specific synoptic conditions. Techniques for analysis, satellite interpretation, and forecasting are presented. The paper will be submitted to a meteorological journal for publication.

7.4 AN EXPLORATORY ANALYSIS OF THE RELATIONSHIP BETWEEN TROPICAL STORM FORMATION IN THE WESTERN NORTH PACIFIC AND EL NINO-SOUTHERN OSCILLATION (ENSO)

Dr. Mark A. Lander
University of Guam

Observed annual tropical cyclone (TC) totals in the western North Pacific are virtually uncorrelated with any ENSO index, a finding which supports earlier work by Ramage and Hori (1981). The only statistically significant relationship found in this study between an ENSO index and a statistic of TC totals was the reduction in the number of Early Season storms during years when the Southern Oscillation index starts out relatively low and rises sharply by the middle of the year.

It is very clear that the ENSO cycle plays a major role in the interannual fluctuation of the annual mean genesis location of TCs in the western North Pacific. In order to show this relationship, the NOAA Climate Analysis Center's monthly values of the Southern Oscillation index were averaged in 11-month (March through January) intervals ($\langle \text{SOI} \rangle$). When the $\langle \text{SOI} \rangle$ is low and the SST in the central and eastern equatorial Pacific is warmer than normal, the genesis region for TCs in the western North Pacific shifts eastward; when the $\langle \text{SOI} \rangle$ is very high and the SST of the central

and eastern equatorial Pacific is cooler than normal (so-called, "la nina" or cold event conditions) the annual average genesis location shifts westward.

During a given year, the TC distribution and the preferred areas for genesis are governed primarily by the location and the behavior of the monsoon trough. ENSO plays a significant part in the complex behavior of the regional circulation of the western North Pacific, particularly with respect to the eastward extent of penetration of monsoonal westerly winds in the western North Pacific. During low $\langle \text{SOI} \rangle$ years, the monsoonal westerly winds penetrate further to the east than during most other years, and the average annual genesis location of the TCs is found east of normal. This eastward displacement of cyclogenesis is greatest during the Late Season of low $\langle \text{SOI} \rangle$ years (Figure 1). During high $\langle \text{SOI} \rangle$ years, the monsoon trough, on average, does not penetrate as far to the east as it does during low $\langle \text{SOI} \rangle$ years, and the annual mean genesis location is found west of normal, particularly during the Early and Late Season. Many of the TCs that form to the east of normal during the Mid Season of high $\langle \text{SOI} \rangle$ years are induced north of 20°N in low-level easterly flow by overlying or peripheral TUTT cells. Most of the TCs that form to the east of normal during low $\langle \text{SOI} \rangle$ years form south of 20°N at the eastern terminus of an eastward-displaced monsoon trough (Figure 1).

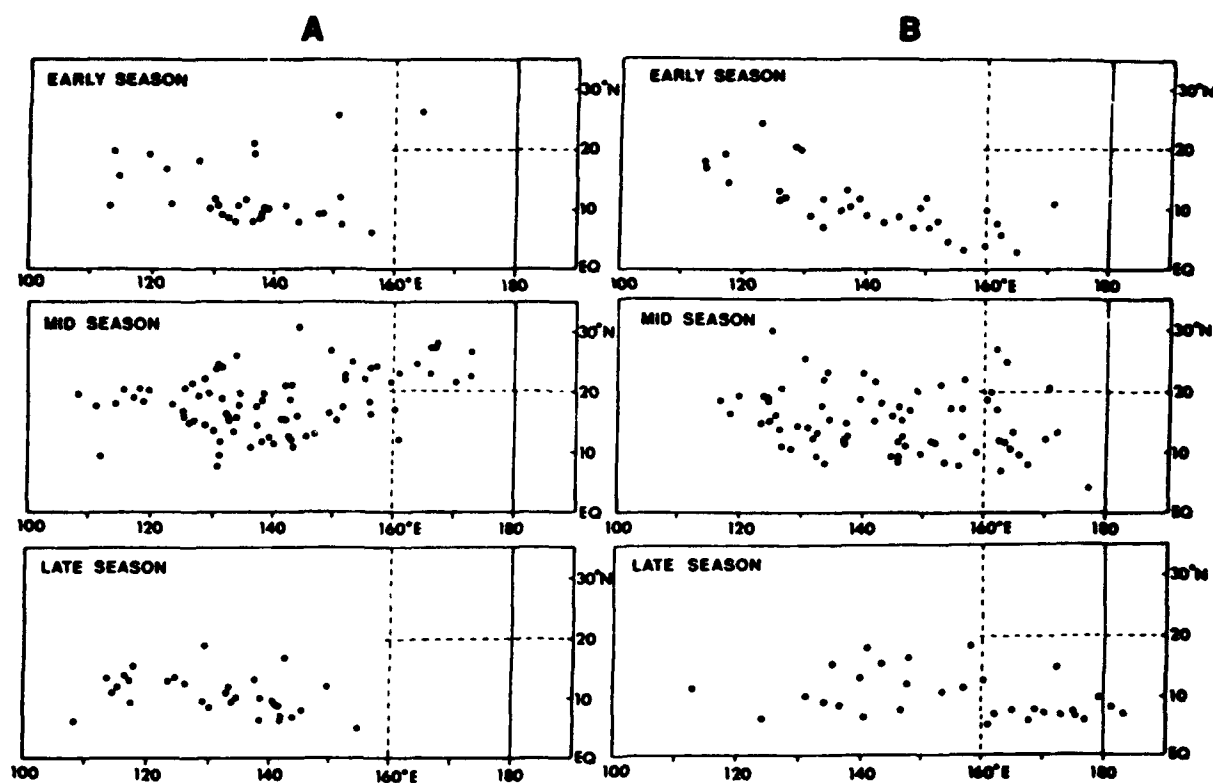


Figure 1. Origins of tropical cyclones by season (Early Season — March through mid-July; Mid-Season — mid-July through mid-October; Late Season — mid-October through January) for the five years during the period 1970-1991 with the five highest values of $\langle \text{SOL} \rangle$ (column A), and for the five years with the lowest values of $\langle \text{SOL} \rangle$ (column B). Note: origin is defined as the location where tropical depression intensity first appears on the JTWC final best track.

7.5 AUTOMATED TROPICAL CYCLONE BINARY INTERACTION ANALYSIS AND FORECASTING

Captain Steven C. Hallin, USAF
Joint Typhoon Warning Center, Guam

7.5.1 ANALYSIS

In order to update existing hand plotted techniques, an automated technique for the analysis of binary systems has been developed. This technique uses analytical techniques developed in previous studies (Brand, 1970; Dong and Neumann, 1983; Lander and Holland, 1993) which have emphasized the importance of plotting the tracks of the two tropical cyclones relative to the centroid, calculating the

separation distance between them, and calculating orbit rates around the centroid. Typical features of a binary interaction, as seen in the centroid-relative tracks, are summarized in Figure 2.

The primary, and most reliable, parameter used in diagnosing the onset of binary interaction is the separation distance. The average distance at which binary interaction is initiated is approximately 750 nm (1400 km or approximately 12° of longitude) (Brand, 1970), although in practice, capture or escape can occur at substantially different distances. A real-time calculation of the orbit rates around the centroid provides another objective measure of the onset of interaction. To use the orbit rate in determining the onset of binary interaction,

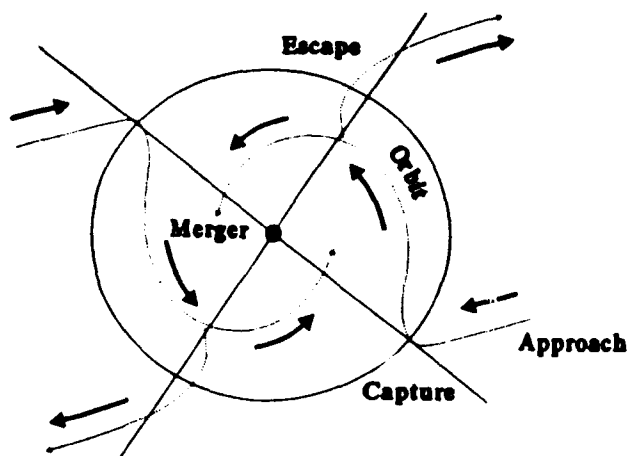


Figure 2. Model of binary interaction of two cyclonic, mesoscale vortices, containing the major elements of approach and capture, followed by mutual orbit, then release and escape, or merger (from Lander and Holland, 1993).

the following rule of thumb is applied: if the separation distance is greater than 750 nm, a delay of the diagnosis of binary interaction is suggested until a cyclonic orbit rate of at least two degrees per six hours has been established for 12 hours. If the separation distance is less than average, then six hours of any amount of cyclonic orbit rate should suffice to establish that interaction has commenced. Deviations from the idealized case shown in Figure 2 can be manifested as periods of transient binary interaction, periods of weak binary interaction, fluctuating orbit rates, and nonstandard capture and escape distances. These deviations may occur due to external influences or size variability in the tropical cyclones.

Figures 3 and 4 show the interaction between Typhoons Brian (25W) and Colleen (26W) in October 1992. Figure 3 is a common centroid-relative pattern for a binary interaction (Lander and Holland, 1993). In earth-relative coordinates, the system to the west will typically exhibit a slow, erratic, looping motion as occurred with Colleen. The other tropical cyclone, in this case Brian, will accelerate toward the northwest after a noticeable bifurcation in its track, and then track around the subtropical

ridge as it escapes and recurves. In Figure 4, the significant cyclonic rotation started on 201200Z October at a greater than average distance, e.g. 12-18 hours before the separation distance reached the 750 nm threshold, and increased as the systems approached. Brian escaped the interaction on 231800Z October as indicated by the increase in separation. The actual tracks of Typhoons Brian (25W) and Colleen (26W) are shown in Chapter 3, Section 3.2 Western North Pacific Tropical Cyclones.

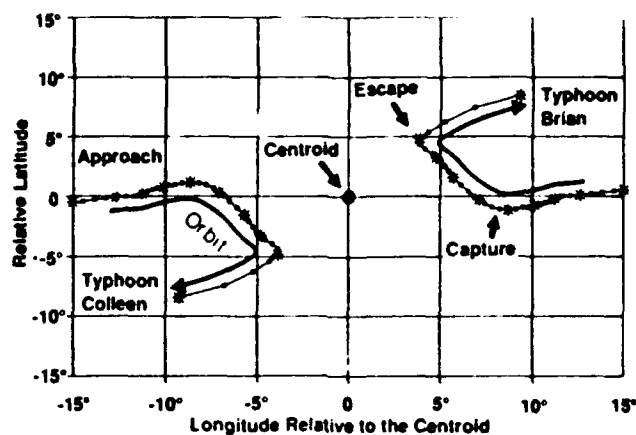


Figure 3 Centroid relative positions for Typhoons Brian (25W) and Colleen (26W).

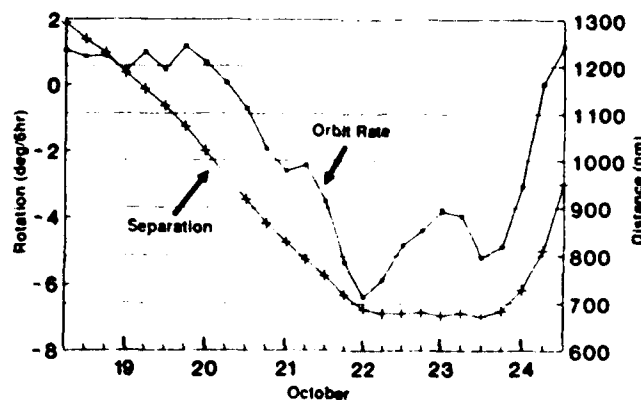


Figure 4. Time series of separation and orbit rate for the interaction between Typhoons Brian (25W) and Colleen (26W). Negative orbit rates indicate cyclone rotation.

The analysis of this particular binary interaction was of considerable operational importance since Brian's track deviation due to the capture in a binary orbit with Colleen directed the typhoon over Guam on 21 October. On 24 October, the interaction ended as Brian escaped into the westerlies.

7.5.2 FORECASTING

After determining that binary interaction is occurring, it is possible to calculate the forecast positions of the binary pair based on the separation distance and the orbit rate coupled with a forecast of the motion of the centroid. For this study, the centroid track forecast is based on CLIPER (Xu and Neumann, 1985). The binary interaction forecast aid developed at JTWC, called FUJI, can then be applied. Its application should be tempered with an understanding that in the western North Pacific very few (less than 25%) of the binary systems merge and, the member of the binary pair to the northeast will most probably be the one to escape the interaction and recurve (Lander and Holland, 1993). Preliminary verification statistics on FUJI show reasonable one to two day guidance, which deteriorates at the three day point. The technique has been expanded to produce centroid track forecasts using other forecast models (e.g. NOGAPS) in addition to CLIPER.

7.6 TROPICAL CYCLONE INTENSITY AND THE LENGTH OF DEEP CONVECTIVE RAINBANDS AS DETECTED BY THE SSM/I SENSOR

Captain Steven C. Hallin, USAF
Joint Typhoon Warning Center, Guam

A set of 26 DMSP satellite passes over 15 western North Pacific tropical cyclones that occurred between 1990 and 1992 was studied to test the hypothesis that the length of rainband signatures on the SSM/I imagery can be related to the intensity of tropical cyclones. After reviewing the work of Glass and Felde (1990), which found a good relationship between the amount of deep convection (as measured on the 85-horizontally-polarized (85h) GHz channel) and intensity, the next step was to see if the length of the deep convective rainbands could be objectively measured on the 85h GHz channel. Each 85h GHz image was processed at a specific threshold temperature that best recovered the rainband detail, the arcs of the deep convective rainbands were curve-fitted to an overlaid 10° logarithmic spiral, and the arc length was measured in tenths of a complete wrap similar to the curved cloud band technique used by Dvorak (1984). The arc lengths were then plotted against the corresponding best track

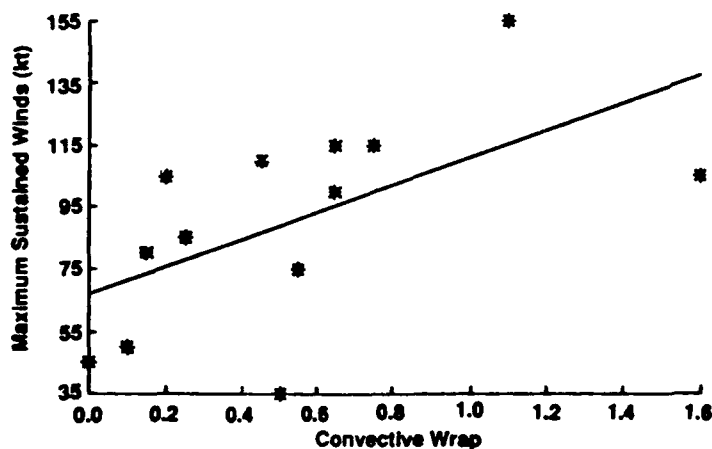


Figure 5. The relationship between the convective wrap of deep convection using a threshold brightness temperature of 205°K and maximum sustained winds for intensifying tropical cyclones. Parameters correlate at 0.82 which explains 90% of the variance. The standard error is 14 kt.

intensities. Separating the intensifying cases from the weakening cases, provided the most useful relationship. For the weakening cases, the use of a colder threshold temperature on the SSM/I data yielded better correlations between arc length and best track intensity. The results of the study are provided in Figures 5 and 6.

In summary, the hypothesis that the length of rainbands on the 85h GHz microwave channel can be related to the intensity of tropical cyclones appears to be valid. Because of the success of the Dvorak technique, which decomposes the visual and infrared satellite images into banding and central cloud features, the application of a Dvorak-like approach to the intensity estimation information latent in the SSM/I rainband signatures is appropriate.

7.7 TROPICAL CYCLONE FORECASTER'S REFERENCE GUIDE

Sampson, C.R., Jan-Hwa Chu

and

Lt. R.A. Jeffries

Naval Research Lab (NRL), Marine

Meteorology Division, Monterey, CA

Development of a Tropical Cyclone Forecaster's Reference Guide continues. The guide consists of seven chapters. They are (1) Tropical Cyclone Warning Support, (2) Tropical Climatology, (3) Tropical Cyclone Formation, (4) Motion, (5) Forecast Aids, (6) Intensity, and (7) Structure. The first three chapters have been published as Technical Notes (available from NRL). The other four chapters are in preparation. The chapter-by-chapter publishing format not only makes the edition and inclusion of updated information easy, but also provides tropical meteorology training notes for aerographers. After all of the chapters are complete, they will be transferred to an interactive video disk format, saving considerable storage space which is especially important for shipboard use.

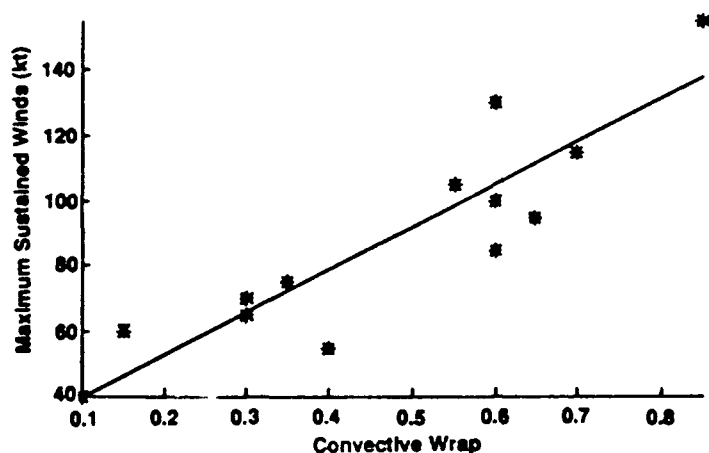


Figure 6. Same as Figure 5 except for weakening tropical cyclones using a threshold brightness temperature of 217°K. Parameters correlate at 0.34 and account for only 58% of the variance. The standard error is 28 kt.

7.8 A REGRESSION MODEL FOR THE WESTERN NORTH PACIFIC TROPICAL CYCLONE INTENSITY FORECAST

Jan-Hwa Chu and C.R. Sampson
Naval Research Lab (NRL), Marine
Meteorology Division, Monterey, CA

A regression model forecasting the tropical cyclone intensity in the western North Pacific was derived by using the nineteen-year (1971-1989) post-analysis best track data from JTWC which includes the date, time and location of the cyclone's circulation center, and the observed maximum sustained wind speed (1-minute average at 10-meter elevation). The term intensity refers to the estimated maximum sustained 1-minute surface wind speed associated with a cyclone. This model provides intensity forecasts for 12-hour intervals up to 72 hours. The verification of the model's forecasts for data from 1990 is discussed. An operational version of this regression model, Statistic Typhoon Intensity Forecast (SHIFOR), was delivered to the Fleet Numerical Oceanography Center for operational testing. This model is based on the SHIFOR model (Jarvinen and Newmann, 1979) used at the National Hurricane Center. A technical report on this model will be published.

7.9 AUTOMATED TROPICAL CYCLONE FORECASTING SYSTEM (ATCF) UPGRADE

T.L. Tsui, A.J. Scrader, Lt R.A. Jeffries
and
C.R. Sampson
Naval Research Lab (NRL), Marine
Meteorology Division, Monterey, CA

The ATCF has been operational at JTWC since 1988. The current system runs on an IBM-DOS operating system. NRL, Monterey is adapting ATCF to the UNIX operating system

under the program direction of the Space Warfare and Systems Command. The new ATCF will use industry standard X-Window/Motif for window management and will communicate with the Tactical Environmental Support System (TESS 3.0). The first phase of the project is expected to be completed in the summer of 1995.

7.10 PROTOTYPE AUTOMATED TROPICAL CYCLONE HANDBOOK (PATCH)

C.R. Sampson and Lt. R.A. Jeffries
Naval Research Lab (NRL)
Marine Meteorology Division, Monterey, CA

PATCH is an expert system designed to provide tropical cyclone forecast and training guidance to JTWC for the western North Pacific Ocean. The scope of the project has expanded to include expertise pertaining to tropical cyclone formation, motion, intensification and dissipation, and structure and structure change. The motion section is under evaluation and in the future will include forecasting expertise currently under development at the Naval Postgraduate School. The expert system is an integral part of the ATCF upgrade.

7.11 TROPICAL CYCLONE MOTION-92 (TCM-92) MINI-FIELD EXPERIMENT

Professor Russell L. Elsberry
Naval Postgraduate School, Monterey, CA

The Naval Postgraduate School (NPS) and the Office of Naval Research (ONR) Marine Meteorology Program co-sponsored a mini-field experiment near Guam during July-August 1992. The Experiment Operations Center was located at JTWC, which provided space, shared its meteorological data bases and facilitated the TCM-92 operations. JTWC TDOs participated in routine meteorological discussions.

The objectives and organization of the experiment were described in the TCM-92 Operations Plan (Elsberry et al., 1992), which also summarized recent research that has investigated short-duration tropical cyclone track deviations. TCM-92 tested the following hypotheses:

1) Long-lived tropical Mesoscale Convective Systems (MCS) have a three-dimensional wind and thermal structure similar to a midtropospheric vortex in the stratiform rain region of a midlatitude MCS, and have sufficient horizontal extent to cause a mutual interaction with a tropical storm or weak typhoon via a Fujiwhara-type effect that results in track deviations of the order of 100 km a day.

2) Long-lived tropical MCSs that maintain a quasi-stationary position relative to an associated tropical cyclone cause approximately 100 km deflections in the cyclone track via a divergent circulation and its interaction with the symmetric vorticity field to create a wavenumber one asymmetric circulation.

3) Relative cyclone track displacement of a MCS and a tropical cyclone can be related to their radial positions within the horizontal wind shear field of an active monsoon trough.

4) Tropical cyclone genesis is caused by the merger of two or more interacting MCSs to create a single system with greater vorticity.

During the period of 21 July 1992 to 21 August 1992, USAF Reserve WC-130 aircraft and crews of the 815th Tactical Airlift Squadron, Keesler Air Force Base, Mississippi deployed to the western North Pacific. Operating from Guam, crews flew nine missions of 9-13 hours duration into tropical cyclones and nearby MCS to collect flight-level and dropwindsonde observations in support of the TCM-92 mini-field experiment as described in the NPS Technical Report (Dunnavan et al., 1992). A M.S. thesis at NPS by Captain Eric McKinley (USAF) compares the observations from the most pronounced MCS during

Intensive Observing Period (IOP) 7 verses a weak MCS during IOP 1. Four papers describing the preliminary results from TCM-92 will appear in the Preprints of the American Meteorological Society 20th Conference on Hurricanes and Tropical Meteorology (Boothe et al., 1993; Dunnavan et al., 1993; McKinley and Elsberry, 1993; and Ritchie, 1993).

BIBLIOGRAPHY

Atkinson, G. D. and C. R. Holliday, 1977: Tropical cyclone minimum sea-level pressure and maximum sustained wind relationship for the western North Pacific. *Monthly Weather Review*, Vol. 105, No. 4, pp 421-427. (also Fleet Weather Central/JTWC Technical Note 75-1).

Boothe, M.A., P.A. Harr and R.L. Elsberry, 1993: Interaction between a mesoscale convective system and the large-scale monsoon flow during TCM-92. Preprints, 20th Conf. on Hurr. and Trop. Meteor., (Paper 15A.3).

Brand, S., 1970: Interaction of binary tropical cyclones of the western North Pacific Ocean. *Journal of Applied Meteorology*, Vol. 9, pp 433-441.

Bureau of Meteorology (Northern Territory Region), 1992: Darwin Tropical Diagnostic Statement(s), Jan through Dec. The Regional Director, Bureau of Meteorology, GPO Box 735, Darwin, Northern Territory 0801, Australia.

Diercks, J. M., R. C. Weir and M. K. Kopper, 1982: Forecast Verification and Reconnaissance Data for Southern Hemisphere Tropical Cyclones (July 1980 through June 1982). NOCC/JTWC Technical Note 82-1, 77 pp.

Dong, K. and C. J. Neumann, 1983: On the relative motion of binary tropical cyclones. *Monthly Weather Review*, Vol. 111, pp 945-953.

Dunnavan, G. M., 1981: Forecasting Intense Tropical Cyclones Using 700 mb Equivalent Potential Temperature and Central Sea-Level Pressure. NOCC/JTWC Technical Note 81-1, 12 pp.

Dunnavan, G. M., E. J. McKinley, P. A. Harr, E. A. Ritchie, M. A. Boothe, M. A. Lander and R. L. Elsberry, 1992: Tropical Cyclone Motion (TCM-92) mini-field experiment summary. Tech. Report NPS-MR-93-001, Naval Postgraduate School, Monterey, CA 93943.

Dunnavan, G.M., R.L. Elsberry, P.A. Harr, E.J. McKinley and M.A. Boothe, 1993: Overview of the 1992 Tropical Cyclone Motion (TCM-92) mini-field experiment. Preprints, 20th Conf. on Hurr. and Trop. Meteor., (Paper 15A.1).

Dvorak, V. F., 1975: TC Intensity Analysis and Forecasting from Satellite Imagery. *Monthly Weather Review*, Vol 103, No. 5, pp 420-430.

Dvorak, V. F., 1984: Tropical Cyclone Intensity Analysis Using Satellite Data. NOAA Technical Report NESDIS 11, 46 pp.

Elsberry, R.L., G.M. Dunnavan and E.J. McKinley, 1992: Operations plan for the tropical cyclone motion (TCM-92) mini-field experiment. Tech. Report NPS-MR-92-002, Naval Postgraduate School, Monterey, CA 93943, 46 pp.

Glass, M., and G.W. Felde, 1990: Tropical storm structure analysis using SSM/I and OLS data. 5th Intl. Conf. on Interactive and Info. Processing Systems for Meteor., Oceanogr. and Hydrol., Anaheim, CA, Amer. Meteor. Soc., 432-437.

Guard, C.P., 1983: A Study of Western North Pacific Tropical Storms and Typhoons that Intensify after Recurvature. First Weather Wing Technical Note-83/002, 28 pp.

Herbert, P. H. and K. O. Poteat, 1975: A Satellite Classification Technique for Subtropical Cyclones. NOAA Technical Memorandum NWS SR-83, 25 pp.

Holland, G. J., 1980: An analytical model of wind and pressure profiles in hurricanes. *Monthly Weather Review*, Vol. 108, No. 8, pp 1212-1218.

Holland, G.J. and M.A. Lander, 1992: On the meandering nature of tropical cyclone tracks. *Journal of the Atmospheric Sciences* (in press).

Holliday, C. R. and A. H. Thompson, 1979: Climatological characteristics of rapidly intensifying typhoons. *Monthly Weather Review*, Vol. 107, pp 1022-1034.

Jarvinen, B.R. and C.J. Neumann, 1979: Statistical forecast of tropical cyclone intensity. NOAA Technical Memorandum NWS NHC-10, 22pp.

Jarrell, J.D., S. Brand and D.S. Nicklin, 1978: An analysis of western Pacific tropical cyclone forecast errors. *Monthly Weather Review*, 106, 925-937.

JTWC, 1991: Tropical Cyclones Affecting Guam (1671-1990). NOCC/JTWC Technical Note 91-2, 45 pp.

Lander, M. A., 1990: Evolution of the cloud pattern during the formation of tropical cyclone twins symmetrical with respect to the equator. *Monthly Weather Review*, Vol. 118, No. 5, pp 1194-1202.

Lander, M.A., 1993: A case study of the low-level summer monsoon circulation of the western North Pacific as a large-scale cyclonic gyre. Preprint Volume of the 20th Conference on Hurricanes and Tropical Meteorology. May 10-14, 1993, San Antonio, TX, pp 463-466.

Lander, M. A. and G. J. Holland, 1993: On the interaction of tropical-cyclone scale vortices: I. Observations. *Quarterly Journal of the Royal Meteorological Society*, (in press).

Matsumoto, C. R., 1984: A Statistical Method for One-to Three-Day Tropical Cyclone Track Prediction. Colorado State University Department of Atmospheric Science, Paper 379, 201 pp.

McKinley, E. J., 1992: An analysis of mesoscale convective systems observed during the 1992 Tropical Cyclone Motion field experiment. M.S. Thesis, Naval Postgraduate School, Monterey, CA 93943, 101 pp.

McKinley, E.J., and R.L. Elsberry, 1993: Observations during TCM-92 of the role of tropical mesoscale convective systems in tropical cyclogenesis. Preprints, 20th Conf. on Hurr. and Trop. Meteor., (Paper 13A.3).

Mundell, D.B., 1990: Prediction of Tropical Cyclone Rapid Intensification Events. Thesis for fulfillment of Master's degree submitted to Colorado State University, 186 pp.

OFCM, 1993: National Hurricane Operations Plan, U.S. Dept. of Commerce, Washington, D.C., p E-1.

Ramage, C.S., and A.M. Hori, 1981: Meteorological aspects of El Nino. *Monthly Weather Review*, 109, 1827-1835.

Ritchie, E.A., 1993: Contributions by mesoscale convective systems to the formation of tropical cyclones. Preprints, 20th Conf. on Hurr. and Trop. Meteor., (Paper 13A.5).

Sadler, J. C. 1979: Tropical Cyclone Initiation by the Upper-Tropospheric Trough. Naval Environmental Prediction Research Facility Technical Paper No. 2-76, 103 pp.

Weatherford, C.L. and W.M. Gray, 1985: Typhoon Structural Variability. Colorado State University Department of Atmospheric Science, Paper No. 391, 77 pp.

Weir, R. C., 1982: Predicting the Acceleration of Northward-moving Tropical Cyclones using Upper-Tropospheric Winds. NAVOCEANCOMCEN/JTWC Tech Note 82-2, 40 pp.

Wirfel, W. P. and S. A. Sandgathe, 1986: Forecast Verification and Reconnaissance Data for Southern Hemisphere Tropical Cyclones (July 1982 through June 1984). NOCC/JTWC Technical Note 86-1, 102 pp.

Xu, Y. and C. J. Neumann, 1985: A Statistical Model for the Prediction of Western North Pacific Tropical Cyclone Motion. NOAA Technical Memorandum NWS NHC 28, 30 pp.

APPENDIX A DEFINITIONS

BEST TRACK - A subjectively smoothed path, versus a precise and very erratic fix-to-fix path, used to represent tropical cyclone movement, and based on an assessment of all available data.

CENTER - The vertical axis or core of a tropical cyclone. Usually determined by cloud vorticity patterns, wind and/or pressure distribution.

EPHEMERIS - Position of a body (satellite) in space as a function of time; used for gridding satellite imagery. Since ephemeris gridding is based solely on the predicted position of the satellite, it is susceptible to errors from vehicle wobble, orbital eccentricity, the oblateness of the Earth, and variation in vehicle speed.

EXPLOSIVE DEEPENING - A decrease in the minimum sea-level pressure of a tropical cyclone of 2.5 mb/hr for at least 12 hours or 5.0 mb/hr for at least six hours (Dunnavan, 1981).

EXTRATROPICAL - A term used in warnings and tropical summaries to indicate that a cyclone has lost its "tropical" characteristics. The term implies both poleward displacement from the tropics and the conversion of the cyclone's primary energy source from the release of latent heat of condensation to baroclinic processes. It is important to note that cyclones can become extratropical and still maintain winds of typhoon or storm force.

EYE - The central area of a tropical cyclone when it is more than half surrounded by wall cloud.

FUJIWHARA EFFECT - A binary interaction where tropical cyclones within about 750 nm (1390 km) of each other begin to rotate about a common midpoint (Brand, 1970; Dong and

Neumann, 1983).

INTENSITY - The maximum sustained 1-minute mean surface wind speed, typically within one degree of the center of a tropical cyclone.

MAXIMUM SUSTAINED WIND - The highest surface wind speed averaged over a 1-minute period of time. (Peak gusts over water average 20 to 25 percent higher than sustained winds.)

MONSOON DEPRESSION - a tropical cyclonic vortex characterized by: 1) its large size, the outermost closed isobar may have a diameter on the order of 600 nm (1000 km); 2) a loosely organized cluster of deep convective elements; 3) a low-level wind distribution which features a 100-nm (200-km) diameter light-wind core which may be partially surrounded by a band of gales; and, 4) a lack of a distinct cloud system center. Note: most monsoon depressions which form in the western North Pacific eventually acquire persistent central convection and accelerated core winds marking its transition into a conventional tropical cyclone.

MONSOON GYRE - a mode of the summer monsoon circulation of the western North Pacific characterized by: 1) a large nearly circular low-level cyclonic vortex that has an outermost closed isobar with diameter on the order of 1200 nm (2500 km); 2) a cloud band rimming the southern through eastern periphery of the vortex/surface low; 3) a relatively long (two week) life span - initially, a subsident regime exists in its core and western and northwestern quadrants with light winds and scattered low cumulus clouds; later, the area within the outer closed isobar may fill with deep convective cloud and become a monsoon depression or

tropical cyclone; and, 4) the large vortex cannot be the result of the expanding wind field of a preexisting monsoon depression or tropical cyclone. Note: a series of small or midget tropical cyclones may emerge from the "head" or leading edge of the peripheral cloud band of a monsoon gyre (Lander, 1993).

RAPID DEEPENING - A decrease in the minimum sea-level pressure of a tropical cyclone of 1.75 mb/hr or 42 mb for 24-hours (Holliday and Thompson, 1979).

RECURVATURE - The turning of a tropical cyclone from an initial path toward the west and poleward to east and poleward, after moving poleward of the mid-tropospheric subtropical ridge axis.

SIGNIFICANT TROPICAL CYCLONE - A tropical cyclone becomes "significant" with the issuance of the first numbered warning by the responsible warning agency.

SIZE - The areal extent of a tropical cyclone, usually measured radially outward from the center to the outer-most closed isobar.

STRENGTH - The average wind speed of the surrounding low-level wind flow, usually measured within one to three degrees of the center of a tropical cyclone (Weatherford and Gray, 1985).

SUBTROPICAL CYCLONE - A low pressure system that forms over the ocean in the subtropics and has some characteristics of a tropical circulation, but not a central dense overcast. Although of upper cold low or low-level baroclinic origins, the system can transition to a tropical cyclone.

SUPER TYPHOON - A typhoon with maximum sustained 1-minute mean surface winds of 130 kt (67 m/sec) or greater.

TROPICAL CYCLONE - A non-frontal, migratory low-pressure system, usually of synoptic scale, originating over tropical or subtropical waters and having a definite organized circulation.

TROPICAL DEPRESSION - A tropical cyclone with maximum sustained 1-minute mean surface winds of 33 kt (17 m/sec) or less.

TROPICAL DISTURBANCE - A discrete system of apparently organized convection, generally 100 to 300 nm (185 to 555 km) in diameter, originating in the tropics or subtropics, having a non-frontal, migratory character and having maintained its identity for 12- to 24-hours. It may or may not be associated with a detectable perturbation of the low-level wind or pressure field. It is the basic generic designation which, in successive stages of development, may be classified as a tropical depression, tropical storm, typhoon or super typhoon.

TROPICAL STORM - A tropical cyclone with maximum 1-minute mean sustained surface winds in the range of 34 to 63 kt (17 to 32 m/sec), inclusive.

TROPICAL UPPER-TROPOSPHERIC TROUGH (TUTT) - A dominant climatological system and a daily upper-level synoptic feature of the summer season, over the tropical North Atlantic, North Pacific and South Pacific Oceans (Sadler, 1979).

TYPHOON (HURRICANE) - A tropical cyclone with maximum sustained 1-minute mean surface winds of 64 to 129 kt (33 to 66 m/sec). West of 180 degrees east longitude they are called typhoons and east of 180 degrees east longitude hurricanes.

WALL CLOUD - An organized band of deep cumuliform clouds that immediately surrounds the central area of a tropical cyclone. The wall cloud may entirely enclose or partially surround the center.

APPENDIX B

NAMES FOR TROPICAL CYCLONES IN THE WESTERN NORTH PACIFIC AND SOUTH CHINA SEA

Column 1		Column 2		Column 3		Column 4	
ANGELA	AN-gel-ah	ABE	ABE	AMY	A-mee	AXEL	AX-ell
BRIAN	BRY-an	BECKY	BECK-ee	BRENDAN	BREN-dan	BOBBIE	BOB-ee
COLLEEN	COL-leen	CECIL	CEE-cil	CAITLIN	KATE-lin	CHUCK	CHUCK
DAN	DAN	DOT	DOT	DOUG	DUG	DEANNA	dee-AN-na
ELSIE	ELL-see	ED	ED	ELLIE	ELL-ee	ELI	EE-lye
FORREST	FOR-rest	FLO	FLO	FRED	FRED	FAYE	FAY
GAY	GAY	GENE	GEEN	GLADYS	GLAD-iss	GARY	GAR-ee
HUNT	HUNT	HATTIE	HAT-ee	HARRY	HAR-ee	HELEN	HELL-en
IRMA	IR-ma	IRA	EYE-ra	IVY	EYE-vee	IRVING	ER-ving
JACK	JACK	JEANA	JEAN-ah	JOEL	JOLE	JANIS	JAN-iss
KORYN	ko-RIN	KYLE	KYE-ell	KINNA	KIN-na	KENT	KENT
LEWIS	LOU-iss	LOLA	LOW-lah	LUKE	LUKE	LOIS	LOW-iss
MARIAN	MAH-rian	MANNY*	MAN-ee	MELISSA*	meh-LISS-ah	MARK	MARK
NATHAN	NAY-than	NELL	NELL	NAT	NAT	NINA	NEE-nah
OFELIA	oh-FEEL-ya	OWEN	OH-en	ORCHID	OR-kid	OSCAR*	OS-car
PERCY	PURR-see	PAGE	PAGE	PAT	PAT	POLLY	PA-lee
ROBYN	ROB-in	RUSS	RUSS	RUTH	RUTH	RYAN	RYE-an
STEVE	STEEV	SHARON	SHAR-on	SETH	SETH	SIBYL	SIB-ill
TASHA	TA-sha	TIM	TIM	TERESA*	teh-REE-sah	TED	TED
VERNON	VER-non	VANESSA	vah-NES-ah	VERNE	VERN	VAL	VAL
WINONA	wi-NO-nah	WALT	WALT	WILDA	WILL-dah	WARD	WARD
YANCY	YAN-see	YUNYA	YUNE-yah	YURI	YOUR-ee	YVETTE	ee-VET
ZOLA	ZO-lah	ZEKE	ZEEK	ZELDA	ZELL-dah	ZACK	ZACK

* Name changes: MANNY replaced MIKE in 1991; MELISSA replaced MIREILLE, TERESA replaced THELMA in 1992, and OSCAR replaced OMAR in 1993.

NOTE 1: Names are assigned in rotation and alphabetically. When the last name in Column 4 (ZACK) has been used, the sequence will begin again with the first name in Column 1 (ANGELA).

NOTE 2: Pronunciation guide for names are italicized.

SOURCE: CINCPACINST 3140.1V

APPENDIX C CONTRACTIONS

A-track	Along-track	ARGOS	International Service for Drifting Buoys	CPHC	Central Pacific Hurricane Center
AB	Air Base				
ABW	Air Base Wing	ATCF	Automated Tropical Cyclone Forecast (System)	CSC	Cloud System Center
ABIO	Significant Tropical Weather Advisory for the Indian Ocean			CSUM	Colorado State University Model
		AUTODIN	Automated Digital Network	DDN	Defense Data Network
ABPW	Significant Tropical Weather Advisory for the Western Pacific Ocean	AWDS	Automated Weather Distribution System	DEG	Degree(s)
		AWN	Automated Weather Network	DET	Detachment
ACCS	Air Control Center Squadron			DFS	Digital Facsimile System
		CCWF	Combined Confidence Weighted Forecast	DMSP	Defense Meteorological Satellite Program
ACFT	Aircraft	CDO	Central Dense Overcast		
ADP	Automated Data Processing	CEC	Circular Exhaust Cloud	DOD	Department of Defense
AFB	Air Force Base	CI	Current Intensity	DSN	Defense Switched Network
AFGWC	Air Force Global Weather Central	CINCPAC	Commander-in-Chief Pacific (AF - Air Force, FLT - Fleet)	DTG	Date Time Group
AFTN	Airfield Fixed Telecommunication Network			EGGR	Bracknell Model
		CIV	Civilian	FBAM	FNOC Beta Advection Model
AIREP	Aircraft (Weather) Report	CLD	Cloud	FI	Forecast Intensity (Dvorak)
		CLIM	Climatology		
AJTWC	Alternate Joint Typhoon Warning Center	CLIP or CLIPER	Climatology and Persistence Technique	FNOC	Fleet Numerical Oceanography Center
AMOS	Automatic Meteorological Observing Station	CM	Centimeter(s)	FT	Feet
		C-MAN	Coastal-Marine Automated Network	GMT	Greenwich Mean Time
AOR	Area of Responsibility			GOES	Geostationary Operational Environmental Satellite
APT	Automatic Picture Transmission	CNOC	Commander Naval Oceanography Command		
ARC	Automated Remote Collection	CPA	Closest Point of Approach	GTS	Global Telecommu- nications System

HPAC	Mean of XTRP and CLIM Techniques (Half Persistence and Climatology)	MBAM	Medium Beta and Advection Model	NEXRAD	Next Generation Weather (Doppler) Radar
HF	High Frequency	MCAS	Marine Corps Air Station	NHC	National Hurricane Center
HR	Hour(s)	MET	Meteorological	NM	Nautical Mile(s)
HRPT	High Resolution Picture Transmission	MIDDAS	Meteorological Imagery, Data Display, and Analysis System	NMC	National Meteorological Center
ICAO	International Civil Aviation Organization	MIN	Minimum	NOAA	National Oceanic and Atmospheric Administration
INIT	Initial	MINI-MET	Mini-Meteorological	NOCC	Naval Oceanography Command Center
INST	Instruction	MISTIC	Mission Sensor Tactical Imaging Computer	NODDES	Naval Environmental Data Network
IR	Infrared	MM	Millimeter(s)		Oceanographic Data Distribution and Expansion System
JTWC	Joint Typhoon Warning Center	MOVG	Moving	NODDS	Navy/NOAA Oceanographic Data Distribution System
JTWC92 or JT92	Statistical-dynamical Objective Technique	MSLP	Minimum Sea-level Pressure	NOGAPS or NGPS	Navy Operational Global Atmospheric Prediction System
JTYM	Japanese Typhoon Model	NARDAC	Naval Regional Data Automation Center	NR	Number
KM	Kilometer(s)	NAS	Naval Air Station	NRL	Naval Research Laboratory
KT	Knot(s)	NASA	National Aeronautics and Space Administration	NRPS or NORAPS	Navy Operational Regional Atmospheric Prediction System
LAN	Local Area Network	NAVOCEANCOM	Naval Oceanography Command	NSDS	Naval Satellite Display System
LAT	Latitude	NEDN	Naval Environmental Data Network	NSDS-G	Naval Satellite Display System - Geostationary
LLCC	Low-Level Circulation Center	NEDS	Naval Environmental Display Station	NSS	Northward-displaced, Self-sustaining, Solitary (monsoon gyre)
LONG	Longitude	NESDIS	National Environmental Satellite, Data, and Information Service	NTCC	Naval Telecommunications Center
LUT	Local User Terminal	NESN	Naval Environmental Satellite Network		
LVL	Level				
M	Meter(s)				
MAX	Maximum				
MB	Millibar(s)				

NWOC	Naval Western Oceanography Center	SFC	Surface	TOTL	Analog Technique based on all acceptable NWP basin analogs (straight and recurvers)
NWP	NorthWest Pacific	SGDB	Satellite Global Data Base		
NWS	National Weather Service	SLP	Sea-Level Pressure	TOVS	TIROS Operational Vertical Sounder
OBS	Observations	SPAWRSYSCOM	Space and Naval Warfare Systems Command	TS	Tropical Storm
OLS	Operational Linescan System		SSM/I	TUTT	Tropical Upper-Tropospheric Trough
ONR	Office of Naval Research	SST	Sea Surface Temperature	TY	Typhoon
OSS	Operations Support Squadron	STNRY	Stationary	TYAN	Typhoon Analog (Program)
OTCM	One-Way (Interactive) Tropical Cyclone Model	ST	Subtropical	TYMNET	Time-Sharing Network: Commercial wide area network connecting micro- and main-frame computers
PACAF	Pacific Air Force	STR	Subtropical Ridge		
PACMEDS	Pacific Meteorological Data System	STY	Super Typhoon	ULCC	Upper-Level Circulation Center
PACOM	Pacific Command	TAPT	Typhoon Acceleration Prediction Technique	US	United States
PCN	Position Code Number	TC	Tropical Cyclone	USAF	United States Air Force
PDN	Public Data Network	TCFA	Tropical Cyclone Formation Alert	USN	United States Navy
PIREP	Pilot Weather Report(s)	TCM-90	Tropical Cyclone Motion Mini-Field Experiment - 1992	VIS	Visual
RADOB	Radar Observation			WESTPAC	Western (North) Pacific
RECON	Reconnaissance	TD	Tropical Depression	WMO	World Meteorological Organization
RRDB	Reference Roster Data Base	TDA	Typhoon Duty Assistant	WRN or WRNG	Warning(s)
RRT	Rapid Response Team	TDO	Typhoon Duty Officer	WS	Weather Squadron
RSDB	Raw Satellite Data Base	TESS	Tactical Environmental Display System	X-track	Cross-track
SAT	Satellite	TIROS	Television Infrared Observational Satellite	XTRP	Extrapolation
SEC	Second	TOGA	Tropical Ocean Global	Z	Zulu time (Greenwich Mean Time/Universal Coordinated Time)
SDHS	Satellite Data Handling System	COARE	Atmosphere Coupled Ocean-Atmosphere Response Experiment		

APPENDIX D

PAST ANNUAL TROPICAL CYCLONE REPORTS

Copies of the past Annual Tropical Cyclone Reports for DOD agencies or contractors can be obtained through:

Defense Technical Information Center
ATTN:FDAC
Cameron Station
Alexandria, VA 22304-6145

Phone: (703)-274-7633
Fax: (703)-274-9307

Copies for non-DOD agencies or users can be obtained from:

National Technical Information Service
5285 Port Royal Road
Springfield, VA 22161

Phone: (703)-487-4650
Fax: (703)-321-8547

Refer to the following numbers when ordering:

<u>YEAR</u>	<u>ACQUISITION NUMBER</u>	<u>YEAR</u>	<u>ACQUISITION NUMBER</u>	<u>YEAR</u>	<u>ACQUISITION NUMBER</u>
1959	AD 786147	1970	AD 785252	1981	AD A112002
1960	AD 786148	1971	AD 768333	1982	AD A124860
1961	AD 786149	1972	AD 768334	1983	AD A137836
1962	AD 786128	1973	AD 777093	1984	AD A153395
1963	AD 786208	1974	AD 010271	1985	AD A168284
1964	AD 786209	1975	AD A023601	1986	AD A184082
1965	AD 786210	1976	AD A038484	1987	AD A191883
1966	AD 785891	1977	AD A055512	1988	AD A207206
1967	AD 785344	1978	AD A070904	1989	AD A232469
1968	AD 785251	1979	AD A082071	1990	AD A239910
1969	AD 785178	1980	AD A094668	1991	AD A251952

APPENDIX E DISTRIBUTION LIST

1 COPY

ACCU-WEATHER, INC.
 AEROMET, INC.
 ANALYSIS & PROCESSING CENTER, INDONESIA
 ARNOLD ASSOCIATES
 ASIAN DISASTER PREPAREDNESS CENTER,
 BANGKOK, THAILAND
 BARRETT CONSULTING GROUP
 BRUNEI SHELL PETROLEUM CO
 CATHOLIC UNIVERSITY OF AMERICA
 CAF WEATHER CENTRAL, TAIWAN
 CENTRAL MET OBSERVATORY, BEIJING
 CENTRAL METEOROLOGICAL OFFICE, SEOUL
 CHULALONGKORN UNIVERSITY, BANGKOK
 CHUNG CHENG INSTITUTE, TAIWAN
 CITIES SERVICES OIL GAS CORP
 CITY POLYTECHNIC OF HONG KONG
 CIUDAD UNIVERSITARIA, MEXICO
 CIVIL DEFENSE, BELAU
 CIVIL DEFENSE, MAJURO
 CIVIL DEFENSE, POHNPEI
 CIVIL DEFENSE, SAIPAN
 CIVIL DEFENSE, TRUK
 CIVIL DEFENSE, YAP
 CINCPACFLT
 CNN
 CNO
 COLORADO STATE UNIVERSITY LIBRARY
 COMMONWEALTH NORTHERN MARIANA
 ISLANDS
 COMNAVMAV
 COMNAVOCEANCOM
 COMNAVSURFPAC
 COMPATRECFOR
 COMPHIBGRU ONE
 COMSC
 COMSEVENTHFLT
 COMSPAWARSTSCOM
 COMSUBGRU SEVEN
 COMTHIRDFLT
 COMUSNAVCENT
 CONGRESSIONAL INFORMATION SERVICE, MD
 DCA GUAM
 DET 1, 15WS WHEELER AFB, HI
 DET 2, 51WS CAMP HUMPHREYS, KOREA
 DISASTER CONTROL OFFICE, SAIPAN
 EDMUNDS COLLEGE SOCIAL SCIENCE DEPT
 FAIRECONRON ONE
 FEDERAL EMERGENCY MANAGEMENT AGENCY,
 GUAM
 FIJI METEOROLOGICAL SERVICE

GEOLOGICAL FLUID DYNAMICS LAB,
 PRINCETON, NJ
 GEOLOGICAL SURVEY, GUAM
 GEOPHYSICS LAB/LYS
 GIFU METEOROLOGICAL OFFICE, JAPAN
 GODDARD SPACE FLIGHT CENTER
 GUAM COMMUNITY COLLEGE
 GUAM POWER AUTHORITY
 GUAM PUBLIC LIBRARY
 HORIZON MARINE, INC
 HQ AIR COMBAT COMMAND/DOW
 HQ AWS
 HQ AWS GROUP, ATC & WX WING JASDF, TOKYO
 HQ US STRATCOM/J3615
 HQ USAF/XOORZ
 INDIAN INSTITUTE OF TROPICAL MET INSTITUO
 DE GEOFISICA, MEXICO
 INTERNATIONAL CENTER FOR DISASTER
 MITIGATION, TOKYO
 JAPAN AIR LINES
 JCS ENV SERVICES DIV (J3(OES))
 JET PROPULSION LAB, PASADENA
 LEND FOUNDATION
 LISD CAMP SPRINGS CENTER, MD
 LOS ANGELES PUBLIC LIBRARY
 MARATHON OIL CO, TX
 MAURITIUS METEOROLOGICAL SERVICE
 MASS INST OF TECH
 MCAS FUTENMA
 MCAS IWAKUNI
 MCAS KANEOHE BAY, HI
 MERCANTILE AND GENERAL REINSURANCE,
 AUSTRALIA
 METEOROLOGICAL DEPARTMENT, PAKISTAN
 METEOROLOGICAL OFFICE, BRACKNELL
 METEOROLOGICAL SERVICE, MADAGASCAR
 METEOROLOGICAL SERVICE, MAURITIUS
 METEOROLOGICAL SERVICE, REUNION
 MIL ASST ENV SCI (R & AT / E & LS)
 MOBIL OIL GUAM, INC
 MONASH UNIVERSITY, AUSTRALIA
 NASA
 NATIONAL CLIMATIC DATA CENTER LIBRARY,
 ASHEVILLE, NC
 NATIONAL METEOROLOGICAL CENTER
 NATIONAL METEOROLOGICAL LIBRARY,
 BRACKNELL, UK
 NATIONAL RESOURCES INSTITUTE, INC, UK
 NATIONAL TAIWAN UNIVERSITY
 NATIONAL TECHNICAL INFORMATION SERVICE

NATIONAL WEATHER SERVICE, PAPUA NEW
 GUINEA
 NAVAL CIVIL ENG LAB, PORT HUENEME, CA
 NAVAL RESEARCH LAB
 NAVEASTOCEANCEN NORFOLK
 NAVHISTCEN
 NAVOCEANCOMCEN ROTA
 NAVOCEANCOMDET AGANA
 NAVOCEANCOMDET ASHEVILLE
 NAVOCEANCOMDET ATSUGI
 NAVOCEANCOMDET KADENA
 NAVOCEANCOMDET MISAWA
 NAVOCEANCOMFACDET SASEBO
 NAVOCEAN COMFAC JACKSONVILLE
 NAVOCEANCOMFAC YOKOSUKA
 NAVOCEANO
 NAVAL POSTGRADUATE SCHOOL LIBRARY
 NAVPOLAROCEANCEN SUITLAND
 NEW ZEALAND INSURANCE
 NEW ZEALAND MET SERVICE
 NOAA/ACQUISITION SECTION, ROCKVILLE, MD
 NOAA/AOML, HRD, MIAMI, FL
 NOAA, ATMOS TURB AND DIFFUSION DIV, OAK
 RIDGE, TN
 NOAA/HYDROMETEOROLOGY BR, SILVER
 SPRINGS, MD
 NOAA/NESDIS, HONOLULU, HI
 NOAA/PMEL, SEATTLE, WA
 NOAA ENVIRONMENTAL RESEARCH LAB
 NOAA LIBRARY, SEATTLE, WA
 NOBEL DENTON
 NRL ATMOSPHERIC DIRECTORATE
 OCEANROUTES, INC, JOLIMENT, WEST
 AUSTRALIA
 OCEANROUTES, INC, SINGAPORE
 OCEANROUTES, INC, SUNNYVALE, CA
 OCEANWEATHER, INC
 OFFICE OF FEDERAL COORDINATOR MET
 OFFICE OF NAVAL RESEARCH
 OFFICE OF THE NAVAL DEPUTY, NOAA
 OL-B, DET 1, 51WS SEOUL, KOREA
 OL-B, DET 3 51WS CAMP CASEY, KOREA
 PACIFIC STARS & STRIPES
 PACNAVFAENGCOM
 QUEENS COLLEGE, DEPT OF GEOLOGY
 PENNSYLVANIA STATE UNIVERSITY
 REUNION METEOROLOGICAL SERVICE
 RUCH WEATHER SERVICE, INC
 SAINT LOUIS UNIVERSITY
 SAT APPL LAB, NOAA/NESDIS, WASHINGTON, DC
 SHANGHAI TYPHOON INSTITUTE
 SRI LANKA METEOROLOGICAL SOCIETY
 SRI LIBRARY
 TAO PROJECT OFFICE

TEXAS A & M UNIVERSITY
 UNIV OF COLORADO, ATMOS SCIENCE
 UNIVERSITY OF CHICAGO
 UNIVERSITY OF GUAM, BIOLOGY DEPT
 UNIVERSITY OF HAWAII LIBRARY
 UNIVERSITY OF WASHINGTON
 USAFETAC/DN
 USCINCPAC
 USCINCPAC REP GUAM
 USCINCPAC REP FIJI
 USNA (OCEANOGRAPHY DEPT/LIBRARY)
 USS AMERICA (CV 66)
 USS BLUE RIDGE (LCC 19)
 USS BELLEAU WOOD (LHA 3)
 USS CARL VINSON (CVN 70)
 USS CONSTELLATION (CV 64)
 USS EISENHOWER (CVN 69)
 USS INDEPENDENCE (CV 62)
 USS J. F. KENNEDY (CV 67)
 USS KITTY HAWK (CV 63)
 USS LINCOLN (CVN 72)
 USS NEW ORLEANS (LPH 11)
 USS NIMITZ (CVN 68)
 USS PELELIU (LHA 5)
 USS RANGER (CV 61)
 USS SARATOGA (CV 60)
 USS TARAWA (LHA 1)
 USS TRIPOLI (LPH 10)
 USS T. ROOSEVELT (CVN 71)
 USS WASP (LHD 1)
 VANUATU METEOROLOGICAL SERVICE
 WORLD DATA CENTER B1, MOSCOW
 AFGWC/WFM
 3 AIR DIVISION HICKAM AFB, HI
 8 OSS/DOW KUNSAN AB, KOREA
 15 WS HICKAM AFB, HI
 18 OSS/DOW KADENA AB, JAPAN
 334 TCHTS/TTMV KEESLER AFB, MS
 374 OSS/DOW YOKOTA AB, JAPAN
 375 WS/OGWA SCOTT AFB, IL
 432 OSS/DOW MISAWA AB, JAPAN
 603 ACCS/WE OSAN AB, KOREA
 633 OSS/DOW ANDERSEN AFB, GU
 652 SPTG/DOW MCCLELLAN AFB, CA
 815 WS (AFRES), KEESLER AFB, MS

2 COPIES

AFGWC/WFMP
 AWS TECH LIBRARY
 BUREAU OF METEOROLOGY, BRISBANE
 BUREAU OF METEOROLOGY, DARWIN
 BUREAU OF METEOROLOGY LIBRARIAN,
 MELBOURNE
 BUREAU OF METEOROLOGY, PERTH

BUREAU OF PLANNING, GUAM
 CIVIL DEFENSE, GUAM
 DEFENSE TECHNICAL INFORMATION CENTER
 DEPARTMENT OF COMMERCE
 ECMWF, BERKSHIRE, UK
 ESCAP LIBRARY, BANGKOK
 FLENUMOCEANCEN MONTEREY
 FLORIDA STATE UNIVERSITY
 INSTITUTE OF PHYSICS, TAIWAN
 MARINERS WEATHER LOG
 MET RESEARCH INST LIBRARY, TOKYO
 MICRONESIAN RESEARCH CENTER UOG, GUAM
 NATIONAL CLIMATIC DATA CENTER
 NATIONAL DATA BUOY CENTER
 NATIONAL HURRICANE CENTER, MIAMI
 NATIONAL WEATHER SERVICE, HONOLULU
 NAVOCEANCOMDET DIEGO GARCIA
 NAVOCEANCOMDET MISAWA
 NAVWF.STOCEANCEN PEARL HARBOR
 NOAA GUAM
 NORA 1570 DALLAS, TX
 OKINAWA METEOROLOGY OBSERVATORY
 SAT APPL LAB, NOAA/NESDIS, CAMP SPRINGS,
 MD
 TYPHOON COMMITTEE SECRATARIAT, MANILA
 UNIVERSITY OF PHILIPPINES
 US ARMY, FORT SHAFTER
 WORLD DATA CENTER A, NOAA
 73 WEATHER GROUP, ROK AF

3 COPIES

BUREAU OF METEOROLOGY, DIRECTOR,
 MELBOURNE, AUSTRALLIA
 CENTRAL WEATHER BUREAU, TAIWAN
 INDIA METEOROLOGICAL DEPT
 INOSHAC, DDGM (WF)
 JAPAN METEOROLOGICAL AGENCY
 KOREAN METEOROLOGY ADMINISTRATION
 NAVPGSCOL DEPT OF METEOROLOGY
 NOAA CORAL GABLES LIBRARY
 PACAF/DOW
 UNIVERSITY OF HAWAII, METEOROLOGY DEPT
 WEATHER CENTRAL, CAF

4 COPIES

COLORADO STATE UNIVERSITY
 METEOROLOGY DEPT, BANGKOK

5 COPIES

PAGASA WEATHER BUREAU, RP
 R & D UNIT, NHC, MIAMI
 ROYAL OBSERVATORY HONG KONG

6 COPIES

NRL WEST
 NATIONAL WEATHER ASSOCIATION

UNCLASSIFIED

SECURITY CLASSIFICATION OF THIS PAGE

REPORT DOCUMENTATION PAGE				
1a. REPORT SECURITY CLASSIFICATION UNCLASSIFIED			1b. RESTRICTIVE MARKINGS	
2a. SECURITY CLASSIFICATION AUTHORITY			3. DISTRIBUTION/AVAILABILITY OF REPORT AS IT APPEARS IN THE REPORT/ DISTRIBUTION UNLIMITED	
2b. DECLASSIFICATION/DOWNGRADING SCHEDULE				
4. PERFORMING ORGANIZATION REPORT NUMBER(S)			5. MONITORING ORGANIZATION REPORT NUMBER(S)	
6a. NAME OF PERFORMING ORGANIZATION NAVOCEANCOMCEN/JTWC		6b. OFFICE SYMBOL (If applicable)	7a. NAME OF MONITORING ORGANIZATION NAVOCEANCOMCEN/JTWC	
6c. ADDRESS (City, State and ZIP Code) COMNAVMAR, PSC 489, BOX 12 FPO AP 96536-0051			7b. ADDRESS (City, State and ZIP Code) COMNAVMAR, PSC 489, BOX 12 FPO AP 96536-0051	
8a. NAME OF FUNDING SPONSORING ORGANIZATION NAVOCEANCOMCEN/JTWC		8b. OFFICE SYMBOL (If applicable)	9. PROCUREMENT INSTRUMENT IDENTIFICATION NUMBER	
8c. ADDRESS (City, State and ZIP Code) COMNAVMAR, PSC 489, BOX 12 FPO AP 96536-0051			10. SOURCE OF FUNDING NOS.	
11. TITLE (Include Security Classification) 1992 ANNUAL TROPICAL CYCLONE REPORT			PROGRAM ELEMENT NO.	PROJECT NO.
			TASK NO.	WORK UNIT NO.
12. PERSONAL AUTHOR(S)				
13a. TYPE OF REPORT ANNUAL		13b. TIME COVERED FROM JAN 92 TO DEC 92	14. DATE OF REPORT (Yr., Mo., Day) 1992	15. PAGE COUNT 269 plus i thru vi
16. SUPPLEMENTARY NOTATION				
17. COSATI CODES			18. SUBJECT TERMS (Continue on reverse if necessary and identify by block number)	
FIELD	GROUP	SUB. GR.	TROPICAL CYCLONES TROPICAL STORMS	
			TROPICAL DEPRESSIONS TYPHOONS/SUPER TYPHOONS	
			TROPICAL CYCLONE RESEARCH METEOROLOGICAL SATELLITES	
19. ABSTRACT (Continue on reverse if necessary and identify by block number)				
ANNUAL PUBLICATION SUMMARIZING TROPICAL CYCLONE ACTIVITY IN THE WESTERN NORTH PACIFIC, BAY OF BENGAL, ARABIAN SEA, WESTERN SOUTH PACIFIC AND SOUTH INDIAN OCEANS. A BEST TRACK IS PROVIDED FOR EACH SIGNIFICANT TROPICAL CYCLONE. A BRIEF NARRATIVE IS GIVEN FOR ALL TROPICAL CYCLONES IN THE WESTERN NORTH PACIFIC AND NORTH INDIAN OCEANS. ALL FIX DATA USED TO CONSTRUCT THE BEST TRACKS ARE PROVIDED, UPON REQUEST, ON DISKETTES. FORECAST VERIFICATION DATA AND STATISTICS FOR THE JOINT TYPHOON WARNING CENTER (JTWC) ARE SUBMITTED.				
20. DISTRIBUTION/AVAILABILITY OF ABSTRACT UNCLASSIFIED/UNLIMITED <input checked="" type="checkbox"/> SAME AS RPT. <input checked="" type="checkbox"/> DTIC USERS <input type="checkbox"/>			21. ABSTRACT SECURITY CLASSIFICATION UNCLASSIFIED	
22a. NAME OF RESPONSIBLE INDIVIDUAL FRANK H. WELLS			22b. TELEPHONE NUMBER (Include Area Code) (671)-344-5240	22c. OFFICE SYMBOL NOCC/JTWC

UNCLASSIFIED

SECURITY CLASSIFICATION OF THIS PAGE

BLOCK 18 (CONTINUED)

RADAR

AUTOMATIC METEOROLOGICAL OBSERVING STATIONS

SYNOPTIC DATA

TROPICAL CYCLONE INTENSITY

TROPICAL CYCLONE BEST TRACK DATA

TROPICAL CYCLONE FORECASTING

TROPICAL CYCLONE RECONNAISSANCE

TROPICAL CYCLONE STEERING MODELS

OBJECTIVE FORECASTING TECHNIQUES

TROPICAL CYCLONE FIX DATA

MICROWAVE IMAGERY

DRIFTING BUOYS

UNCLASSIFIED

SECURITY CLASSIFICATION OF THIS PAGE